

SHEAR STRENGTH BEHAVIOR OF GRANULAR FILL-CLAYEY SOIL  
INTERFACES AND IMPROVEMENT WITH DOWELS

A THESIS SUBMITTED TO  
THE GRADUATE SCHOOL OF NATURAL AND APPLIED SCIENCES  
OF  
MIDDLE EAST TECHNICAL UNIVERSITY

BY

ŞEVKİ ÖZTÜRK

IN PARTIAL FULFILLMENT OF THE REQUIREMENTS  
FOR  
THE DEGREE OF DOCTOR OF PHILOSOPHY  
IN  
CIVIL ENGINEERING

FEBRUARY 2015



Approval of the thesis:

**SHEAR STRENGTH BEHAVIOR OF GRANULAR FILL-CLAYEY SOIL  
INTERFACES AND IMPROVEMENT WITH DOWELS**

submitted by **ŞEVKİ ÖZTÜRK** in partial fulfillment of the requirements for the degree of **Doctor of Philosophy in Civil Engineering Department, Middle East Technical University** by,

Prof. Dr. Gülbin Dural Ünver  
Dean, Graduate School of **Natural and Applied Sciences**

\_\_\_\_\_

Prof. Dr. Ahmet Cevdet Yalçın  
Head of Department, **Civil Engineering**

\_\_\_\_\_

Prof. Dr. M. Ufuk Ergun  
Supervisor, **Civil Engineering Dept., METU**

\_\_\_\_\_

**Examining Committee Members:**

Prof. Dr. Erdal Çokca  
Civil Engineering Dept., METU

\_\_\_\_\_

Prof. Dr. M. Ufuk Ergun  
Civil Engineering Dept., METU

\_\_\_\_\_

Prof. Dr. Reşat Ulusay  
Geological Engineering Dept., Hacettepe University

\_\_\_\_\_

Asst. Prof. Dr. Nejan Huvaj Sarıhan  
Civil Engineering Dept., METU

\_\_\_\_\_

Asst. Prof. Dr. Kartal Toker  
Civil Engineering Dept., METU

\_\_\_\_\_

**Date:** 06.02.2015

**I hereby declare that all information in this document has been obtained and presented in accordance with academic rules and ethical conduct. I also declare that, as required by these rules and conduct, I have fully cited and referenced all material and results that are not original to this work.**

Name, Last Name : Şevki Öztürk

Signature :

## **ABSTRACT**

### **SHEAR STRENGTH BEHAVIOR OF GRANULAR FILL-CLAYEY SOIL INTERFACES AND IMPROVEMENT WITH DOWELS**

Öztürk, Şevki  
Ph.D., Department of Civil Engineering  
Supervisor: Prof. Dr. M. Ufuk Ergun

February 2015, 268 pages

Shear failures of interfaces between granular material and clay are frequently encountered in engineering practice. In earthfill dams, road embankments and spoil piles in mining operations, granular materials are placed on clay, and shear failures and/or large movements are observed along interfaces. When dealing with this type of a problem selecting representative shear strength parameters is difficult. Furthermore in the literature no accepted procedure is available to select these parameters.

This study aims to assess the shear strength behavior of interfaces between granular materials and clay soils. For this purpose, drained direct shear (small and large scale) tests and triaxial tests have been conducted on samples composed of clay, granular soil and granular soil-clay interfaces. All of the experiments were continued up to large displacements to determine large strain behavior.

The results of all experiments are presented in the thesis, and comparisons have been made among all test results, the main focus being directed to select shear strength parameters for the interfaces. Sand-clay and gravel-clay interfaces yielded several degrees of additional friction angle compared to drained friction angle of clay at large strains.

The effect of dowels that reinforce the gravel-clay interface is also studied through model experiments in large shear box. Depending on the length and number of the dowels, shear strength increased considerably especially in case of longer dowels, and it proved to be an effective way to increase the shear strength of granular soil-clay interfaces.

**Keywords:** Interface, Direct Shear Test, Shear Strength, Large Shear Box, Improvement with Dowels

## ÖZ

### DANELİ DOLGU-KİLLİ ZEMİN ARAYÜZEYİ KAYMA MUKAVEMETİ DAVRANIŞI VE KISA KAZIKLAR İLE İYİLEŞTİRME

Öztürk, Şevki  
Doktora, İnşaat Mühendisliği Bölümü  
Tez Yöneticisi: Prof. Dr. M. Ufuk Ergun

Şubat 2015, 268 sayfa

Daneli (granüler) malzeme-kil arayüzeylerinde kayma (makaslama) yenilmesi mühendislik uygulamalarında sıklıkla karşılaşılan bir durumdur. Baraj, yol ve madencilik uygulamalarında daneli malzemeler kilin üzerine yerleştirilir ve bu yüzeylerde kayma yenilmeleri ve/veya büyük hareketler olabilir. Bu tip problemlerin çözümünde gerçekçi bir kayma mukavemeti (makaslama dayanımı) parametresi seçmek güçtür. Ayrıca literatürde bu parametrelerin seçimi için kabul edilmiş bir yöntem bulunmamaktadır.

Bu çalışma, daneli malzeme-kil arayüzeyinde kayma mukavemeti davranışının belirlenmesini amaçlamaktadır. Bu amaçla kil, daneli malzeme ve daneli malzeme-kil arayüzeylerinde drenajlı direkt kesme (doğrudan makaslama) deneyleri (hem büyük, hem küçük ölçekli) ve üç eksenli deneyler yapılmıştır. Tüm deneyler yüksek birim deformasyon davranışını inceleyebilmek amacıyla büyük yer değiştirmelere kadar sürdürülmüştür.

Tüm deney sonuçları tezde sunulmuş olup; arayüzeyler için kayma mukavemeti parametrelerinin seçimine odaklanılarak deney sonuçları arasında gerekli karşılaştırmalar yapılmıştır. Büyük birim deformasyonlarda kum-kil ve çakıl-kil arayüzeylerinin kil ile mukayese edildiğinde birkaç dereceden daha fazla sürtünme açısı verdiği görülmüştür.

Çakıl-kil arayüzeyini güçlendiren kısa kazıkların etkisi de büyük direkt kesme kutusunda model deneyler yapılarak araştırılmıştır. Kısa kazıkların sayısına ve boyuna bağlı olarak kayma mukavemetinin özellikle daha uzun kazıklar kullanıldığında önemli ölçüde arttığı ve kısa kazıkların daneli malzeme-kil arayüzeylerinde kayma mukavemetini arttırmak için etkili bir yöntem olduğu gösterilmiştir.

Anahtar Kelimeler: Arayüzey, Direkt Kesme Deneyi, Kayma Mukavemeti, Büyük Ölçekli Direkt Kesme Kutusu, Kısa Kazıklarla İyileştirme

*To Enes Ilgar and Nehir Ilgim*

## ACKNOWLEDGMENTS

The author wishes to express his deepest appreciation to his supervisor Prof. Dr. M. Ufuk Ergun for his guidance, advice, encouragements and insight throughout the research.

The author would like to thank Prof. Dr. Reşat Ulusay and Asst.Prof. Dr. Nejan Huvaj Sarihan for their valuable supports and contributions during the progress of the thesis.

For continuous support during this research, the author is grateful to Asst. Prof. Dr. Volkan Kalpakcı.

Mr. Ali Bal and METU Civil Engineering Geotechnical Laboratory Staff are appreciated for their valuable technical assistances.

For the scholarship provided to the author during the research TÜBİTAK is appreciated.

The author is grateful to his family, especially to his brother Özgür and his wife Serap, for their continuous support, encouragement and patience.

## TABLE OF CONTENTS

ABSTRACT .....	v
ÖZ.....	vi
ACKNOWLEDGMENTS .....	viii
TABLE OF CONTENTS.....	ix
LIST OF TABLES .....	xii
LIST OF FIGURES .....	xiii
LIST OF SYMBOLS AND ABBREVIATIONS .....	xviii
CHAPTERS	
1. INTRODUCTION .....	1
1.1 Problem Statement.....	1
1.2 Research Methodology and Objectives .....	2
1.3 Thesis Outline.....	3
2. LITERATURE REVIEW .....	5
2.1 Introduction .....	5
2.2 Shear Strength Studies.....	5
3. EXPERIMENTAL STUDY I - DIRECT SHEAR TESTS .....	31
3.1 Introduction .....	31
3.2 Materials Used in Experiments.....	32
3.2.1 Clay .....	32
3.2.2 Granular Material .....	33
3.3 Large Shear Box Tests.....	35
3.3.1 Experimental Setup .....	35
3.3.2 Results of Large Shear Box Tests .....	37
3.3.2.1 Large Shear Box Tests of Gravel.....	37
3.3.2.2 Large Shear Box Tests of Clay-Gravel Interfaces .....	39
3.4 Small Shear Box Tests.....	44
3.4.1 Shearing Rate Effect.....	45
3.4.2 Results of Small Shear Box Tests .....	46
3.4.2.1 Small Shear Box Tests of Clay.....	47
3.4.2.2 Small Shear Box Tests of Sand .....	50

3.4.2.3	Small Shear Box Tests of Clay-Sand Interfaces .....	52
3.5	Discussion of Results .....	54
4.	EXPERIMENTAL STUDY II - TRIAXIAL TESTS .....	59
4.1	Introduction.....	59
4.2	Triaxial Testing Equipment .....	59
4.3	Triaxial Tests of Intact Clay Specimen.....	61
4.4	Triaxial Tests of Interfaces .....	64
4.4.1	Triaxial Tests of Clay-Clay Interface .....	70
4.4.2	Granular Material-Clay Interface Triaxial Tests.....	75
4.4.2.1	Gravel-Clay Interface.....	76
4.4.2.2	Sand-Clay Interface.....	81
4.5	Triaxial Tests of Granular Material .....	85
4.6	Discussion of Results .....	87
5.	EXPERIMENTAL STUDY III - IMPROVEMENT WITH DOWELS.....	91
5.1	Introduction.....	91
5.2	Shear Tests of Interfaces Improved with Model Dowels.....	91
5.3	Results and Discussion.....	98
5.4	Effect of Continuous Improvement.....	108
6.	SUMMARY OF RESULTS AND CONCLUSIONS .....	111
6.1	Introduction.....	111
6.2	Results in Direct Shear Tests .....	111
6.2.1	Peak Friction Angles.....	111
6.2.2	Friction Angles at Large Deformation.....	112
6.2.3	Cohesion Values .....	112
6.3	Results in Triaxial Tests.....	112
6.3.1	Peak Friction Angles.....	112
6.3.2	Friction Angles at Large Deformation.....	113
6.3.3	Cohesion Values .....	113
6.4	Results in Improvement Tests.....	113
6.5	Conclusions.....	114
6.6	Recommendations for Future Studies .....	115

REFERENCES .....	117
APPENDICES	
A. DIRECT SHEAR TESTS .....	121
B. TRIAXIAL TESTS .....	159
C. IMPROVEMENT TESTS .....	205
D. UNCONSOLIDATED UNDRAINED (UU) TESTS OF CLAY .....	253
E. AREA AND MEMBRANE CORRECTION IN TRIAXIAL TESTS.....	263
VITA.....	267

## LIST OF TABLES

### TABLES

Table 2.1 Shear Test Results of Different Materials (Kasmer and Ulusay, 2006) .....	19
Table 3.1 Mineralogical and Chemical Properties of Clay (Şengör, 2013) .....	32
Table 3.2 Basic Parameters of Granular Materials.....	34
Table 3.3 Summary of Direct Shear Tests-Shear Strength Parameters.....	55
Table 4.1 Summary of Triaxial Shear Tests-Shear Strength Parameters .....	87
Table 5.1 Model Dowels Used in Improvement Tests .....	91
Table 5.2 Improvement Test Sets Conducted.....	95
Table 5.3 Results of Improvement Tests .....	99
Table 5.4 Summary of Improvement Test Results (Average) for $\sigma_n'=111$ kPa.....	103
Table 5.5 Summary of Improvement Test Results (Average) for $\sigma_n'=222$ kPa.....	104
Table 5.6 Summary of Improvement Test Results (Average) for $\sigma_n'=333$ kPa.....	104
Table 5.7 Summary of Unconsolidated Undrained (UU) Test Results .....	105
Table 5.8 Shear Contribution of Dowels- $\sigma_n'=111$ kPa.....	106
Table 5.9 Shear Contribution of Dowels- $\sigma_n'=222$ kPa.....	107
Table 5.10 Shear Contribution of Dowels- $\sigma_n'=333$ kPa.....	107
Table 5.11 Properties of Fiberglass Used in Continuous Improvement Tests ....	108
Table 5.12 Continuous Improvement Experiments.....	108

## LIST OF FIGURES

### FIGURES

Figure 1.1 Shear Failures along Interfaces (Kasmer and Ulusay, 2006) .....	1
Figure 2.1 Influence of Confining Pressure ( $\sigma_3$ ) on Maximum Principal Stress Ratio $(\sigma_1/\sigma_3)_f$ (Charles and Watts, 1980) .....	5
Figure 2.2 Failure Envelope of Rockfills (Charles and Watts, 1980).....	6
Figure 2.3 Change in Friction Angle and Cohesion with Sand Content (Miller and Sowers, 1957) .....	7
Figure 2.4 Failure Envelope for Different Gravel Content (Holtz, 1960) .....	8
Figure 2.5 Shear Resistance vs. Coarse Fraction (Patwardhan et al., 1970).....	9
Figure 2.6 Shear Strength of Sand-Clay-Gravel Mixtures (Donagne and Torrey, 1979) .....	9
Figure 2.7 Effect of Crushed Rock Content on Shear Strength (Irfan and Tang, 1992).....	10
Figure 2.8 Change of Shear Strength with Coarse Fraction Content in a) Large Shear Box b) Small Shear Box (Irfan and Tang, 1992) .....	11
Figure 2.9 Control of Shear Strength (Irfan and Tang, 1992).....	12
Figure 2.10 Stress-Strain Curves for Two Different Gradations (Indraratna et al.,1993) .....	13
Figure 2.11 Influence of Effective Confining Pressure on Sample Strains at Peak Deviator Stress (Indraratna et al.,1993) .....	14
Figure 2.12 a) Failure Envelope of Greywacke b) Effect of Confining Stress on Friction Angle (Indraratna et al., 1993) .....	14
Figure 2.13 Stress-Strain Curves for Spoil Material (Ulusay et al., 1995) .....	15
Figure 2.14 Failure Envelopes for Spoil Material (Ulusay et al., 1995).....	16
Figure 2.15 Roughness Effect on Shear Strength (Barton, 2008).....	16
Figure 2.16 Failure Envelope and Change of Friction Angle with Confining Stress (Wang, 2006) .....	17
Figure 2.17 Failures and Combined Failure Surface (Kasmer and Ulusay, 2006) .....	18
Figure 2.18 Direct Shear Testing of Interface (Kasmer and Ulusay, 2006) .....	19
Figure 2.19 Experimental Setup (Zhang et al., 2007) .....	20
Figure 2.20 Typical Test Results for CS-FS Interface (Zhang et al., 2007) .....	21
Figure 2.21 Typical Test Results for SS-FS Interface (Zhang et al., 2007).....	22
Figure 2.22 Combined Failure Envelope (Zhang et al., 2007).....	22

Figure 2.23 Laminar Ring Displacements (Zhang et al., 2007) .....	23
Figure 2.24 In-situ Sample Preparation (Xu et al., 2007) .....	24
Figure 2.25 Particle Movements (Bareither et al., 2008) .....	25
Figure 2.26 Typical Test Results (Bareither et al., 2008) .....	26
Figure 2.27 Tests Results of Nakao and Fityus, 2008 .....	27
Figure 2.28 Effects of Particle Size and Size of the Shear Box (Nakao and Fityus, 2008) .....	28
Figure 2.29 Tests Results of Fakhimi and Hosseinpour, 2008 .....	29
Figure 2.30 Change of Friction Angle and Cohesion with Gravel Content (Mollamahmutoğlu and Yılmaz, 2009) .....	30
Figure 3.1 Gradation of the Clay Specimen (Result of Hydrometer Test) .....	33
Figure 3.2 Gradation of the Granular Material .....	34
Figure 3.3 General View of Large Shear Box .....	35
Figure 3.4 Instrumentation on Large Shear Box .....	36
Figure 3.5 Shear Stress-Shear Displacement Graphs of Gravel in Large Shear Box .....	38
Figure 3.6 Settlement of Gravel during Shearing in Large Shear Box .....	38
Figure 3.7 Shear Strength Envelope of Gravel in Large Shear Box .....	39
Figure 3.8 Large Shear Box Tests of Gravel-Clay Interface .....	40
Figure 3.9 Gravel-Clay Interface in Large Shear Box Tests .....	40
Figure 3.10 Consolidation Graph of Interface (Sample) .....	41
Figure 3.11 Shear Stress-Shear Displacement Graphs of Gravel-Clay Interface .....	41
Figure 3.12 Settlement of Gravel-Clay Interface in Large Shear Box during Shear .....	42
Figure 3.13 Peak Shear Strength Envelope of Gravel-Clay Interface (All Tests) .....	43
Figure 3.14 Peak Shear Strength Envelope of Gravel-Clay Interface .....	43
Figure 3.15 Large Deformation Shear Strength Envelope of Gravel-Clay Interface .....	44
Figure 3.16 General View of Small Shear Box Machine .....	45
Figure 3.17 Effect of Shearing Rate for $\sigma_n' = 173.30$ kPa .....	46
Figure 3.18 Effect of Shearing Rate for $\sigma_n' = 108.30$ kPa .....	46
Figure 3.19 Settlement of Clay in Consolidation Stage .....	47
Figure 3.20 Stress-Displacement Graphs of Clay .....	48
Figure 3.21 Settlement of Clay during Shearing .....	48
Figure 3.22 Peak Shear Strength Envelope of Clay .....	49

Figure 3.23 Residual Shear Strength Envelope of Clay.....	49
Figure 3.24 Stress-Displacement Curves of Clay in Residual Tests.....	50
Figure 3.25 Stress-Displacement Graphs of Sand in Small Shear Box .....	50
Figure 3.26 Vertical Displacement of Sand during Shearing .....	51
Figure 3.27 Shear Strength Envelope of Sand .....	51
Figure 3.28 Small Shear Box Tests of Sand-Clay Interface .....	52
Figure 3.29 Shear Stress-Shear Displacement Curves of Sand-Clay Interface .....	52
Figure 3.30 Settlement of Sand-Clay Interface during Shearing .....	53
Figure 3.31 Peak Shear Strength Envelope of Sand-Clay Interface .....	53
Figure 3.32 Large Deformation Envelopes of Sand-Clay Interface .....	54
Figure 3.33 Summary of Direct Shear Tests.....	55
Figure 3.34 Secant Friction Angles Obtained from Peak Shear Strengths of Direct Shear Tests.....	57
Figure 3.35 Secant Friction Angles Obtained from Large Deformation Shear Strengths of Direct Shear Tests .....	58
Figure 4.1 Triaxial Testing Apparatus .....	60
Figure 4.2 Clay Specimens after Triaxial Tests.....	61
Figure 4.3 Volume Change during Consolidation Stage of Clay .....	62
Figure 4.4 Stress-Strain Graphs of Clay in Triaxial Tests .....	62
Figure 4.5 Change in Volume during Triaxial Tests of Clay.....	63
Figure 4.6 p-q Plot of Clay in Triaxial Tests .....	63
Figure 4.7 Mohr Circles and Peak Shear Strength Envelope of Clay .....	64
Figure 4.8 Transferring Clay from Specimen Mold to “Pre-Cut Mold” (a) 10x20 cm Specimen (b) 5x10 cm Specimen.....	65
Figure 4.9 Cutting Clay Symmetrically with 56° Angle Using Fret Saw (a) 10x20 cm Specimen (b) 5x10 cm Specimen.....	66
Figure 4.10 Pre-Cut Clay (Lower Part of the Interface) (a) 10x20 cm Specimen (b) 5x10 cm Specimen.....	66
Figure 4.11 Transferring Pre-Cut Clay to Triaxial Mold (a) 10x20 cm Specimen (b) 5x10 cm Specimen.....	67
Figure 4.12 Filling Upper Part of Gravel-Clay Interface with Gravel.....	67
Figure 4.13 Filling Upper Part of Sand-Clay Interface Specimen with Sand.....	68
Figure 4.14 Triaxial Testing of Interfaces.....	68
Figure 4.15 Stresses on Pre-Cut Surface.....	69
Figure 4.16 Clay-Clay Specimen after Triaxial Tests.....	70
Figure 4.17 Stress-Strain Graphs of Clay-Clay Interfaces in Triaxial Tests.....	71

Figure 4.18 Volume Change during Triaxial Tests of Clay-Clay Interfaces.....	72
Figure 4.19 Peak Shear Strength Envelope of Clay-Clay Interfaces 5x10 cm Specimen .....	73
Figure 4.20 Peak Shear Strength Envelope of Clay-Clay Interfaces 10x20 cm Specimen .....	73
Figure 4.21 Mohr Circles of Clay-Clay Interface Triaxial Tests .....	74
Figure 4.22 Peak Shear Strength Envelope of Clay-Clay Interfaces.....	74
Figure 4.23 Shear Strength Envelope of Clay-Clay Interface for Large Deformation .....	75
Figure 4.24 Gravel-Clay Interface Triaxial Tests during and after Experiments .....	76
Figure 4.25 Gravel-Clay Interface Triaxial Tests-Shear Surface after Experiments .....	77
Figure 4.26 Stress-Strain Graphs of Gravel-Clay Interface in Triaxial Tests .....	78
Figure 4.27 Volume Change during Triaxial Tests of Gravel-Clay Interface.....	78
Figure 4.28 Mohr Circles- of Gravel-Clay Interface.....	79
Figure 4.29 Peak Shear Strength Envelope of Gravel-Clay Interface.....	80
Figure 4.30 Shear Strength Envelope of Gravel-Clay Interface at Large Deformation .....	80
Figure 4.31 Sand-Clay Interfaces after Triaxial Tests.....	81
Figure 4.32 Stress-Strain Graphs of Sand-Clay Interface in Triaxial Tests .....	82
Figure 4.33 Volume Change in Sand-Clay Interface Tests (5x10 cm Specimen) .....	82
Figure 4.34 Volume Change in Sand-Clay Interface Tests (10x20 cm Specimen) .....	83
Figure 4.35 Mohr Circles of Sand-Clay Interface .....	83
Figure 4.36 Peak Shear Strength Envelope of Sand-Clay Interface.....	84
Figure 4.37 Large Deformation Shear Strength Envelope of Sand-Clay Interface.....	84
Figure 4.38 Stress-Strain Graphs of Gravel Specimen.....	85
Figure 4.39 Peak Shear Strength of Gravel .....	86
Figure 4.40 Stress-Strain Graphs of Sand .....	86
Figure 4.41 Peak Shear Strength of Sand.....	87
Figure 4.42 Summary of Triaxial Tests.....	88
Figure 4.43 Secant Friction Angles at Large Deformation in Triaxial Tests .....	89
Figure 5.1 Gravel in the Lower Part of the Large Shear Box.....	92
Figure 5.2 Filling Clay up to Dowel Installation Level.....	93

Figure 5.3 Drilling Model Dowel Holes .....	93
Figure 5.4 Dowels Placed to the Drilled Holes.....	94
Figure 5.5 Shear Tests with Dowels .....	94
Figure 5.6 Improvement Tests with 1 Model Dowel-Dowel Length=8cm (I-1).....	95
Figure 5.7 Improvement Tests with 3 Model Dowels-Dowel Length=8cm (I-2).....	96
Figure 5.8 Improvement Tests with 9 Model Dowels-Dowel Length=8cm (I-3).....	96
Figure 5.9 Improvement Tests with 9 Model Dowels-Dowel Length=4cm (I-4).....	97
Figure 5.10 Improvement Tests with 9 Model Dowels-Dowel Length=12cm (I-5) .....	97
Figure 5.11 Improvement Tests with 36 Model Dowels-Dowel Length=6cm (I-6) .....	98
Figure 5.12 Improvement Tests with 36 Model Dowels-Dowel Length=12cm (I-7) .....	98
Figure 5.13 Effect of Number of Dowels in Improvement Tests .....	100
Figure 5.14 Effect of Number of Dowels for Different Normal Stresses .....	101
Figure 5.15 Effect of Dowel Lengths in Improvement Tests.....	102
Figure 5.16 Effect of Dowel Lengths for Different Normal Stresses .....	102
Figure 5.17 a) Taking Specimen for UU Tests b) Specimen after UU Tests.....	105
Figure 5.18 Filling Clay on Gravel in Continuous Improvement Tests.....	109
Figure 5.19 Improvement Tests with Continuous Wall.....	109
Figure 5.20 Results of Continuous Wall Experiments.....	110
Figure 6.1 Flow Chart for Granular Material-Clay Interface Studies.....	115

## LIST OF SYMBOLS AND ABBREVIATIONS

$c$	: Cohesion
CD	: Consolidated Drained
$C_u$	: Undrained Shear Strength
$c_v$	: Coefficient of Consolidation
$d$	: Diameter of Dowel
DR	: Relative Density
$E$	: Elastic Modulus
$\phi$	: Friction Angle
$\phi_{sec}$	: Secant Friction Angle
$H$	: Height
$k$	: Bearing Capacity Factor
$L$	: Length of Dowel
LL	: Liquid Limit
$n$	: Number of Dowels
PL	: Plastic Limit
PI	: Plastic Index
$\rho_{max}$	: Maximum Density
$\rho_{min}$	: Minimum Density
$s$	: Spacing of Dowels
$\sigma_1'$	: Axial Stress
$\sigma_3'$	: Confining Stress
$\sigma, \sigma_n'$	: Normal Stress
$t_{90}$	: Time for 90% Consolidation
$\theta$	: Angle from Horizontal (Pre-cut Surface)
UU	: Unconsolidated Undrained

# CHAPTER 1

## INTRODUCTION

### 1.1 Problem Statement

Shear failures of interfaces between granular material and clay are frequently encountered in engineering practice. In earth fill dams, road embankments and spoil piles constructed during mining operations, granular material can be placed on clay layer and there may be movements along the interfaces (Figure 1.1).

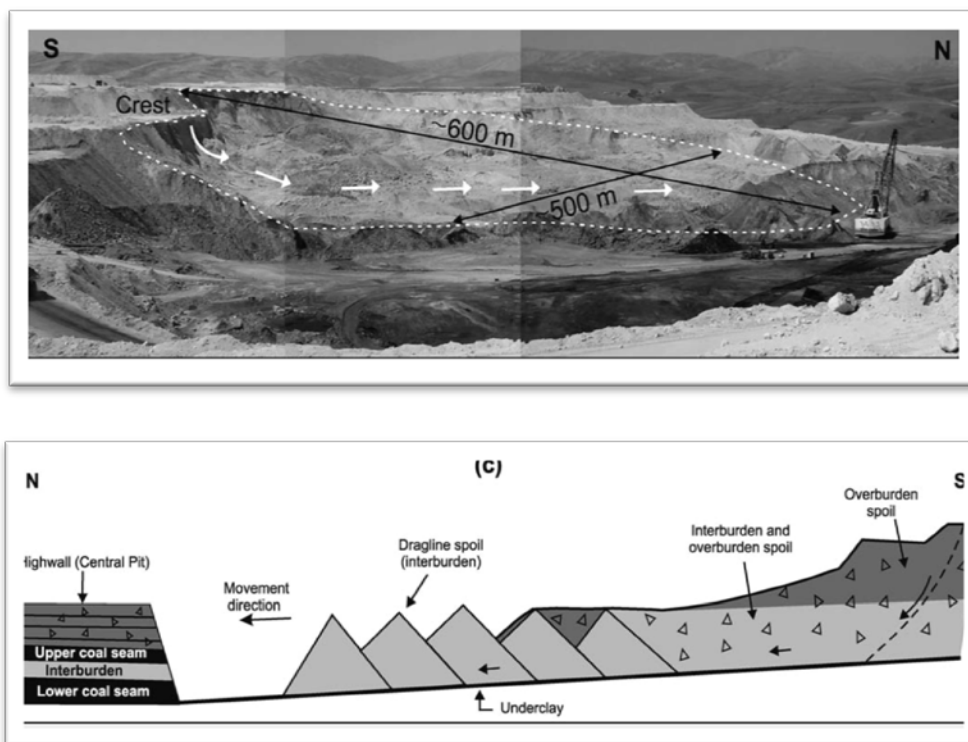


Figure 1.1 Shear Failures along Interfaces (Kasmer and Ulusay, 2006)

Slope movements due to shear failure of interfaces may result in considerable economic losses. When dealing with movements on this type of interfaces,

selecting representative shear strength parameters has a great importance. Shear strength parameters should be selected correctly in order to construct stable engineering structures.

Mixture of clay and granular materials has been studied in several other research programs in detail as referenced in Chapter 2 however there has not been efforts in the literature on interfaces, and there is no available method on how to select shear strength parameters of interfaces. Therefore an experimental study concerning the shear strength properties of granular materials and clay interfaces would provide an understanding of the shearing mechanism, which, in the Author's opinion, would be an interesting contribution to this practically significant issue. In fact the subject was also faced in a couple of engineering design problems by professional groups where shear strength parameters at granular fill-soft clay contacts were assumed without much technical basis.

## **1.2 Research Methodology and Objectives**

In order to study the failure mechanism and to determine the shear strength parameters of granular material and clay interfaces, direct shear tests (using small shear box and large shear box) and triaxial tests have been conducted. The details of direct shear and triaxial tests are given in the related sections of the thesis.

Another important topic is the selection of suitable improvement method for interface instabilities. This part of the study aims to study the effect of dowels (short piles) on the shear strength of interfaces. For this purpose, the large direct shear box tests were repeated with dowels having different lengths, diameters and placed with different spacing and layouts.

The following are objectives of this research:

- a) Determine shear strength properties of clay, granular material and granular material-clay interfaces, through direct shear and triaxial tests.

- b) Determine and discuss the shear strength differences in triaxial and direct shear testing.
- c) Investigate use of dowels on the interfaces as an improvement technique.

Since interfaces are being widely encountered, shear strength of interfaces and the strength parameters to be used have become more important. Because of the economic losses due to instability problems on interfaces and the lack of detailed investigations on shear strength of interfaces; the results of the study shall provide a significant contribution both to the literature and engineering practice.

### **1.3 Thesis Outline**

This thesis is composed of six chapters. In Chapter 2, literature review is presented. The results and discussion of direct shear tests and triaxial tests are given in Chapter 3 and Chapter 4, respectively. The results of the improvement tests (with dowels) are described in Chapter 5. Finally, the conclusions are provided in Chapter 6.



## CHAPTER 2

### LITERATURE REVIEW

#### 2.1 Introduction

In the literature, granular fill and clayey soil contacts have not been studied in detail. The existing studies are mainly about investigation of shear strength characteristics of granular material-clayey soil mixtures and rockfills. Generally, the effect of granular content in a mixture has been investigated.

#### 2.2 Shear Strength Studies

*Charles and Watts (1980)* carried out large-scale triaxial compression tests on well graded and dense rockfill. Four rockfill materials were tested with maximum particle size of 38 mm. At low confining stresses, dilation was observed and principal effective stress ratio at failure,  $(\sigma_1/\sigma_3)_f$  was found to be greater (Figure 2.1). The authors obtained non-linear failure envelopes from triaxial tests (Figure 2.2) making surface stability non-critical. Since stability of rockfills was related to the strength of rockfill at low stresses, it was concluded that rockfill embankments could be built with steeper slopes.

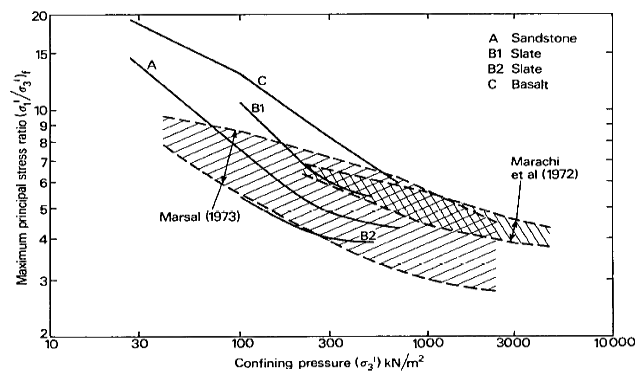


Figure 2.1 Influence of Confining Pressure ( $\sigma_3$ ) on Maximum Principal Stress Ratio  $(\sigma_1/\sigma_3)_f$  (Charles and Watts, 1980)

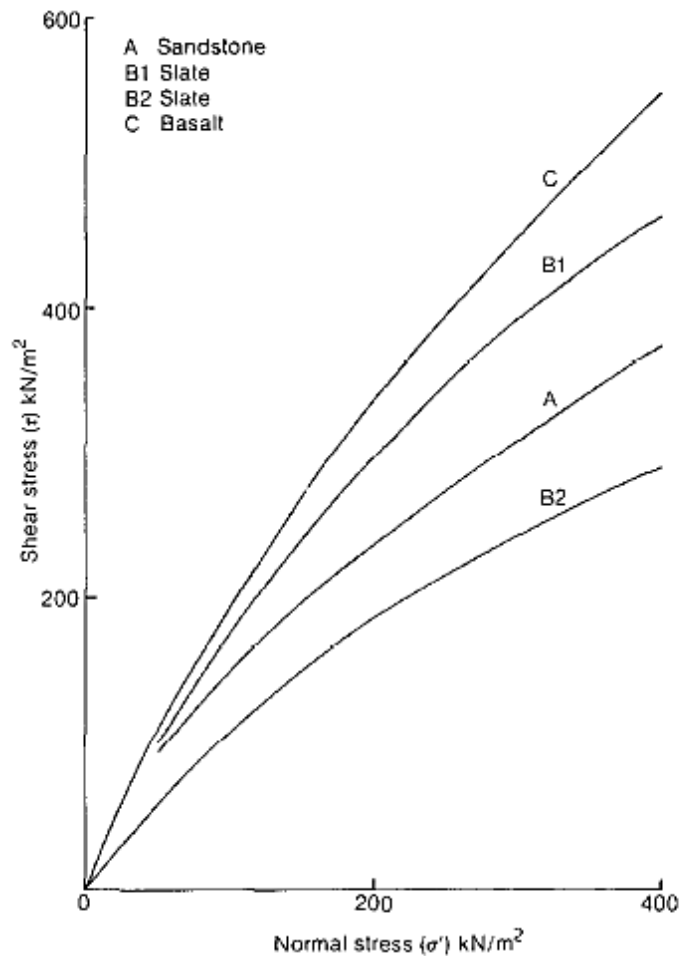


Figure 2.2 Failure Envelope of Rockfills (Charles and Watts, 1980)

*Lupini et al. (1981)* studied the effect of granular material content on drained residual strength of clays. The authors called sliding mechanisms as “turbulent, sliding and translational” modes depending on granular material content. According to Lupini et al. (1981), residual shear strength depended on fine and granular material contents and if granular material content was greater than a specific value, shear strength was affected considerably.

*Irfan and Tang (1992)* prepared a geotechnical report concerning the effect of the coarse fraction on the shear strength. The authors summarized the early studies and investigated the granular material content effect with laboratory experiments and back analyses of existing slopes.

Miller and Sowers (1957) investigated the effect of sand content on the strength of the sand-clay mix according to the report of Irfan and Tang (1992). Up to 67% sand content, no apparent change in strength was observed. For sand content ranging between 67%-74%, rapid increase of friction angle and decrease of cohesion were reported (Figure 2.3). It was also mentioned that for a sand content between 67%-74% the strength of mixture was dominated by granular material rather than clay.

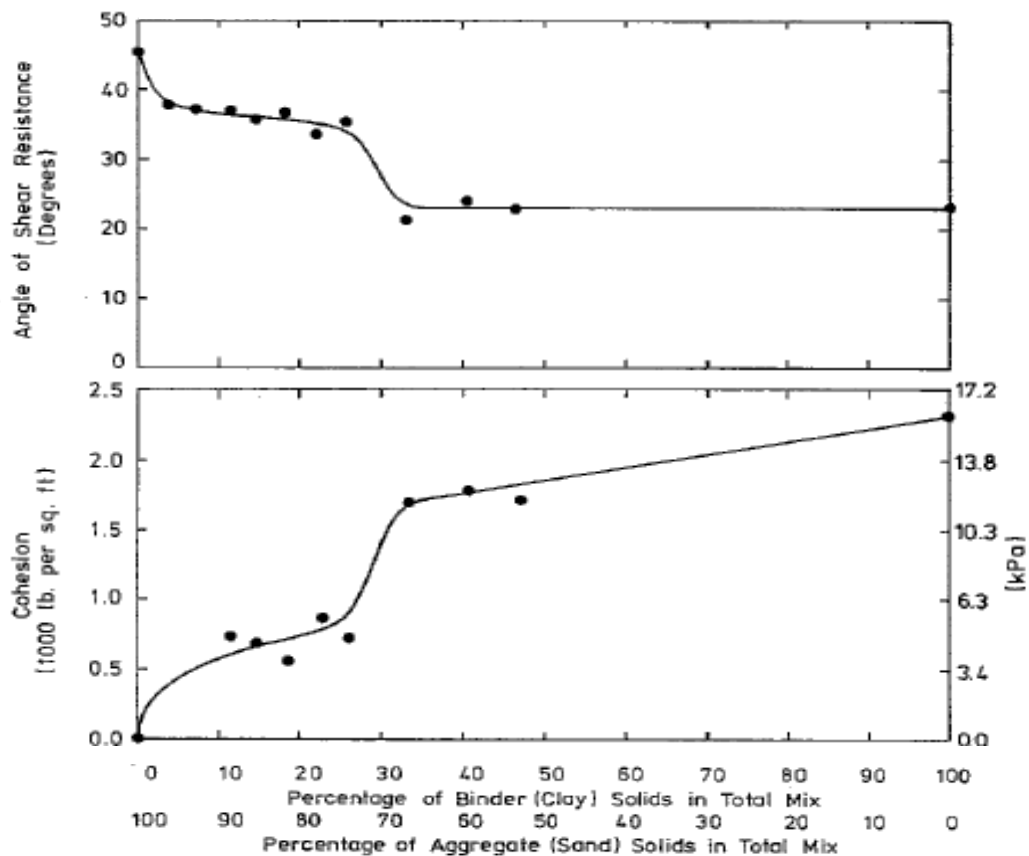


Figure 2.3 Change in Friction Angle and Cohesion with Sand Content (Miller and Sowers, 1957)

In the same report, the results of Holtz (1960), who conducted triaxial tests on clay-gravel mixtures and investigated effect of gravel content on shear strength, were also given. It was reported that up to 35% of gravel content, change in shear

strength was not significant. Shear strength was observed to increase sharply for gravel content between 35%- 50% (Figure 2.4).

Shear Strength Envelope	Percentage of Gravel by Weight	$\phi'$ (deg)	$c'$ (kPa)
-----	0	24	60
- - - - -	20	26	48
-----	35	25	57
- - - - -	50	32	31
-----	65	34	34

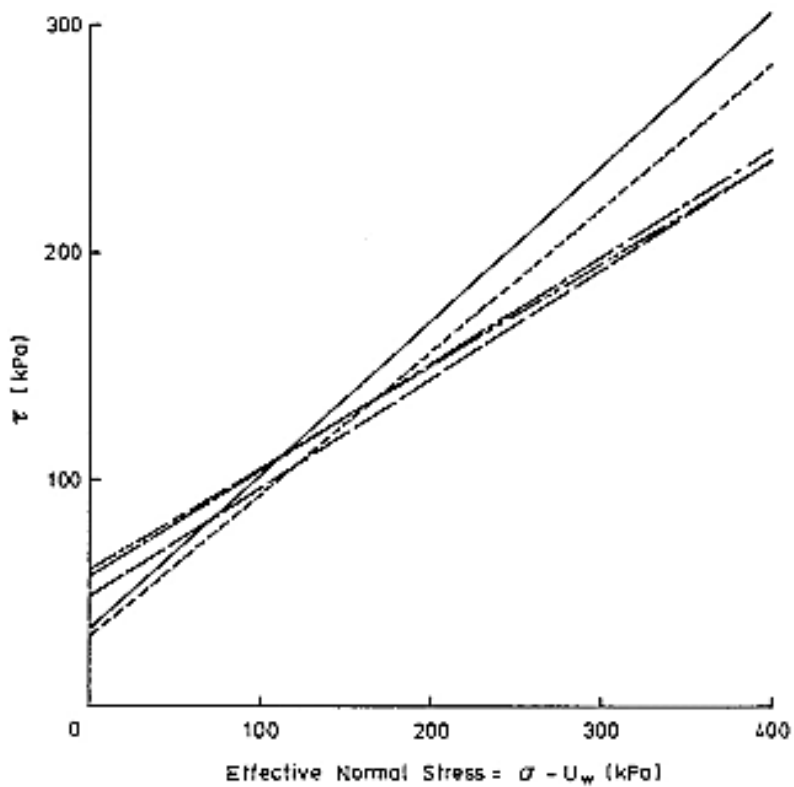


Figure 2.4 Failure Envelope for Different Gravel Content (Holtz, 1960)

Irfan and Tang (1992) reviewed the results of large direct shear box tests performed by Patwardhan et al. (1970) on cobble-clay mixture. In this study, a gradual increase was observed up to 30%-40% cobble content followed by a sharper increase for more cobble content (Figure 2.5).

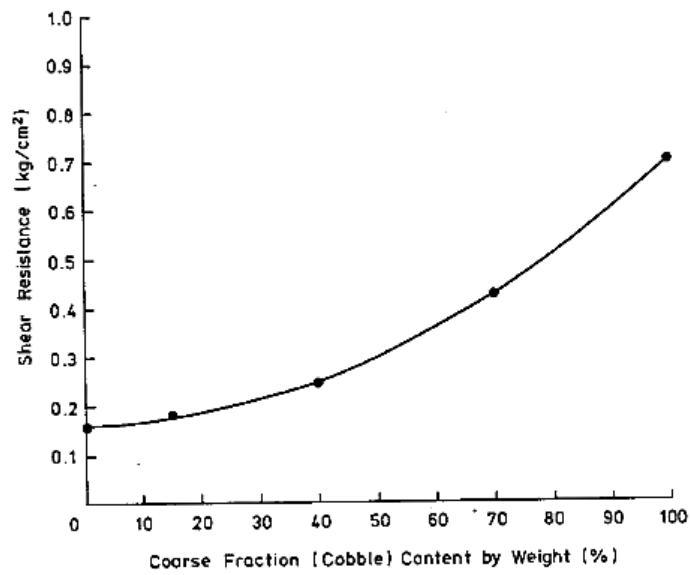


Figure 2.5 Shear Resistance vs. Coarse Fraction (Patwardhan et al., 1970)

Large diameter triaxial tests on gravel-sand-clay mixtures conducted by Donagne and Torrey (1979) were also reviewed by Irfan and Tang (1992). It was reported that shear strength of the mixture increased with increasing gravel content and particle size (Figure 2.6).

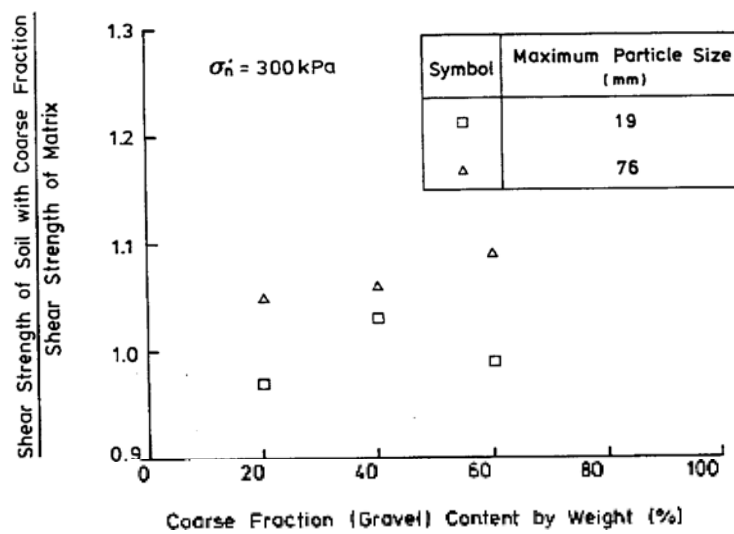


Figure 2.6 Shear Strength of Sand-Clay-Gravel Mixtures (Donagne and Torrey, 1979)

Irfan and Tang (1992) carried out back analyses for eighteen sections of fifteen existing slopes in Hong Kong and the results showed no regular pattern of shear strength increase with coarse fraction content. These authors concluded that the factors other than the coarse fraction content affected the stability of slopes.

Irfan and Tang (1992) conducted laboratory tests in order to assess the effect of crushed rock content on the shear strength of silty sand matrix. For this purpose, triaxial tests and direct shear box tests were conducted. Direct shear box tests were executed in small scale and large scale direct shear box. Maximum aggregate size was chosen as 7 mm for 100x100x43 mm shear box and 25 mm for 300x300x148 mm shear box.

In consolidated undrained triaxial tests, no change in shear strength was observed up to 10% crushed rock content. Above 25% crushed rock content, shear strength increased rapidly (Figure 2.7).

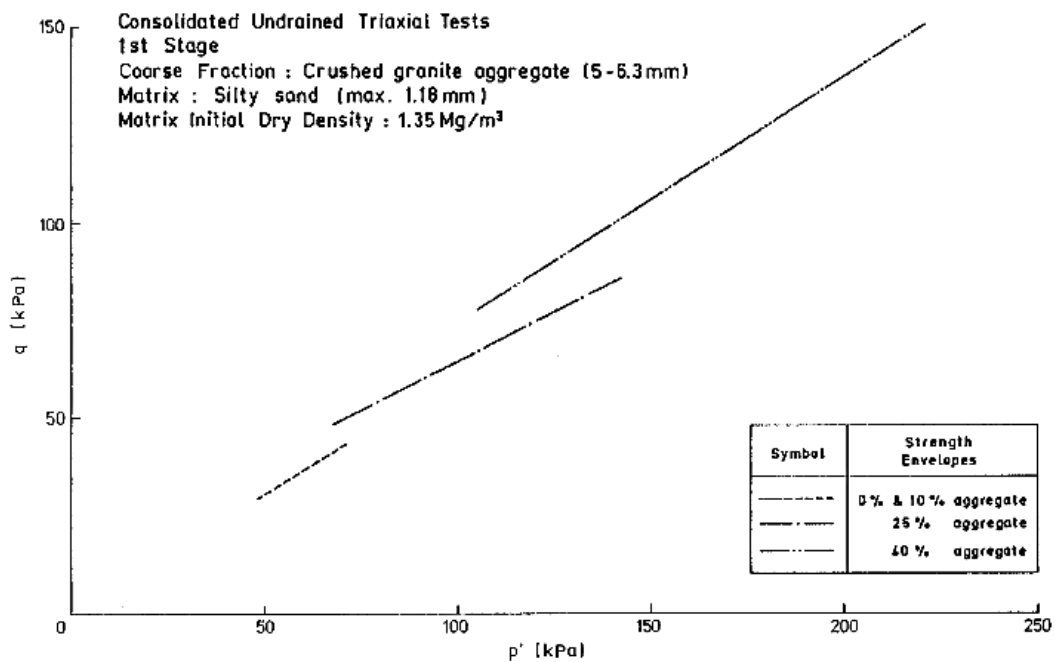


Figure 2.7 Effect of Crushed Rock Content on Shear Strength (Irfan and Tang, 1992)

In large direct shear tests conducted by Irfan and Tang (1992), small increase in shear strength was observed from 20% to 30% coarse fraction content. The increase became significant after 30% coarse fraction content (Figure 2.8a). In small direct shear tests, shear strength was observed to increase sharply with increasing coarse fraction content (Figure 2.8b). Soil behavior changed from compressive to dilative when a coarse fraction content of 20% was exceeded.

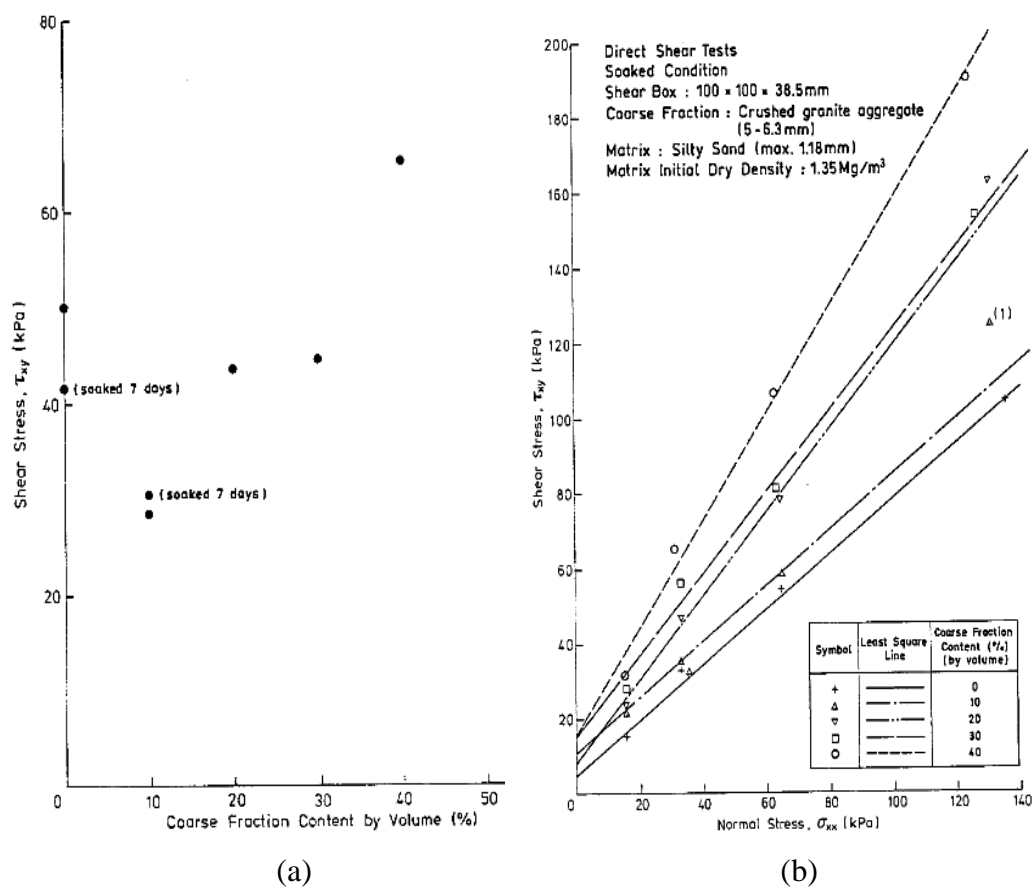


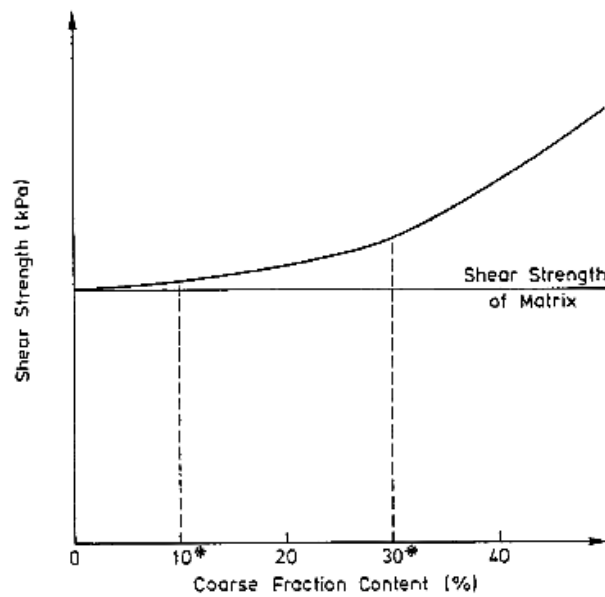
Figure 2.8 Change of Shear Strength with Coarse Fraction Content in a) Large Shear Box b) Small Shear Box (Irfan and Tang, 1992)

Irfan and Tang (1992) concluded that at low coarse fraction contents (below 10%), the effect of coarse particles on shear strength was negligible and shear strength was governed by matrix whereas at coarse fraction content greater than 30%, shear strength increased rapidly with increasing coarse fraction content and

coarse fraction started to become dominant in controlling the shear strength behavior (Figure 2.9).

*Indraratna et al. (1993)* conducted large-scale triaxial tests on greywacke rockfill in order to determine strength and deformation behavior from low to medium confining pressures.

Grain size curve of the rockfill used in experiments was chosen to be similar to the field conditions considered in *Indraratna et al. (1993)*. The authors summarized the results of *Marachi (1969)* who concluded a size ratio (the diameter of the triaxial divided by the mean diameter of particle size) of at least 6 must be employed in order to minimize size effects. Size ratio was chosen as 8 and 12 in large-triaxial tests of *Indraratna et al. (1993)*.



Primary Control	Matrix	Matrix	Coarse Fraction	Coarse Fraction
Secondary Control	-	Coarse Fraction	Matrix	-

Figure 2.9 Control of Shear Strength (Irfan and Tang, 1992)

Ductile strain-softening of rockfill was observed by Indraratna et al. (1993) from triaxial tests (Figure 2.10). At small confining pressures, dilation was observed whereas at higher pressures dilation was suppressed. It was concluded that volumetric strains increase linearly with confining pressure being independent of particle gradation (Figure 2.11). The effect of confining stress on the shear strength was found to be more important than the effect of particle size and angularity.

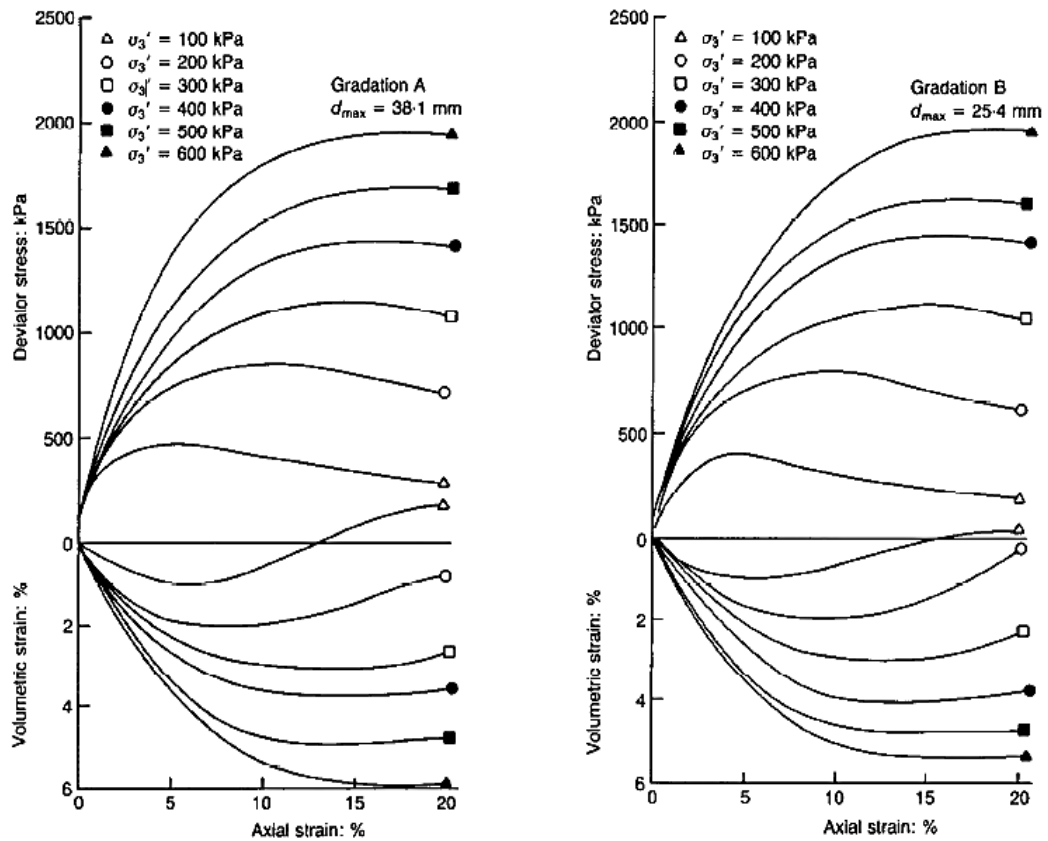


Figure 2.10 Stress-Strain Curves for Two Different Gradations (Indraratna et al.,1993)

Failure envelopes corresponding to low confining stress region showed non-linearity (Figure 2.12a). As the confining stress was increased, the drained friction angle of the rockfill was found to decrease (Figure 2.12b).

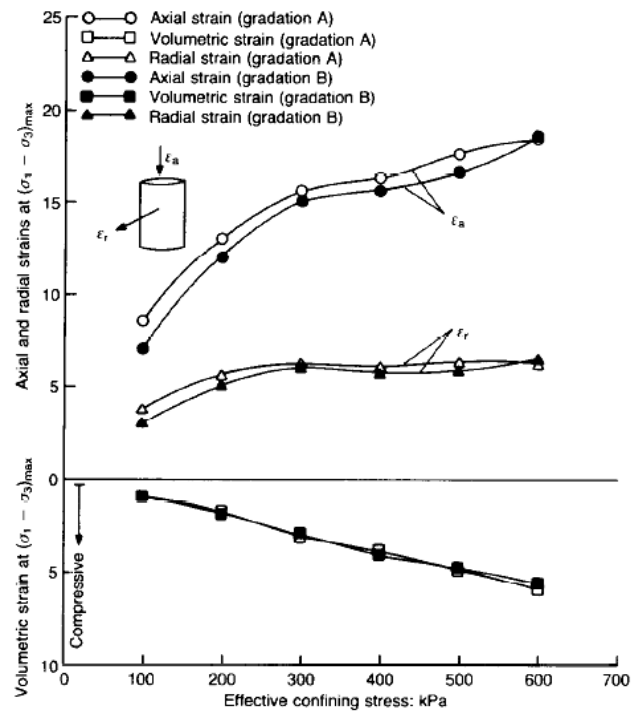


Figure 2.11 Influence of Effective Confining Pressure on Sample Strains at Peak Deviator Stress (Indraratna et al., 1993)

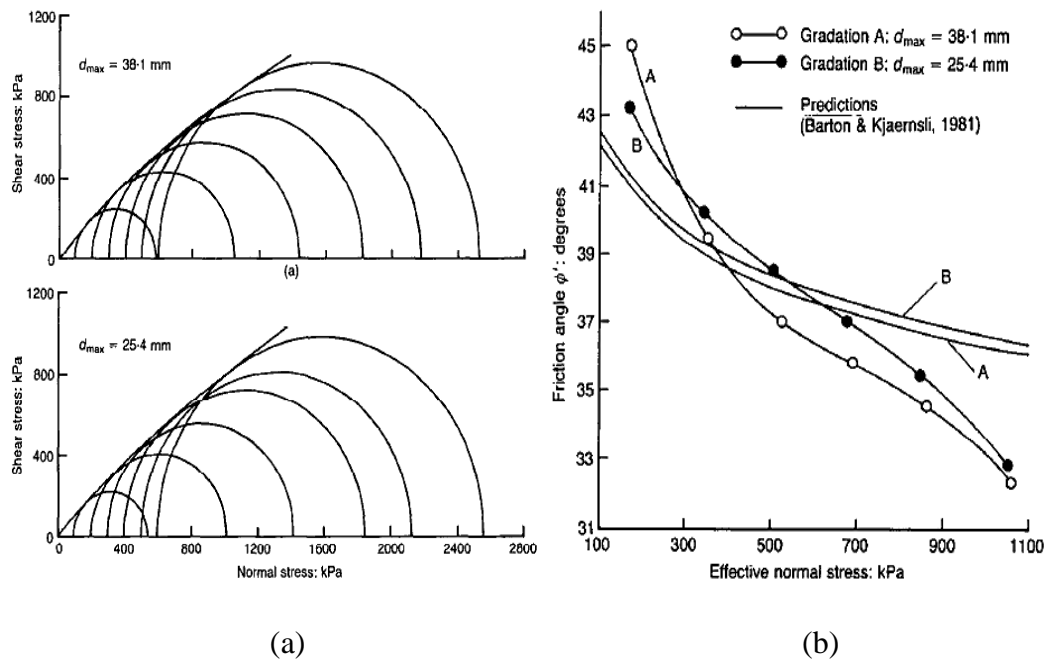


Figure 2.12 a) Failure Envelope of Greywacke b) Effect of Confining Stress on Friction Angle (Indraratna et al., 1993)

*Ulusay et al. (1995)* examined the geotechnical characteristics of the spoil material at the Eskihsar open pit coal mine located in southwest part of Turkey. Shallow-seated small circular failures and bi-linear wedge failures occurred through the spoil piles containing approximately same amount of fine and coarse materials.

In order to obtain shear strength characteristics, direct shear tests and consolidated drained triaxial compression tests were conducted by the investigators on undisturbed spoil samples which were collected using 100 mm square by 30 mm thick specimen cutters.

Stress-strain curves of spoil material from direct shear tests are shown in Figure 2.13.

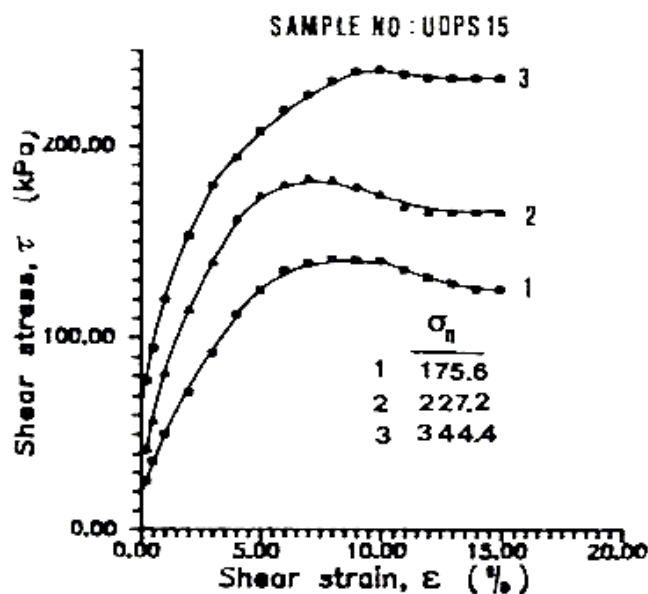


Figure 2.13 Stress-Strain Curves for Spoil Material (Ulusay et al., 1995)

Linear and power failure envelopes obtained with high correlation coefficients were reported not to have great differences (Figure 2.14). Back analysis results of observed spoil pile failures were in good agreement with laboratory results.

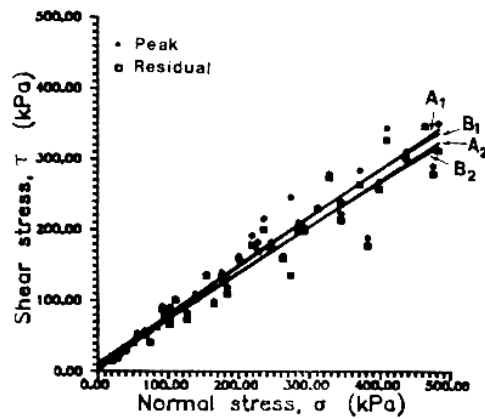


Figure 2.14 Failure Envelopes for Spoil Material (Ulusay et al., 1995)

*Iannacchione and Vallejo (2000)* reviewed 31 technical papers in order to investigate the shear strength of clay-rock mixtures. The authors concluded that great concentration of rock particles within mixture causes particles to be in contact which results in higher friction angles and higher shear strength values.

*Barton (2008)* investigated shear strength of rockfill, interfaces and rock joints. He concluded that the shear strength of interface was governed by the Joint Roughness Coefficient (JRC) if roughness of the interface was too low. It is also mentioned that if there is a good interlock between interface and rockfill, the strength would be determined by the weak foundation (Figure 2.15).

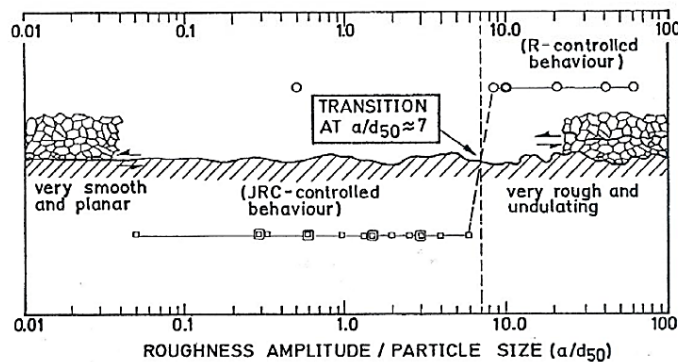


Figure 2.15 Roughness Effect on Shear Strength (Barton, 2008)

*Wang and Ling (2006)* investigated stress-strain behavior of sand-clay mixtures. Triaxial compression tests were conducted at different confining pressures. The behavior of sand-clay mixtures were reported to resemble that of dense sand or overconsolidated clay. At small strain levels, specimen contraction was observed whereas at large strains dilative behavior was observed. The mixture showed non-linear failure envelope and friction angle decreased with increasing confining pressure (Figure 2.16).

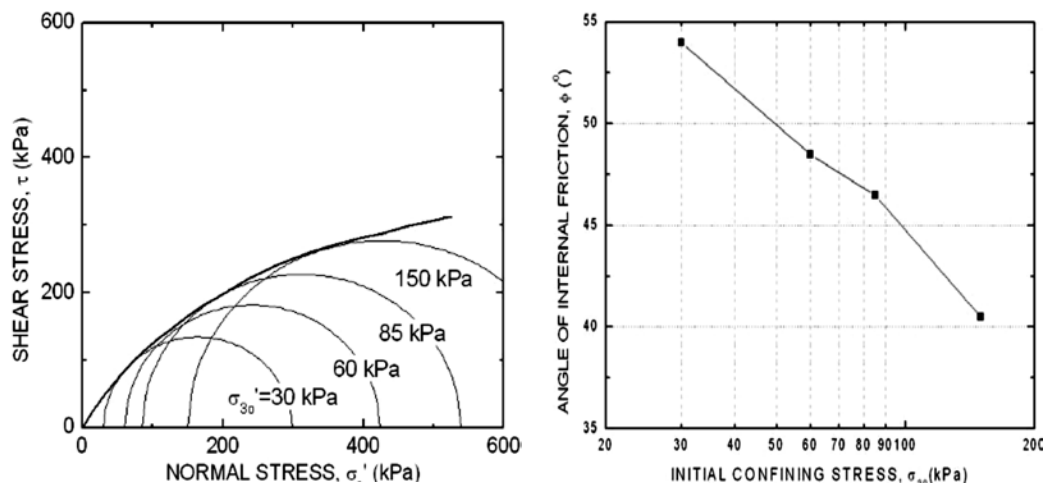


Figure 2.16 Failure Envelope and Change of Friction Angle with Confining Stress (Wang, 2006)

*Kasmer and Ulusay (2006)* studied the stability of spoil piles at an open pit coal mine in Central Anatolia, Turkey. This study includes the assessment of large-scale spoil pile instability occurred in June 2001 at the central pit and gives recommendations about the stability of south pit. In order to describe the geotechnical properties of the spoil material and the failure mechanism, laboratory and field investigations were performed.

The failure surface was reported to pass through both spoil material and along foundation soil (bottom clay). Combined failure surface consisting of circular surface passing through the overburden spoil material and a planar surface along

the interface between spoil material and underclay were observed at the central pit (Figure 2.17).

For laboratory testing, undisturbed samples were collected with an orientation parallel to the displacement from the spoils and underclay interface. For index and soil classification tests, disturbed samples were also collected from the field. Spoil material was found to contain brown silty soil and green marl being mainly composed of illite mineral.

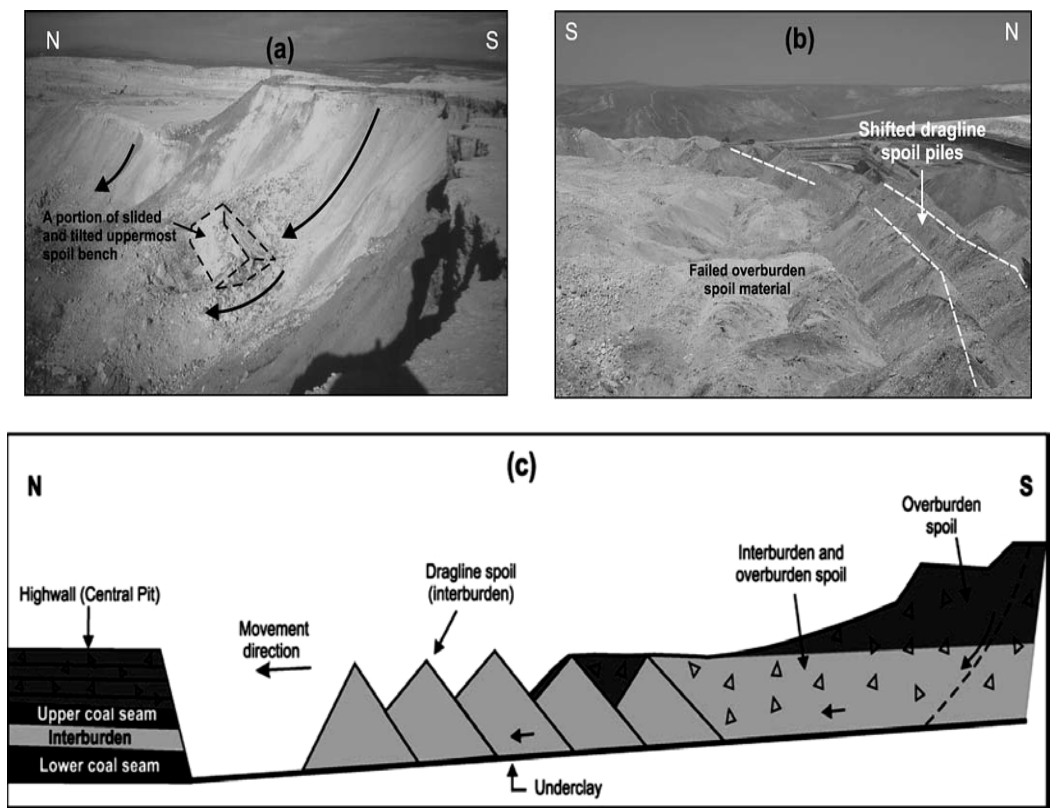


Figure 2.17 Failures and Combined Failure Surface (Kasmer and Ulusay, 2006)

Consolidated-drained direct shear tests were performed on undisturbed samples of silty soil, green marl, underclay, dragline spoil and spoil/underclay interface. In order to determine the shear strength of interface between spoil and underclay, undisturbed underclay and spoil material were placed into the lower and upper

parts of the shear box, respectively (Figure 2.18). Very small shearing rate (0.05 mm/s) in order to allow drainage and stress range of 50-850 kPa were used during shear tests.

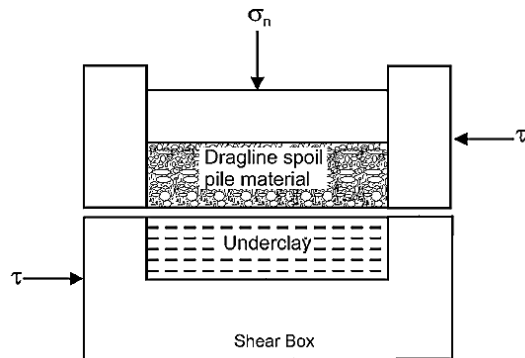


Figure 2.18 Direct Shear Testing of Interface (Kasmer and Ulusay, 2006)

The failure envelopes obtained using linear and power curve relationship resulted in high correlation coefficients. Shear strength of the interface was found to be lower than underclay which makes interface the weakest surface for the stability of spoil piles. Results of shear tests for different materials are given in Table 2.1.

Table 2.1 Shear Test Results of Different Materials (Kasmer and Ulusay, 2006)

Material	Peak Shear Strength		Residual Shear Strength	
	$c_p$ (kPa)	$\phi_p$ (°)	$c_r$ (kPa)	$\phi_r$ (°)
S	16–26	31.1–32.4	3.3–11.7	26.2–29.8
GM	25.3–34.4	33–33.8	2.5–5.9	32.5–32.7
DS	17.5	30.5	10.1	23.6
UC	46.5–65.5	19.4–23.7	11.5–22.1	13.7–16.3
DS/UC	7.9–14.8	22.2–23.8	1.4–8.9	10.5–13.8

S = silty material (overburden spoil); GM = green marl (overburden spoil); UC = underclay; DS = dragline spoil; DS/UC = interface between spoil and underclay.

As can be seen from Table 2.1, peak cohesion of the interface is close to peak cohesion of dragline spoil and peak friction angle of the interface is close to the friction angle of underclay. Same situation is valid for the residual shear strength parameters. Therefore, it can be concluded that cohesion and friction angle of the interface are close to the weakest cohesion and friction angle of the interface-making materials.

Limit equilibrium back-analysis results indicated 45-50 percent saturation at the time of failure that makes the heavy rainfall as an important triggering factor. For the south pit, based on the results of finite element analysis and limit equilibrium calculations, the authors concluded that there was no spoil pile instability risk.

*Zhang et al. (2007)* investigated shear strength of interfaces between core and filter soils in rock-fill dams by using a large shear box that was constructed in Tsinghua University. The shear box (250 mm x 250 mm) is capable of 2500 kN and it consists of laminar-ring system, the loading piston, upper and lower boxes (Figure 2.19).

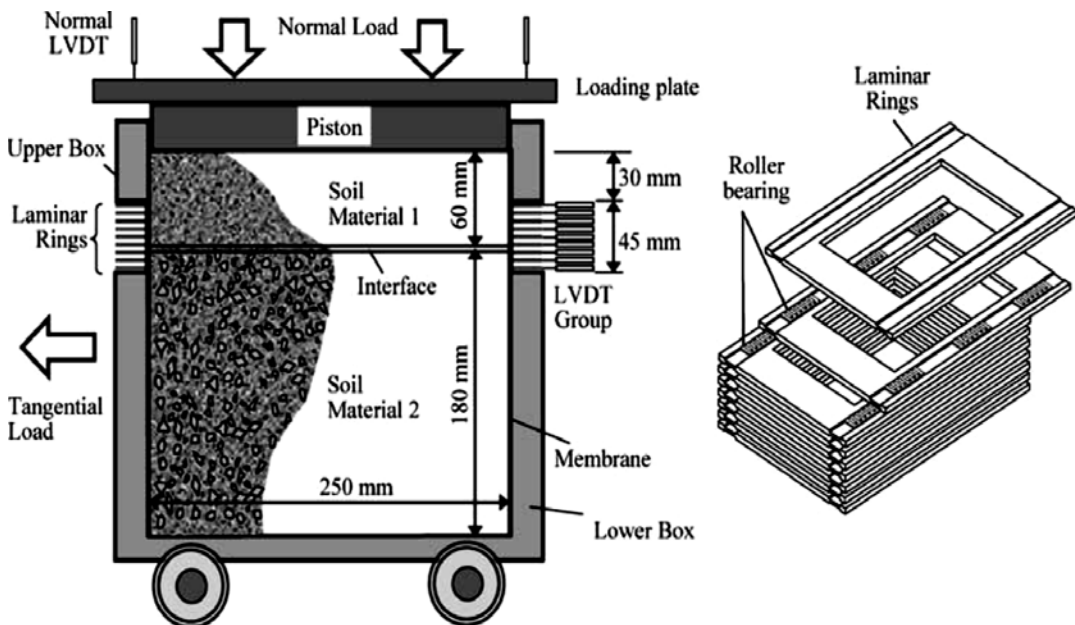


Figure 2.19 Experimental Setup (Zhang et al., 2007)

The laminar ring system consisted of nine steel laminar rings having 5 mm thickness. Each steel rings had roller bearings with a diameter of 3 mm in order to minimize the friction between steel rings. The laminar ring system was placed between the upper box and lower box. With the laminar rings, failure occurred along the weakest plane which resulted in the strength and failure characteristics of the interface to be simulated well.

Three types of soil were used in the large shear box tests: filter soil (FS), composite soil (CS) and synthetic soil (SS). The filter soil was crushed granite gravel ( $c=0$ ,  $\phi=35^\circ$ ), composite soil was collected from the construction site ( $c=200$  kPa,  $\phi=17.7^\circ$ ) and synthetic soil included 65% composite soil and 35% gravel. Using these soils, shear tests were conducted for composite soil-filter soil (CS-FS) and synthetic soil- filter soil (SS-FS) interfaces.

Zhang et al. (2007) reported that the shear tests resulted in dilative behavior for small normal stresses (100 kPa and 300 kPa) and contractive behavior for normal stresses greater than 600 kPa (Figure 2.20). High strength, strong dilatancy and less compressibility were observed for SS-FS interface due to increased gravel content in the synthetic soil (Figure 2.21).

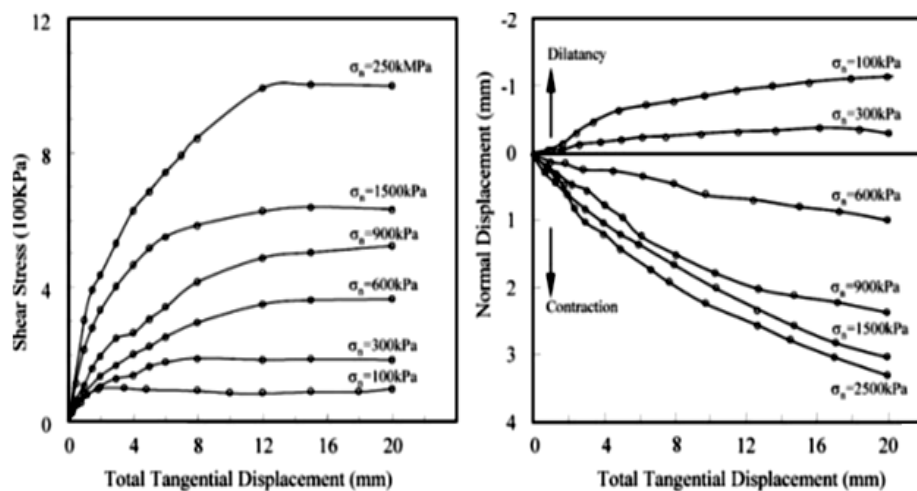


Figure 2.20 Typical Test Results for CS-FS Interface (Zhang et al., 2007)

In CS-FS interface, it was observed that when the normal stress is less than 500 kPa, the interface strength was consistent with that of the filter soil. When the normal stress was greater than 500 kPa, the interface strength was found to be close to the strength of composite soil. Figure 2.22 was suggested as the combined failure envelope for the interface by Zhang et al. (2007).

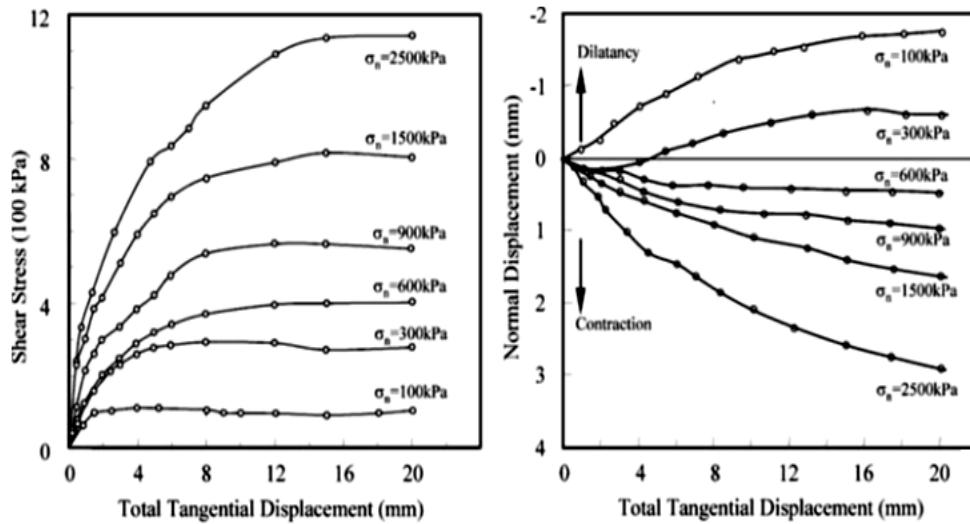


Figure 2.21 Typical Test Results for SS-FS Interface (Zhang et al., 2007)

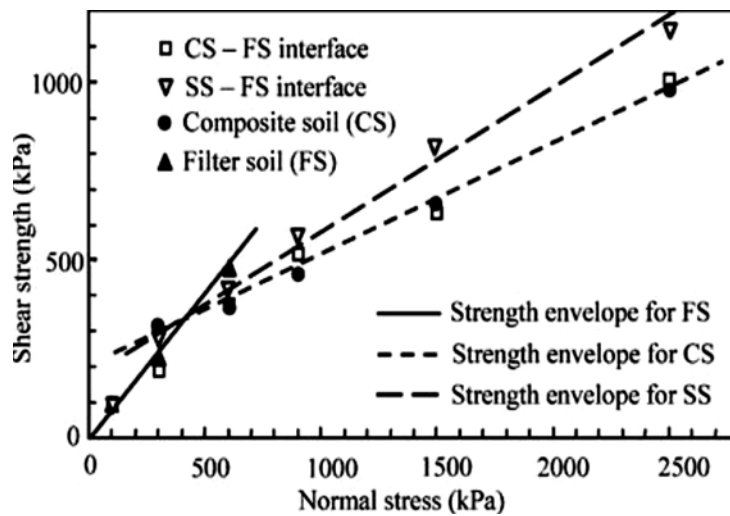


Figure 2.22 Combined Failure Envelope (Zhang et al., 2007)

Using laminar ring displacements, the position of failure zone was also determined. It was found that at 100 kPa and 300 kPa normal stresses, failure planes were found to be developed in filter soil. When the normal stress was 500 kPa, the failure plane was observed to be close to the interface between the two soils. For normal stresses greater than 900 kPa, failure occurred in the upper composite soils (Figure 2.23).

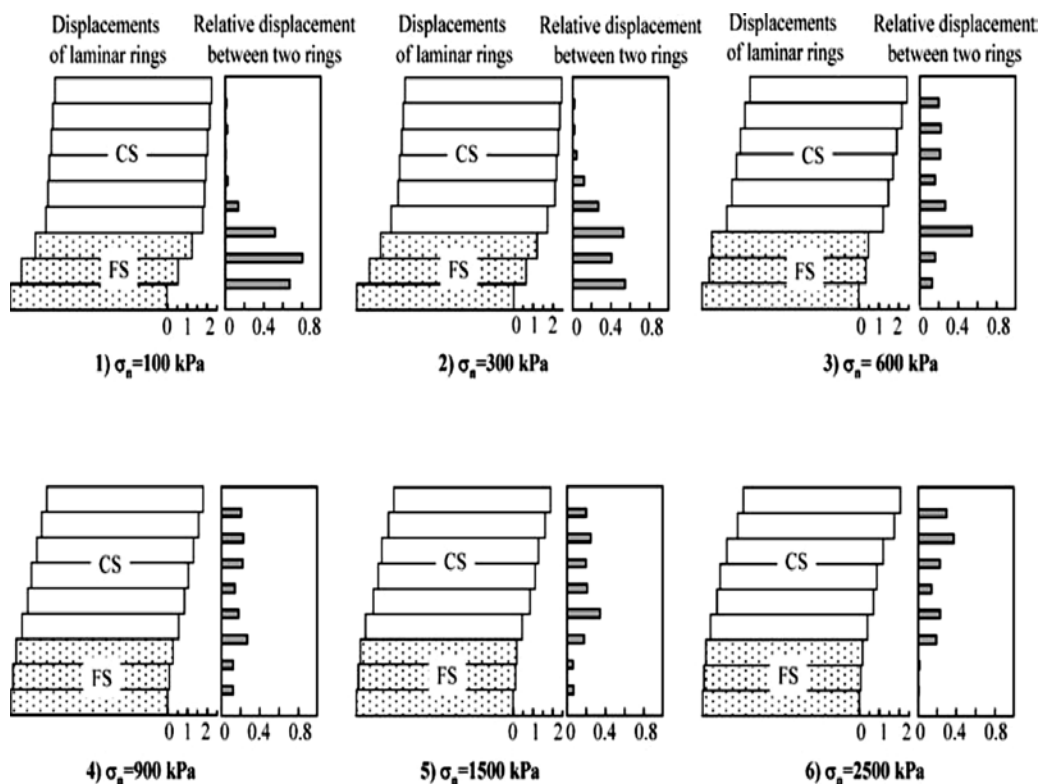


Figure 2.23 Laminar Ring Displacements (Zhang et al., 2007)

By using the results of shear tests, Zhang et al. (2007) concluded that shear strength of interfaces were consistent with lowest strength of the surrounding soils and strength envelope could be expressed as a bi-linear curve. According to the authors, when the normal stress was small, failure would occur in a soil having lower cohesion, while for higher normal stresses failure would occur in a soil with smaller internal friction.

*Xu et al. (2007)* performed in-situ tests in order to examine geomechanical properties of soil-rock mixtures. The in-situ shear tests were conducted on six samples prepared as shown in Figure 2.24. First three tests were performed under natural conditions and remaining tests were conducted under simulated rain.

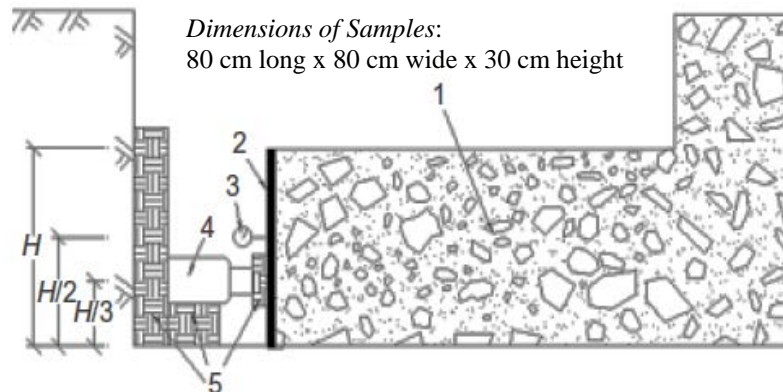


Figure 2.24 In-situ Sample Preparation (Xu et al., 2007)

At natural conditions, it was found that the internal friction angle depends on the weight proportion of rock being higher for high rock proportions. It was reported that cohesion changed with weight proportion and particle size of the rock. Rock fragments were found to control the deformation and failure mechanism of soil-rock mixtures.

Soil-rock mixtures were observed to be very sensitive to water. Xu et al. (2007) found that cohesion decreased sharply whereas internal friction angle increased for samples under simulated rain conditions when compared to samples at natural condition.

*Bareither et al. (2008)* conducted direct shear tests on 30 sand backfill materials having gravel contents up to 30% in a small-scale (64 mm square) and in a large scale (305 mm square) direct shear boxes. Triaxial compression tests were also conducted for comparison purposes.

Sands tested in small-scale direct shear box were sieved from 4.75 mm sieve in order to ensure that box length to maximum particle diameter was at least 10.

Direct shear tests were conducted at constant rate of shearing of 0.24 mm/min. Large shear box tests were corrected for box friction at the shear box interface. An increase in shear stress at larger displacements was observed in large direct shear box tests due to particle-box interactions.

The authors observed dilation in front of the box and contraction at the back of the box during large shear box tests due to particle movements and concluded that these particle movements were transferred to particle-box interface that increased the shear resistance (Figure 2.25). The increase due to particle-box interaction was ignored during the determination of shearing resistance.

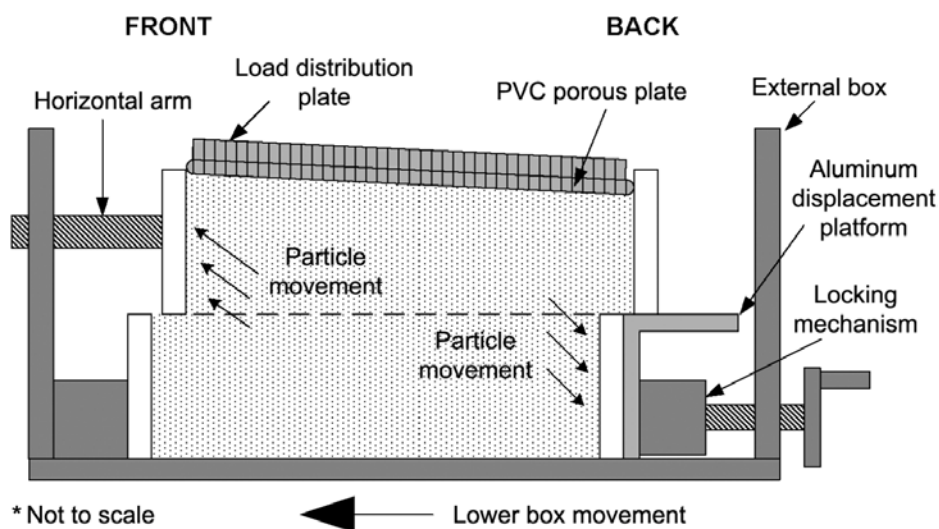


Figure 2.25 Particle Movements (Bareither et al., 2008)

By comparing the results of small-scale direct shear tests and large-scale direct shear tests, Bareither et al. (2008) found that friction angles did not differ more than  $4^\circ$ , the difference being less than  $2^\circ$  in most cases. Triaxial test results were also agreed with those obtained from direct shear tests (Figure 2.26). It was then

concluded that for sands with gravel contents less than 30%, friction angle can be measured with similar accuracy using large-scale or small-scale direct shear test or triaxial test.

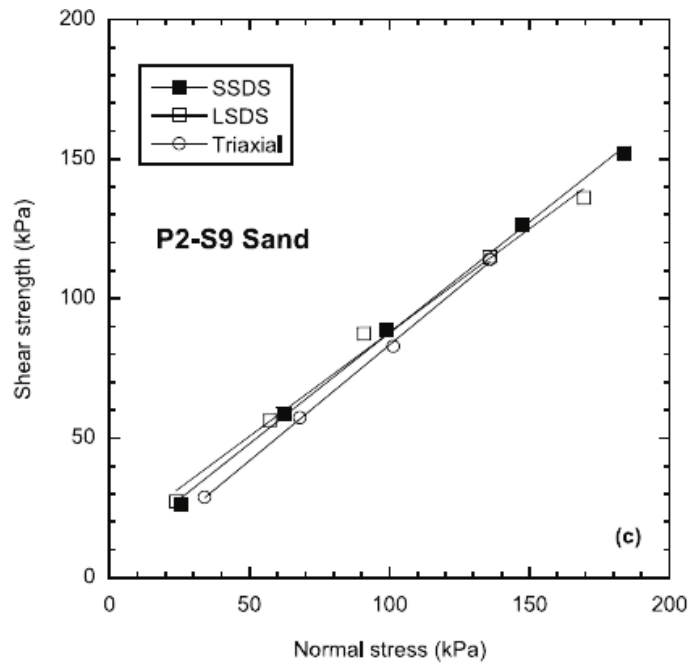


Figure 2.26 Typical Test Results (Bareither et al., 2008)

*Nakao and Fityus (2008)* investigated the effects of shearing rate, shear box dimensions and particle size to the shear strength of rock materials.

In order to see the effect of shearing rate, shear tests were conducted at different shearing rates. For large shear box, tests were conducted at 7.06, 0.63 and 0.05 mm/min shearing rates whereas for small shear box, the shearing rates of 6.03 and 0.42 mm/min were used.

Nakao and Fityus (2008) observed that for large shear box effective friction angle was underestimated by over  $3.5^\circ$  and residual friction angle was underestimated by around  $2^\circ$  at faster shearing rates (Figure 2.27).

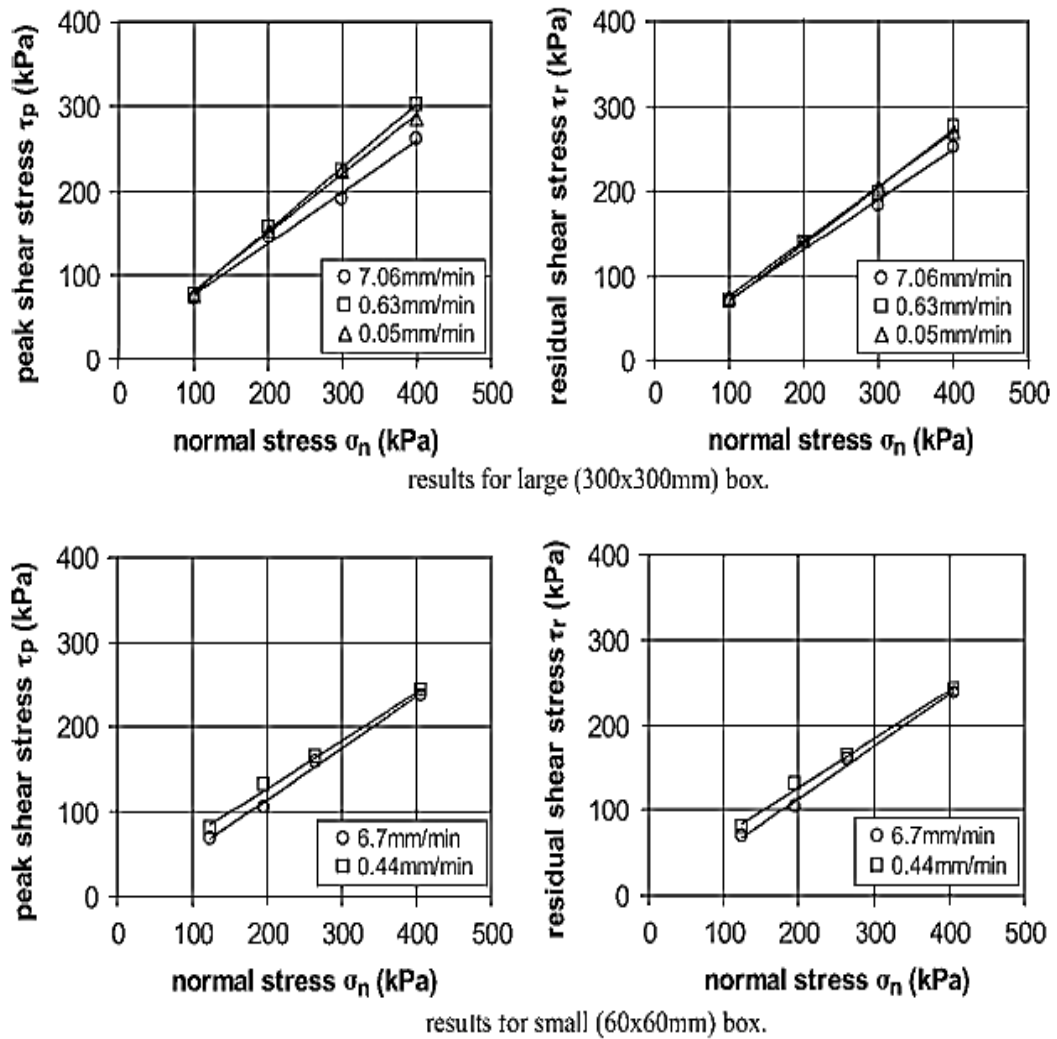


Figure 2.27 Tests Results of Nakao and Fityus, 2008

For examining the effect of shear box size, Nakao and Fityus (2008) conducted shear tests using small and large shear boxes. In order to see the effect of particle size, specimens having maximum particle sizes of 4.75 mm and 19 mm were tested.

At same shearing rate and for 4.75 mm maximum particle size, large shear box and small shear box tests were reported to give close friction angles. However, samples having different maximum particle sizes showed great differences in friction angle when tested in different sized shear boxes (Figure 2.28).

Nakao and Fityus (2008) concluded that higher effective strength measured in large shear box was mainly as a result of presence of larger particles. The authors also observed some amount of peak strength behavior in large shear box.

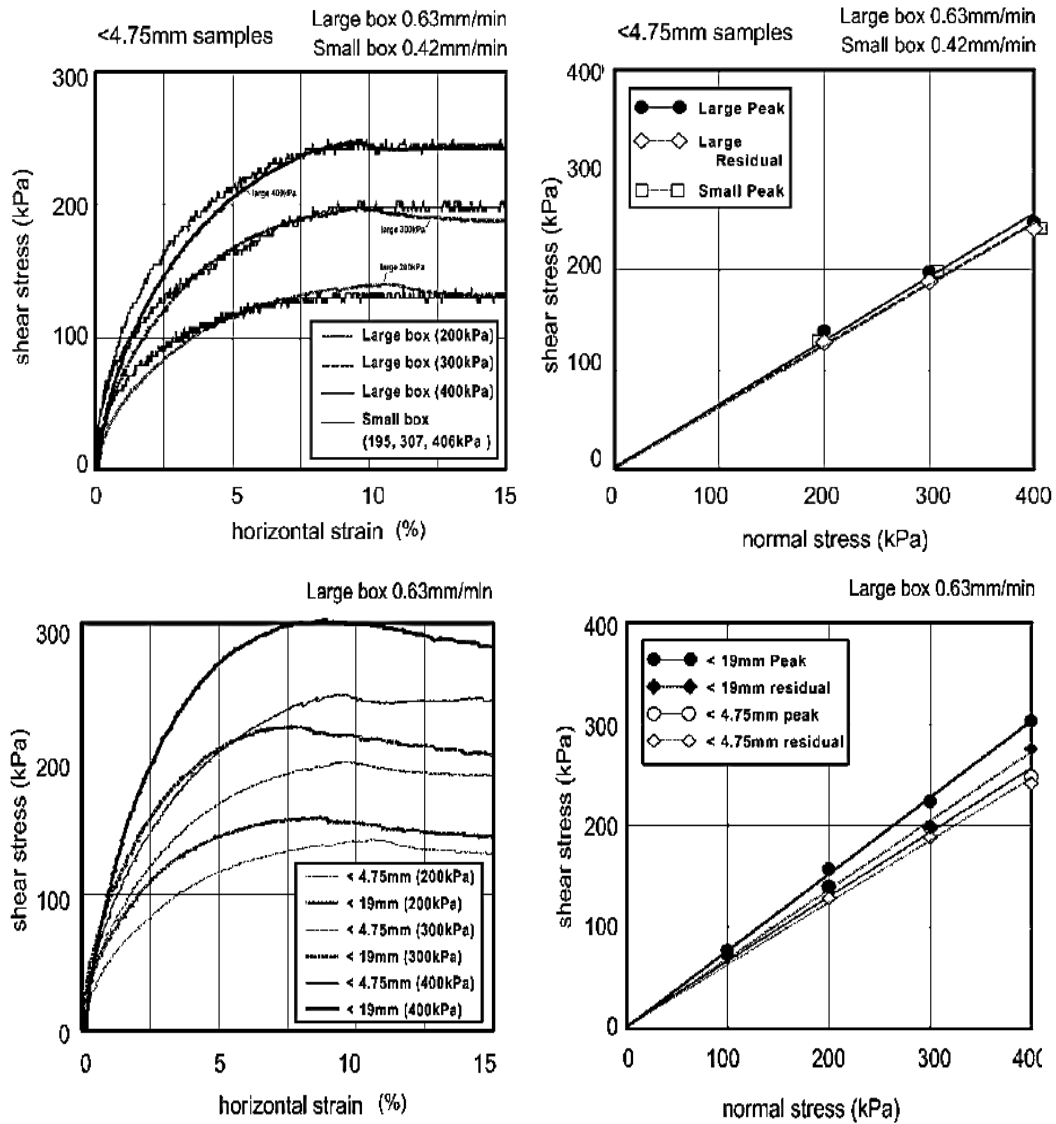


Figure 2.28 Effects of Particle Size and Size of the Shear Box (Nakao and Fityus, 2008)

*Fakhimi and Hosseinpour (2008)* studied the role of oversized particles on the shear strength of a rock pile material. The authors conducted direct shear tests

using steel balls of three different sizes (0.66 cm, 2.28 cm and 2.90 cm) in a 60 mm shear box.

As a result of direct shear tests, it was found that the presence of oversized particles changed the shear strength of the material. The biggest ball diameter results in more dilative behavior and higher strength values (Figure 2.29). In this study, friction angle was found to be increased and cohesion was observed to be decreased as a result of oversized particles.

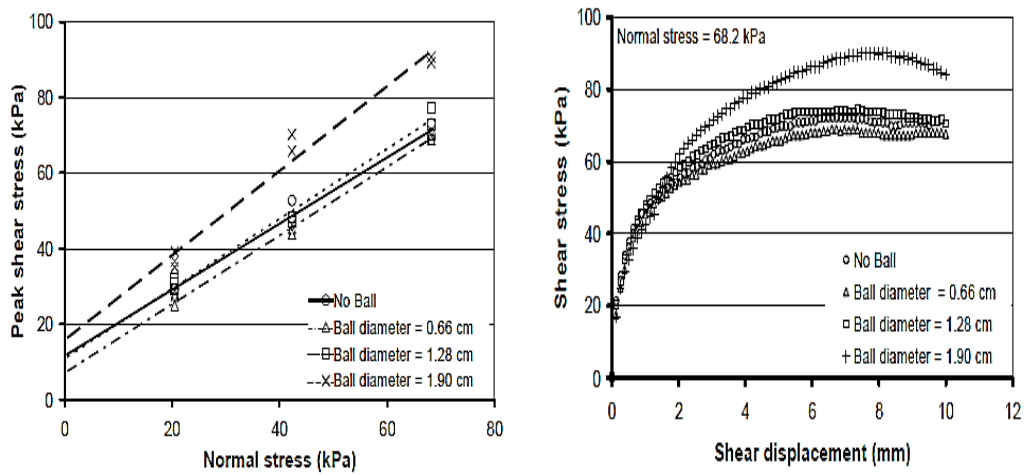


Figure 2.29 Tests Results of Fakhimi and Hosseinpour, 2008

*Mollamahmutoğlu and Yılmaz (2009)* mixed highly plastic clayey soil (Ankara clay) with different amounts of fine gravel and investigated the effect of gravel content on the undrained shear strength through unconsolidated-undrained triaxial tests.

The authors observed that as the gravel content increased friction angle of the mixture also increased. Cohesion of the mixture was reported to decrease for increasing gravel content being significant for gravel contents beyond 50% (Figure 2.30).

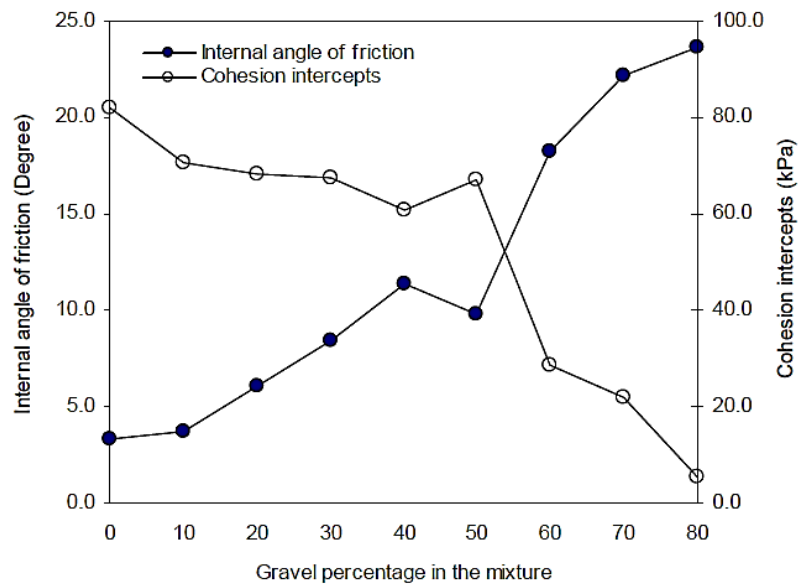


Figure 2.30 Change of Friction Angle and Cohesion with Gravel Content (Mollamahmutoglu and Yilmaz, 2009)

As discussed throughout this chapter, there are very limited studies on shear strength properties of granular fill-clay materials. Moreover, all of these studies are concentrated on the shear strength properties of granular fill-clay mixtures while no study is available in the literature investigating the shear strength properties of granular material-clay interfaces. The aim is to make contribution in this lacking part to the available literature based on the results of this study.

## CHAPTER 3

### EXPERIMENTAL STUDY I - DIRECT SHEAR TESTS

#### 3.1 Introduction

In many engineering applications granular material can be seen on soft clay layers and there may be some instability problems on interfaces of strong granular material and soft clay layer.

In order to prevent movements along such interfaces or in order to suggest an improvement, some slope stability computations are performed in the design stage. In this stage, selecting representative shear strength parameters has a great importance for an accurate design and in order to have stable engineering structures. However in the literature no accepted method is available on how to select these parameters.

Generally when dealing with instability problems of interfaces, the design is based on the strength parameters of the soft layer encountered. However, the shear strength characteristics of the interfaces may be stronger than the soft layer due to the intrusion of the granular materials to the lower soft layer in the interface zone.

Since coarse grained granular material is being used in practice, interface should be tested in large shear boxes. However, it is difficult to provide large shear box in order to obtain shear strength parameters. Shear tests are generally performed in small shear boxes due to traceability. In small shear box, large grains can not be used and the maximum particle size of the granular material to be used is arranged according to small shear box limitations. In this study, shear box tests of the interfaces were conducted both using large and small shear boxes. A total of 38 direct shear tests were conducted, 13 of which were on large shear box while the remaining 25 experiments were executed on small shear box.

Since interfaces are being widely encountered, shear strength of interfaces and the strength parameters to be used have become more important. The economic losses due to instability problems on interfaces and the lack of detailed investigations on shear strength of interfaces makes the results of this study more important for scientific literature.

### 3.2 Materials Used in Experiments

#### 3.2.1 Clay

The mineralogical and chemical properties of the clay specimen used in experiments are given in Table 3.1 (Şengör, 2013).

Table 3.1 Mineralogical and Chemical Properties of Clay (Şengör, 2013)

Mineralogical Structure	Volumetric Content	%	Chemical Analysis	%	
kaolinite	Clay Mineral	90.5	(loss on ignition)	12.73	
Quartz	Free Quartz	2.71	SiO <sub>2</sub>	47.89	
Illite	Sodium Feldspar	0.08	Al <sub>2</sub> O <sub>3</sub>	36.75	
		4.45	TiO <sub>2</sub>	0.61	
				Fe <sub>2</sub> O <sub>3</sub>	0.40
				CaO	0.39
				MgO	0.09
				Na <sub>2</sub> O	0.01
				K <sub>2</sub> O	0.75
				SO <sub>4</sub>	0.37

Clay content of the specimen is 38 % according to the hydrometer tests as can be seen in Figure 3.1. Plastic limit (PL) and liquid limit (LL) of the specimen were found to be 26% and 44% respectively. Plastic index (PI) of clay is calculated as 18%. The specimen can be classified as low plastic clay with silts (CL).

Same procedure described in Şengör (2013) was applied while preparing the clay specimens. Dry powder kaolinite was mixed with sufficient water providing water content  $w=43\%$  corresponding to a liquidity index of 0.94. Prepared clay

specimen was placed in moisture room for at least 2 days to obtain a homogenous specimen.

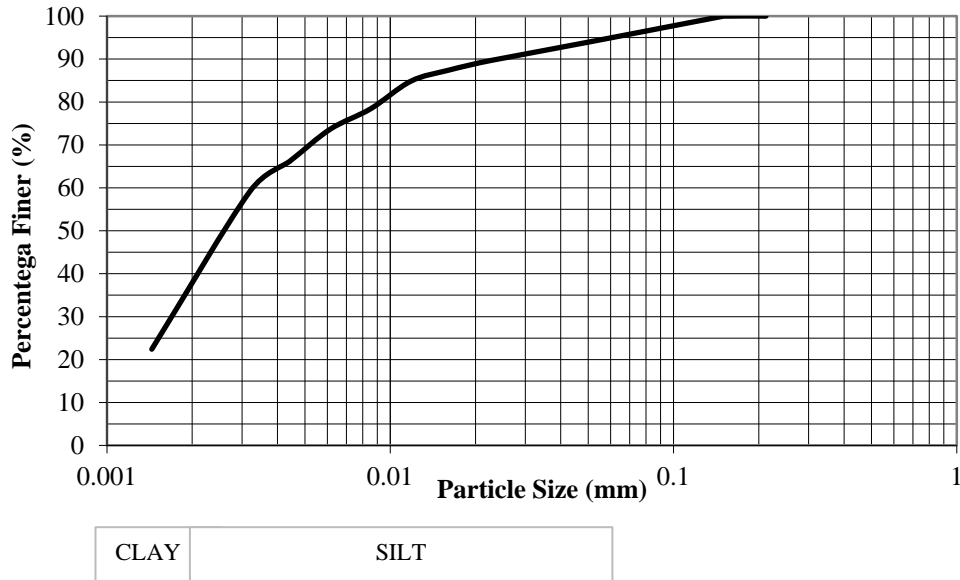


Figure 3.1 Gradation of the Clay Specimen (Result of Hydrometer Test)

### 3.2.2 Granular Material

In ASTM D3080 (2011) “it is recommended that the minimum specimen width should not be less than ten times the maximum particle-size diameter and the initial specimen thickness should not be less than six times the maximum particle diameter” (Cerato and Lutenegeger, 2006). Two types of granular material were used in experiments due to size limitations of ASTM D3080 (2011).

In small shear box tests, medium to coarse sand was used since the maximum aggregate size that can be used is around 3 mm. Gradation of the sand used can be seen in Figure 3.2. Basic parameters of sand determined from Figure 3.2 are summarized in Table 3.2. Sand can be classified as poorly graded sand (SP). Density of sand was  $1.75 \text{ g/cm}^3$  in all tests performed indicating a relative density (DR) of 72% ( $\rho_{\max}=1.85 \text{ g/cm}^3$ ,  $\rho_{\min}=1.54 \text{ g/cm}^3$ ).

In large shear box tests, fine to medium gravels can be used. The maximum aggregate size used was 13 mm in that case. Gradation curve of the gravel used in large shear box tests can be seen in Figure 3.2 and basic parameters of gravel are given in Table 3.2. Gravel can be classified as poorly graded gravel (GP). Density of gravel was  $1.85 \text{ g/cm}^3$  in all tests performed resulting in a relative density (DR) of 67% ( $\rho_{\max}=1.95 \text{ g/cm}^3$ ,  $\rho_{\min}=1.65 \text{ g/cm}^3$ ).

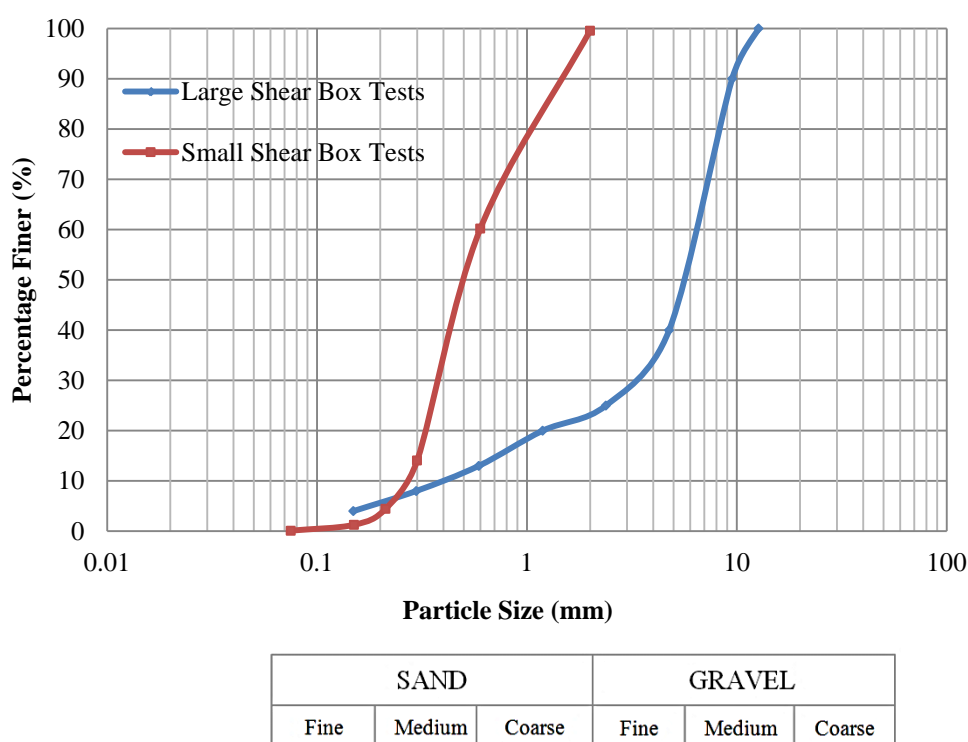


Figure 3.2 Gradation of the Granular Material

Table 3.2 Basic Parameters of Granular Materials

Granular Material	$D_{60}$	$D_{30}$	$D_{10}$	Uniformity Coefficient, $C_u$	Coefficient of Curvature, $C_c$	Soil Classification
				$(D_{60} / D_{10})$	$(D_{30}^2 / D_{60}D_{10})$	
Sand	0.60	0.38	0.27	2.22	0.89	SP
Gravel	6.56	3.35	0.40	16.40	4.28	GP

### 3.3 Large Shear Box Tests

In order to determine the shear strength parameters of granular material and clay interface, shear tests were conducted in a large shear box machine, which is available at the Rock Mechanics Laboratory of the Mining Engineering Department at M.E.T.U.

The experimental setup and the tests conducted are given in following parts of this section.

#### 3.3.1 Experimental Setup

“Wykeham Farrance” large shear box machine consists of shear box, horizontal and vertical loading systems and instrumentation system (displacement and load measurement). Figure 3.3 shows general view of large shear box used.



Figure 3.3 General View of Large Shear Box

The shear box of the machine has dimensions of 300 mm x 300 mm in plan and has a height of 150 mm. The vertical and horizontal capacity of the shear box is

100 kN. The horizontal loading system provides constant rate of displacement using a motor with 0.5 horse power capacity. Maximum shearing rate is 5 mm/min, minimum shearing rate is 0.00001 mm/min and maximum travel length of the shear box is 60 mm. Vertical load is applied by a hydraulic piston.

Horizontal loading system applies force to the bottom half of the shear box and this force can be instrumented with a proving ring attached (Figure 3.4). “Wykeham Farrance” (Ring No:14338) special alloy steel proving ring having 100 kN capacity was supplied with a “Mitutoya” digital indicator having a range of 12 mm and 0.001 mm resolution. The factor used to convert readings to the loads (kg) is 3.8.



Figure 3.4 Instrumentation on Large Shear Box

Vertical and horizontal displacements are measured with digital indicators attached to shear box at suitable positions having measurement ranges of 25 mm and 50 mm, respectively. These digital indicators manufactured by “Mitutoya America Co.” have a resolution of 0.01 mm.

Shear tests were conducted in drained conditions which take a long time (especially in consolidation stage) making mechanical measurements difficult. In order to have continuous records, a data acquisition system was needed. A data system consisted of a computer, data logger and three digital indicators (to measure vertical and horizontal displacements together with the applied horizontal load) were used in the large shear box experiments (Figure 3.3).

“TDG TestBOX 1001” was used as data logger which have a 16 bit system and 0.0003 Volt bit resolution. The data system has 4 channels to which digital indicators can be connected. All connected data can be measured with an interval of at least 0.125 s. The data system has a signal-to noise ratio (SNR)  $\geq 72$ .

### 3.3.2 Results of Large Shear Box Tests

In large shear box, gravel and gravel-clay interface were tested and the results of these experiments are given in this section. Area correction was applied to the results of the experiments.

#### 3.3.2.1 Large Shear Box Tests of Gravel

Granular material (gradation is shown in Figure 3.2) was sheared in large shear box. Stress-displacement graphs are shown in Figure 3.4. Peak shear strength values were obtained at large deformations (30 mm - 45 mm).

Vertical displacement during shearing can be seen in Figure 3.6. At small initial normal stresses (111 kPa, 222 kPa) settlement at small horizontal displacements and heaving at large deformations was observed whereas for high initial normal stress (333 kPa) settlement continued during shearing as expected.

Both non-linear and linear failure envelopes were investigated. As it can be seen in Figure 3.6, these two envelopes revealed very similar behavior. Based on this finding, linear failure envelopes are utilized throughout the study.

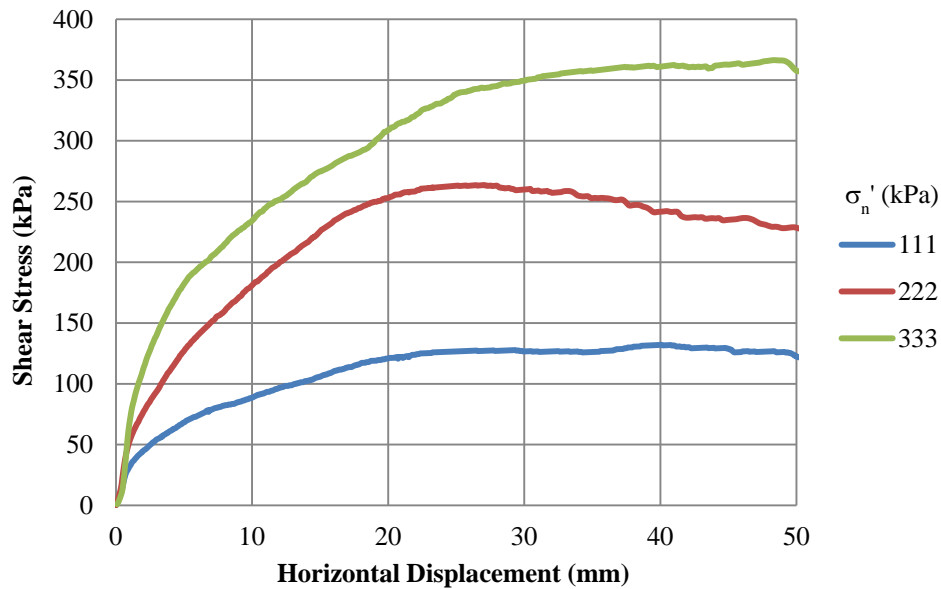


Figure 3.5 Shear Stress-Shear Displacement Graphs of Gravel in Large Shear Box

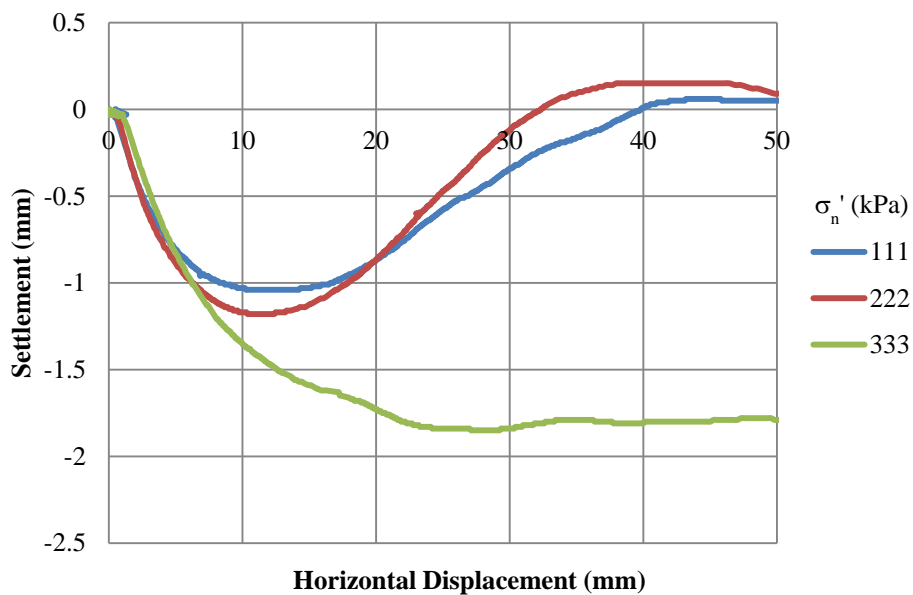


Figure 3.6 Settlement of Gravel during Shearing in Large Shear Box

Shear strength parameters of the granular material were obtained as  $c=0$  kPa and  $\phi=44.8^\circ$  (Figure 3.7) from the large shear box tests.

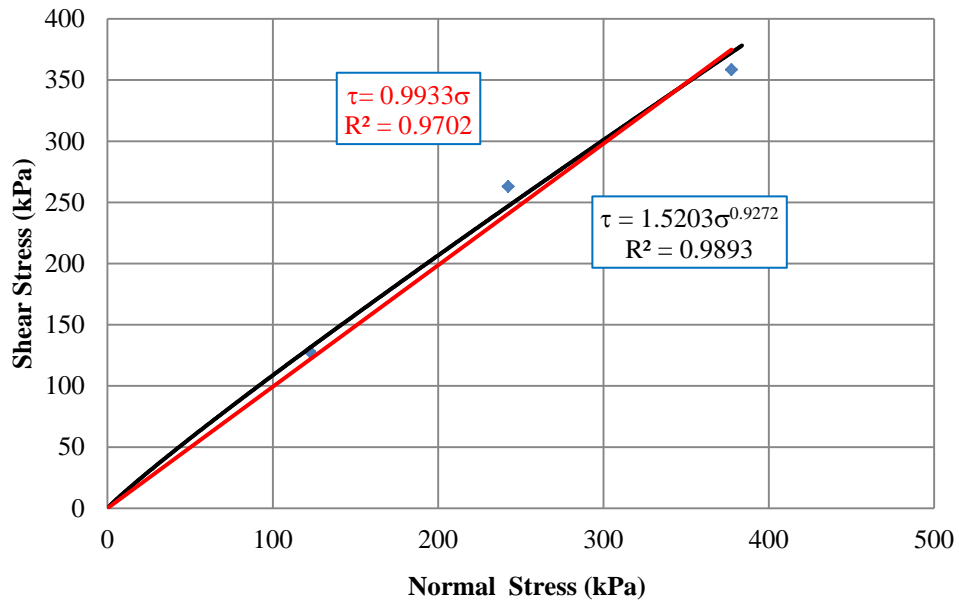


Figure 3.7 Shear Strength Envelope of Gravel in Large Shear Box

### 3.3.2.2 Large Shear Box Tests of Clay-Gravel Interfaces

For gravel-clay interface tests, gravel was placed in lower part of the shear box with a constant density and clay was placed on gravel (Figure 3.8 and 3.9)

Shear tests were conducted at five different normal stresses (55.5 kPa, 111 kPa, 222 kPa, 333 kPa and 444 kPa) and some of the tests were repeated in order to check results. Strain rate was chosen to be 0.5 mm/min since smaller rates caused some problems related with the shear box (i.e. shear motor stopped during experiments).

Consolidation pressure was increased to the desired pressure in stages since it was observed that consolidation in one stage caused some failures within the specimen that lead to misleading results.



Figure 3.8 Large Shear Box Tests of Gravel-Clay Interface



Figure 3.9 Gravel-Clay Interface in Large Shear Box Tests

A typical consolidation graph is shown in Figure 3.10. Stress-displacement and settlement graphs obtained are presented in Figure 3.11 and Figure 3.12, respectively.

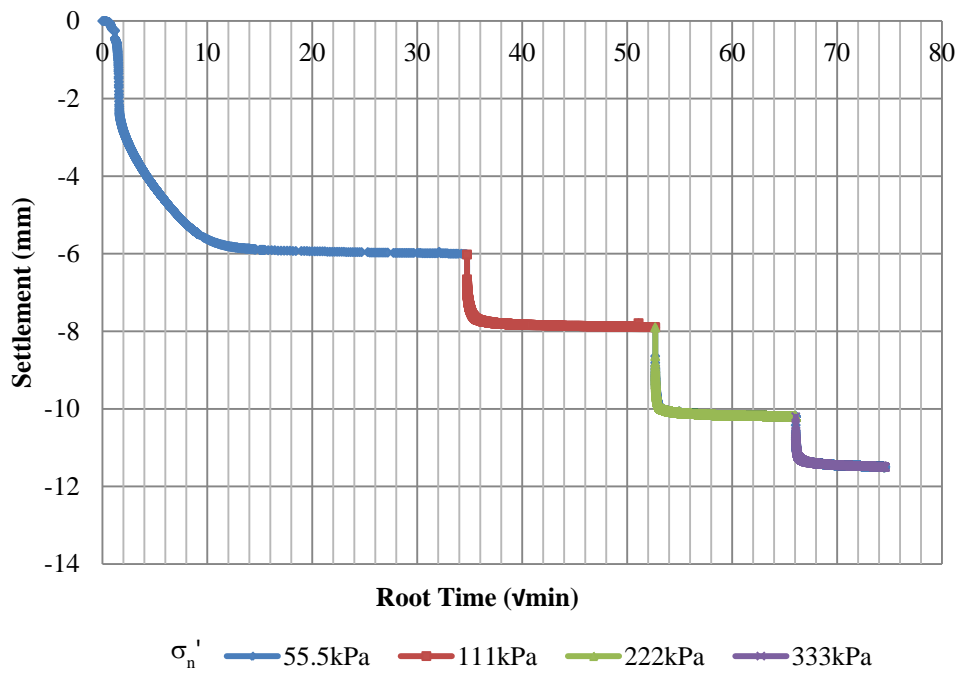


Figure 3.10 Consolidation Graph of Interface (Sample)

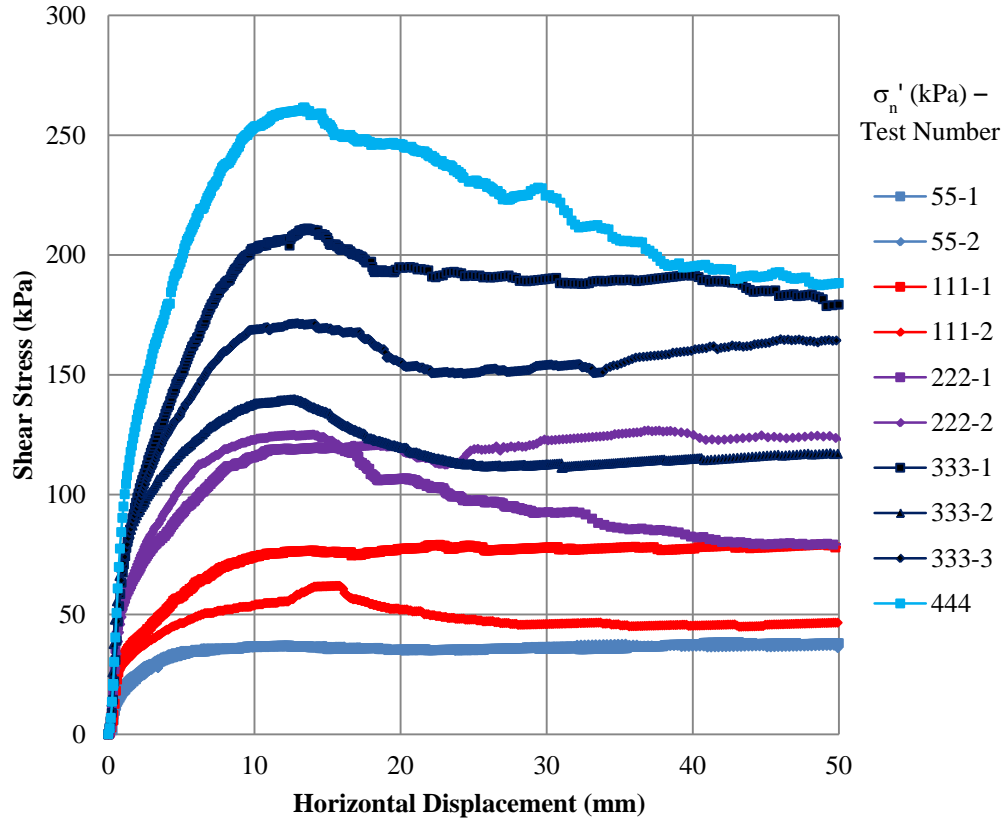


Figure 3.11 Shear Stress-Shear Displacement Graphs of Gravel-Clay Interface

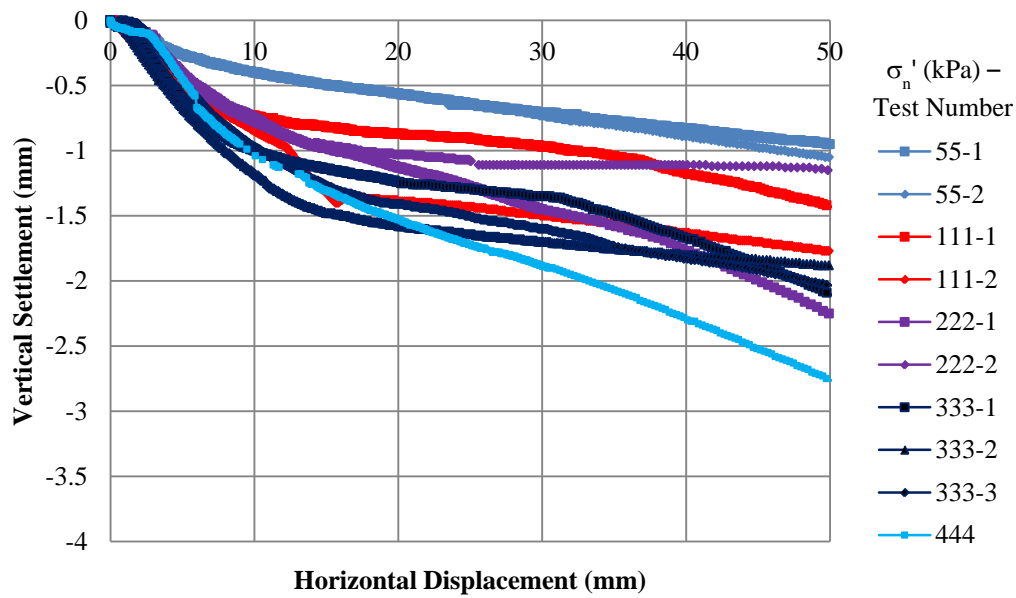


Figure 3.12 Settlement of Gravel-Clay Interface in Large Shear Box during Shear

According to Figure 3.11, peak shear strengths were obtained at 5 mm shear displacement for smallest normal stress (55 kPa) and 10-15 mm shear displacement for remaining normal stresses.

The peak shear strength envelope is shown in Figure 3.13 considering the all shear tests conducted. According to these results, peak shear strength parameters of the interface was found to be  $c=6.1$  kPa and  $\phi=26.8^\circ$  in large shear box tests.

As can be seen from Figure 3.13, there is some scatter at normal stress  $\sigma'_n=333$  kPa and stress-displacement behavior of the tests conducted at  $\sigma'_n=444$  kPa is different from other tests at large horizontal displacements as shown in Figure 3.11. All small direct shear tests (Sec. 3.4) and triaxial tests (Chapter 4) were conducted at normal stresses up to  $\sim 200$  kPa. Due to these reasons, the shear strength envelope can be redrawn for normal stresses 55, 111 and 222 kPa as shown in Figure 3.14 which gives envelopes having higher regression coefficients ( $R^2$ ). Considering Figure 3.14, peak shear strength parameters of the interface was found to be  $c=10.4$  kPa and  $\phi=25.8^\circ$  in large shear box tests.

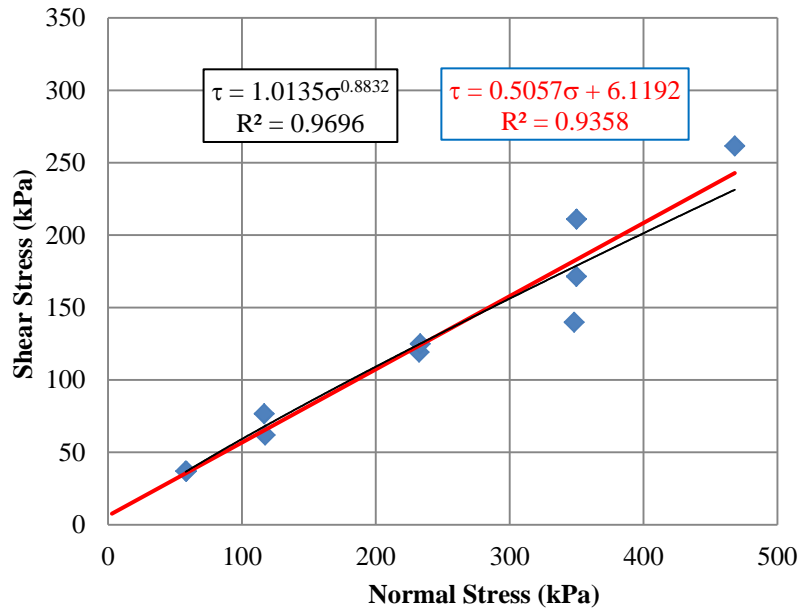


Figure 3.13 Peak Shear Strength Envelope of Gravel-Clay Interface (All Tests)

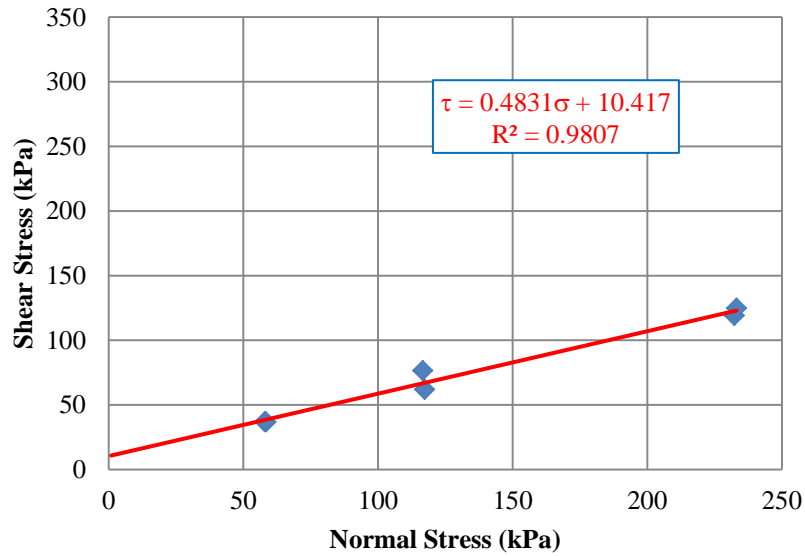


Figure 3.14 Peak Shear Strength Envelope of Gravel-Clay Interface

For large deformations (30 mm shear displacement=10% of sample size and 36 mm shear displacement=12% of sample size), shear strength envelope is shown in Figure 3.15 and the shear strength parameters are found as **c=14.2 kPa**,  $\phi=20.6^\circ$  and **c=15.2 kPa**,  $\phi=19.8^\circ$ , respectively.

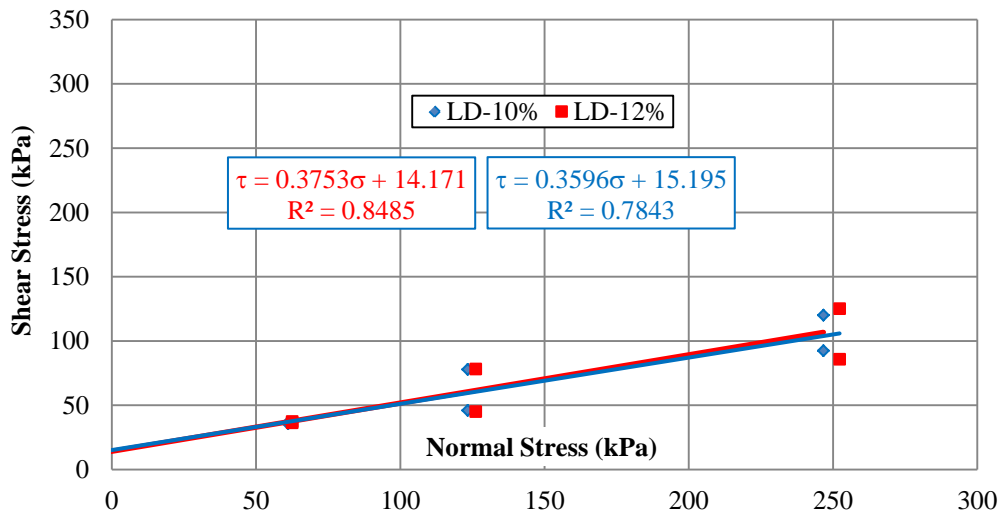


Figure 3.15 Large Deformation Shear Strength Envelope of Gravel-Clay Interface

### 3.4 Small Shear Box Tests

Direct shear tests were performed in order to obtain shear strength properties of clay, sand and clay-sand interfaces in small shear box. Specimens having a diameter of 6 cm and a thickness of 2 cm were tested in small shear box.

In interface shear tests performed using small shear box, the lower part of the shear box was filled with sand and clay was placed on that layer in such a way that enables shearing along the interface. Each test was performed for two normal stress levels and with at least two specimens.

“VJ Tech 9500 ShearTest” direct shear machine (Figure 3.16) was used for small shear tests. The machine is microprocessor controlled with data system and data processing software. Strain rate ranging between 0.00001 mm/min and 10 mm/min can be used in experiments. Maximum displacement of the shear box machine is 20 mm.

Vertical load (up to 5 kN) is given using a load hanger with 10 / 1 lever loading unit. Lateral load is measured with “VJTS 0361 S-Beam” load cell having a capacity of 5 kN and 2N resolution.

Horizontal displacement is measured with “VJT 0271” displacement transducer having a range of 25 mm and 0.01 mm resolution. The displacement transducer for vertical settlement measurement, “VJT 0270” has a range of 10 mm and a resolution of 0.01 mm.



Figure 3.16 General View of Small Shear Box Machine

#### 3.4.1 Shearing Rate Effect

In order to see the effect of shearing rate, shear tests were performed in small shear box with different shearing rates for clay specimen. The results are shown in Figure 3.17 and Figure 3.18 for different normal stress values.

Small differences were observed in shear strength values for different experiments having different shearing rates. It can be concluded that in all experiments the clay specimen showed drained behavior and shear strength was not influenced from the shear rate (for a range of shearing rate between 0.0049 and 0.183 mm/min).

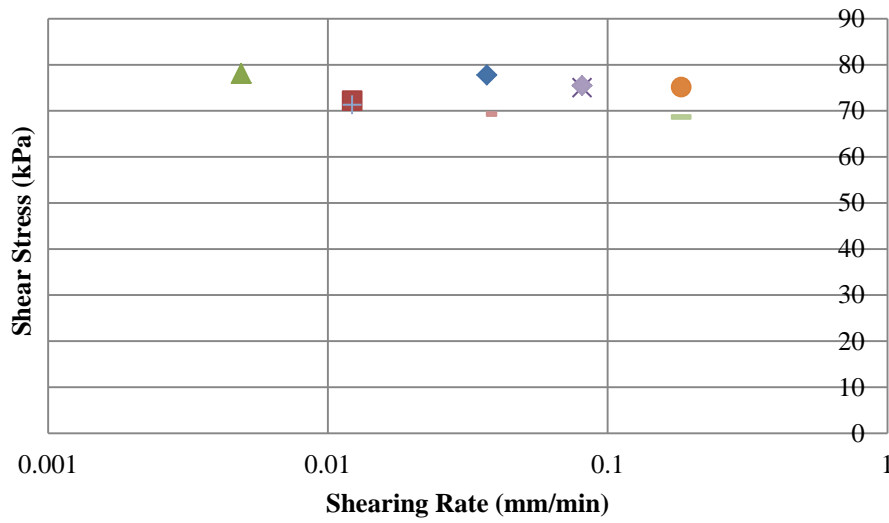


Figure 3.17 Effect of Shearing Rate for  $\sigma'_n=173.30$  kPa

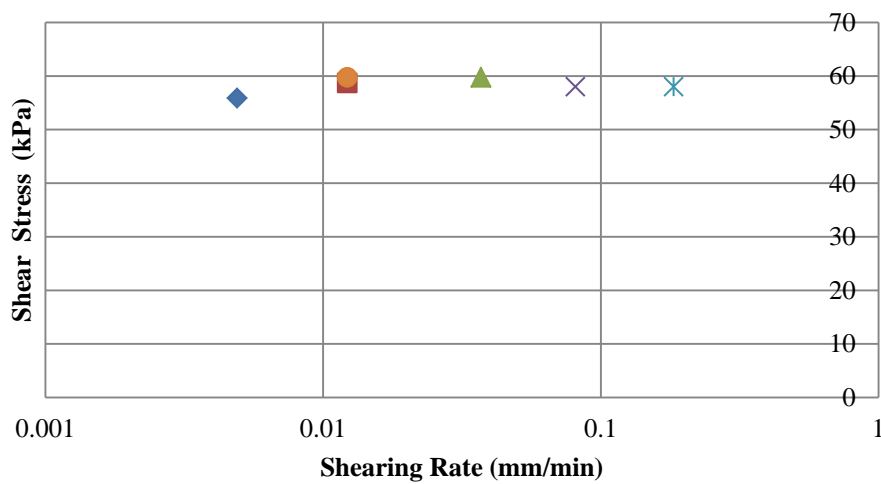


Figure 3.18 Effect of Shearing Rate for  $\sigma'_n=108.30$  kPa

### 3.4.2 Results of Small Shear Box Tests

Small shear box tests were performed for clay, sand and clay-sand interface. Peak and residual parameters were obtained.

The results of experiments conducted on each type of specimen are given in separate parts of this section. Area correction was applied to the results of the tests performed.

### 3.4.2.1 Small Shear Box Tests of Clay

Shear strength tests in small shear box were performed for three normal stresses (53, 108 and 197 kPa).

The settlement graph obtained during consolidation stage is given in Figure 3.19. From Figure 3.19, time for 90% consolidation,  $t_{90}$  is calculated as 4 min indicating a coefficient of consolidation,  $c_v = 0.21 \text{ cm}^2 / \text{min}$ . Shear rate was calculated according to ASTM D3080 (2011) using the consolidation data and shear tests were performed at a rate of 0.035 mm/min which is smaller than the calculated value.

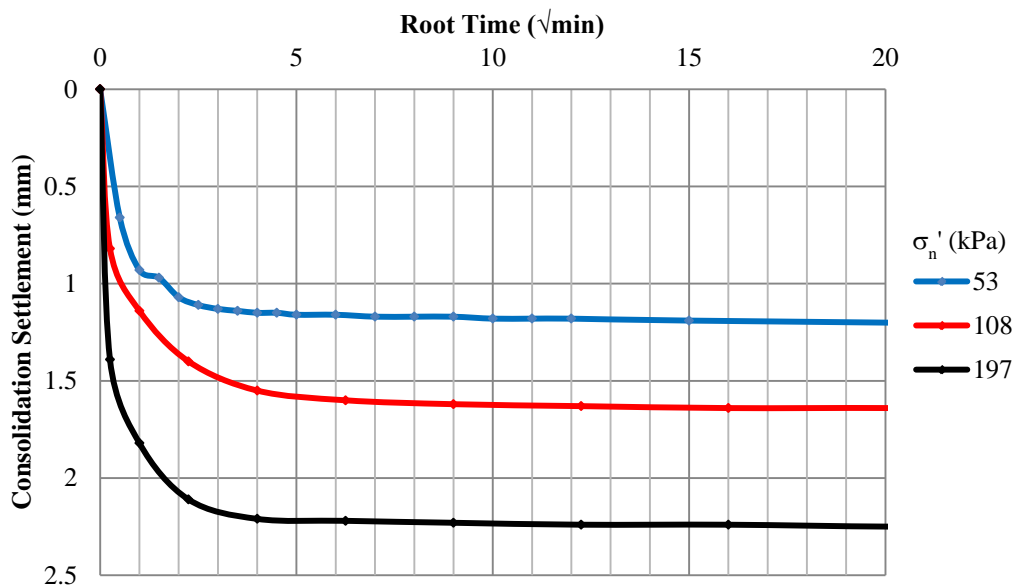


Figure 3.19 Settlement of Clay in Consolidation Stage

Stress-displacement graphs and vertical displacement during shearing are shown in Figure 3.20 and Figure 3.21, respectively. As can be seen, shear stresses increase and become constant. Settlement during shearing was also observed.

Peak shear strength envelope is given in Figure 3.22. Peak shear strength parameters were obtained as  $c=8.8 \text{ kPa}$  and  $\phi=22.4^\circ$ .

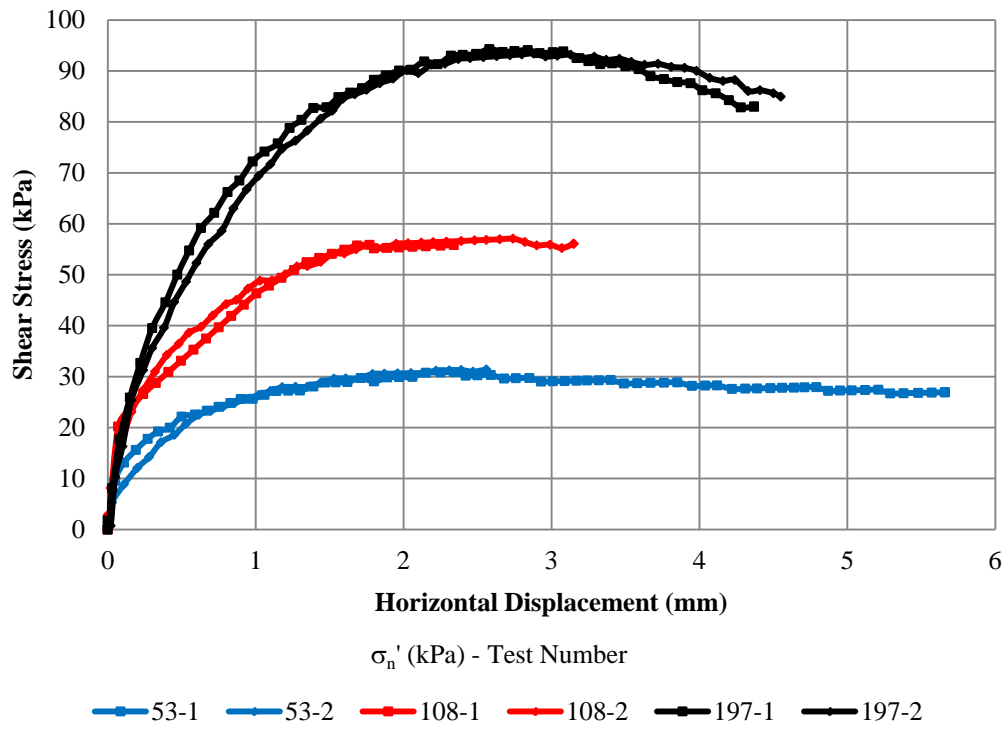


Figure 3.20 Stress-Displacement Graphs of Clay

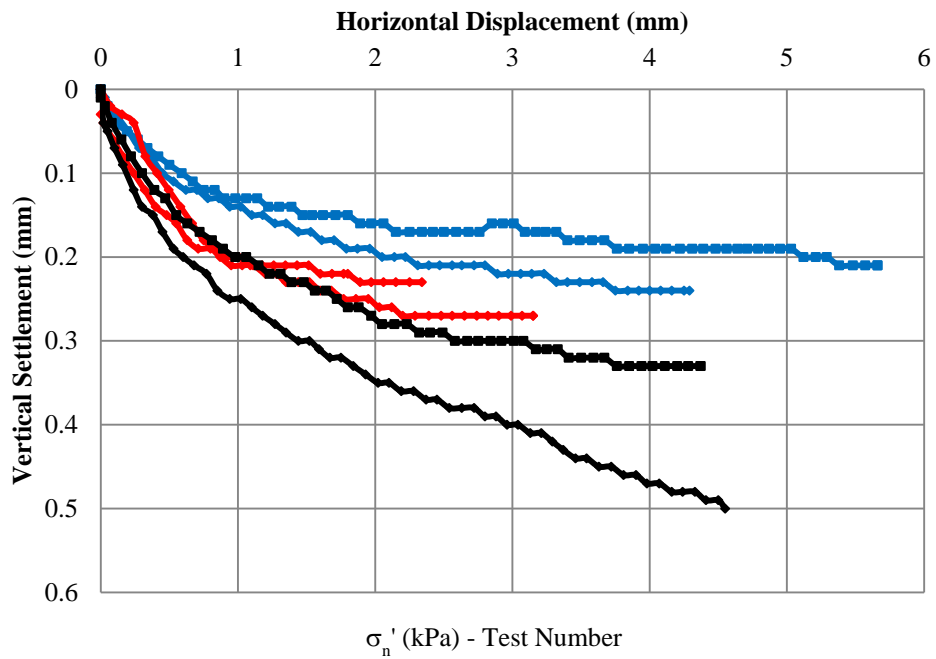


Figure 3.21 Settlement of Clay during Shearing

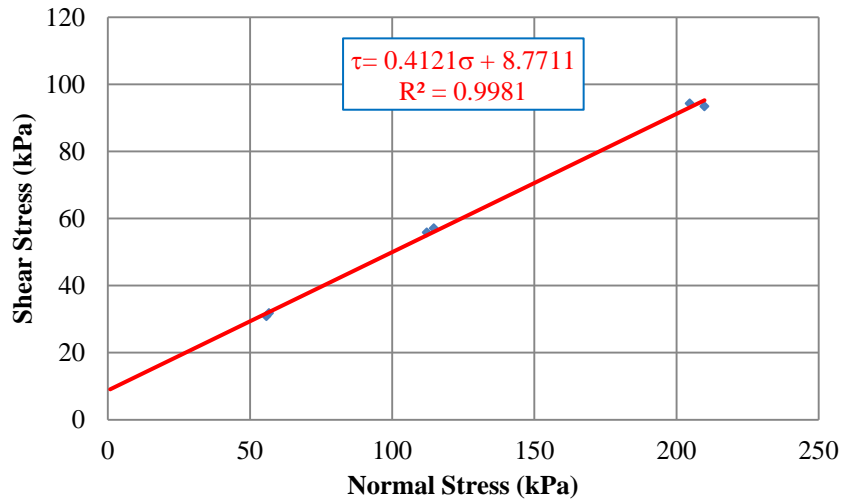


Figure 3.22 Peak Shear Strength Envelope of Clay

In shear tests, after peak shear strengths were obtained, specimen was sheared continuously (at higher strain rates) and a residual surface was obtained. Residual shear strength tests were then conducted for a shear rate of 0.035 mm/min.

Shear strength envelope is given in Figure 3.23 for clay in residual state. Residual shear strength parameters were obtained as  $c=7.3$  kPa and  $\phi=12.9^\circ$ . Shear stress-shear displacement graphs are shown in Figure 3.24.

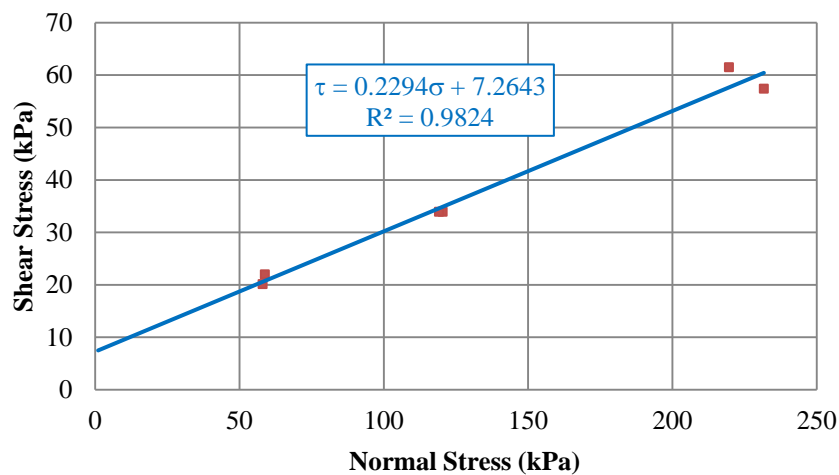


Figure 3.23 Residual Shear Strength Envelope of Clay

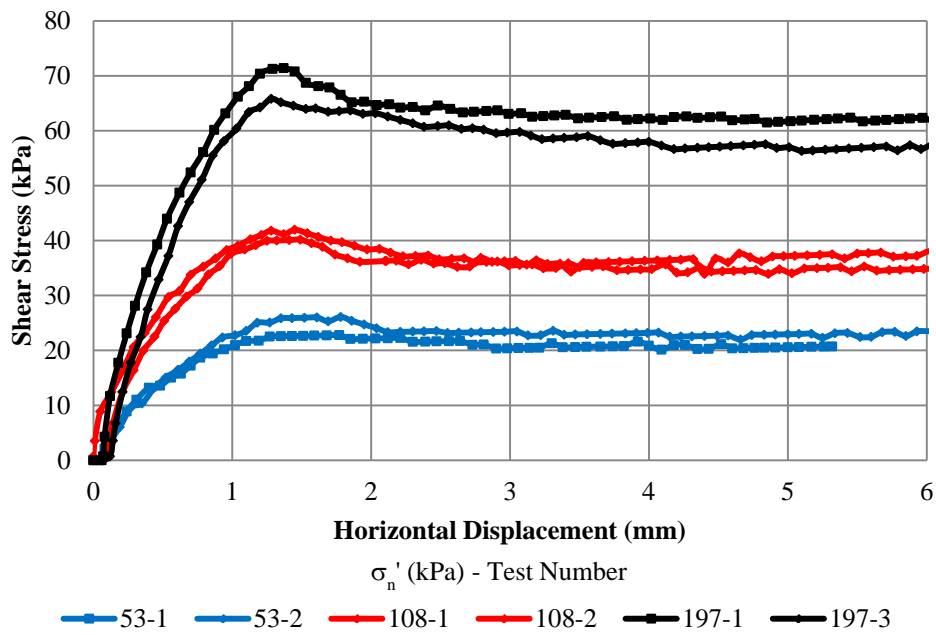


Figure 3.24 Stress-Displacement Curves of Clay in Residual Tests

### 3.4.2.2 Small Shear Box Tests of Sand

Sand was sheared at a rate of 0.5 mm/min. Stress-displacement graph is shown in Figure 3.25. Vertical displacement during shearing can be seen in Figure 3.26.

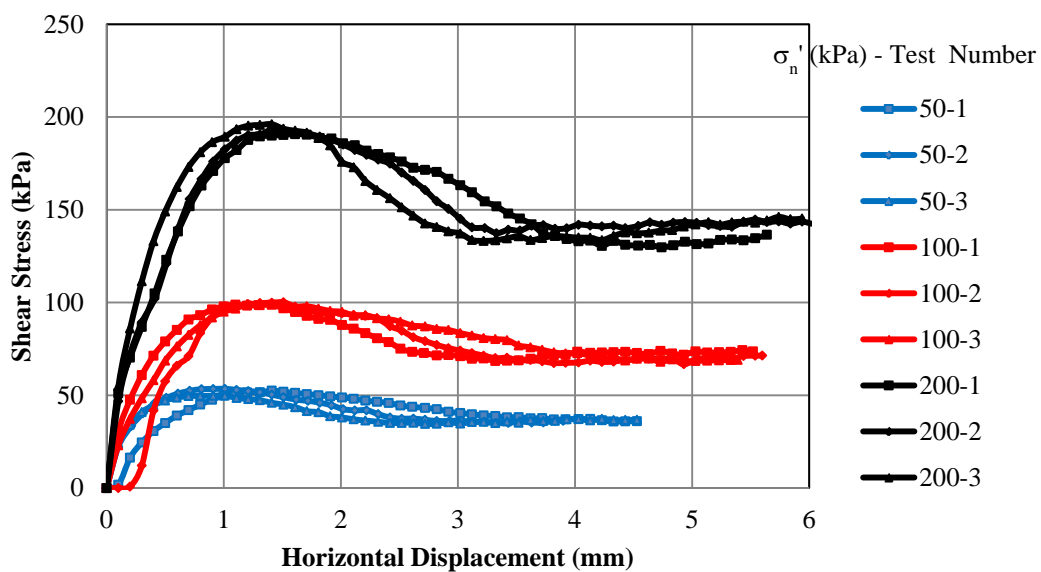


Figure 3.25 Stress-Displacement Graphs of Sand in Small Shear Box

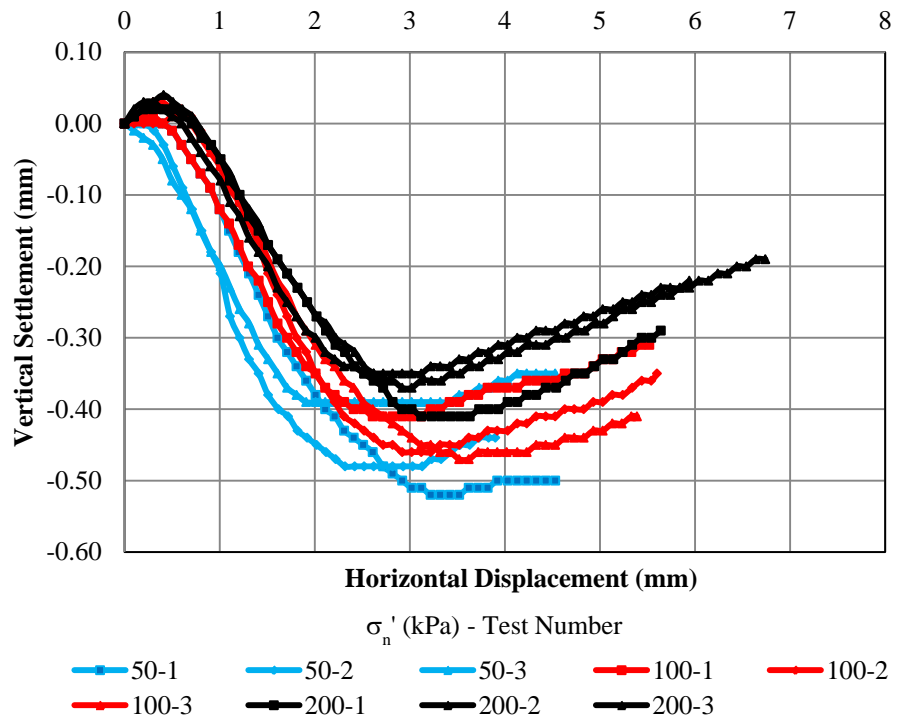


Figure 3.26 Vertical Displacement of Sand during Shearing

Shear strength envelope of the sand is given in Figure 3.27. Peak shear strength parameters of the sand was found to be  $c=0$  kPa and  $\phi=43.2^\circ$ .

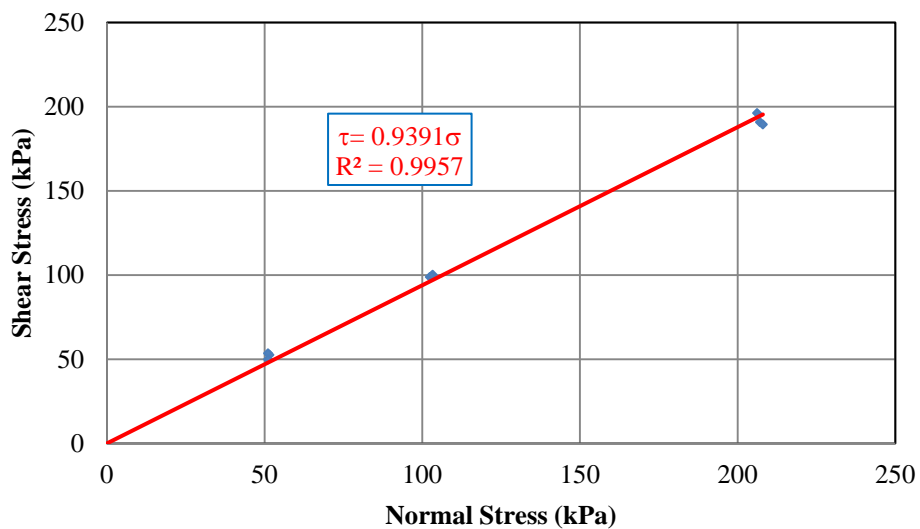


Figure 3.27 Shear Strength Envelope of Sand

### 3.4.2.3 Small Shear Box Tests of Clay-Sand Interfaces

As previously discussed, shear tests for interfaces were performed by filling sand to the lower part of the shear box and placing clay on sand (Figure 3.28).

Shear tests were performed at 0.5 mm/min shearing rate and with normal stresses of 100 kPa and 200 kPa. Stress-displacement curves and settlement graphs during shearing are given in Figure 3.29 and Figure 3.30, respectively.

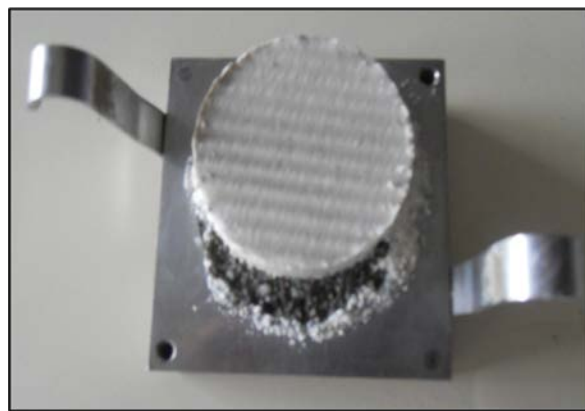


Figure 3.28 Small Shear Box Tests of Sand-Clay Interface

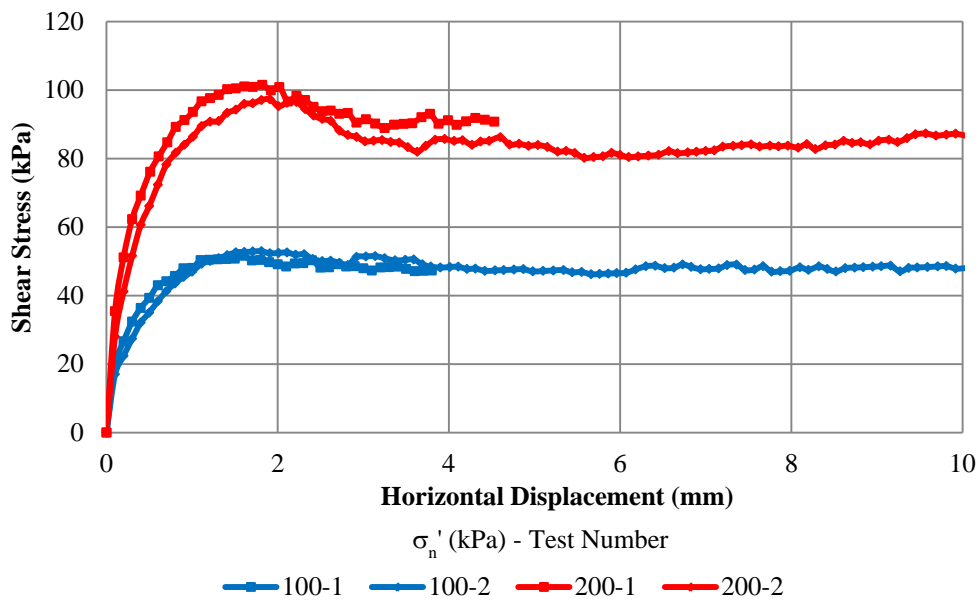


Figure 3.29 Shear Stress-Shear Displacement Curves of Sand-Clay Interface

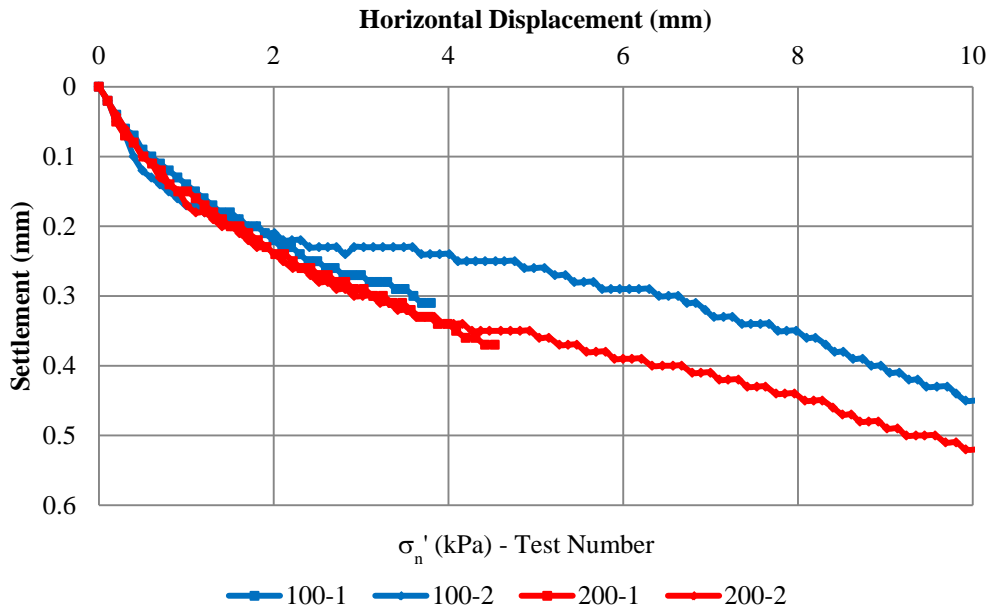


Figure 3.30 Settlement of Sand-Clay Interface during Shearing

Peak shear strength envelope of the interface is given in Figure 3.31. Based on these results, shear strength parameters of the interface was found to be  $c=5.5 \text{ kPa}$  and  $\phi=24.3^\circ$  in small shear box tests indicating a decrease in cohesion and an increase in friction angle when compared to peak clay parameters.

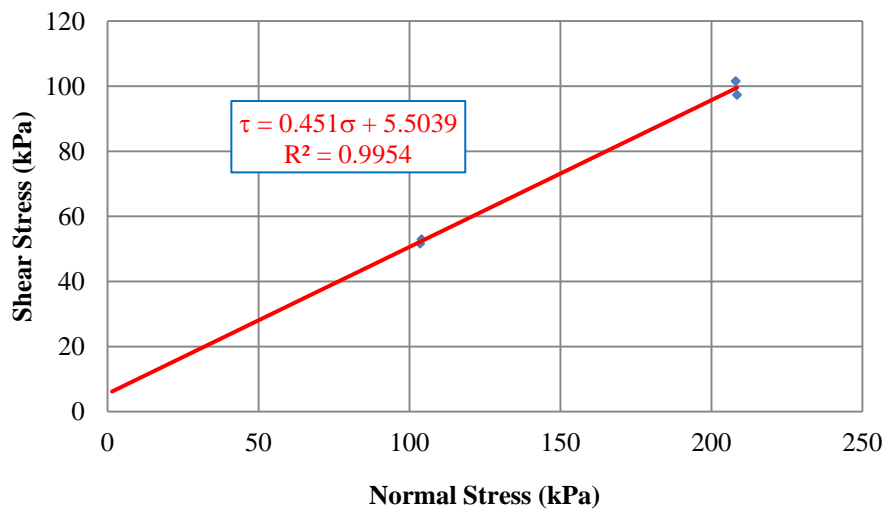


Figure 3.31 Peak Shear Strength Envelope of Sand-Clay Interface

For large deformations (6 mm shear displacement=10% of sample size and 7.2 mm shear displacement=12% of sample size), shear strength values were found as  $c=12.2$  kPa,  $\phi=16.7^\circ$  and as  $c=14.2$  kPa,  $\phi=16.4^\circ$  as shown in Figure 3.32.

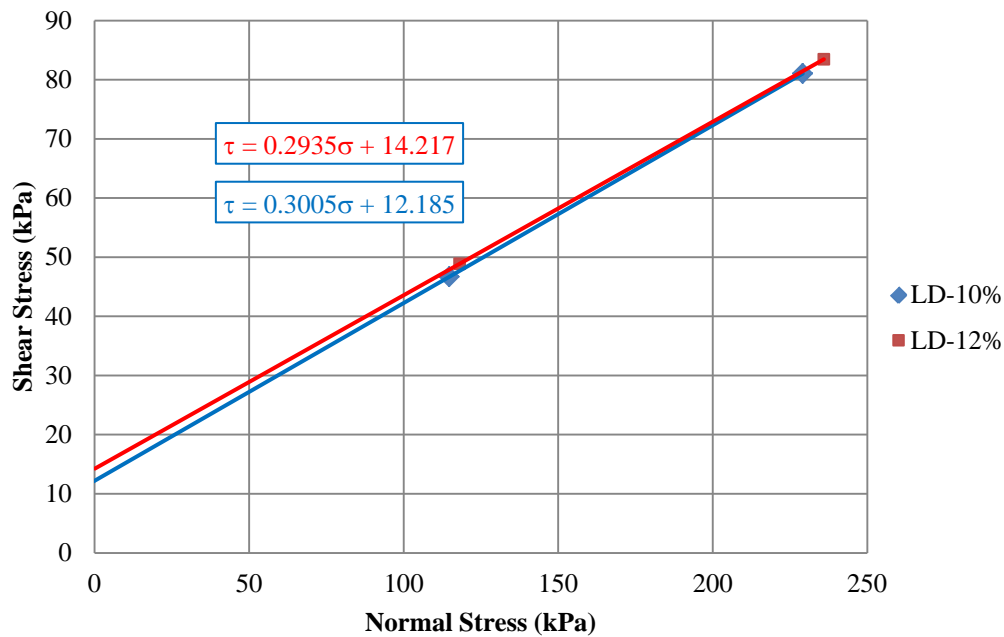


Figure 3.32 Large Deformation Envelopes of Sand-Clay Interface

### 3.5 Discussion of Results

As discussed in previous sections of this chapter, the direct shear tests were conducted both in small and large shear boxes. The experiments conducted are summarized in Appendix A.

Sand, clay and sand-clay interface shear strength tests were conducted in small shear box and gravel sized granular material and gravel-clay interface were tested in large shear box. The results were summarized in Table 3.3 and in Figure 3.33. Large deformation parameters in the table were chosen as the smallest of the previously presented values.

Table 3.3 Summary of Direct Shear Tests-Shear Strength Parameters

Material	Test Type	Strength Type	c (kPa)	$\phi$ (°)
Sand	SSB	Peak	0.00	43.20
Gravel	LSB	Peak	0.00	44.80
Clay	SSB	Peak	8.80	22.40
		Res	7.30	12.90
Sand-Clay	SSB	Peak	5.50	24.30
		LD	12.20	16.70
Gravel-Clay	LSB	Peak	10.40*	25.80*
		LD	15.20	19.80

LSB: Large Shear Box    SSB: Small Shear Box    Res:Residual    LD:Large Deformation

\*Strength parameters were obtained considering the compatible tests conducted.

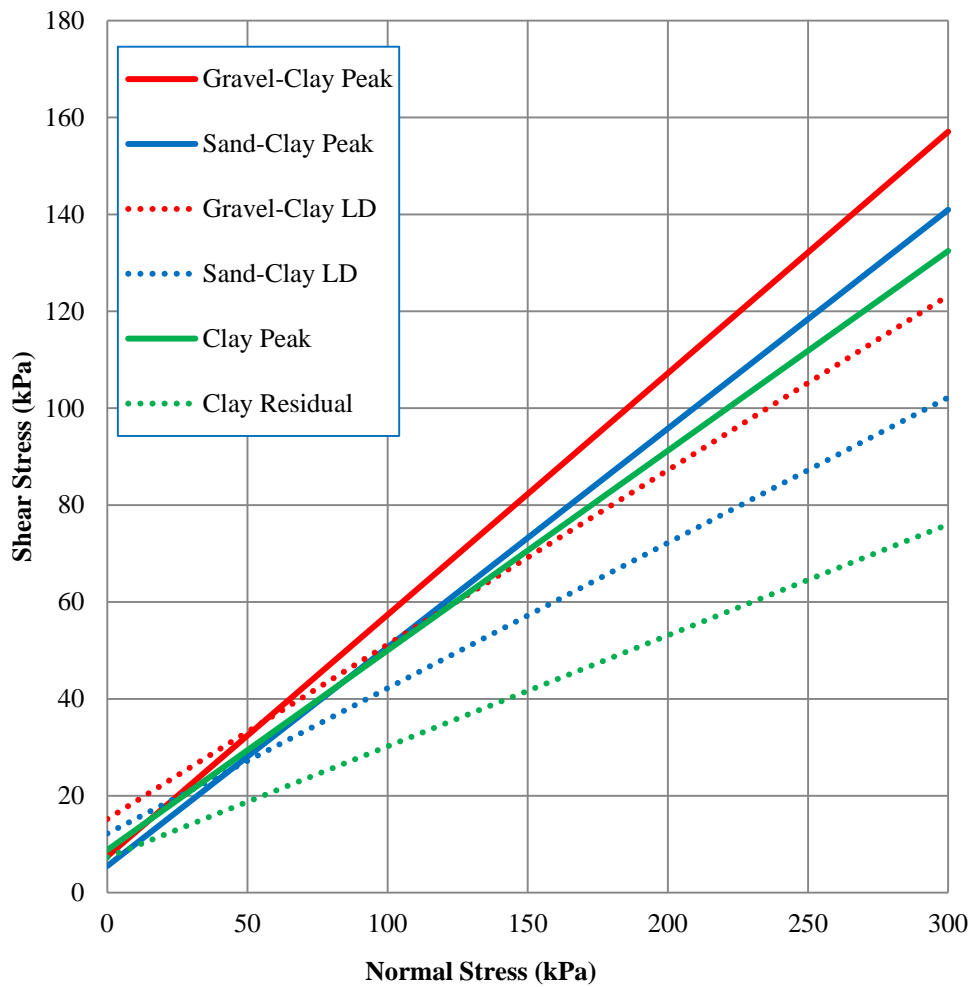


Figure 3.33 Summary of Direct Shear Tests

The friction angle of gravel was found to have a friction angle that is 1.6° higher than the friction angle of sand.

The peak shear strength of gravel-clay interface and sand-clay interface were obtained to be greater than the peak shear strength of clay especially at large normal stress values as can be seen in Figure 3.33. In large shear box tests, peak friction angle of gravel-clay interface is obtained as 3.4° higher than the peak friction angle of clay. In small shear box tests, peak friction angle of sand-clay interface is found to be 1.9° greater than the peak friction angle of clay. So, peak friction angle of gravel-clay interface is 1.5° higher than peak friction angle of sand-clay interface.

At the peak shear strength, cohesion intercept of gravel-clay interface is higher than the peak cohesion value of clay whereas this is not the case for sand-clay interface. In small shear box tests, peak cohesion of sand-clay interface is found to be smaller than the peak cohesion of clay.

In order to make a better comparison, secant friction angles for peak shear strength values are obtained and presented in Figure 3.34 for different normal stresses.

$$\tau = \sigma \tan \phi_{\text{sec}} \quad (3.1)$$

As discussed above, shear strength increase at interfaces can be seen from Figure 3.34. Gravel-clay interfaces showed 3.6°-3.9° increase in secant friction angle when compared to secant friction angle of clay at peak shear strength. This increase is at most 1.3° for sand-clay interfaces being very small at small normal stresses. So the difference of secant friction angles of gravel-clay and sand-clay interface at peak state is 2.2°-3.5°.

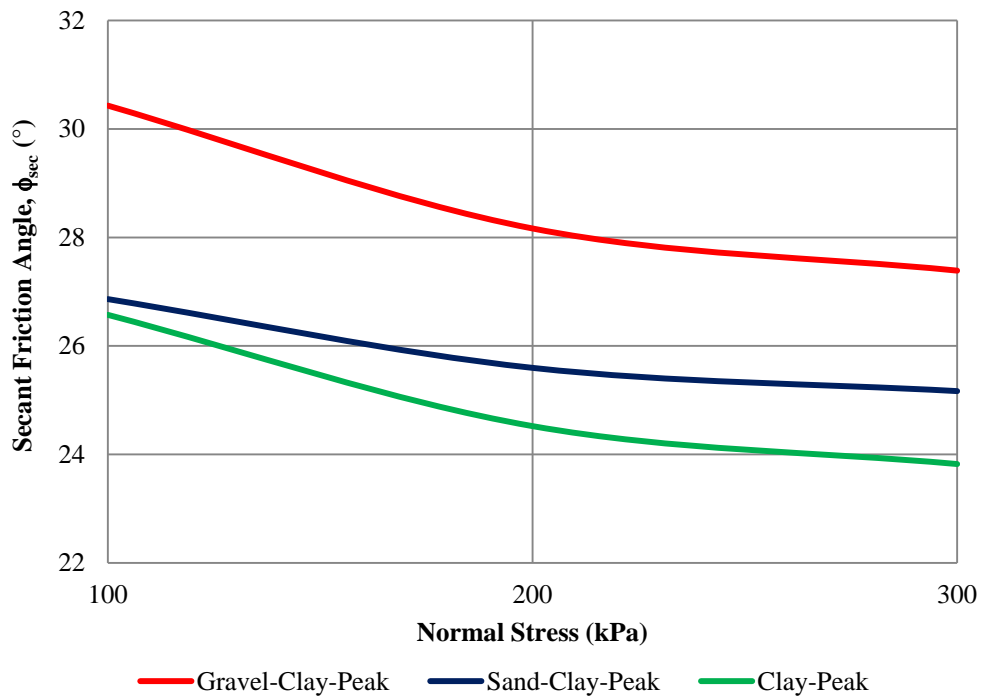


Figure 3.34 Secant Friction Angles Obtained from Peak Shear Strengths of Direct Shear Tests

The large deformation shear strength of gravel-clay interface and sand-clay interface were obtained to be greater than the residual shear strength of clay. In large shear box tests, large deformation friction angle of gravel-clay interface is obtained  $6.9^\circ$  greater than the residual friction angle of clay. In small shear box tests, peak friction angle of sand-clay interface is found to be almost  $3.8^\circ$  higher than the residual friction angle of clay. So, large deformation friction angle of gravel-clay interface is  $3.1^\circ$  greater than large deformation friction angle of sand-clay interface.

At large deformation, cohesion intercepts of gravel-clay interface and sand-clay interface are higher than the residual cohesion value of clay.

Secant friction angles for large deformation shear strength values are given in Figure 3.35. Gravel-clay interfaces showed  $8.1^\circ$ - $10.3^\circ$  increase in secant friction angle when compared to secant friction angle of clay at large deformation. This

increase is between 4.6°-6.1° for sand-clay interfaces. The difference of secant friction angles of gravel-clay and sand-clay interface is 3.5°-4.2°.

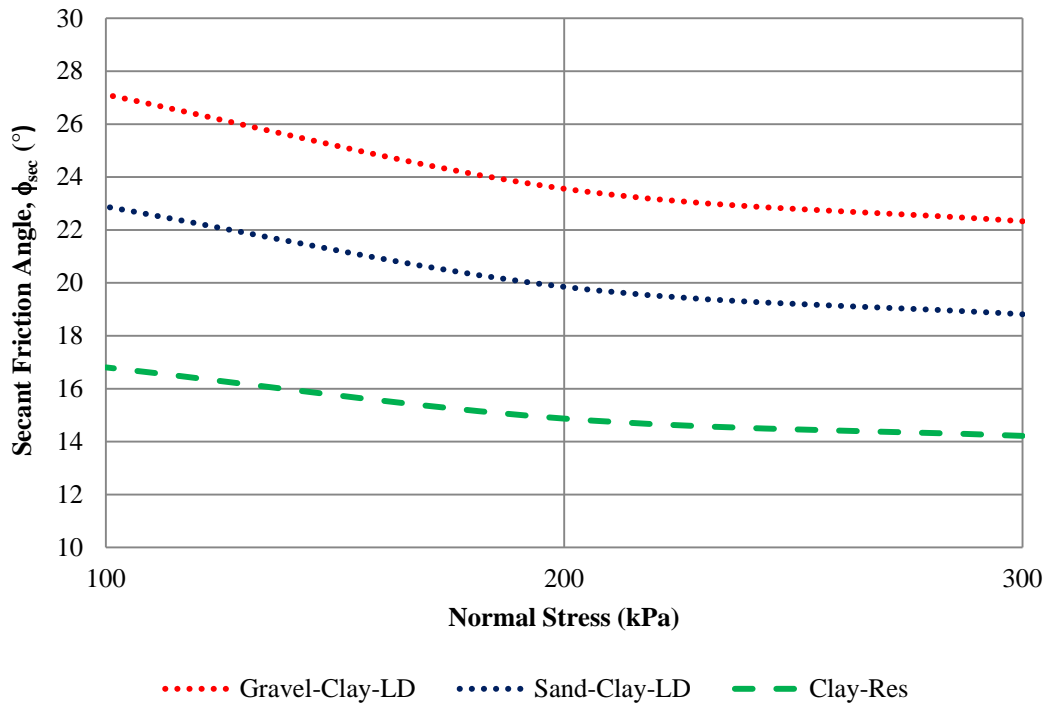


Figure 3.35 Secant Friction Angles Obtained from Large Deformation Shear Strengths of Direct Shear Tests

From direct shear tests, angle of shearing resistance is found to increase consistently at the interface both at peak and large deformation states for the two types of granular materials used.

## CHAPTER 4

### EXPERIMENTAL STUDY II - TRIAXIAL TESTS

#### 4.1 Introduction

Shear strength of interfaces were studied through triaxial tests. Clay-clay, gravel-clay and sand-clay interfaces were tested in triaxial cell and shear strength properties were determined. Apart from the interface tests, for comparison purposes, triaxial tests were also conducted on one material specimens composed of either clay, sand or gravel. A total of 45 triaxial tests were conducted.

For triaxial tests of clay, axial strain rate was chosen as 0.04 mm/min according to ASTM D7181 (2011). Interfaces were tested at the same shearing rate whereas granular material (sand and gravel) tests were conducted at a rate of 0.5 mm/min.

In all triaxial tests, clay specimen prepared as discussed in Sec. 3.2.1 was consolidated to 30 kPa in a large box (25 cm x 25 cm). After consolidation stage, clay specimen was taken from the box with cutters at desired sizes.

Granular material (sand and gravel) used in direct shear tests was used in triaxial tests with the same density as in the direct shear tests. Properties of granular materials are given in Sec. 3.2.2.

#### 4.2 Triaxial Testing Equipment

In triaxial tests, “ELE Digital Tritest 50” triaxial apparatus was used. A general view of the triaxial testing apparatus is given in Figure 4.1.

The triaxial testing apparatus is microprocessor controlled and can give a strain rate ranging between 0.00001 mm/min and 10 mm/min.



Figure 4.1 Triaxial Testing Apparatus

Axial load is measured with a proving ring manufactured from special alloy steel. “ELE International” proving ring having a capacity of 4.5 kN is supplied with a dial gauge having 8 mm range and 0.001 mm resolution. In triaxial tests of gravel “Wykeham Farrance” proving ring having a range of 25 kN is used. The factors used to convert readings to the loads (kg) are 0.3 and 1.337 for the two types of proving rings used.

Axial displacement is measured with a dial gauge having a range of 25 mm and a resolution of 0.005 mm which was manufactured by “ELE International”.

A twin-burette unit was used in order to measure the volume change during triaxial tests. The volume change unit has a capacity of 100 cm<sup>3</sup> and a resolution of 0.2 cm<sup>3</sup>.

“ELE Pressure Test 1700 Oil/Water Constant Pressure System” which can provide variable pressures up to 1700 kPa is used with pressure gauges as pressure system in triaxial tests.

### 4.3 Triaxial Tests of Intact Clay Specimen

Consolidated Drained (CD) triaxial tests were conducted on the clay specimens in order to obtain peak shear strength of clay.

In order to obtain peak shear strength of clay, clay specimen having dimensions of 5x10 cm was used. Specimen was taken from the box where consolidated to 30 kPa with a cutter having a diameter of 5 cm and a height that was slightly greater than the desired specimen size (10 cm). Specimen was trimmed and put into triaxial cell. After saturation and consolidation stages tests were conducted at three different confining effective stresses (50 kPa, 150 kPa and 250 kPa).

In saturation stage, back pressuring of the specimen pore-water was applied following the saturation of drainage system. When the specimen drainage valves were closed, change in the specimen pore pressure as a result of increase in the chamber pressure was measured and pore pressure parameter (B) was calculated. Saturation stage was considered to be completed when pore pressure parameter is equal to or greater than 0.95.

A view of clay specimens after performed tests is given in Figure 4.2. In this figure, shear surfaces developed within clay specimen can be seen clearly.



Figure 4.2 Clay Specimens after Triaxial Tests

Volume change during consolidation phase is shown in Figure 4.3. Time for 90% consolidation ( $t_{90}$ ) was obtained from these graphs as 20 minutes and strain rate is calculated considering  $t_{90}$  value and the recommendations given in ASTM D7181 (2011) as 0.04 mm/min.

Stress-strain graphs of performed triaxial tests are given in Figure 4.4. Change in volume during testing is presented in Figure 4.5 for the all of the tests performed.

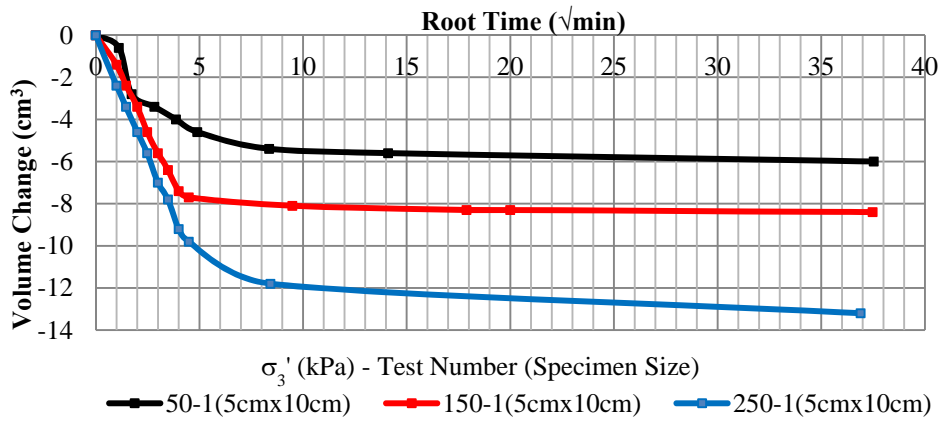


Figure 4.3 Volume Change during Consolidation Stage of Clay

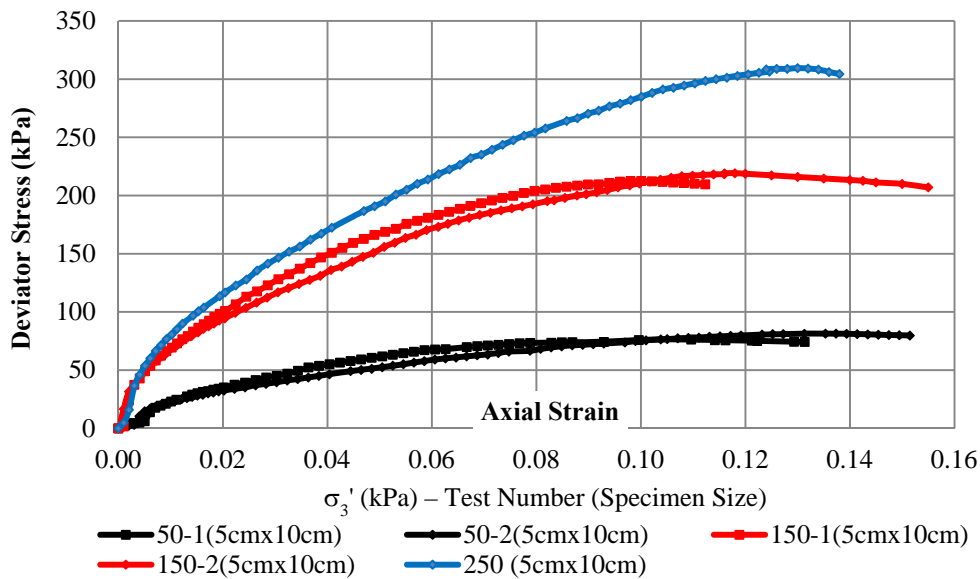


Figure 4.4 Stress-Strain Graphs of Clay in Triaxial Tests

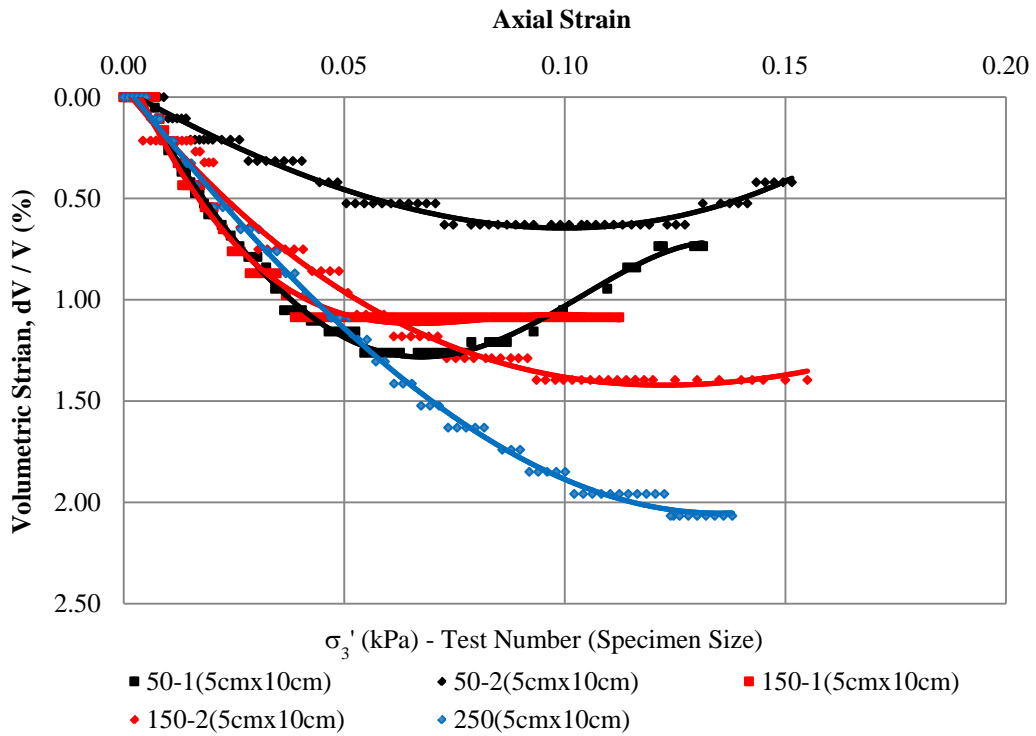


Figure 4.5 Change in Volume during Triaxial Tests of Clay

Using the experimental data, p-q plots (Figure 4.6) and Mohr circles (Figure 4.7) were drawn and peak shear strength parameters were obtained.

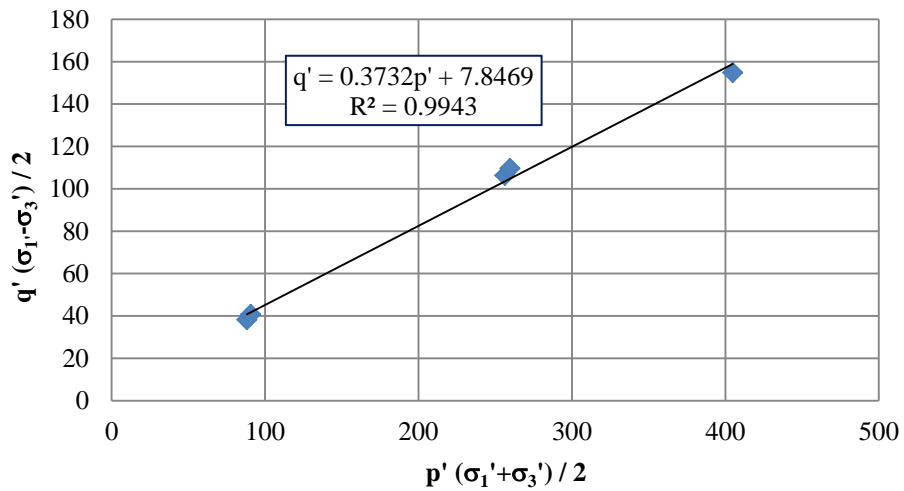


Figure 4.6 p-q Plot of Clay in Triaxial Tests

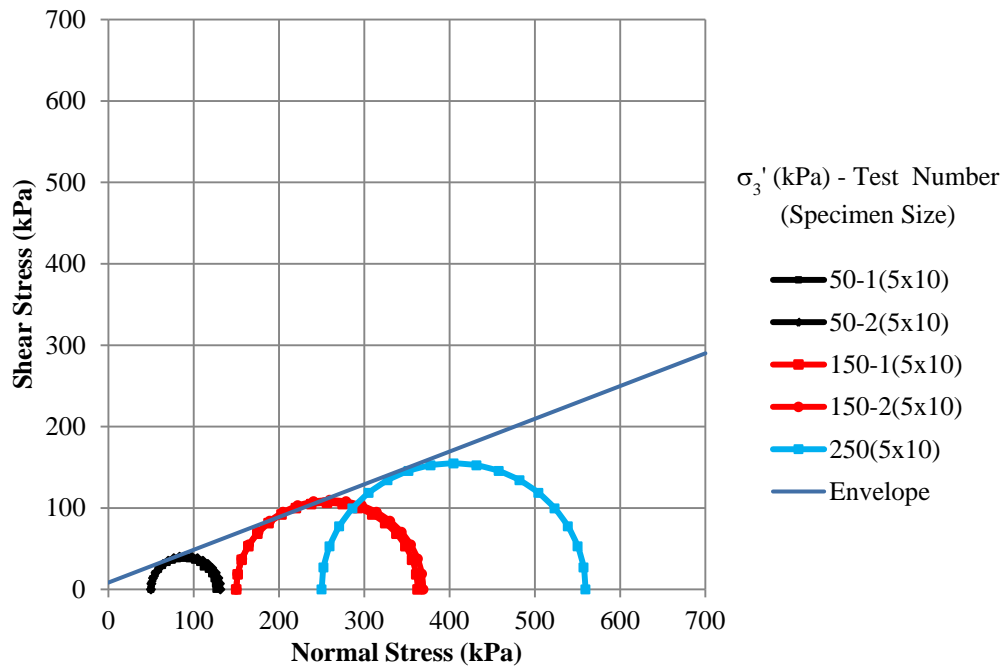


Figure 4.7 Mohr Circles and Peak Shear Strength Envelope of Clay

As a result of triaxial tests, drained peak shear strength parameters of clay were obtained as  $c=8.5 \text{ kPa}$  and  $\phi=21.9^\circ$ .

#### 4.4 Triaxial Tests of Interfaces

Clay-clay, gravel-clay and sand-clay interfaces were tested in triaxial cell in order to determine the shear strength properties.

Specimen preparation procedures for interfaces can be summarized as follows:

- a. Clay specimen was taken from the box where consolidated to 30 kPa with cutters.
- b. From cutters, the specimen was transferred to the “pre-cut mold”. (Figure 4.8)
- c. Clay specimen was cut with an angle of  $56^\circ$  ( $=45+\phi/2$  where  $\phi$ : peak friction angle of clay) from horizontal using fret saw (Figure 4.9). Pre-cut clay (lower part of the interface) is shown in Figure 4.10.

- d. Upper clay was put on lower clay in clay-clay interface tests.
- e. Pre-cut clay(s) was transferred to triaxial mold. (Figure 4.11)
- f. In gravel-clay interface tests, gravel used in large shear box tests was filled on top of clay layer. Granular material was gently compacted on clay layer to obtain the same density value with granular material tested in large shear box tests. (Figure 4.12)
- g. In sand-clay interface tests, sand used in small shear tests was filled on top of clay layer. Sand specimen was compacted on clay layer to obtain the same density value with sand used in small shear tests (Figure 4.13).
- h. After saturation and consolidation stages, triaxial tests were performed at the desired effective confining stresses (Figure 4.14).

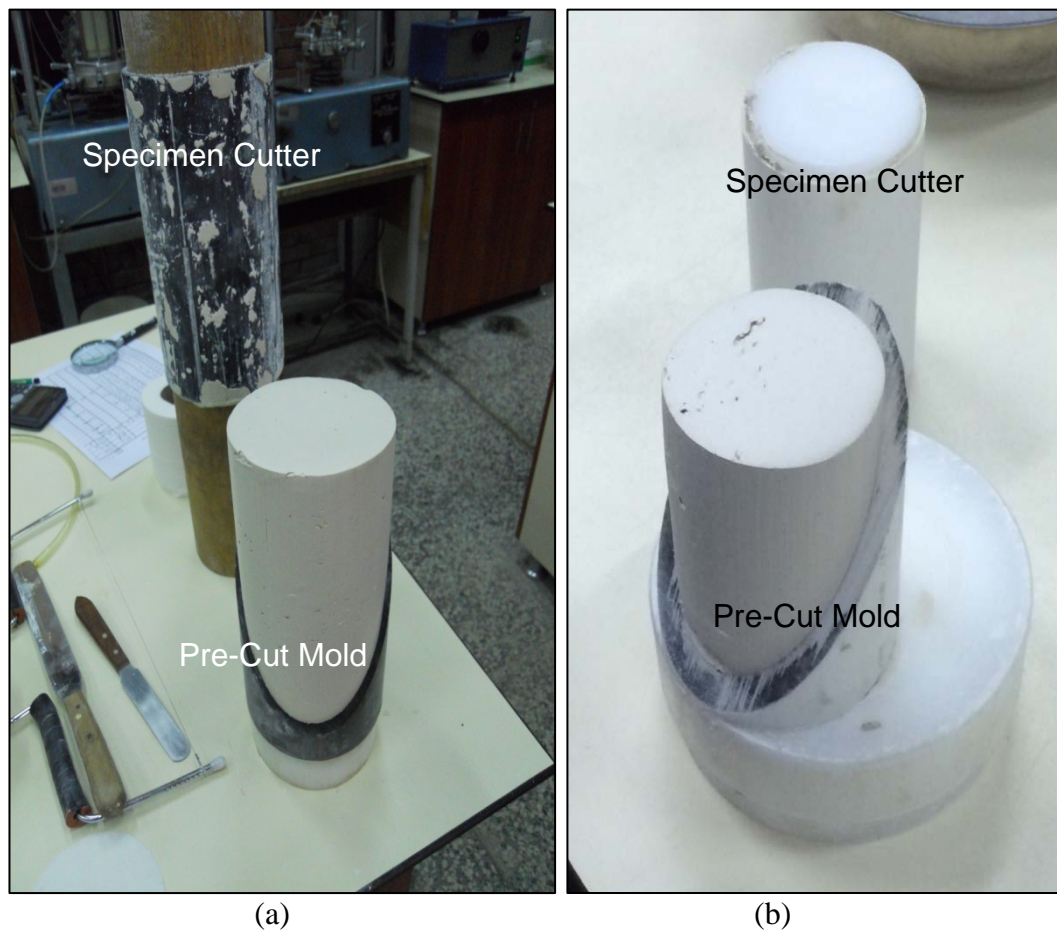


Figure 4.8 Transferring Clay from Specimen Mold to “Pre-Cut Mold”  
(a) 10x20 cm Specimen (b) 5x10 cm Specimen



(a)



(b)

Figure 4.9 Cutting Clay Symmetrically with  $56^\circ$  Angle Using Fret Saw  
(a) 10x20 cm Specimen (b) 5x10 cm Specimen



(a)



(b)

Figure 4.10 Pre-Cut Clay (Lower Part of the Interface)  
(a) 10x20 cm Specimen (b) 5x10 cm Specimen



(a)



(b)

Figure 4.11 Transferring Pre-Cut Clay to Triaxial Mold  
(a) 10x20 cm Specimen (b) 5x10 cm Specimen



Figure 4.12 Filling Upper Part of Gravel-Clay Interface with Gravel



Figure 4.13 Filling Upper Part of Sand-Clay Interface Specimen with Sand



Figure 4.14 Triaxial Testing of Interfaces

During the interface experiments (clay-clay, gravel-clay and sand-clay), it was observed that the upper specimen moved on the lower clay part along the interface. However, it was difficult to observe the starting time of this action during experiments. Since the sliding along the interface could not be measured exactly after each test, this action was not estimated from back calculations based on measurements. Due to sliding of upper specimen moving on lower clay, area correction for interface tests differs from area correction methodology of the standard triaxial tests. There are also some differences between clay-clay, sand-clay and gravel-clay experiments. The corrected area for interface triaxial tests was calculated according to the details given in Appendix E.

Although the effect of membrane correction is very minor, it was also considered in the calculations based on the details given in Appendix E.

After applying area and membrane correction to the experimental data, Mohr circles were drawn for each test. In order to obtain shear strength parameters of the interfaces, the shear stress and the normal stress on the pre-defined surface (pre-cut surface) were determined as shown in Figure 4.15.

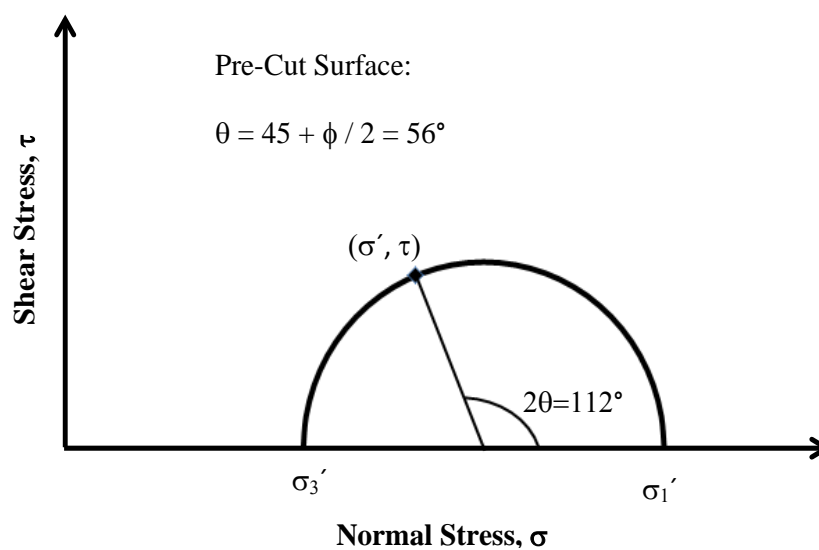


Figure 4.15 Stresses on Pre-Cut Surface

Shear stress and normal stress on pre-cut surface can be determined graphically as shown in figure 4.15 or can be calculated using equations 4.1 and 4.2 below.

$$\sigma' = \frac{\sigma_1' + \sigma_3'}{2} - \frac{\sigma_1' - \sigma_3'}{2} \cos (180 - 2\theta) \quad (4.1)$$

$$\tau = \frac{\sigma_1' - \sigma_3'}{2} \sin (180 - 2\theta) \quad (4.2)$$

For the determined shear stresses and normal stresses on the pre-cut surface, shear strength envelopes can be drawn and shear strength parameters can be calculated.

#### 4.4.1 Triaxial Tests of Clay-Clay Interface

For obtaining the shear strength of clay-clay interface, triaxial tests were performed both with 5x10 cm and 10x20 cm specimens. Clay-clay specimen after triaxial tests is shown in Figure 4.16.



Figure 4.16 Clay-Clay Specimen after Triaxial Tests

Applying area correction and membrane correction methods described in Appendix E, stress-strain graphs of the tests conducted were obtained and shown in Figure 4.17.

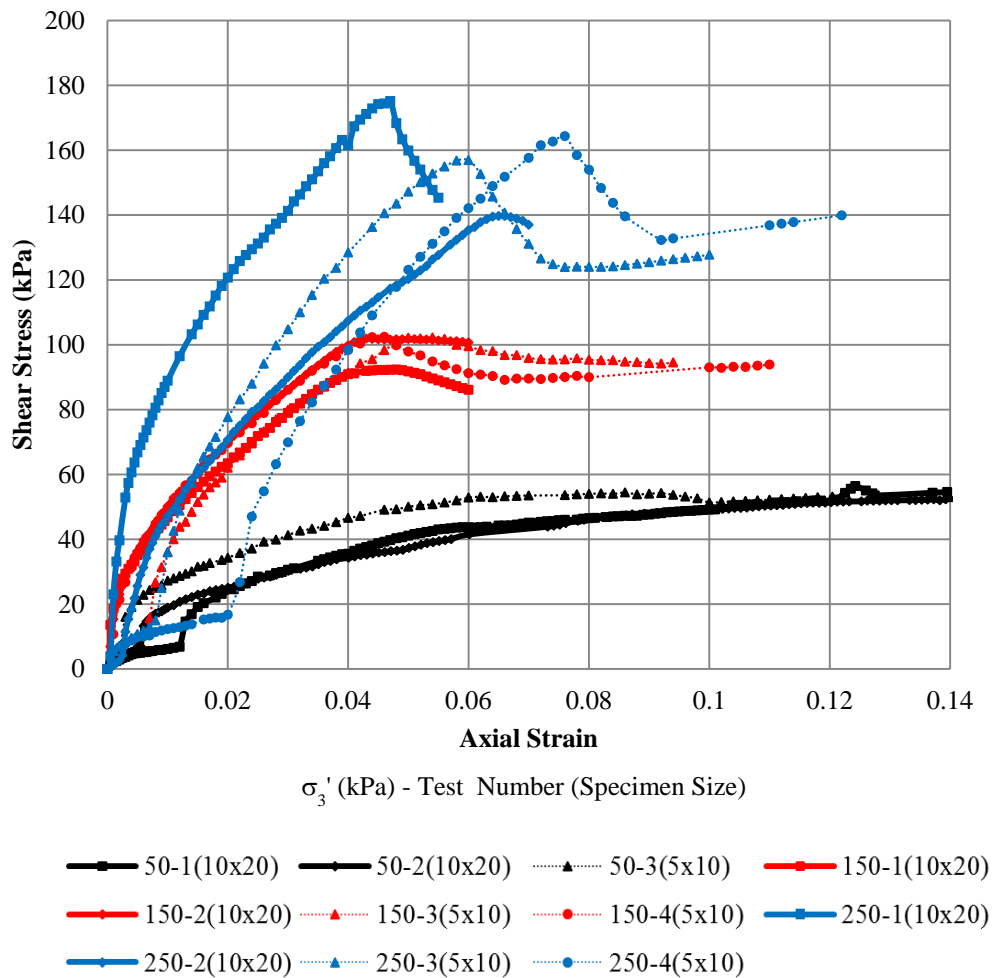


Figure 4.17 Stress-Strain Graphs of Clay-Clay Interfaces in Triaxial Tests

Change in volume during testing of clay-clay interfaces can be seen in Figure 4.18. In Figure 4.18, for high confining stresses (150 kPa and 250 kPa) large scale experiments (10x20 cm specimen) showed small volume change when compared to small scale experiments (5x10 cm specimen). Also in small scale experiments, volume change decreased and became constant whereas this is not the case for large scale experiments.

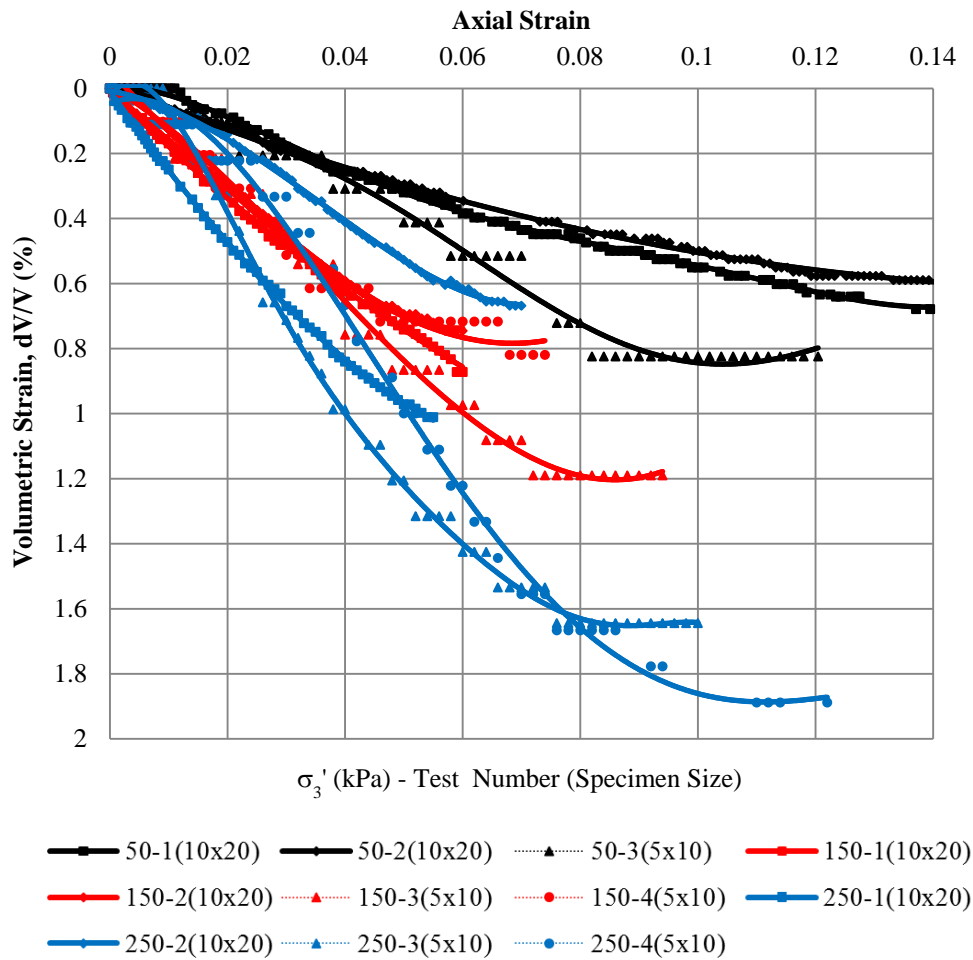


Figure 4.18 Volume Change during Triaxial Tests of Clay-Clay Interfaces

In order to see the scale effect, peak shear strength envelopes were drawn separately for 5x10 cm and 10x20 cm specimen in Figure 4.19 and Figure 4.20, respectively.

Peak shear strength parameters were obtained as  $c=9.8$  kPa and  $\phi=12.0^\circ$  for 5x10 cm specimen, and  $c=9.9$  kPa and  $\phi=11.7^\circ$  for 10x20 cm specimen.

Although there were some differences in volume change behavior of small scale and large scale experiments, peak shear strength values were found to be very close to each other. Therefore peak shear strength of clay-clay interfaces were obtained considering all experiments conducted.

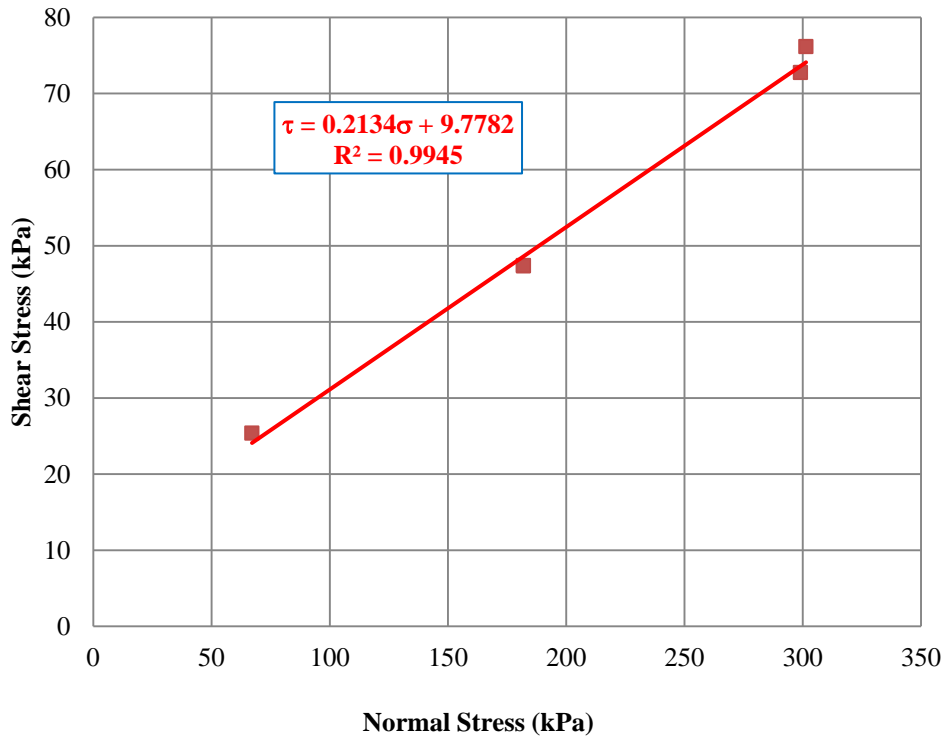


Figure 4.19 Peak Shear Strength Envelope of Clay-Clay Interfaces  
5x10 cm Specimen

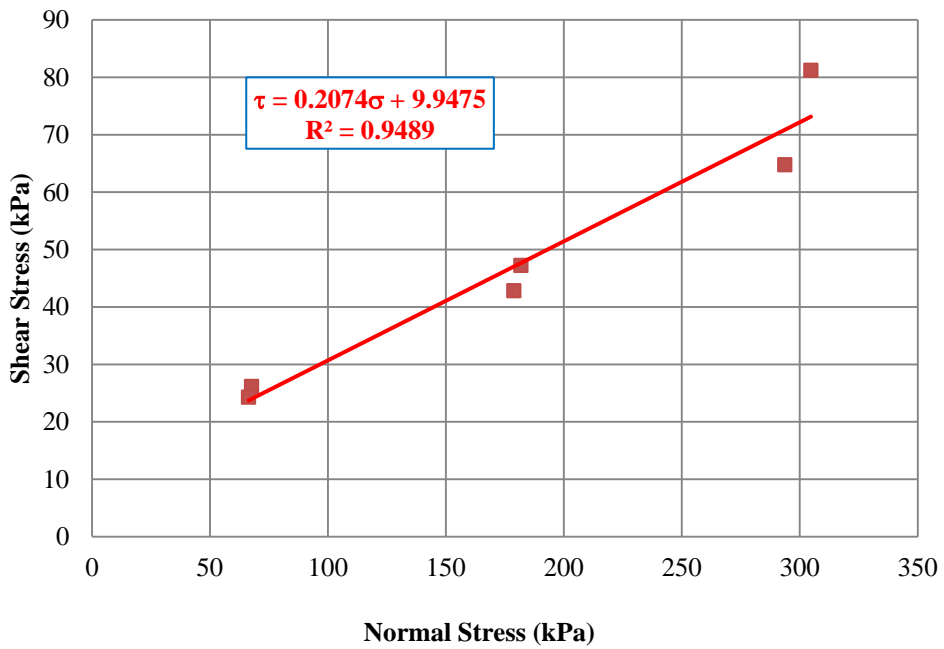


Figure 4.20 Peak Shear Strength Envelope of Clay-Clay Interfaces  
10x20 cm Specimen

Using all of the experimental data, Mohr circles were drawn in Figure 4.21. Using the peak shear strength envelope shown in Figure 4.22, peak shear strength of clay-clay interface was obtained as  $c=9.8 \text{ kPa}$  and  $\phi=11.9^\circ$ .

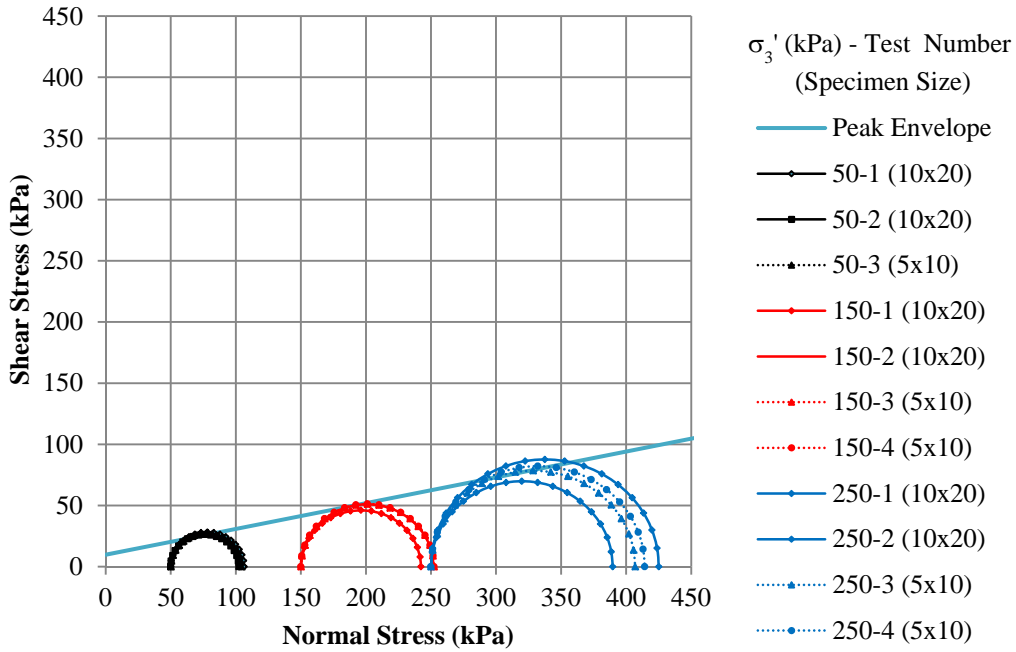


Figure 4.21 Mohr Circles of Clay-Clay Interface Triaxial Tests

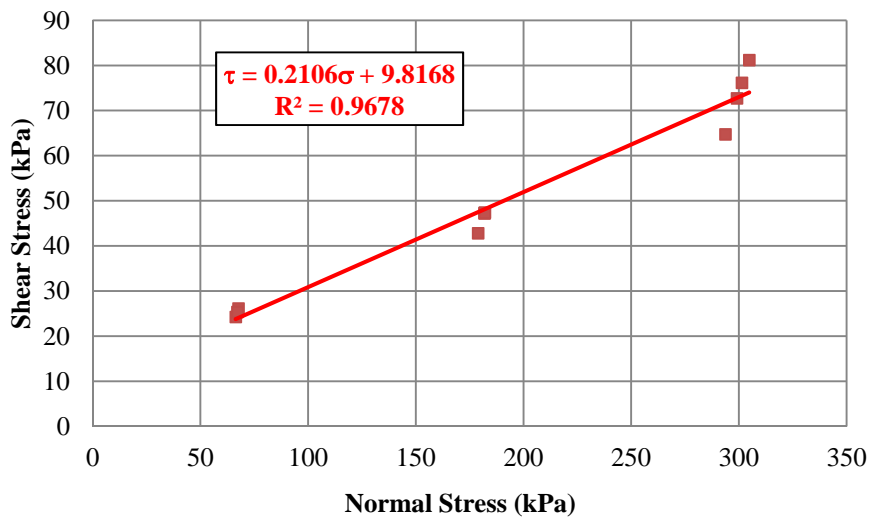


Figure 4.22 Peak Shear Strength Envelope of Clay-Clay Interfaces

In Figure 4.23, shear strength envelopes for large deformation were shown. For 10% and 12% axial strain, the shear strength parameters were obtained as  $c=12.2$  kPa,  $\phi=9.6^\circ$  and  $c=12.7$  kPa,  $\phi=10.1^\circ$ , respectively.

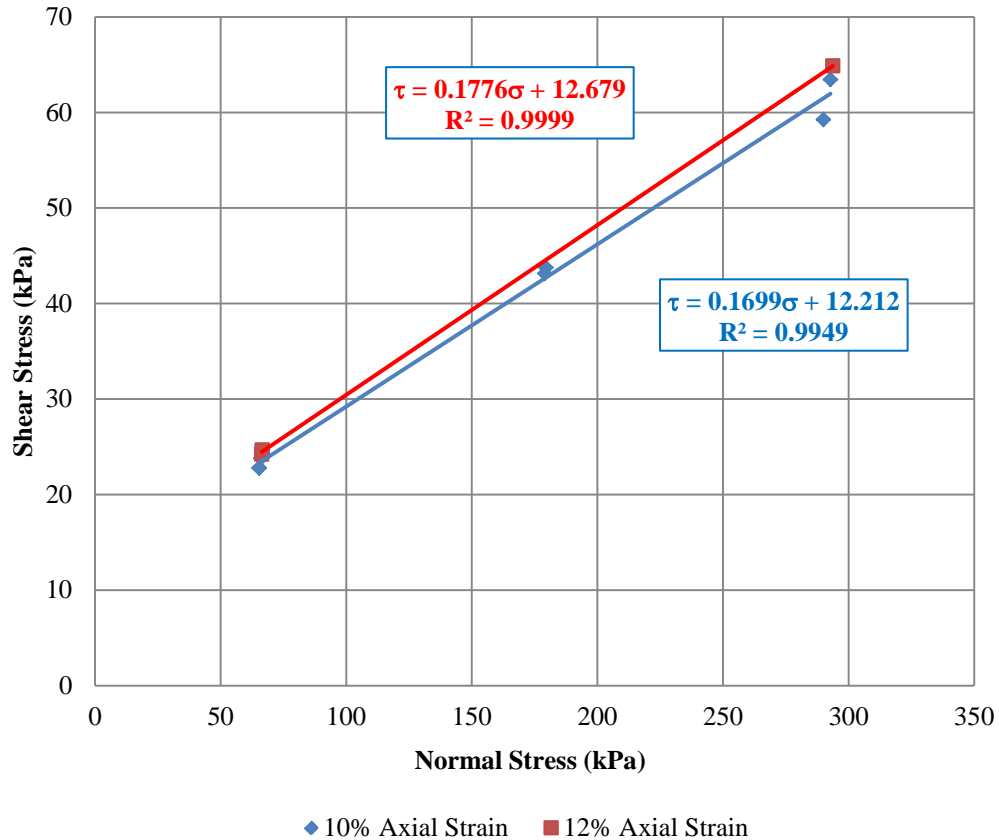


Figure 4.23 Shear Strength Envelope of Clay-Clay Interface for Large Deformation

#### 4.4.2 Granular Material-Clay Interface Triaxial Tests

Shear strength of interfaces was studied on specimens which were formed by filling granular material (a. gravel and b. sand) on clay in triaxial cell.

Consolidated Drained (CD) tests were conducted to obtain shear strength of interfaces. Large deformation shear strength parameters were also studied.

#### 4.4.2.1 Gravel-Clay Interface

Drained triaxial tests of interfaces were performed for three different confining effective stresses (50 kPa, 150 kPa and 250 kPa) and the tests were repeated at least two times. All tests were performed with 10x20 cm specimens with an axial strain rate of 0.04 mm/min.

Interface specimens during and after triaxial tests are shown in Figure 4.24 and shear surface after experiments are presented in Figure 4.25. No shear cracks were observed in lower clay portion of the gravel-clay specimen after experiments.



Figure 4.24 Gravel-Clay Interface Triaxial Tests during and after Experiments



Figure 4.25 Gravel-Clay Interface Triaxial Tests-Shear Surface after Experiments

Stress-strain behavior of gravel-clay interfaces are given in Figure 4.26. Volume change during experiments can be seen in Figure 4.27.

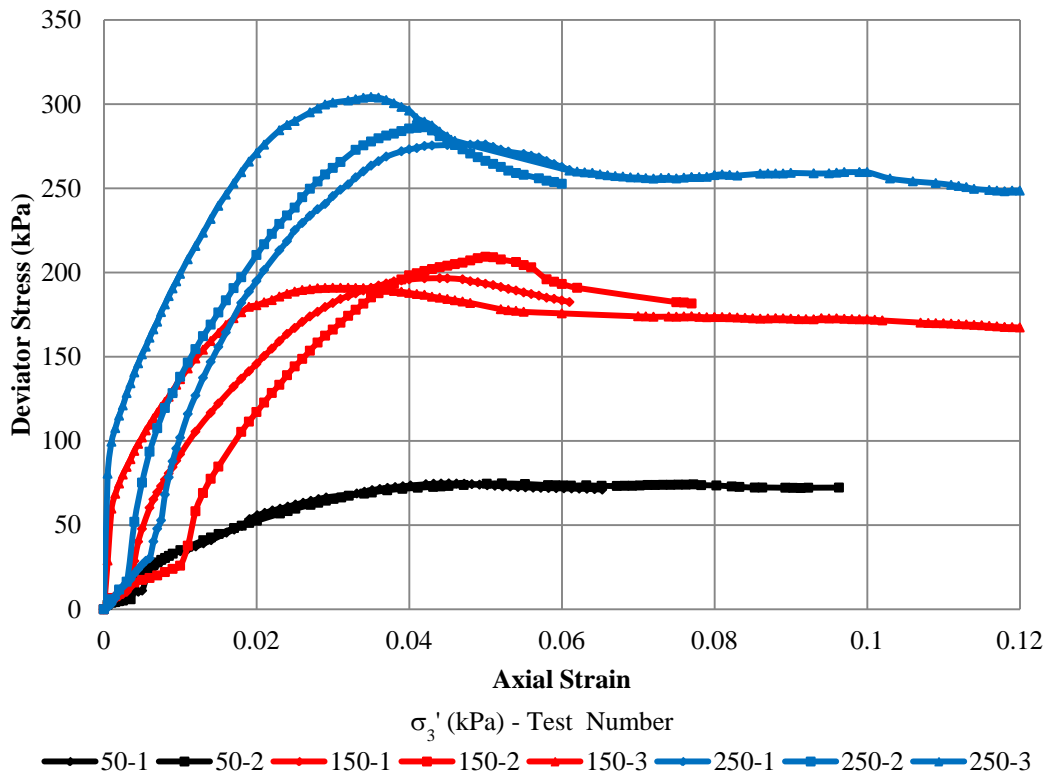


Figure 4.26 Stress-Strain Graphs of Gravel-Clay Interface in Triaxial Tests

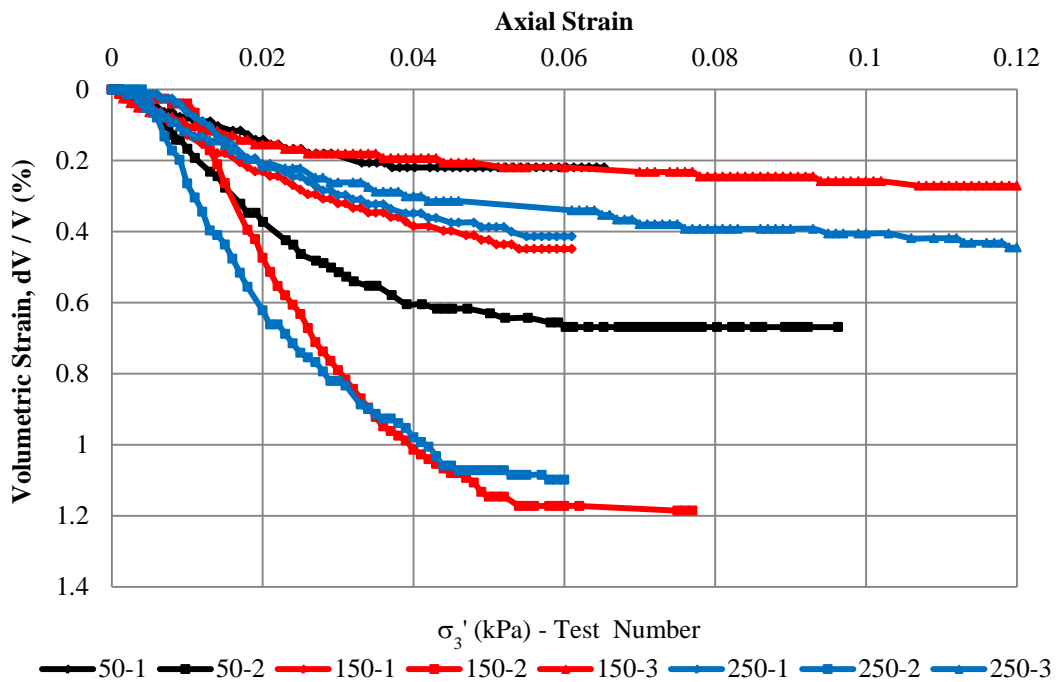


Figure 4.27 Volume Change during Triaxial Tests of Gravel-Clay Interface

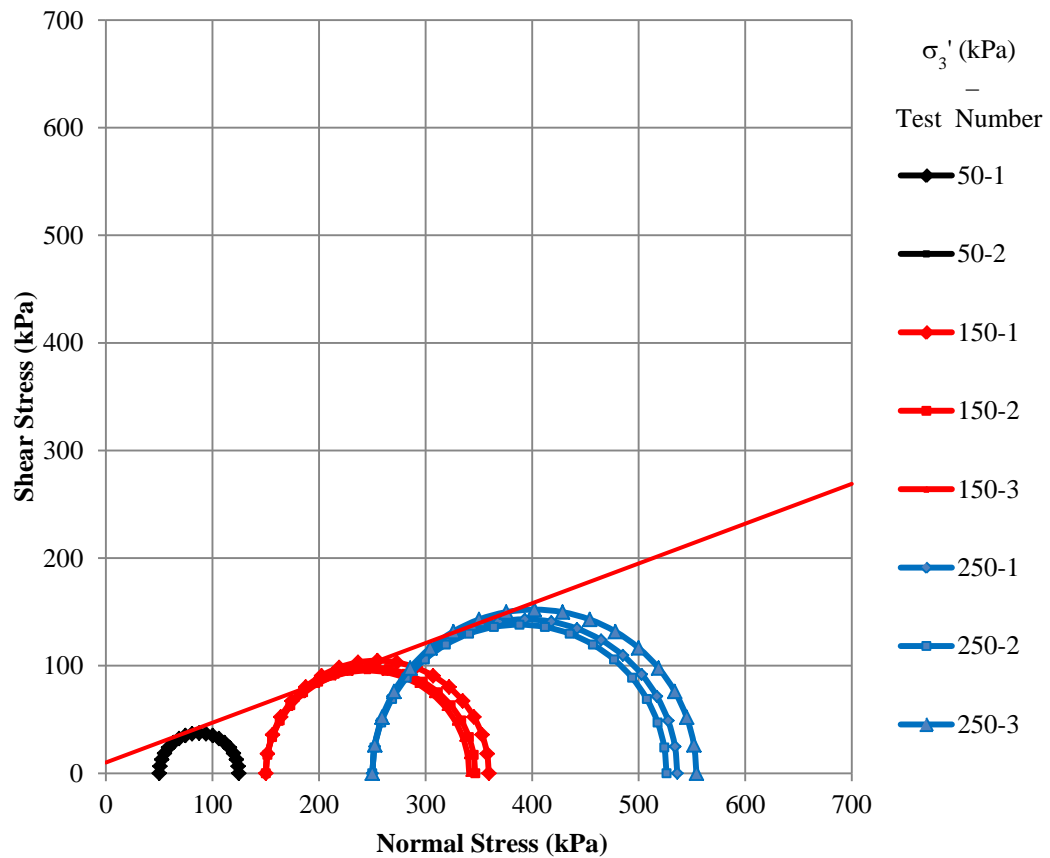


Figure 4.28 Mohr Circles- of Gravel-Clay Interface

Using the experimental data, Mohr circles were obtained and drawn in Figure 4.28. Stresses (normal stress and shear stress) on pre-cut surface ( $56^\circ$  from horizontal) were calculated as previously discussed and peak shear strength envelope was drawn as shown in Figure 4.29.

Peak shear strength parameters of gravel-clay interface was found to be as  $c=10.0 \text{ kPa}$  and  $\phi =20.3^\circ$ .

The large deformation shear strength parameters are presented in Figure 4.30. Shear strength found for 10% and 12% axial strain are very close to each other.

The shear strength parameters were obtained as  $c=9.8 \text{ kPa}$  and  $\phi=18.6^\circ$  for large deformation.

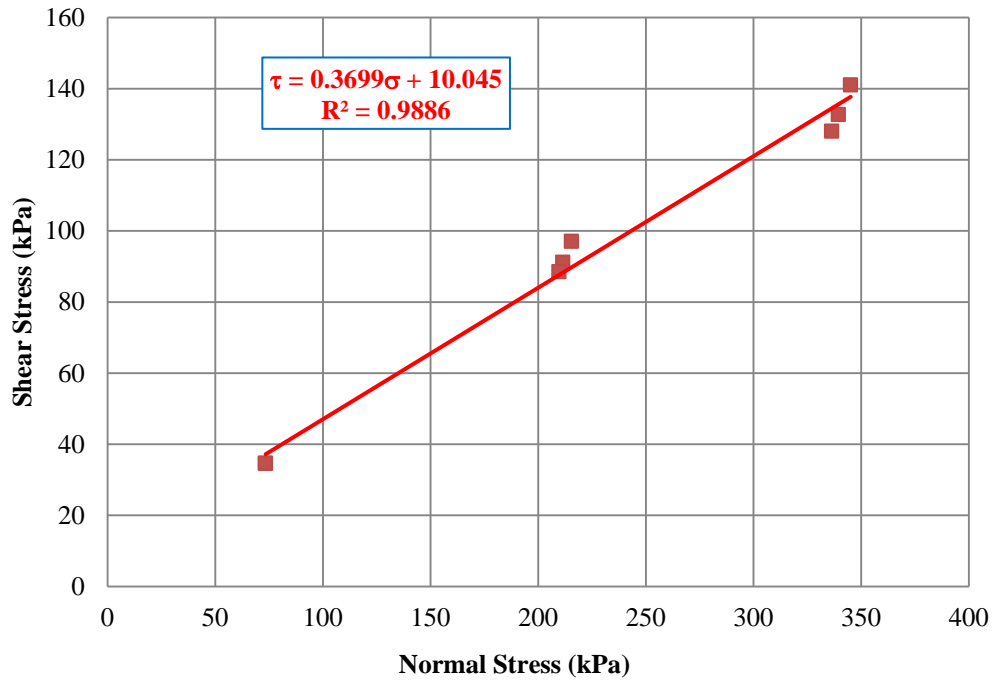


Figure 4.29 Peak Shear Strength Envelope of Gravel-Clay Interface

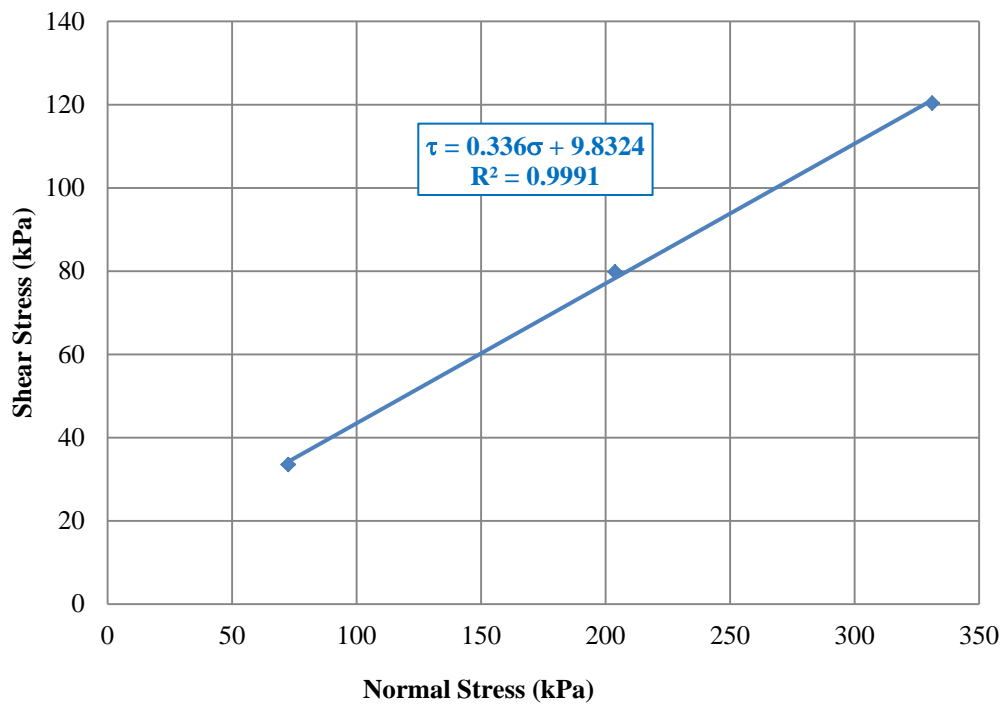


Figure 4.30 Shear Strength Envelope of Gravel-Clay Interface at Large Deformation

#### 4.4.2.2 Sand-Clay Interface

Drained triaxial tests of sand-clay interfaces were performed for three different confining effective stresses (50 kPa, 150 kPa and 250 kPa) and the tests were repeated at least two times.

Tests were conducted using both small (5x10 cm) and large (10x20 cm) specimens. Interfaces were tested with an axial strain rate of 0.04 mm/min.

Sand-clay interfaces after triaxial tests can be seen in Figure 4.31.



Figure 4.31 Sand-Clay Interfaces after Triaxial Tests

Stress-strain plots of sand-clay interface are given in Figure 4.32. Volume change during experiments is shown in Figure 4.33 and 4.34 for small scale and large scale specimen, respectively.

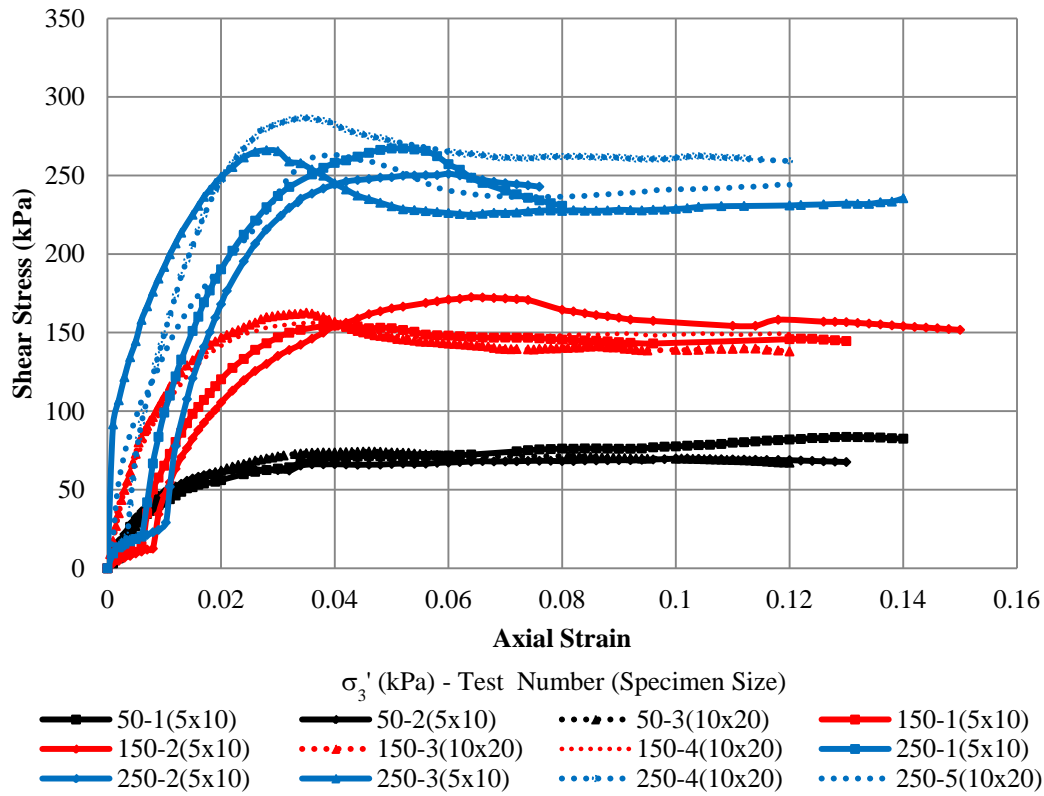


Figure 4.32 Stress-Strain Graphs of Sand-Clay Interface in Triaxial Tests

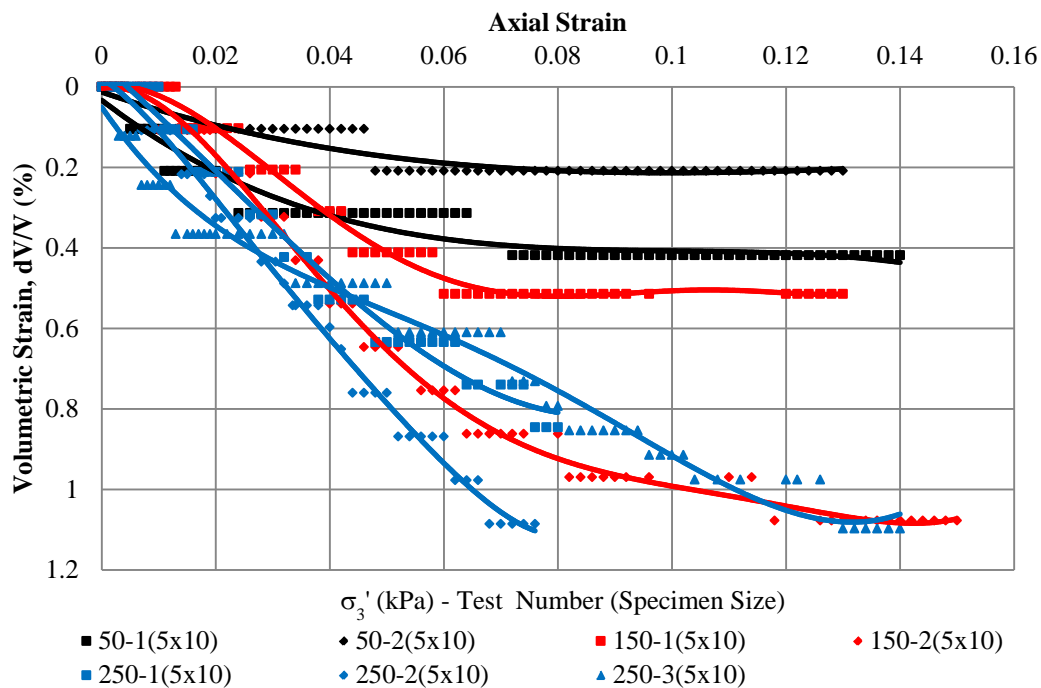


Figure 4.33 Volume Change in Sand-Clay Interface Tests (5x10 cm Specimen)

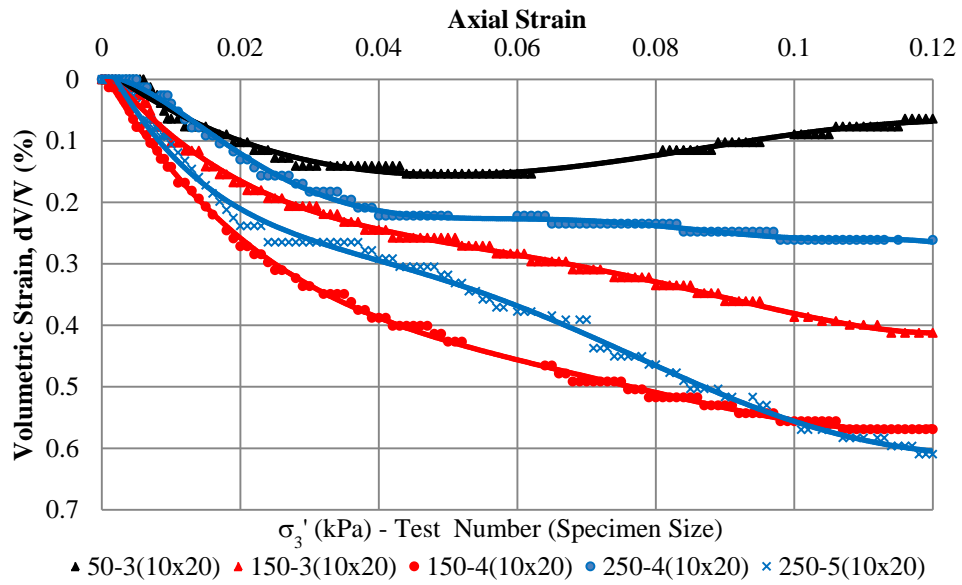


Figure 4.34 Volume Change in Sand-Clay Interface Tests (10x20 cm Specimen)

Using the experimental data, Mohr circles were obtained and drawn in Figure 4.35. Stresses on the pre-cut surface ( $56^\circ$  from horizontal) were calculated and peak shear strength envelope was drawn as shown in Figure 4.36.

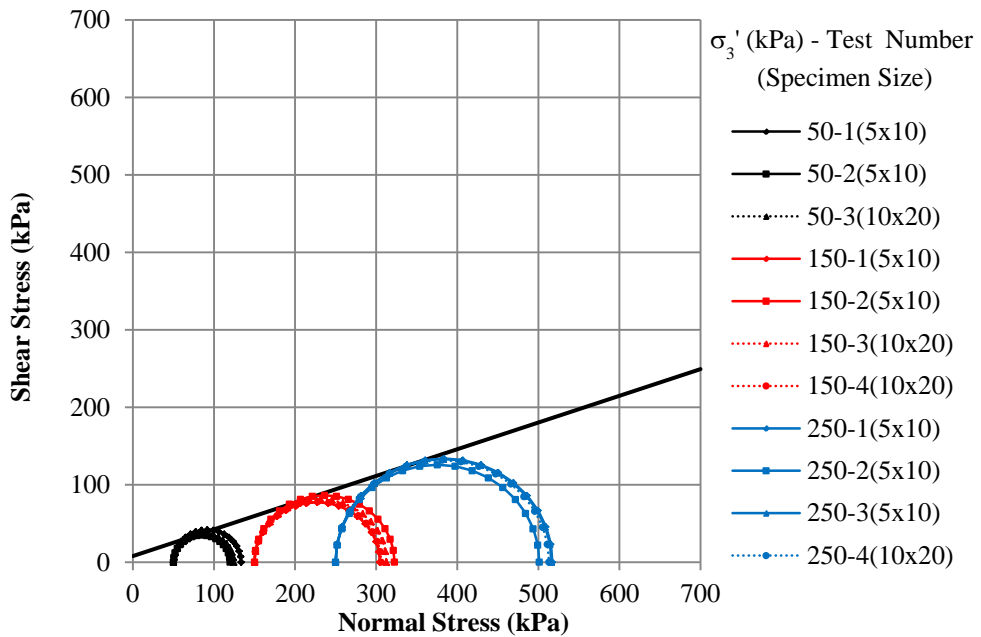


Figure 4.35 Mohr Circles of Sand-Clay Interface

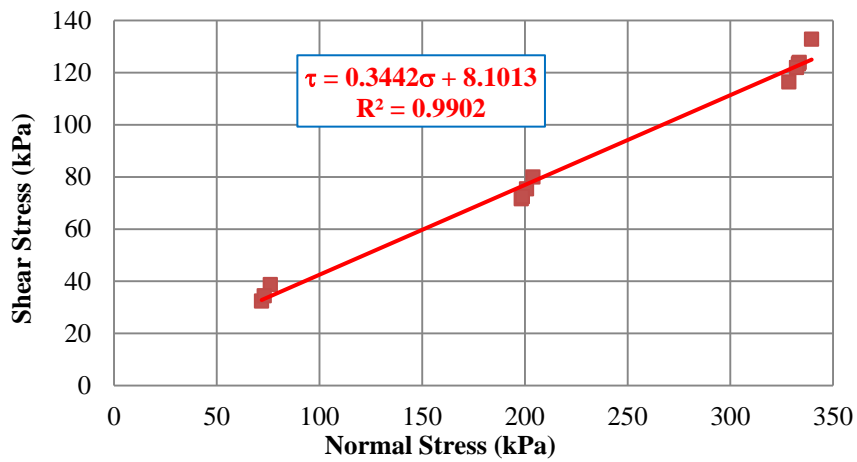


Figure 4.36 Peak Shear Strength Envelope of Sand-Clay Interface

Peak shear strength parameters of sand-clay interface was found to be as  $c=8.1 \text{ kPa}$   $\phi =19.0^\circ$ .

The large deformation shear strength parameters are presented in Figure 4.37 for 10% and 12% axial strain. Both from stress-strain graphs presented in Figure 4.32 and strength envelope given in Figure 4.37, it is obvious that shear strength found for 10% and 12% axial strain are very close to each other. The shear strength parameters were obtained as  $c=8.9 \text{ kPa}$  and  $\phi =17.5^\circ$  for large deformation.

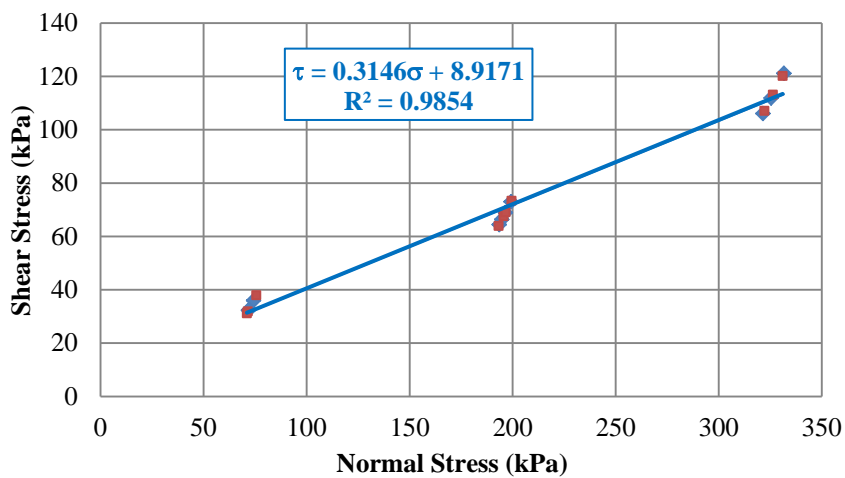


Figure 4.37 Large Deformation Shear Strength Envelope of Sand-Clay Interface

#### 4.5 Triaxial Tests of Granular Material

Drained triaxial tests of granular material were performed for sand and gravel specimens used in triaxial tests.

Gravel specimen was tested for three different confining effective stresses (50 kPa, 150 kPa and 250 kPa). Sand specimens were tested for two different confining effective stresses (100 kPa and 200 kPa) and the tests were repeated two additional times.

Stress-strain behavior of gravel is given in Figure 4.38 and the strength envelope is given in Figure 4.39. Peak shear strength parameters of gravel was found as  $c=0$  kPa and  $\phi=43.9^\circ$ .

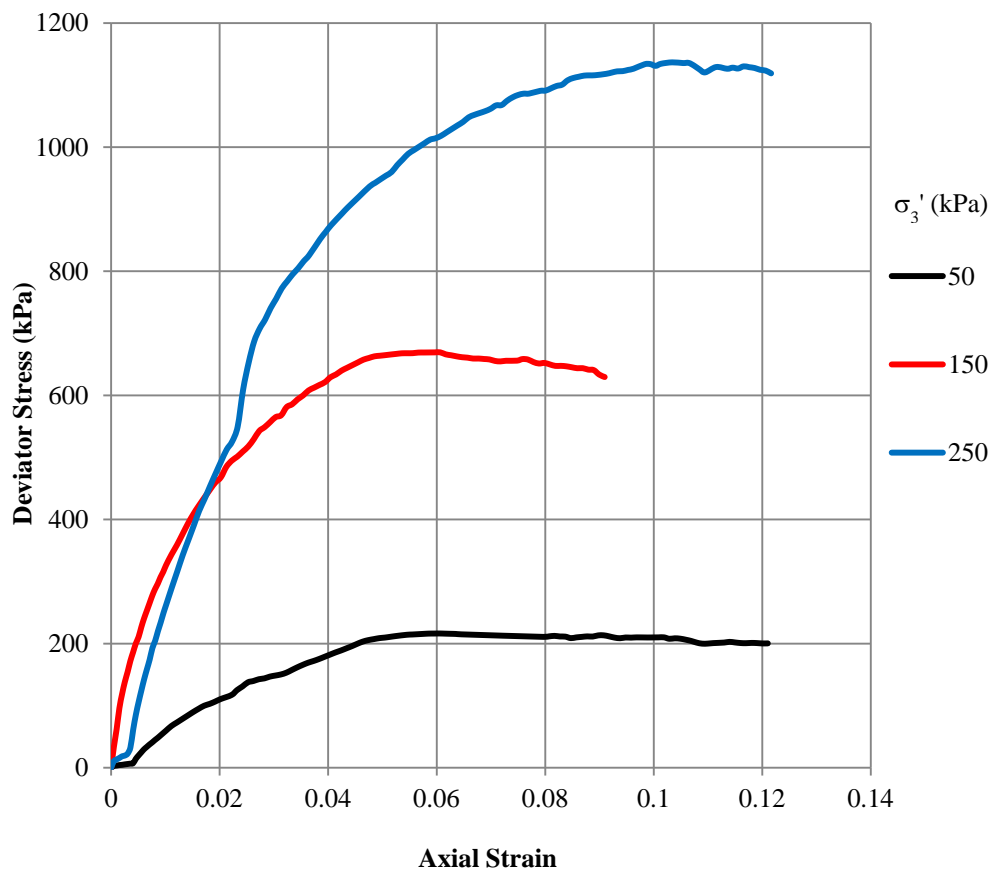


Figure 4.38 Stress-Strain Graphs of Gravel Specimen

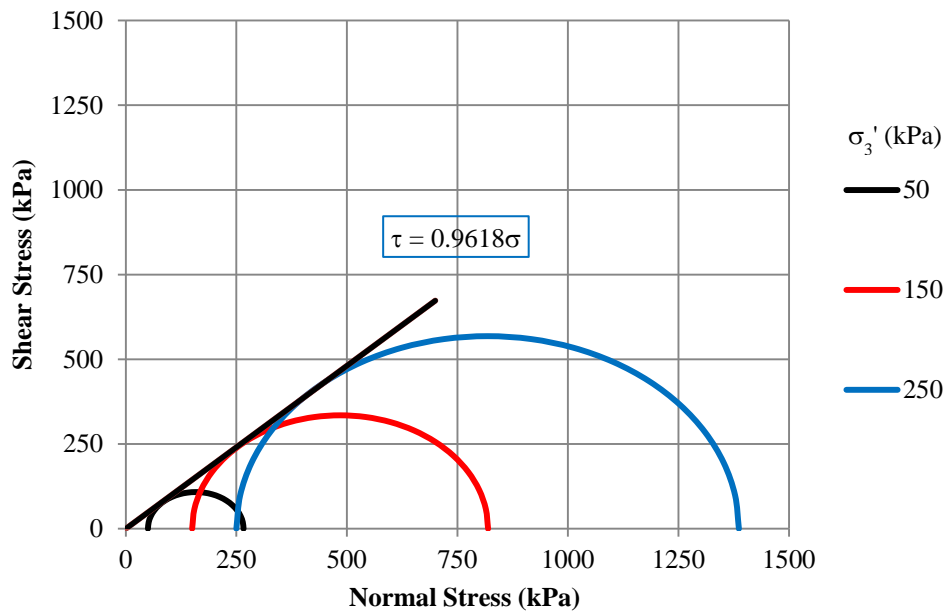


Figure 4.39 Peak Shear Strength of Gravel

Stress-strain behavior of sand is revealed in Figure 4.40 and the strength envelope is presented in Figure 4.41. Peak shear strength parameters of sand was found as  $c=0$  kPa and  $\phi=43.0^\circ$ .

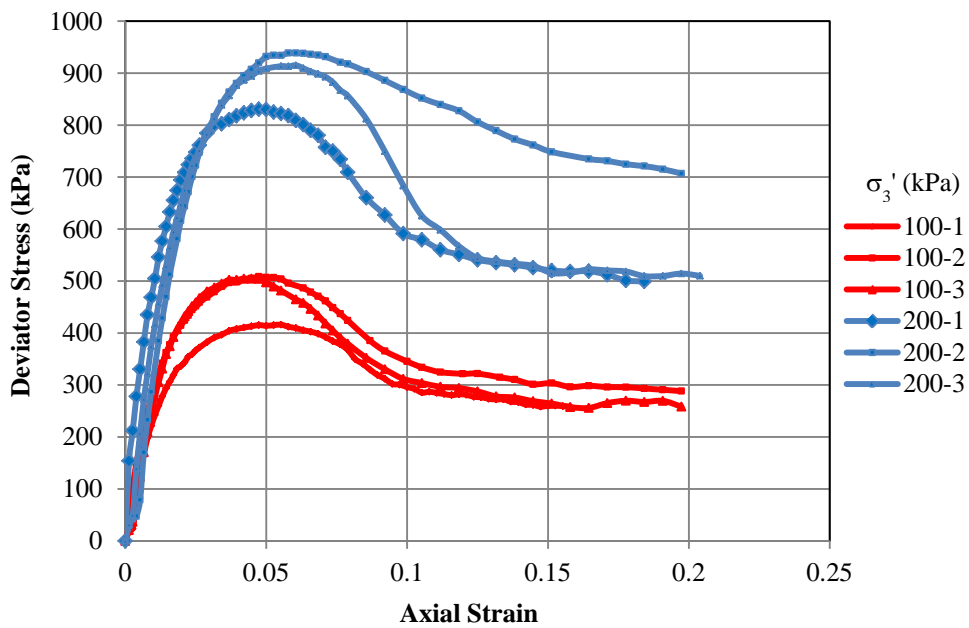


Figure 4.40 Stress-Strain Graphs of Sand

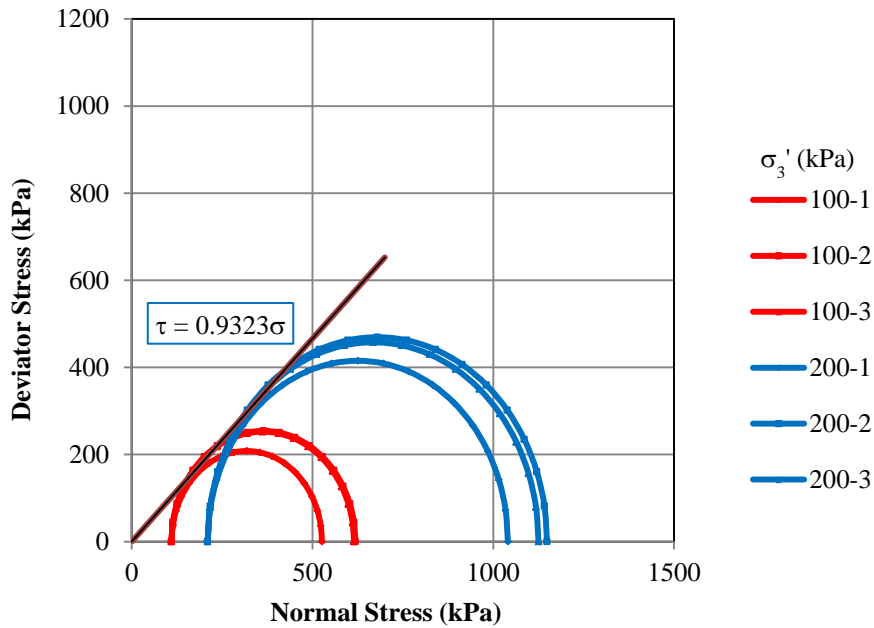


Figure 4.41 Peak Shear Strength of Sand

#### 4.6 Discussion of Results

Triaxial tests were conducted for clay-clay, gravel-clay and sand-clay interfaces. The results of all experiments are given in Appendix B. Summary of triaxial test results are shown in Table 4.1. Results are also presented in Figure 4.42.

Table 4.1 Summary of Triaxial Shear Tests-Shear Strength Parameters

Material	Test Type	Strength Type	c (kPa)	$\phi$ (°)
Sand	Triaxial	Peak	0	43.0
Gravel	Triaxial	Peak	0	43.9
Clay	Triaxial	Peak	8.5	21.9
Clay-Clay	Triaxial	Peak	9.8	11.9
		LD*	12.7	10.1
Sand-Clay	Triaxial	Peak	8.1	19.0
		LD*	8.9	17.5
Gravel-Clay	Triaxial	Peak	10.0	20.3
		LD*	9.8	18.6

\*LD: Large Deformation

When gravel-clay and sand-clay interface results were compared, shear strength of gravel-clay interface was found to be higher as expected. Friction angle of gravel-clay interface is  $1.3^\circ$  higher than the friction angle of sand-clay interface.

Large deformation shear strength parameters were obtained for clay-clay, sand-clay and gravel-clay interfaces. At large deformation, friction angle of gravel-clay interface was found to be  $8.5^\circ$  higher than the friction angle of clay-clay interface in triaxial tests. The increase in friction angle is  $7.4^\circ$  for sand-clay interface at large deformation when compared to clay-clay interface.

Cohesion values of interfaces are generally between 8-10 kPa.

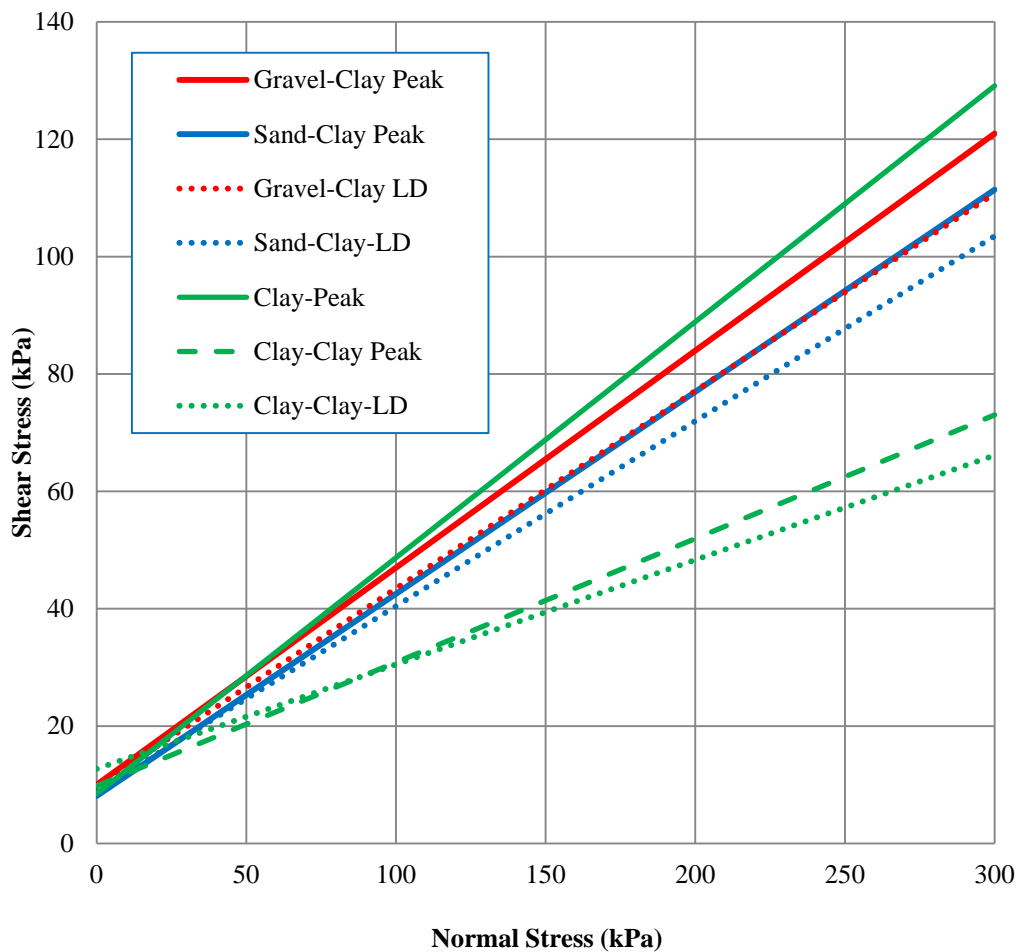


Figure 4.42 Summary of Triaxial Tests

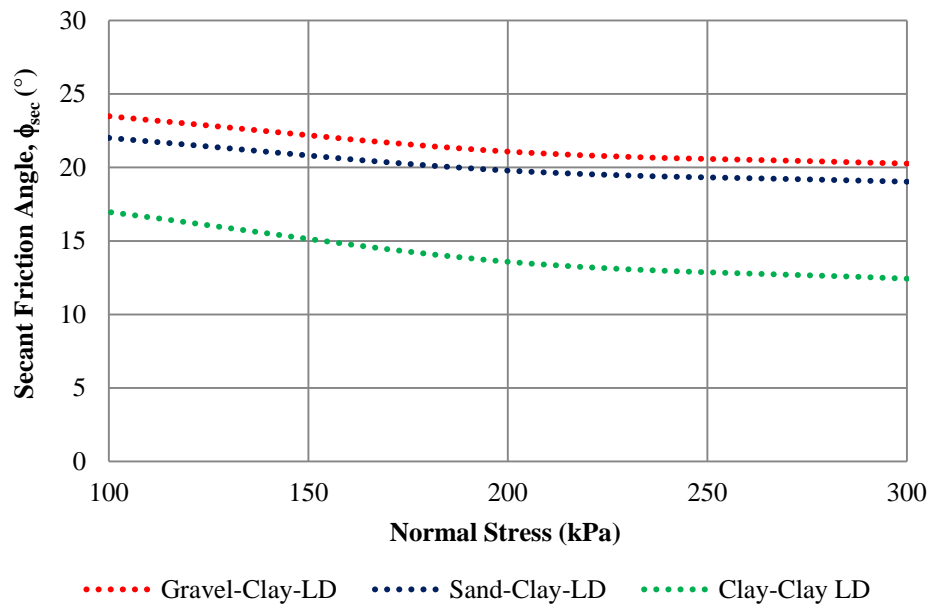


Figure 4.43 Secant Friction Angles at Large Deformation in Triaxial Tests

Secant friction angles for large deformation shear strength values are given in Figure 4.43. Gravel-clay interfaces showed 6.5°-7.8° increase in secant friction angle when compared to secant friction angle of clay at large deformation. This increase is between 5.0°-6.6° for sand-clay interfaces. The difference of secant friction angles of gravel-clay and sand-clay interface is 1.2°-1.5°.

Like in direct shear tests, triaxial tests indicate higher friction angles for interfaces for large deformations. Friction angles of gravel, sand and clay obtained in triaxial tests are close to the friction angles obtained in direct shear tests as indicated by Castellanos and Brandon (2013) who concluded shear strength to be identical in triaxial and direct shear tests for remolded samples.



## CHAPTER 5

### EXPERIMENTAL STUDY III - IMPROVEMENT WITH DOWELS

#### 5.1 Introduction

There are many geotechnical engineering cases where relatively stronger fill materials (rock fill or granular fill) are placed on clay soils as counter-measure for slope movements, to provide passive resistance for walls or uncontrolled fills deposited near mining areas. Slope stability analyses are required in such cases, and shear strength parameters at fill/clay base contact is needed. Straightforward way may be to use clay properties conservatively resulting in flatter slopes. Study of interface shear strength parameters was the main theme in this thesis.

In engineering practice long passive piles are frequently used in order to eliminate instability problems. Alternatively, using short dowels for improvement purposes can give sufficient support. In order to see the effect of short dowels on stability at the fill-clay contact, shear tests with short model dowels were planned and performed in large shear box.

#### 5.2 Shear Tests of Interfaces Improved with Model Dowels

In order to study improvement on interfaces, large shear box tests with model dowels were conducted. Properties of the model dowels are given in Table 5.1.

Table 5.1 Model Dowels Used in Improvement Tests

Material	Elastic Modulus (E)	Diameter (d)	Length (L)
Brass (solid)	100 GPa	2 cm	4 cm (2d)
			8 cm (4d)
			12 cm (8d)
		1 cm	6 cm (6d)
			12 cm (12d)

In shear tests with model dowels, dowel holes were drilled and dowels were placed in such a way that half of the dowel was in upper clay layer and the remaining half of the dowel was in the underlying granular material.

The procedure can be summarized as follows:

- a) Granular material was filled in the lower part of large shear box. (Figure 5.1)
- b) Clay was filled up to a level from where dowels will be inserted. (Figure 5.2)
- c) Dowel holes were drilled using a hand auger. (Figure 5.3)
- d) Dowels were placed from drilled holes resulting in half of dowel to be in upper clay layer and the remaining half of the dowel to be in the underlying granular material. (Figure 5.4)
- e) After consolidation stage, shear tests were performed. (Figure 5.5)



Figure 5.1 Gravel in the Lower Part of the Large Shear Box



Figure 5.2 Filling Clay up to Dowel Installation Level



Figure 5.3 Drilling Model Dowel Holes



Figure 5.4 Dowels Placed to the Drilled Holes



Figure 5.5 Shear Tests with Dowels

All tests were conducted for at least two normal stresses (111, 222 and in some tests 333 kPa) and repeated at least two times. Same shear rate (0.5 mm/min) with the earlier tests was used, and the same consolidation procedure was applied.

Table 5.2 summarizes the improvement tests conducted. In improvement tests, two types of model dowels with different diameters and lengths were used.

Table 5.2 Improvement Test Sets Conducted

Test Set	Dowel Diameter (d)	Dowel Length (L)	# of Dowels (n)	Spacing of Dowels (s)
I-1	2 cm	8 cm (4d)	1	-
I-2		8 cm (4d)	3x1=3	8 cm (4d)
I-3		8 cm (4d)	3x3=9	8 cm (4d)
I-4		4 cm (2d)	3x3=9	8 cm (4d)
I-5		12 cm (6d)	3x3=9	8 cm (4d)
I-6	1 cm	6 cm (6d)	6x6=36	4 cm (4d)
I-7		12 cm (12d)	6x6=36	4 cm (4d)

The views of dowels after the improvement tests summarized in Table 5.2 are shown between Figure 5.6 and Figure 5.12.



Figure 5.6 Improvement Tests with 1 Model Dowel-Dowel Length=8cm (I-1)



Figure 5.7 Improvement Tests with 3 Model Dowels-Dowel Length=8cm (I-2)



Figure 5.8 Improvement Tests with 9 Model Dowels-Dowel Length=8cm (I-3)



Figure 5.9 Improvement Tests with 9 Model Dowels-Dowel Length=4cm (I-4)



Figure 5.10 Improvement Tests with 9 Model Dowels-Dowel Length=12cm (I-5)



Figure 5.11 Improvement Tests with 36 Model Dowels-Dowel Length=6cm (I-6)



Figure 5.12 Improvement Tests with 36 Model Dowels-Dowel Length=12cm (I-7)

### 5.3 Results and Discussion

A total of 36 improvement tests were conducted with dowels and the experiments were summarized in Appendix C. Results of improvement tests with dowels are given in Table 5.3.

Table 5.3 Results of Improvement Tests

Test Set	Experiment No	# of Dowels (n)	Dowel Length (L)	Dowel Diameter (d)	Normal Stress, $\sigma_n'$ (kPa)	Shear Stress, $\tau$ (kPa)
I-1	1	1	4d	2 cm	117.48	75.52
	2	1	4d	2 cm	117.34	83.02
	3	1	4d	2 cm	234.49	131.12
	4	1	4d	2 cm	231.62	118.50
	5	1	4d	2 cm	349.71	164.06
I-2	6	3	4d	2 cm	121.97	86.76
	7	3	4d	2 cm	119.26	85.74
	8	3	4d	2 cm	234.58	136.52
	9	3	4d	2 cm	236.06	138.28
	10	3	4d	2 cm	352.04	209.79
	11	3	4d	2 cm	350.26	191.41
I-3	12	9	4d	2 cm	120.89	109.44
	13	9	4d	2 cm	123.71	101.64
	14	9	4d	2 cm	238.14	153.54
	15	9	4d	2 cm	235.73	169.47
	16	9	4d	2 cm	235.63	149.23
	17	9	4d	2 cm	350.32	207.88
I4	18	9	2d	2 cm	116.46	79.74
	19	9	2d	2 cm	117.71	81.04
	20	9	2d	2 cm	233.71	133.79
	21	9	2d	2 cm	234.70	121.86
I5	22	9	6d	2 cm	135.80	106.41
	23	9	6d	2cm	133.47	108.14
	24	9	6d	2 cm	272.97	199.36
	25	9	6d	2 cm	276.74	194.22
I6	26	36	6d	1 cm	117.70	89.54
	27	36	6d	1 cm	121.18	78.82
	28	36	6d	1 cm	235.35	145.92
	29	36	6d	1 cm	235.03	120.69
	30	36	6d	1 cm	235.92	136.85
I7	31	36	12d	1 cm	131.49	131.04
	32	36	12d	1 cm	135.09	143.37
	33	36	12d	1 cm	260.78	268.82
	34	36	12d	1 cm	264.82	259.39
	35	36	12d	1 cm	267.75	256.65

In order to see the effect of number of dowels resisting shear movement (i.e. effect of dowel spacing), the shear tests performed with 1, 3 and 9 dowels having same length and diameter ( $d=2$  cm,  $L=8$  cm), i.e. improvement tests I-1, I-2 and I-3, were compared. Tests were conducted at least two times and repeated for three normal stresses (111, 222 and 333 kPa). The results were given in Figure 5.13.

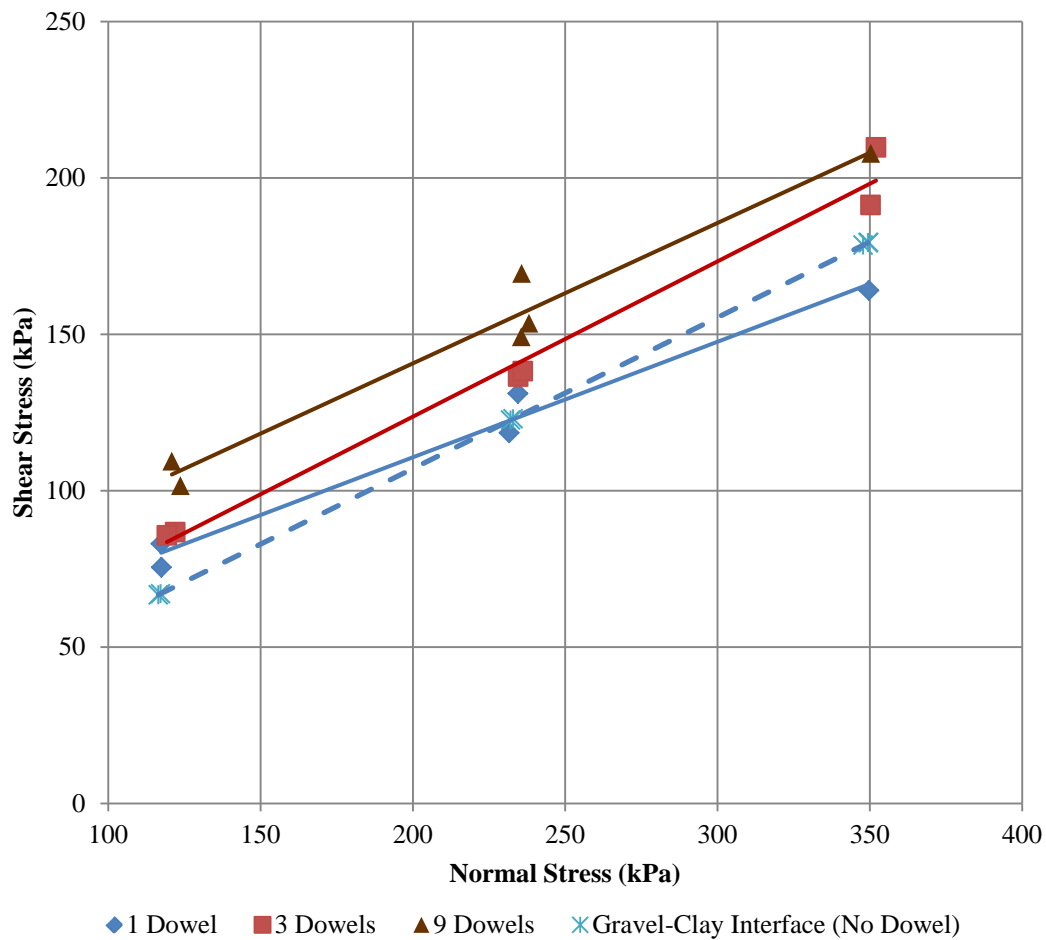


Figure 5.13 Effect of Number of Dowels in Improvement Tests

In Figure 5.13, it can be seen that the results of experiments with 1 dowel is questionable especially for 111 kPa and 333 kPa. For 3 dowels, considerable improvement was obtained whereas 9 dowels resulted in higher increase of shear strength.

In Figure 5.14, change in shear strength with number of dowels is summarized for different normal stresses and the shear strength of the gravel-clay interface improved with dowels is related to the number of piles and effective normal stresses.

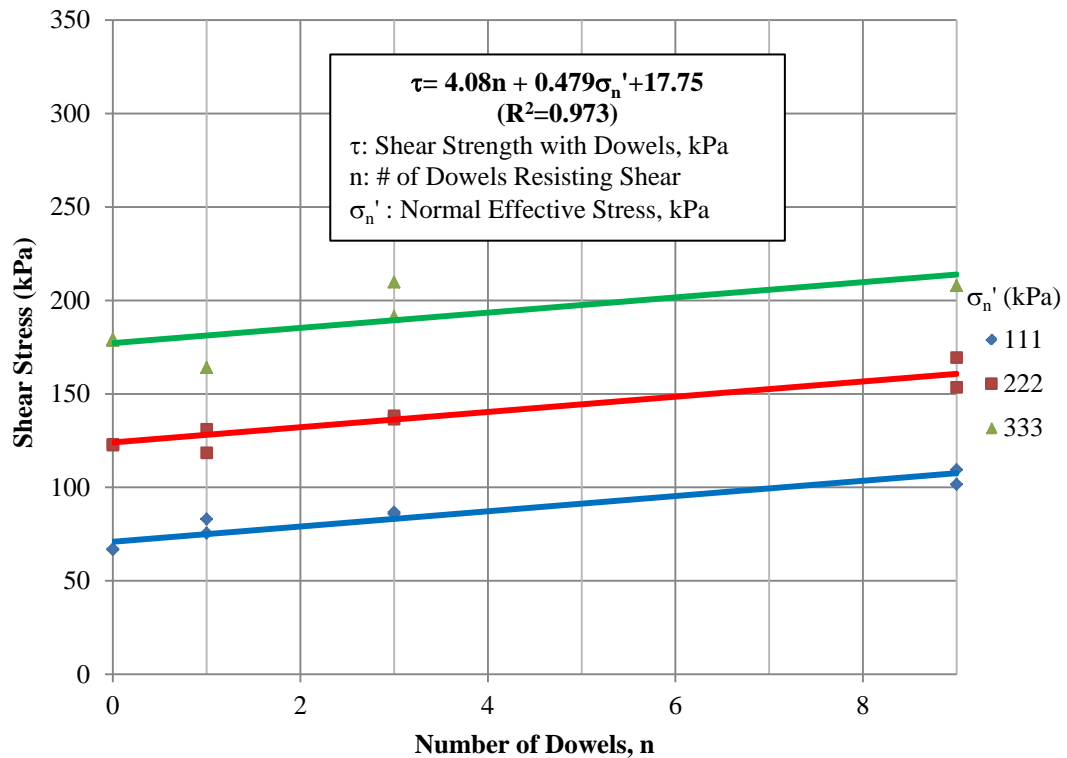


Figure 5.14 Effect of Number of Dowels for Different Normal Stresses

In order to see the effect of dowel length, improvement shear tests conducted with model dowels having different dowel lengths that were placed with same spacing (4d) were compared, i.e. improvement tests I-3, I-4, I-5, I-6 and I-7. In these tests 9 dowels with a diameter of 2 cm and lengths of 4 cm, 8 cm and 12 cm or 36 dowels with a diameter of 1 cm and lengths of 6 cm and 12 cm were used and all dowels were placed with 4d spacing.

Tests were conducted at least two times and repeated for two normal stresses (111 and 222 kPa). Results are shown in Figure 5.15 and Figure 5.16.

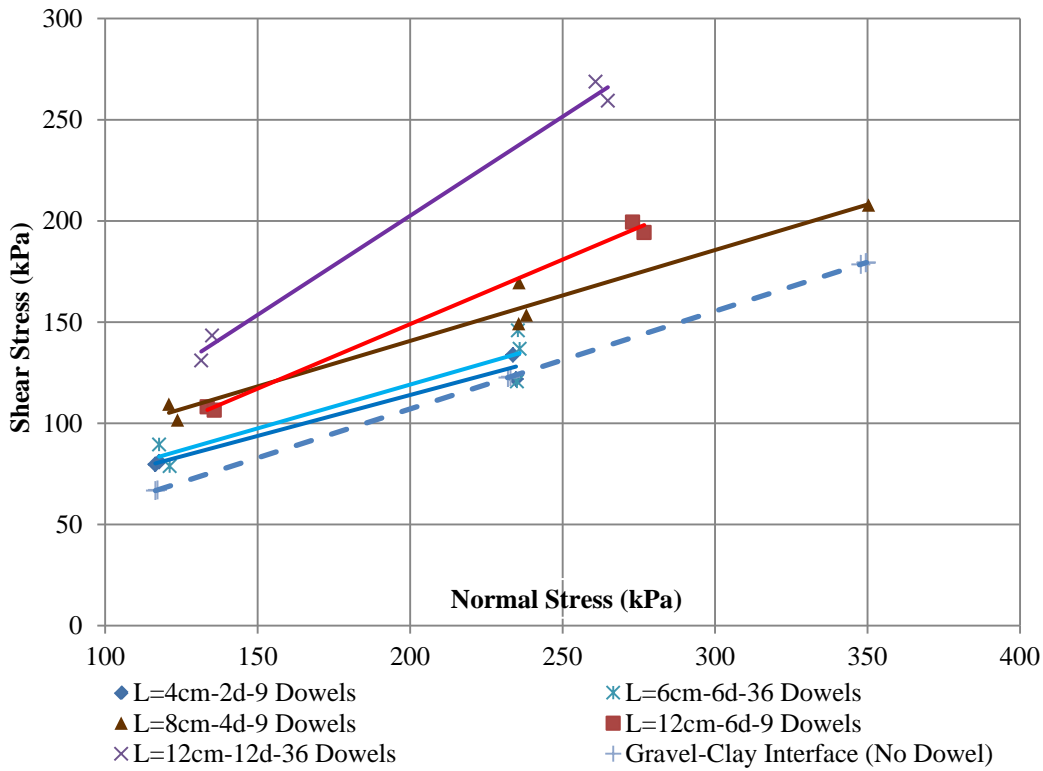


Figure 5.15 Effect of Dowel Lengths in Improvement Tests

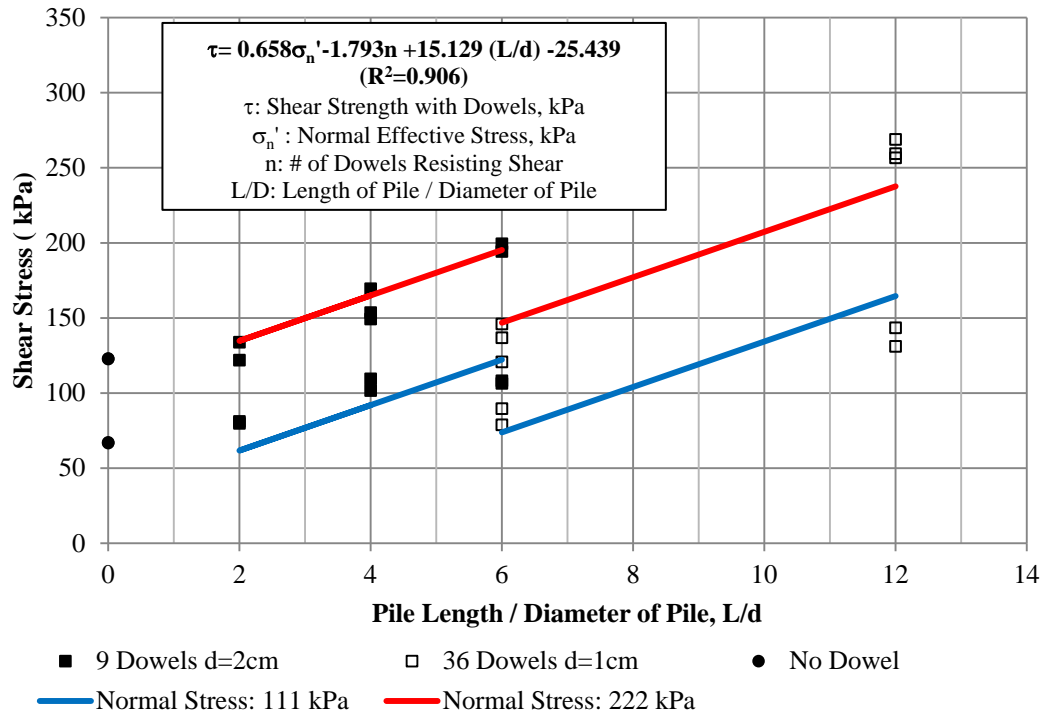


Figure 5.16 Effect of Dowel Lengths for Different Normal Stresses

As a result of the improvement tests with different dowel lengths, improvement increased as the dowel length increased as expected. Dowels having a length of 4 cm (2d) showed very small increase indicating insufficient improvement. From the dowels having same length of 12 cm, 36 dowels with 1 cm diameter showed large improvement against 9 dowels with 2 cm diameter.

In Table 5.4, Table 5.5 and Table 5.6 the results obtained from improvement tests were summarized for different normal stresses and compared with large shear box tests of gravel-clay interface and small direct shear tests of clay.

For 2d and 3d dowel penetrations (4d and 6d total length) improvements are observed. It was seen that with increasing penetrations into clay shearing resistances increase significantly.

Table 5.4 Summary of Improvement Test Results (Average) for  $\sigma_n'=111$  kPa

Normal Stress $\sigma_n'=111$ kPa							
Test Set	Dowel Diameter (d)	Dowel Length (L)	# of Dowels (n)	Spacing of Dowels (s)	Shear Strength, $\tau$ (kPa)	Increase in Shear Strength Compared to Clay (%)	Increase in Shear Strength Compared to Gravel-Clay (%)
Peak Shear Strength of Gravel-Clay					66.88		-
Peak Shear Strength of Clay					54.55		
I-1	2 cm	8 cm (4d)	1	-	79.27	45%	19%
I-2	2 cm	8 cm (4d)	3x1=3	8 cm (4d)	86.25	58%	29%
I-3	2 cm	8 cm (4d)	3x3=9	8 cm (4d)	105.54	93%	58%
I-4	2 cm	4 cm (2d)	3x3=9	8 cm (4d)	80.39	47%	20%
I-5	2 cm	12 cm (6d)	3x3=9	8 cm (4d)	107.28	97%	60%
I-6	1 cm	6 cm (6d)	6x6=36	4 cm (4d)	84.18	54%	26%
I-7	1 cm	12 cm (12d)	6x6=36	4 cm (4d)	137.21	152%	105%

Table 5.5 Summary of Improvement Test Results (Average) for  $\sigma_n'=222$  kPa

Normal Stress $\sigma_n'=222$ kPa							
Test Set	Dowel Diameter (d)	Dowel Length (L)	# of Dowels (n)	Spacing of Dowels (s)	Shear Strength, $\tau$ (kPa)	Increase in Shear Strength Compared to Clay (%)	Increase in Shear Strength Compared to Gravel-Clay (%)
Peak Shear Strength of Gravel-Clay					122.80	-	-
Peak Shear Strength of Clay					100.30	-	-
I-1	2 cm	8 cm (4d)	1	-	124.81	24%	2%
I-2	2 cm	8 cm (4d)	3x1=3	8 cm (4d)	137.40	37%	12%
I-3	2 cm	8 cm (4d)	3x3=9	8 cm (4d)	157.41	57%	28%
I-4	2 cm	4 cm (2d)	3x3=9	8 cm (4d)	127.83	27%	4%
I-5	2 cm	12 cm (6d)	3x3=9	8 cm (4d)	196.79	96%	60%
I-6	1 cm	6 cm (6d)	6x6=36	4 cm (4d)	134.49	34%	10%
I-7	1 cm	12 cm (12d)	6x6=36	4 cm (4d)	261.62	161%	113%

Table 5.6 Summary of Improvement Test Results (Average) for  $\sigma_n'=333$  kPa

Normal Stress $\sigma_n'=333$ kPa							
Test Set	Dowel Diameter (d)	Dowel Length (L)	# of Dowels (n)	Spacing of Dowels (s)	Shear Strength, $\tau$ (kPa)	Increase in Shear Strength Compared to Clay (%)	Increase in Shear Strength Compared to Gravel-Clay (%)
Peak Shear Strength of Gravel-Clay					179.32	-	-
Peak Shear Strength of Clay					146.05	-	-
I-1	2 cm	8 cm (4d)	1	-	164.06	12%	-9%
I-2	2 cm	8 cm (4d)	3x1=3	8 cm (4d)	200.60	37%	12%
I-3	2 cm	8 cm (4d)	3x3=9	8 cm (4d)	207.88	42%	16%

Viggiani (1981) suggested a formula for ultimate load per unit length of a passive dowel ( $P_u$ ) which is related with undrained shear strength of clay ( $C_u$ ), diameter of dowel (d) and a bearing capacity factor (k) and defined as given in equation 5.1. Bearing capacity factor, k was given between 4 and 8 for moving and stable soils, respectively by Viggiani (1981).

$$P_u = k C_u d \quad (5.1)$$

In order to compare the contribution of dowels with undrained shear strength of clay, clay samples were taken at the end of improvement tests and Unconsolidated Undrained (UU) shear tests were performed (Figure 5.17).

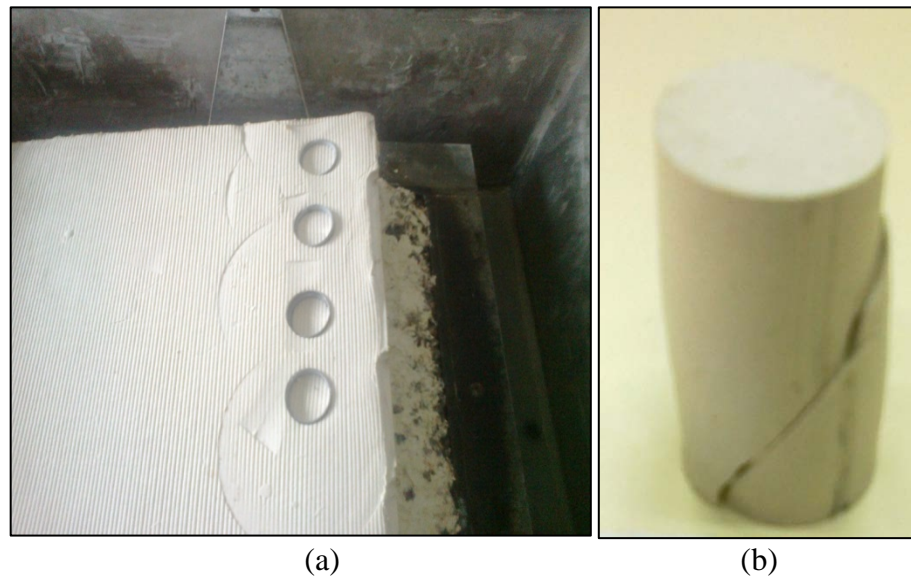


Figure 5.17 a) Taking Specimen for UU Tests b) Specimen after UU Tests

The results of UU tests performed were summarized in Table 5.7 and attached in Appendix D.

Table 5.7 Summary of Unconsolidated Undrained (UU) Test Results

Test Set	Experiment No	# of Dowels (n)	Dowel Length (L)	Dowel Diameter (d)	Normal Stress, $\sigma_n'$ (kPa)	Undrained Shear Strength, $C_u$ (kPa)
I-1	2	1	4d	2 cm	111	64.00
I-1	3	1	4d	2 cm	222	94.00
I-1	4	1	4d	2 cm	222	86.00
I-2	6	3	4d	2 cm	111	76.00
I-2	7	3	4d	2 cm	111	57.00

Table 5.7 Summary of Unconsolidated Undrained (UU) Test Results-continued

Test Set	Experiment No	# of Dowels (n)	Dowel Length (L)	Dowel Diameter (d)	Normal Stress, $\sigma_n'$ (kPa)	Undrained Shear Strength, $C_u$ (kPa)
I-2	8	3	4d	2 cm	222	87.50
I-2	9	3	4d	2 cm	222	99.00
I-2	10	3	4d	2 cm	333	122.00
I-2	11	3	4d	2 cm	333	101.00
I-3	12	9	4d	2 cm	111	75.00
I-3	13	9	4d	2 cm	111	83.00
I-3	14	9	4d	2 cm	222	86.00
I-3	15	9	4d	2 cm	222	88.00
I-4	18	9	2d	2 cm	111	58.50
I-4	19	9	2d	2 cm	111	59.80
I-4	20	9	2d	2 cm	222	113.00

In Table 5.8, Table 5.9 and Table 5.10 shear contribution of dowels were compared with the undrained shear strength of clay and bearing capacity factors were calculated. Average values of undrained shear strength were used for that comparison.

Table 5.8 Shear Contribution of Dowels- $\sigma_n'=111$  kPa

For $\sigma_n'=111$ kPa-Average $C_u=67$ kPa							
# of Dowels (n)	Dowel Length in Clay, L (m)	Dowel Diameter, d (m)	Shear Strength, $\tau$ (kPa)	Shear Increase due to Dowels, $\Delta S$ (kPa)	Shear Contribution of One Dowel, $F = (\Delta S.A)/n$ (kN)	Load for One Dowel, $P_u = F/L$ (kN/m)	Bearing Capacity Factor, $k = \frac{P_u}{C_u \cdot d}$
0	-	-	66.88	-	-		
1	0.04	0.02	79.27	12.39	1.115	27.879	20.805
3	0.04	0.02	86.25	19.37	0.581	14.528	10.842
9	0.04	0.02	105.54	38.66	0.387	9.665	7.213
9	0.02	0.02	80.39	13.51	0.135	6.755	5.041
9	0.06	0.02	107.28	40.40	0.404	6.733	5.024
36	0.06	0.01	137.21	70.33	0.176	2.930	4.373
36	0.03	0.01	84.18	17.30	0.043	1.442	<b>2.152</b>

\*A=Area of Shear Box=0.09 m<sup>2</sup>

Bearing capacity factors calculated from experiments conducted are mostly between 4-6 for experiments where large improvements were obtained which is consistent with the findings of Viggiani (1981).

Bearing capacity factor decrease to 1-2 range in experiments with shortest dowels indicating ineffectiveness of improvement as can be seen in Table 5.9.

Table 5.9 Shear Contribution of Dowels- $\sigma_n'=222$  kPa

For $\sigma_n'=222$ kPa-Average $C_u=96$ kPa							
# of Dowels (n)	Dowel Length in Clay, L (m)	Dowel Diameter, d (m)	Shear Strength, $\tau$ (kPa)	Shear Increase due to Dowels, $\Delta S$ (kPa)	Shear Contribution of One Dowel, $F = (\Delta S.A)/n$ (kN)	Load for One Dowel, $P_u=F/L$ (kN/m)	Bearing Capacity Factor, $k=\frac{P_u}{C_u.d}$
0	-	-	122.80	-	-		
1	0.04	0.02	124.81	2.01	0.181	4.533	<b>2.361</b>
3	0.04	0.02	137.40	14.60	0.438	10.954	5.705
9	0.04	0.02	157.41	34.62	0.346	8.655	4.508
9	0.02	0.02	127.83	5.03	0.050	2.515	<b>1.310</b>
9	0.06	0.02	196.79	73.99	0.740	12.332	6.423
36	0.06	0.01	261.62	138.82	0.347	5.784	6.025
36	0.03	0.01	134.49	11.69	0.029	0.974	<b>1.015</b>

Table 5.10 Shear Contribution of Dowels- $\sigma_n'=333$  kPa

For $\sigma_n'=333$ kPa-Average $C_u=112$ kPa							
# of Dowels (n)	Dowel Length in Clay, L (m)	Dowel Diameter, d (m)	Shear Strength, $\tau$ (kPa)	Shear Increase due to Dowels, $\Delta S$ (kPa)	Shear Contribution of One Dowel, $F = (\Delta S.A)/n$ (kN)	Load for One Dowel, $P_u=F/L$ (kN/m)	Bearing Capacity Factor, $k=\frac{P_u}{C_u.d}$
0	-	-	179.32	-	-		
3	0.04	0.02	200.60	21.28	0.638	15.961	7.125
9	0.04	0.02	207.88	28.56	0.286	7.140	3.188

## 5.4 Effect of Continuous Improvement

In order to see the effect of a continuous improvement, direct shear tests were performed with a fiberglass having 2 cm thickness and a length which is slightly shorter than the size of shear box (30 cm) to prevent friction between fiberglass and shear box. A total number of 12 experiments were conducted as summarized in Appendix C.

Table 5.11 Properties of Fiberglass Used in Continuous Improvement Tests

Material	Elastic Modulus (E)	Dimensions	Height (H)
Fiberglass	80 GPa	30 cm x 2 cm	4 cm-8 cm-12 cm

Fiberglass wall having different heights shown in Table 5.11 is placed in such a way that half of it is in the lower granular material and remaining part is in the upper clay specimen (Figure 5.18 and Figure 5.19). The tests conducted are summarized in Table 5.12 and Figure 5.20.

Table 5.12 Continuous Improvement Experiments

Test Set	Experiment No	Height, H (cm)	Normal Stress, $\sigma_n'$ (kPa)	Shear Stress, $\tau$ (kPa)
W1	1	4	117.43	53.60
W1	2	4	120.91	52.89
W1	3	4	232.20	95.39
W1	4	4	239.58	101.61
W2	5	8	127.36	69.76
W2	6	8	121.05	73.67
W2	7	8	235.40	119.54
W2	8	8	275.26	147.63
W3	9	12	111.00	78.96
W3	10	12	111.00	89.09
W3	11	12	222.00	141.44
W3	12	12	222.00	152.00



Figure 5.18 Filling Clay on Gravel in Continuous Improvement Tests



Figure 5.19 Improvement Tests with Continuous Wall

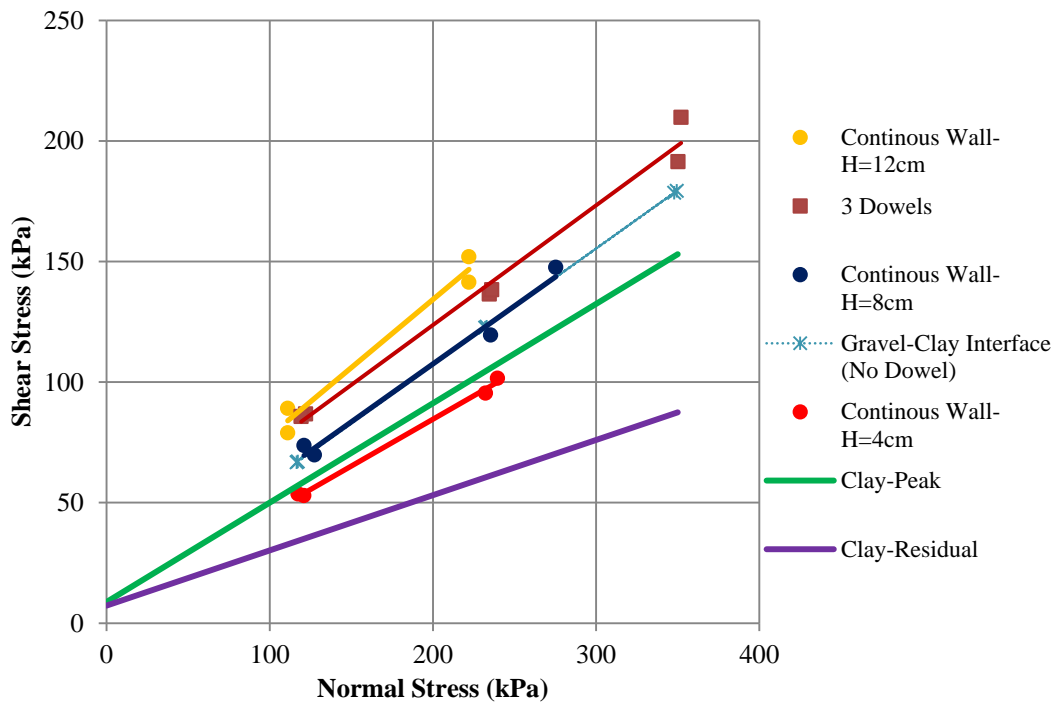


Figure 5.20 Results of Continuous Wall Experiments

According to results given in Figure 5.20, no improvement was obtained from continuous improvement tests conducted for 8 cm wall height.

It is interesting that, tests with smallest wall height (4 cm) gave a shear strength which is very close to peak shear strength of clay indicating that continuous improvement with small heights forced failure to be in the clay layer below improvement.

Continuous improvement with largest height (12 cm) resulted in very close shear strength to 3-dowel improvement tests.

It is well known that when the spacing of piles or dowels decreases, increase in shear strength also decreases due to interaction between piles or dowels. Brown and Shie (1991), Wang and Reese (1986), Cox et al. (1984), Barradas and Correiga (1995) are some of the researchers studying this effect. In continuous improvement experiments, reduction in improvement was clearly seen.

## CHAPTER 6

### SUMMARY OF RESULTS AND CONCLUSIONS

#### 6.1 Introduction

In order to determine the shear strength parameters of granular materials and clayey soil interfaces, shear strength tests were performed. Both granular material (sand and gravel) and interface (sand-clay and gravel-clay) parameters were measured in direct shear tests and triaxial tests for that purpose.

The results of the shear strength tests are given in the previous sections of the thesis. In this chapter, the results from experiments are summarized and general conclusions obtained from the research study are given.

#### 6.2 Results in Direct Shear Tests

##### 6.2.1 Peak Friction Angles

-Gravel and sand were tested in large shear box and small shear box, respectively. The friction angle of gravel is found to be  $1.6^\circ$  greater than the friction angle of sand ( $44.8^\circ$  vs  $43.2^\circ$ ).

-In large shear box tests, peak friction angle of gravel-clay interface is obtained  $3.4^\circ$  greater than the peak friction angle of clay obtained in small shear box tests ( $25.8^\circ$  vs  $22.4^\circ$ ).

-In small shear box tests, peak friction angle of sand-clay interface is found to be  $1.9^\circ$  higher than the peak friction angle of clay ( $24.3^\circ$  vs  $22.4^\circ$ ).

-Peak friction angle of gravel-clay interface is  $1.5^\circ$  higher than peak friction angle of sand-clay interface.

## 6.2.2 Friction Angles at Large Deformation

-In large shear box tests, large deformation friction angle of gravel-clay interface is obtained  $6.9^\circ$  greater than the residual friction angle of clay ( $19.8^\circ$  vs  $12.9^\circ$ ). In small shear box tests, large deformation friction angle of sand-clay interface is found to be  $3.8^\circ$  greater than the residual friction angle of clay ( $16.7^\circ$  vs  $12.9^\circ$ ).

-Large deformation friction angle of gravel-clay interface is  $3.1^\circ$  greater than large deformation friction angle of sand-clay interface.

## 6.2.3 Cohesion Values

-At the peak shear strength, cohesion intercept of gravel-clay interface is greater than the cohesion value of clay (10.4 kPa vs 8.8 kPa). In small shear box tests, peak cohesion of sand-clay interface is obtained to be smaller than the peak cohesion of clay (5.5 kPa vs 8.8 kPa).

-At large deformation, cohesion intercepts of gravel-clay interface and sand-clay interface are higher than the residual cohesion value of clay (15.2 kPa vs 7.3 kPa and 12.2 kPa vs 7.3 kPa).

## 6.3 Results in Triaxial Tests

### 6.3.1 Peak Friction Angles

-The friction angle of gravel is  $0.9^\circ$  greater than the friction angle of sand in triaxial tests ( $43.9^\circ$  vs  $43^\circ$ ).

-Friction angle of gravel-clay interface is  $1.3^\circ$  higher than the friction angle of sand-clay interface ( $20.3^\circ$  vs  $19^\circ$ ).

-Drained triaxial peak friction angle of clay ( $21.9^\circ$ ) is  $2.9^\circ$  and  $1.6^\circ$  greater than peak friction angles of sand-clay interface ( $19.0^\circ$ ) and gravel-clay interface ( $20.3^\circ$ ), respectively. Pre-cut clay samples yield a peak angle of  $11.9^\circ$ .

### 6.3.2 Friction Angles at Large Deformation

-Sand-clay interface and gravel-clay interface friction angles at large strains are 17.5° and 18.6°, respectively.

-At large deformation, friction angle of clay-clay interface is found as 10.1°. Note that the friction angle in direct shear tests on clay at large strains (residual) is 12.9°.

### 6.3.3 Cohesion Values

-Peak cohesion value of clay in the drained tests is 8.5 kPa. Peak cohesion in the sand-clay interface and gravel clay interface triaxial tests are 8.1 kPa and 10 kPa, respectively. Peak cohesion intercept in the clay-clay pre-cut tests is 9.8 kPa.

-Large deformation cohesion intercepts in the sand-clay interface and gravel-clay interface tests are 8.9 kPa and 9.8 kPa, respectively and it is 12.7 kPa in the pre-cut clay tests.

## 6.4 Results in Improvement Tests

- For 2d and 3d dowel penetrations (4d and 6d total length) improvements are observed. It was seen that with increasing penetrations into clay shearing resistance increases significantly.

- 4 to 6 diameter spacing between dowels or piles is usually regarded sufficient for development of single pile behavior. Field application should follow such a spacing for efficient improvement. Closer spacing is known to decrease lateral capacity. That was the reason for 4d spacing selected in the improvement tests. In continuous improvement experiments, decrease in lateral capacity is seen clearly.

- As the number of dowels resisting to the shear movement increases, shear strength increased as expected.

## 6.5 Conclusions

Starting point for the comparisons is strength of clay. In this experimental study, peak friction angle of clay with PI=18% prepared at liquidity index of 0.94 in direct shear tests and triaxial tests are almost identical (22.4° and 21.9°). Sand-clay and gravel-clay interfaces in direct shear show peak angles of 24.3° and 25.8°, respectively.

Residual friction angle of clay is 12.9° in direct shear tests and large deformation friction angle of clay-clay interface is 10.1°. Sand-clay interface large strain friction angle was obtained as 16.7° in direct shear tests and 17.5° in triaxial tests. Gravel-clay friction angle is 19.8° in direct shear tests and 18.6° in triaxial tests at large deformation.

Clearly, angle of shearing resistance increases consistently at the interface. It is 2 to 4 degrees in peak and 4 to 6 degrees in residual strengths for the two types of granular materials (GP with DR=67% and SP prepared at DR=72%) in direct shear and triaxial experiments. This is believed to be a significant finding.

Cohesion values in almost all type of tests at peak and large strains are about 8-10 kPa.

Friction angles are more influential on stability in case of high fills compared to cohesion values. Since factors of safety in remediation works related to slope instabilities are low, peak strengths may be at least partly exceeded, and large strain resistances may govern the stability.

Dowels are observed to be highly effective in increasing the shear resistance and recommended for field applications. 4d spacing between dowels and 3d penetration into clay seem to be minimum required. Trial field tests should be accompanied.

Considering the results of this study, the following flow chart (Figure 6.1) is recommended for granular material-clay interface studies.

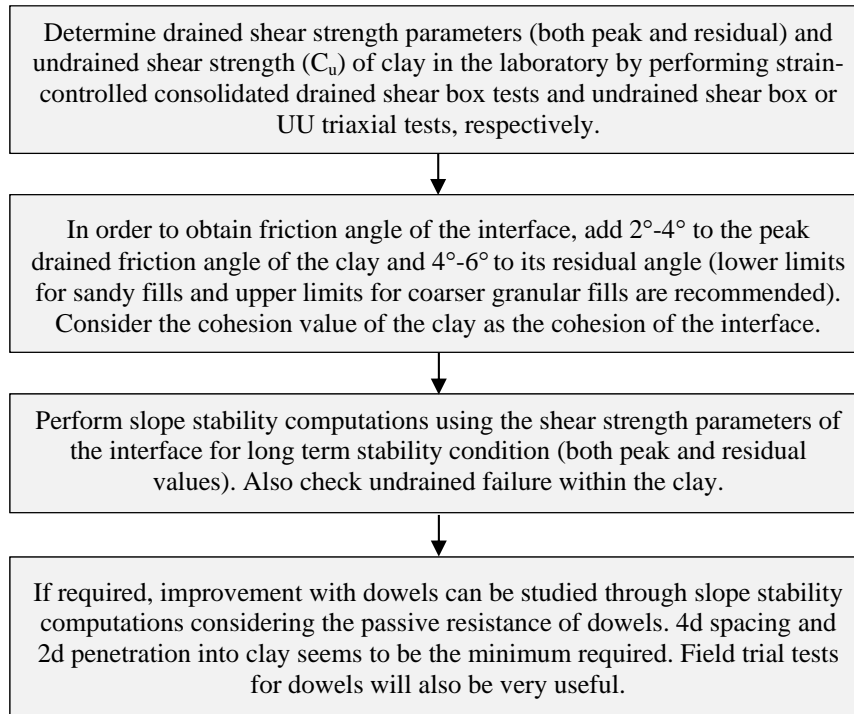


Figure 6.1 Flow Chart for Granular Material-Clay Interface Studies

## 6.6 Recommendations for Future Studies

- The shear strength tests may be repeated for different types of granular material. The effect of gradation, particle shape, density of granular fill can be studied in detail.
- The tests can be repeated for clay-sized materials having different plasticity values in order to see the effect of soil plasticity. The effect of consolidation states, i.e. normally consolidated, slightly overconsolidated or highly overconsolidated, can be studied in detail.
- Triaxial tests should be specially instrumented and area correction must be focused on for interface studies.

- Single and group tests on dowels seem to be a promising research field. Improvement using dowels can be studied with field tests which will make a valuable contribution to the improvement techniques used for interface instabilities.

## REFERENCES

- ASTM D7181 (2011). *Standard Test Method for Consolidated Drained Triaxial Compression Tests for Soils*. ASTM International, West Conshohocken, PA.
- ASTM D3080 (2011). *Standard Test Method for Direct Shear Test of Soils Under Consolidated Drained Conditions*. ASTM International, West Conshohocken, PA.
- Bareither, C.A, Benson, C.H., and Edil, T.B. (2008). Comparison of Shear Strength of Sand Backfills Measured in Small-Scale and Large-Scale Direct Shear Tests. *Canadian Geotechnical Journal*, Vol: 45, pp. 1224-1236.
- Baradas, J., and Correia, R. (1995). Numerical and Physical Modeling of Slope Soil Nailing. *The Interplay Between Geotechnical Engineering and Engineering Geology*, Copenhagen, Vol:4, pp. 4.13-4.18.
- Barton, N.R. (2008). Shear Strength of Rockfill, Interfaces and Rock Joints and Their Points of Contact in Rock Dump Design. *Rock Dumps 2008*, Australian Centre for Geomechanics, Perth, pp. 3-8.
- Brown, D.A., and Shie, C. (1991). Modification of p-y Curves to Account for Group Effects on Laterally Loaded Piles. *Proceedings of the Congress Sponsored by the Geotechnical Engineering Division of A.S.C.E.*, Geotechnical Special Publication, No: 27, pp. 479-490.
- Castellanos, B.A.and Brandon , T.L. (2013). A Comparison Between the Shear Stregnth Measured with Direct Shear and Triaxial Devices on Undisturbed and Remolded Soils. *Proceedings of the 18th International Conference on Soil Mechanics and Geotechnical Engineering*, Paris, pp. 317-320.
- Cerato, A.B., and Lutenegro, A.J. ( 2006). Specimen Size and Scale Effects of Direct Shear Box Tests of Sands. *Geotechnical Testing Journal*, Vol: 29, No: 6, pp. 1-10.
- Chandler, R. J. (1966). The Measurement of Residual Strength in Triaxial Compression. *Geotechnique*, Vol:16, No:3, pp. 181–186.
- Charles, J.A., and Watts, K.S. (1980.). The Influence of Confining Pressure on the Shear Strength of Mine Waste Rock. *Geotechnique*, Vol: 30, pp. 353-367.

- Cox, W.R., Dixon, D.A., and Murphy, B.S. (1984). Lateral Load Tests of 25.4 mm. Diameter Piles in Very Soft Clay in Side-by-Side and In-Line Groups. *Laterally Loaded Deep Foundations: Analysis and Performance*, ASTM, SPT835.
- Donaghe, R.T., and Torrey, W.H. (1979). Scalping and Replacement Effects on Strength Parameters of Earh-Rock Mixtuures. *Proceedings of the Seventh European Conference on Soil Mechanics and Foundation Engineering*, Brington, England, Vol:2, pp. 29-34.
- Fakhimi, A., and Hosseinpour, H. (2008). The Role of Oversize Particles on the Shear Strength and Deformational Behavior of Rock Pile Material. ARMA08-204. *The 42nd US Rock Mechanics Symposium and 2nd US-Canada Rock Mechanics Symposium*, San Francisco, USA.
- Holtz, W. G. (1960). Discussion to session "Testing Equipment, Techniques, and Errors". *Proceedings of the Research Conference on Shear Strength of Cohesive Soils*, Boulder, Colorado, pp. 997-1002.
- Iannacchione, A.T., and Vallejo, L.E. (2000). Shear Strength Evaluation of Clay-Rock Mixtures. *Slope Stability 2000*, pp. 209-223.
- Indraratna, B., Wijewardena, L.S.S., and Balasubramaniam, A.S. (1993). Large Scale Triaxial Testing of Greywacke Rockfill. *Geotechnique*, Vol: 40, No: 1, pp. 37-51.
- Irfan, T.Y., and Tang, K.Y. (1992). *Effect of the Coarse Fractions on the Shear Strength of Colluvium*. Hong Kong: Geotechnical Engineering Office, Civil Engineering Department, Report No. SPR 15/92.
- Kasmer, O., and Ulusay, R. (2006). Stability of Spoil Piles at Two Coal Mines in Turkey: Geotechnical Characterization and Design Considerations. *Enviromental and Engineering Geoscience*, Vol: 12, No: 4, pp. 337-352.
- La Rochelle P. (1967). Membrane, Drain, and Area Correction in Triaxial Tests on Soil Samples Failing along a Single Shear Plane. *Proc. 3rd Pan-American Conference on Soil Mechanics and Foundation Engineering*, Caracas, Venezuela, Vol:1, pp. 273–292.
- Lupini, J.F., Skinner, A.E., and Vaughan, P.R. (1981). The Drained Residual Strength of Cohesive Soils. *Geotechnique*, Vol: 31, No: 2, pp. 181–213.
- Marachi, N. D. (1969). *Strength and Deformation Characteristics of Rockfill Materials*. PhD. Thesis. University of California.
- Meehan, C.L., Tiwari, B., Brandon T.L., and Duncan J.M. (2011). Triaxial Shear Testing of Polished Slickensided Surfaces. *Landslides*, Vol:8, pp. 449-458.

- Miller, E.A., and Sowers, G.F. (1957). The Strength Characteristics of Soil-Aggregate Mixture. *Highway Research Board Bulletin*, No: 183, pp. 16-23.
- Mollamahmutoglu, M., and Yılmaz, Y. (2009). Fine Gravel Content Effect on the Undrained Shear Strength Characteristics of Highly Plastic Clayey Soils. *2nd International Conference on New Developments in Soil Mechanics and Geotechnical Engineering*, Nicosia, North Cyprus.
- Nakao, T., and Fityus, S. (2008). Direct Shear Testing of a Marginal Material Using a Large Shear Box. *Geotechnical Testing Journal*, Vol: 31, No: 5, pp. 1-11.
- Patwardhan, A.S., J.S. Rao, and R.B. Gaidhane. (1970). Interlocking Effects and Shearing Resistance of Boulders and Large Size Particles in a Matrix of Fines on the Basis of Large Scale Direct Shear Tests. *Proceedings of the 2nd Southeast Asian Conference on Soil Mechanics*. Singapore, pp. 265-273.
- Şengör, M. Y. (2013). *The Deformation Characteristics of Deep Mixed Columns in Soft Clayey Soils: A Model Study*. Ph.D Thesis, M.E.T.U.
- Ulusay, R., Arıkan, F., Yoleri, M.F., and Çağlan, D. (1995). Engineering Geological Characterization of Coal Mine Waste Material and An Evaluation in the Context of Back-Analysis of Spoil Pile Instabilities in a Strip Mine, SW Turkey. *Engineering Geology*, Vol: 40, pp. 77-101.
- Viggiani, C. (1981). Ultimate Lateral Load on Piles Used to Stabilize Landslides. *Proc. 10th Journal of Soil Mechanics and Foundation Engineering*. Stockholm, Vol:3, pp. 555-560.
- Wang, S.T., and Reese, L.C. (1986). Study of Design Method for Vertical Drilled Shaft Retaining Walls. *Research Report 415-2F, Center of Transportation Research, Bureau of Engineering Research, The University of Texas at Austin*.
- Wang, J.P., and Ling, H.I. (2006). Stress-Strain Behavior of a Compacted Sand-Clay Mixture. *Soil Stress-Strain Behavior: Measurement, Modeling and Analysis Geotechnical Symposium*. Roma, pp. 491-502.
- Xu, W.J., Hu, R.L., and Tan, R.J. (2007). Some Geomechanical Properties of Soil-Rock Mixtures in the Hutiao Gorge Area, China. *Geotechnique*, Vol: 57, No: 3, pp. 255-264.
- Zhang, B., Yu, Y., Fu, J., and Hu, L. (2007). Simple Shear Test for Interfaces Between Core and Filler Soils in Rock-Fill Dams. *Geotechnical Testing Journal*, Vol: 31, No: 3, pp. 252-260.



## APPENDIX A

### DIRECT SHEAR TESTS

#### 1. Large Shear Box Tests

##### a. Large Shear Tests of Gravel

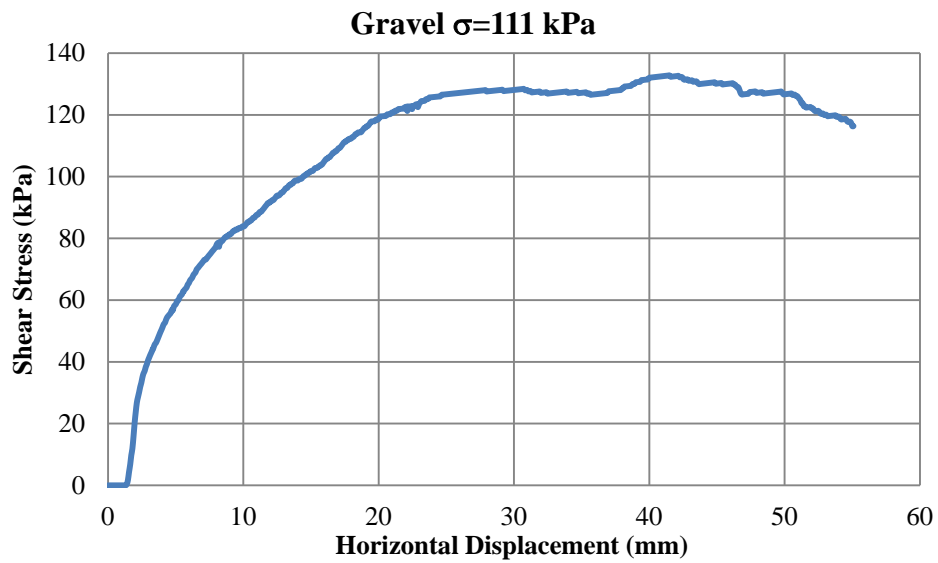


Figure A.1 Shear Stress vs. Displacement Graph-Experiment 1

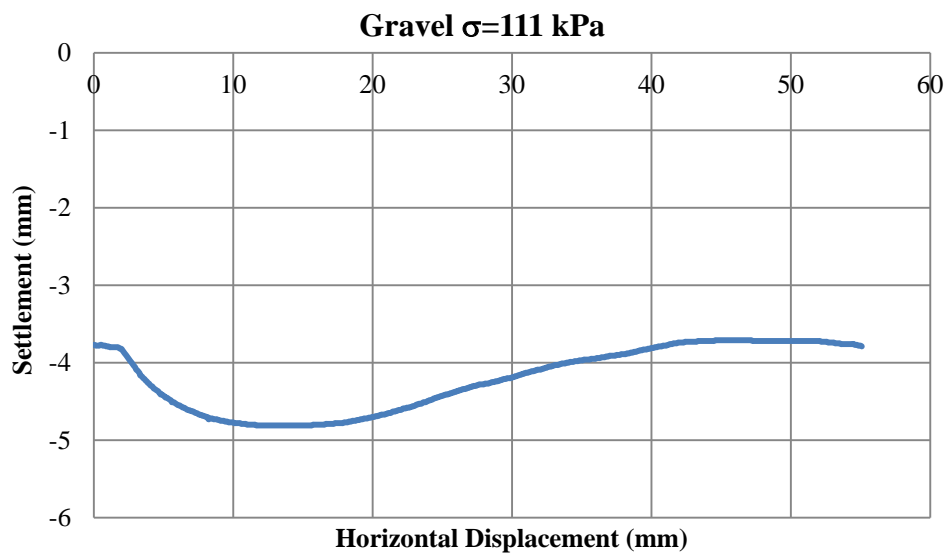


Figure A.2 Settlement vs. Displacement Graph- Experiment 1

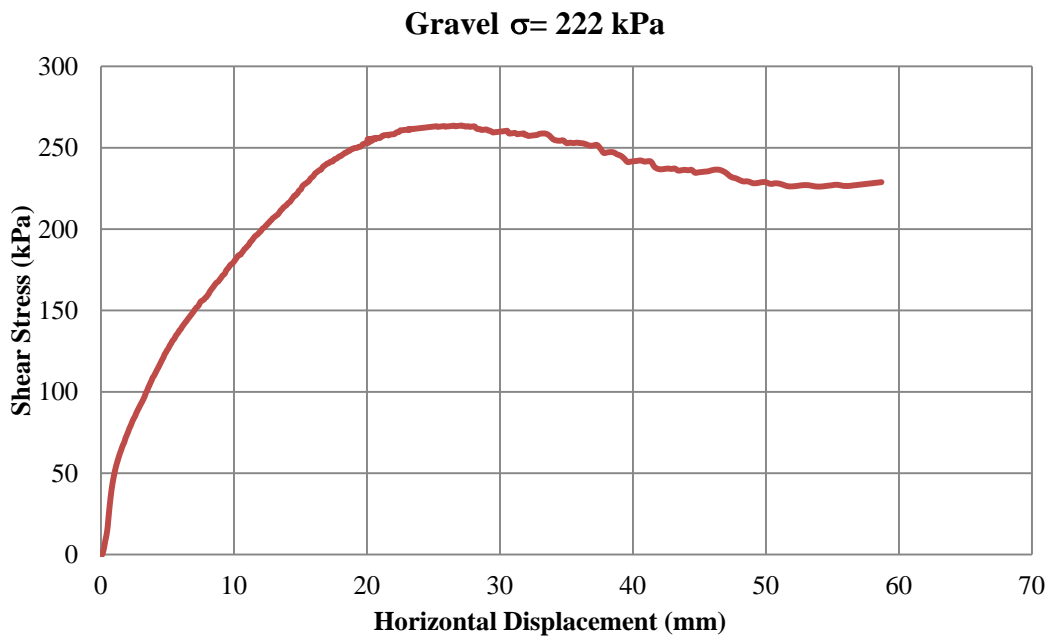


Figure A.3 Shear Stress vs. Displacement Graph-Experiment 2

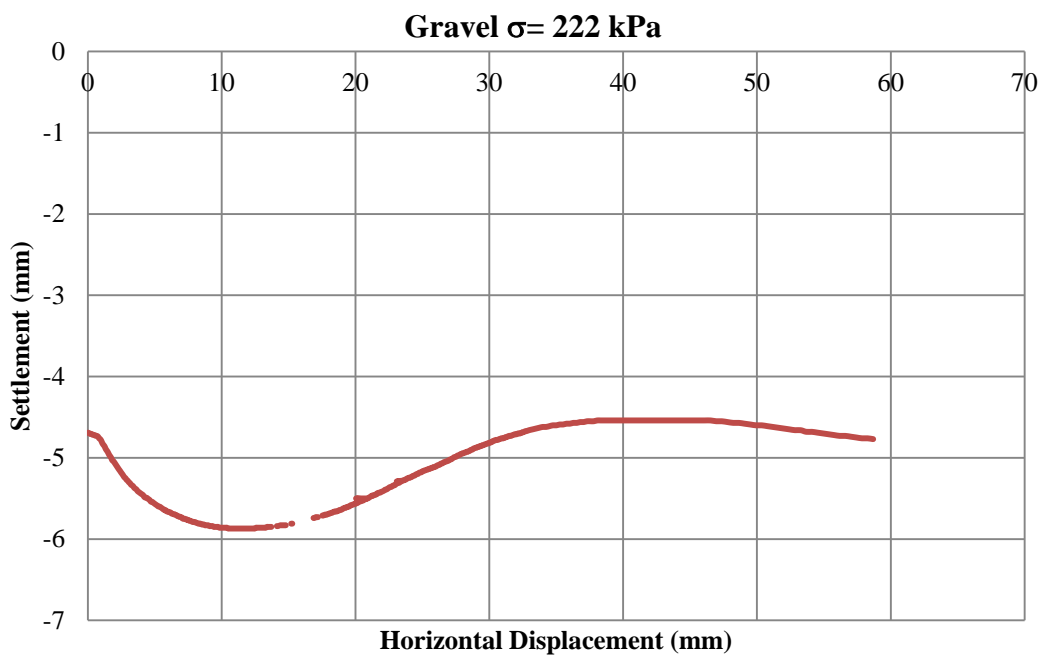


Figure A.4 Settlement vs. Displacement Graph- Experiment 2

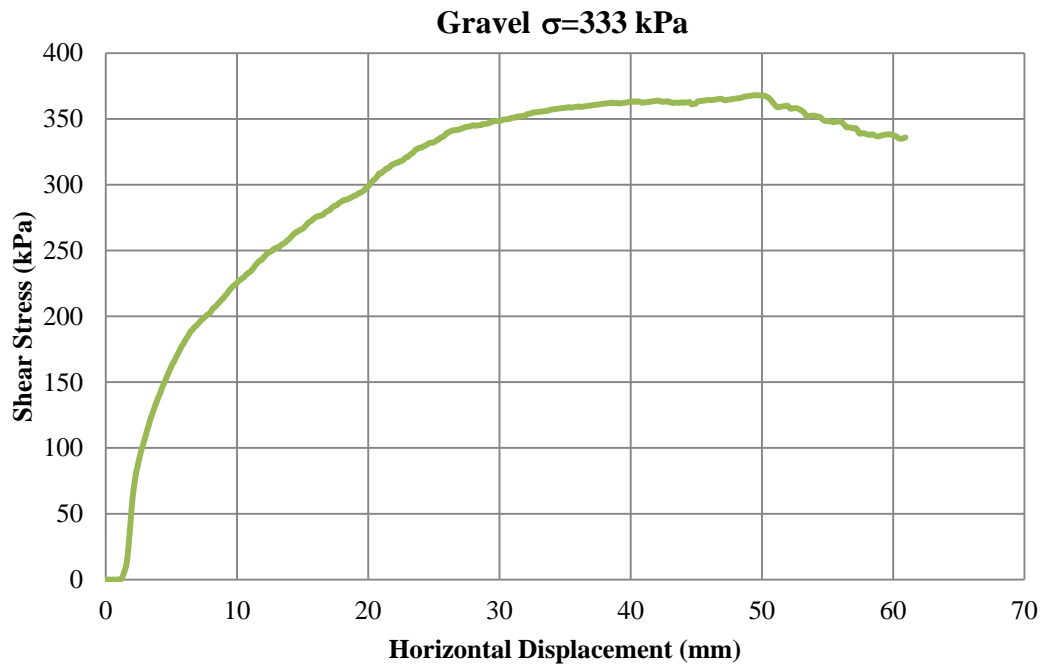


Figure A.5 Shear Stress vs. Displacement Graph-Experiment 3

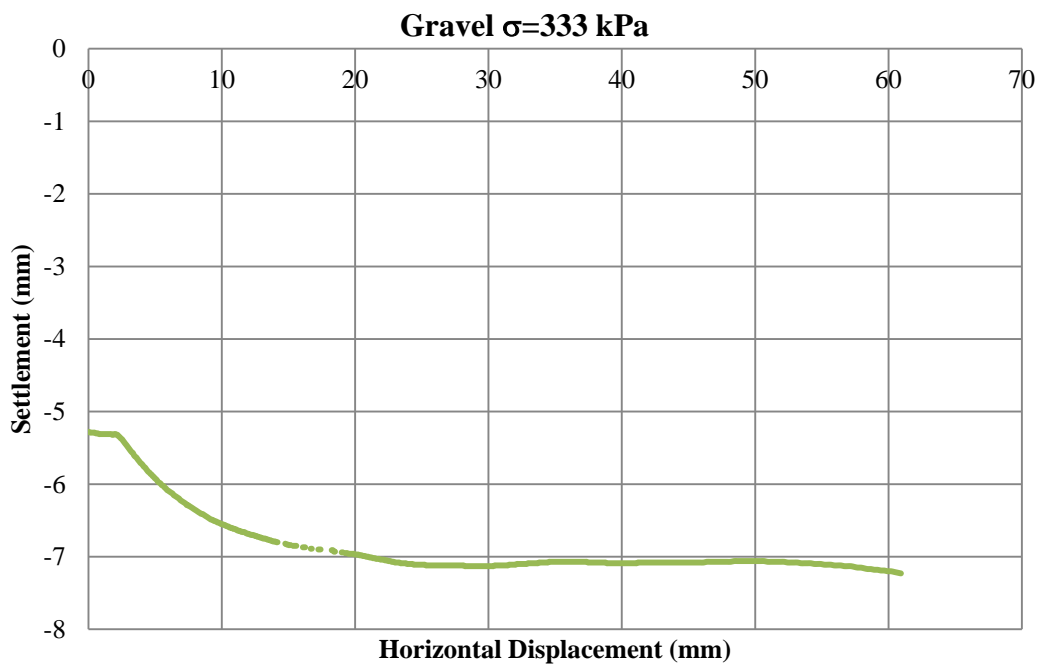


Figure A.6 Settlement vs. Displacement Graph- Experiment 3

**b. Large Shear Tests of Gravel-Clay Interface**

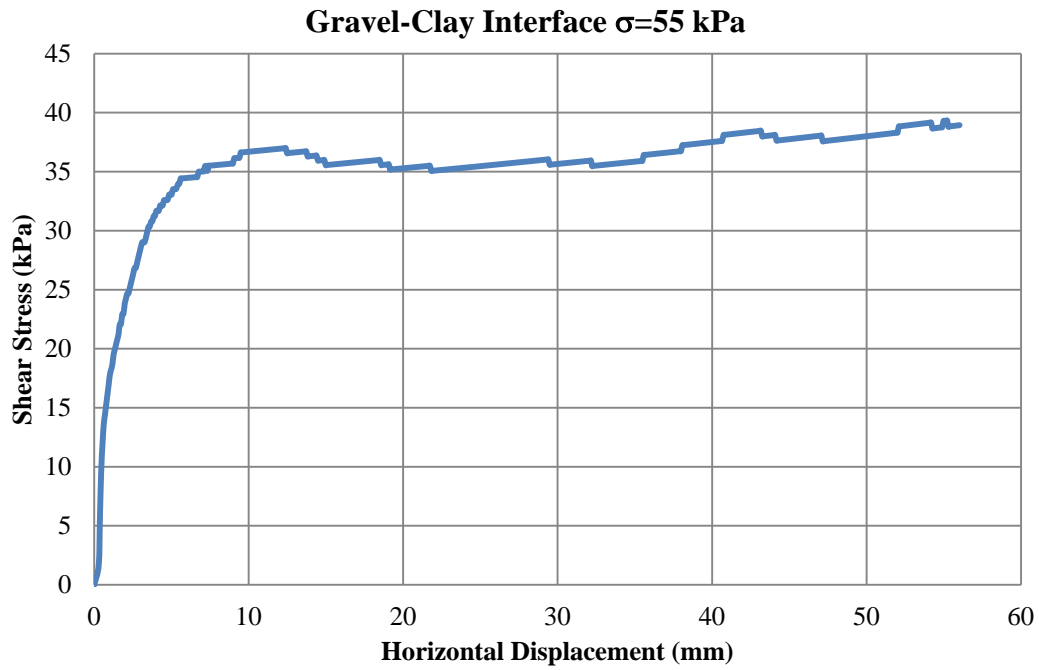


Figure A.7 Shear Stress vs. Displacement Graph-Experiment 1

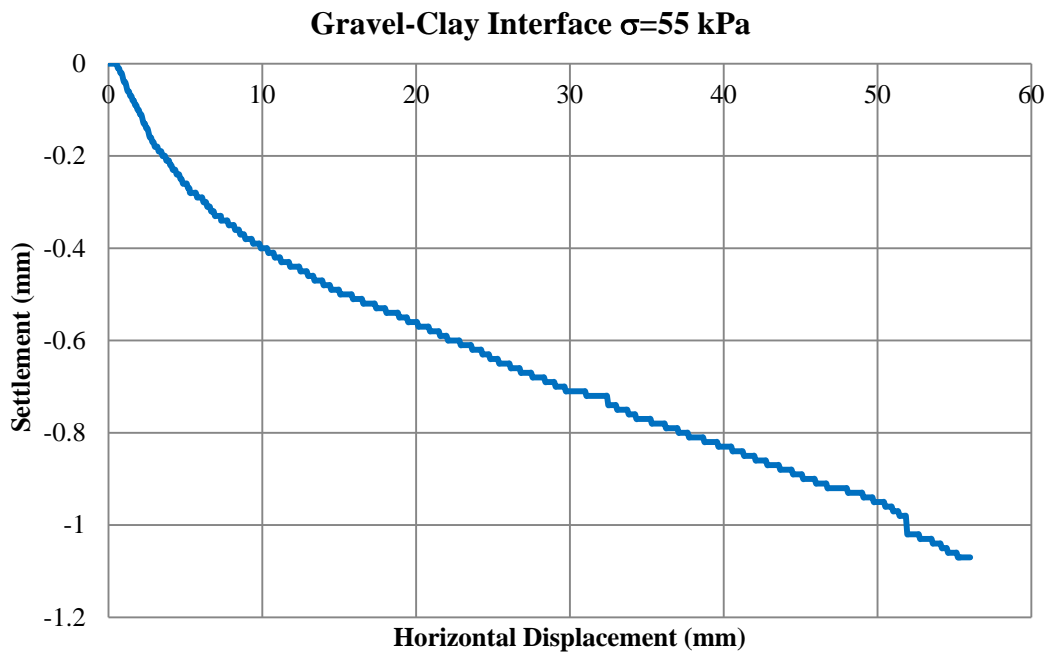


Figure A.8 Settlement vs. Displacement Graph- Experiment 1

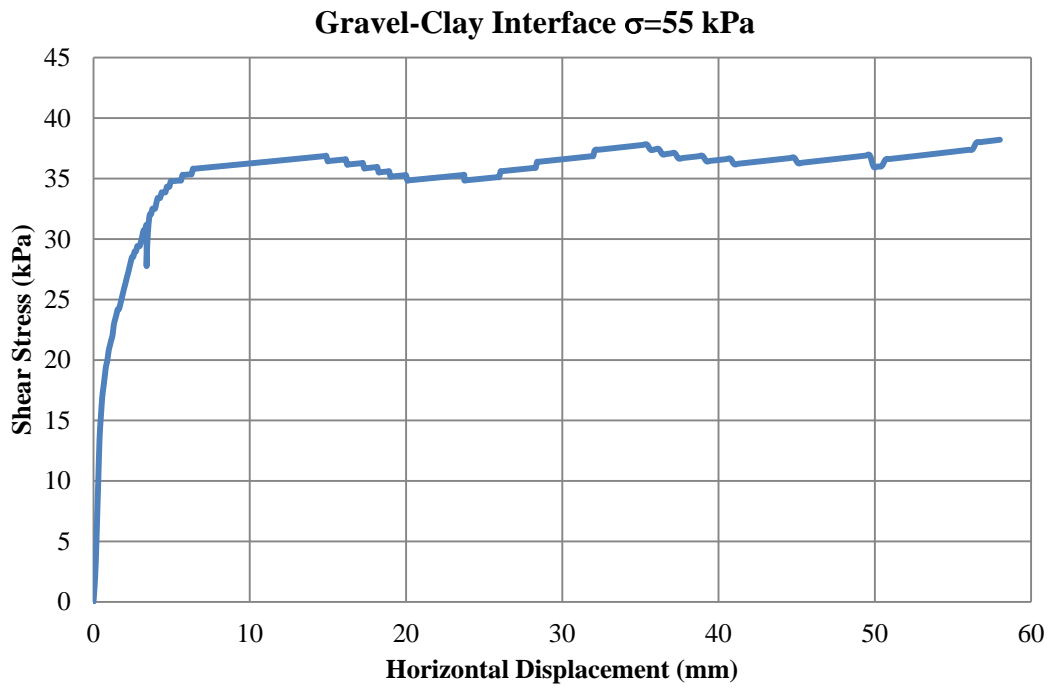


Figure A.9 Shear Stress vs. Displacement Graph-Experiment 2

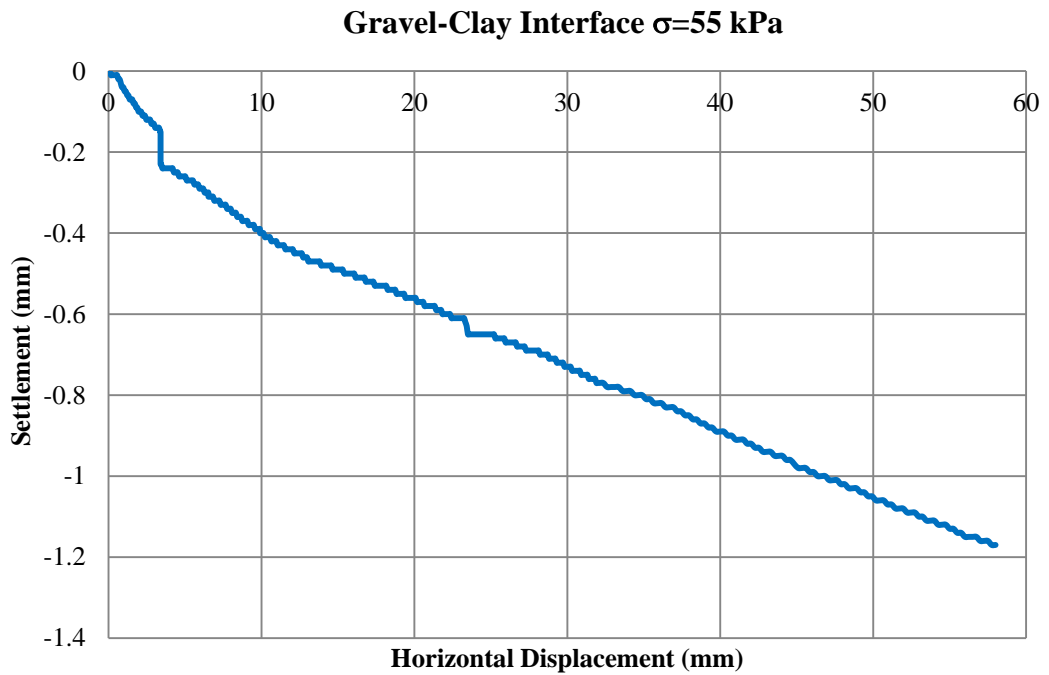


Figure A.10 Settlement vs. Displacement Graph- Experiment 2

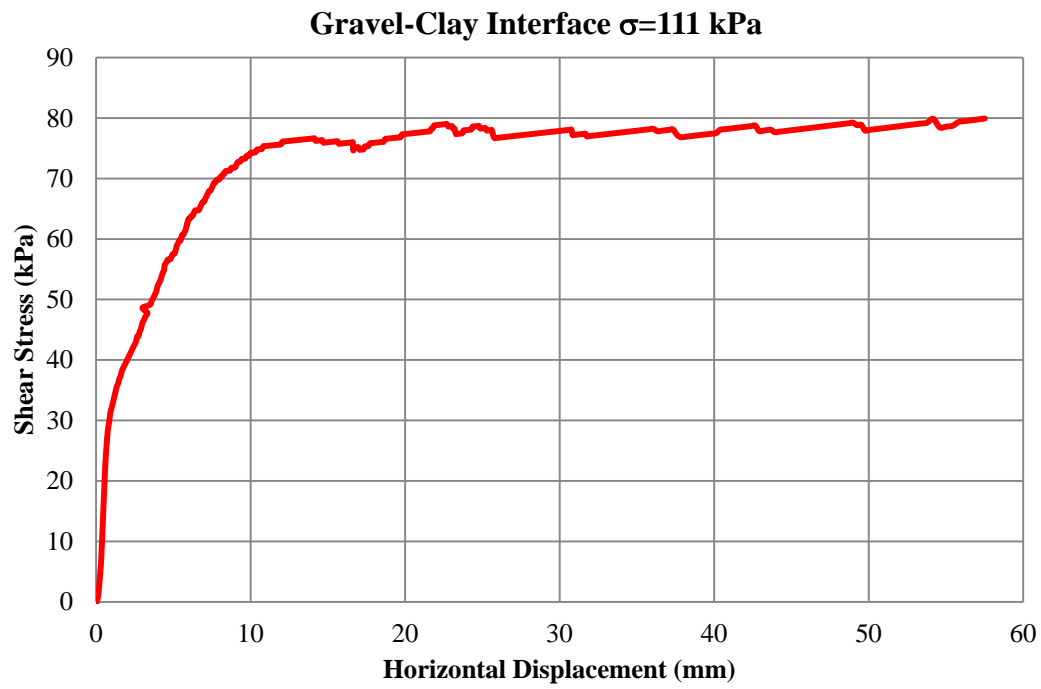


Figure A.11 Shear Stress vs. Displacement Graph-Experiment 3

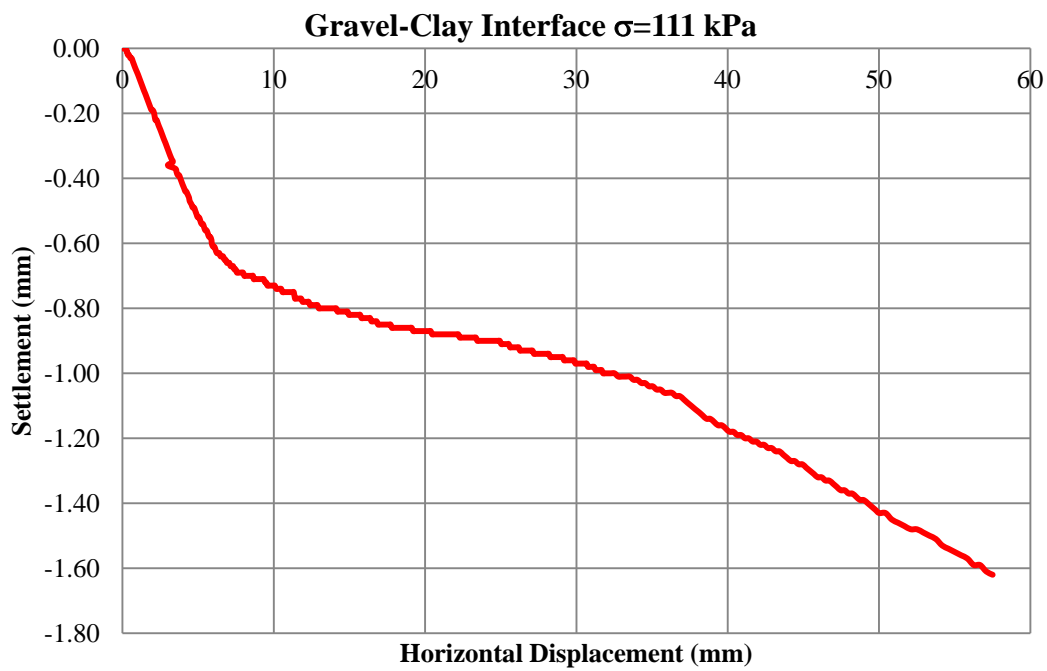


Figure A.12 Settlement vs. Displacement Graph- Experiment 3

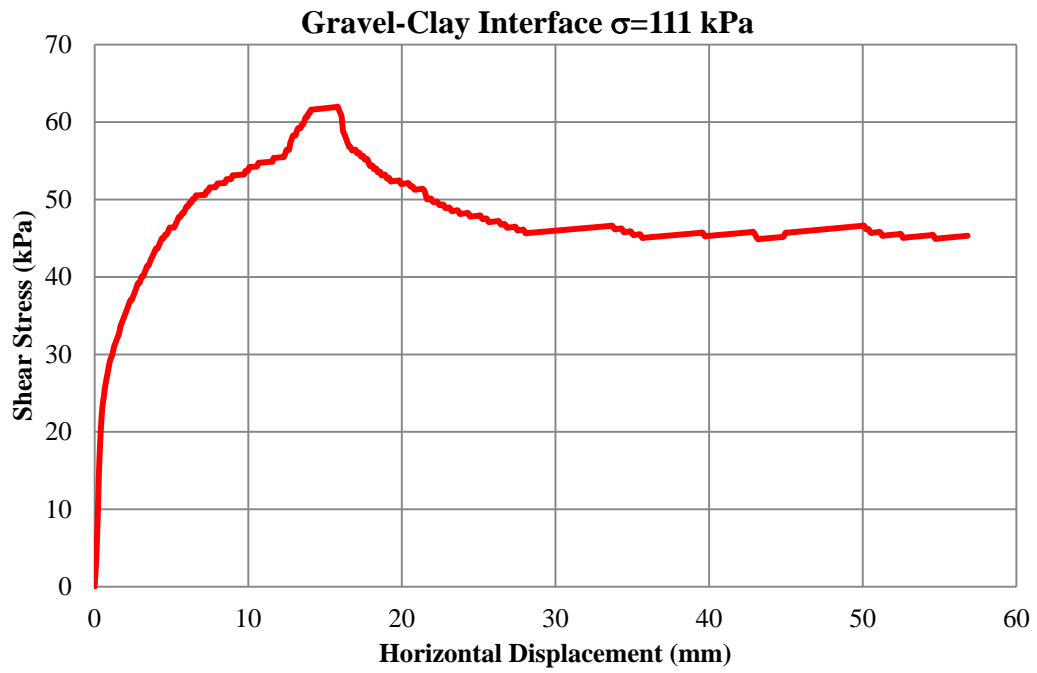


Figure A.13 Shear Stress vs. Displacement Graph-Experiment 4

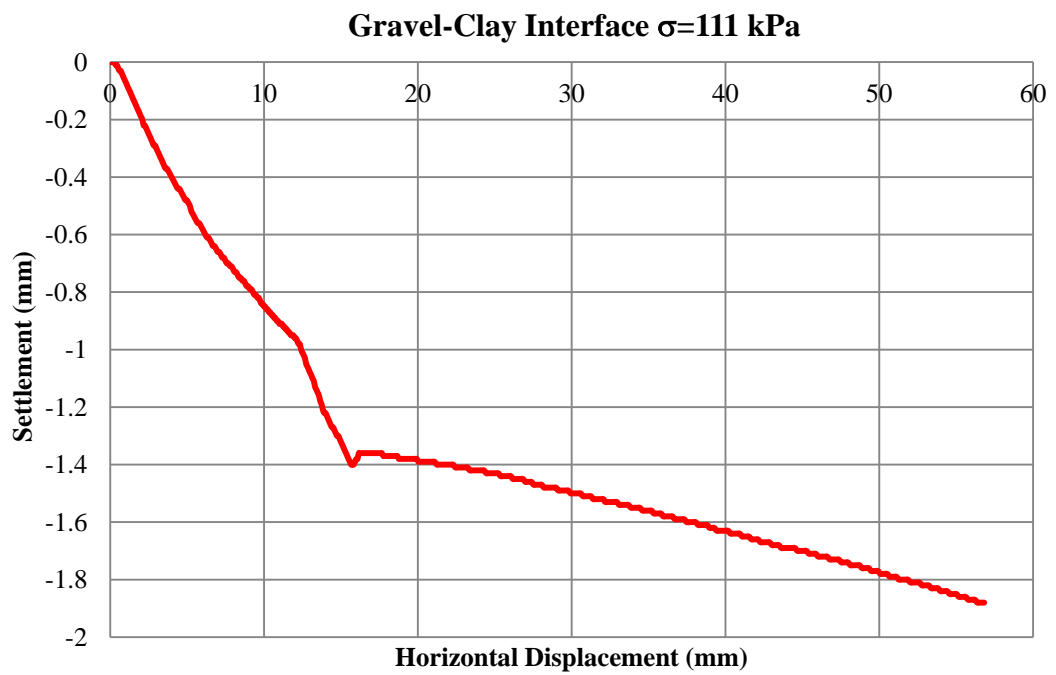


Figure A.14 Settlement vs. Displacement Graph- Experiment 4

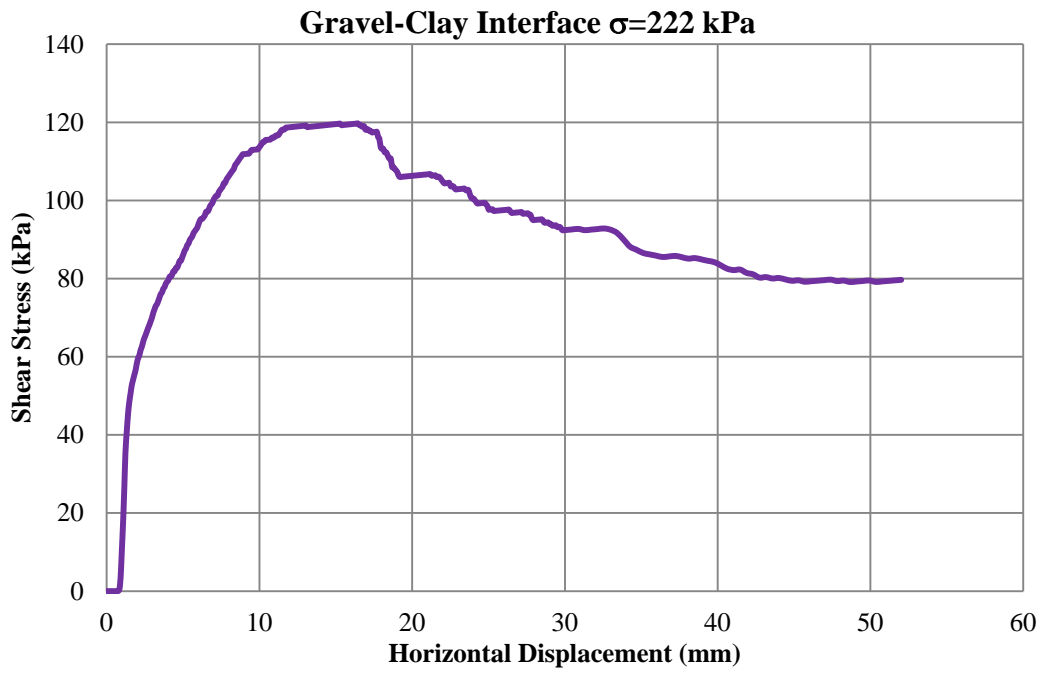


Figure A.15 Shear Stress vs. Displacement Graph-Experiment 5

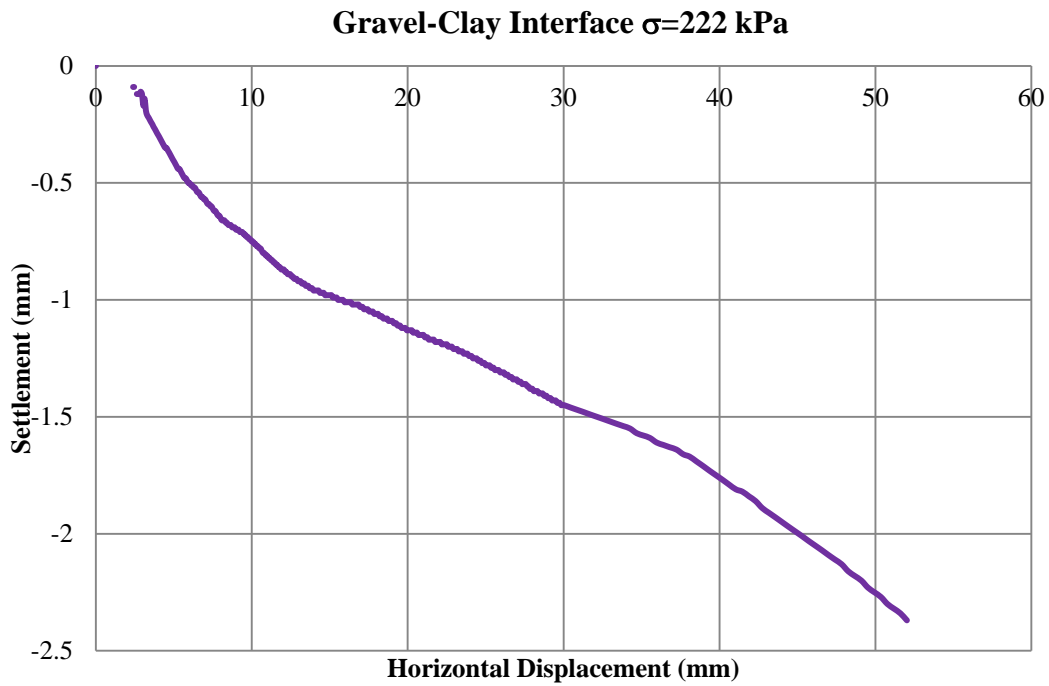


Figure A.16 Settlement vs. Displacement Graph- Experiment 5

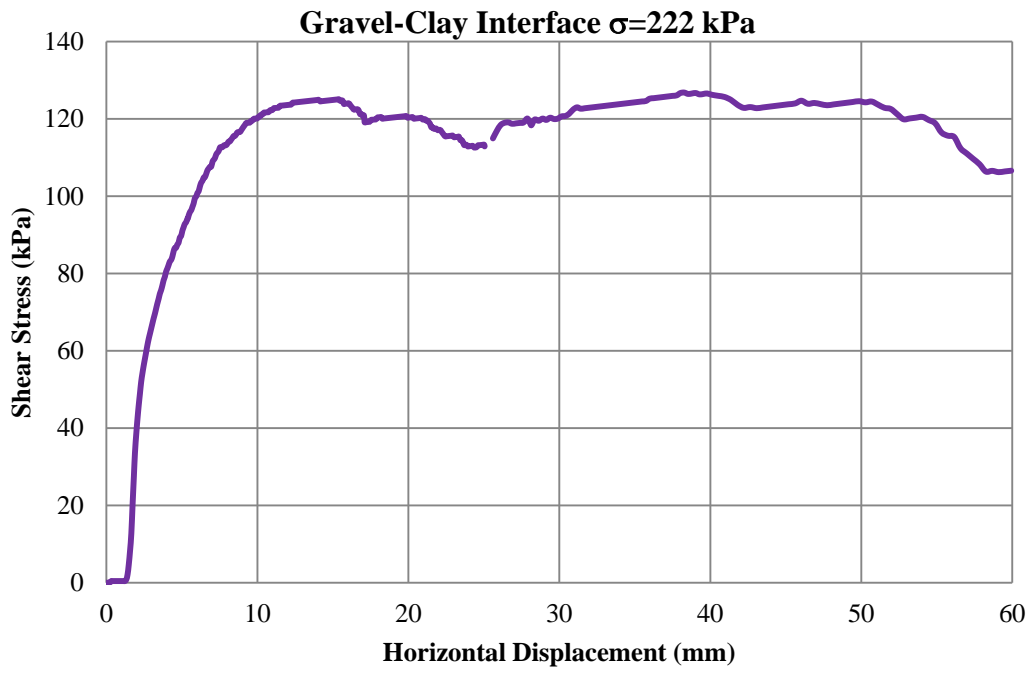


Figure A.17 Shear Stress vs. Displacement Graph-Experiment 6

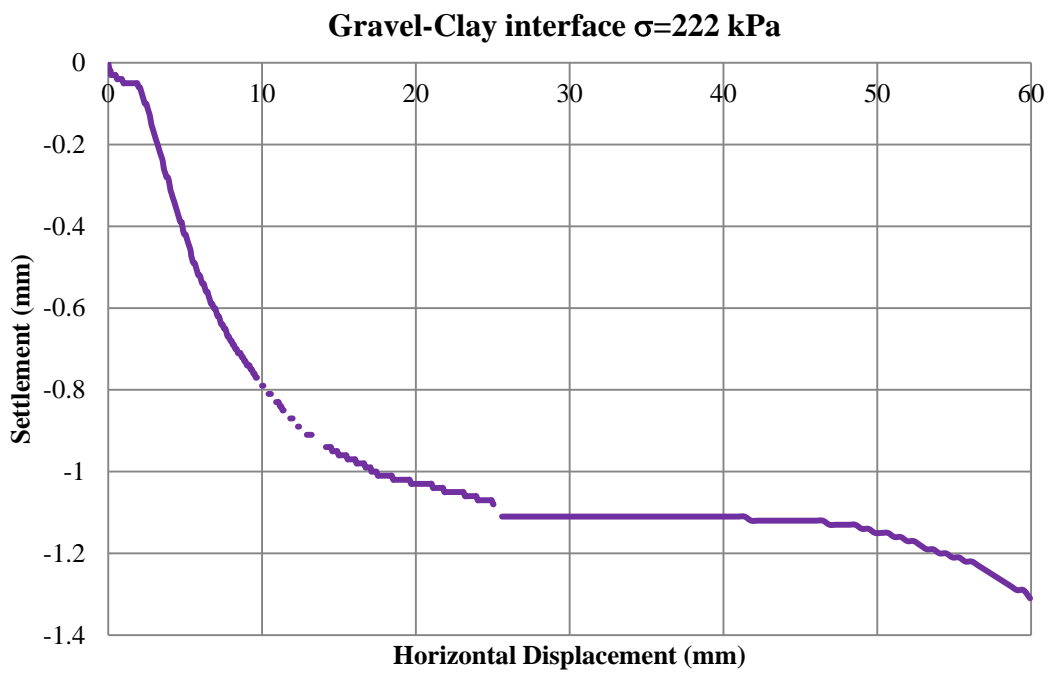


Figure A.18 Settlement vs. Displacement Graph- Experiment 6

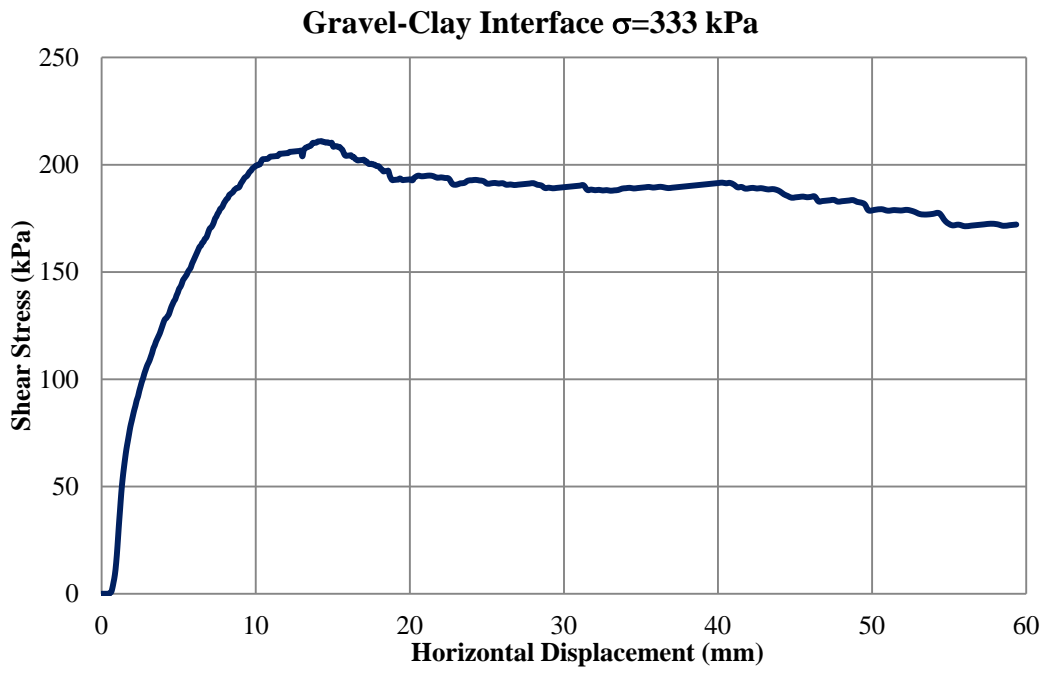


Figure A.19 Shear Stress vs. Displacement Graph-Experiment 7

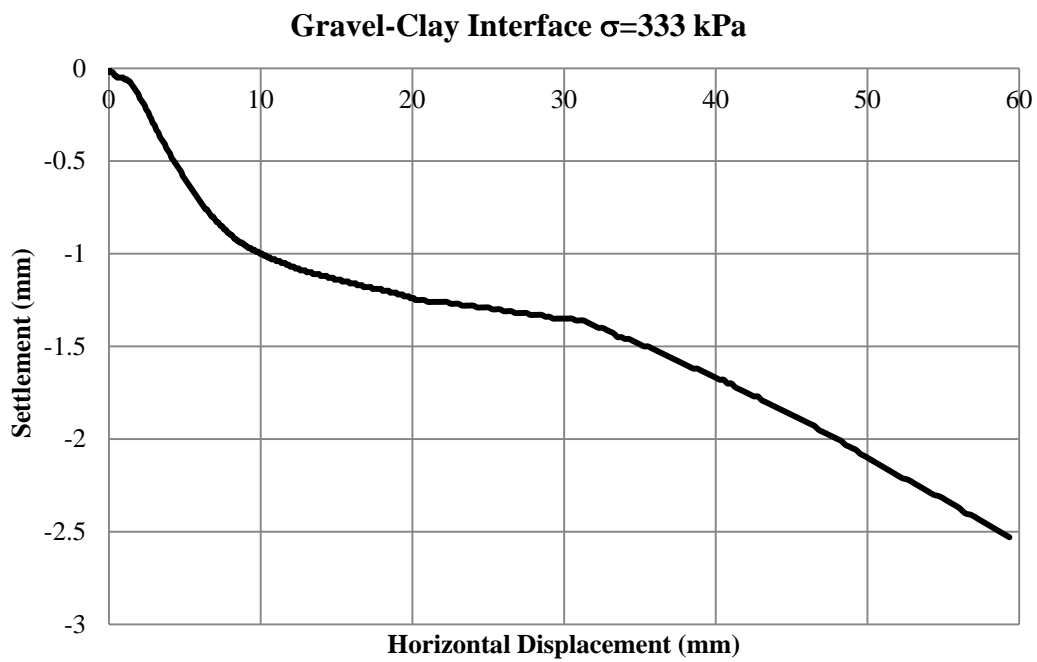


Figure A.20 Settlement vs. Displacement Graph- Experiment 7

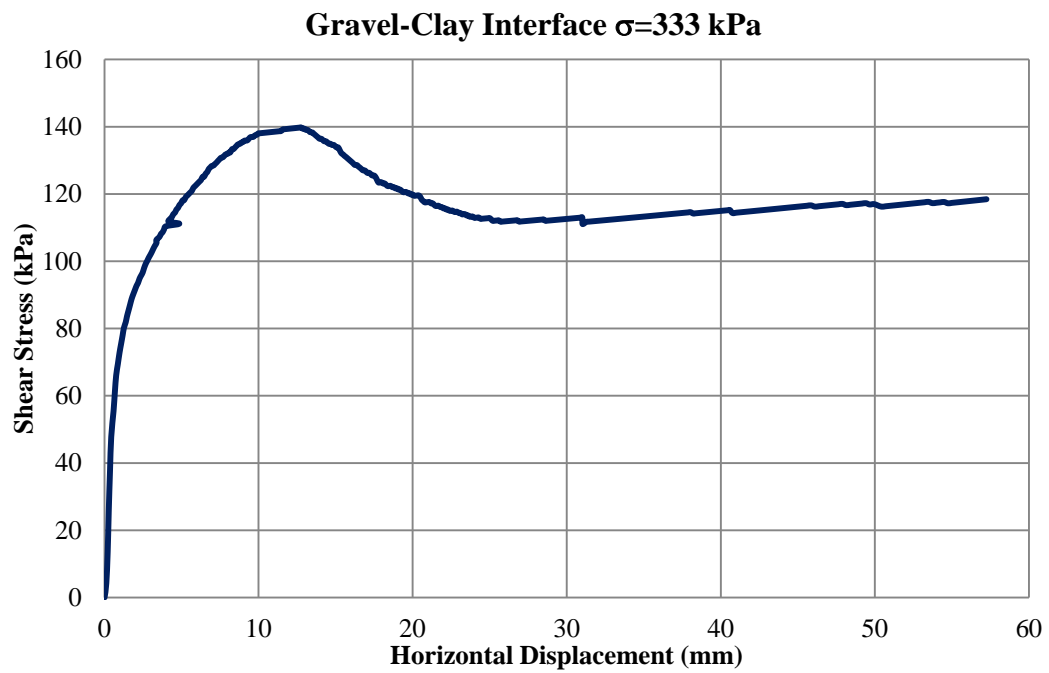


Figure A.21 Shear Stress vs. Displacement Graph-Experiment 8

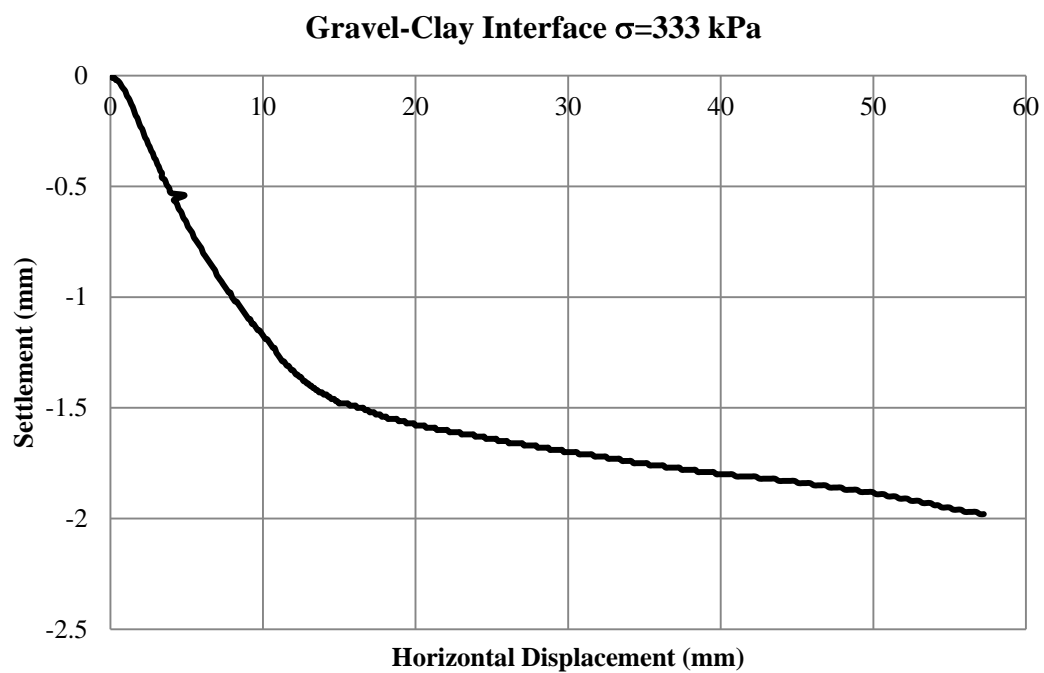


Figure A.22 Settlement vs. Displacement Graph- Experiment 8

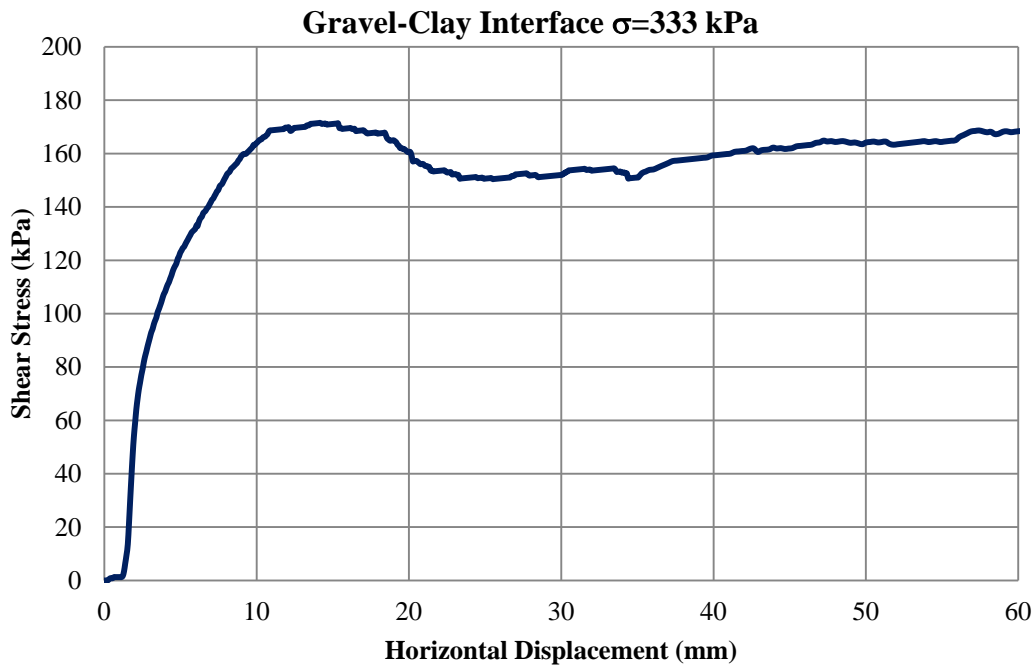


Figure A.23 Shear Stress vs. Displacement Graph-Experiment 9

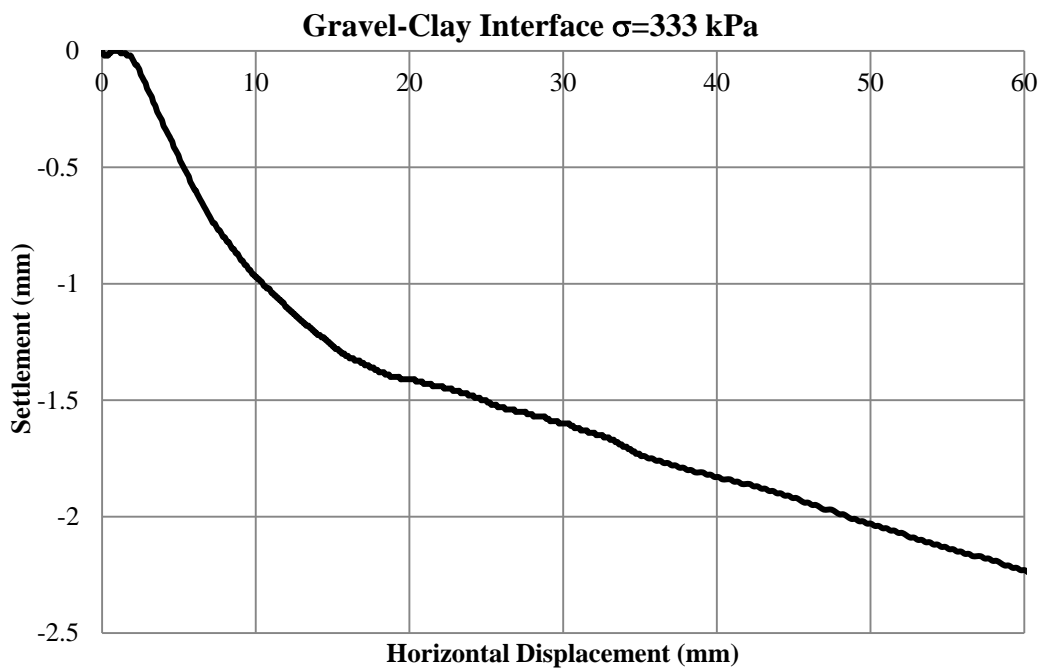


Figure A.24 Settlement vs. Displacement Graph- Experiment 9

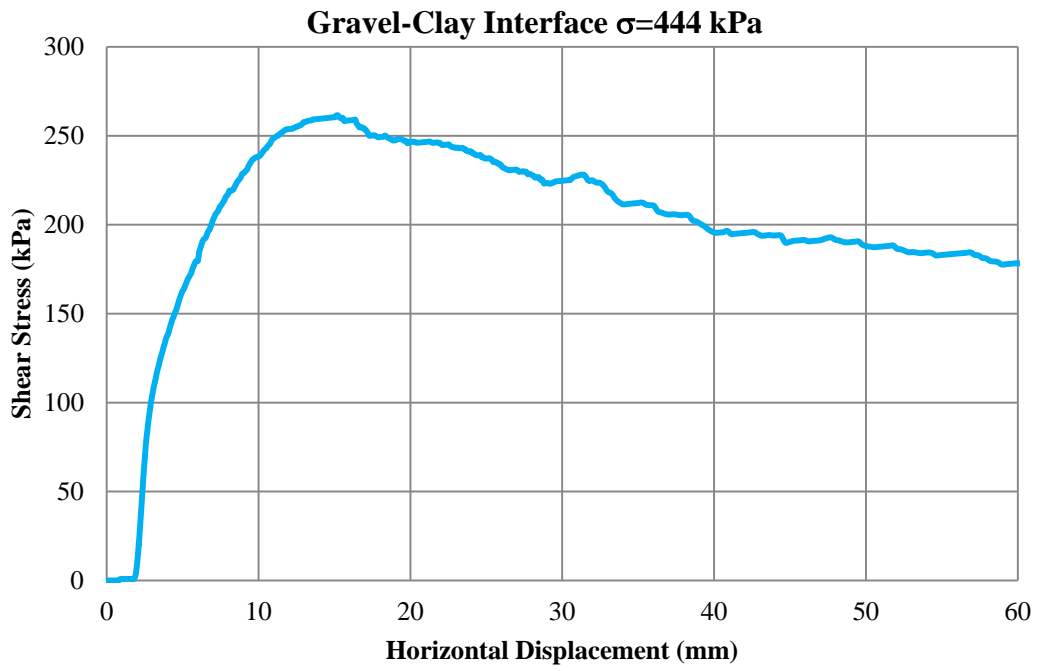


Figure A.25 Shear Stress vs. Displacement Graph-Experiment 10

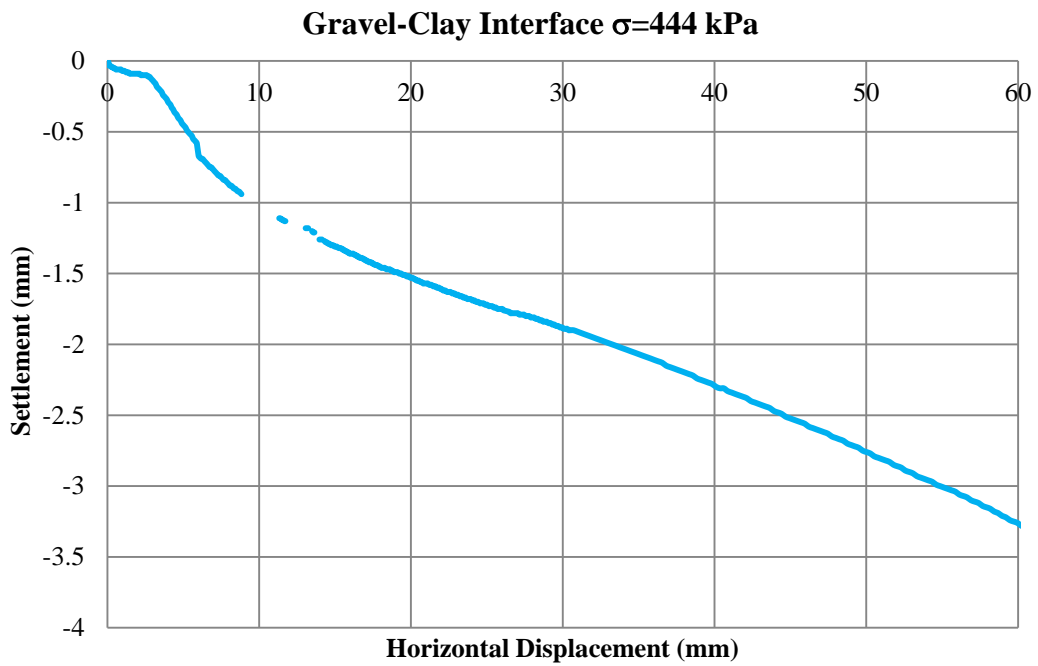


Figure A.26 Settlement vs. Displacement Graph- Experiment 10

## 2. Small Shear Box Tests

### a. Small Shear Tests of Clay

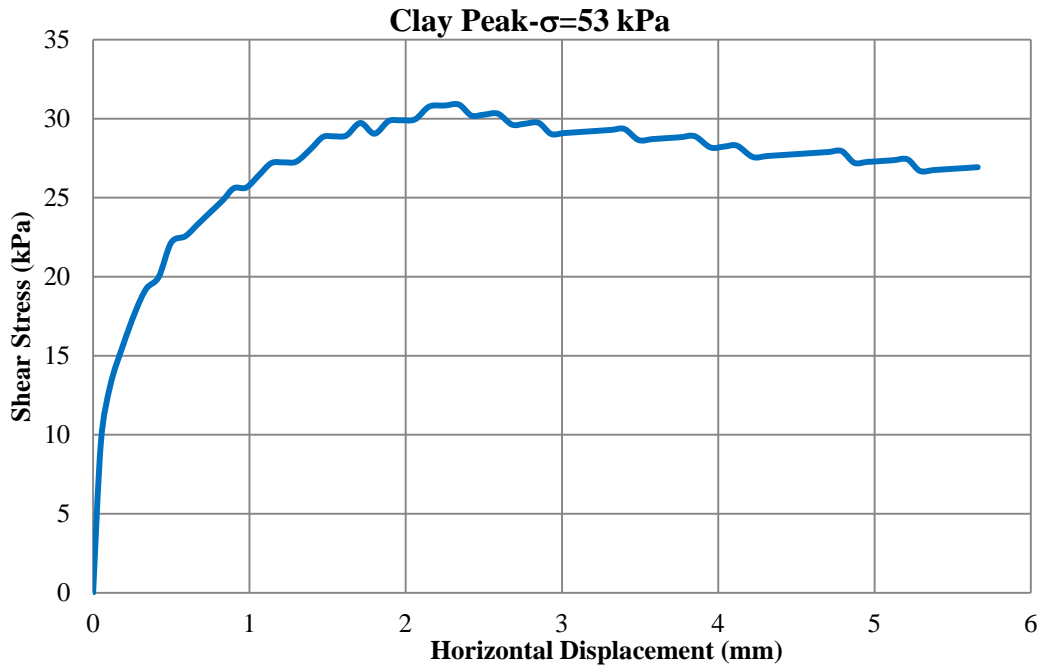


Figure A.27 Shear Stress vs. Displacement Graph-Experiment 1

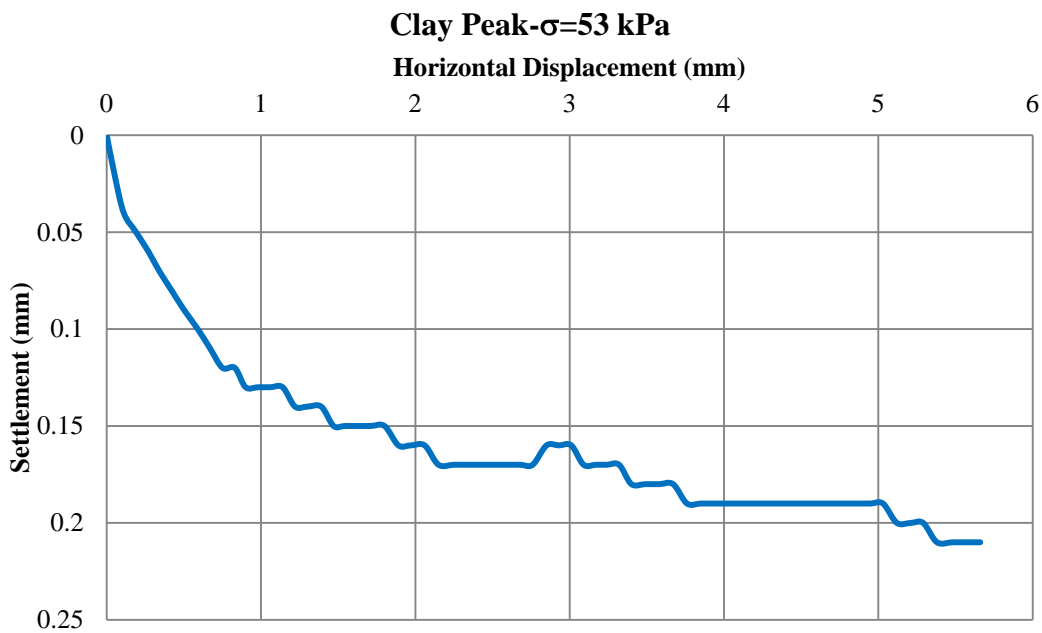


Figure A.28 Settlement vs. Displacement Graph- Experiment 1

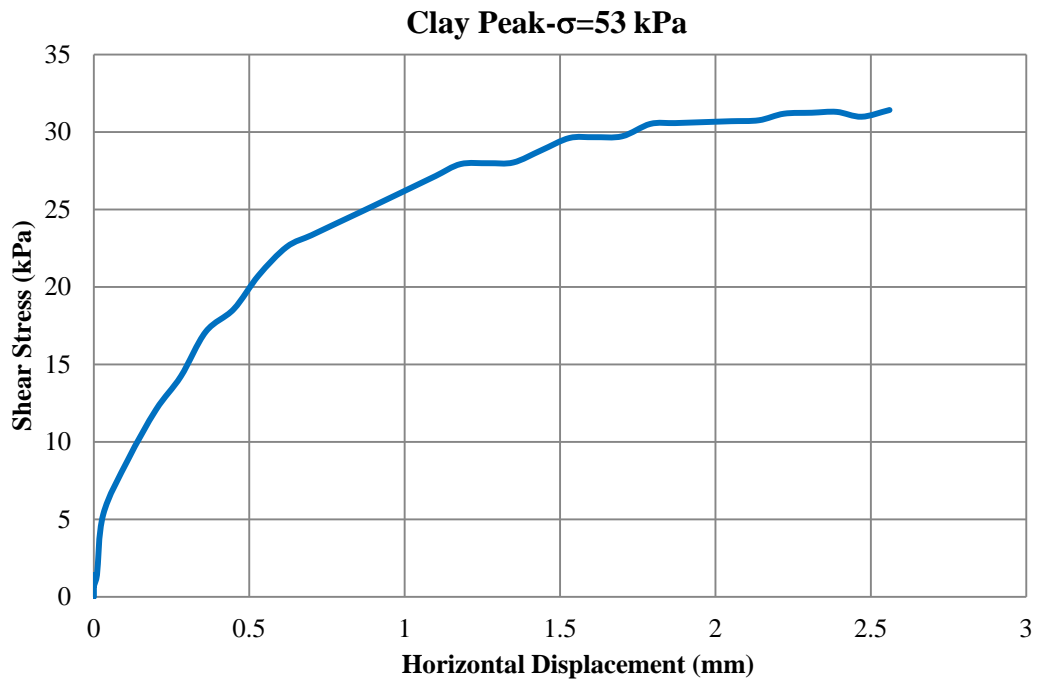


Figure A.29 Shear Stress vs. Displacement Graph-Experiment 2

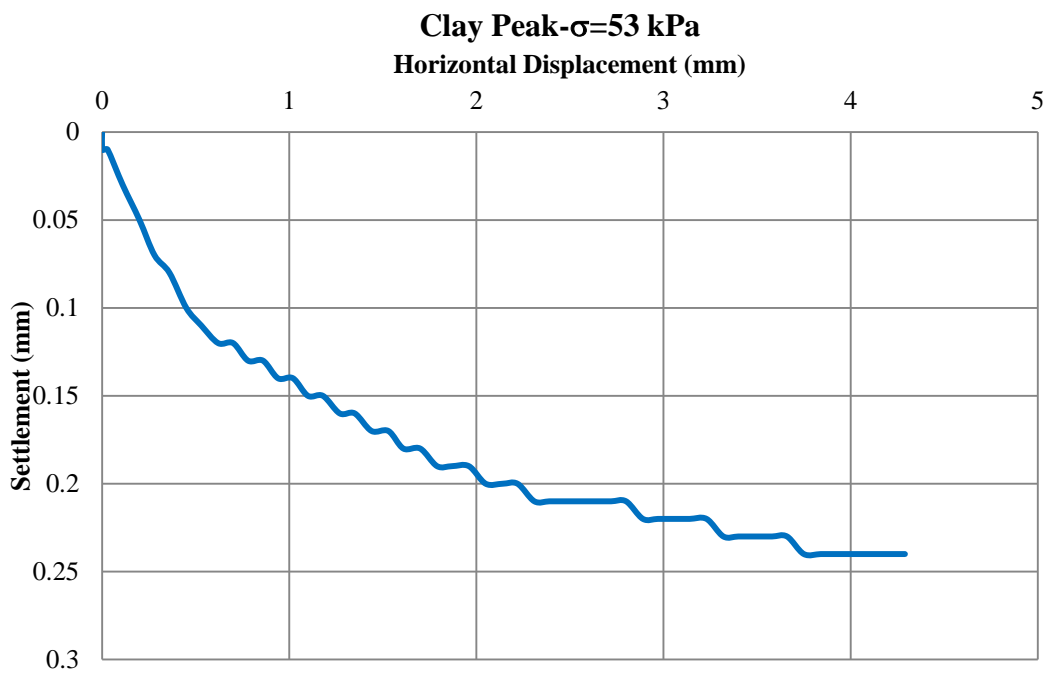


Figure A.30 Settlement vs. Displacement Graph- Experiment 2

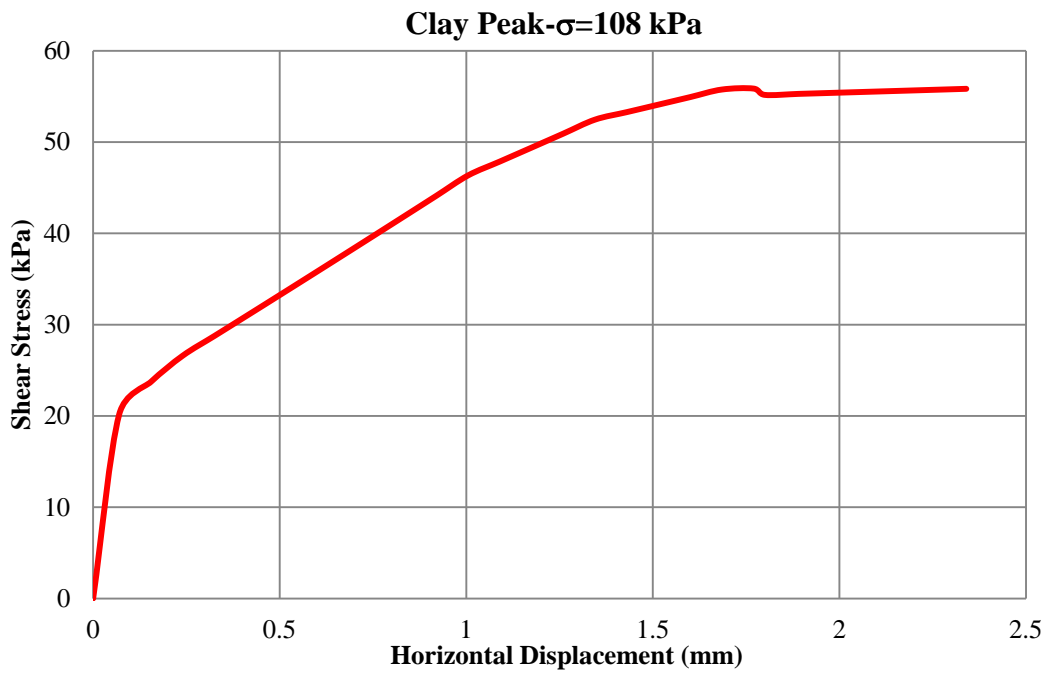


Figure A.31 Shear Stress vs. Displacement Graph-Experiment 3

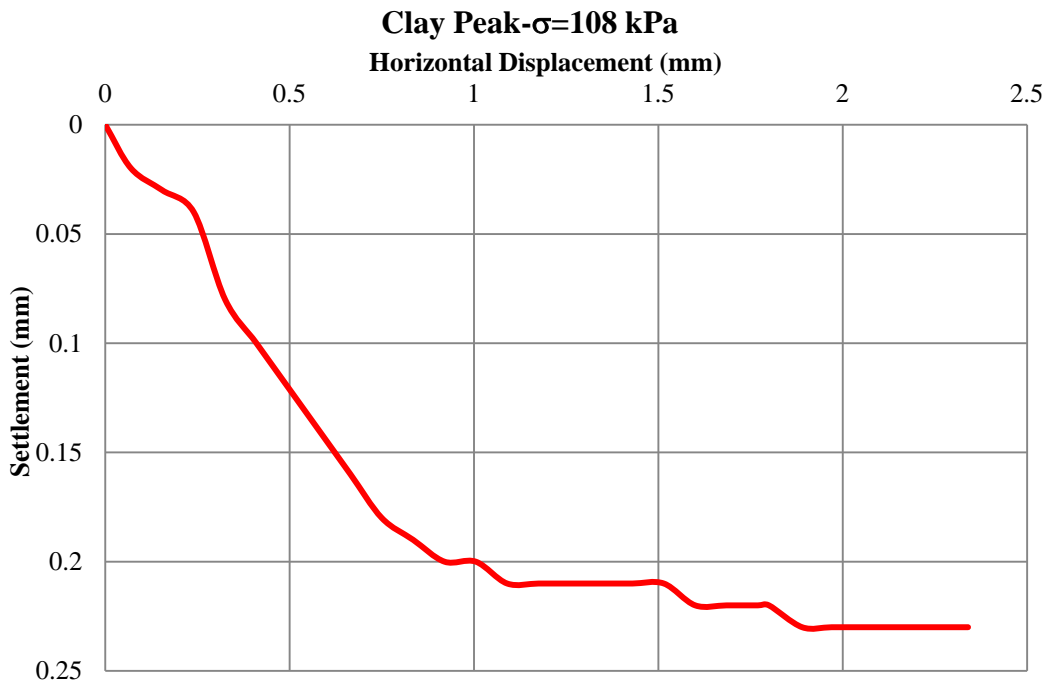


Figure A.32 Settlement vs. Displacement Graph- Experiment 3

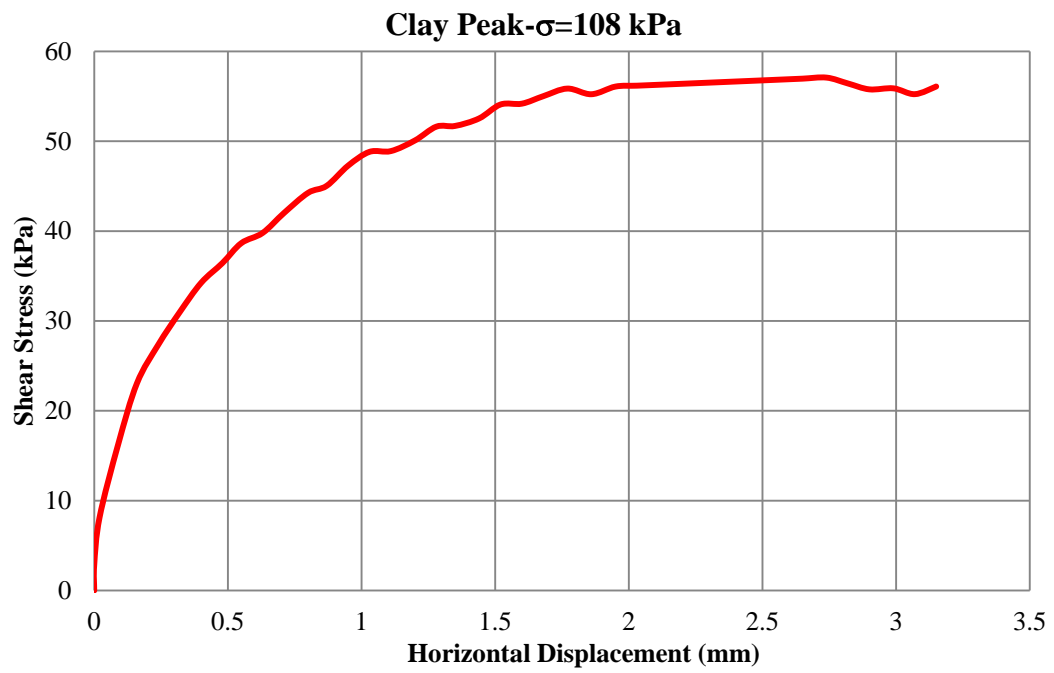


Figure A.33 Shear Stress vs. Displacement Graph-Experiment 4

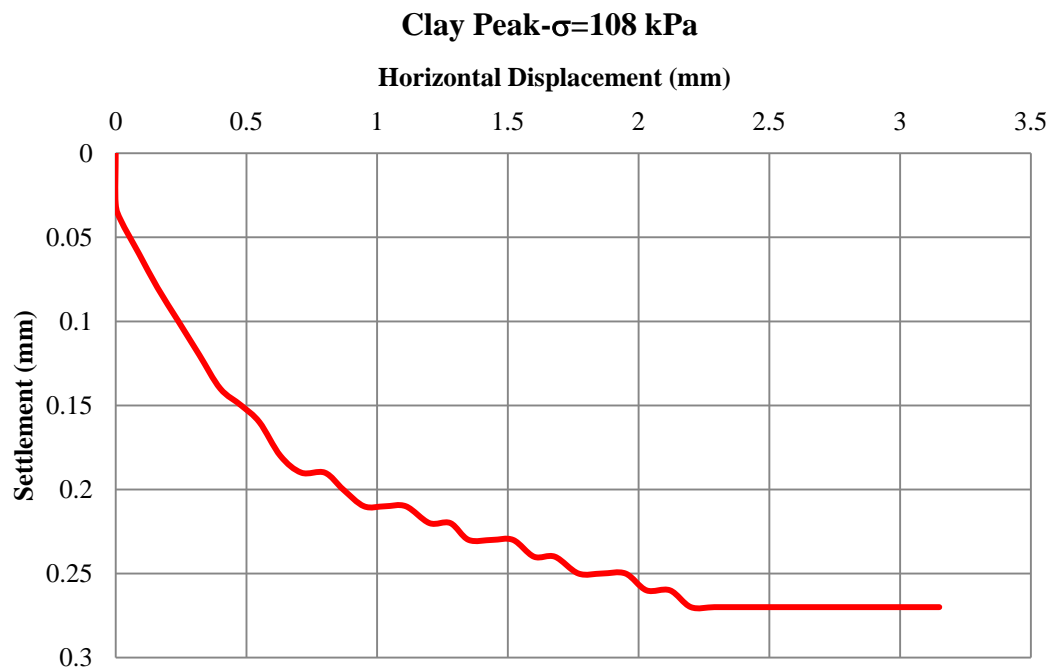


Figure A.34 Settlement vs. Displacement Graph- Experiment 4

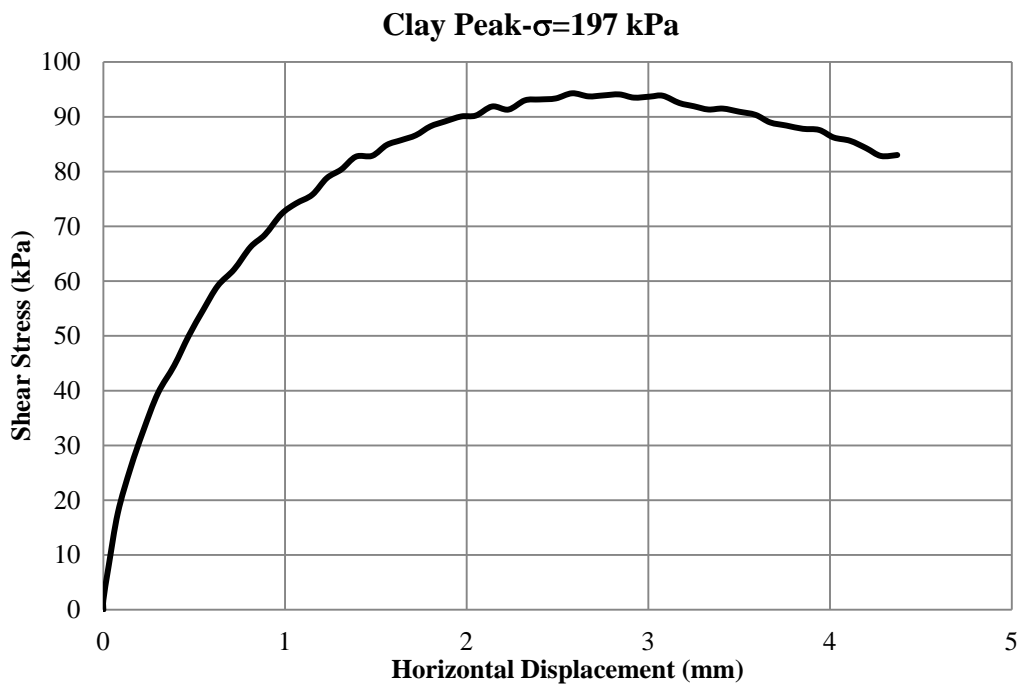


Figure A.35 Shear Stress vs. Displacement Graph-Experiment 5

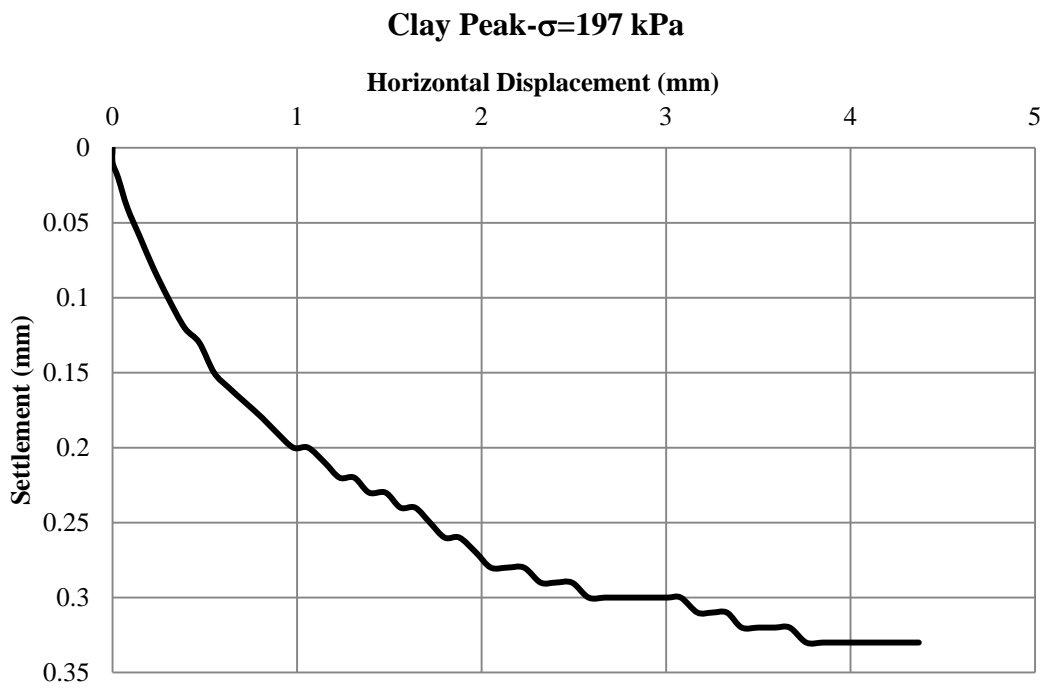


Figure A.36 Settlement vs. Displacement Graph- Experiment 5

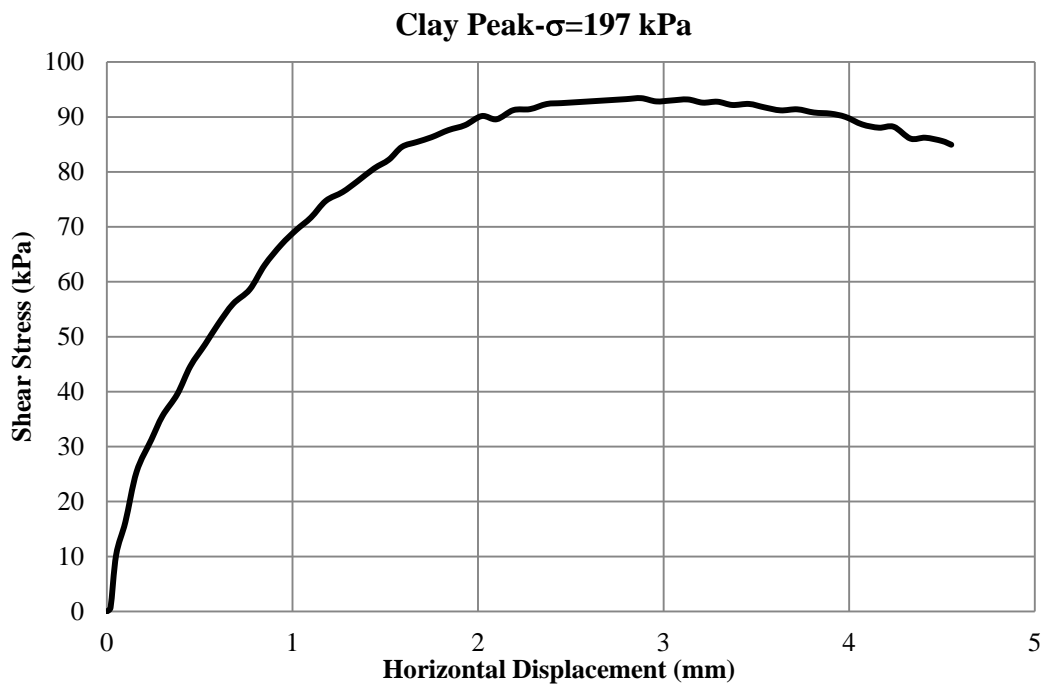


Figure A.37 Shear Stress vs. Displacement Graph-Experiment 6

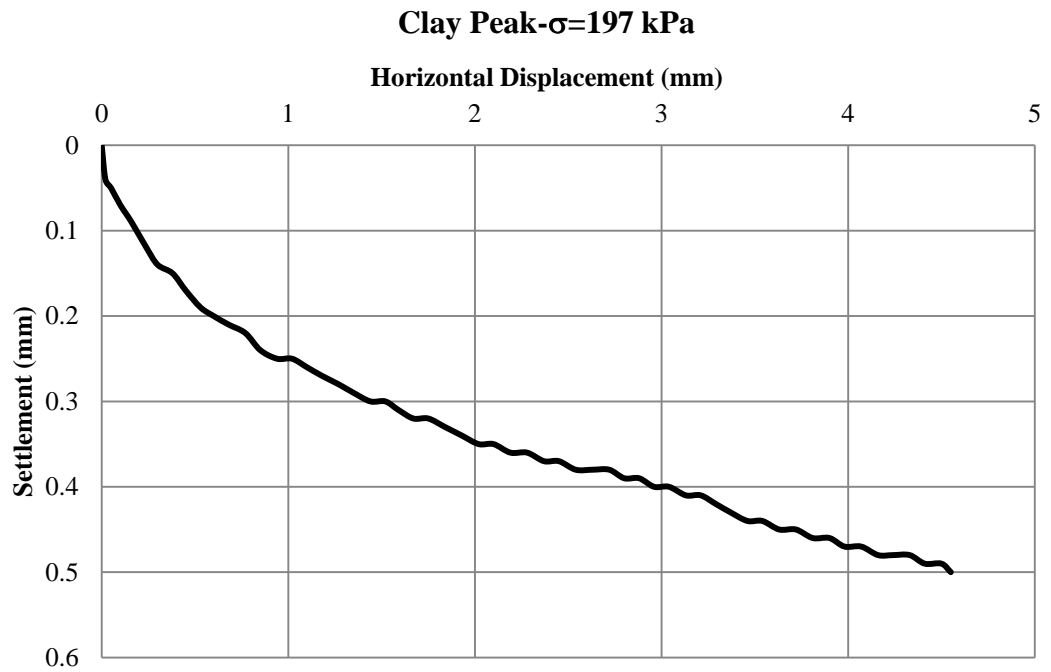


Figure A.38 Settlement vs. Displacement Graph- Experiment 6

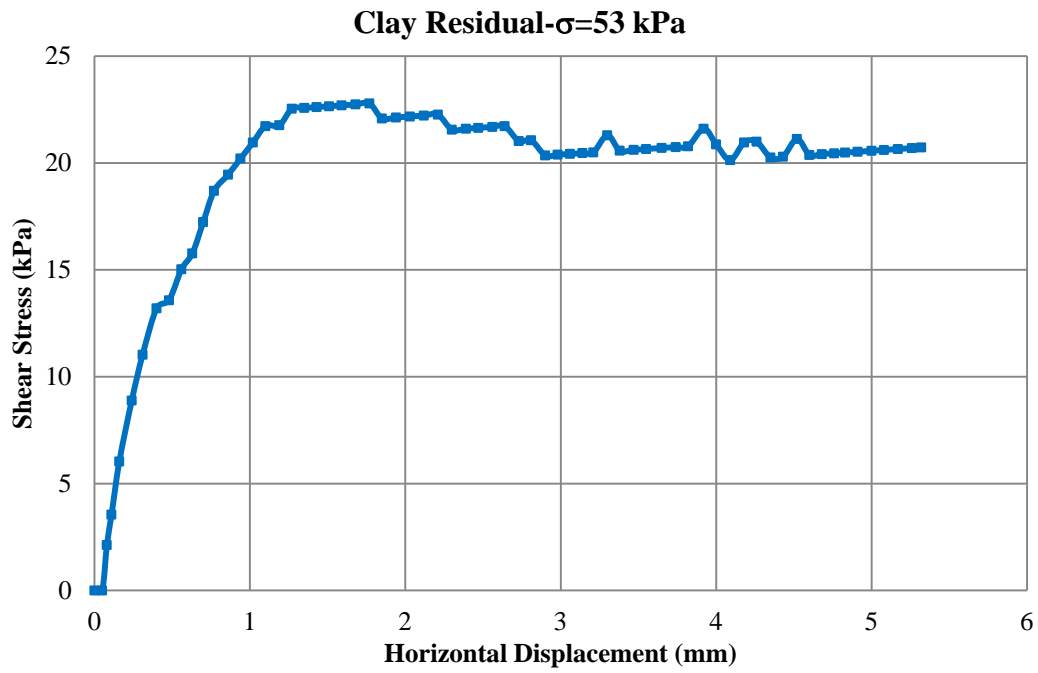


Figure A.39 Shear Stress vs. Displacement Graph-Experiment 7

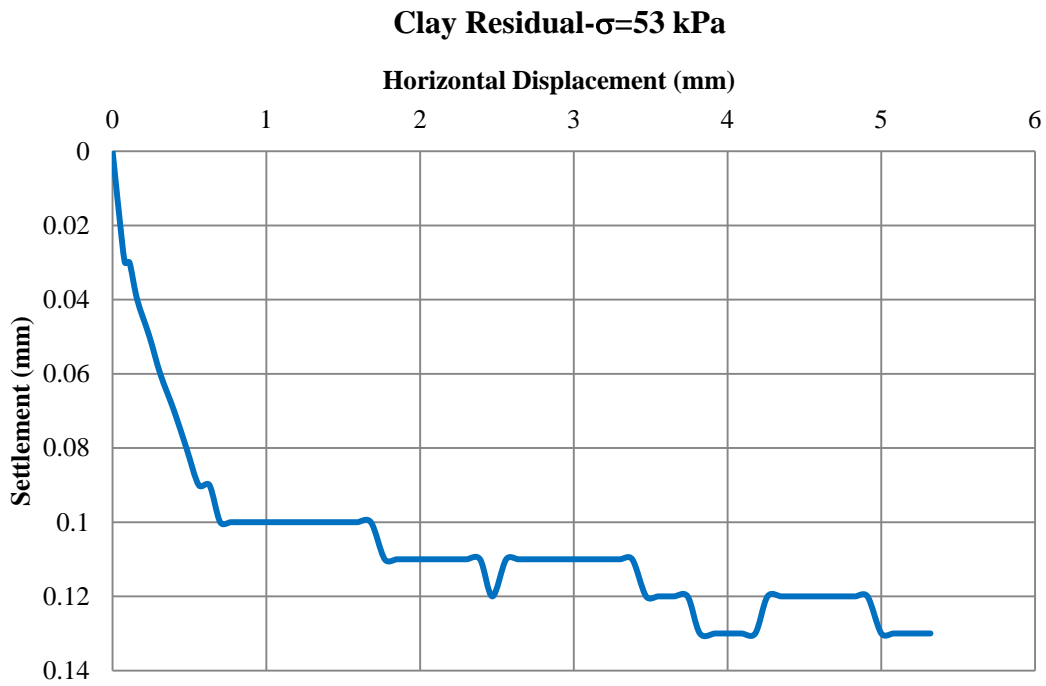


Figure A.40 Settlement vs. Displacement Graph- Experiment 7

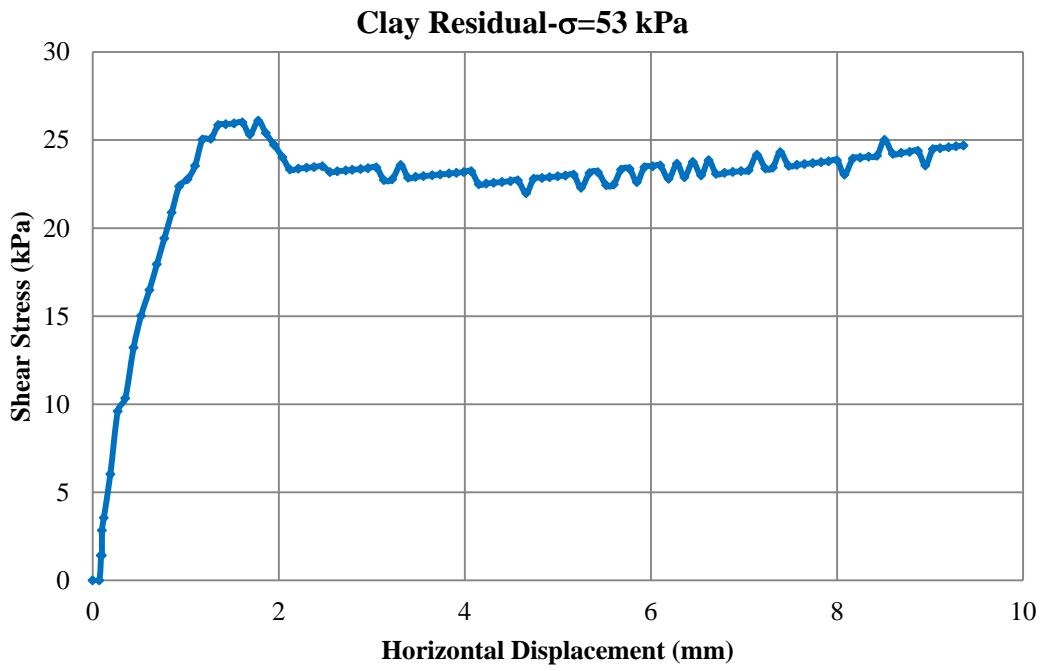


Figure A.41 Shear Stress vs. Displacement Graph-Experiment 8

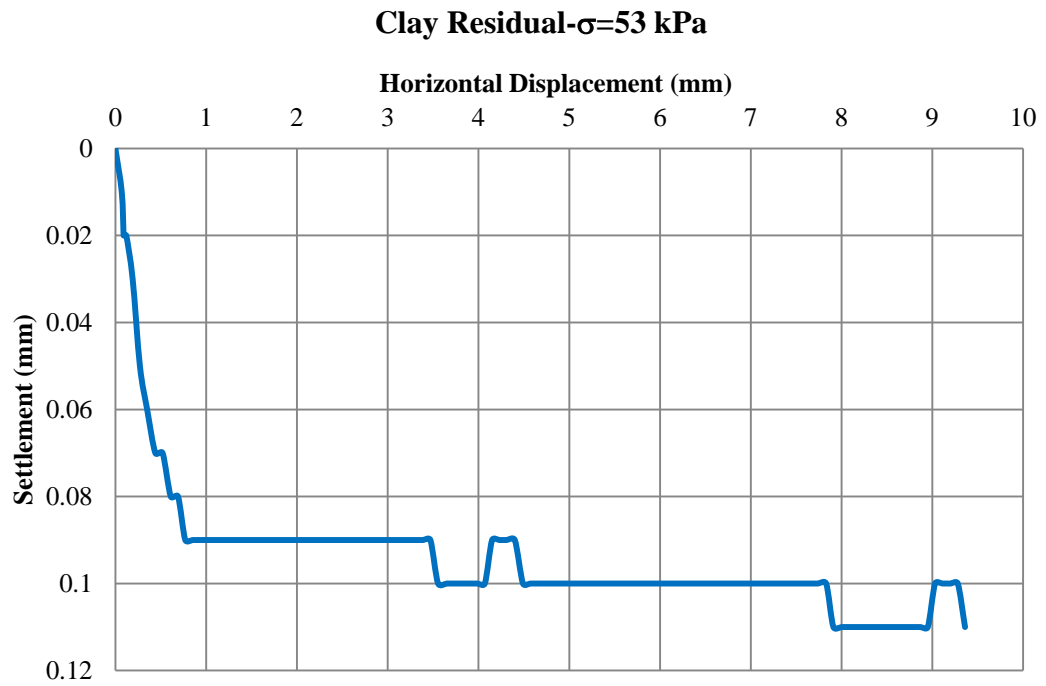


Figure A.42 Settlement vs. Displacement Graph- Experiment 8

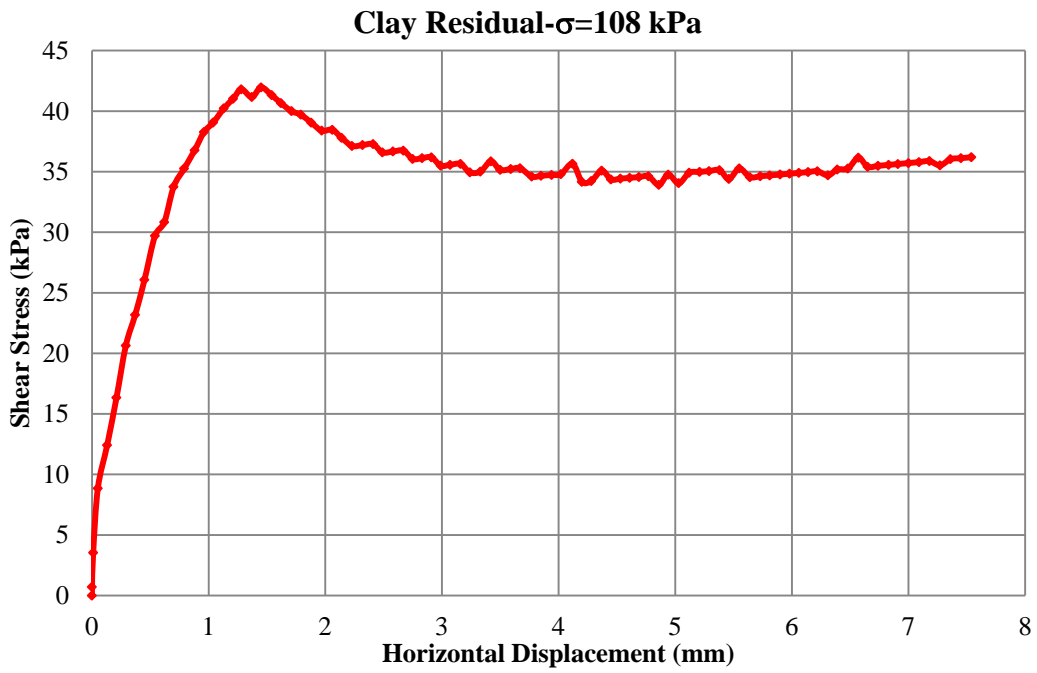


Figure A.43 Shear Stress vs. Displacement Graph-Experiment 9

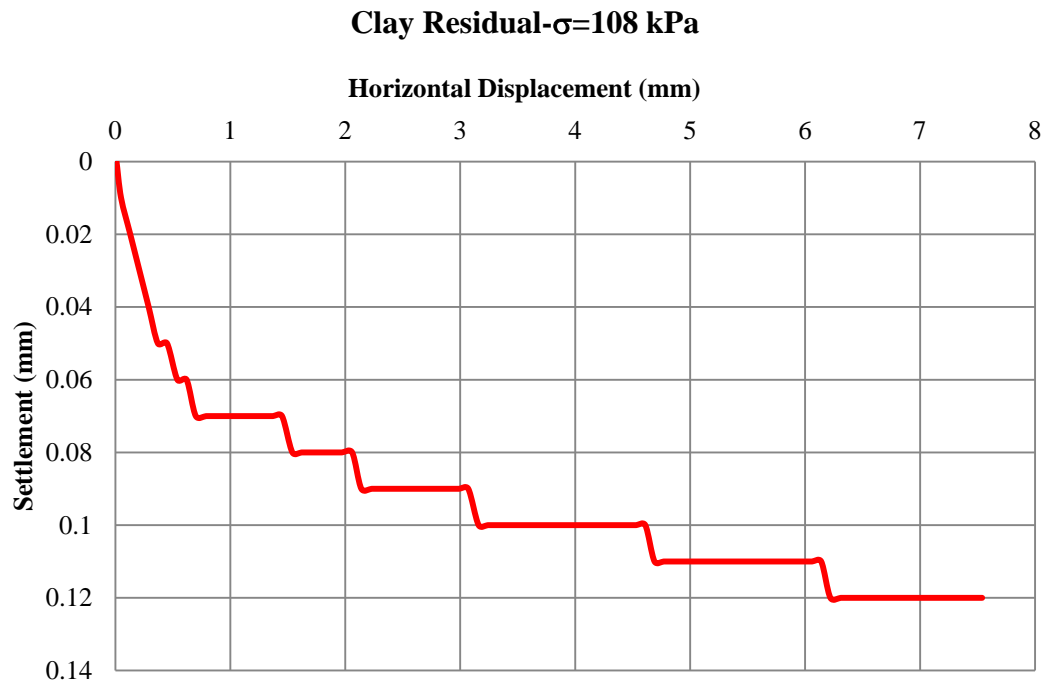


Figure A.44 Settlement vs. Displacement Graph- Experiment 9

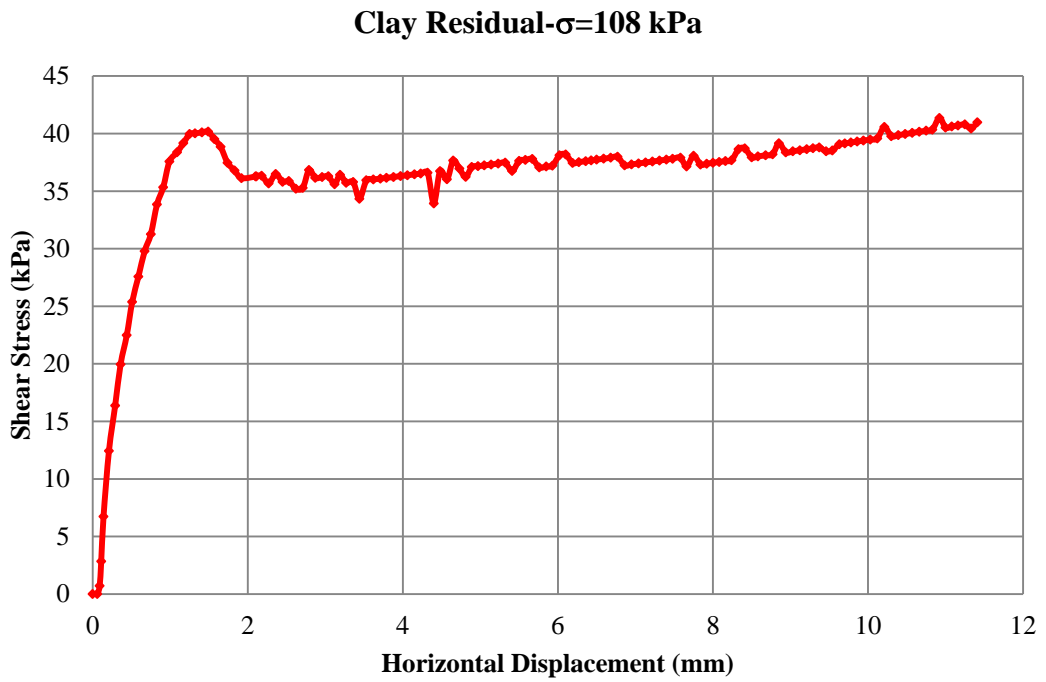


Figure A.45 Shear Stress vs. Displacement Graph-Experiment 10

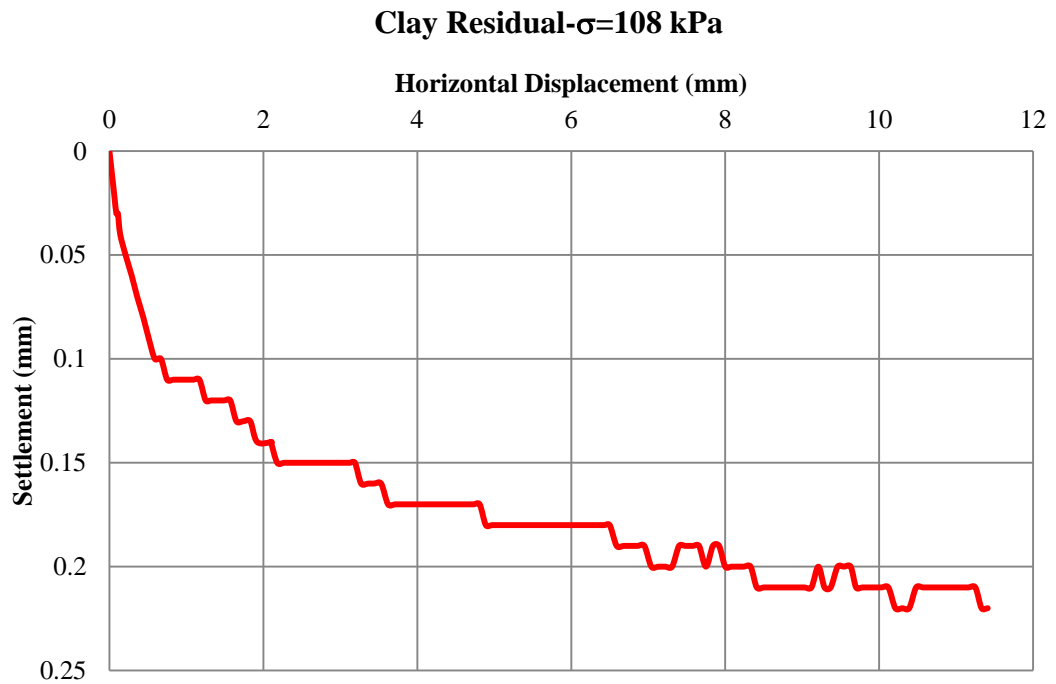


Figure A.46 Settlement vs. Displacement Graph- Experiment 10

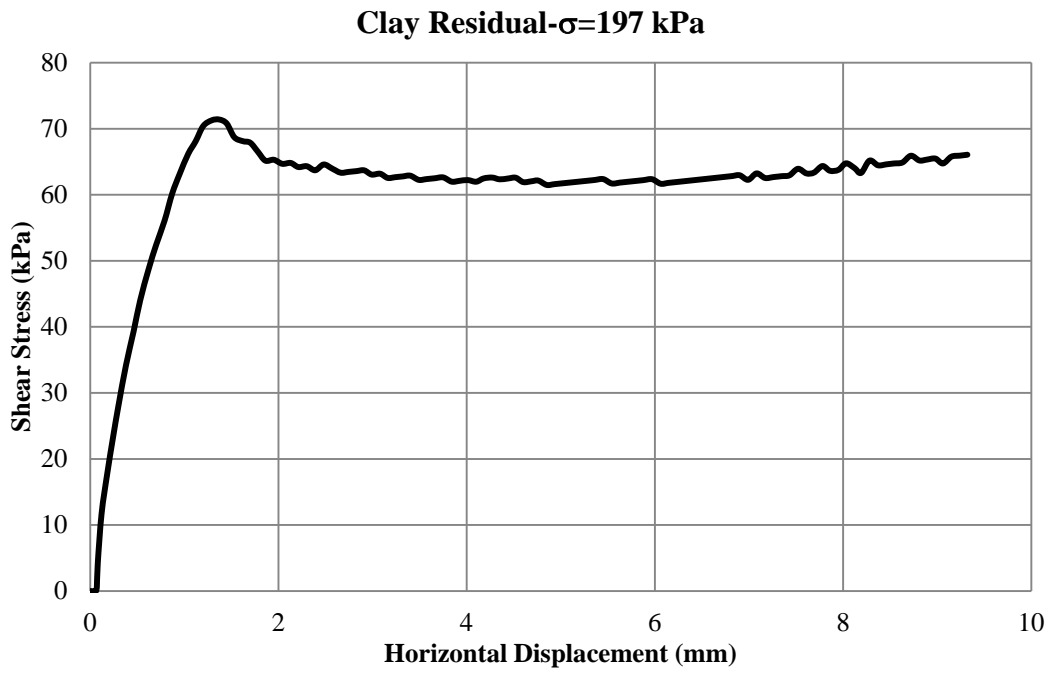


Figure A.47 Shear Stress vs. Displacement Graph-Experiment 11

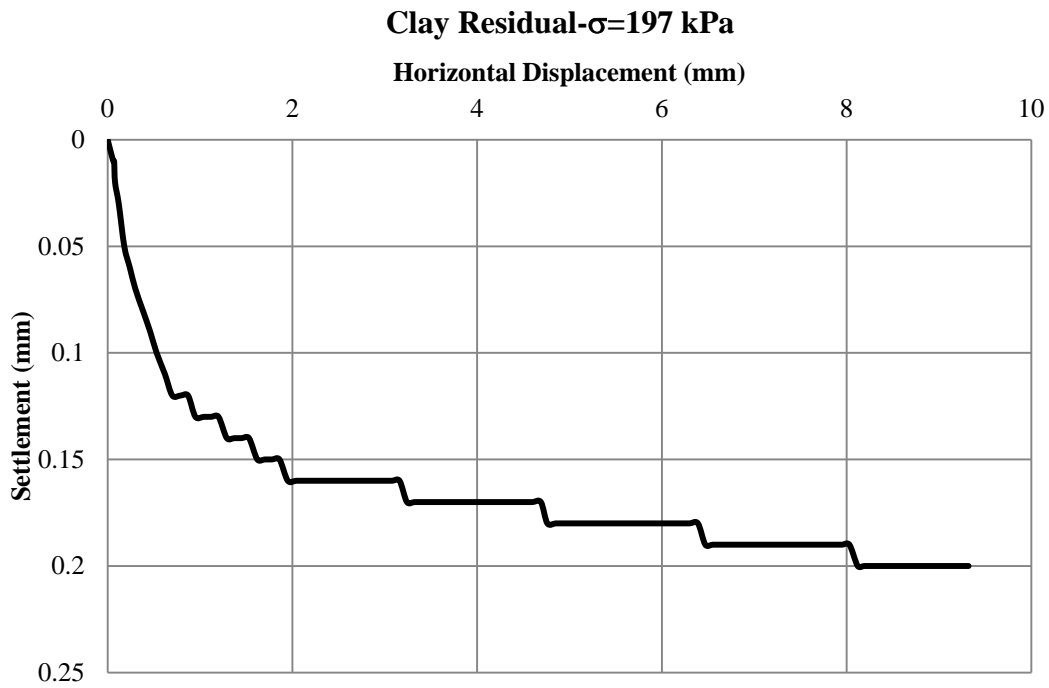


Figure A.48 Settlement vs. Displacement Graph- Experiment 11

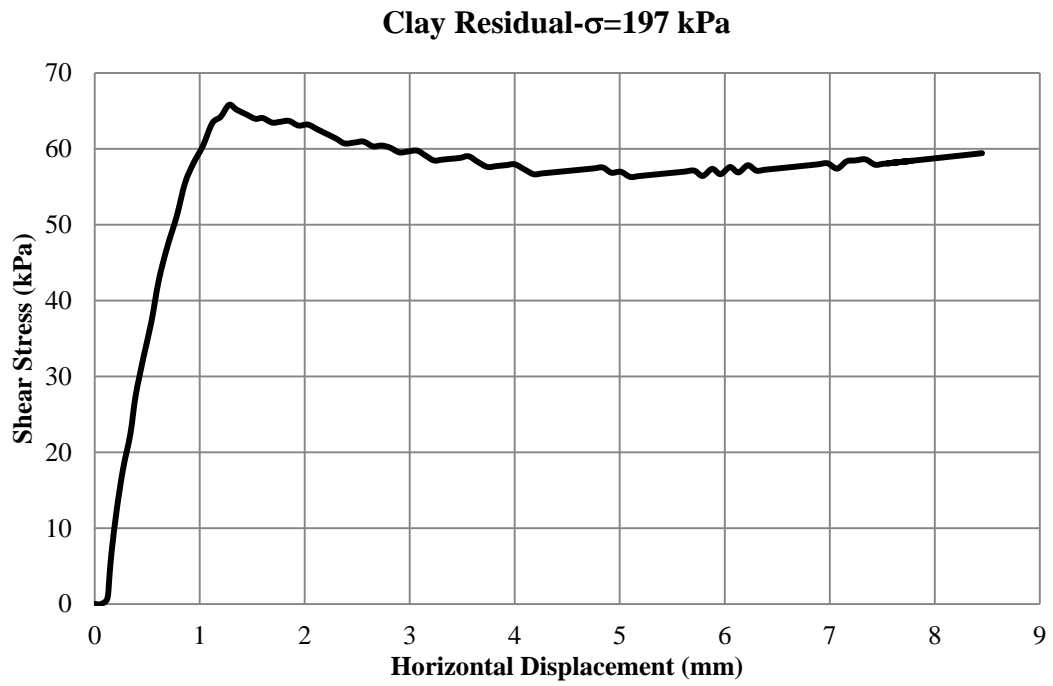


Figure A.49 Shear Stress vs. Displacement Graph-Experiment 12

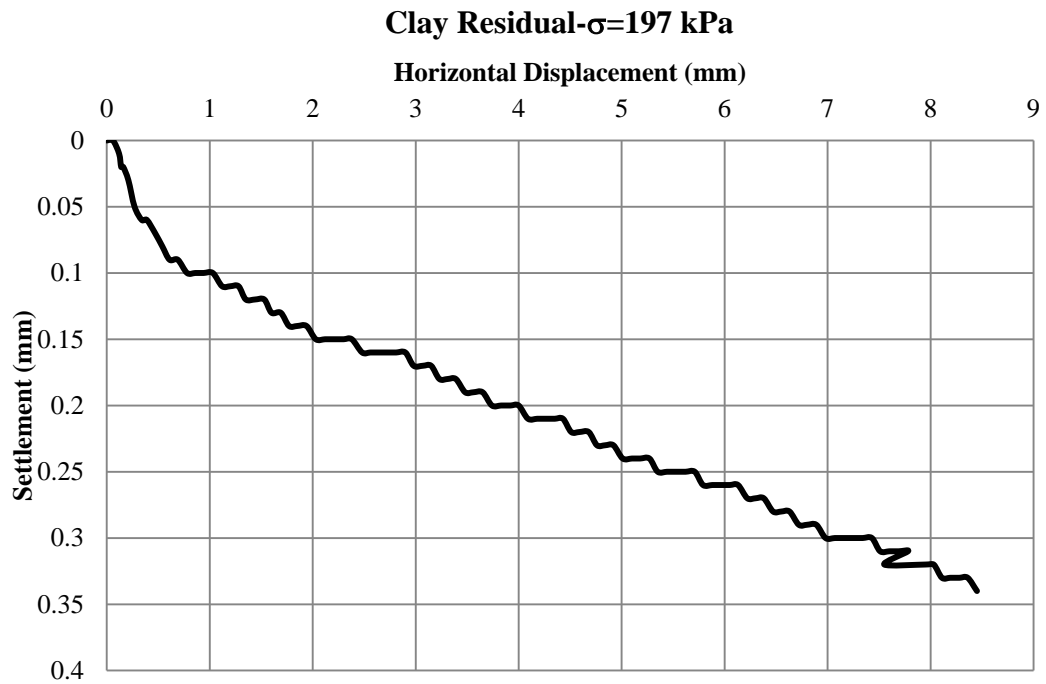


Figure A.50 Settlement vs. Displacement Graph- Experiment 12

**b. Small Shear Tests of Sand**

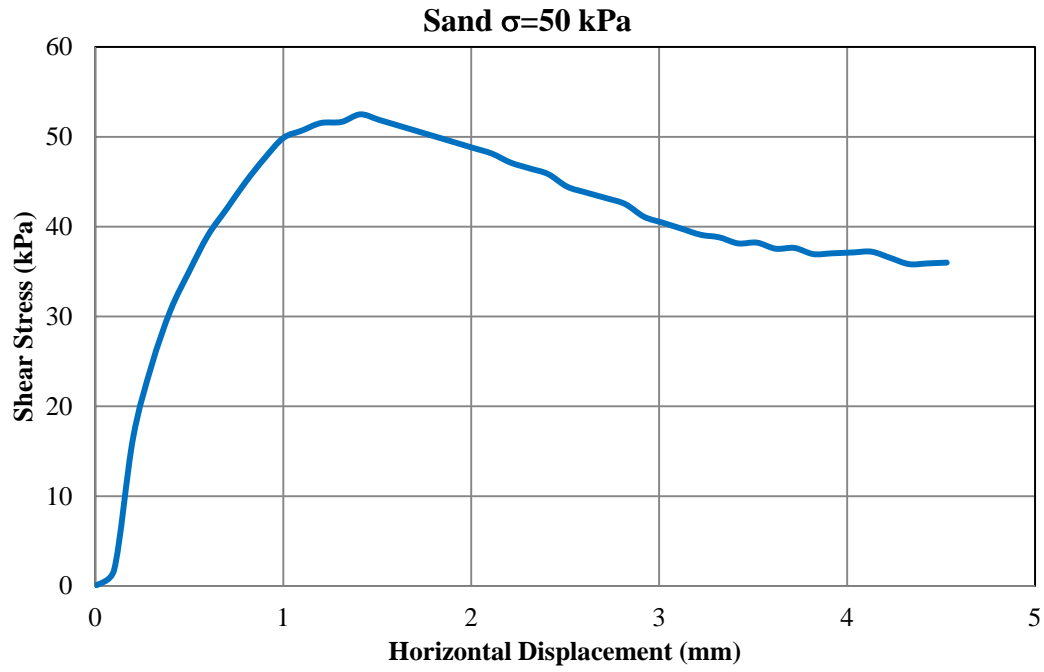


Figure A.51 Shear Stress vs. Displacement Graph-Experiment 1

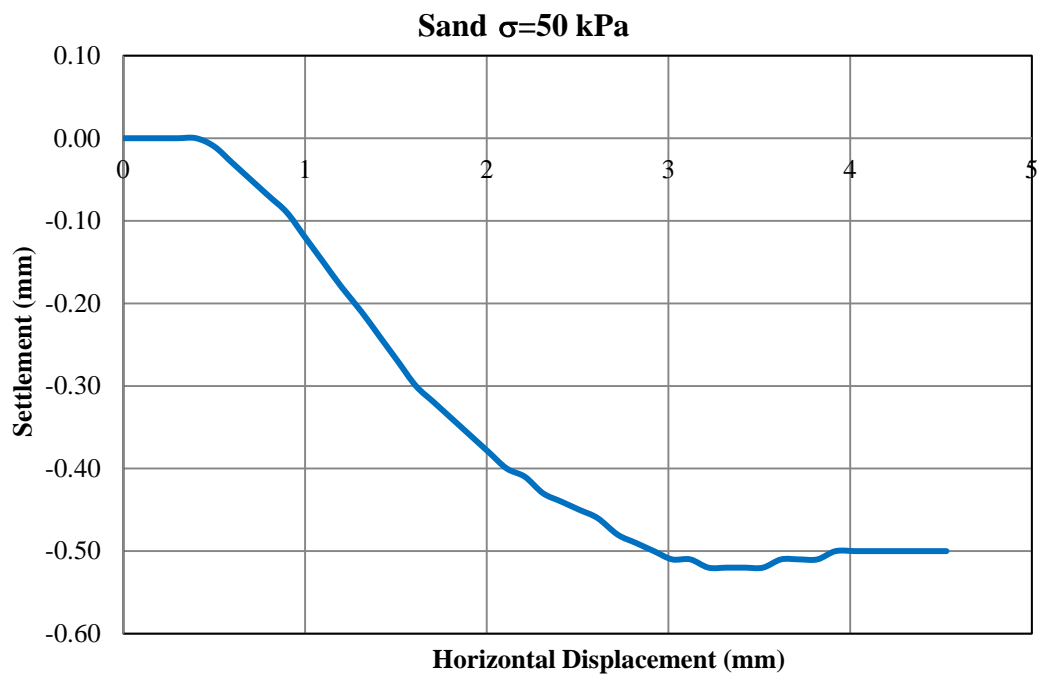


Figure A.52 Settlement vs. Displacement Graph- Experiment 1

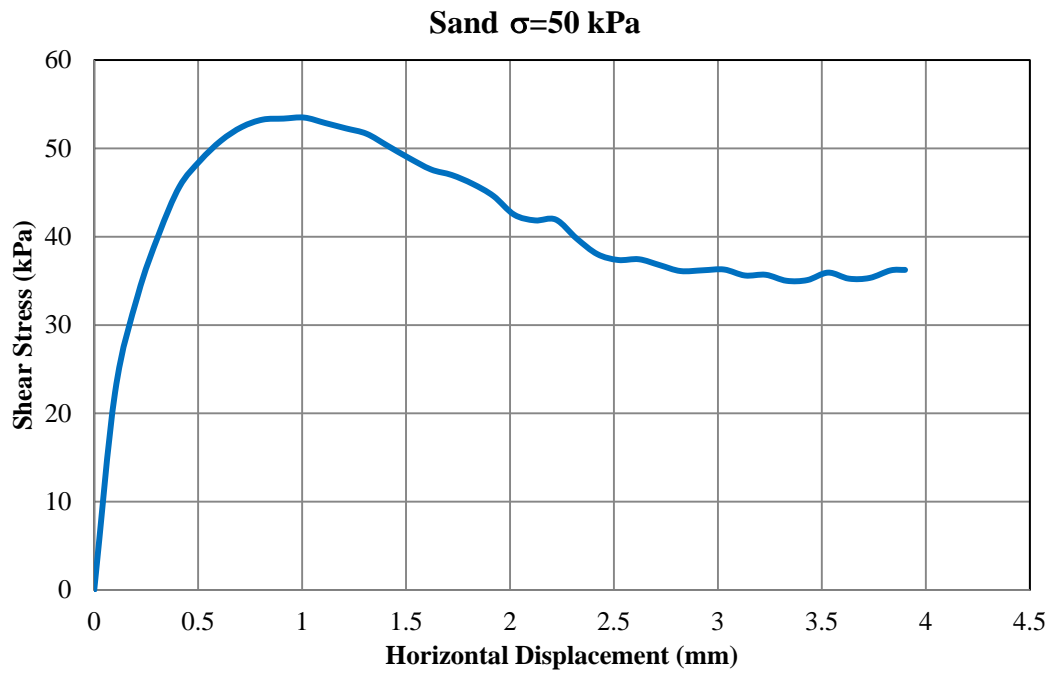


Figure A.53 Shear Stress vs. Displacement Graph-Experiment 2

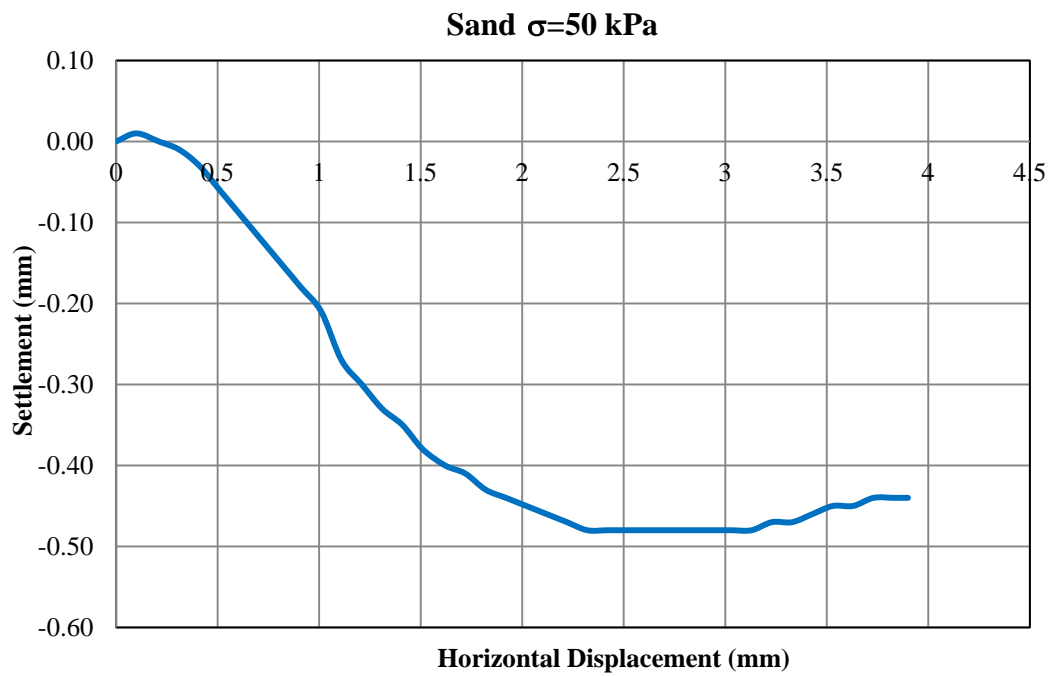


Figure A.54 Settlement vs. Displacement Graph- Experiment 2

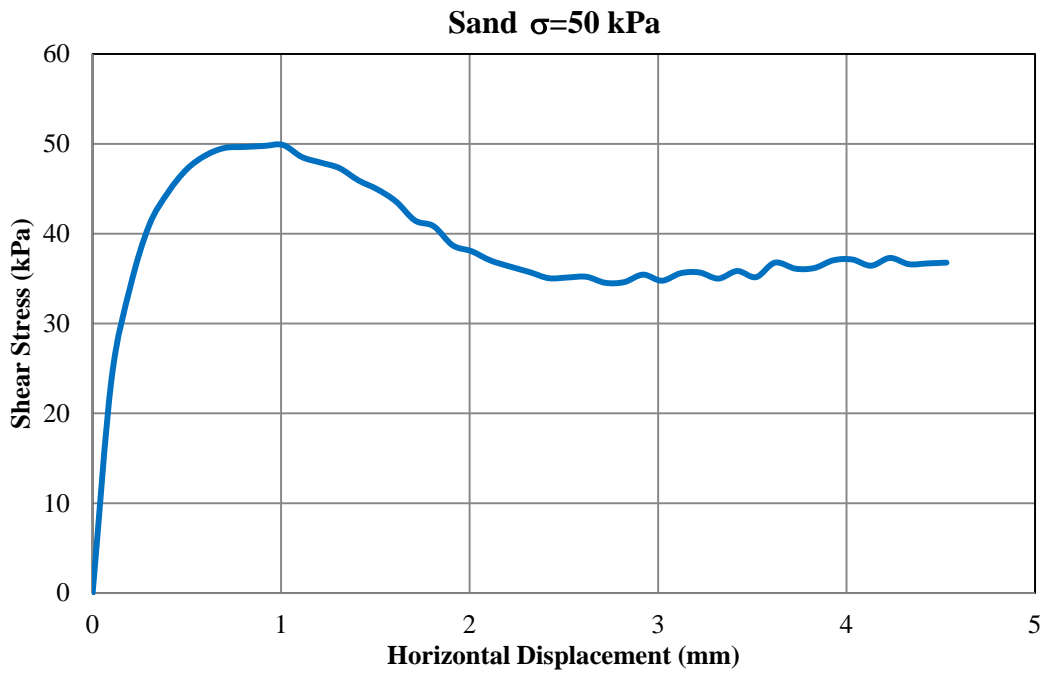


Figure A.55 Shear Stress vs. Displacement Graph-Experiment 3

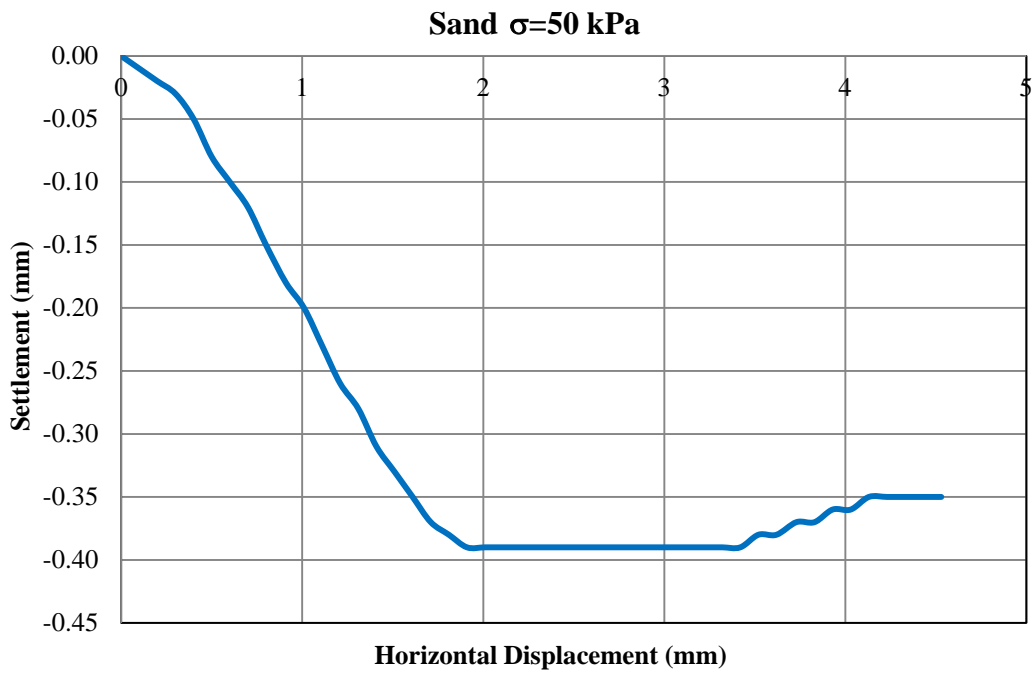


Figure A.56 Settlement vs. Displacement Graph- Experiment 3

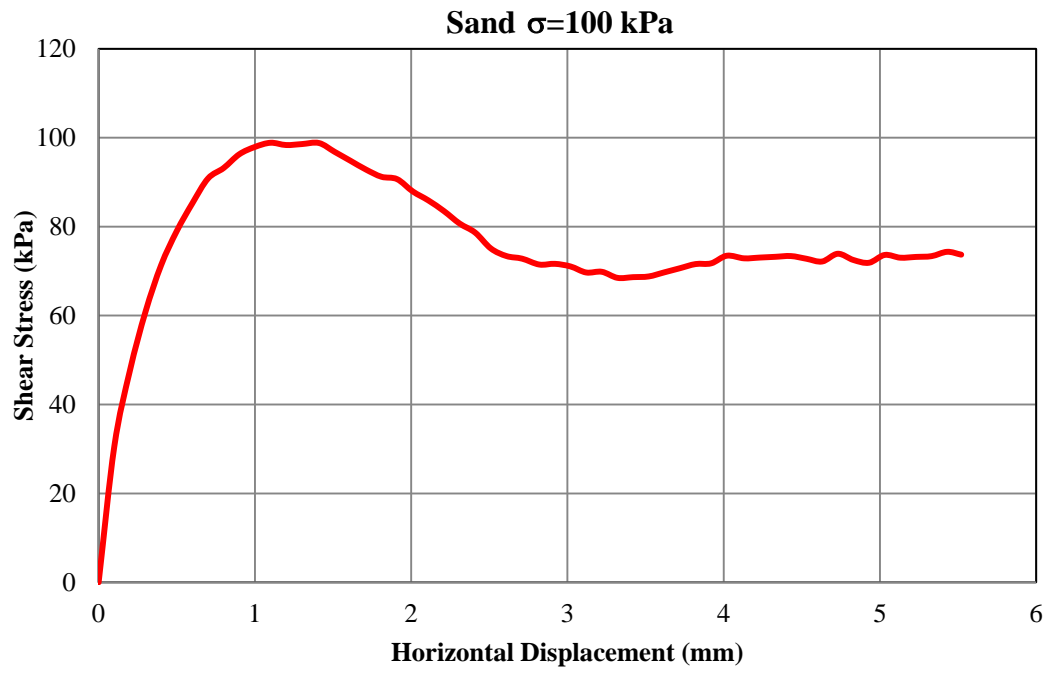


Figure A.57 Shear Stress vs. Displacement Graph-Experiment 4

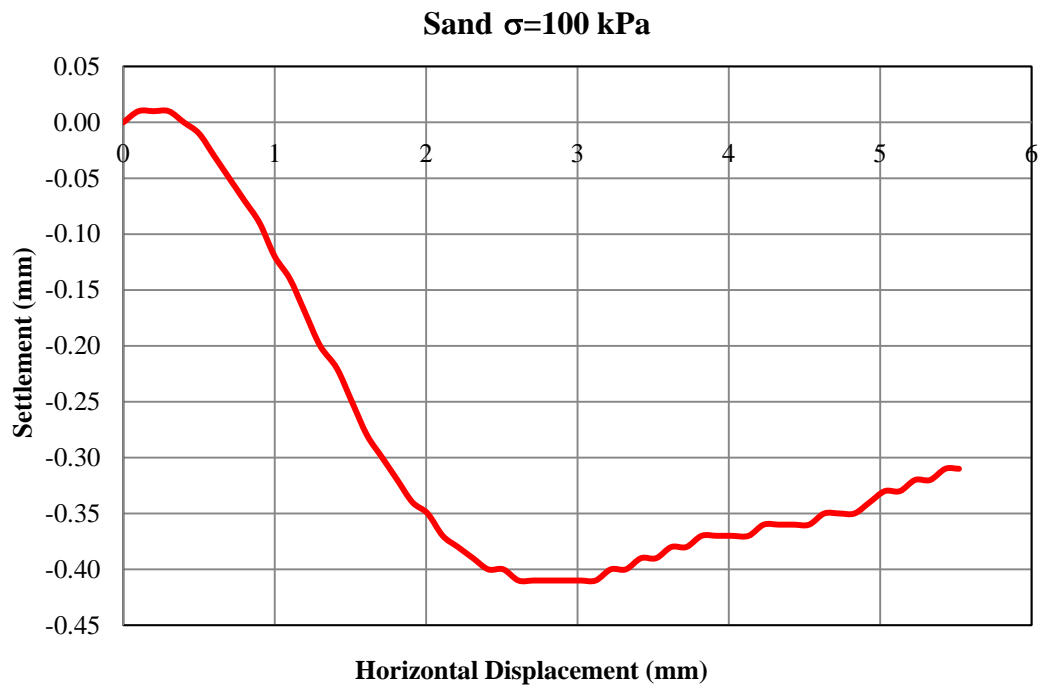


Figure A.58 Settlement vs. Displacement Graph- Experiment 4

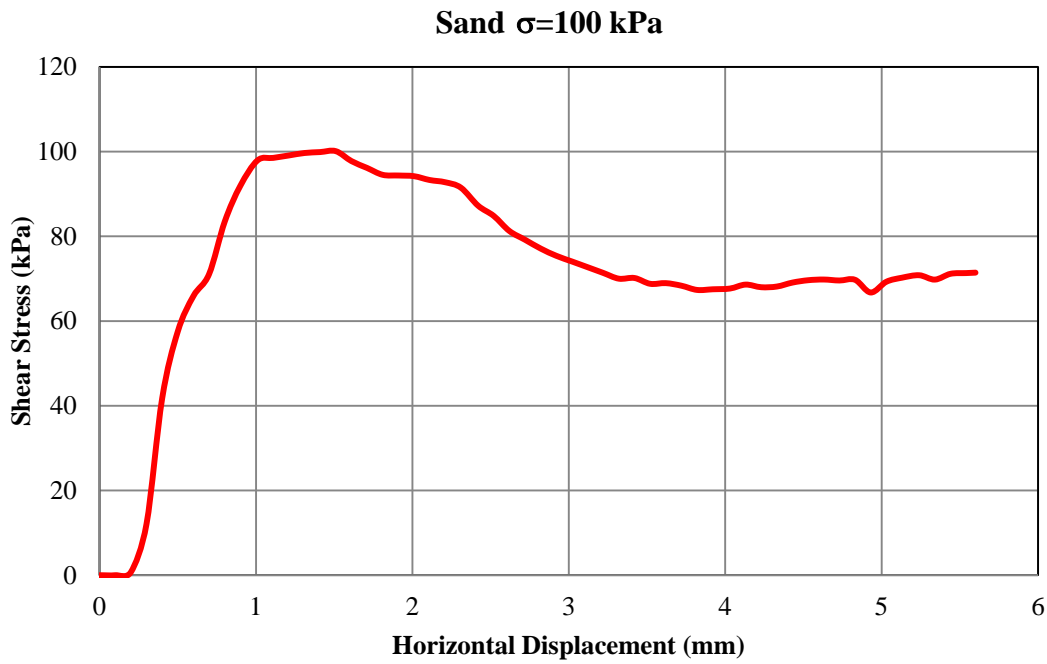


Figure A.59 Shear Stress vs. Displacement Graph-Experiment 5

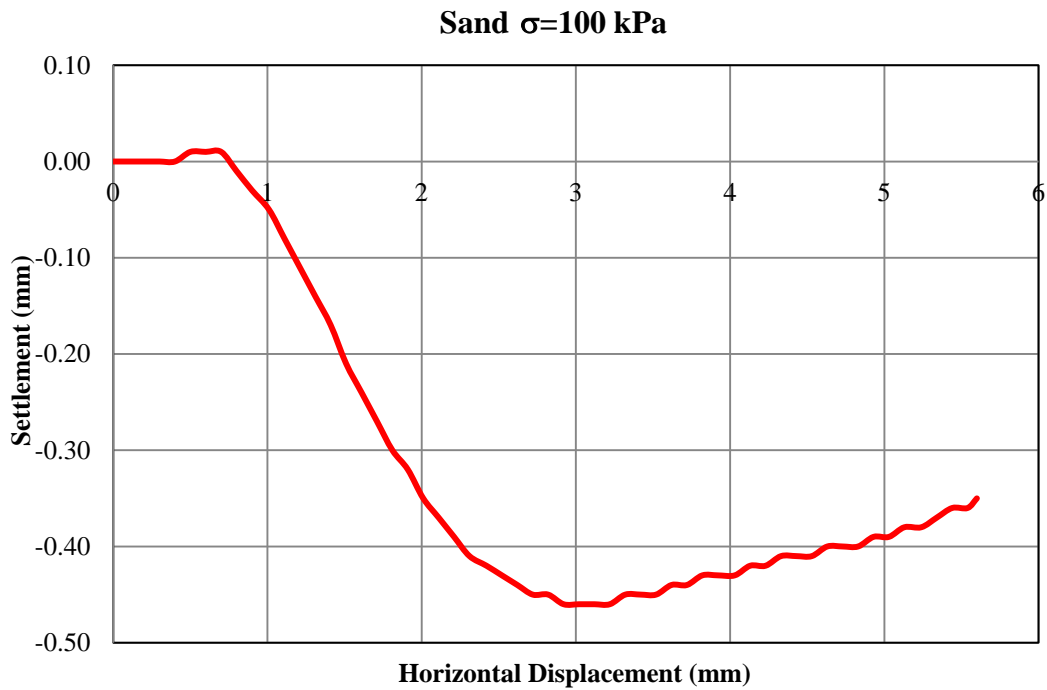


Figure A.60 Settlement vs. Displacement Graph- Experiment 5

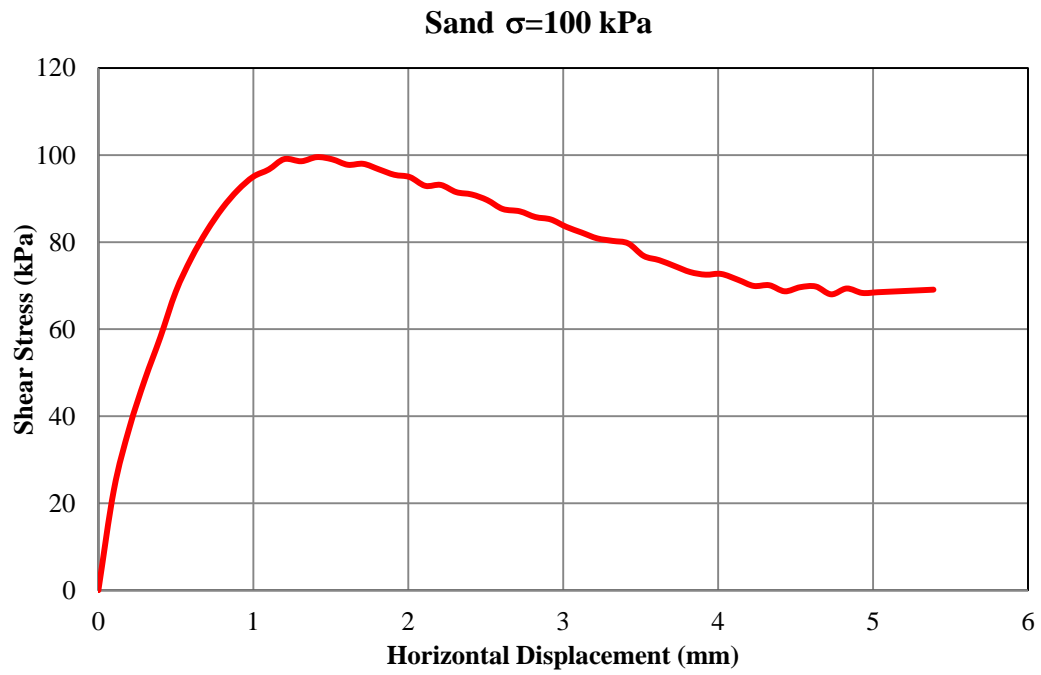


Figure A.61 Shear Stress vs. Displacement Graph-Experiment 6

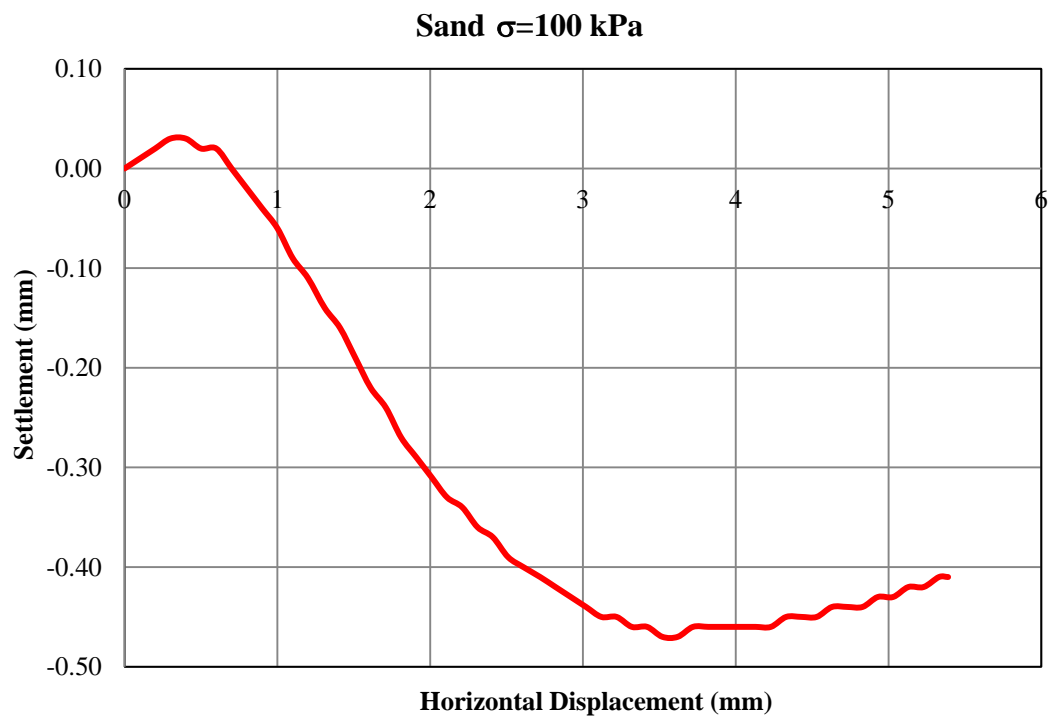


Figure A.62 Settlement vs. Displacement Graph- Experiment 6

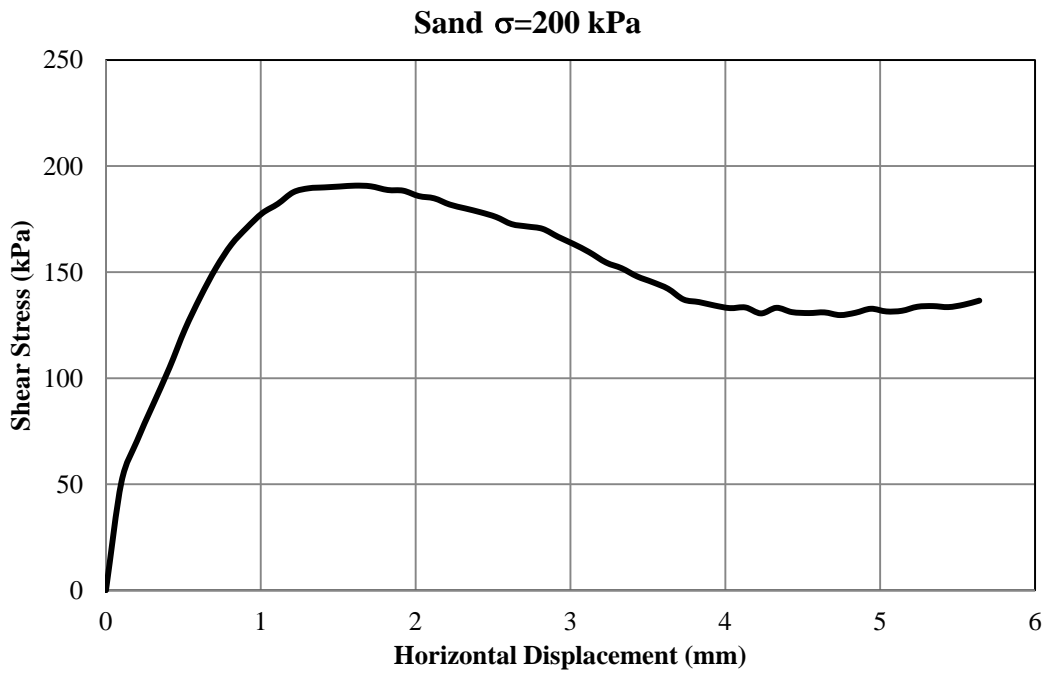


Figure A.63 Shear Stress vs. Displacement Graph-Experiment 7

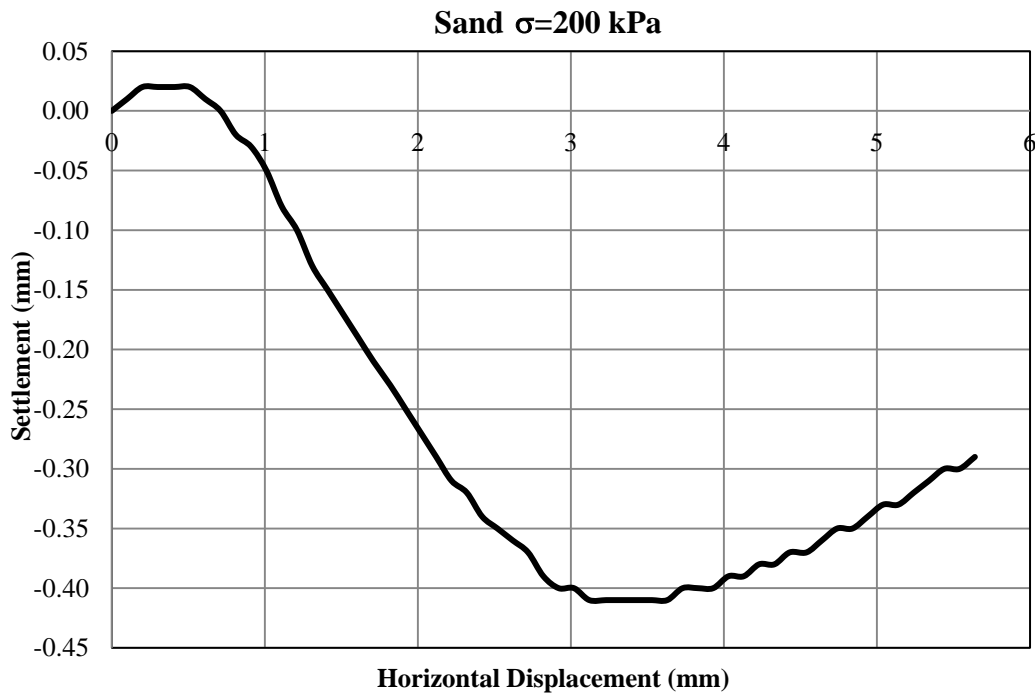


Figure A.64 Settlement vs. Displacement Graph- Experiment 7

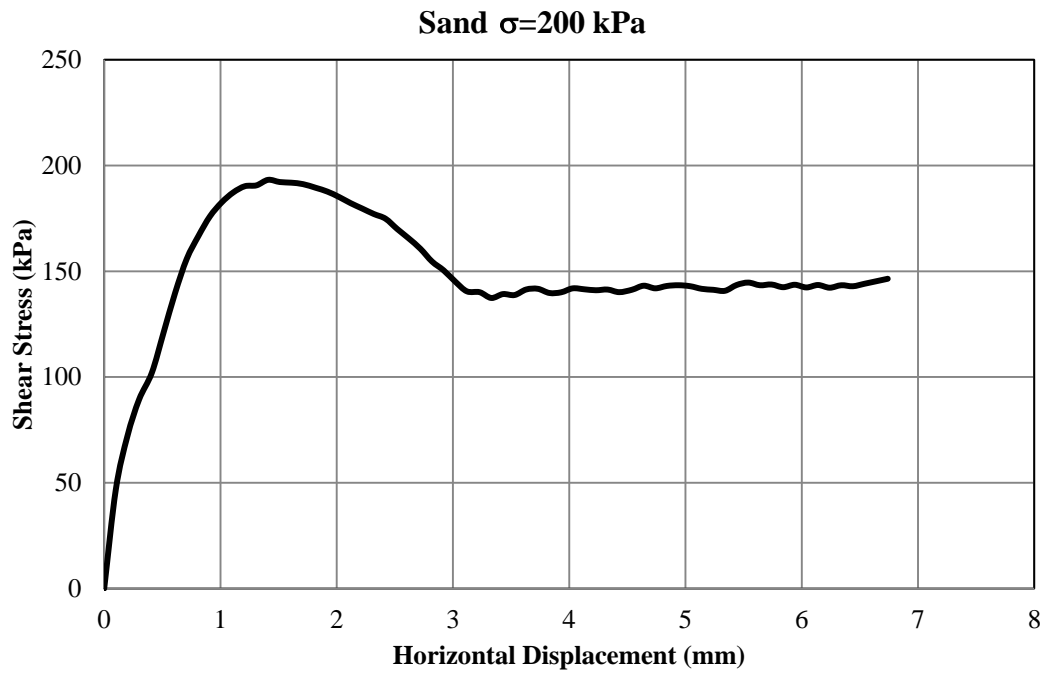


Figure A.65 Shear Stress vs. Displacement Graph-Experiment 8

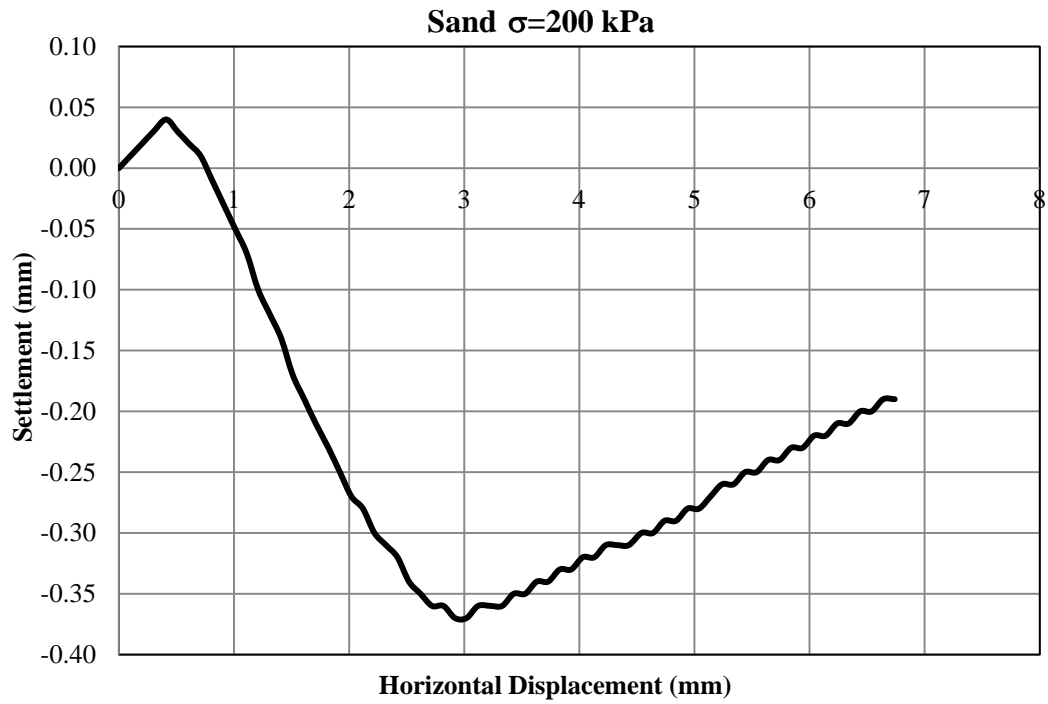


Figure A.66 Settlement vs. Displacement Graph- Experiment 8

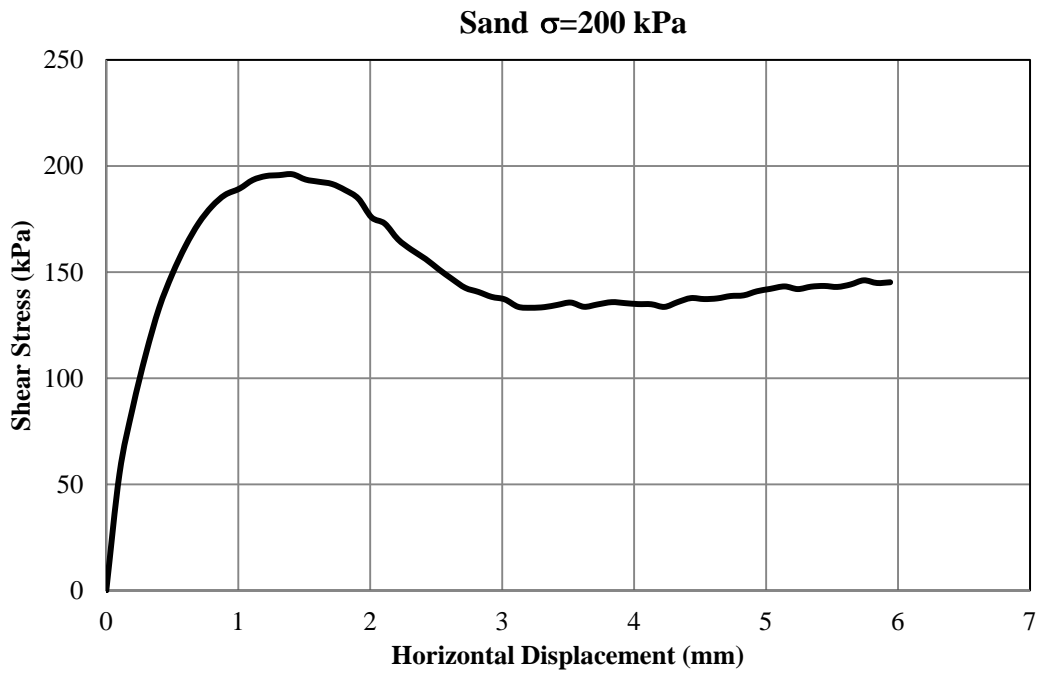


Figure A.67 Shear Stress vs. Displacement Graph-Experiment 9

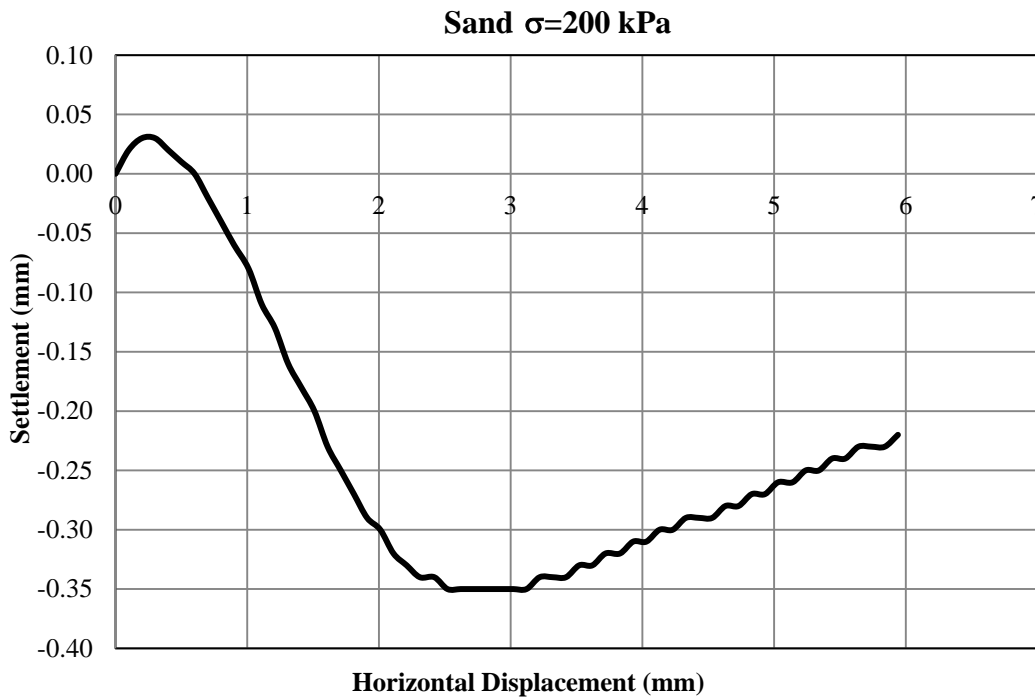


Figure A.68 Settlement vs. Displacement Graph- Experiment 9

**c. Small Shear Tests of Sand-Clay Interface**

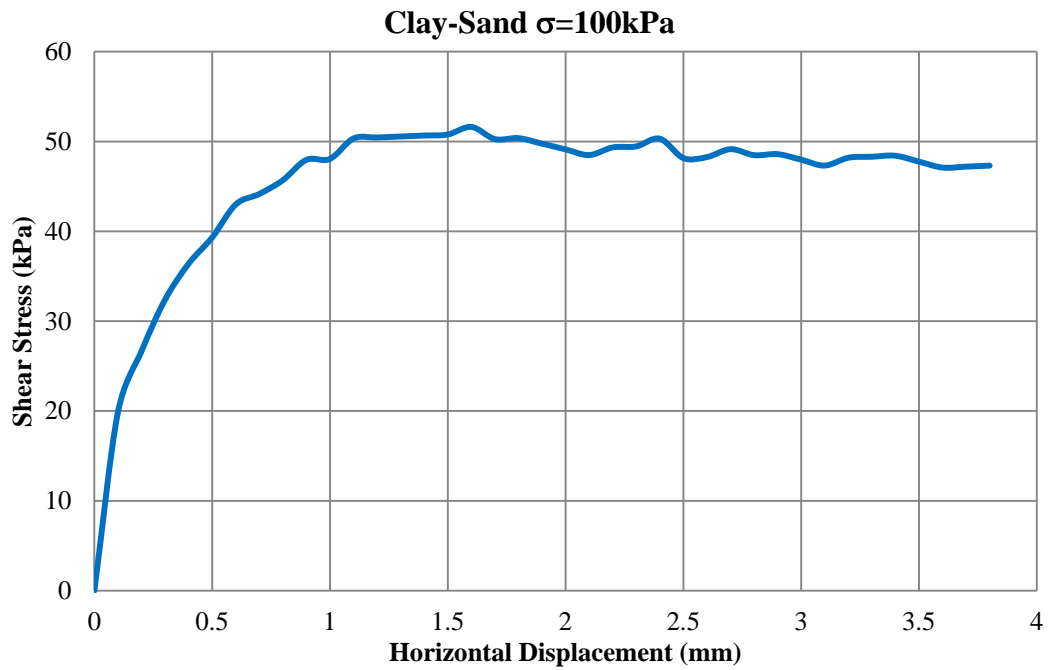


Figure A.69 Shear Stress vs. Displacement Graph-Experiment 1

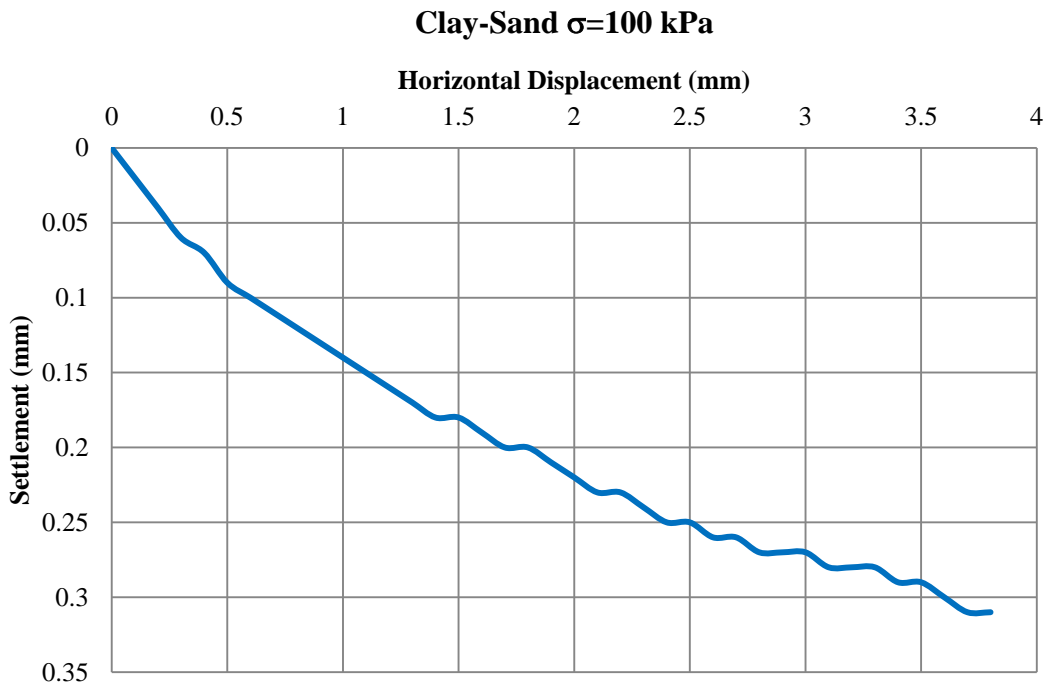


Figure A.70 Settlement vs. Displacement Graph- Experiment 1

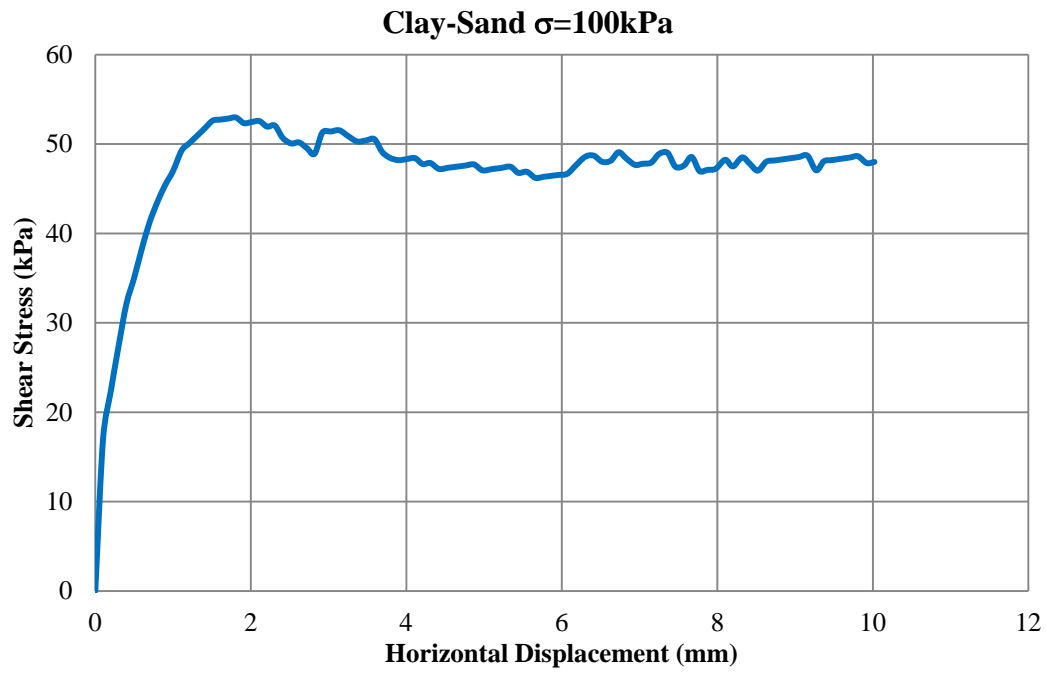


Figure A.71 Shear Stress vs. Displacement Graph-Experiment 2

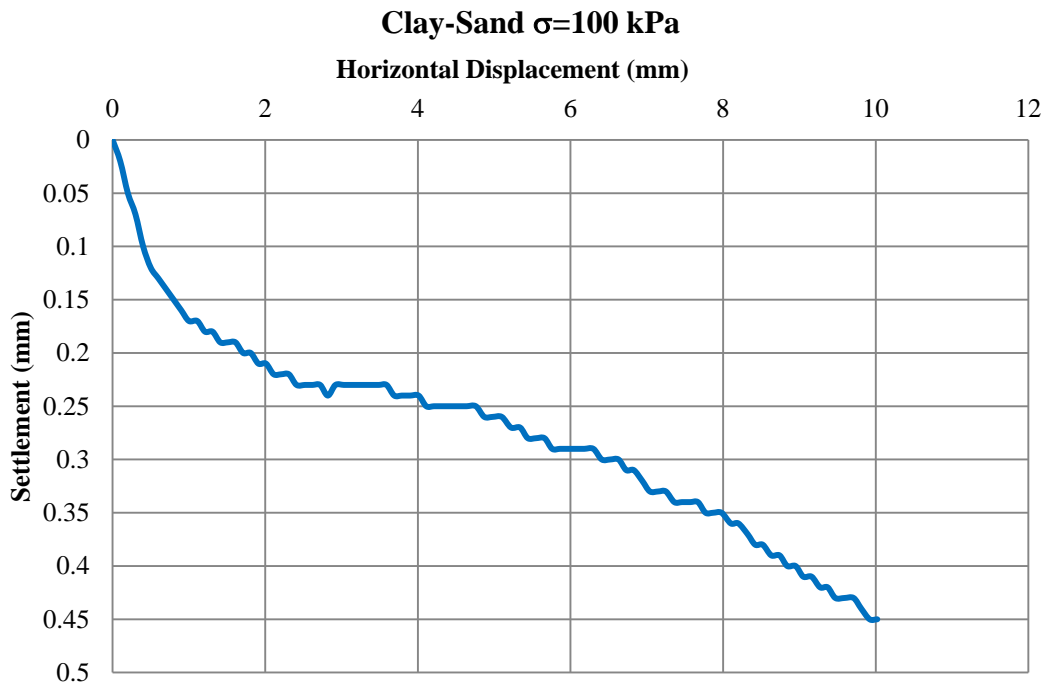


Figure A.72 Settlement vs. Displacement Graph- Experiment 2

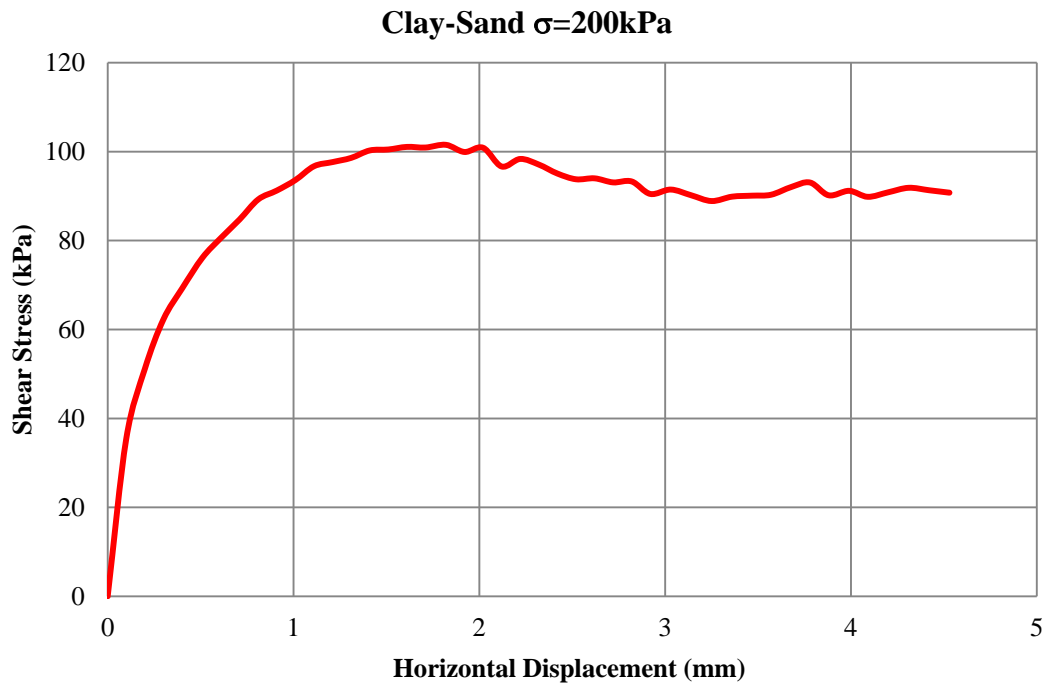


Figure A.73 Shear Stress vs. Displacement Graph-Experiment 3

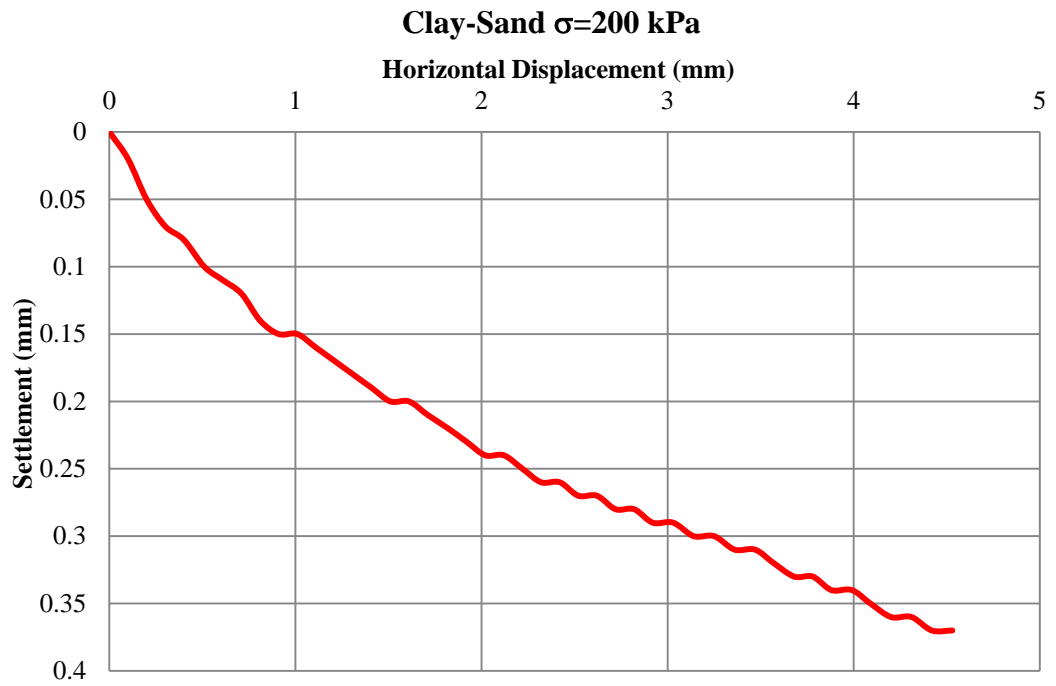


Figure A.74 Settlement vs. Displacement Graph- Experiment 3

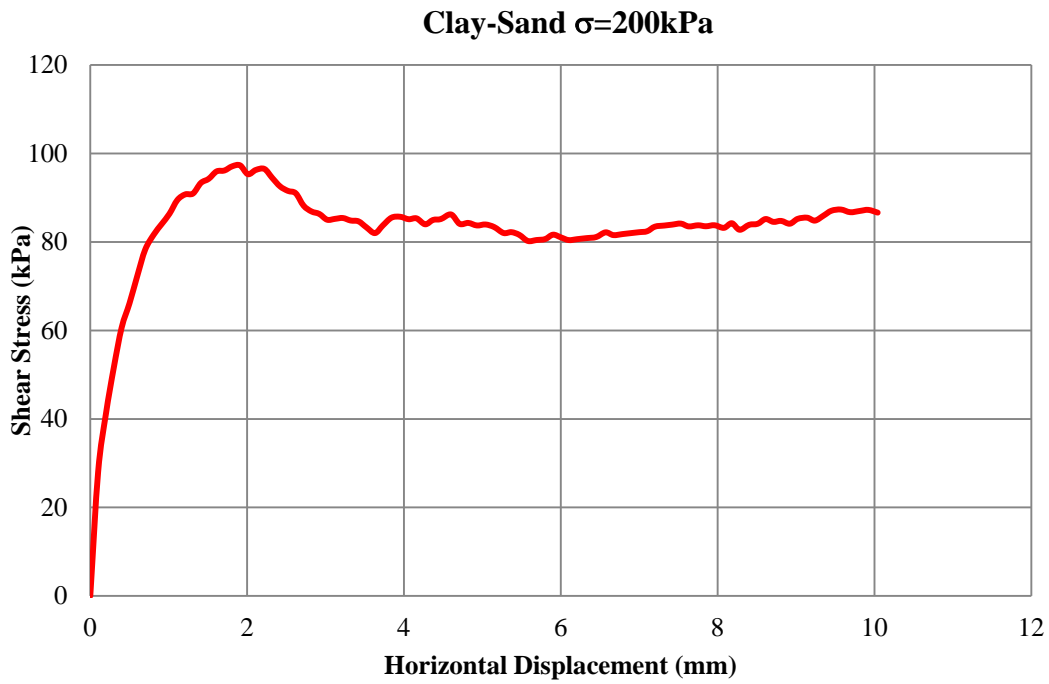


Figure A.75 Shear Stress vs. Displacement Graph-Experiment 4

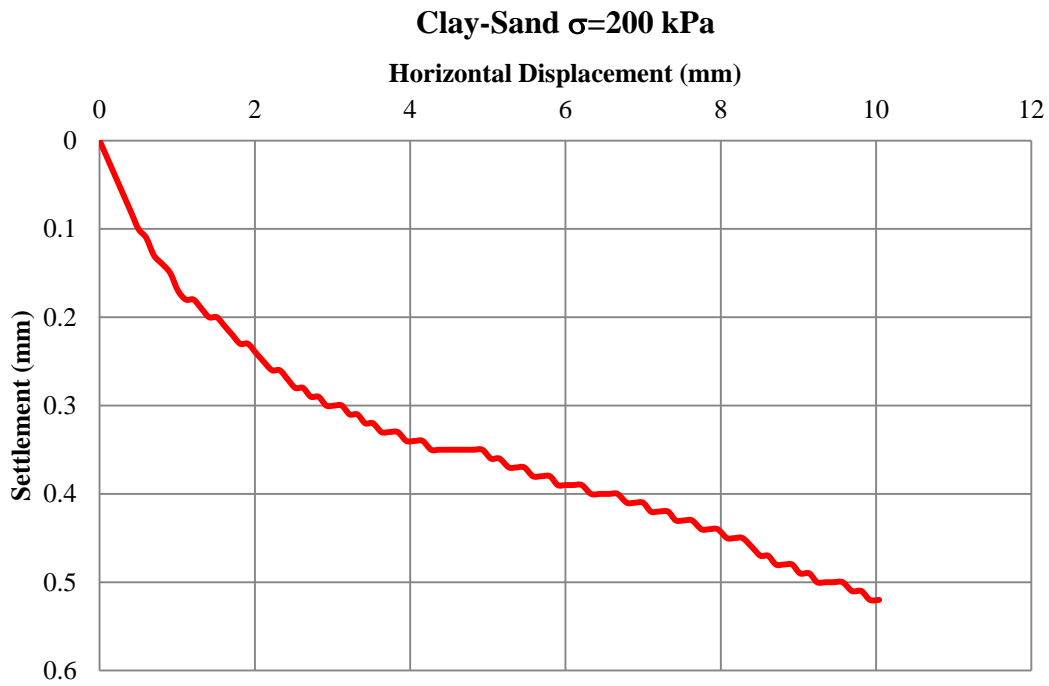


Figure A.76 Settlement vs. Displacement Graph- Experiment 4

## APPENDIX B

### TRIAXIAL TESTS

#### 1. Triaxial Tests of Clay

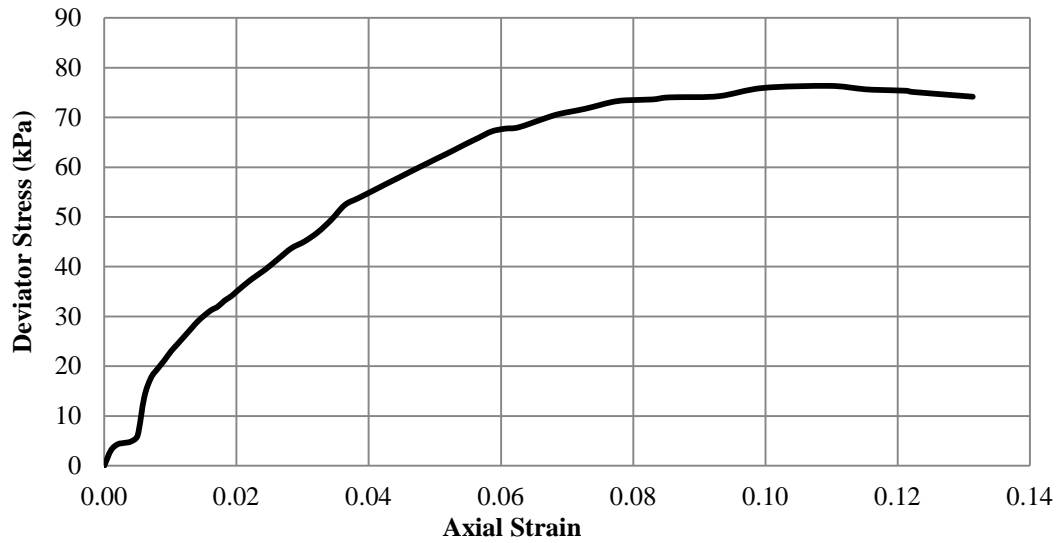


Figure B.1 Axial Strain vs. Deviator Stress-Experiment 1  
Confining Effective Stress=50 kPa

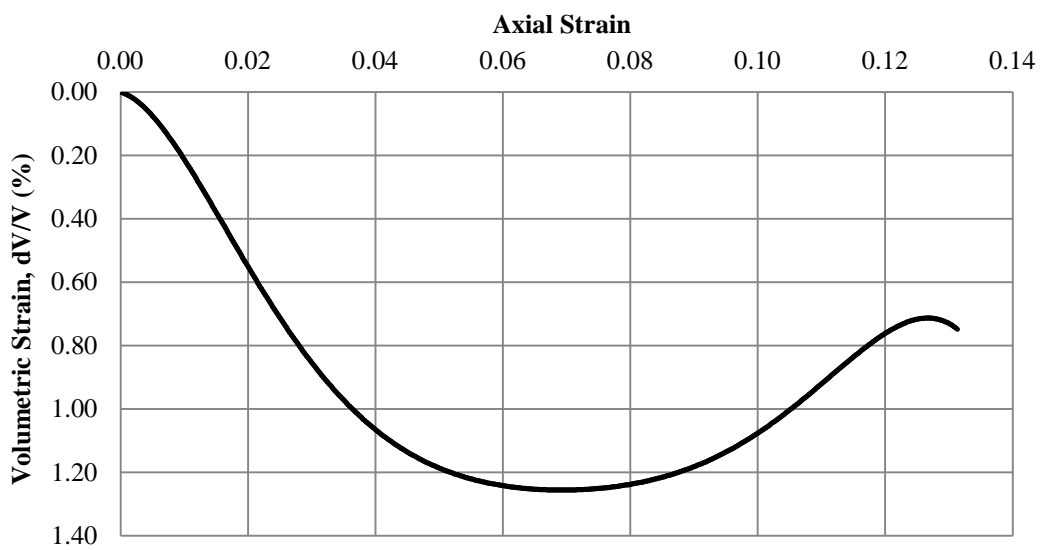


Figure B.2 Axial Strain vs. Volumetric Strain-Experiment 1  
Confining Effective Stress=50 kPa

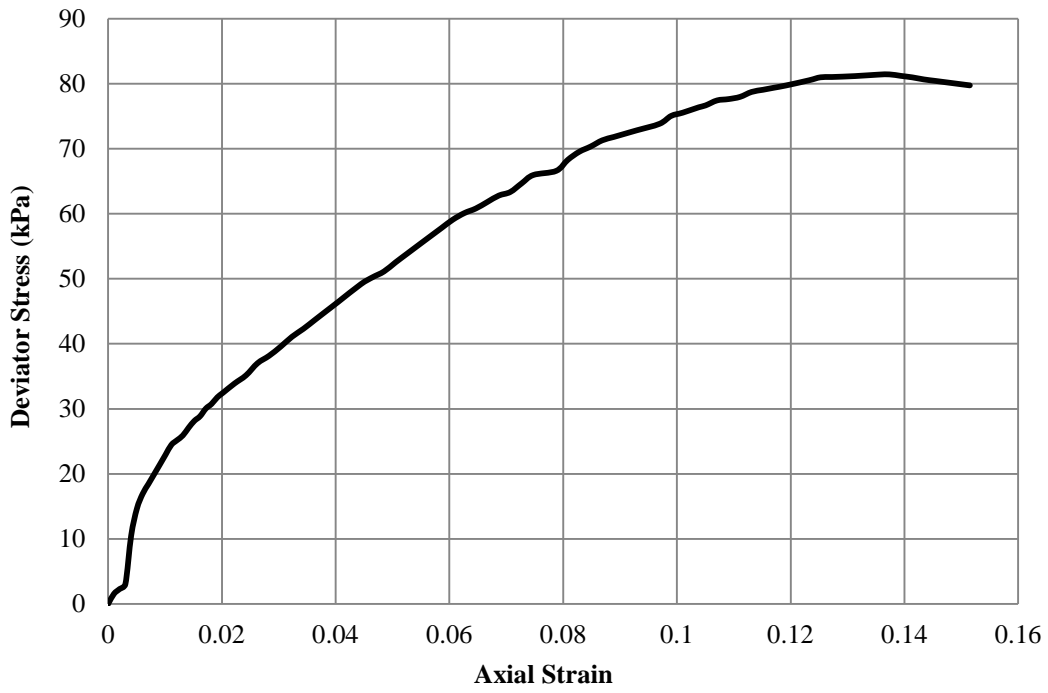


Figure B.3 Axial Strain vs. Deviator Stress-Experiment 2  
Confining Effective Stress=50 kPa

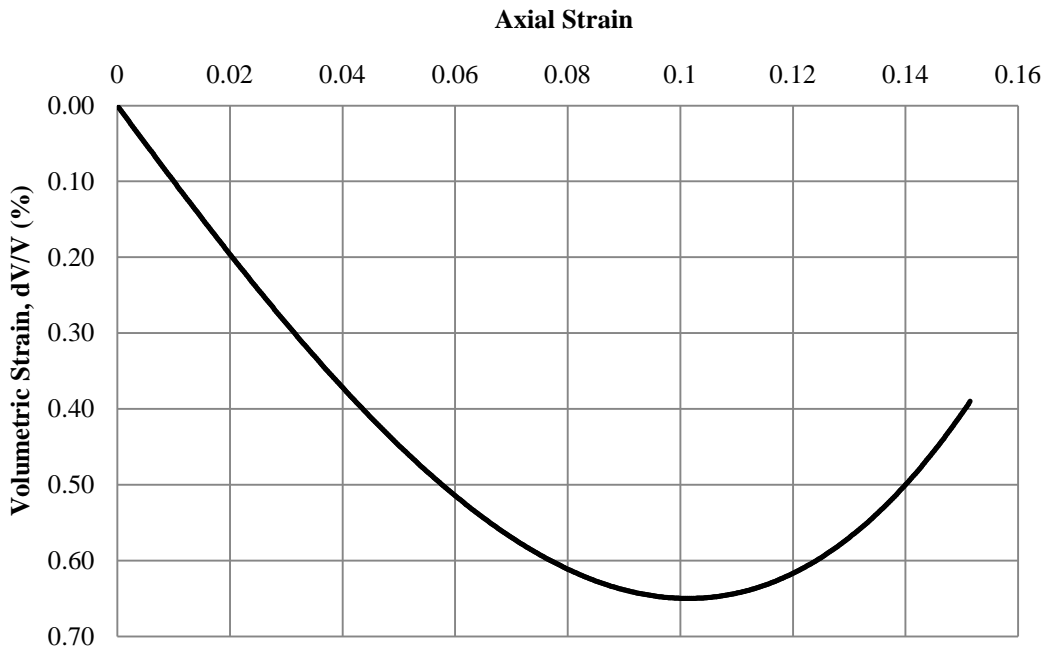


Figure B.4 Axial Strain vs. Volumetric Strain-Experiment 2  
Confining Effective Stress=50 kPa

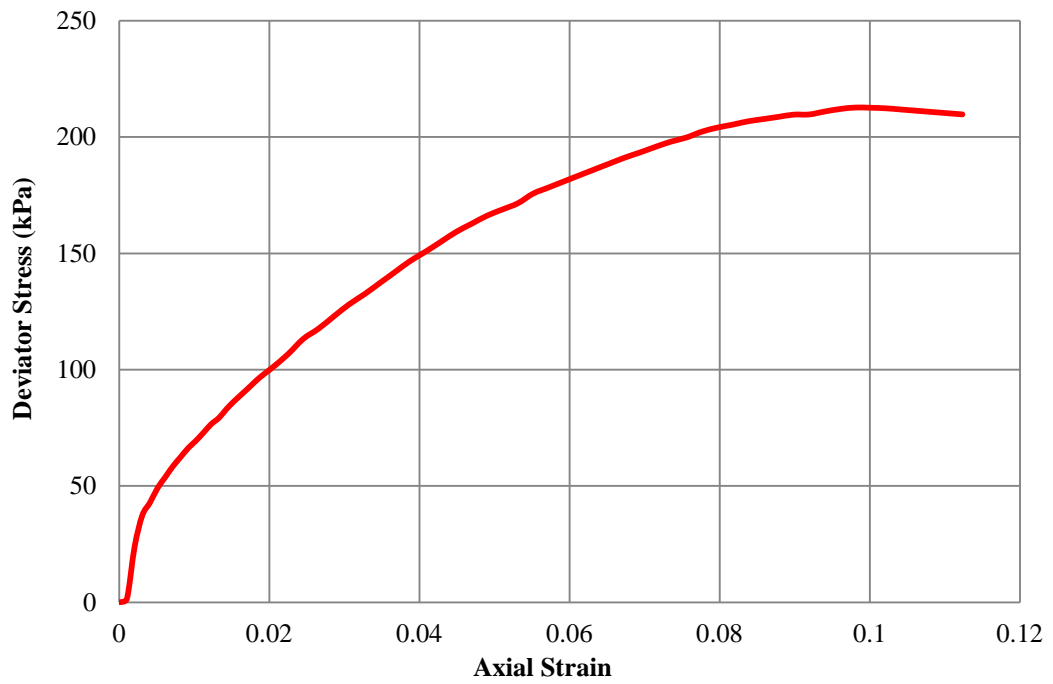


Figure B.5 Axial Strain vs. Deviator Stress-Experiment 1  
 Confining Effective Stress=150 kPa

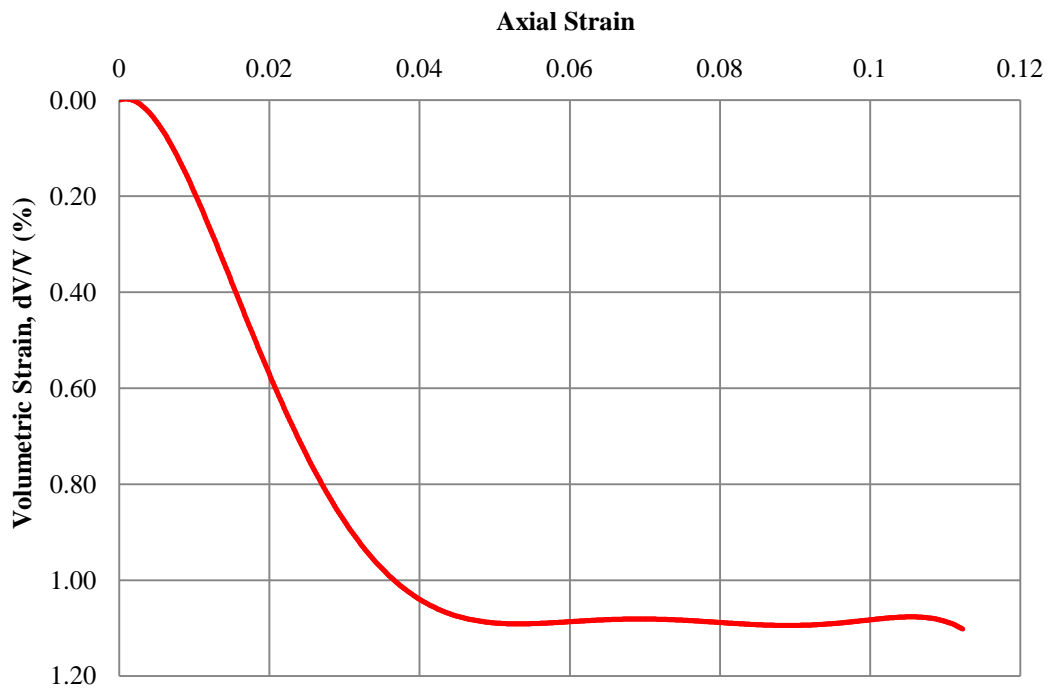


Figure B.6 Axial Strain vs. Volumetric Strain-Experiment 1  
 Confining Effective Stress=150 kPa

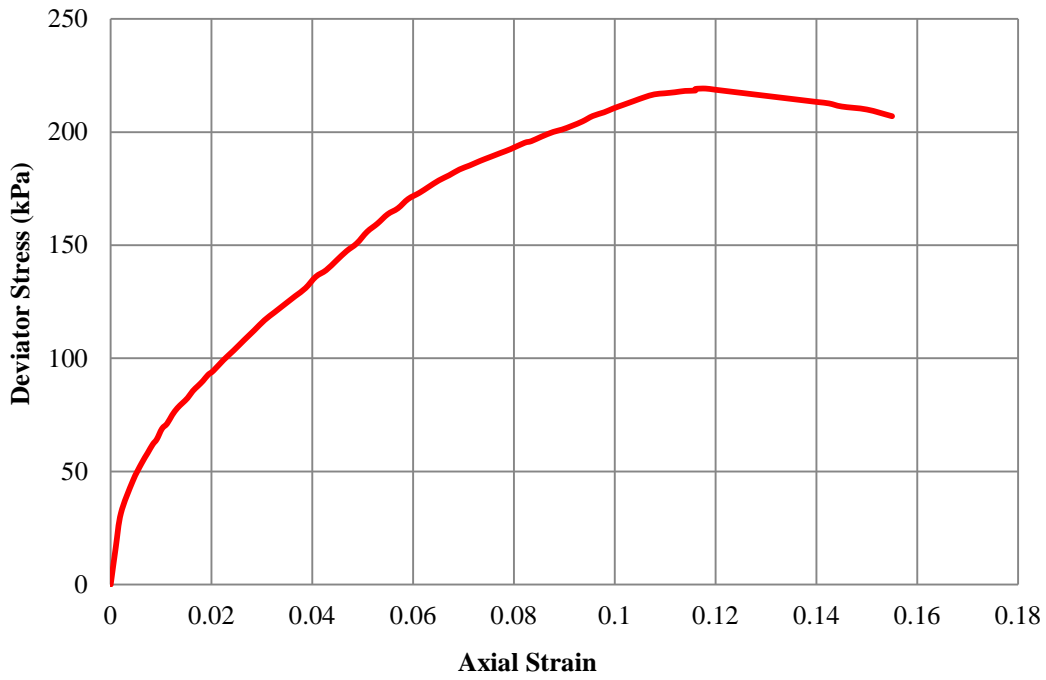


Figure B.7 Axial Strain vs. Deviator Stress-Experiment 2  
 Confining Effective Stress=150 kPa

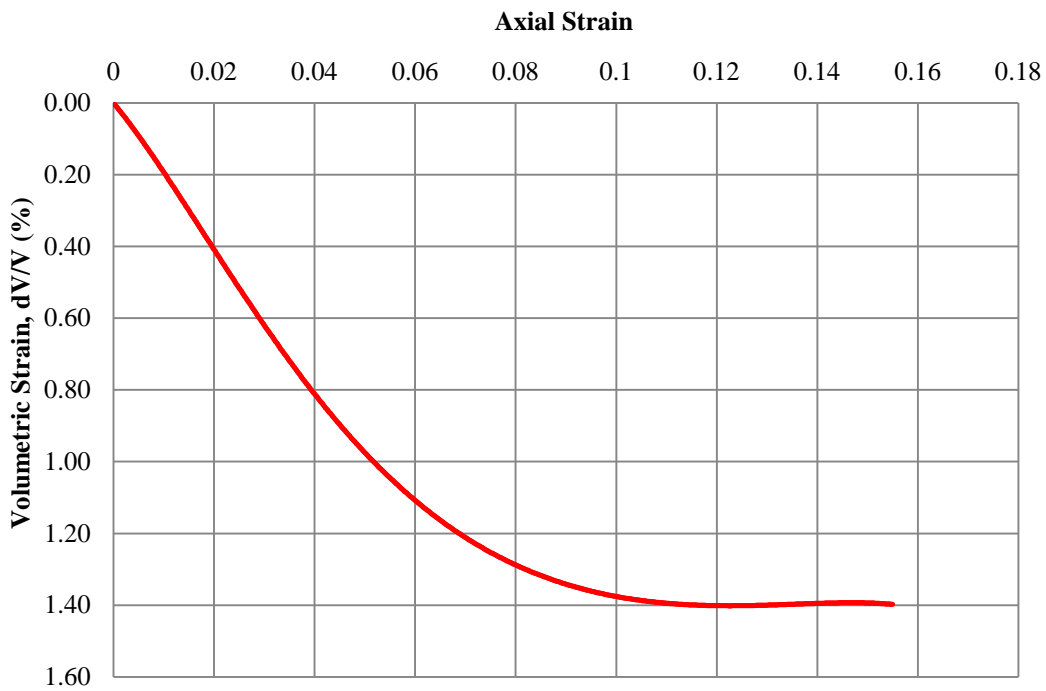


Figure B.8 Axial Strain vs. Volumetric Strain-Experiment 2  
 Confining Effective Stress=150 kPa

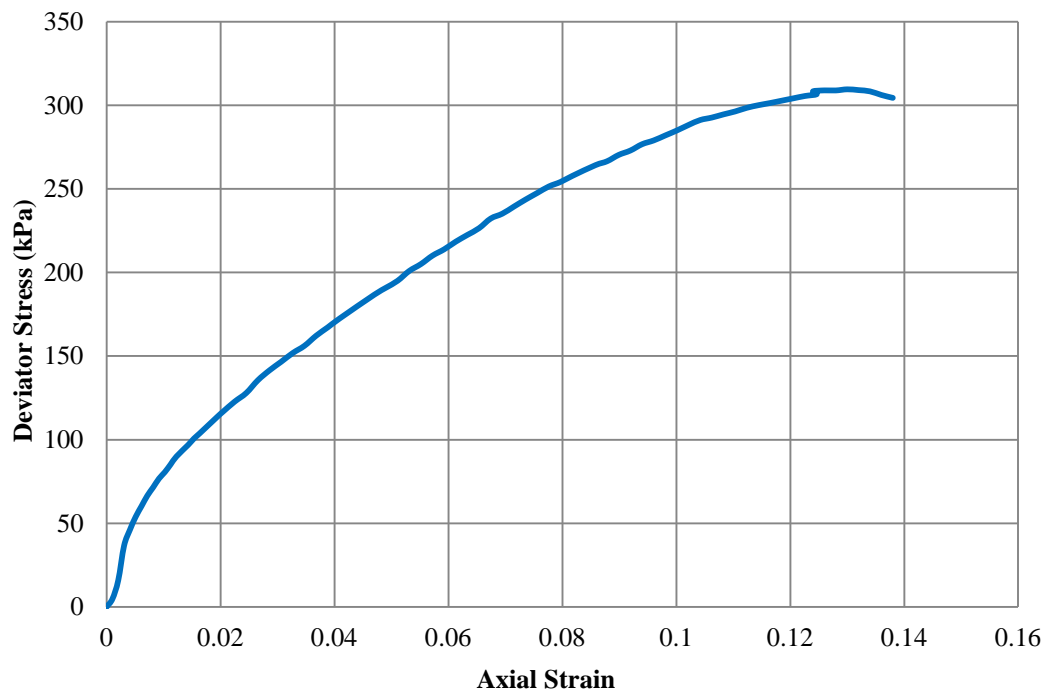


Figure B.9 Axial Strain vs. Deviator Stress-Experiment 1  
 Confining Effective Stress=250 kPa

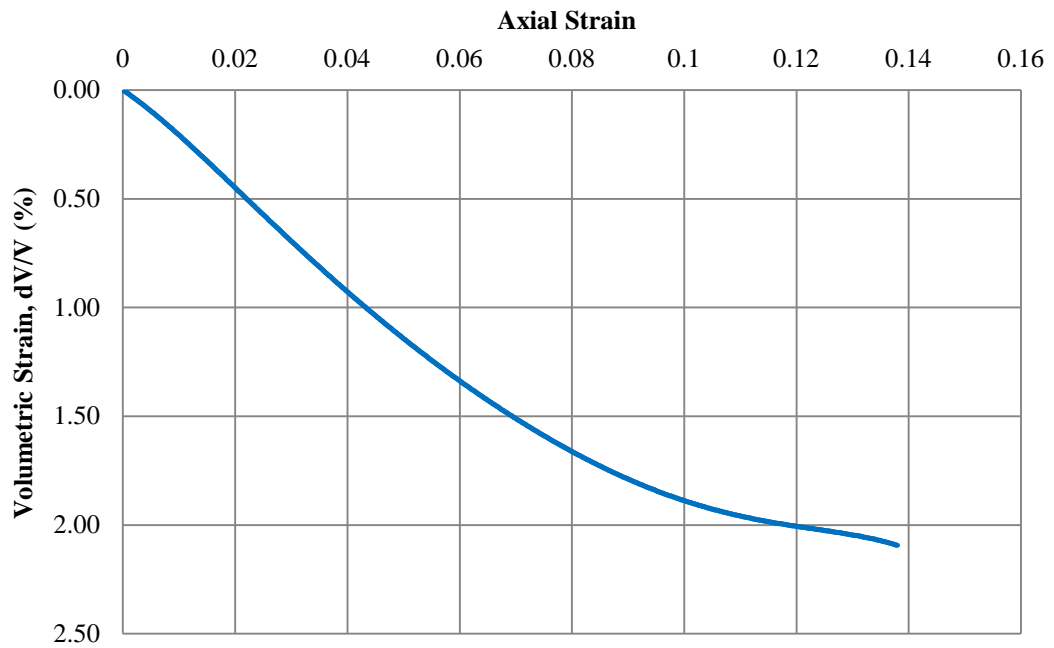


Figure B.10 Axial Strain vs. Volumetric Strain-Experiment 1  
 Confining Effective Stress=250 kPa

## 2. Triaxial Tests of Clay-Clay

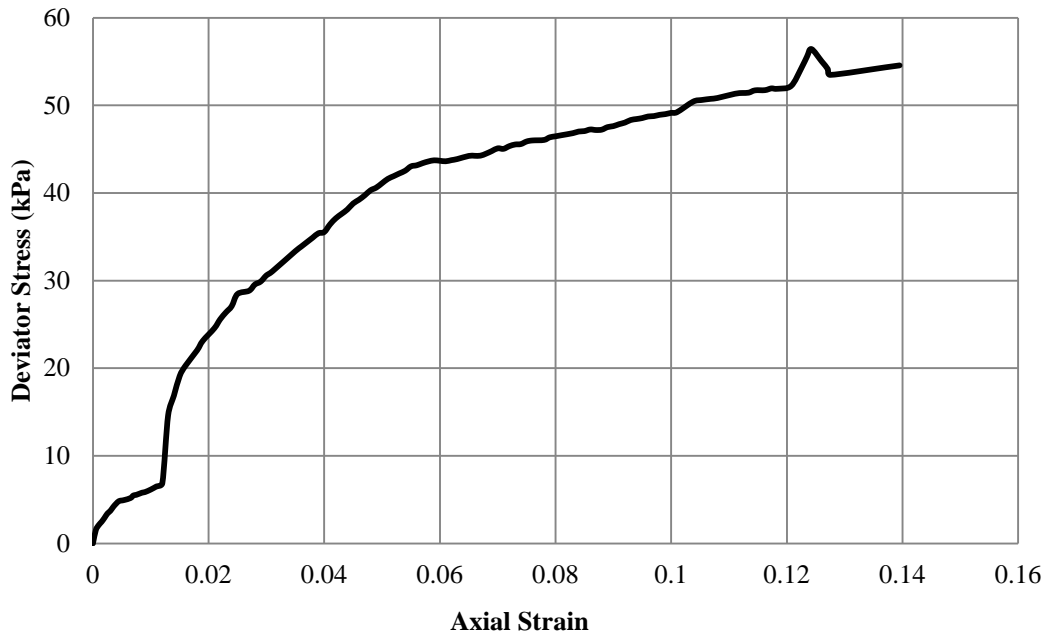


Figure B.11 Axial Strain vs. Deviator Stress-Experiment 1  
Confining Effective Stress=50 kPa-10x20 cm

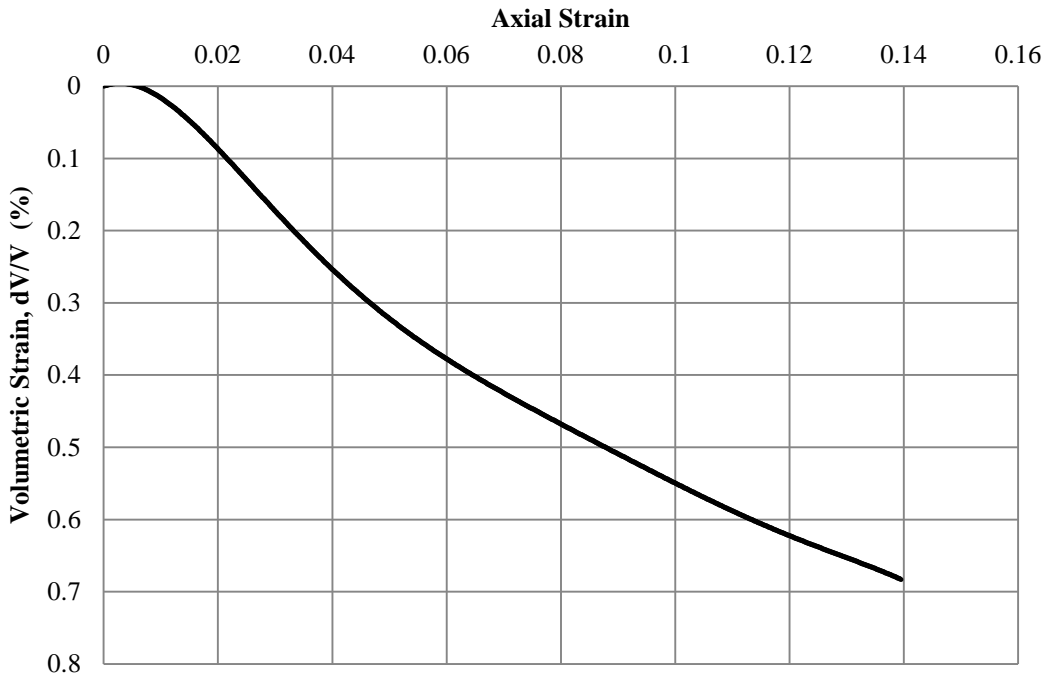


Figure B.12 Axial Strain vs. Volumetric Strain-Experiment 1  
Confining Effective Stress=50 kPa-10x20 cm

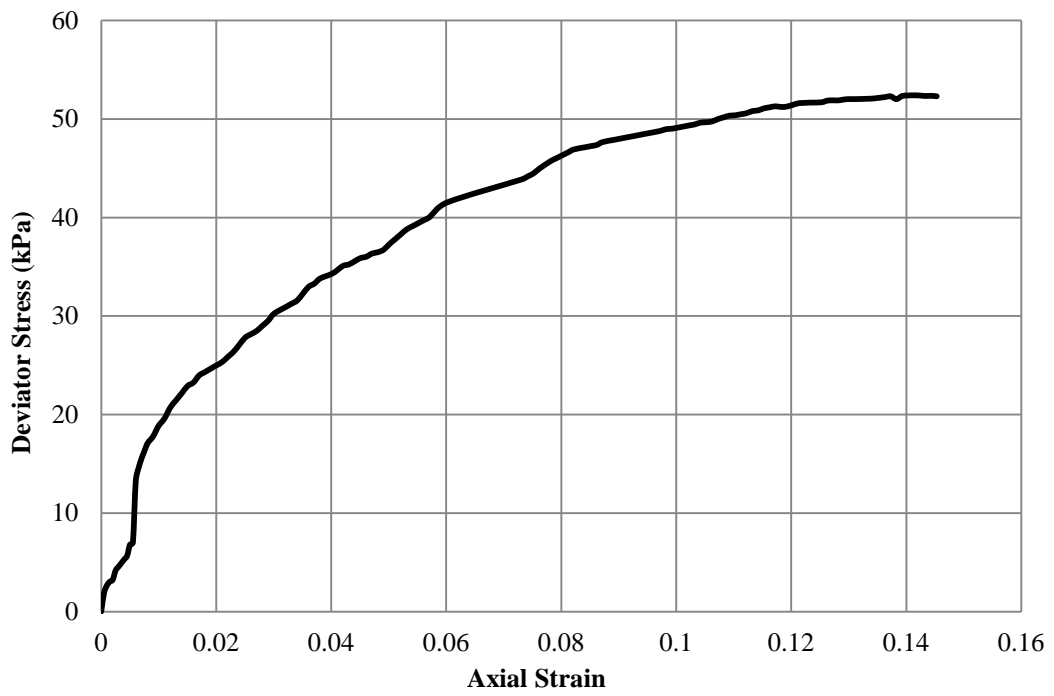


Figure B.13 Axial Strain vs. Deviator Stress-Experiment 2  
 Confining Effective Stress=50 kPa 10x20 cm

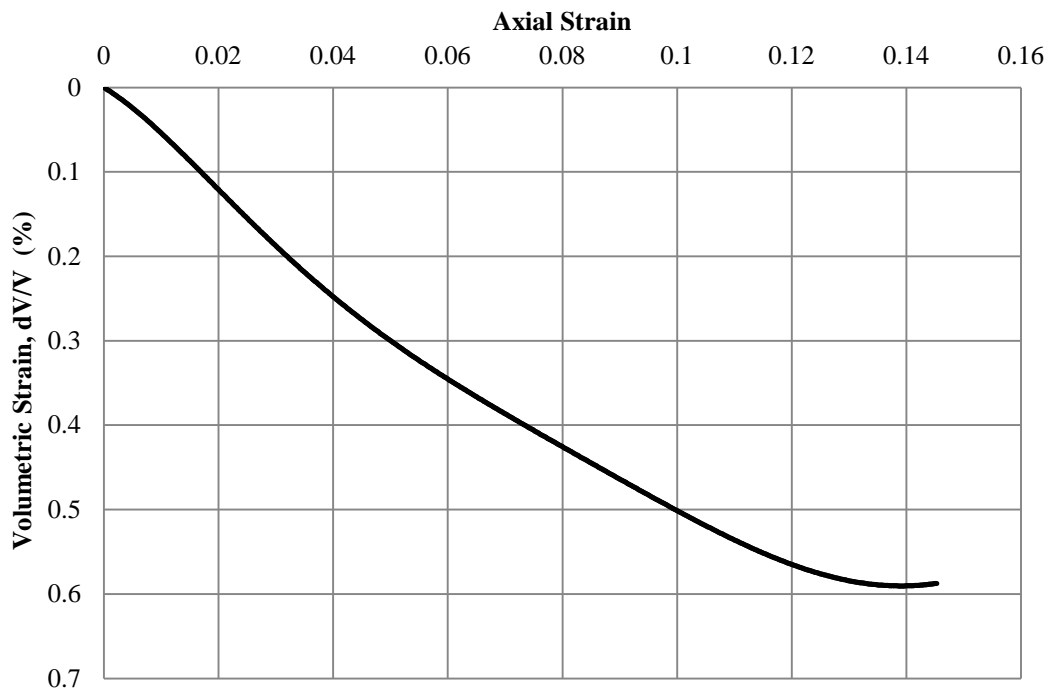


Figure B.14 Axial Strain vs. Volumetric Strain-Experiment 2  
 Confining Effective Stress=50 kPa-10x20 cm

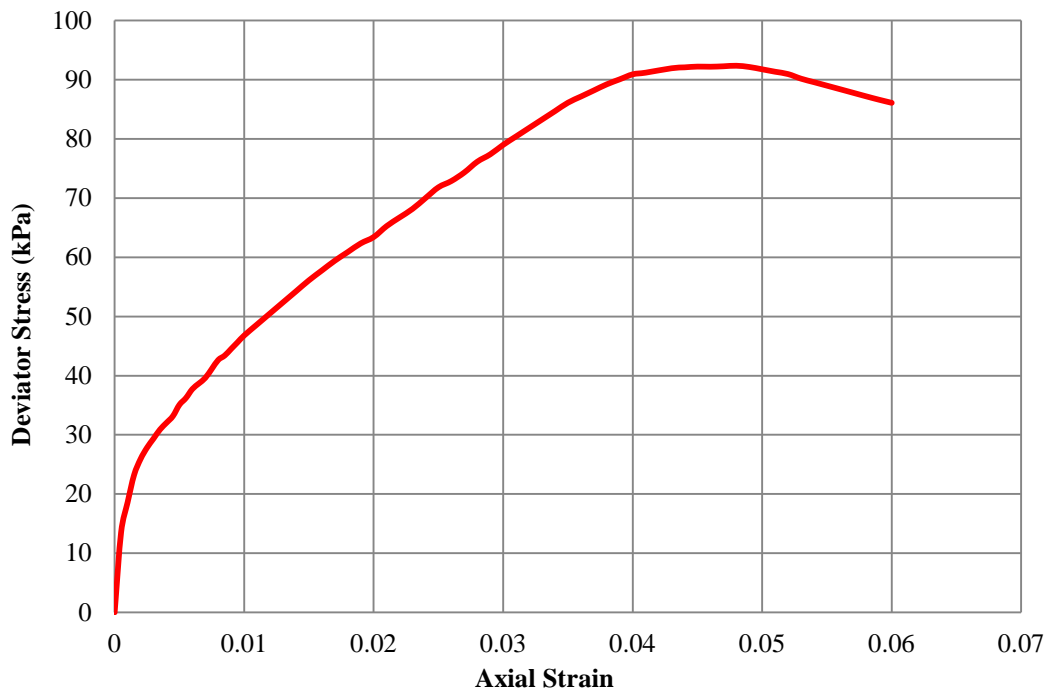


Figure B.15 Axial Strain vs. Deviator Stress-Experiment 3  
 Confining Effective Stress=150 kPa 10x20 cm

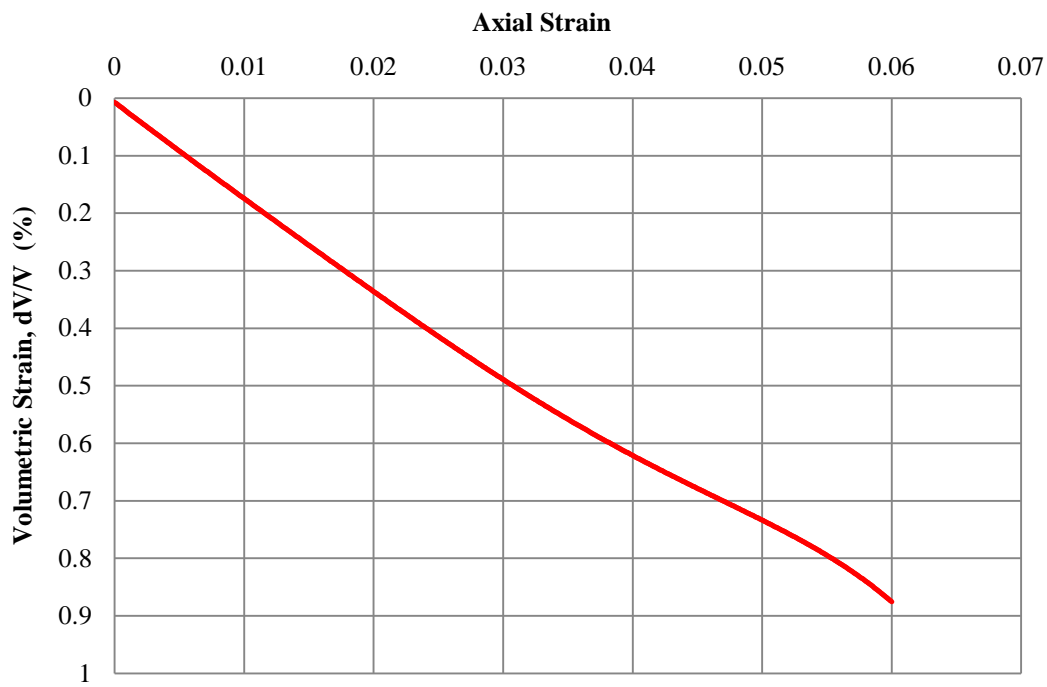


Figure B.16 Axial Strain vs. Volumetric Strain-Experiment 3  
 Confining Effective Stress=150 kPa-10x20 cm

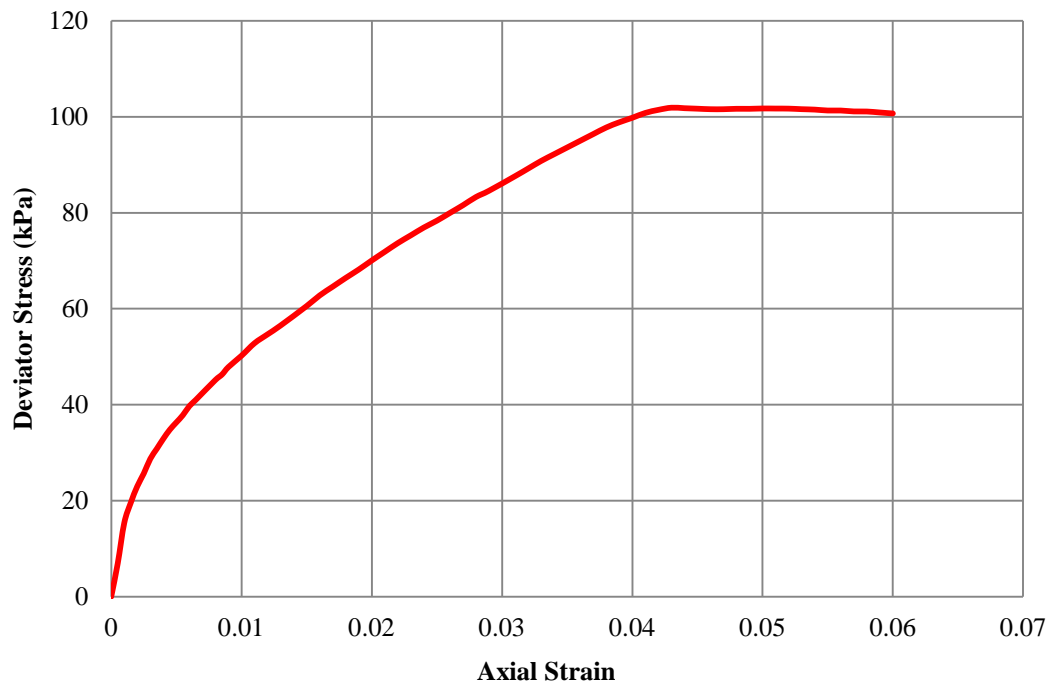


Figure B.17 Axial Strain vs. Deviator Stress-Experiment 4  
 Confining Effective Stress=150 kPa 10x20 cm

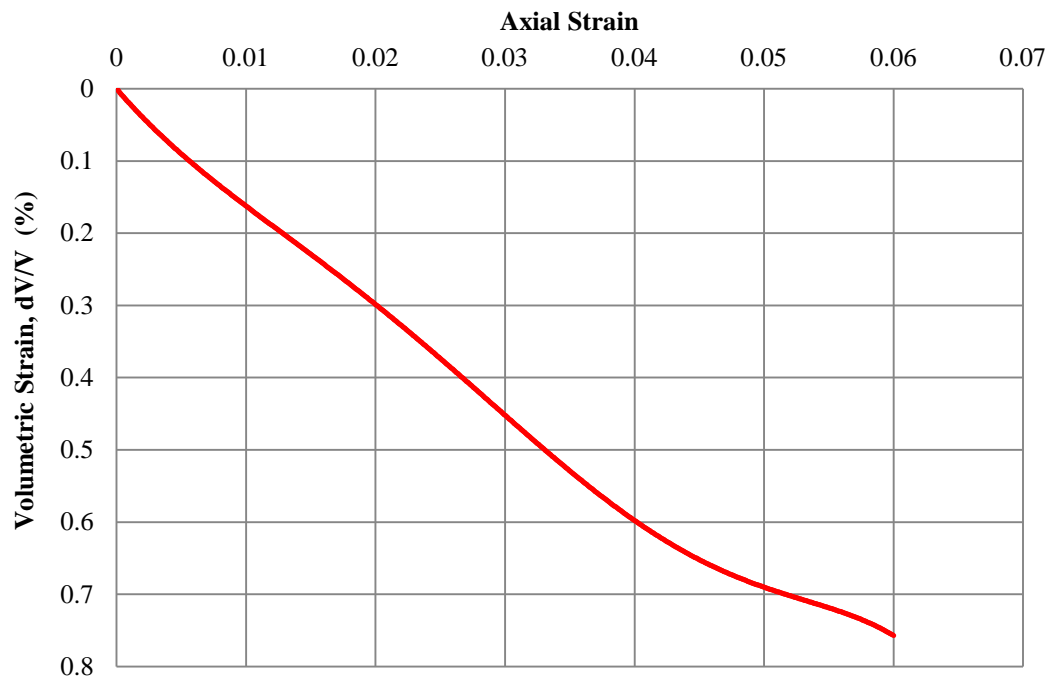


Figure B.18 Axial Strain vs. Volumetric Strain-Experiment 4  
 Confining Effective Stress=150 kPa-10x20 cm

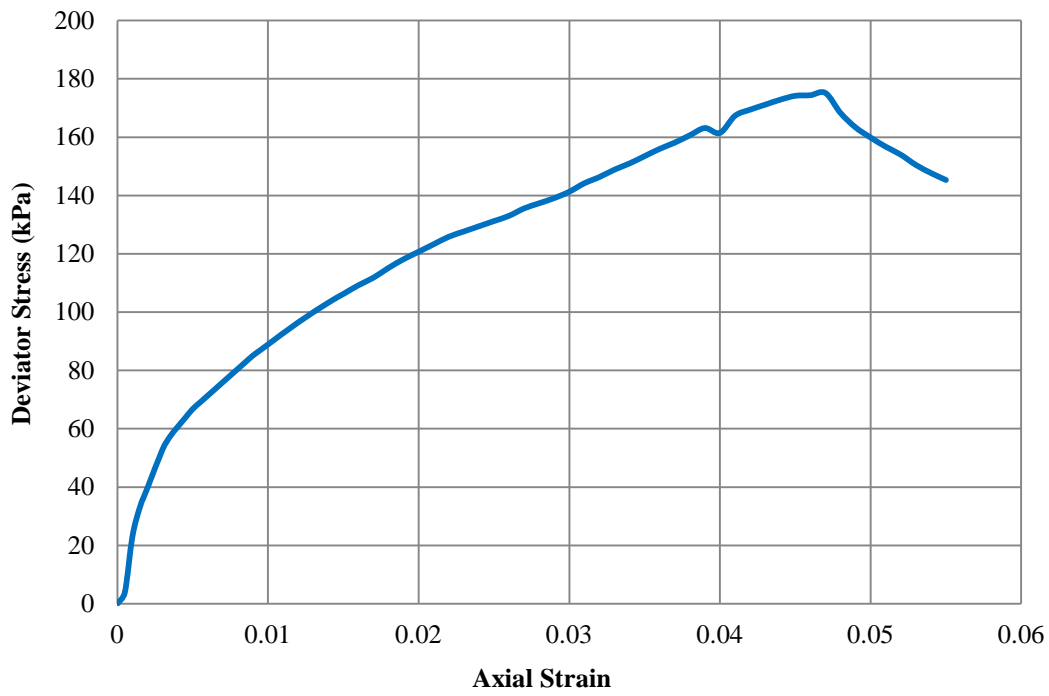


Figure B.19 Axial Strain vs. Deviator Stress-Experiment 5  
 Confining Effective Stress=250 kPa 10x20 cm

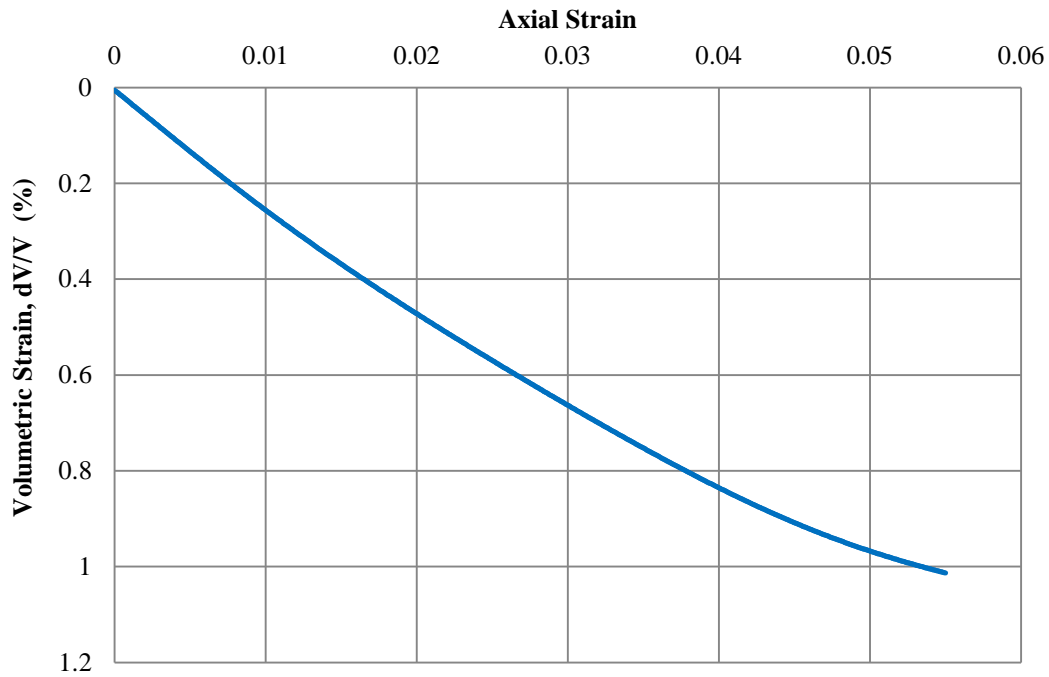


Figure B.20 Axial Strain vs. Volumetric Strain-Experiment 5  
 Confining Effective Stress=250 kPa-10x20 cm

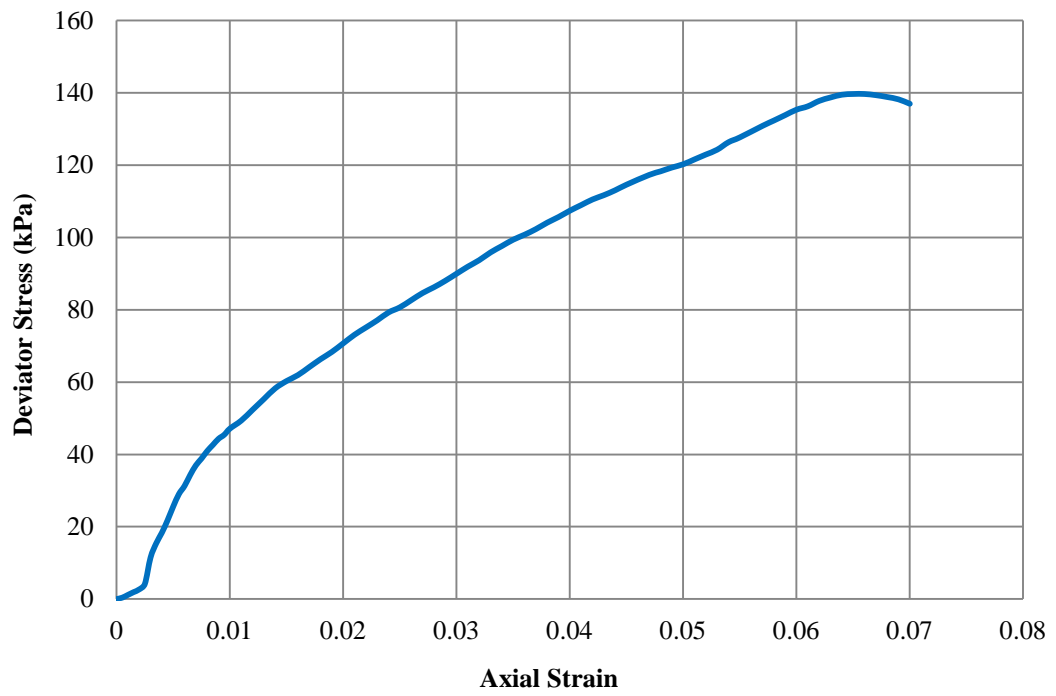


Figure B.21 Axial Strain vs. Deviator Stress-Experiment 6  
 Confining Effective Stress=250 kPa 10x20 cm

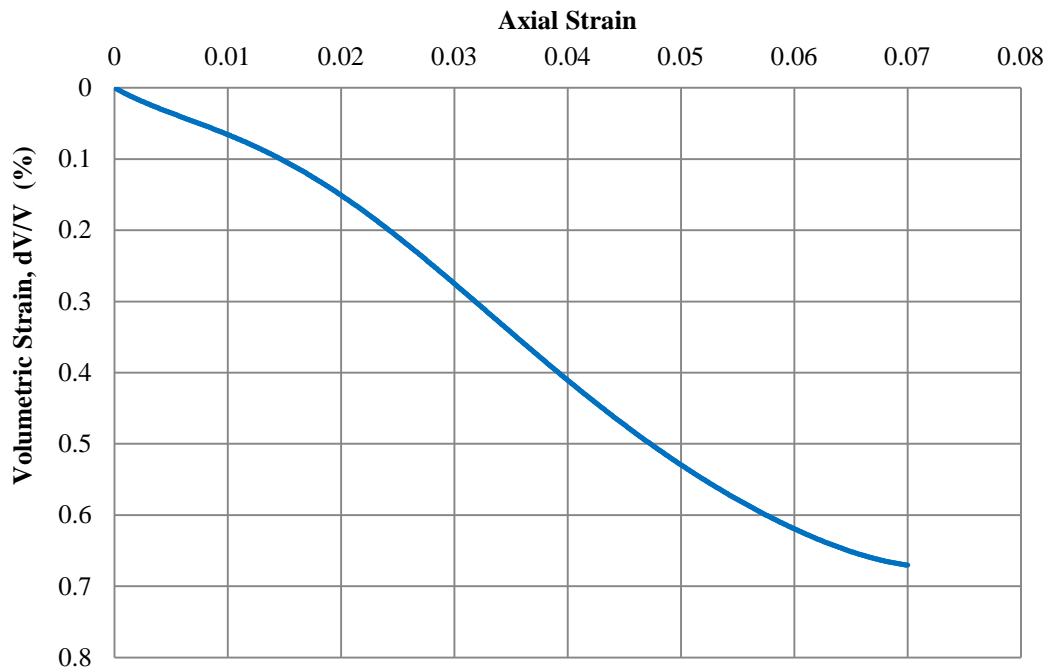


Figure B.22 Axial Strain vs. Volumetric Strain-Experiment 6  
 Confining Effective Stress=250 kPa-10x20 cm

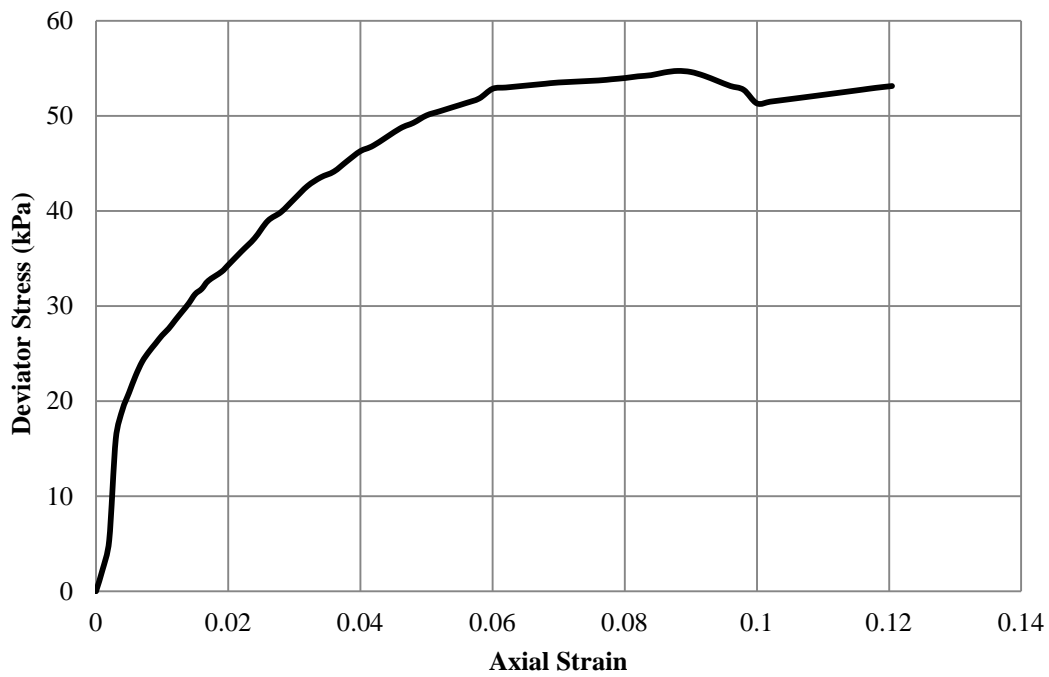


Figure B.23 Axial Strain vs. Deviator Stress-Experiment 7  
 Confining Effective Stress=50 kPa 5x10 cm

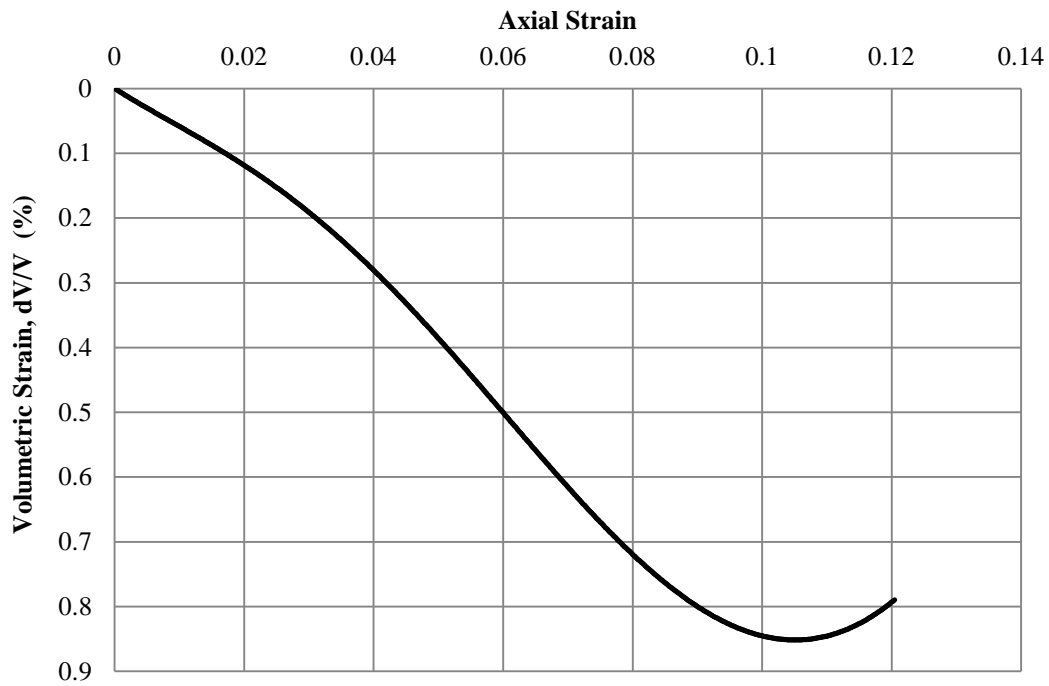


Figure B.24 Axial Strain vs. Volumetric Strain-Experiment 7  
 Confining Effective Stress=50 kPa-5x10 cm

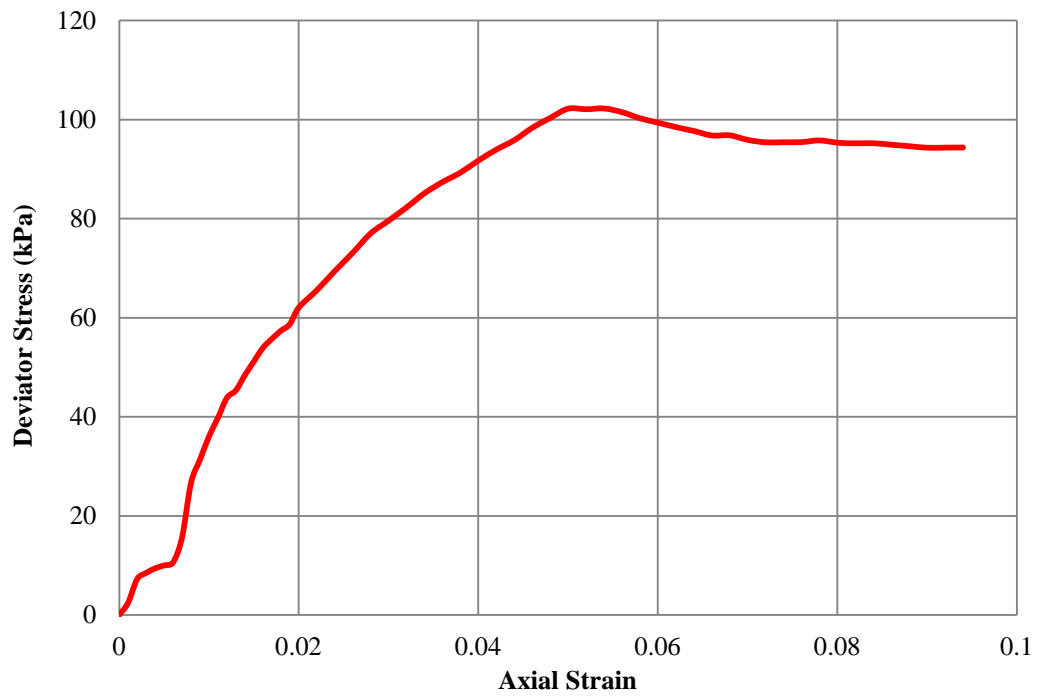


Figure B.25 Axial Strain vs. Deviator Stress-Experiment 8  
 Confining Effective Stress=150 kPa 5x10 cm

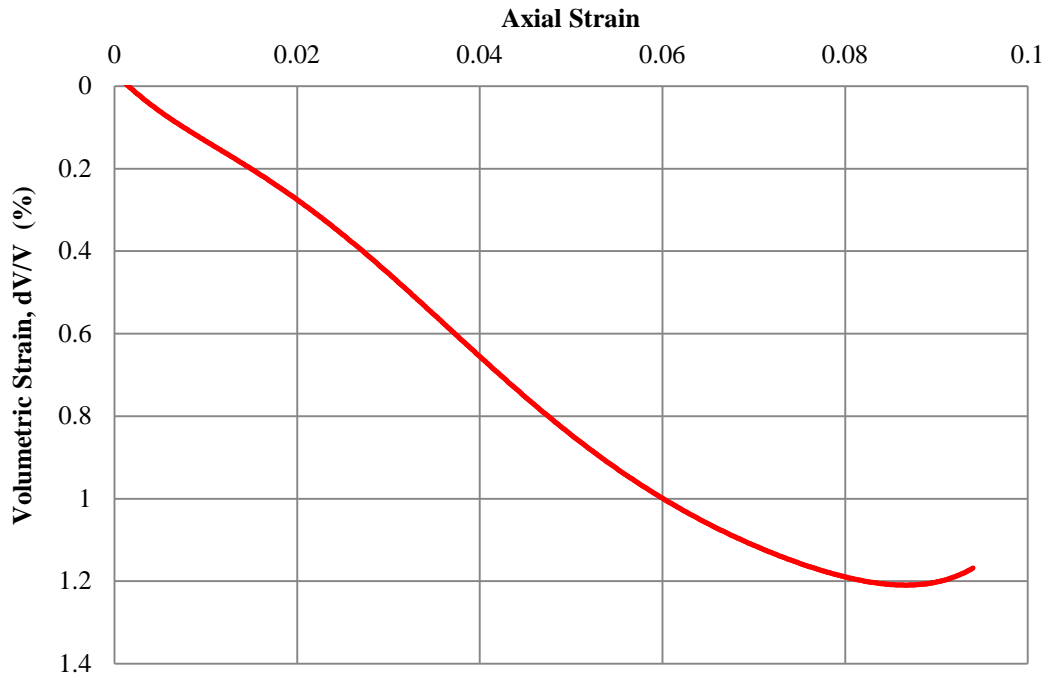


Figure B.26 Axial Strain vs. Volumetric Strain-Experiment 8  
 Confining Effective Stress=150 kPa-5x10 cm

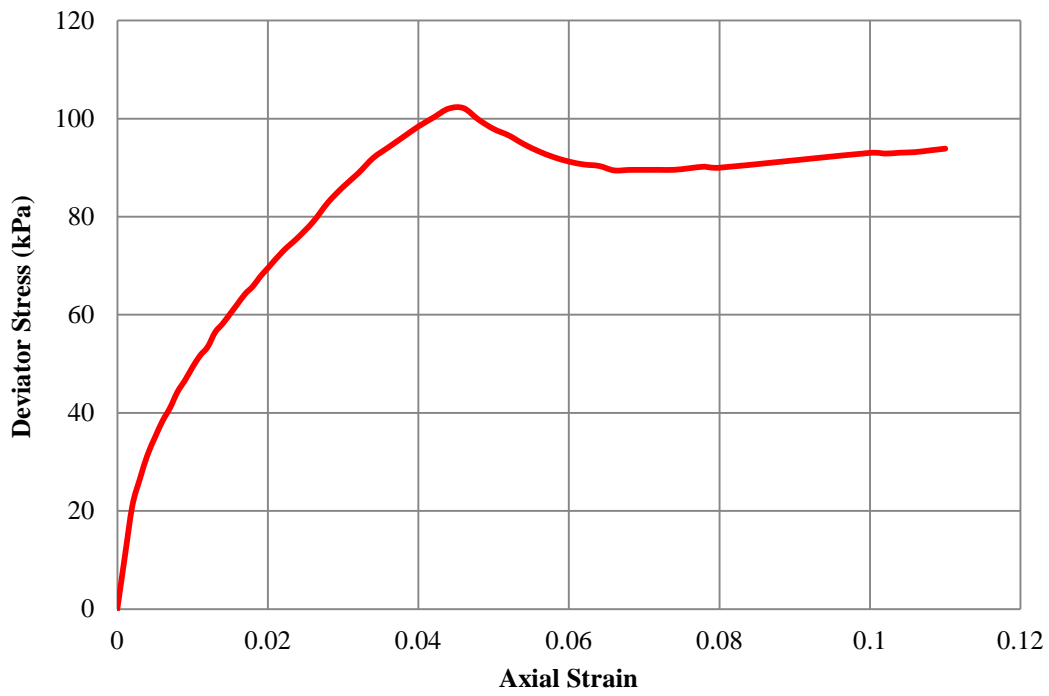


Figure B.27 Axial Strain vs. Deviator Stress-Experiment 9  
 Confining Effective Stress=150 kPa 5x10 cm

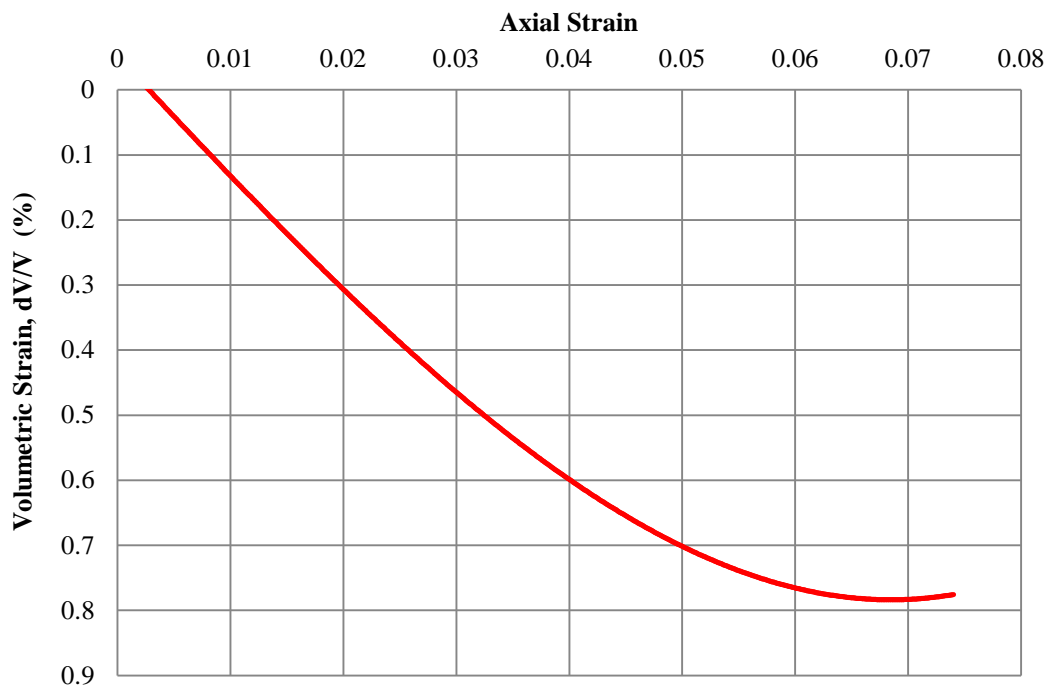


Figure B.28 Axial Strain vs. Volumetric Strain-Experiment 9  
 Confining Effective Stress=150 kPa-5x10 cm

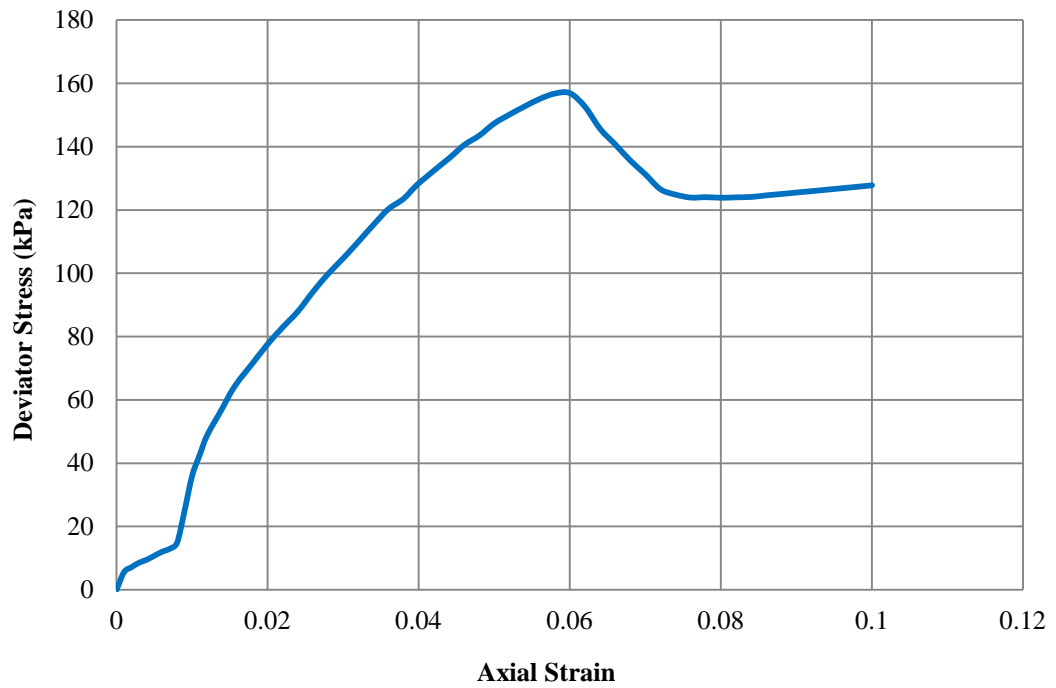


Figure B.29 Axial Strain vs. Deviator Stress-Experiment 10  
 Confining Effective Stress=250 kPa 5x10 cm

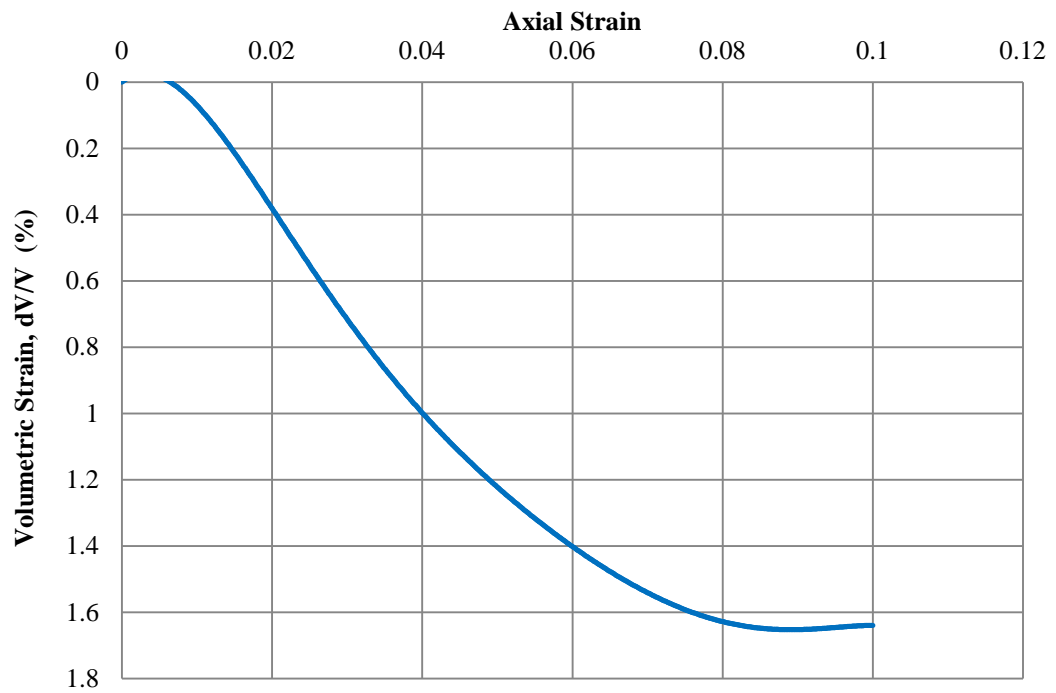


Figure B.30 Axial Strain vs. Volumetric Strain-Experiment 10  
 Confining Effective Stress=250 kPa-5x10 cm

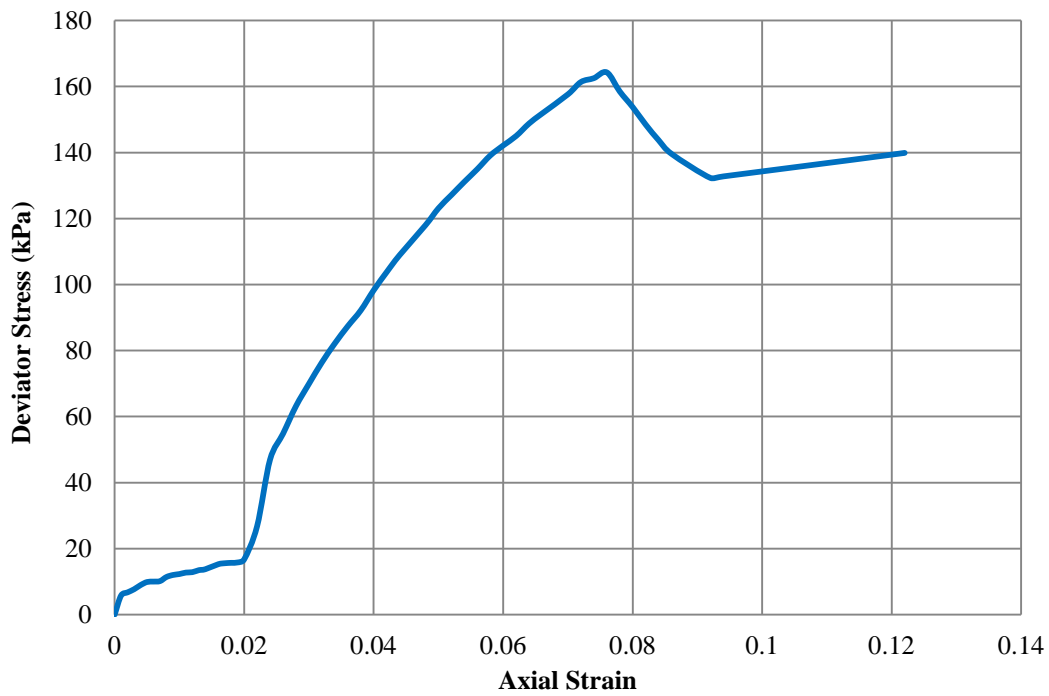


Figure B.31 Axial Strain vs. Deviator Stress-Experiment 11  
 Confining Effective Stress=250 kPa 5x10 cm

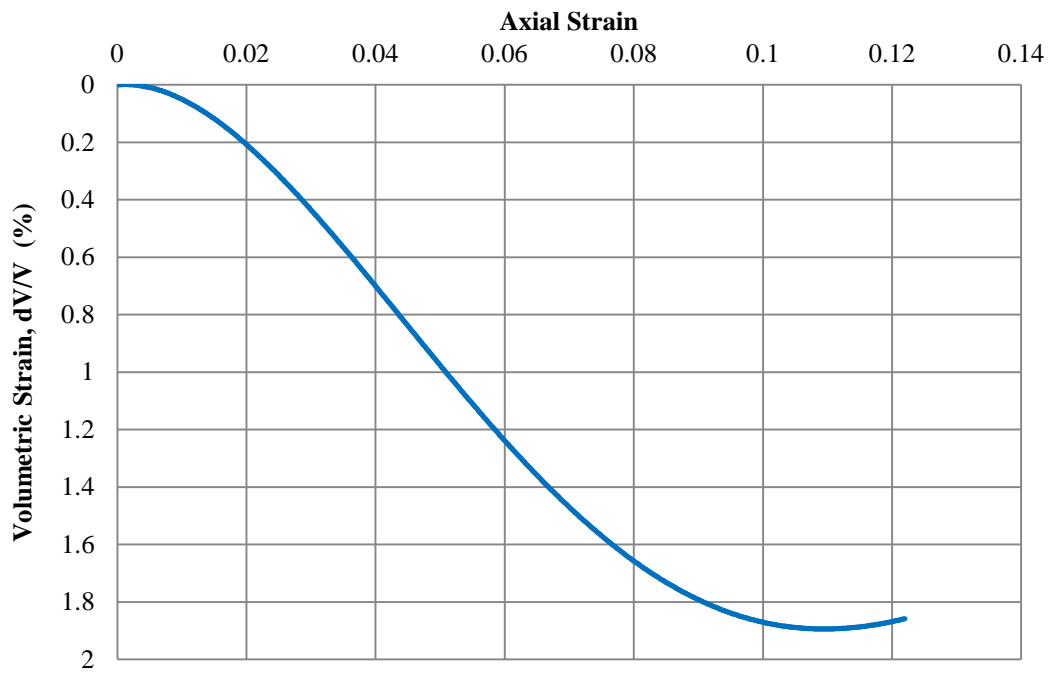


Figure B.32 Axial Strain vs. Volumetric Strain-Experiment 11  
 Confining Effective Stress=250 kPa-5x10 cm

### 3. Triaxial Tests of Gravel-Clay

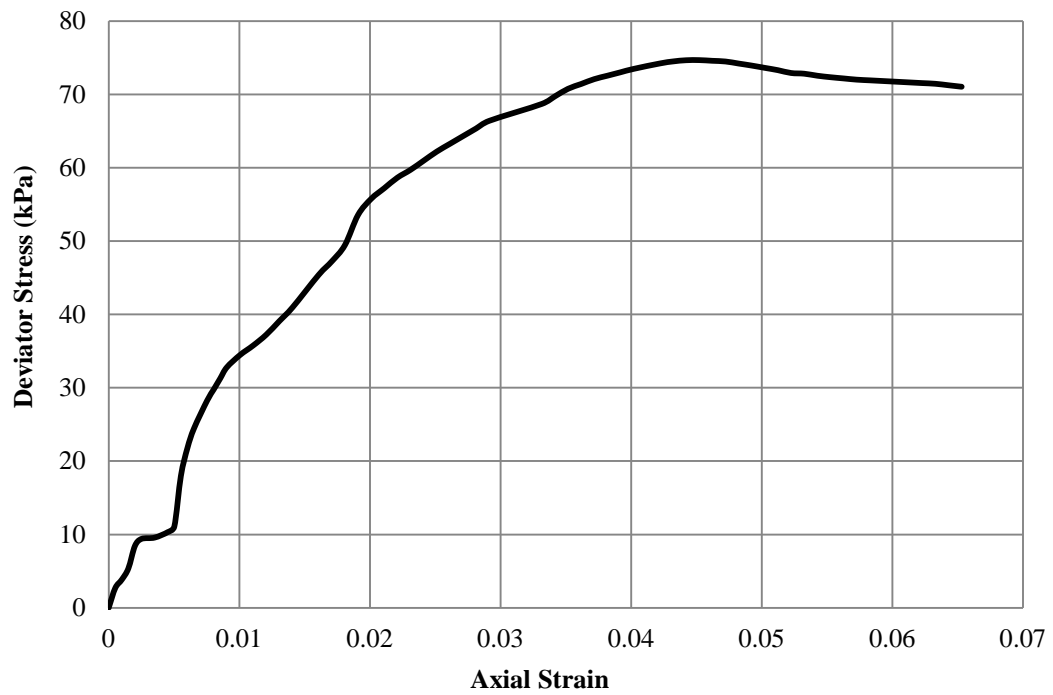


Figure B.33 Axial Strain vs. Deviator Stress-Experiment 1  
Confining Effective Stress=50 kPa

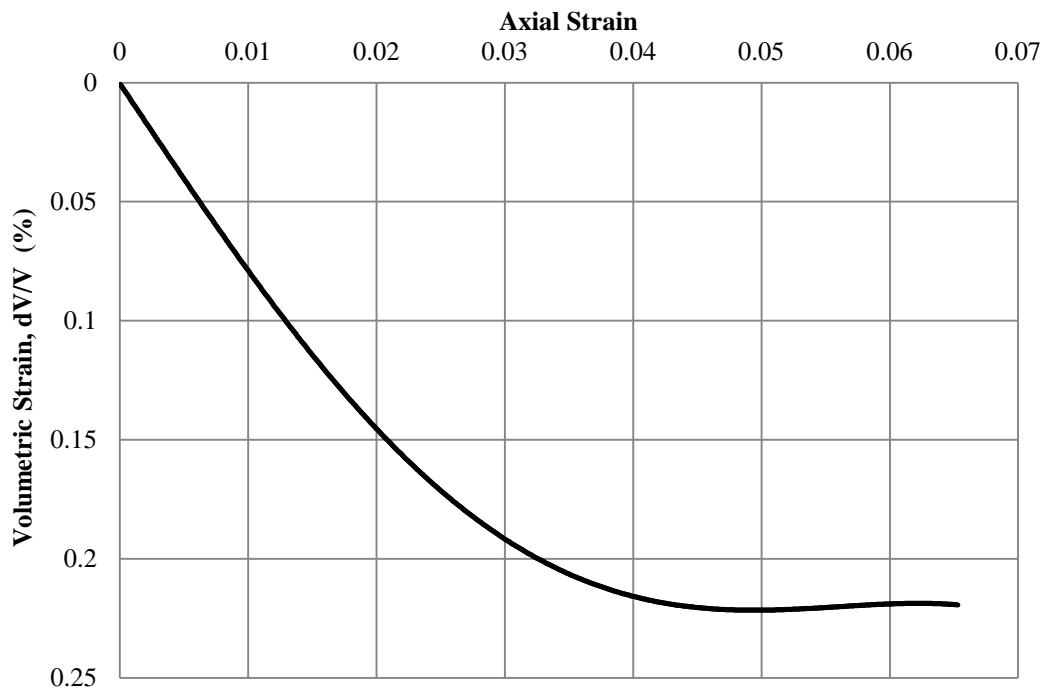


Figure B.34 Axial Strain vs. Volumetric Strain-Experiment 1  
Confining Effective Stress=50 kPa

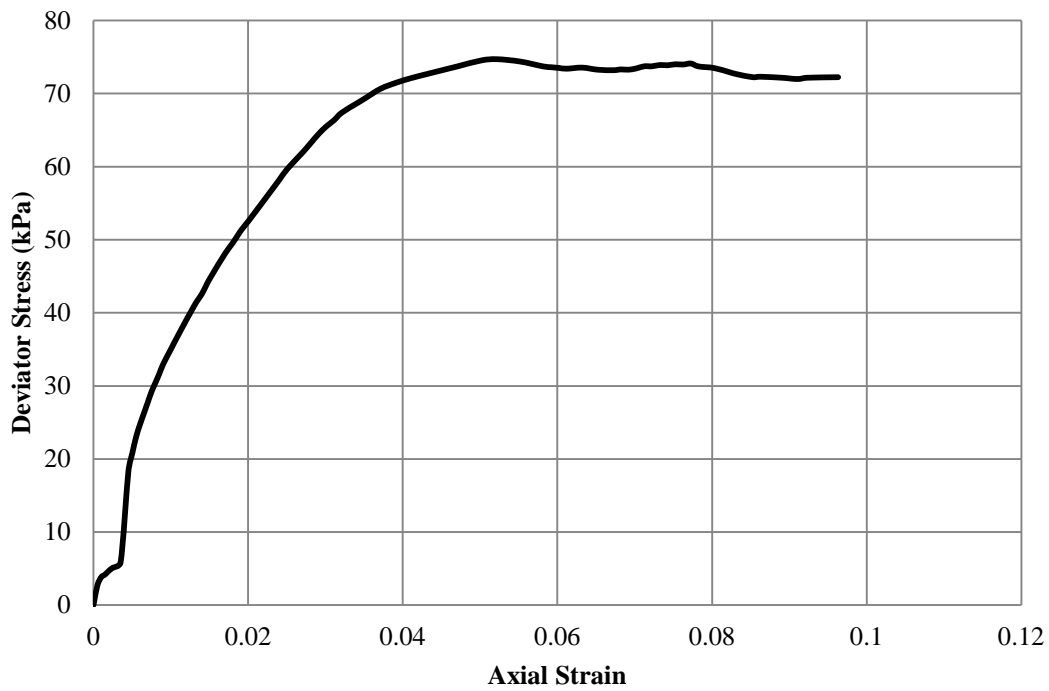


Figure B.35 Axial Strain vs. Deviator Stress-Experiment 2  
 Confining Effective Stress=50 kPa

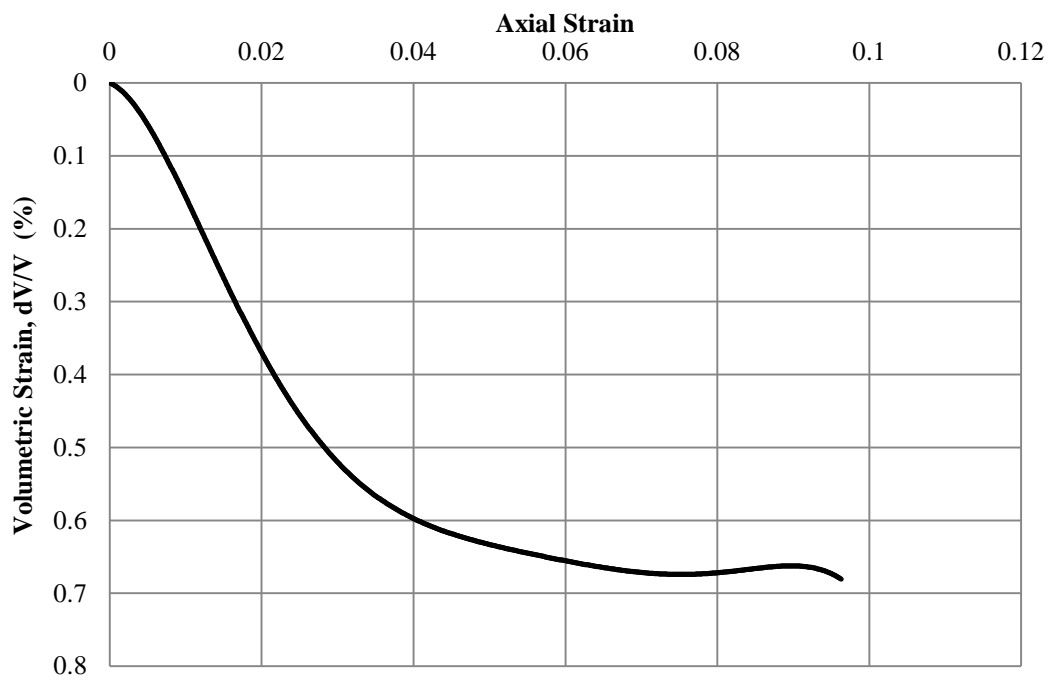


Figure B.36 Axial Strain vs. Volumetric Strain-Experiment 2  
 Confining Effective Stress=50 kPa

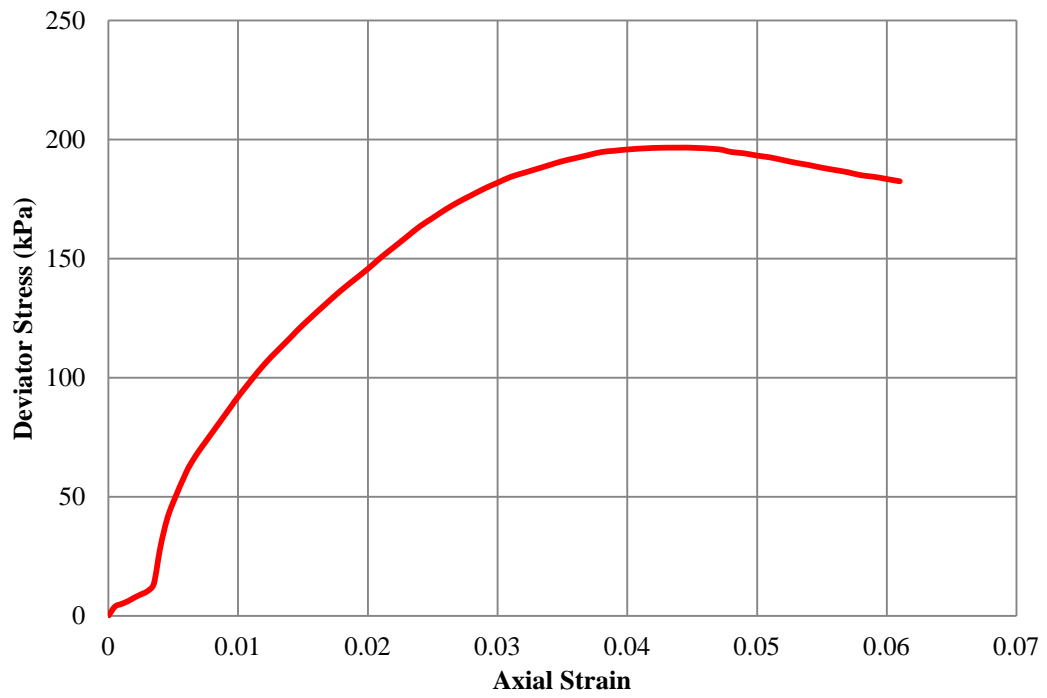


Figure B.37 Axial Strain vs. Deviator Stress-Experiment 3  
 Confining Effective Stress=150 kPa

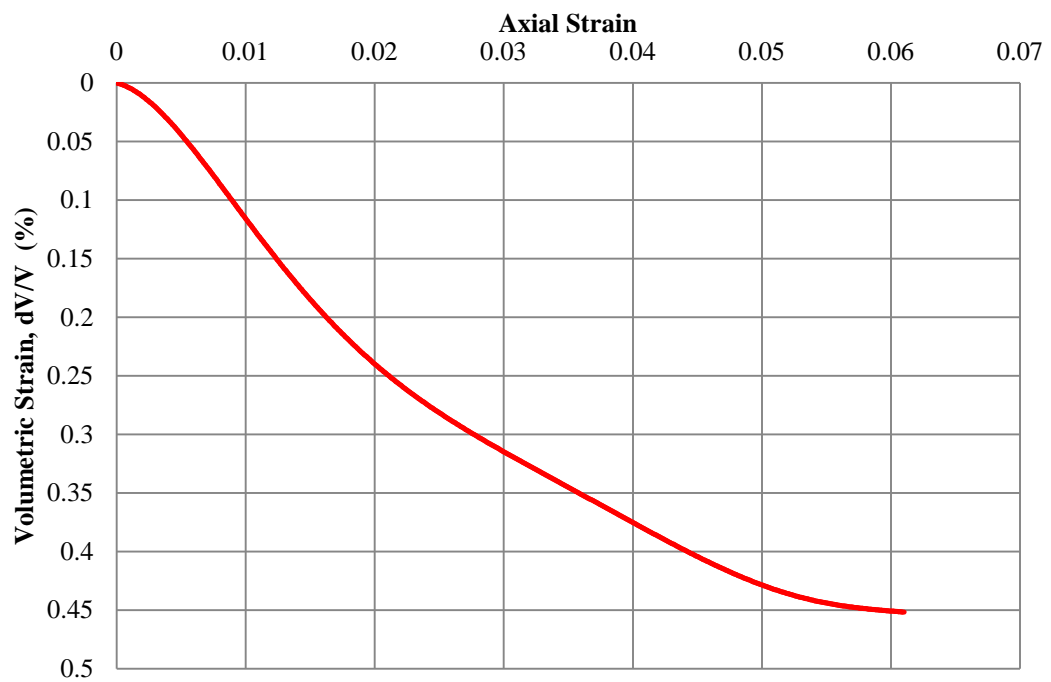


Figure B.38 Axial Strain vs. Volumetric Strain-Experiment 3  
 Confining Effective Stress=150 kPa

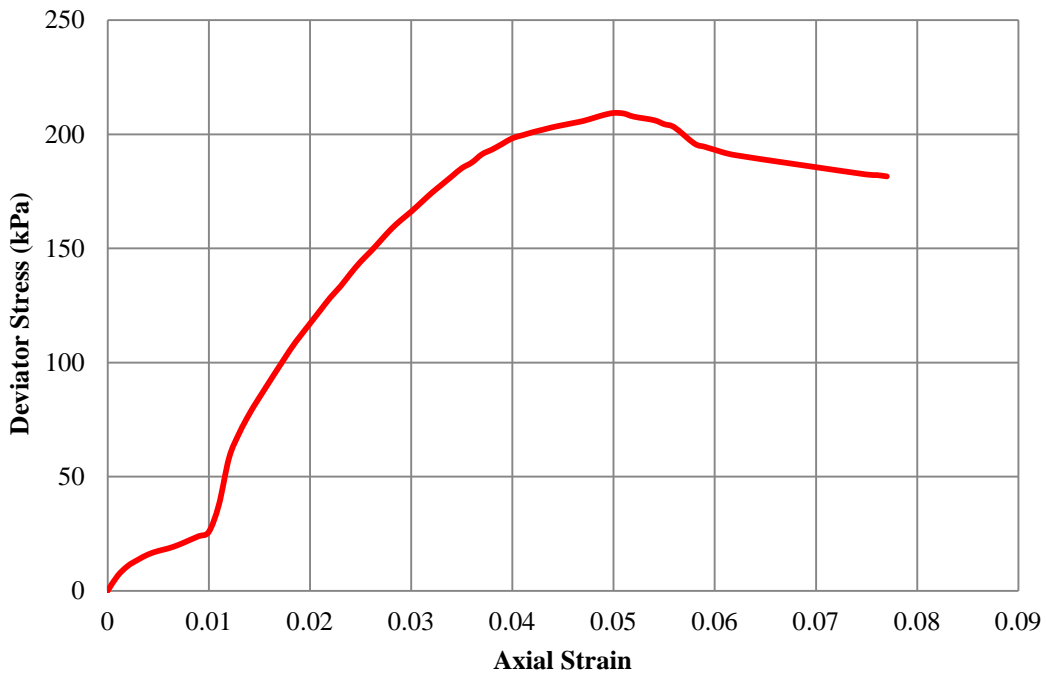


Figure B.39 Axial Strain vs. Deviator Stress-Experiment 4  
 Confining Effective Stress=150 kPa

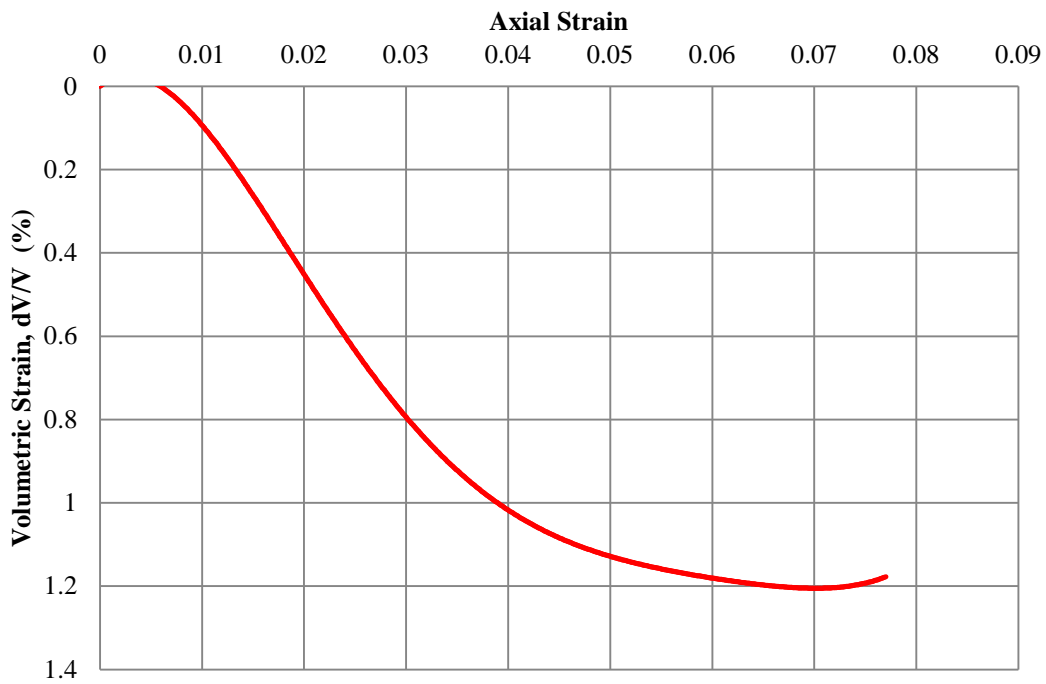


Figure B.40 Axial Strain vs. Volumetric Strain-Experiment 4  
 Confining Effective Stress=150 kPa

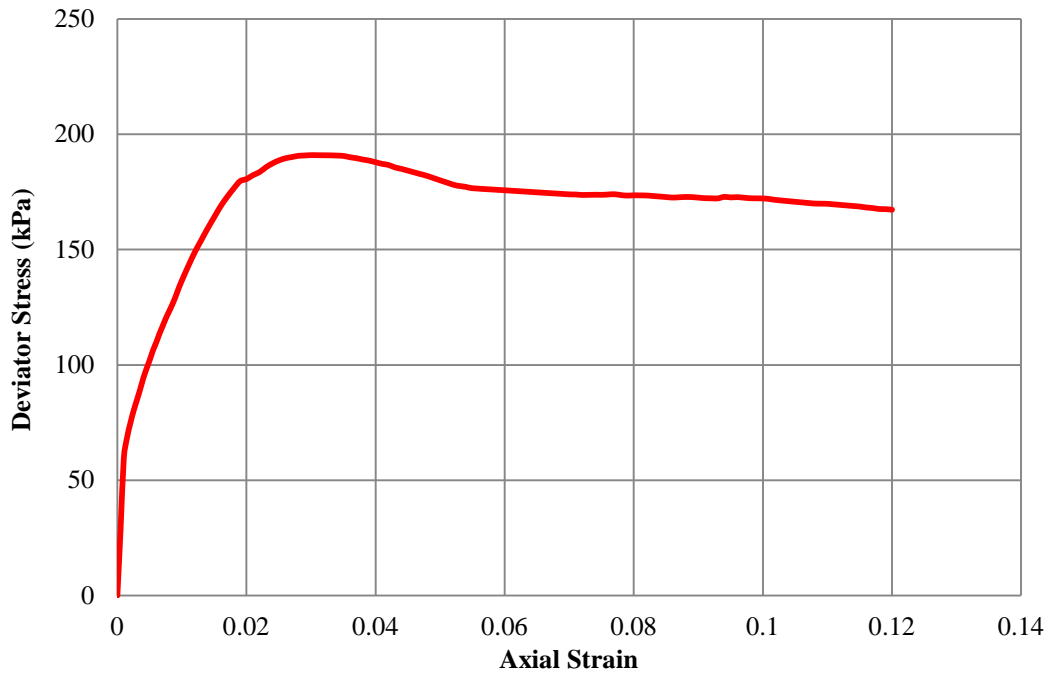


Figure B.41 Axial Strain vs. Deviator Stress-Experiment 5  
 Confining Effective Stress=150 kPa

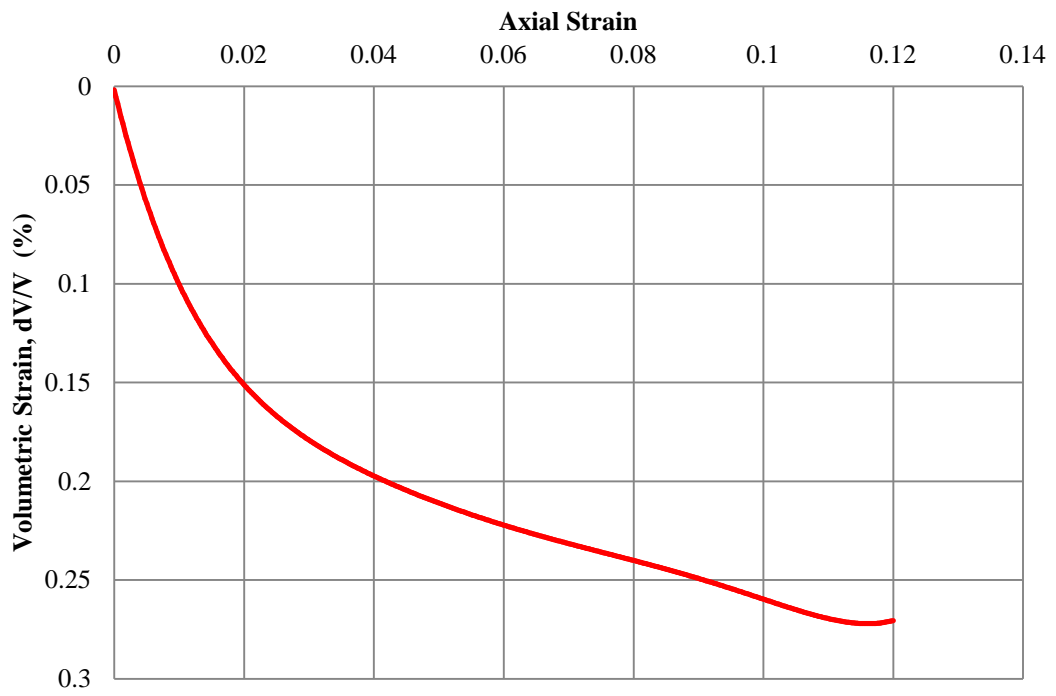


Figure B.42 Axial Strain vs. Volumetric Strain-Experiment 5  
 Confining Effective Stress=150 kPa

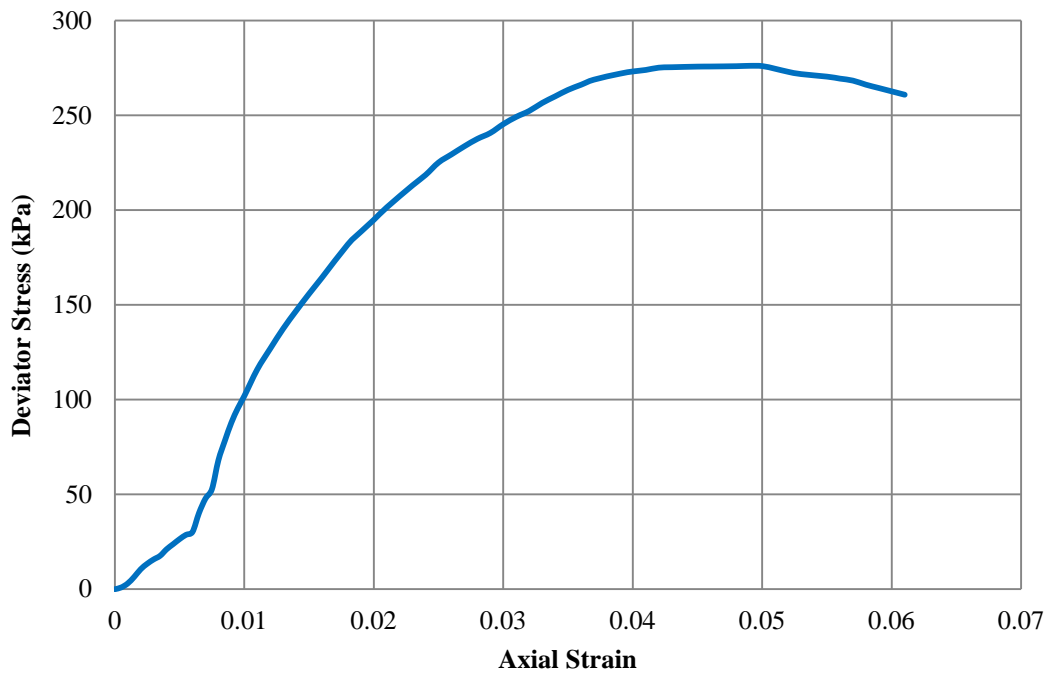


Figure B.43 Axial Strain vs. Deviator Stress-Experiment 6  
 Confining Effective Stress=250 kPa

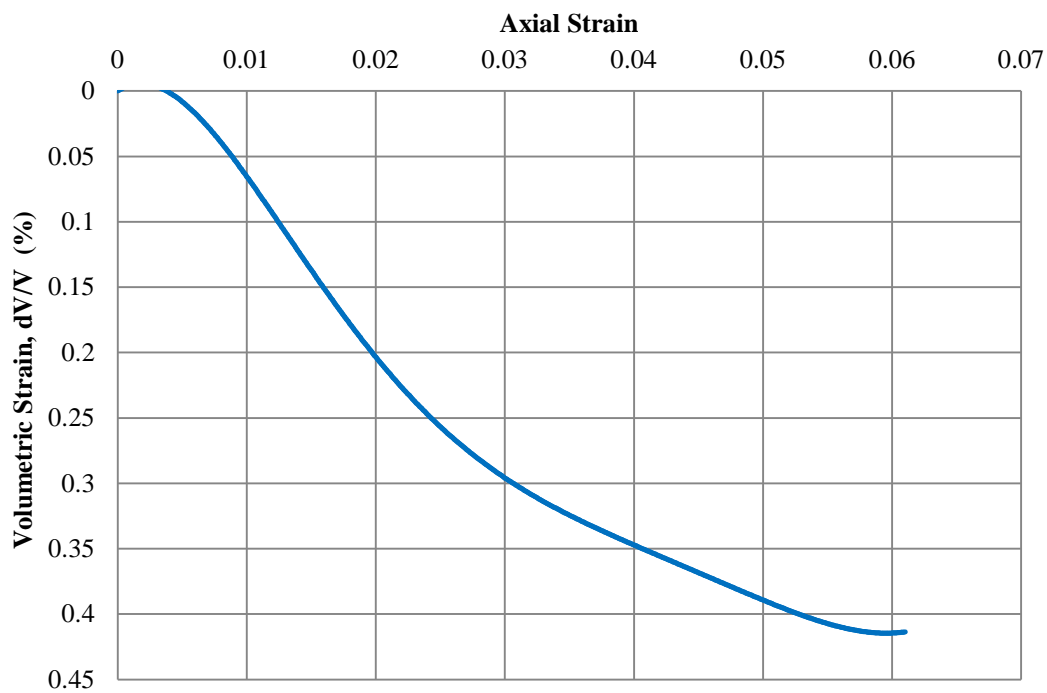


Figure B.44 Axial Strain vs. Volumetric Strain-Experiment 6  
 Confining Effective Stress=250 kPa

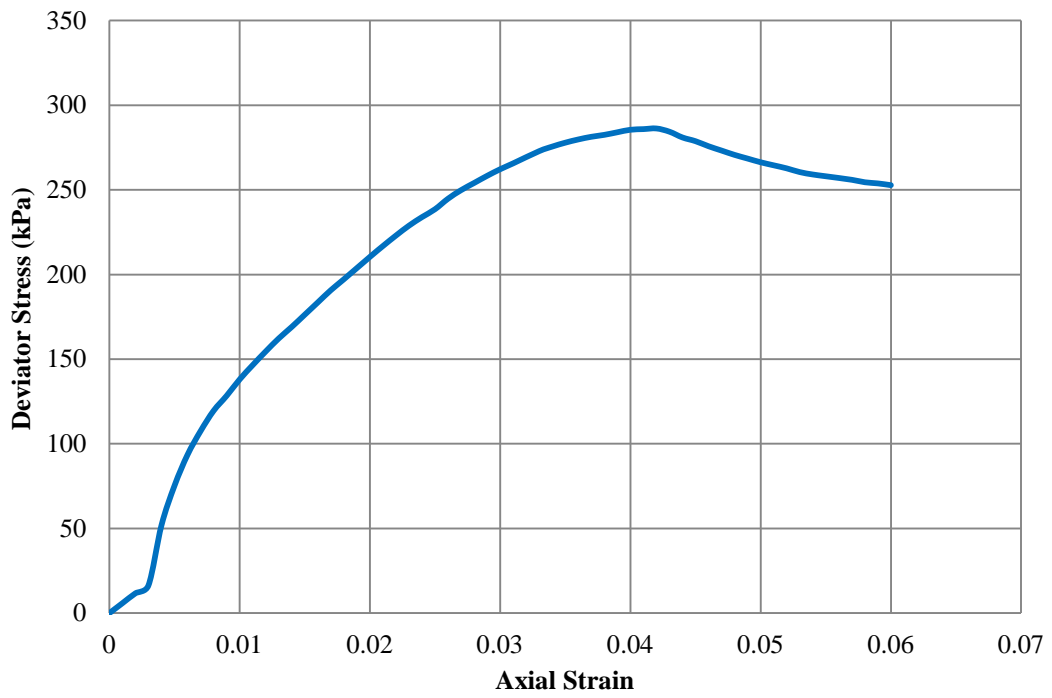


Figure B.45 Axial Strain vs. Deviator Stress-Experiment 7  
 Confining Effective Stress=250 kPa

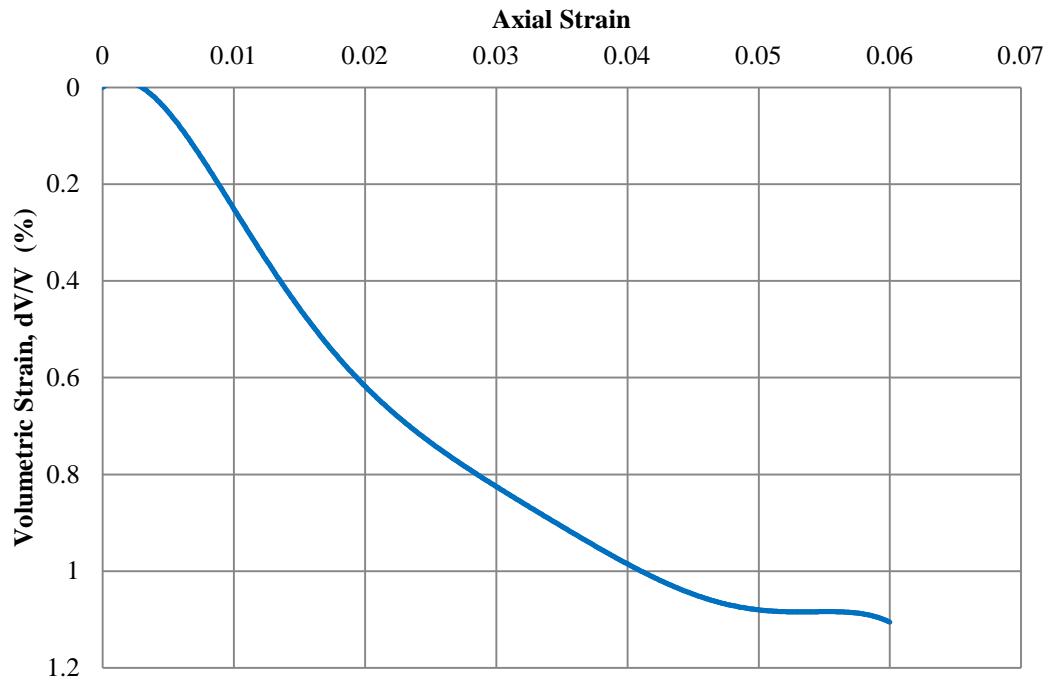


Figure B.46 Axial Strain vs. Volumetric Strain-Experiment 7  
 Confining Effective Stress=250 kPa

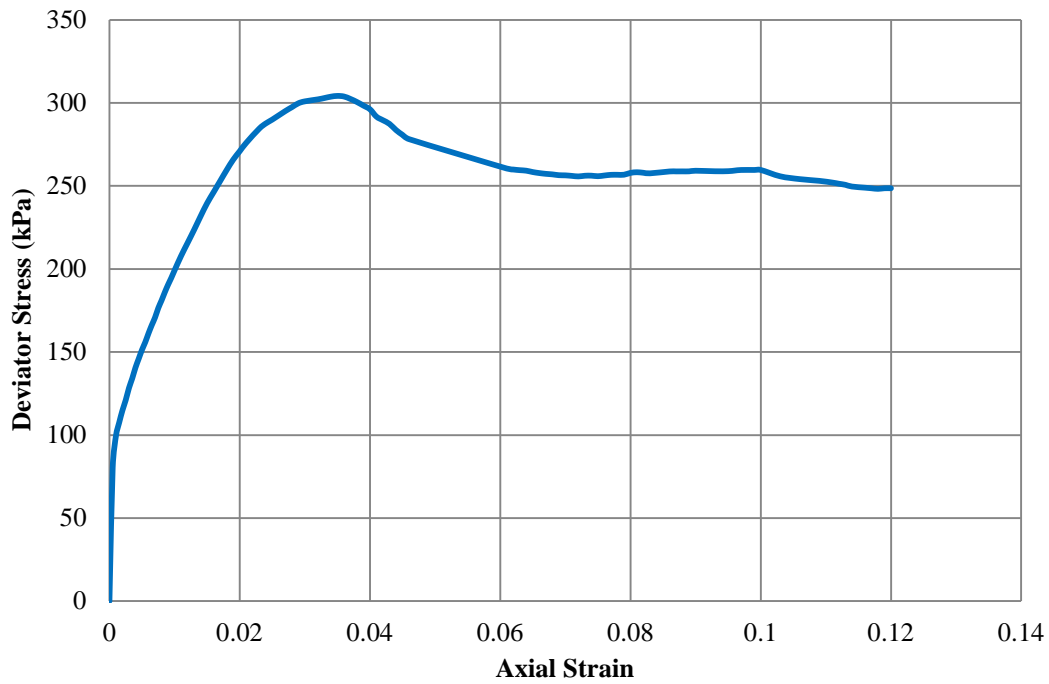


Figure B.47 Axial Strain vs. Deviator Stress-Experiment 8  
 Confining Effective Stress=250 kPa

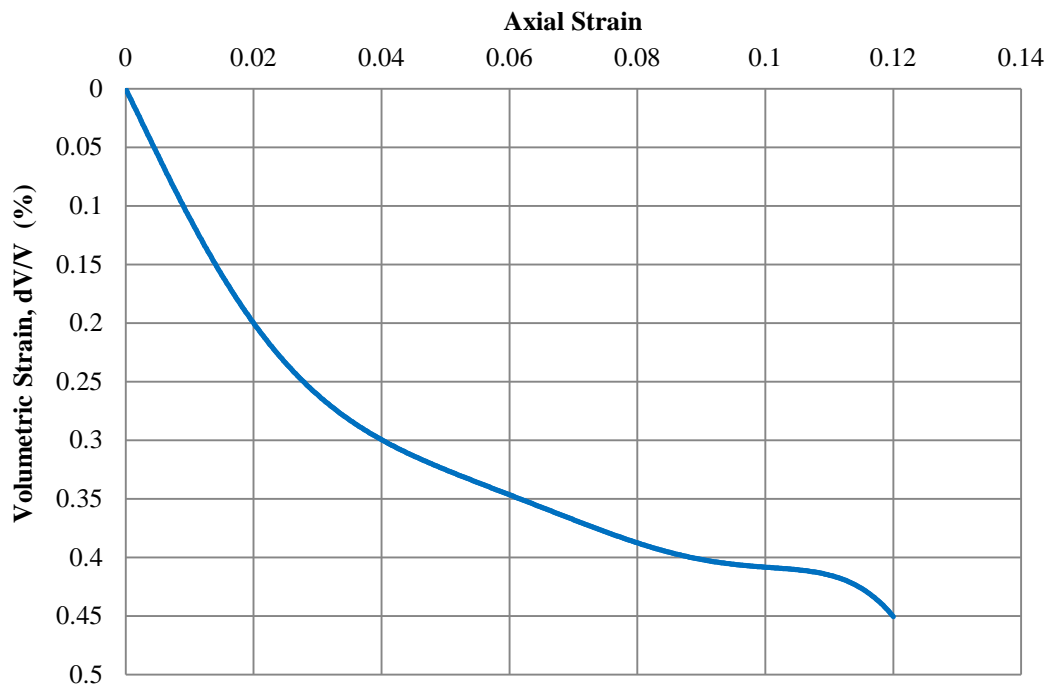


Figure B.48 Axial Strain vs. Volumetric Strain-Experiment 8  
 Confining Effective Stress=250 kPa

#### 4. Triaxial Tests of Sand-Clay

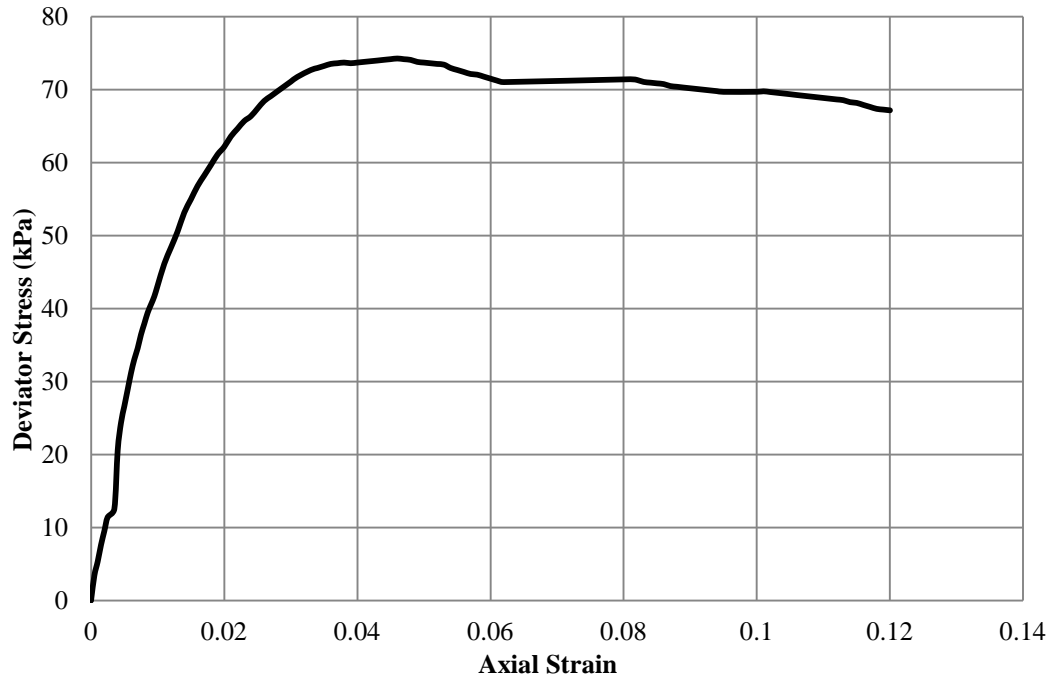


Figure B.49 Axial Strain vs. Deviator Stress-Experiment 1  
Confining Effective Stress=50 kPa 10x20 cm

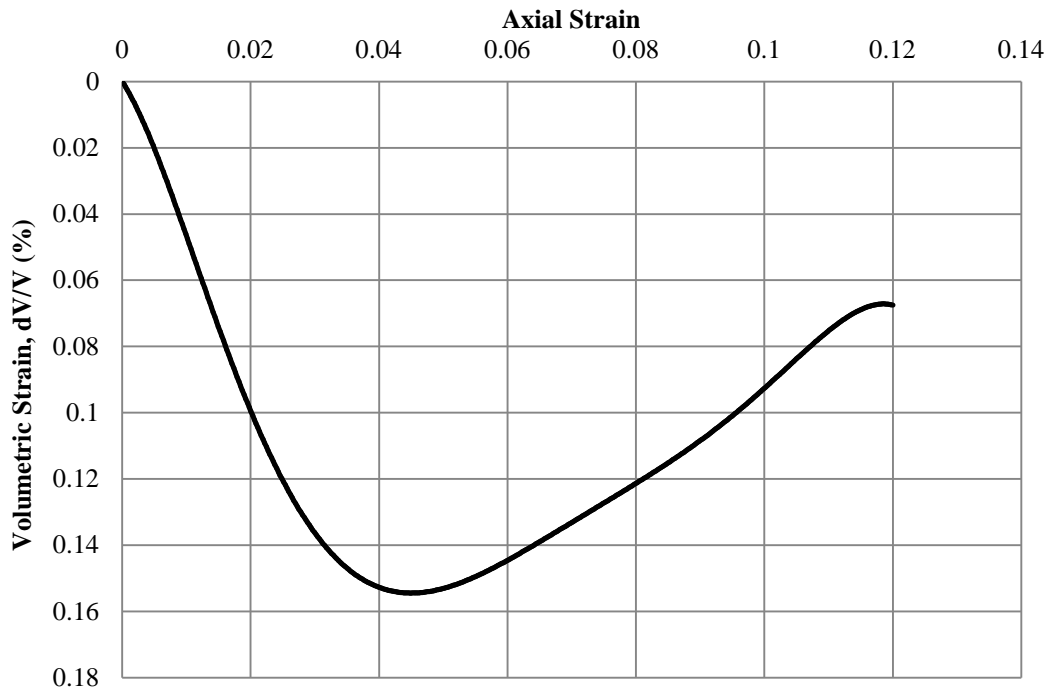


Figure B.50 Axial Strain vs. Volumetric Strain-Experiment 1  
Confining Effective Stress=50 kPa-10x20 cm

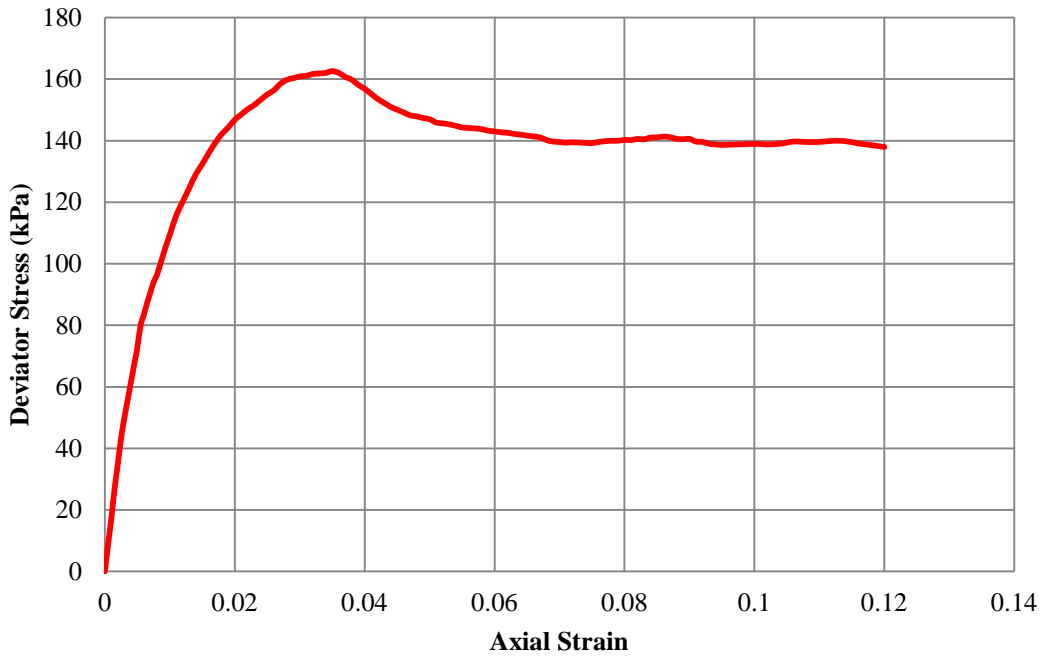


Figure B.51 Axial Strain vs. Deviator Stress-Experiment 2  
 Confining Effective Stress=150 kPa 10x20 cm

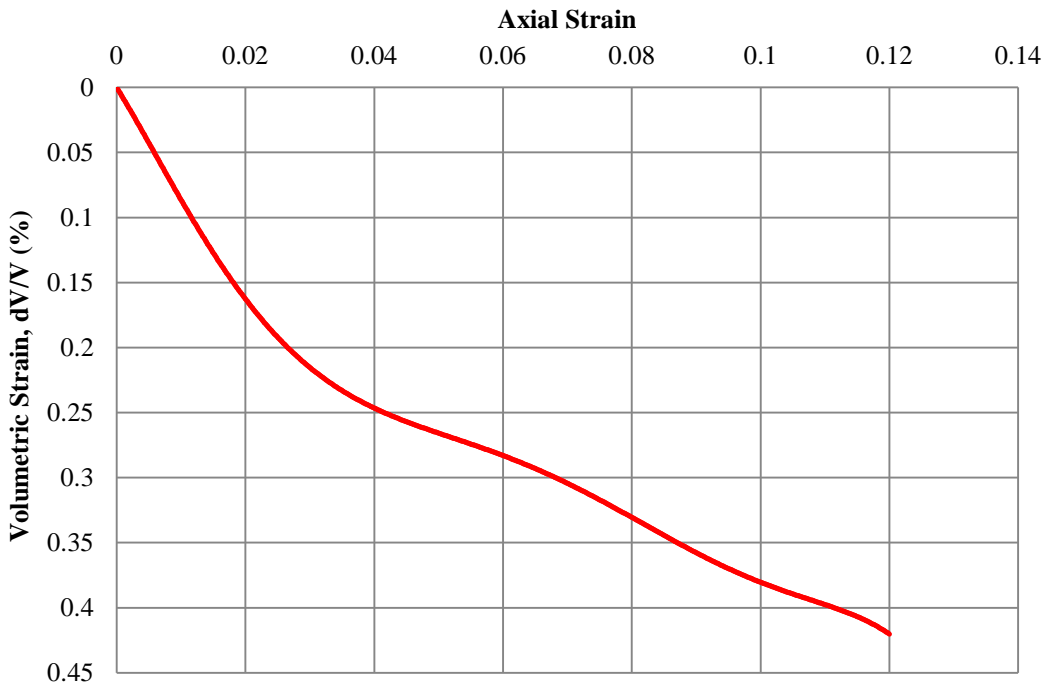


Figure B.52 Axial Strain vs. Volumetric Strain-Experiment 2  
 Confining Effective Stress=150 kPa-10x20 cm

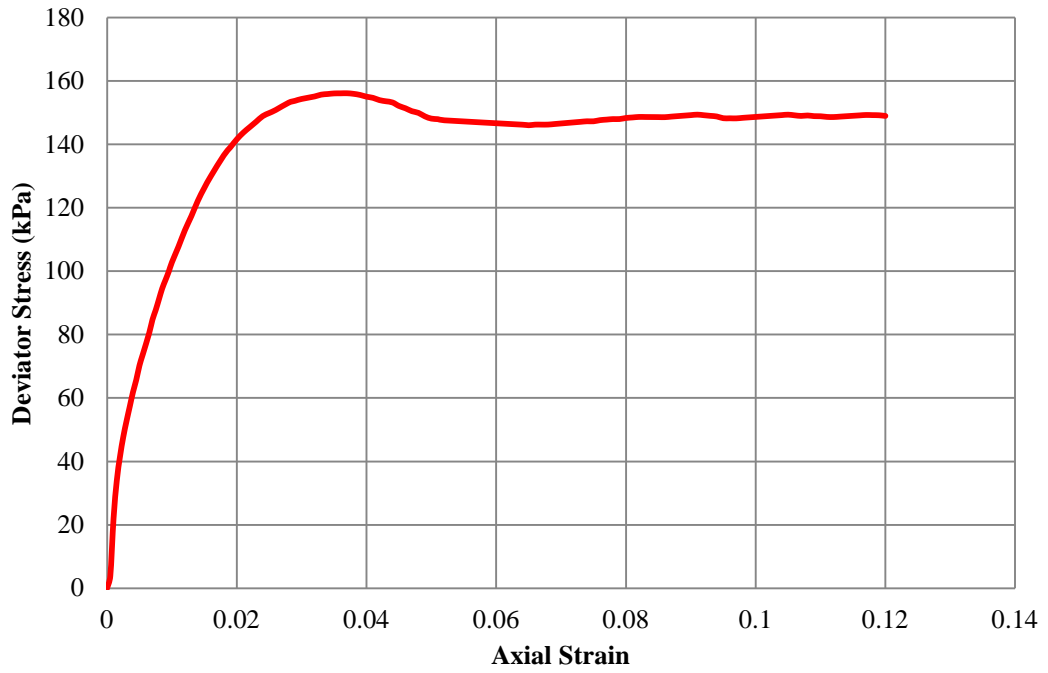


Figure B.53 Axial Strain vs. Deviator Stress-Experiment 3  
 Confining Effective Stress=150 kPa 10x20 cm

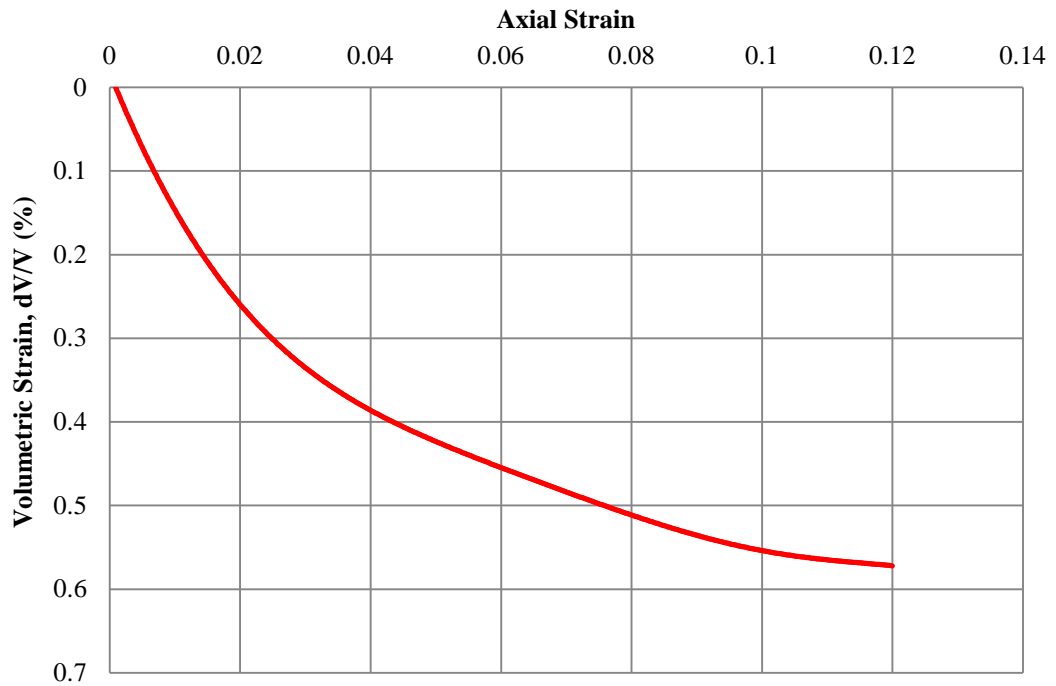


Figure B.54 Axial Strain vs. Volumetric Strain-Experiment 3  
 Confining Effective Stress=150 kPa-10x20 cm

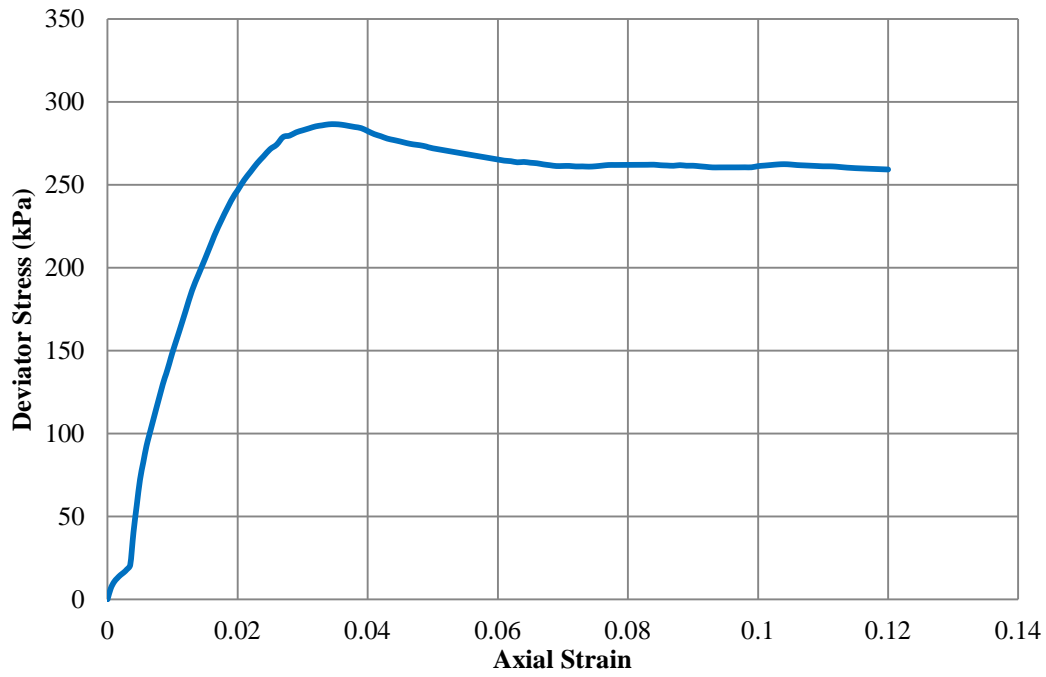


Figure B.55 Axial Strain vs. Deviator Stress-Experiment 4  
 Confining Effective Stress=250 kPa 10x20 cm

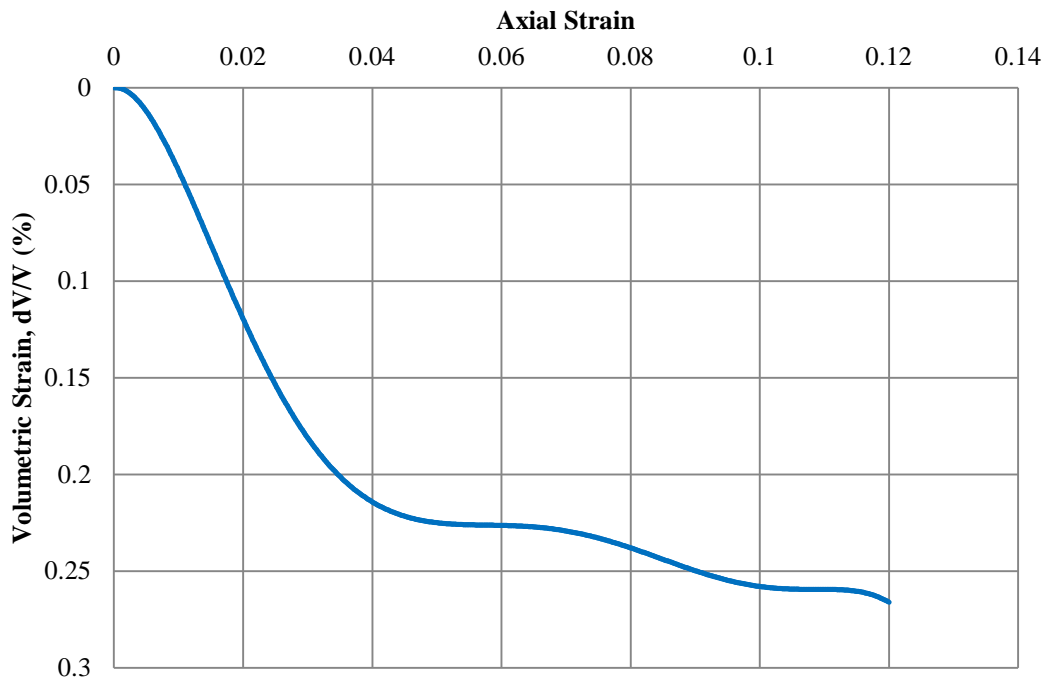


Figure B.56 Axial Strain vs. Volumetric Strain-Experiment 4  
 Confining Effective Stress=250 kPa-10x20 cm

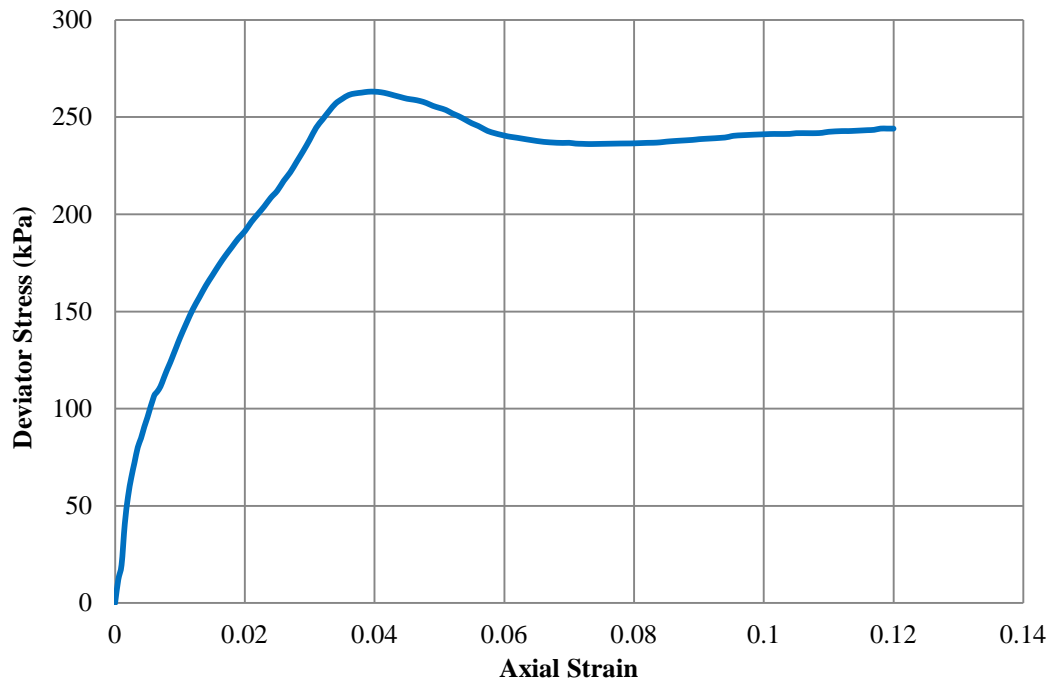


Figure B.57 Axial Strain vs. Deviator Stress-Experiment 5  
 Confining Effective Stress=250 kPa 10x20 cm

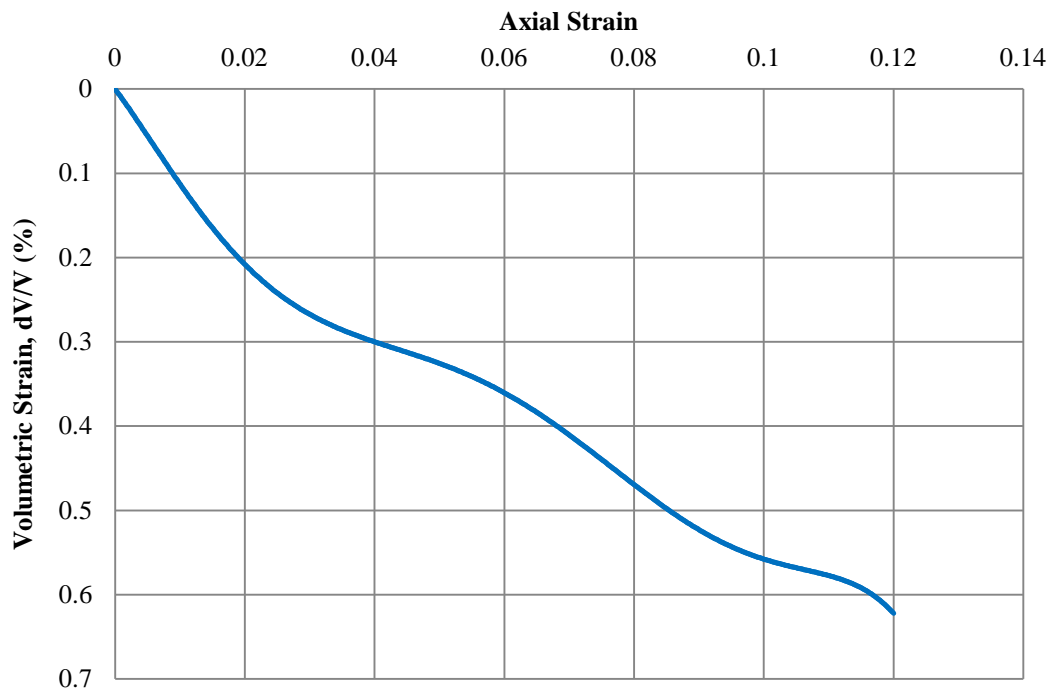


Figure B.58 Axial Strain vs. Volumetric Strain-Experiment 5  
 Confining Effective Stress=250 kPa-10x20 cm

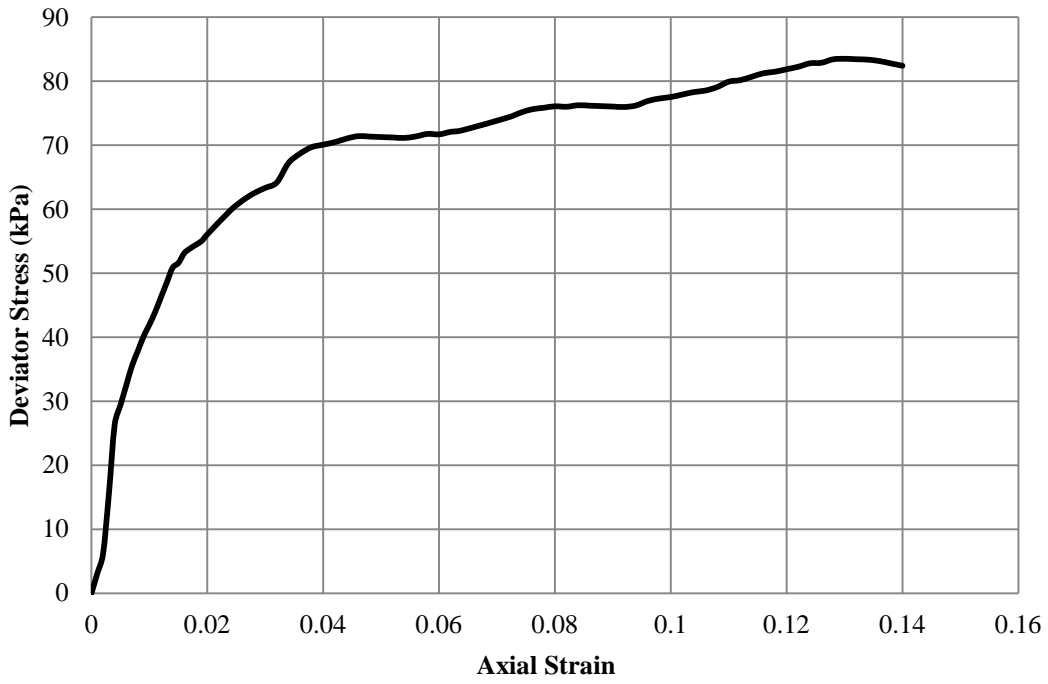


Figure B.59 Axial Strain vs. Deviator Stress-Experiment 6  
 Confining Effective Stress=50 kPa 5x10 cm

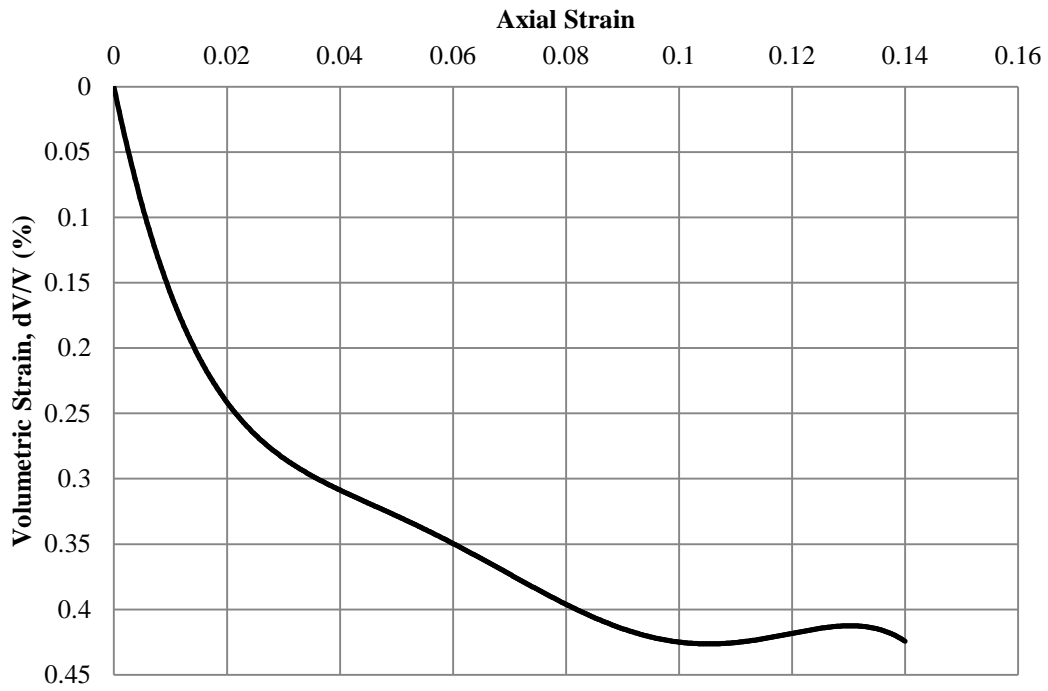


Figure B.60 Axial Strain vs. Volumetric Strain-Experiment 6  
 Confining Effective Stress=50 kPa-5x10 cm

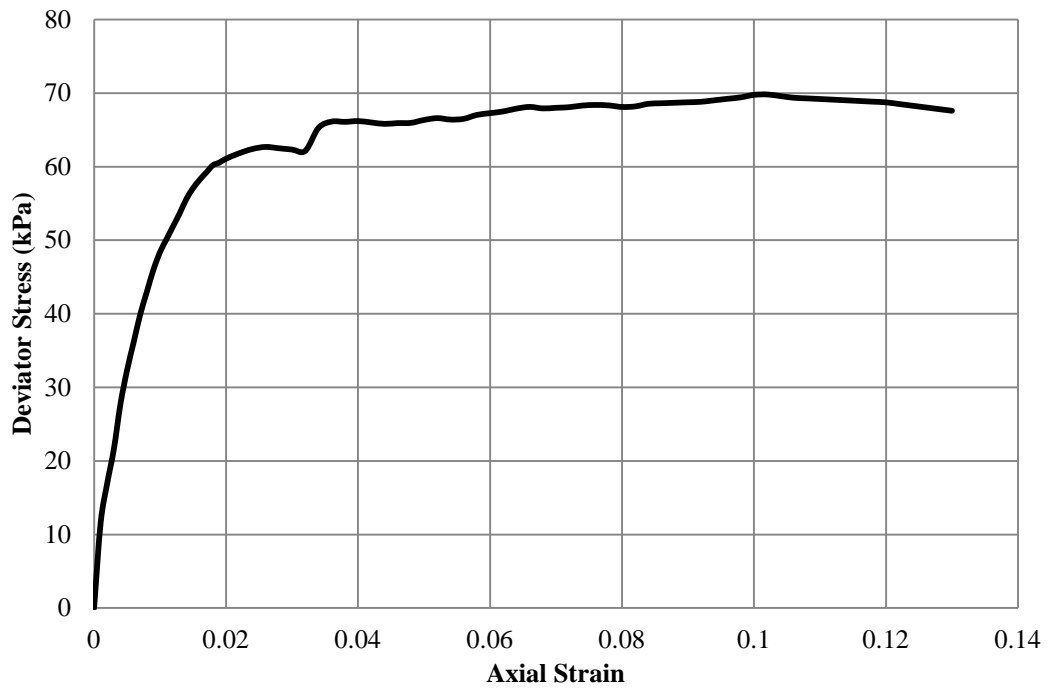


Figure B.61 Axial Strain vs. Deviator Stress-Experiment 7  
 Confining Effective Stress=50 kPa 5x10 cm

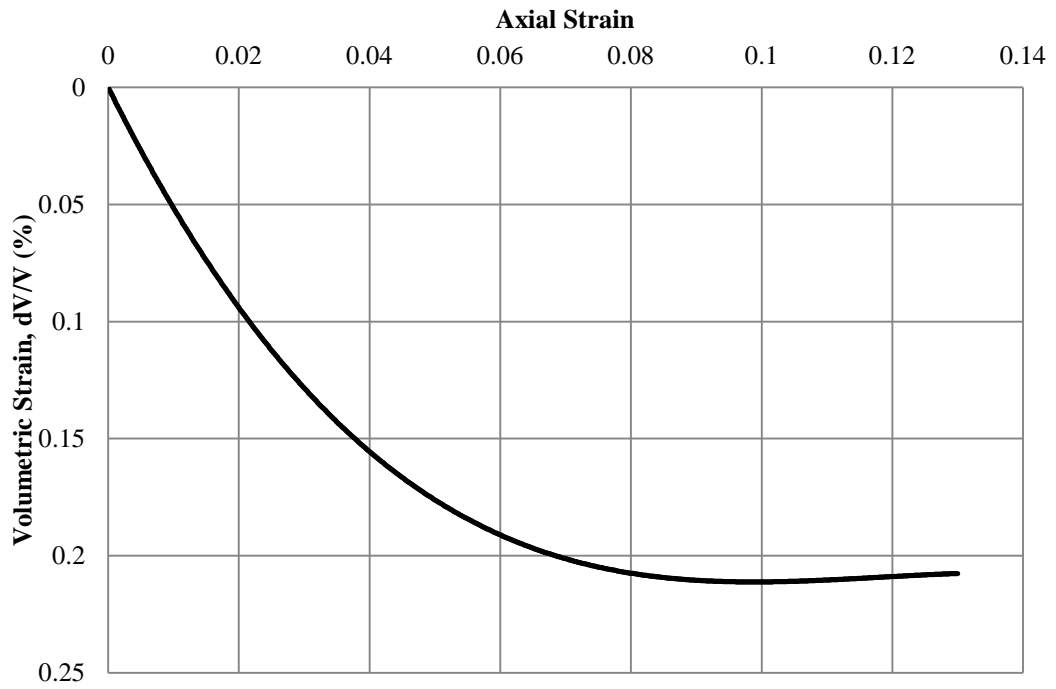


Figure B.62 Axial Strain vs. Volumetric Strain-Experiment 7  
 Confining Effective Stress=50 kPa-5x10 cm

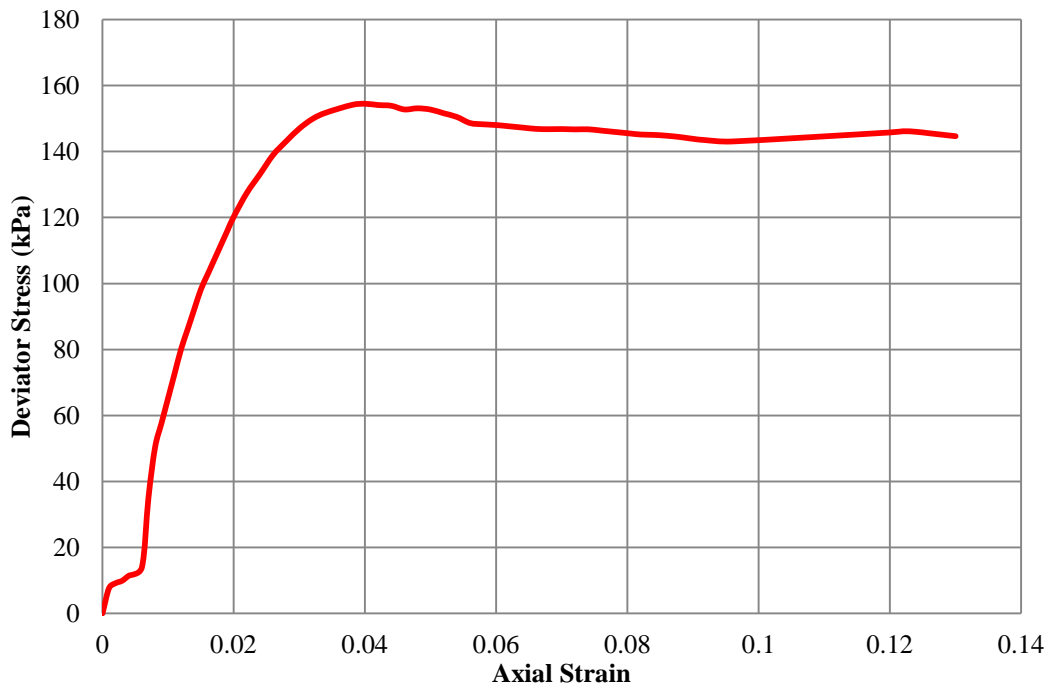


Figure B.63 Axial Strain vs. Deviator Stress-Experiment 8  
 Confining Effective Stress=150 kPa 5x10 cm

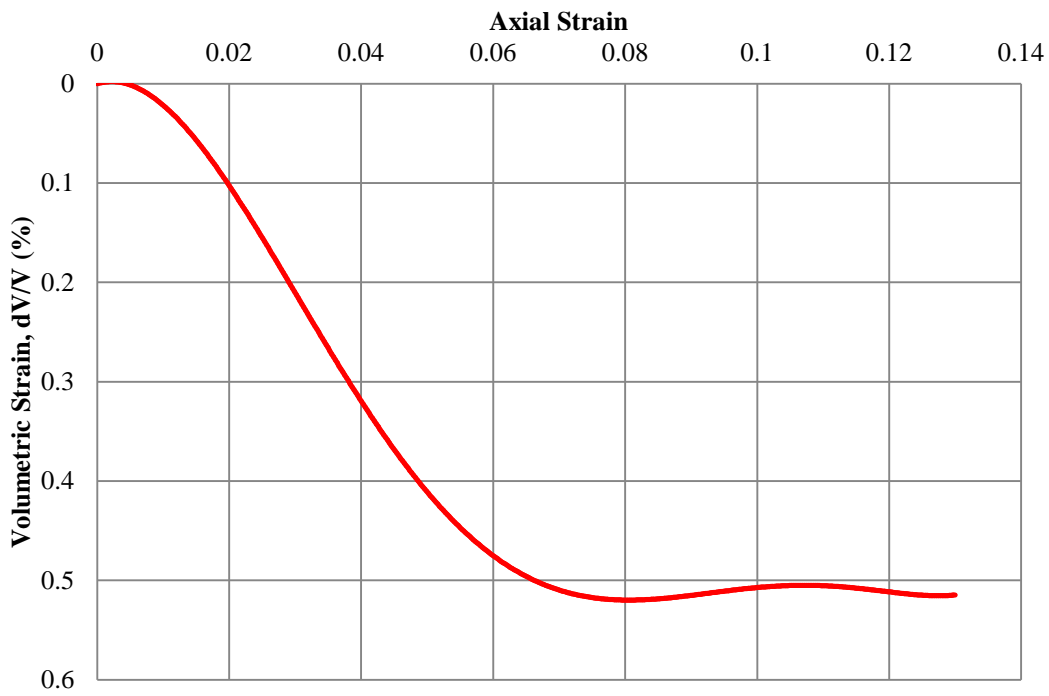


Figure B.64 Axial Strain vs. Volumetric Strain-Experiment 8  
 Confining Effective Stress=150 kPa-5x10 cm

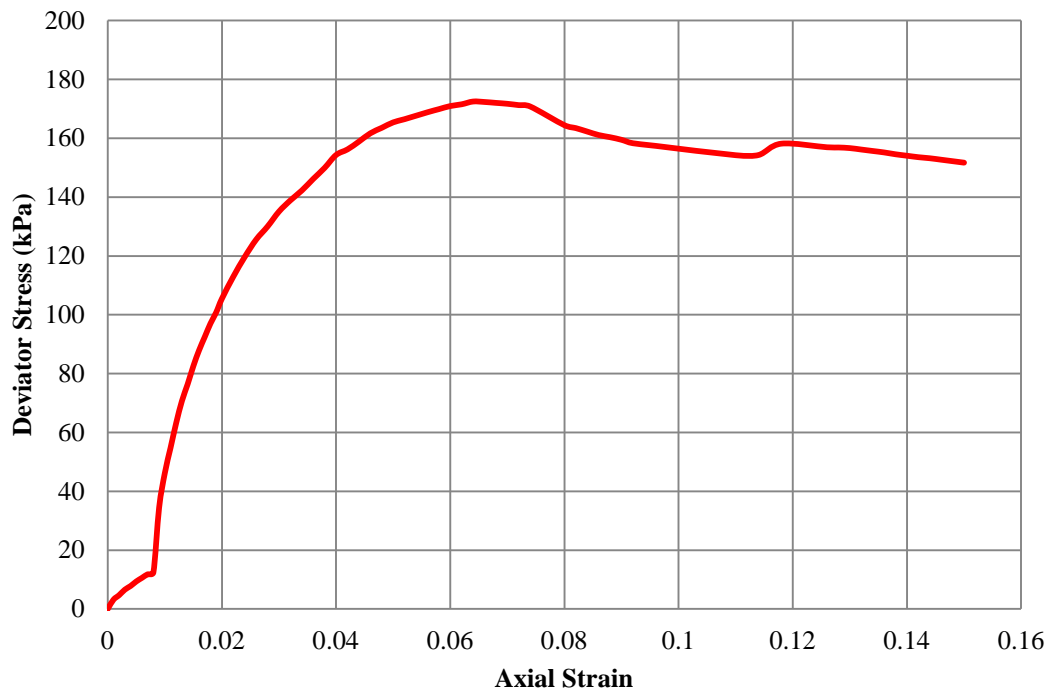


Figure B.65 Axial Strain vs. Deviator Stress-Experiment 9  
 Confining Effective Stress=150 kPa 5x10 cm

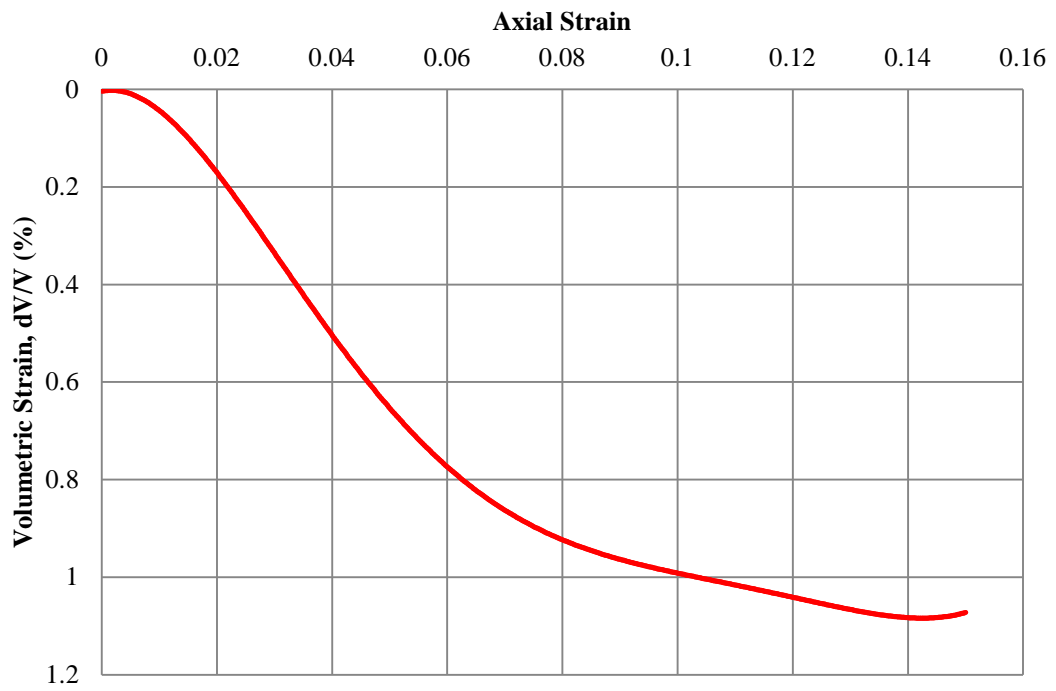


Figure B.66 Axial Strain vs. Volumetric Strain-Experiment 9  
 Confining Effective Stress=150 kPa-5x10 cm

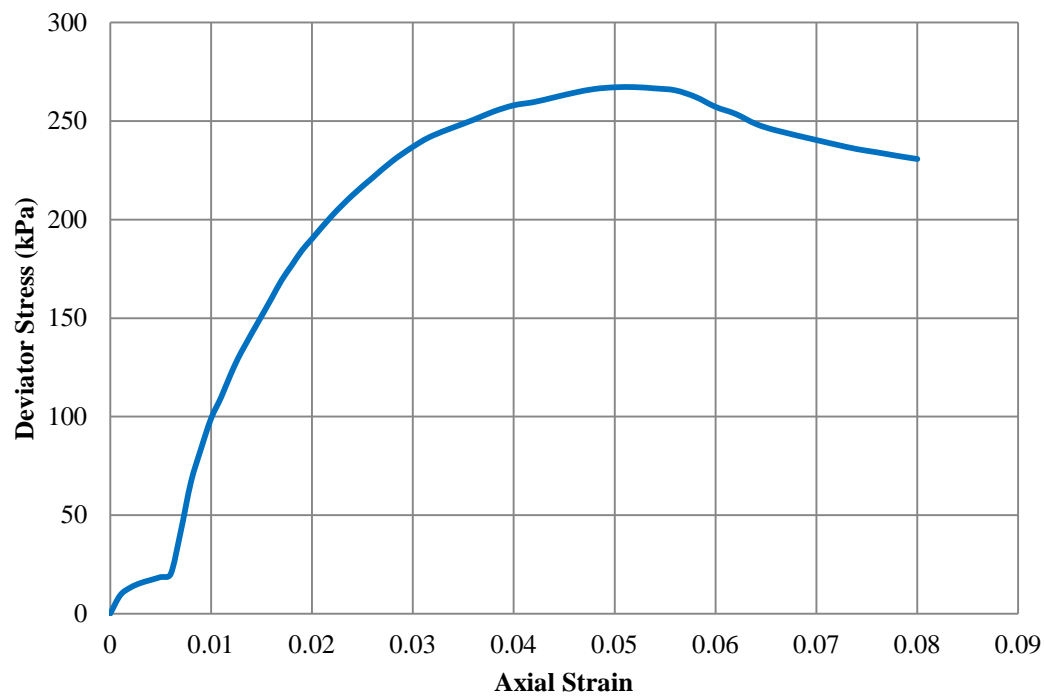


Figure B.67 Axial Strain vs. Deviator Stress-Experiment 10  
 Confining Effective Stress=250 kPa 5x10 cm

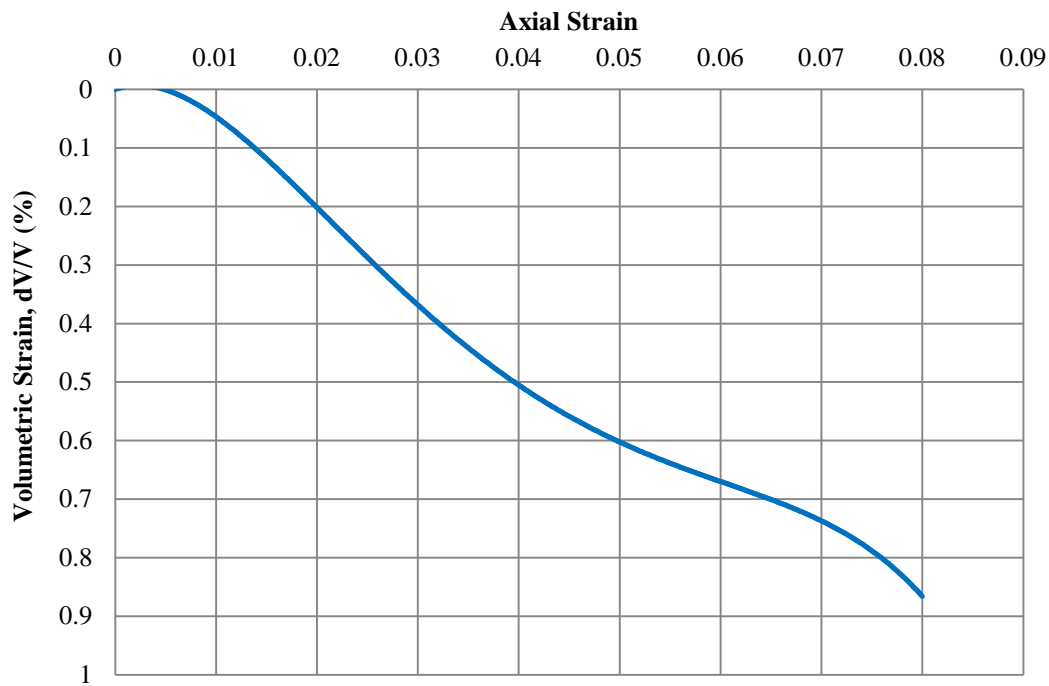


Figure B.68 Axial Strain vs. Volumetric Strain-Experiment 10  
 Confining Effective Stress=250 kPa-5x10 cm

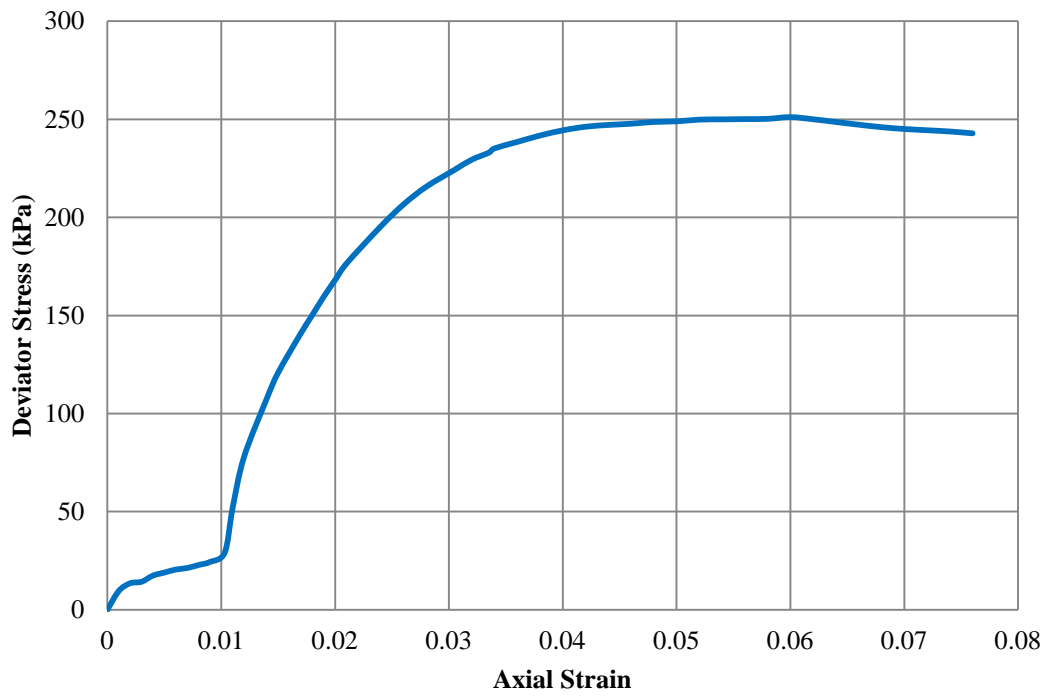


Figure B.69 Axial Strain vs. Deviator Stress-Experiment 11  
 Confining Effective Stress=250 kPa 5x10 cm

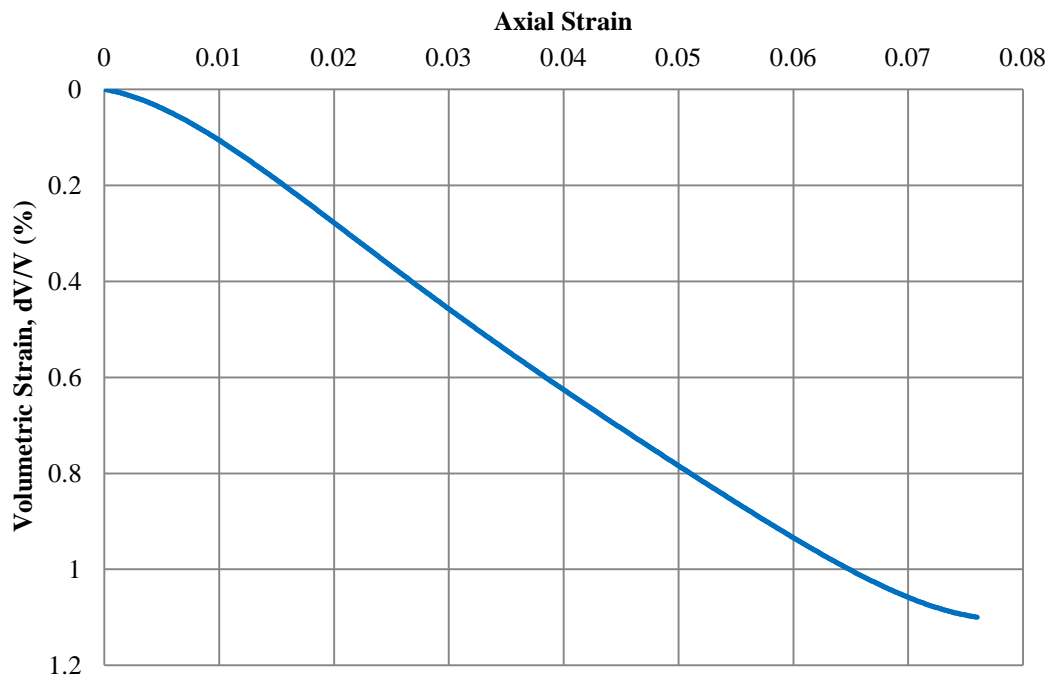


Figure B.70 Axial Strain vs. Volumetric Strain-Experiment 11  
 Confining Effective Stress=250 kPa-5x10 cm

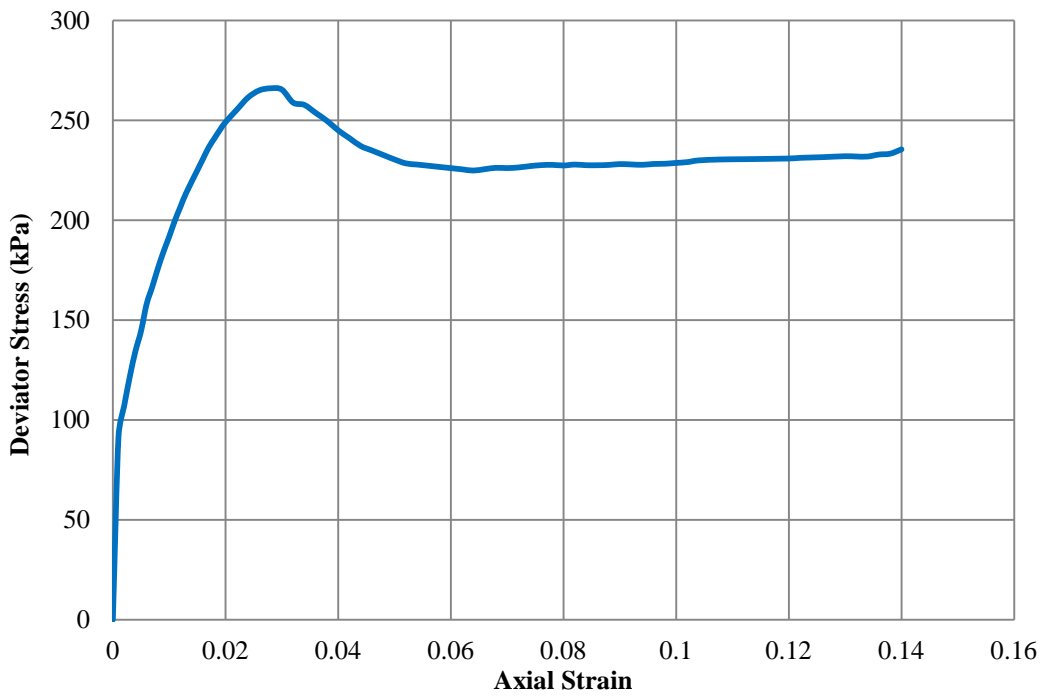


Figure B.71 Axial Strain vs. Deviator Stress-Experiment 12  
 Confining Effective Stress=250 kPa 5x10 cm

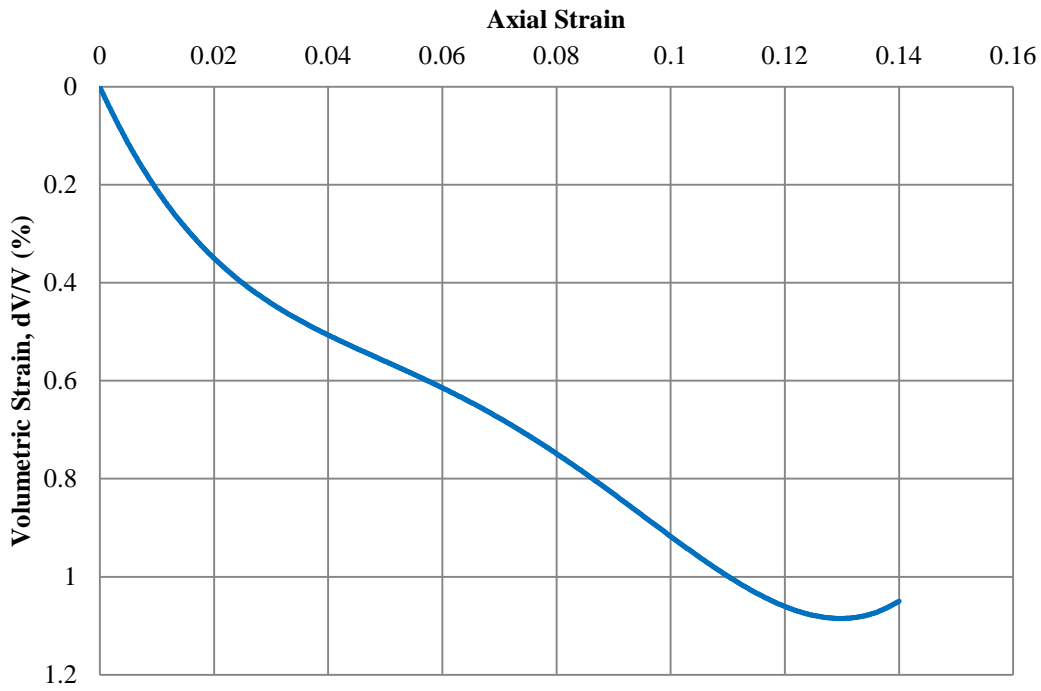


Figure B.72 Axial Strain vs. Volumetric Strain-Experiment 12  
 Confining Effective Stress=250 kPa-5x10 cm

## 5. Triaxial Tests of Gravel

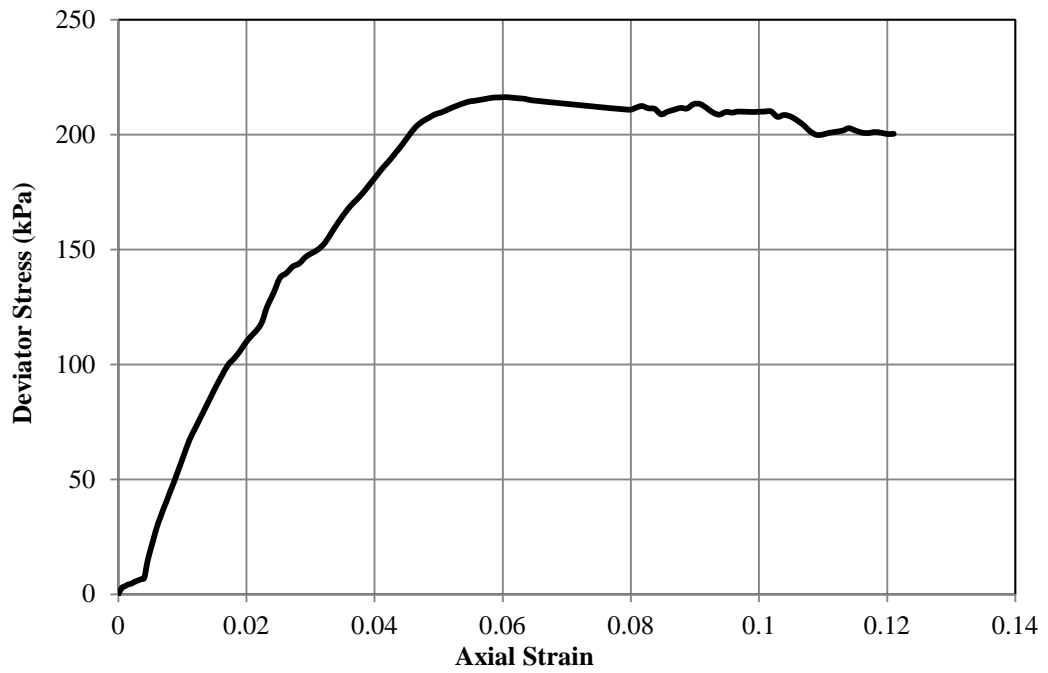


Figure B.73 Axial Strain vs. Deviator Stress-Experiment 1  
Confining Effective Stress=50 kPa

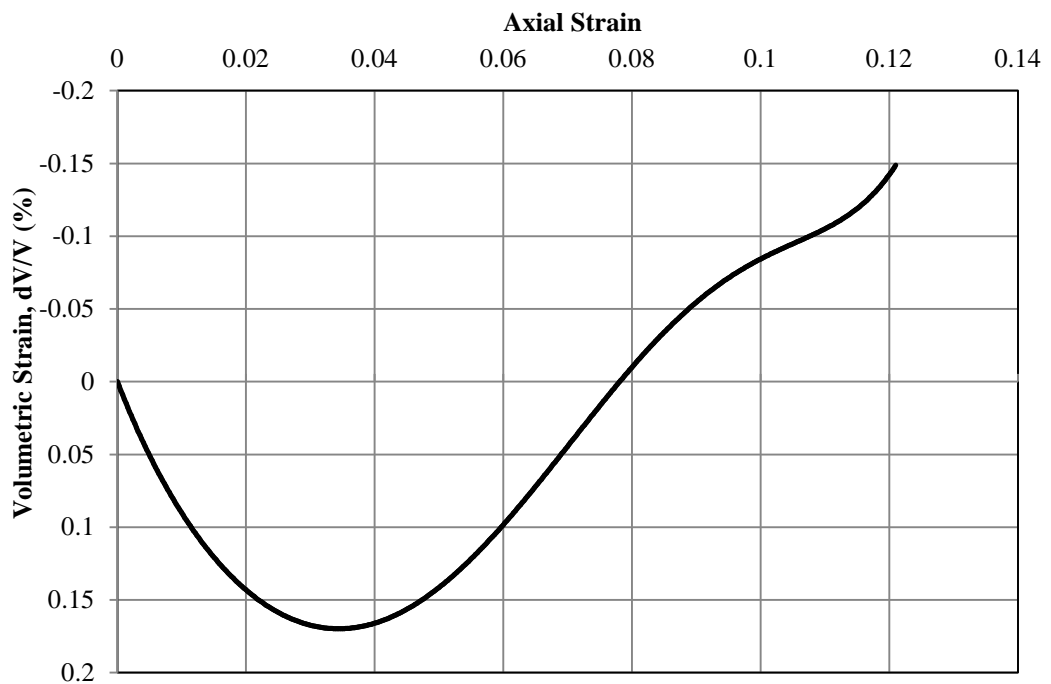


Figure B.74 Axial Strain vs. Volumetric Strain-Experiment 1  
Confining Effective Stress=50 kPa

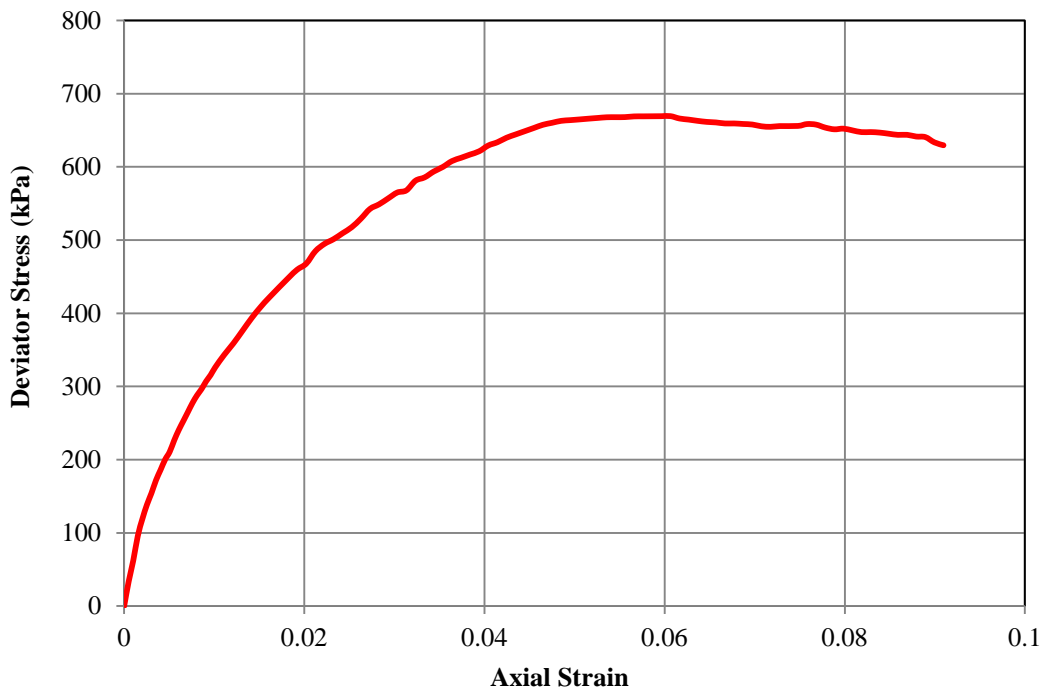


Figure B.75 Axial Strain vs. Deviator Stress-Experiment 2  
 Confining Effective Stress=150 kPa

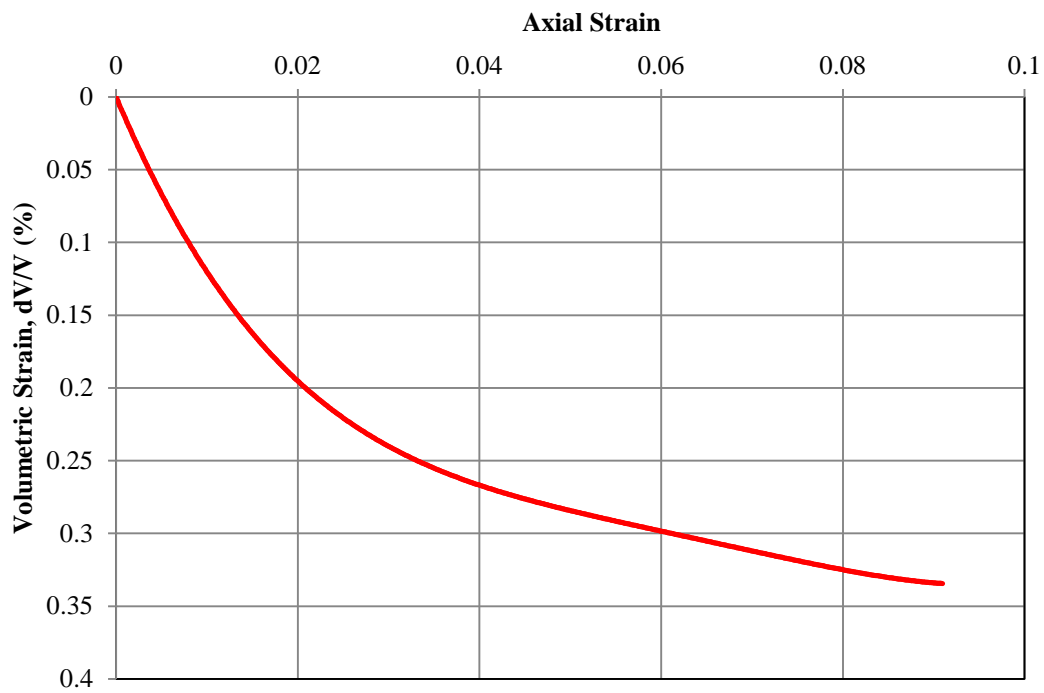


Figure B.76 Axial Strain vs. Volumetric Strain-Experiment 2  
 Confining Effective Stress=150 kPa

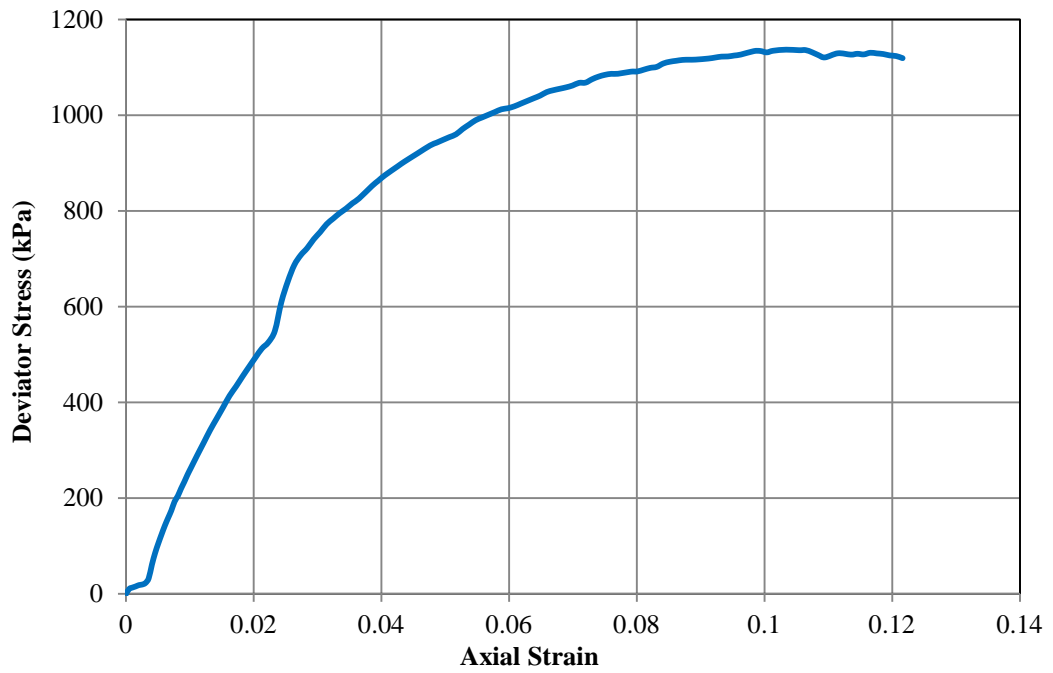


Figure B.77 Axial Strain vs. Deviator Stress-Experiment 3  
 Confining Effective Stress=250 kPa

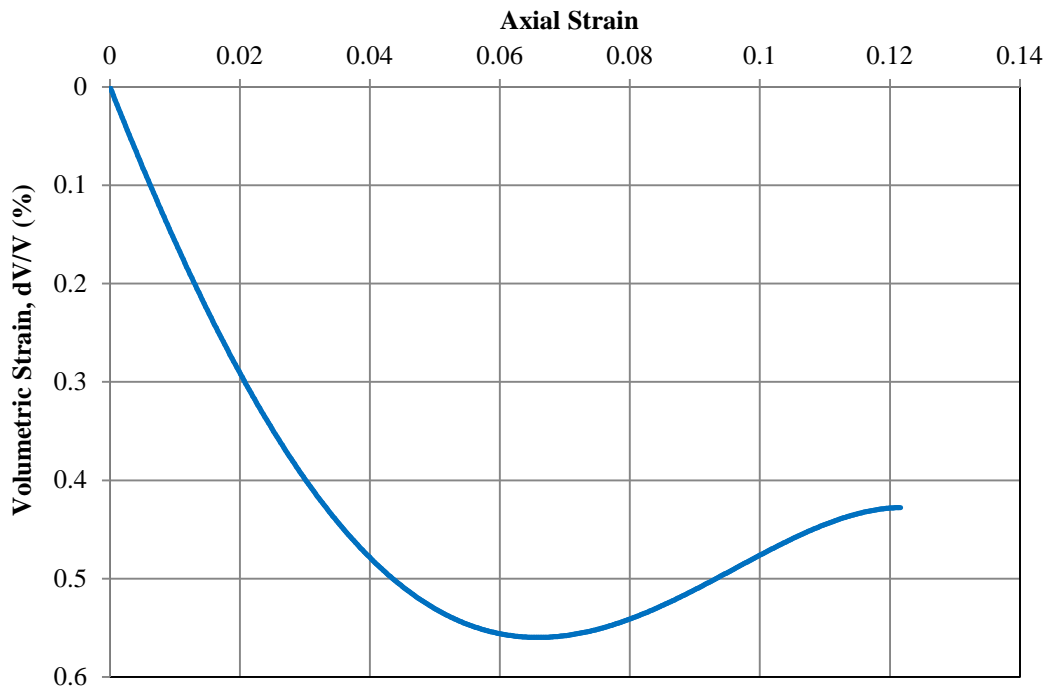


Figure B.78 Axial Strain vs. Volumetric Strain-Experiment 3  
 Confining Effective Stress=250 kPa

## 6. Triaxial Tests of Sand

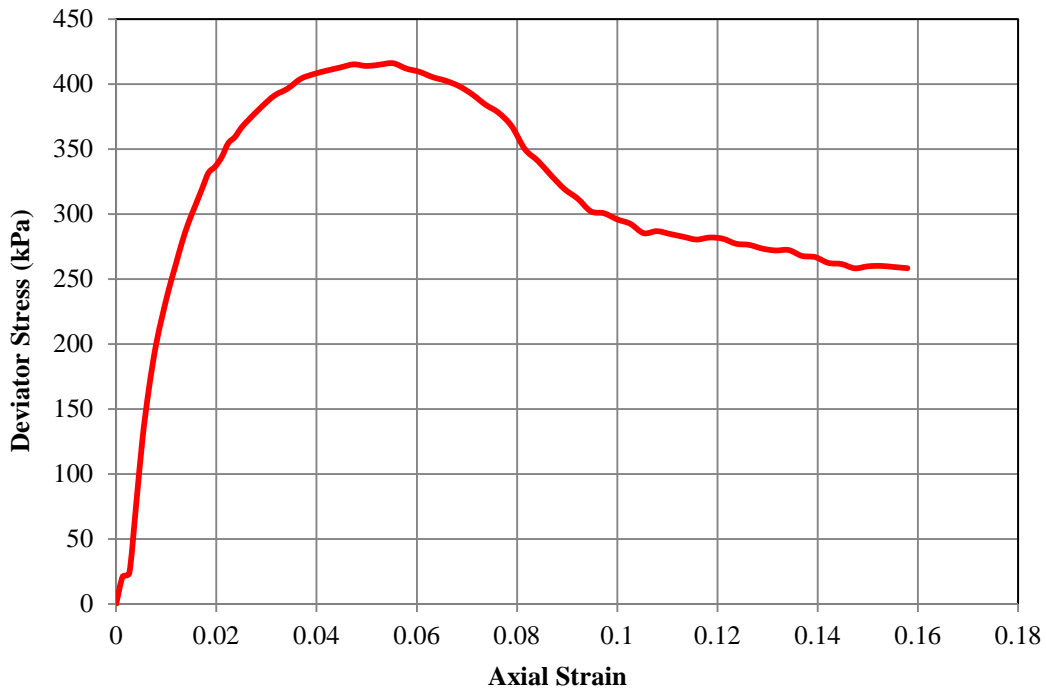


Figure B.79 Axial Strain vs. Deviator Stress-Experiment 1  
Confining Effective Stress=100 kPa

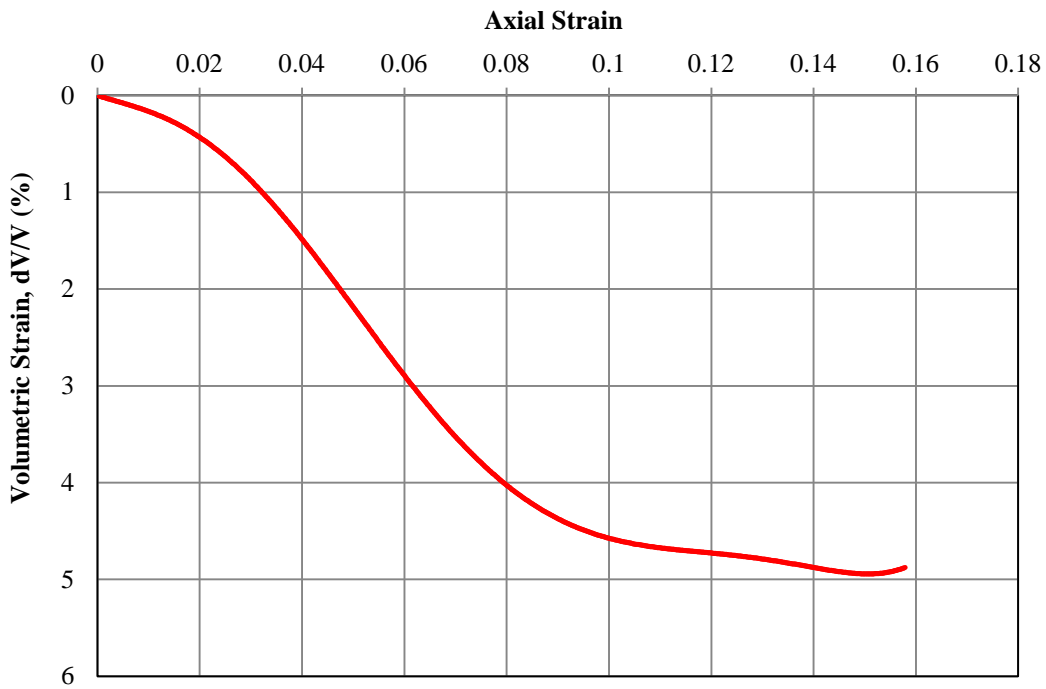


Figure B.80 Axial Strain vs. Volumetric Strain-Experiment 1  
Confining Effective Stress=100 kPa

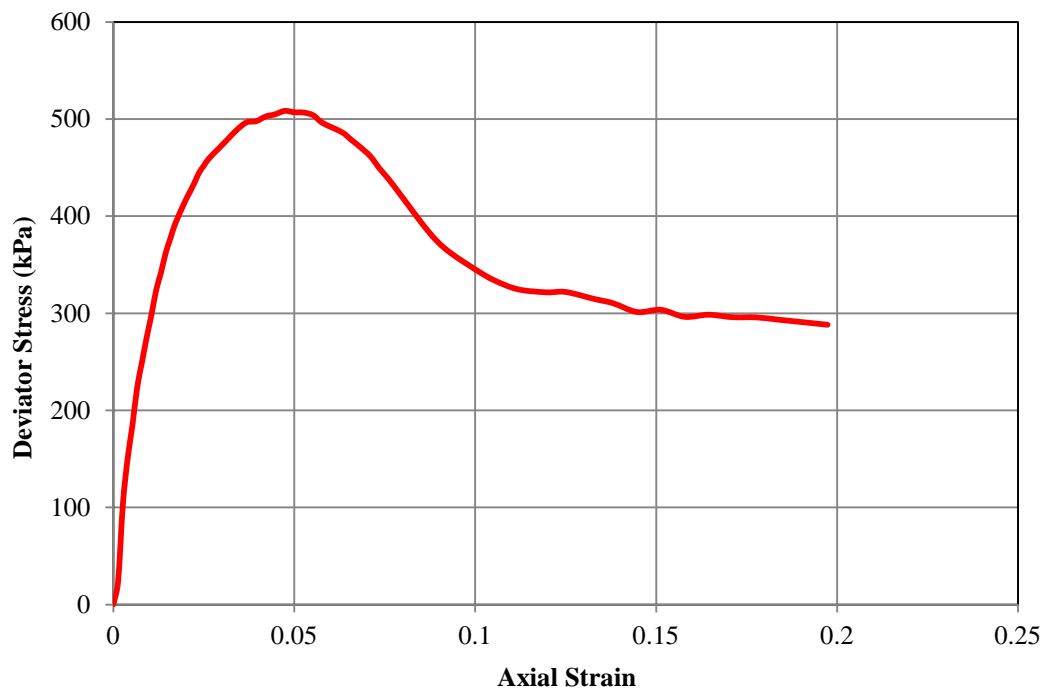


Figure B.81 Axial Strain vs. Deviator Stress-Experiment 2  
 Confining Effective Stress=100 kPa

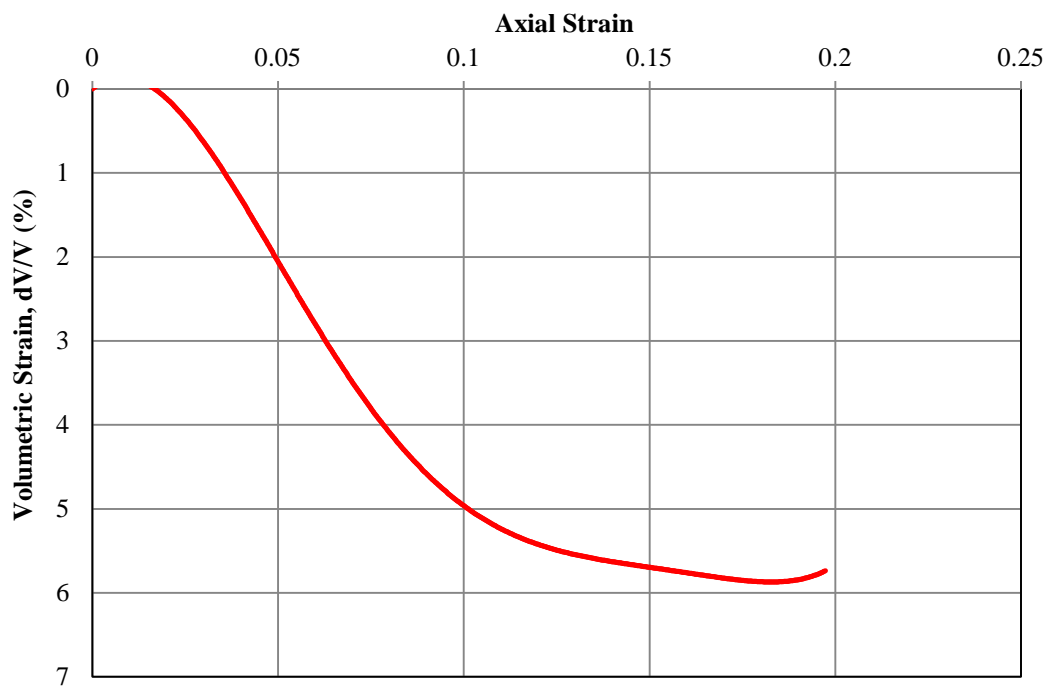


Figure B.82 Axial Strain vs. Volumetric Strain-Experiment 2  
 Confining Effective Stress=100 kPa

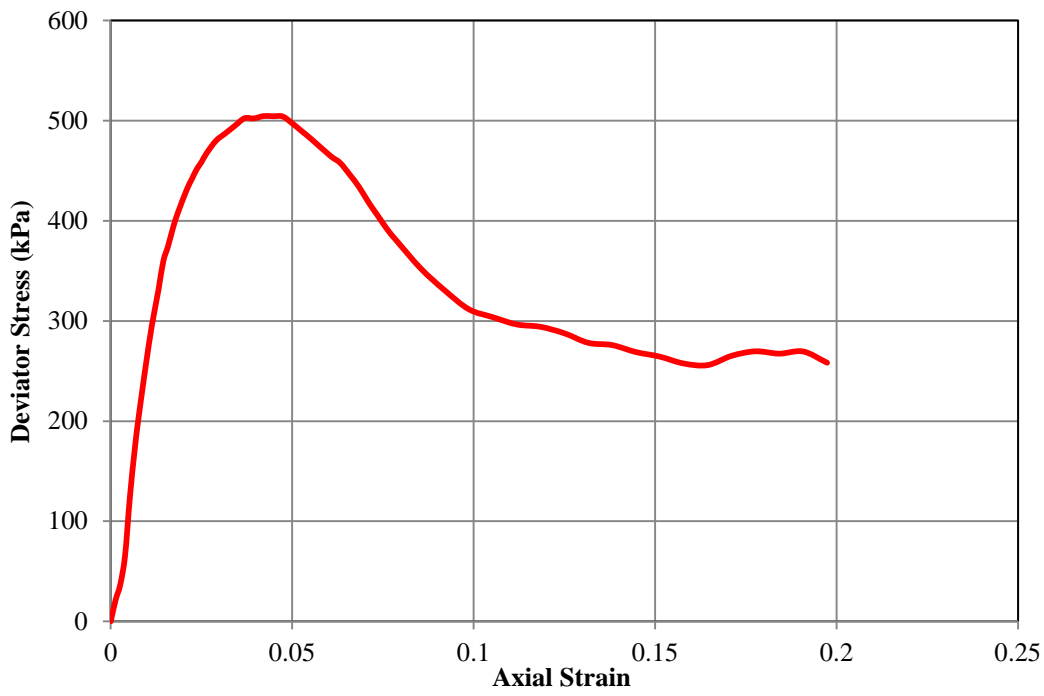


Figure B.83 Axial Strain vs. Deviator Stress-Experiment 3  
 Confining Effective Stress=100 kPa

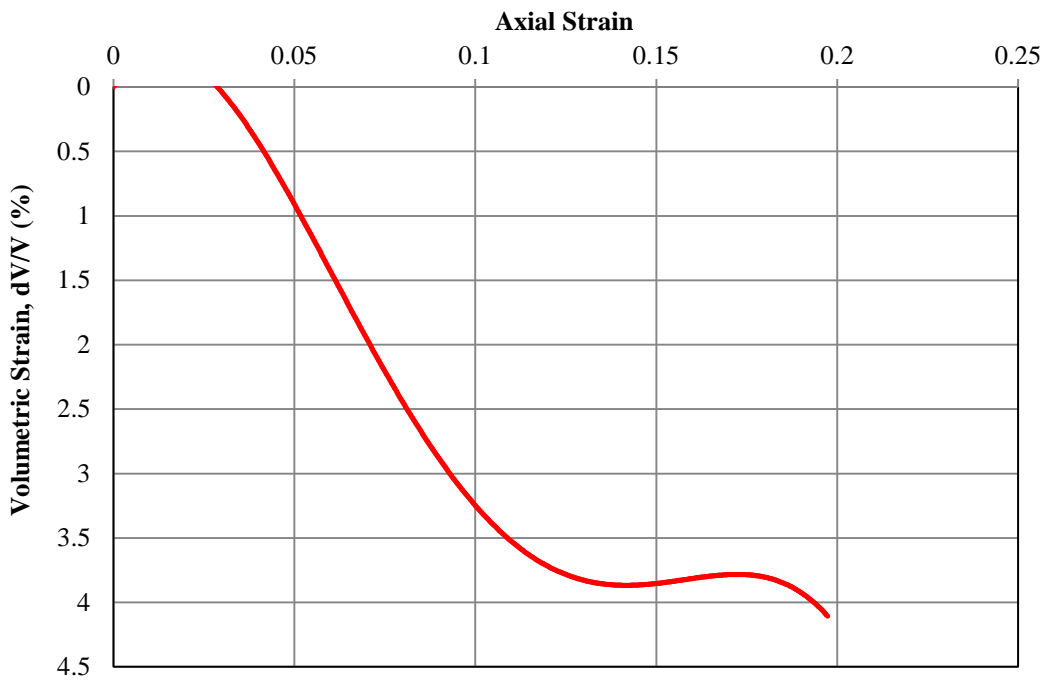


Figure B.84 Axial Strain vs. Volumetric Strain-Experiment 3  
 Confining Effective Stress=100 kPa

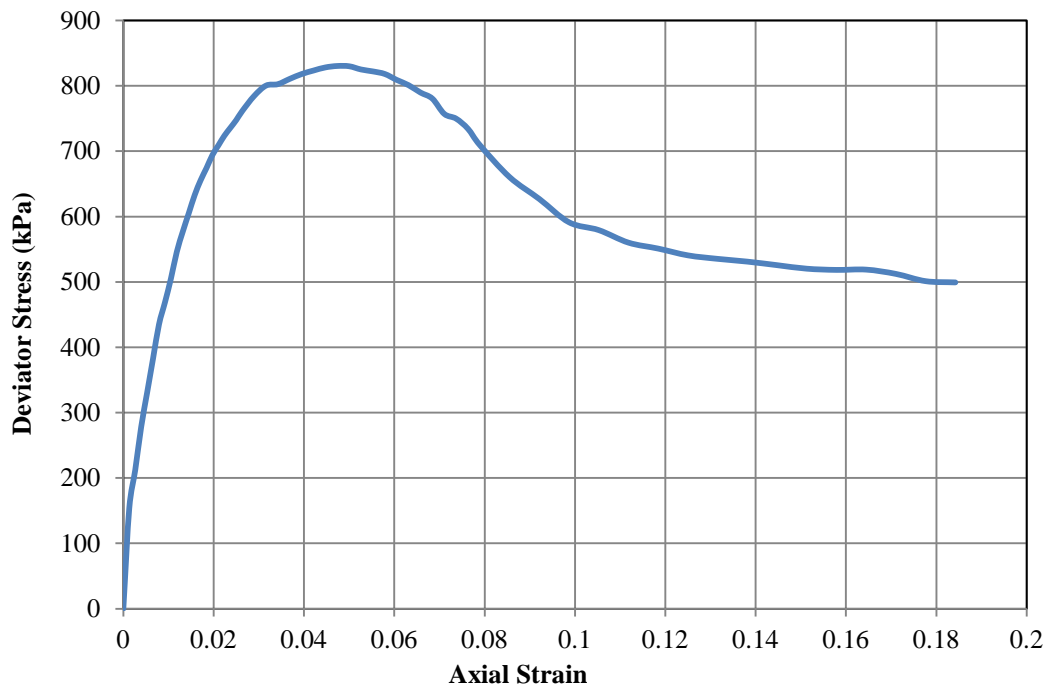


Figure B.85 Axial Strain vs. Deviator Stress-Experiment 4  
 Confining Effective Stress=200 kPa

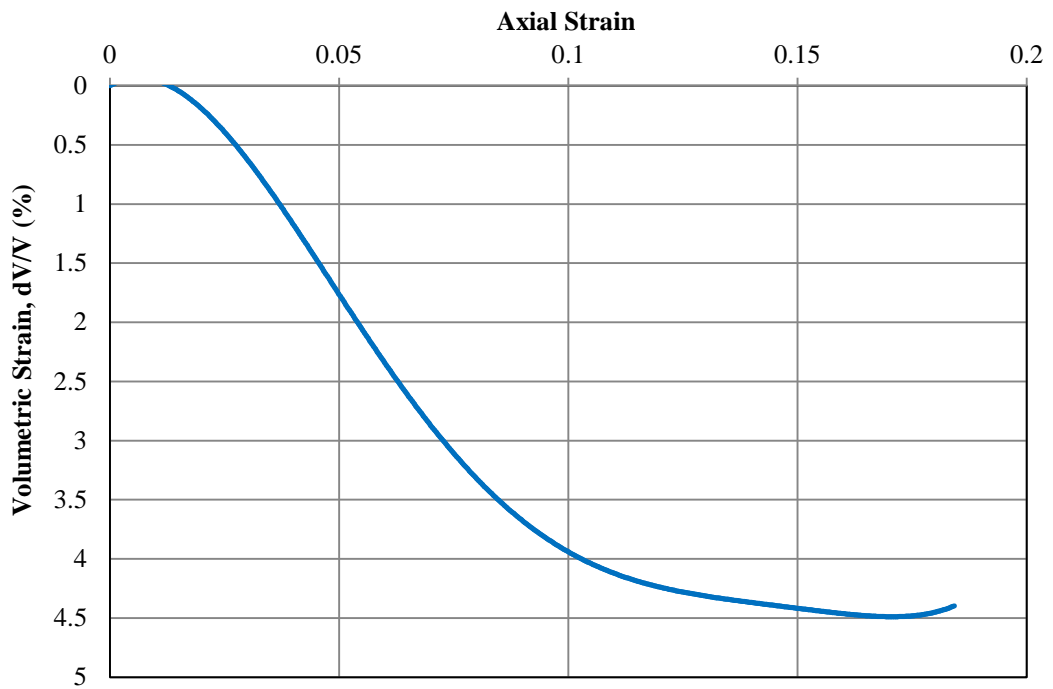


Figure B.86 Axial Strain vs. Volumetric Strain-Experiment 4  
 Confining Effective Stress=200 kPa

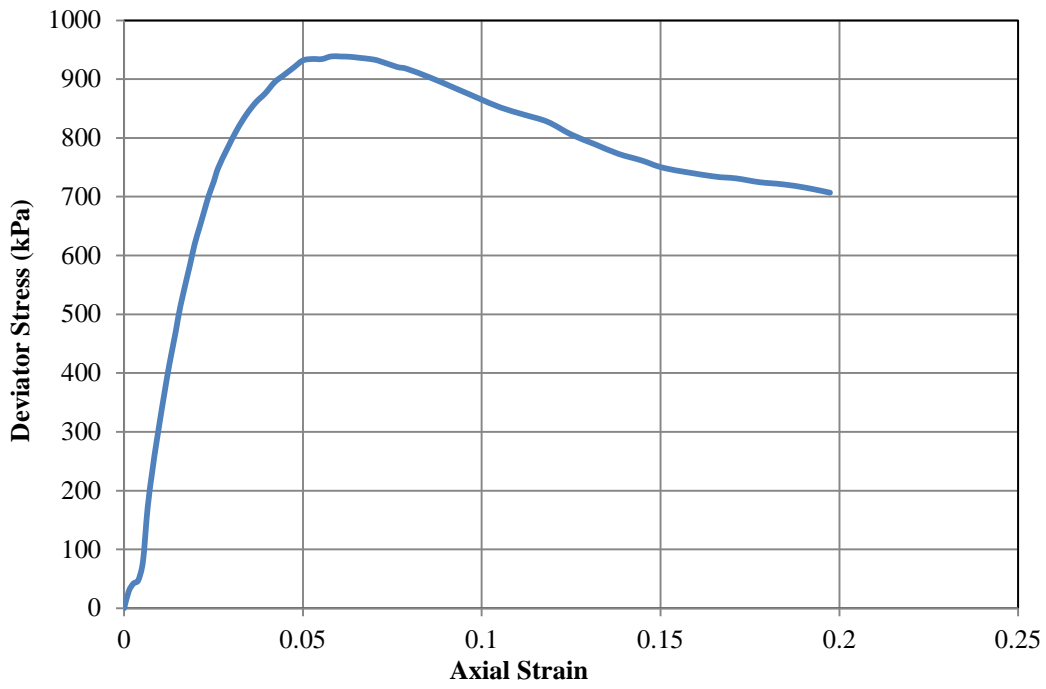


Figure B.87 Axial Strain vs. Deviator Stress-Experiment 5  
 Confining Effective Stress=200 kPa

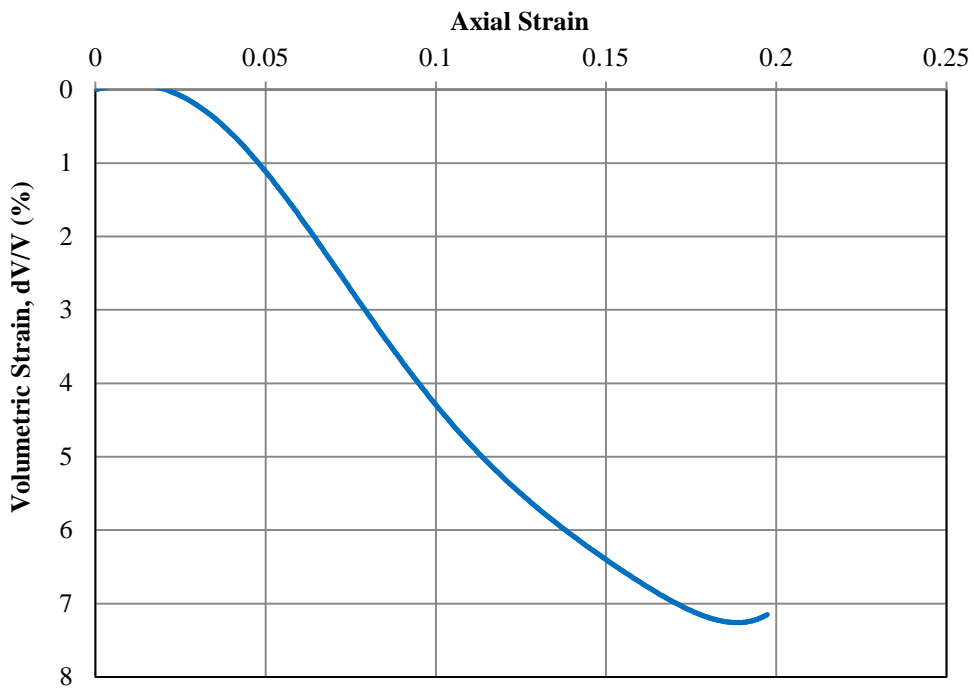


Figure B.88 Axial Strain vs. Volumetric Strain-Experiment 5  
 Confining Effective Stress=200 kPa

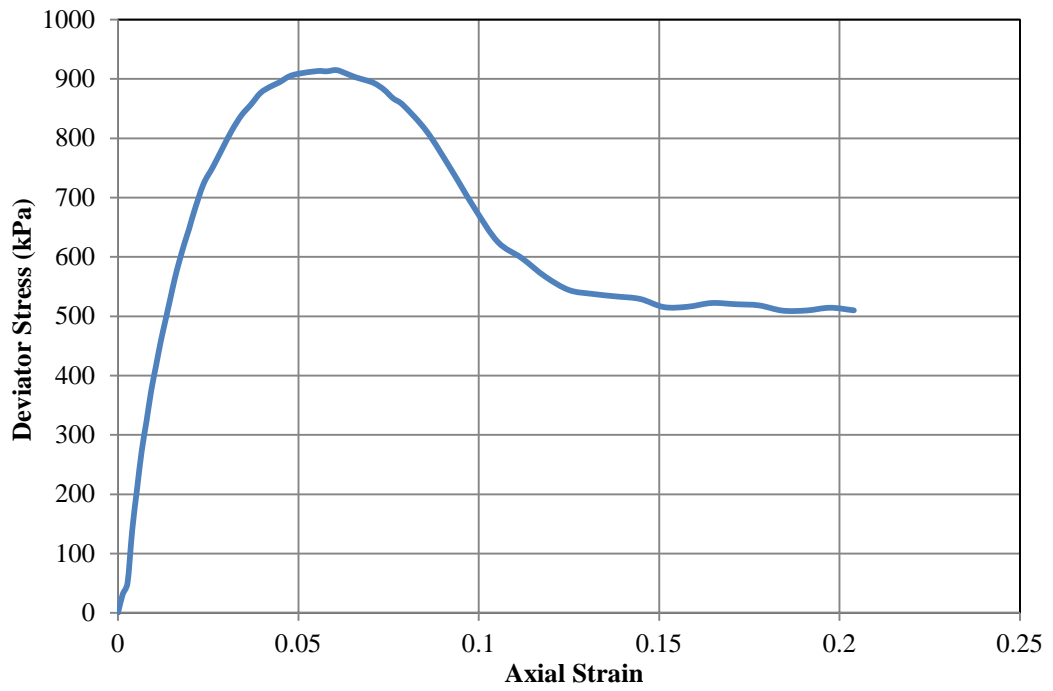


Figure B.89 Axial Strain vs. Deviator Stress-Experiment 6  
 Confining Effective Stress=200 kPa

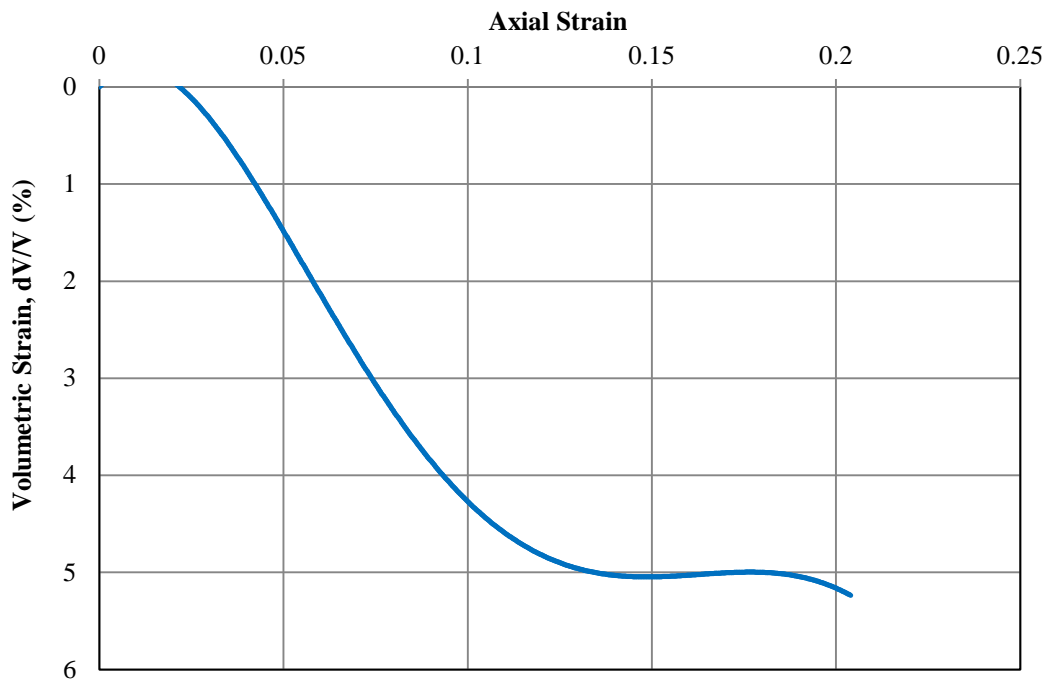


Figure B.90 Axial Strain vs. Volumetric Strain-Experiment 6  
 Confining Effective Stress=200 kPa



## APPENDIX C

### IMPROVEMENT TESTS

#### 1. Improvement Tests- I-1

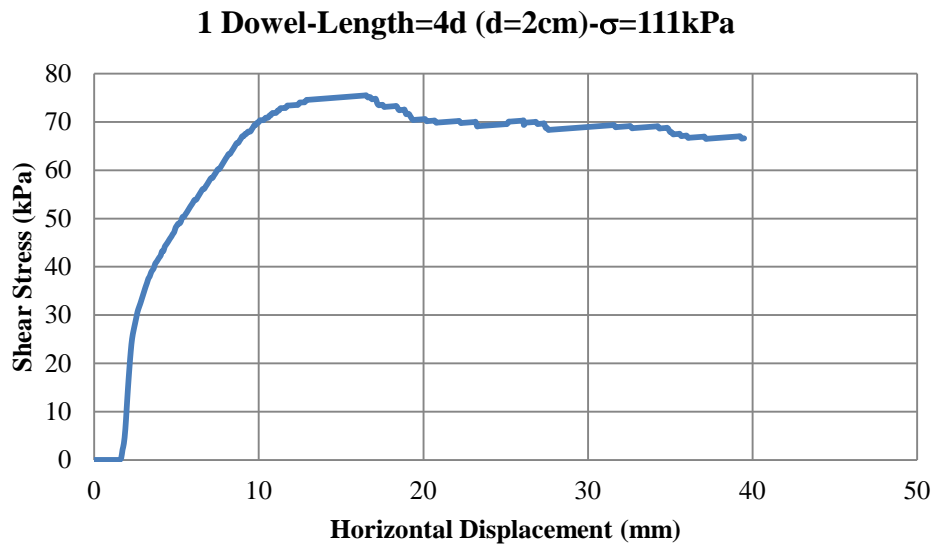


Figure C.1 Shear Stress vs. Displacement Graph-Experiment 1

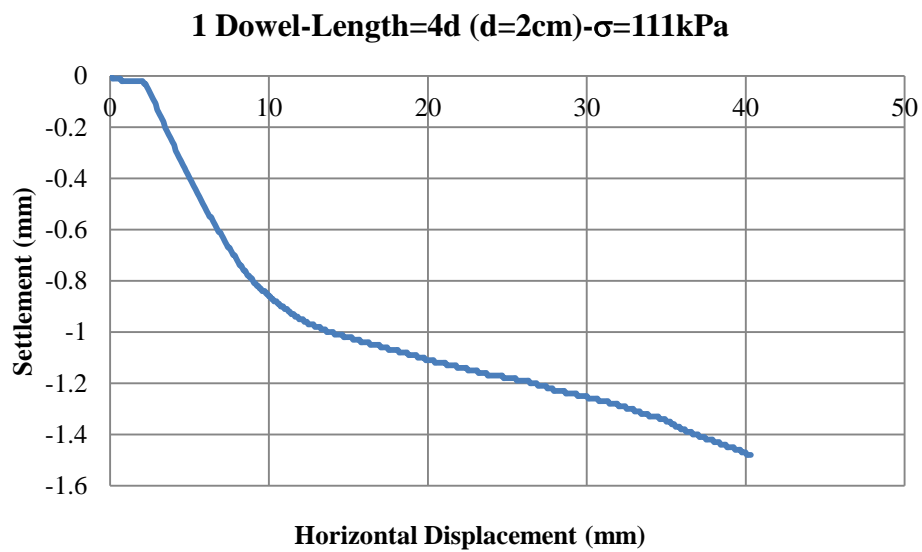


Figure C.2 Settlement vs. Displacement Graph- Experiment 1

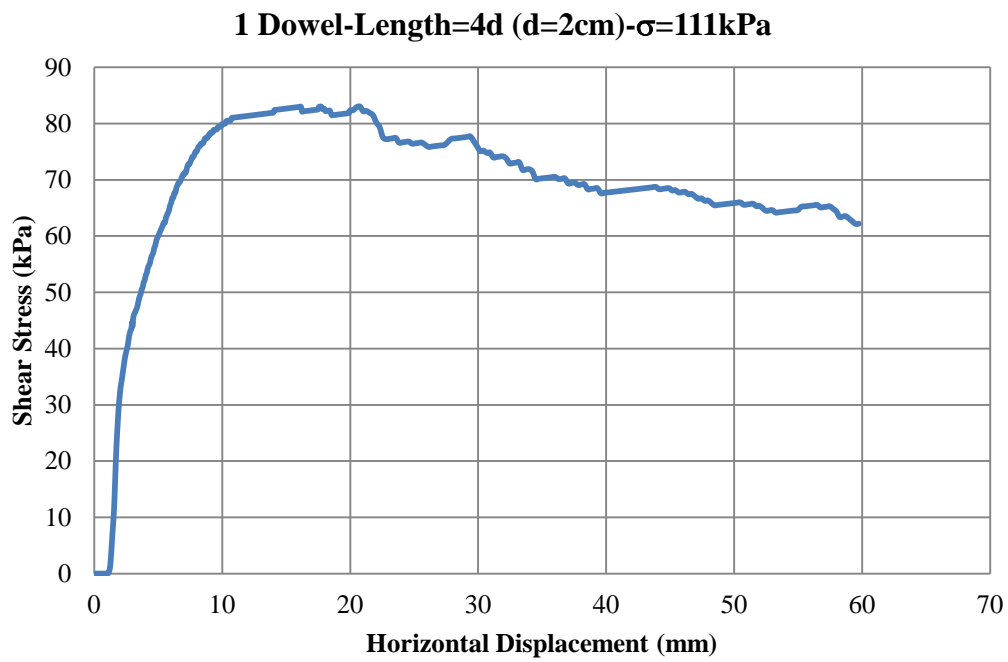


Figure C.3 Shear Stress vs. Displacement Graph-Experiment 2

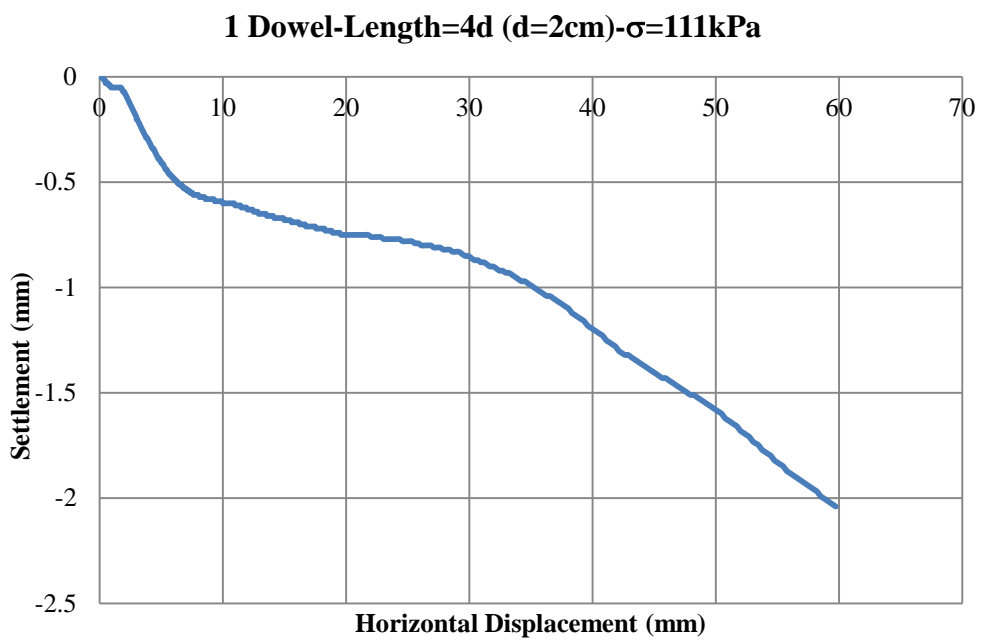


Figure C.4 Settlement vs. Displacement Graph- Experiment 2

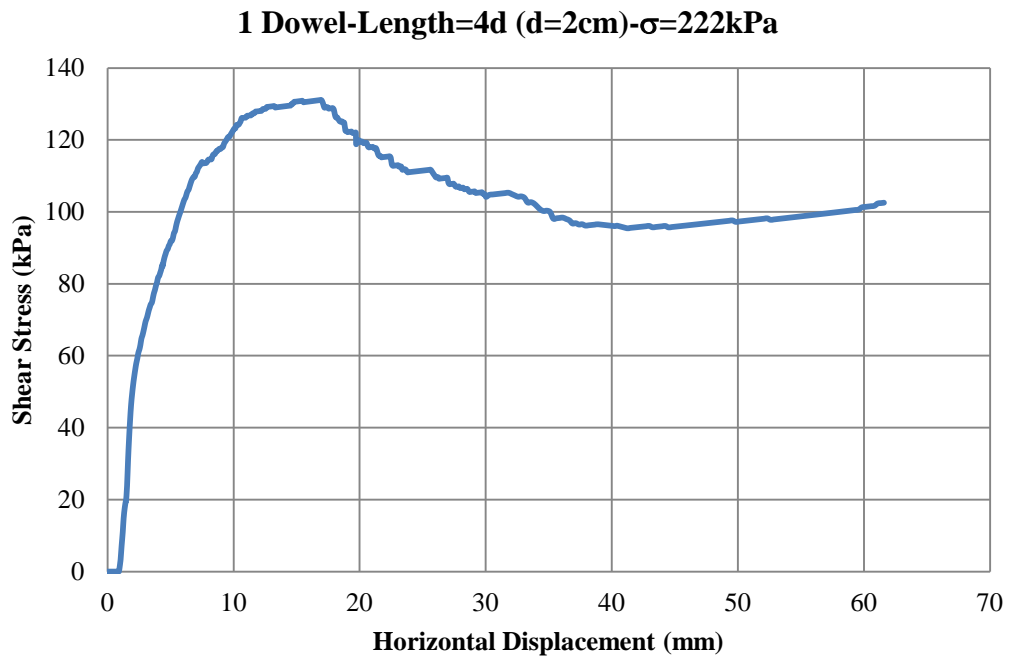


Figure C.5 Shear Stress vs. Displacement Graph-Experiment 3

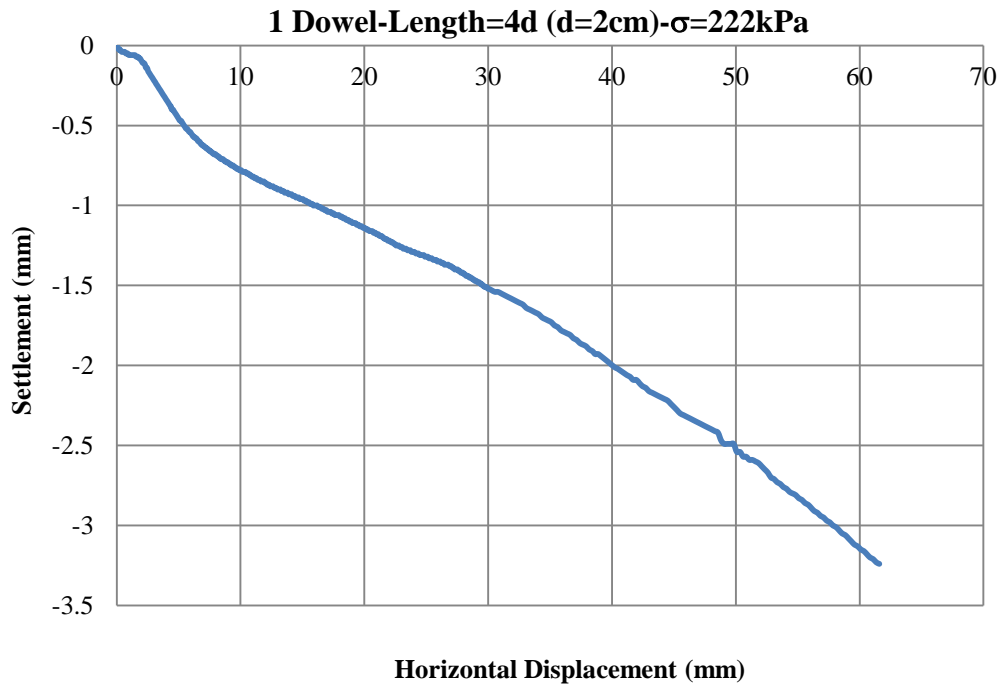


Figure C.6 Settlement vs. Displacement Graph- Experiment 3

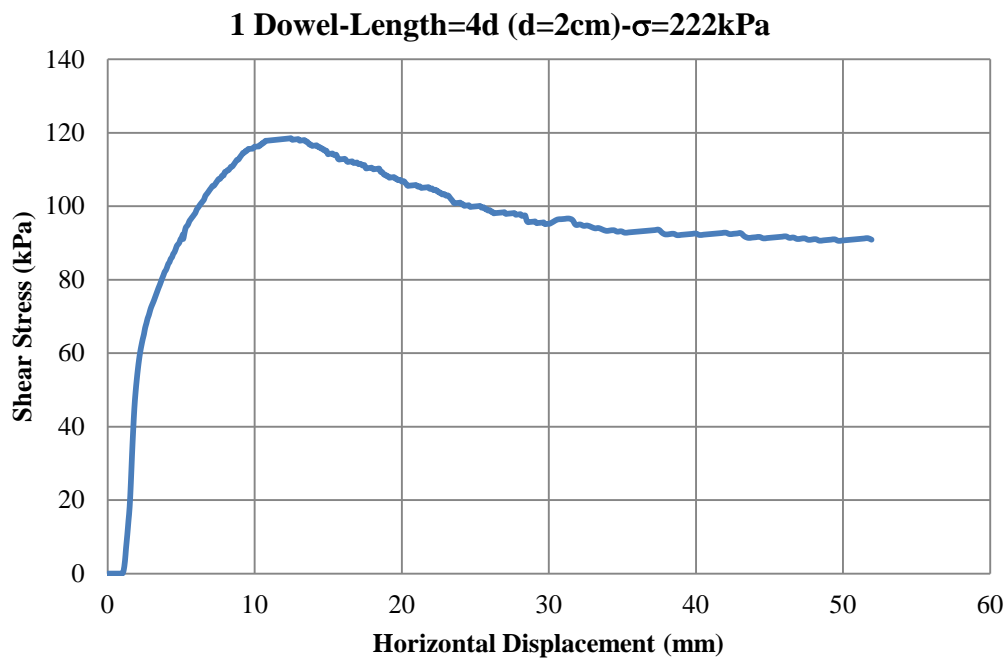


Figure C.7 Shear Stress vs. Displacement Graph-Experiment 4

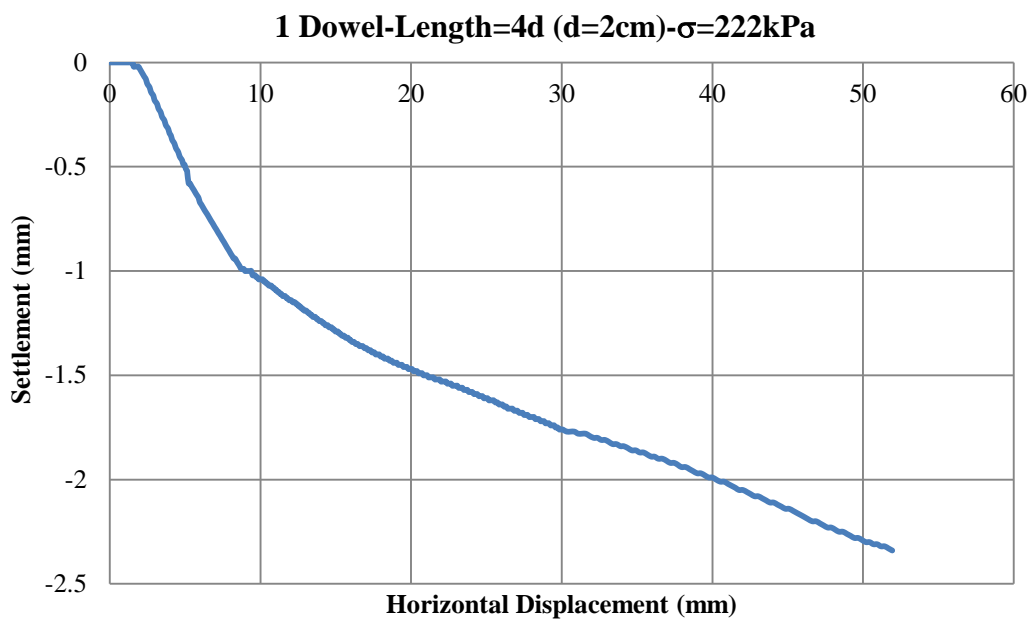


Figure C.8 Settlement vs. Displacement Graph- Experiment 4

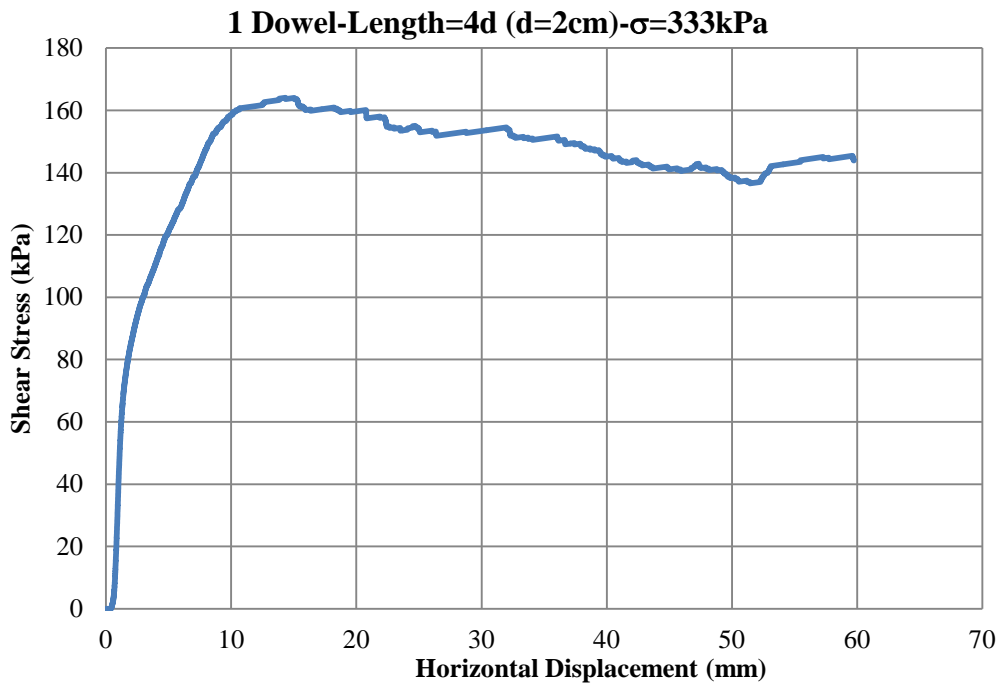


Figure C.9 Shear Stress vs. Displacement Graph-Experiment 5

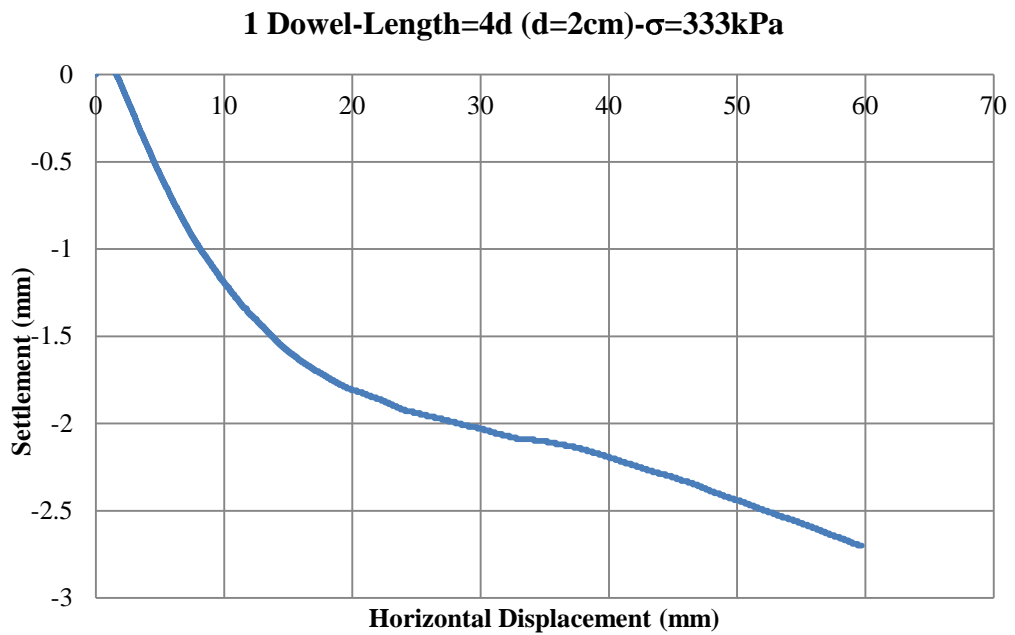


Figure C.10 Settlement vs. Displacement Graph- Experiment 5

## 2. Improvement Tests- I-2

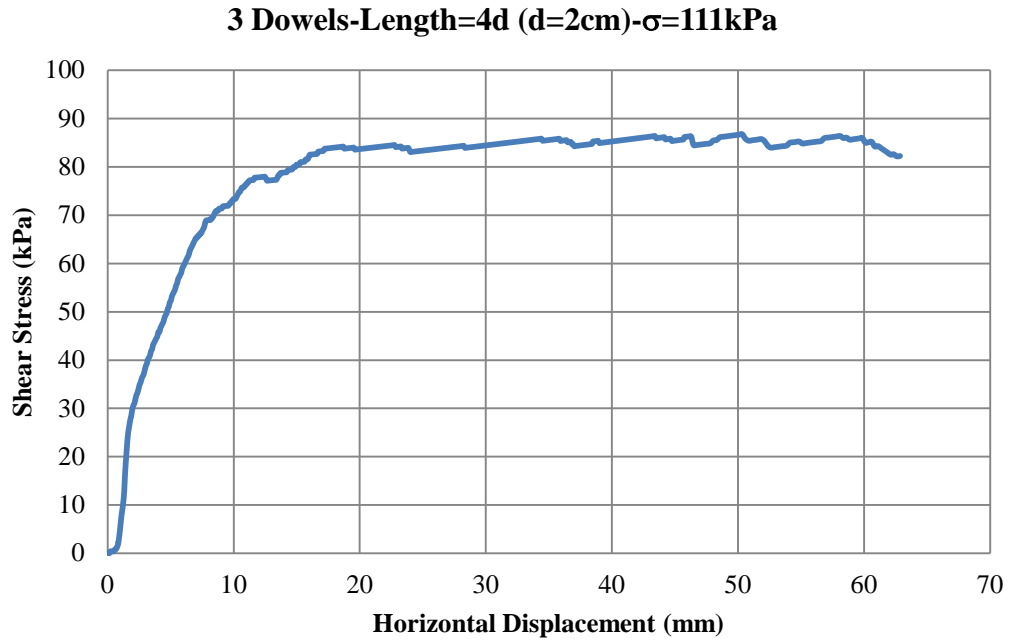


Figure C.11 Shear Stress vs. Displacement Graph-Experiment 6

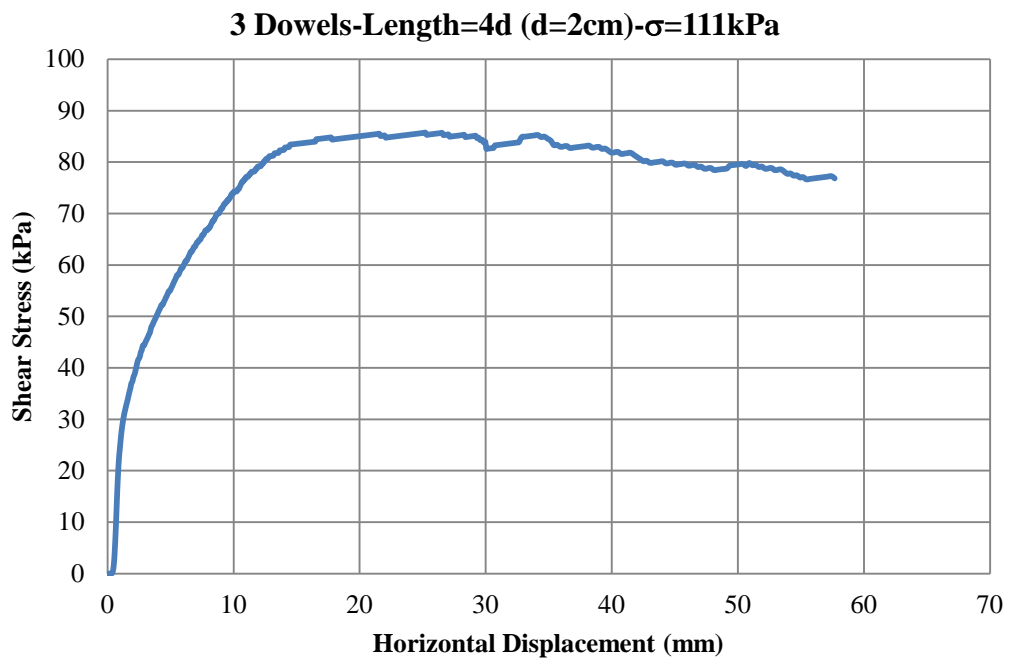


Figure C.12 Shear Stress vs. Displacement Graph-Experiment 7

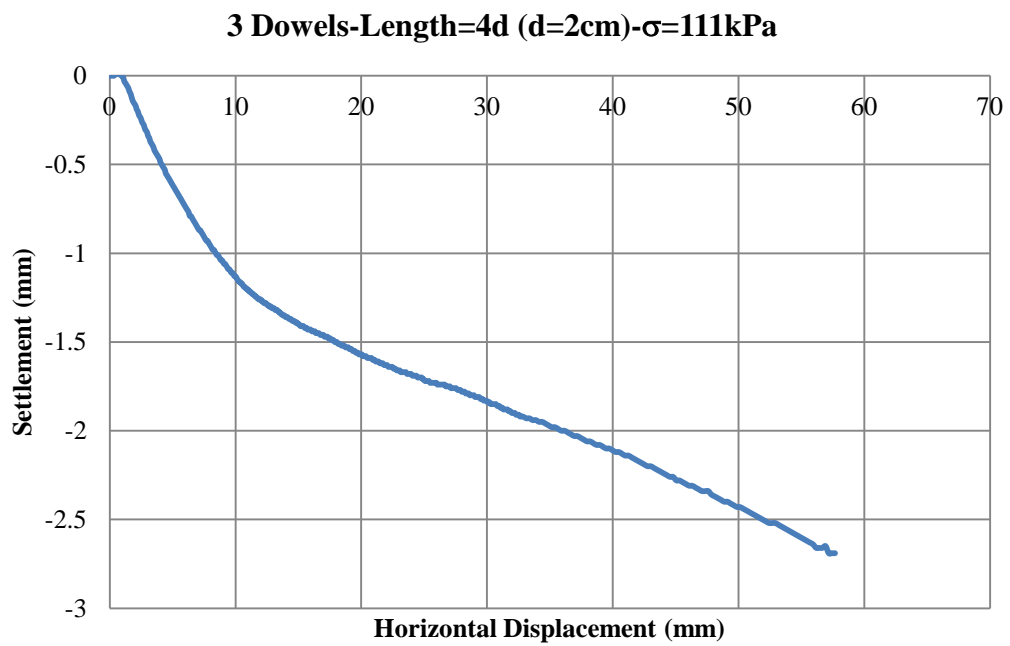


Figure C.13 Settlement vs. Displacement Graph-Experiment 7

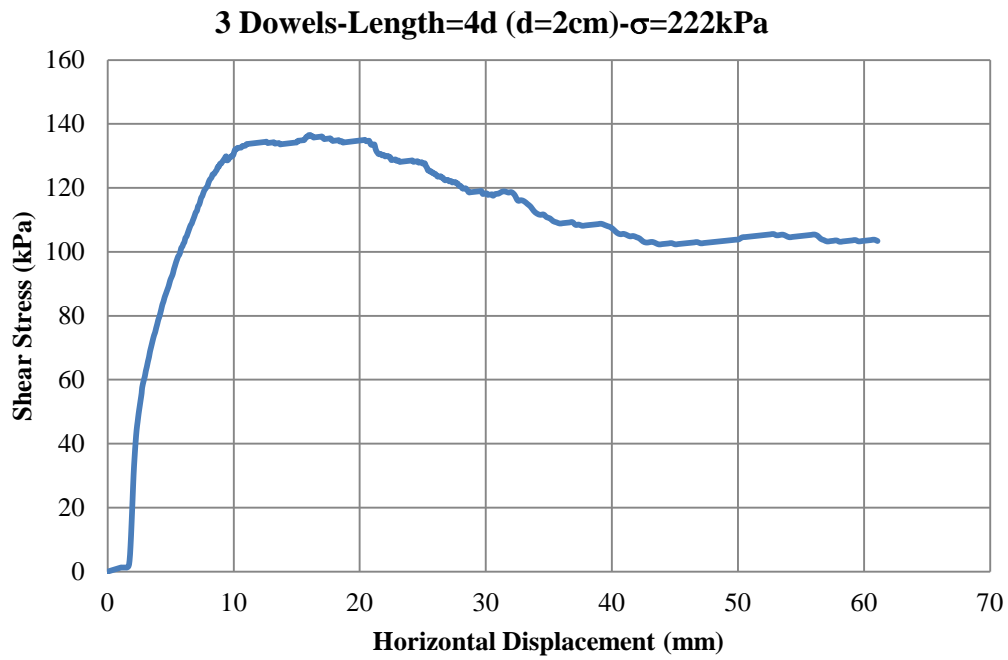


Figure C.14 Shear Stress vs. Displacement Graph-Experiment 8

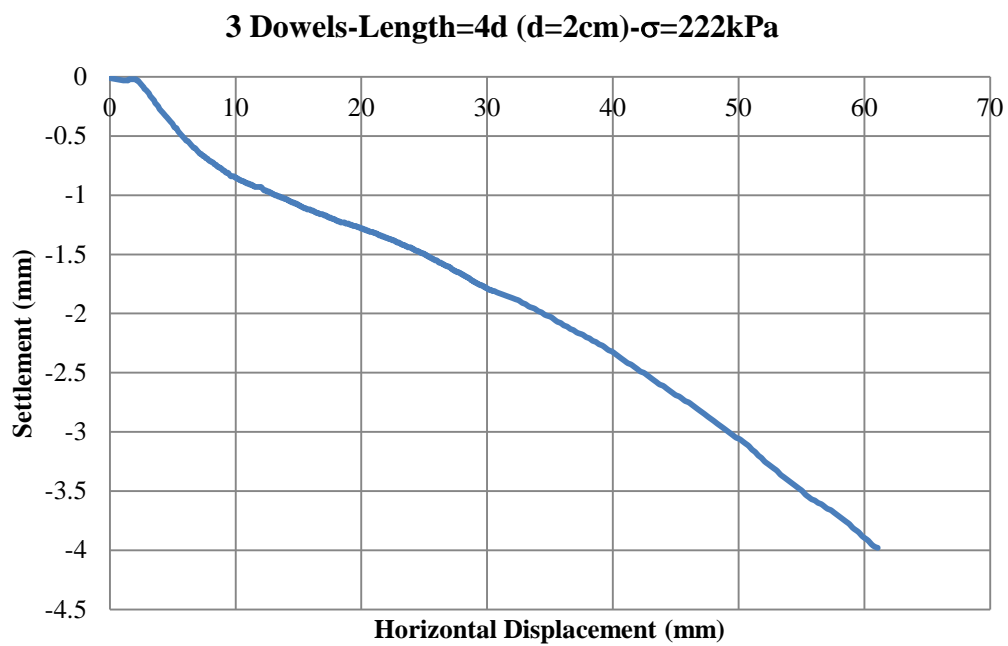


Figure C.15 Settlement vs. Displacement Graph-Experiment 8

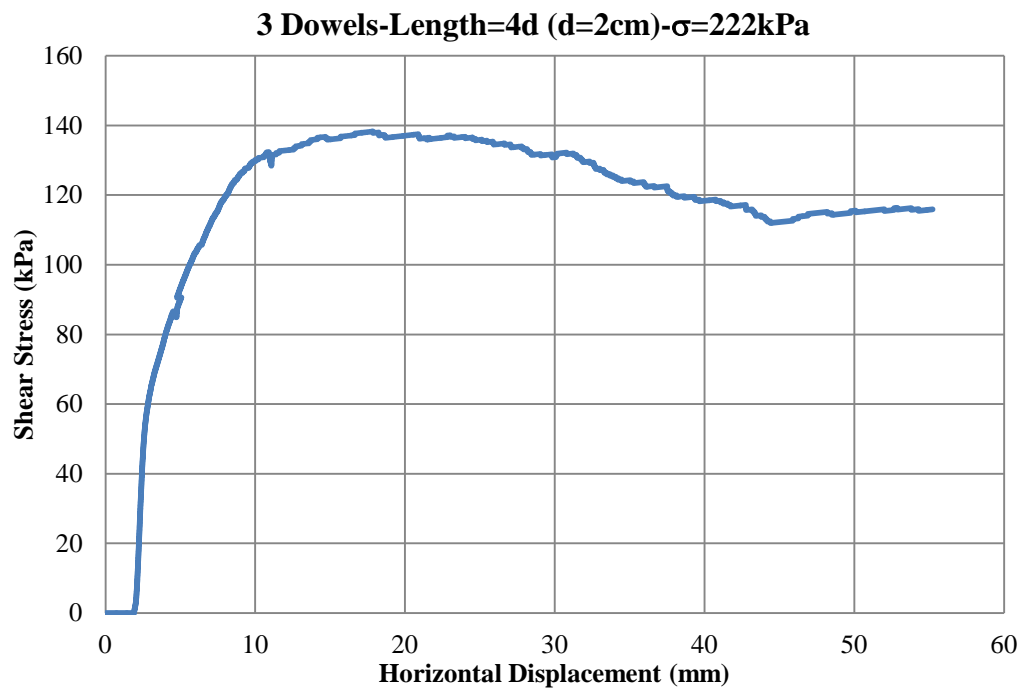


Figure C.16 Shear Stress vs. Displacement Graph-Experiment 9

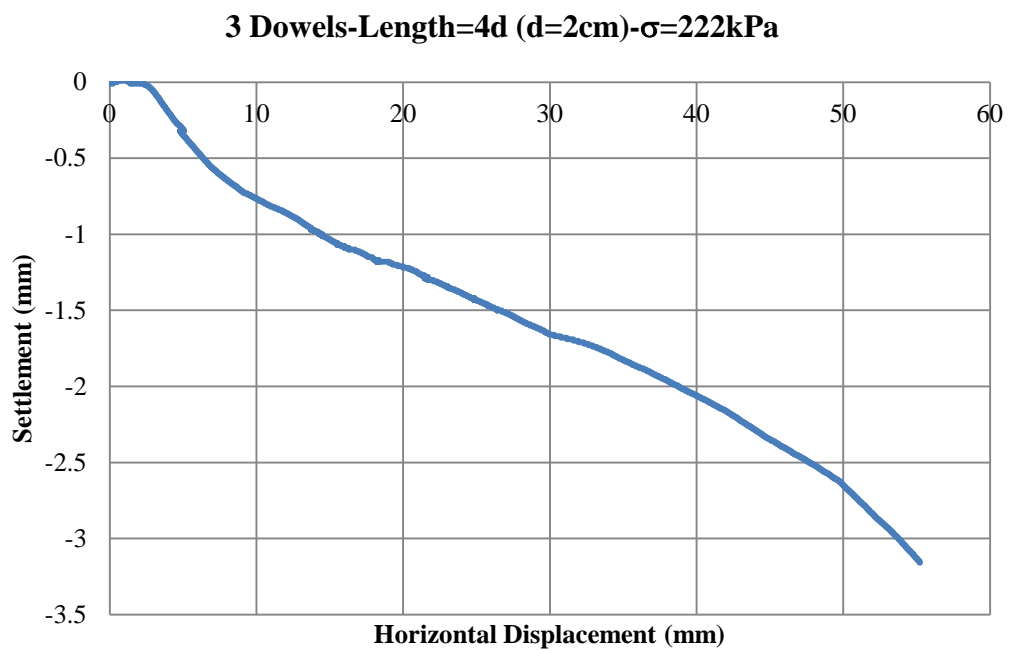


Figure C.17 Settlement vs. Displacement Graph-Experiment 9

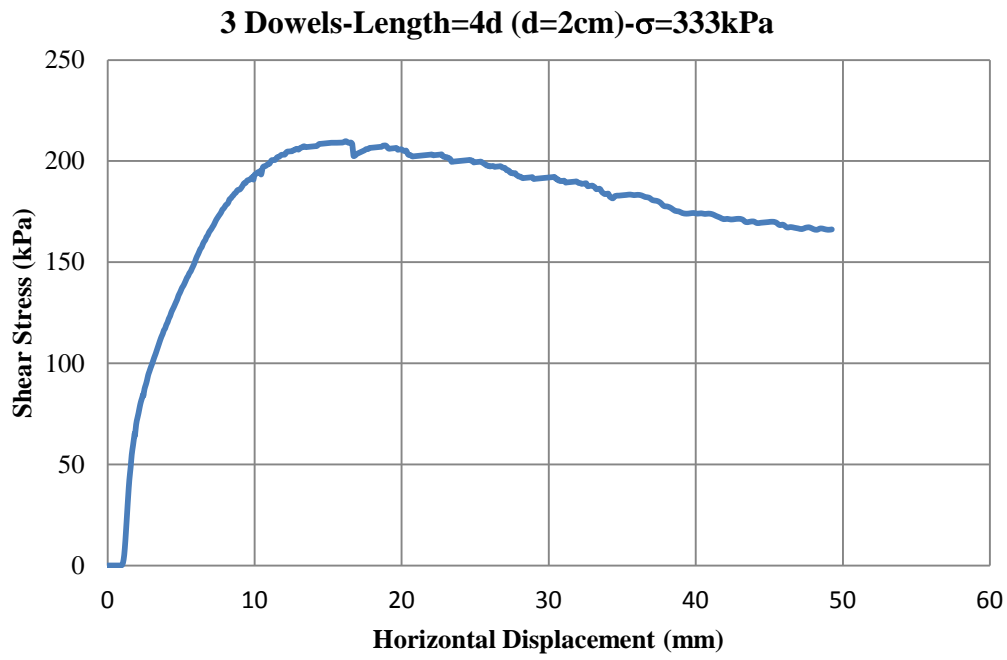


Figure C.18 Shear Stress vs. Displacement Graph-Experiment 10

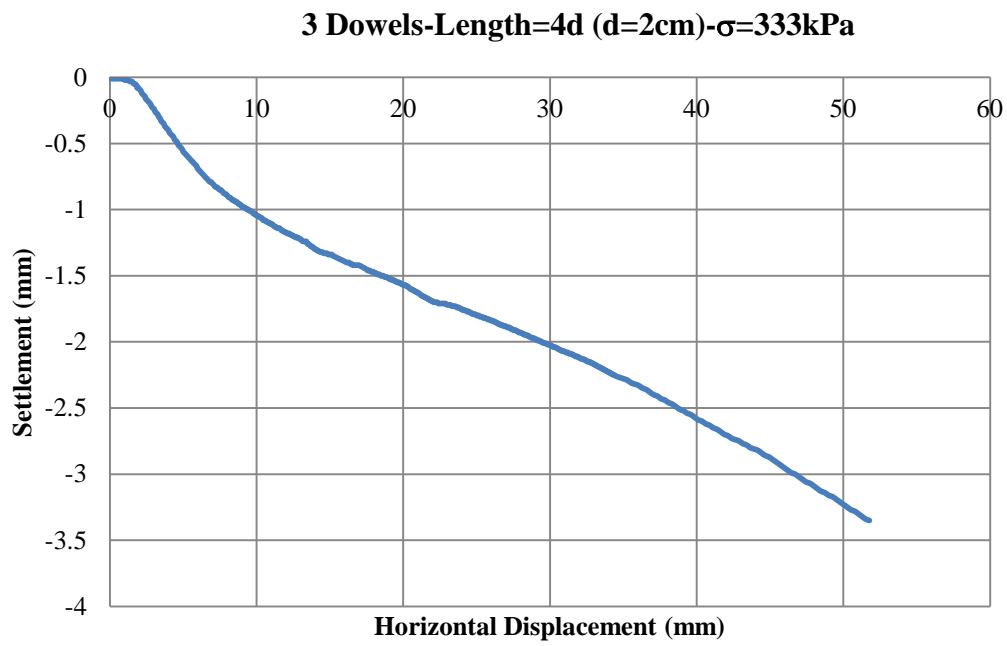


Figure C.19 Settlement vs. Displacement Graph-Experiment 10

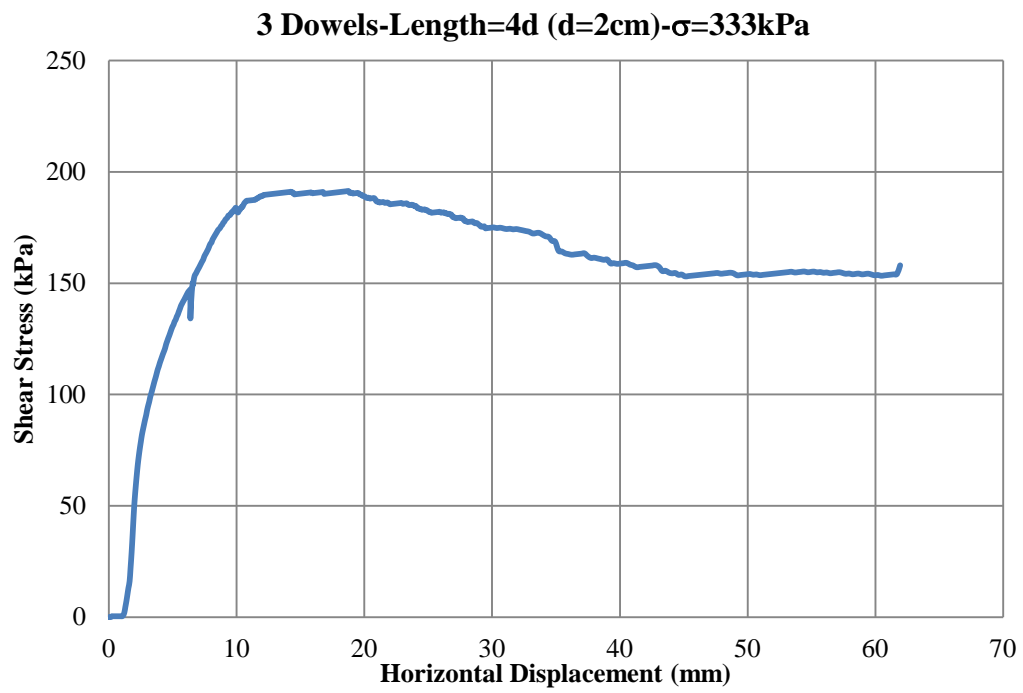


Figure C.20 Shear Stress vs. Displacement Graph-Experiment 11

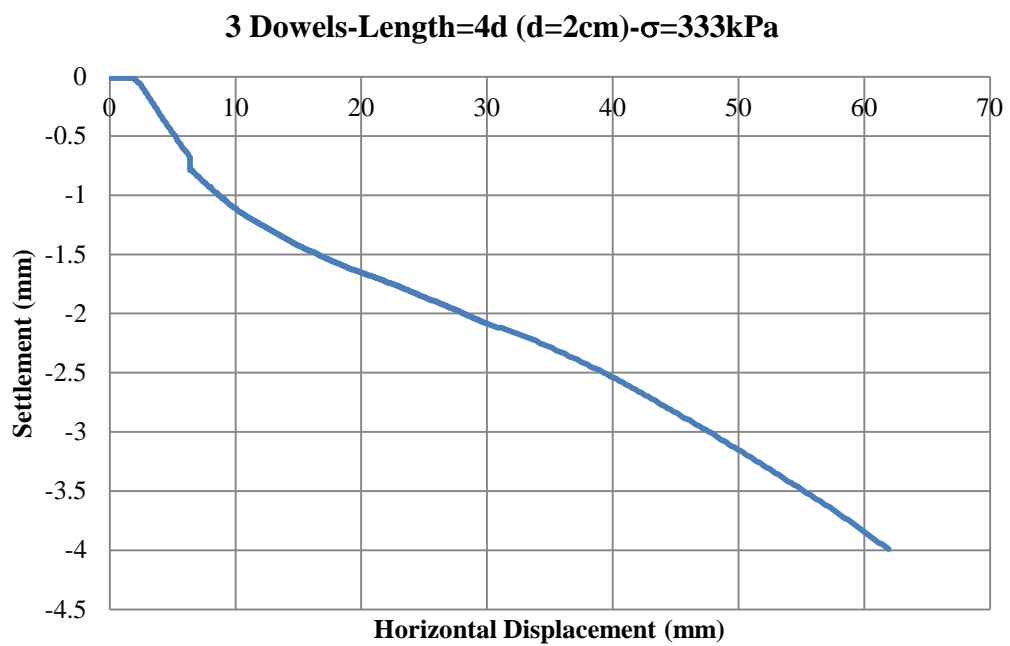


Figure C.21 Settlement vs. Displacement Graph-Experiment 11

### 3. Improvement Tests- I-3

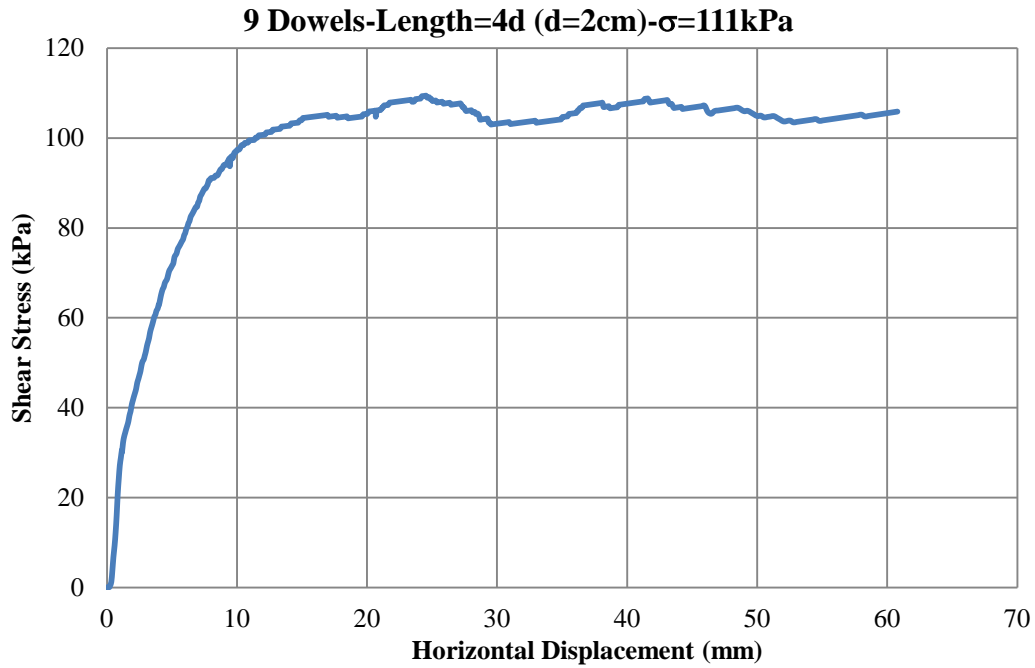


Figure C.22 Shear Stress vs. Displacement Graph-Experiment 12

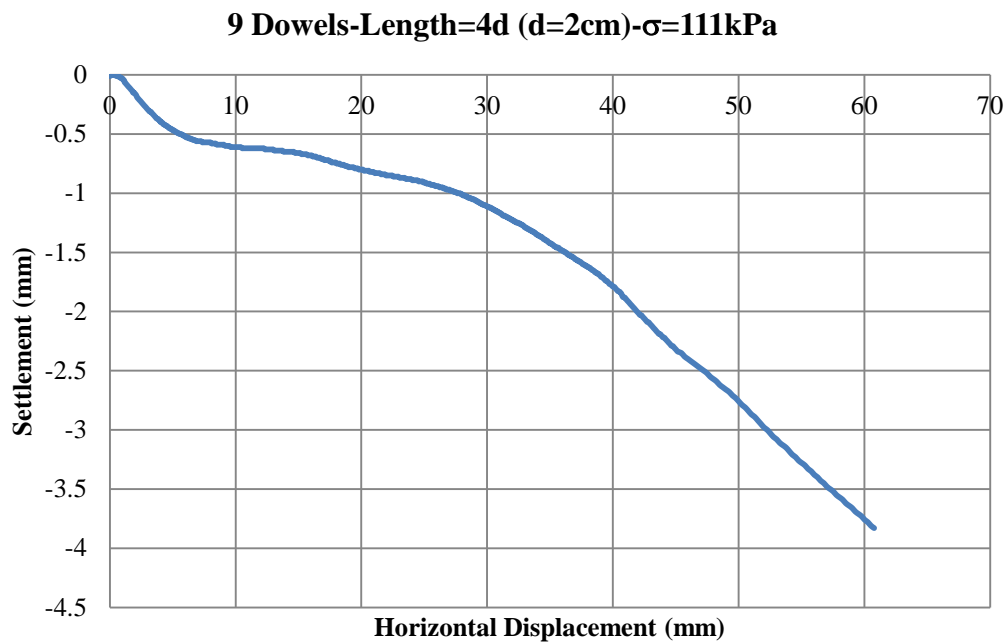


Figure C.23 Settlement vs. Displacement Graph-Experiment 12

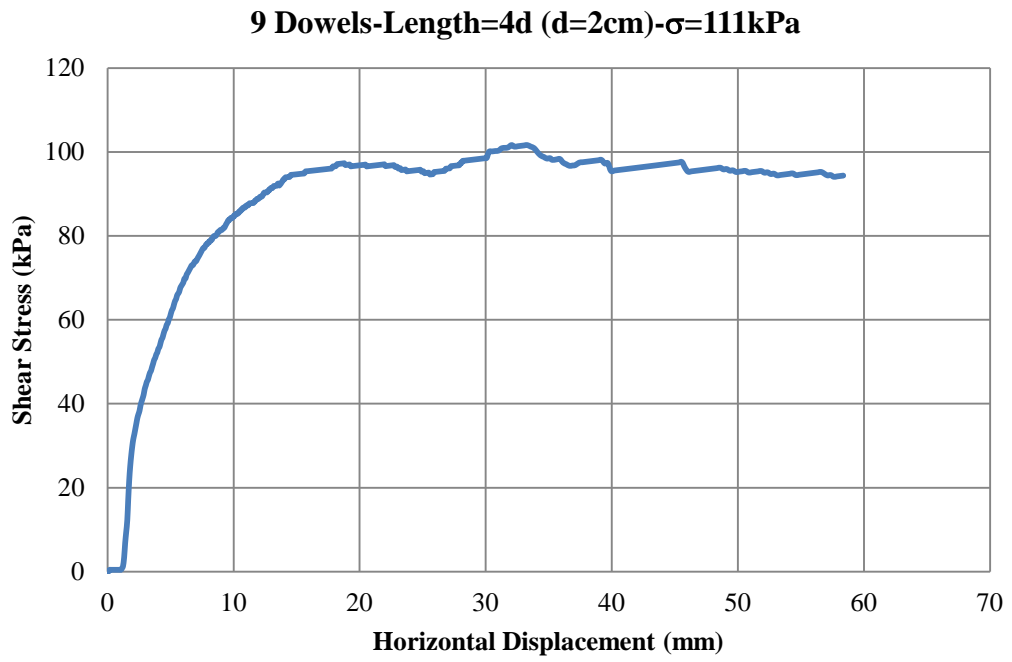


Figure C.24 Shear Stress vs. Displacement Graph-Experiment 13

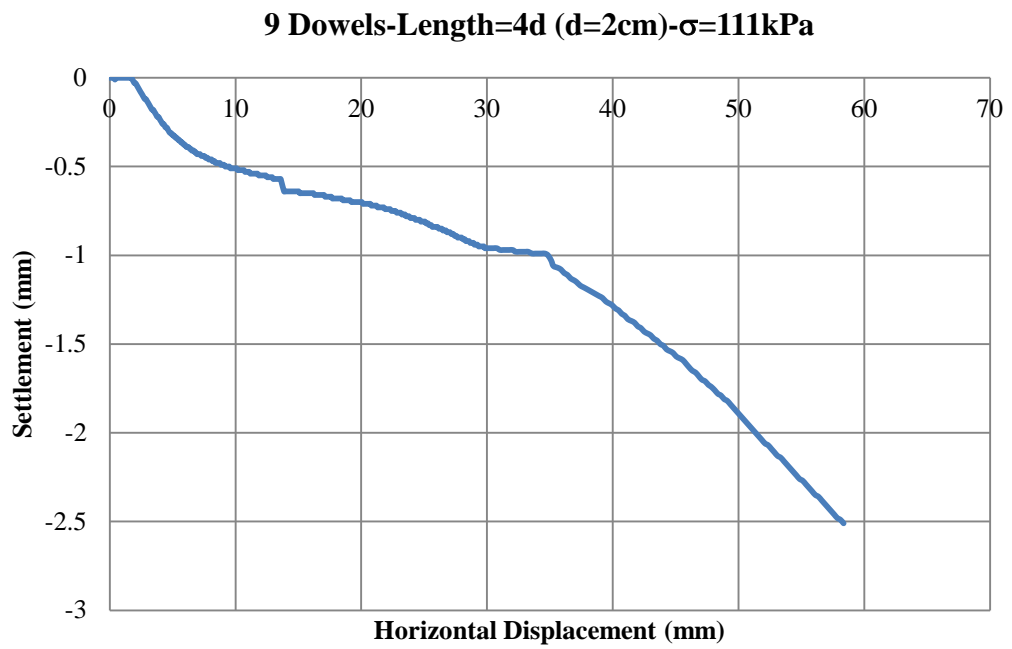


Figure C.25 Settlement vs. Displacement Graph-Experiment 13

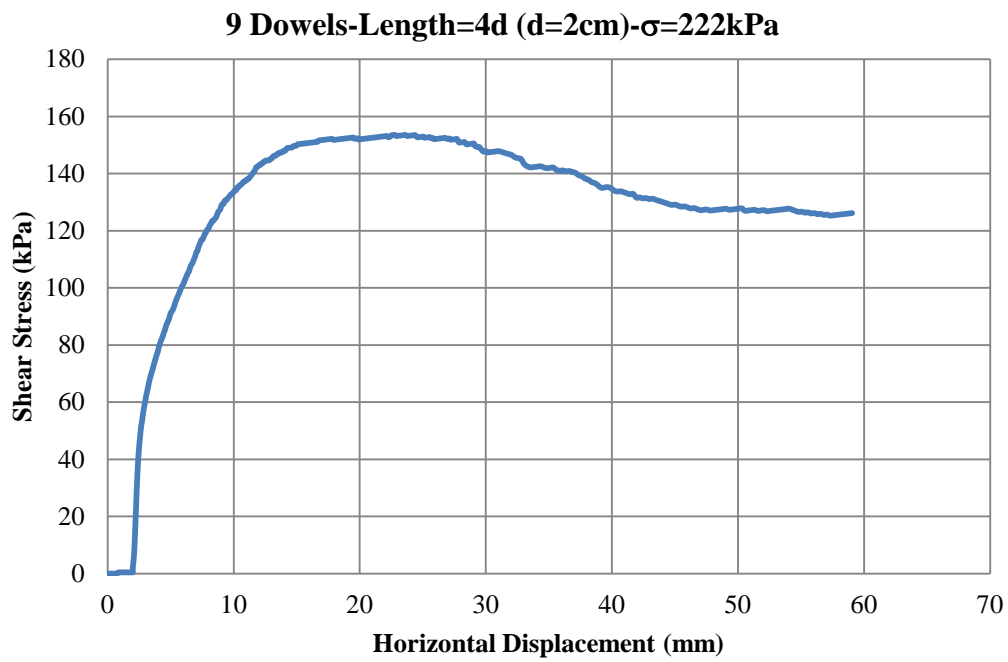


Figure C.26 Shear Stress vs. Displacement Graph-Experiment 14

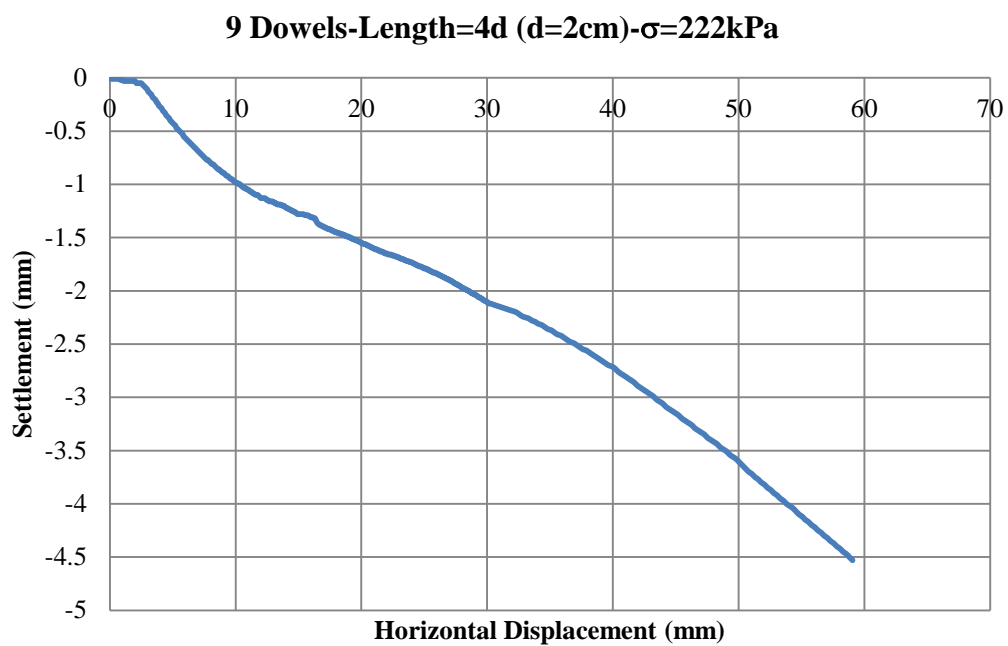


Figure C.27 Settlement vs. Displacement Graph-Experiment 14

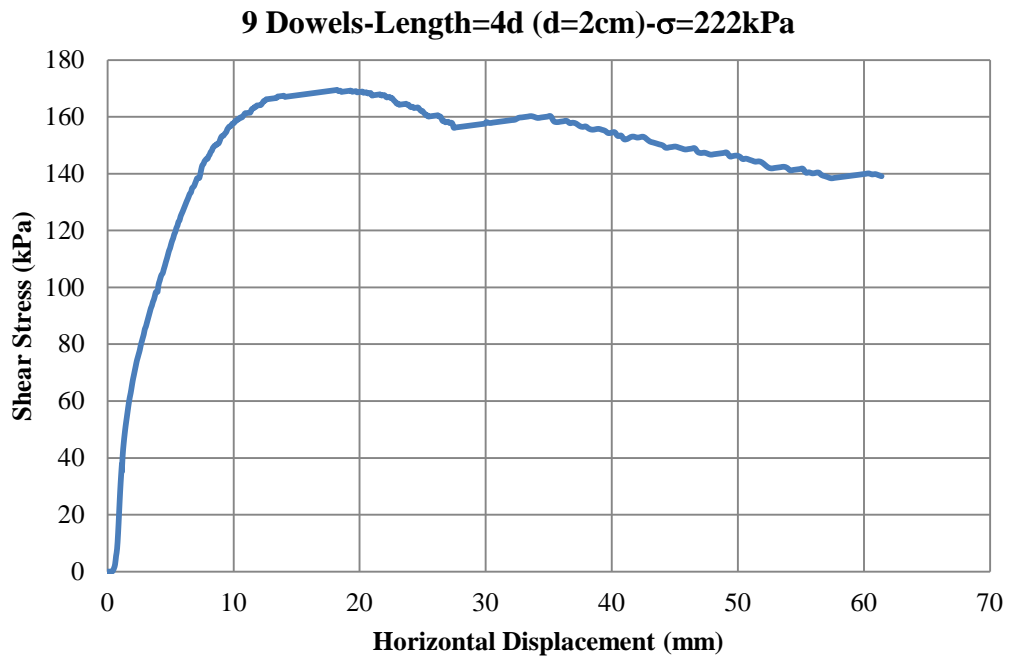


Figure C.28 Shear Stress vs. Displacement Graph-Experiment 15

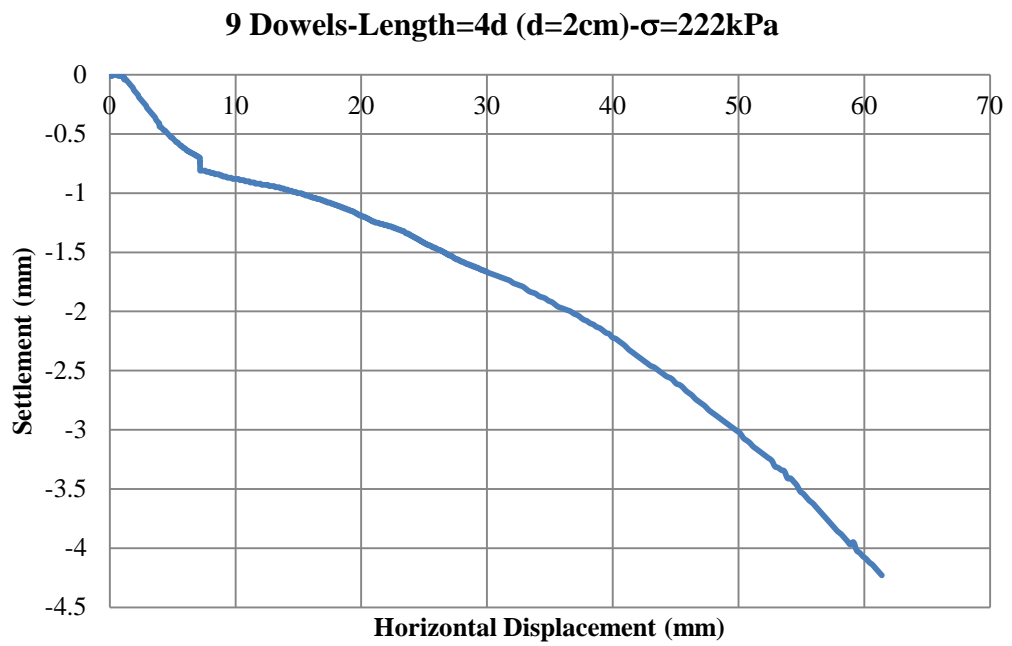


Figure C.29 Settlement vs. Displacement Graph-Experiment 15

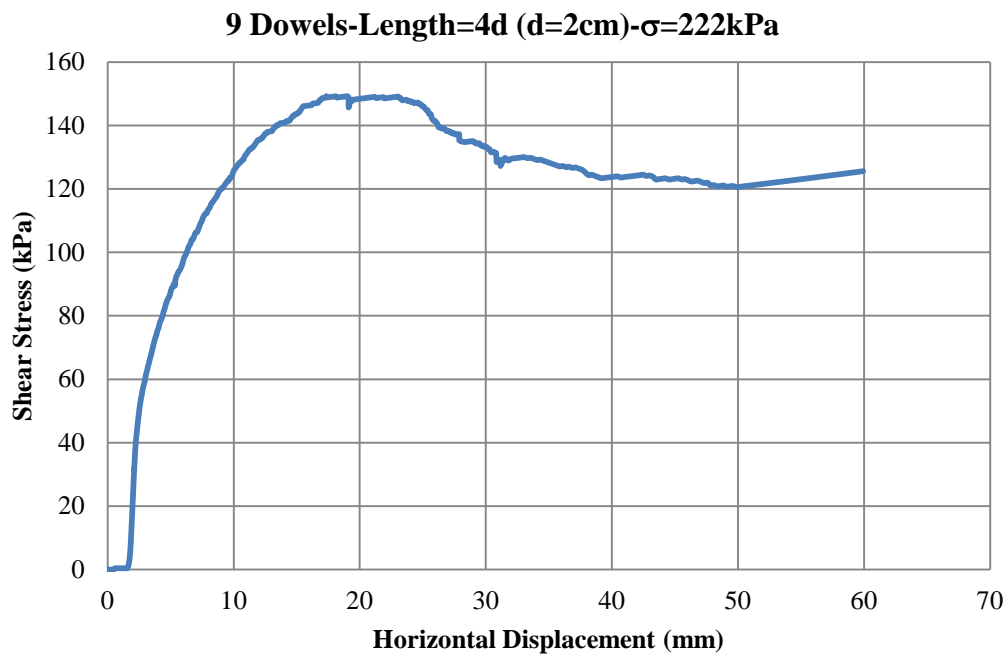


Figure C.30 Shear Stress vs. Displacement Graph-Experiment 16

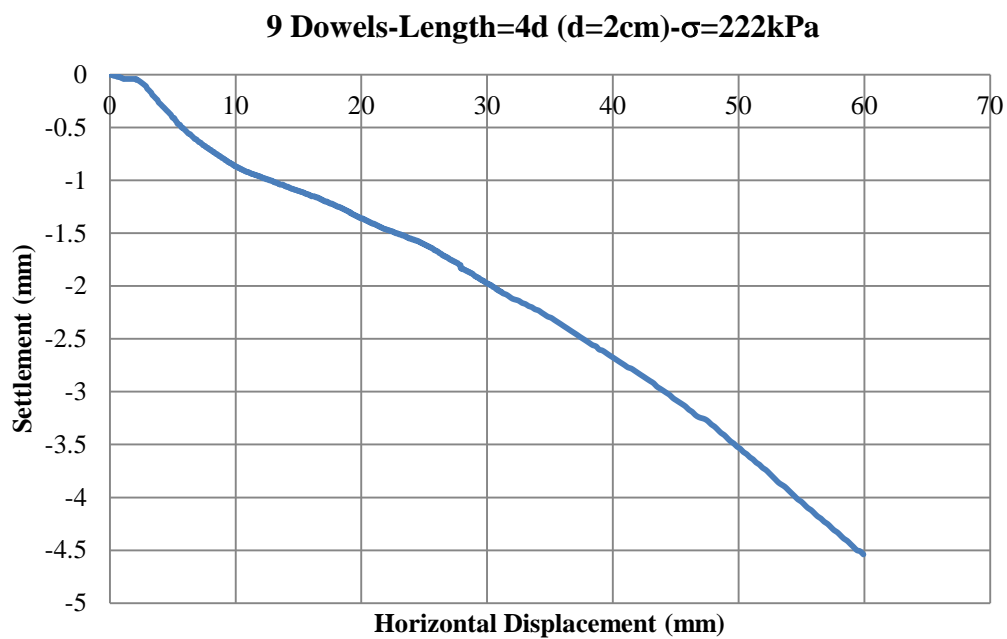


Figure C.31 Settlement vs. Displacement Graph-Experiment 16

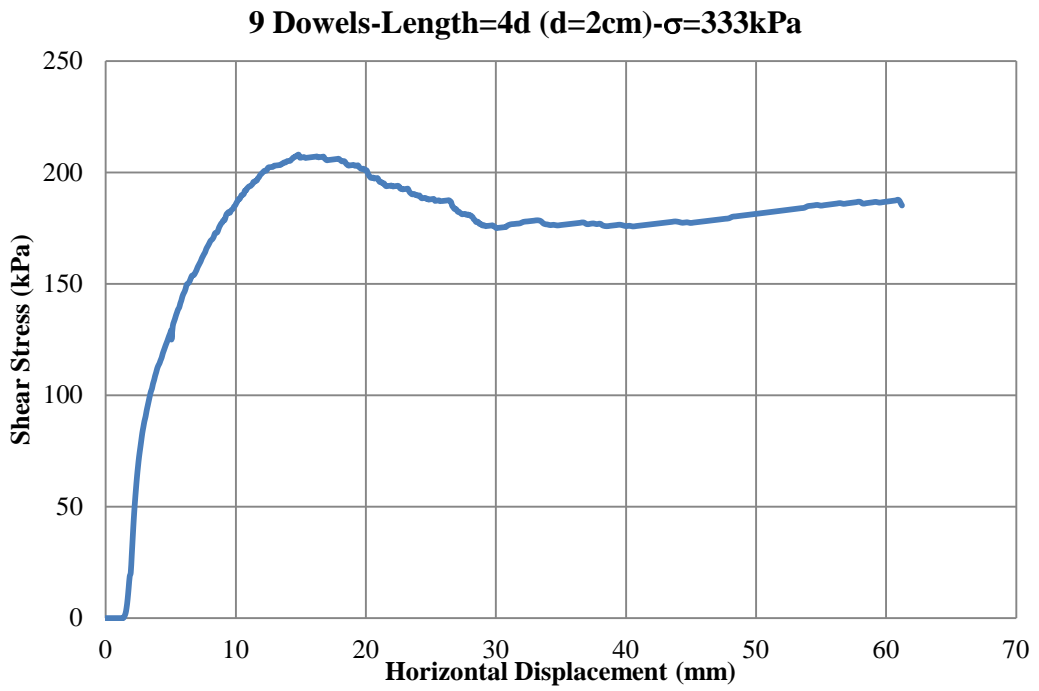


Figure C.32 Shear Stress vs. Displacement Graph-Experiment 17

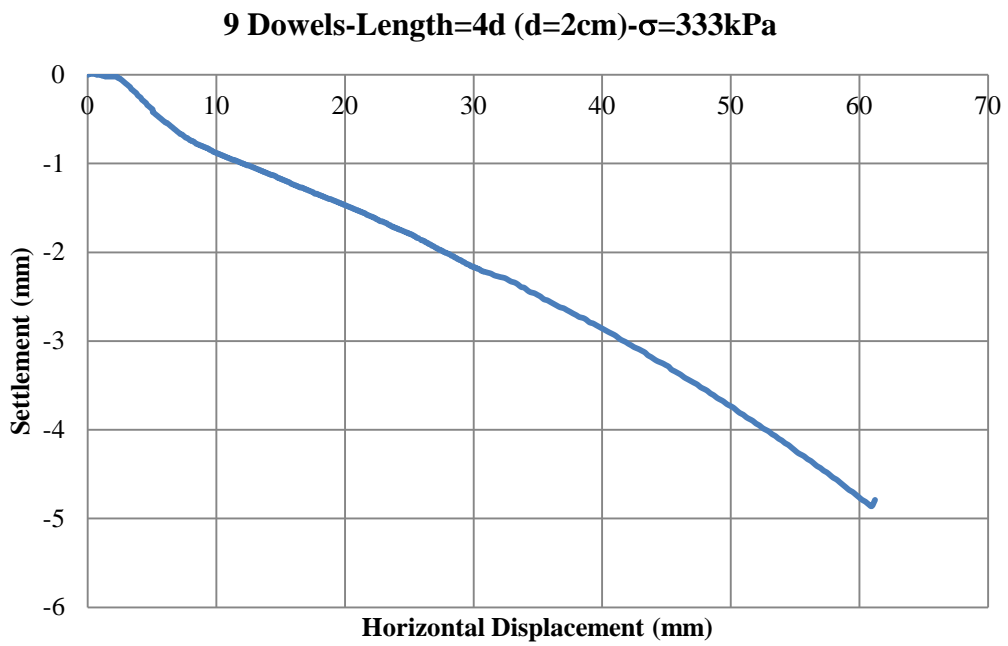


Figure C.33 Settlement vs. Displacement Graph-Experiment 17

#### 4. Improvement Tests- I-4

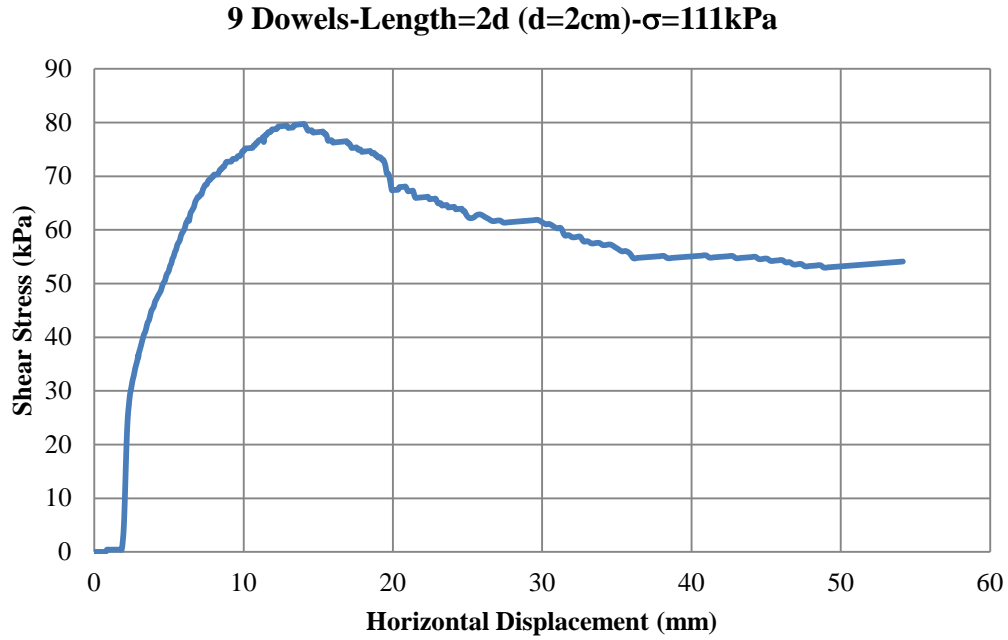


Figure C.34 Shear Stress vs. Displacement Graph-Experiment 18

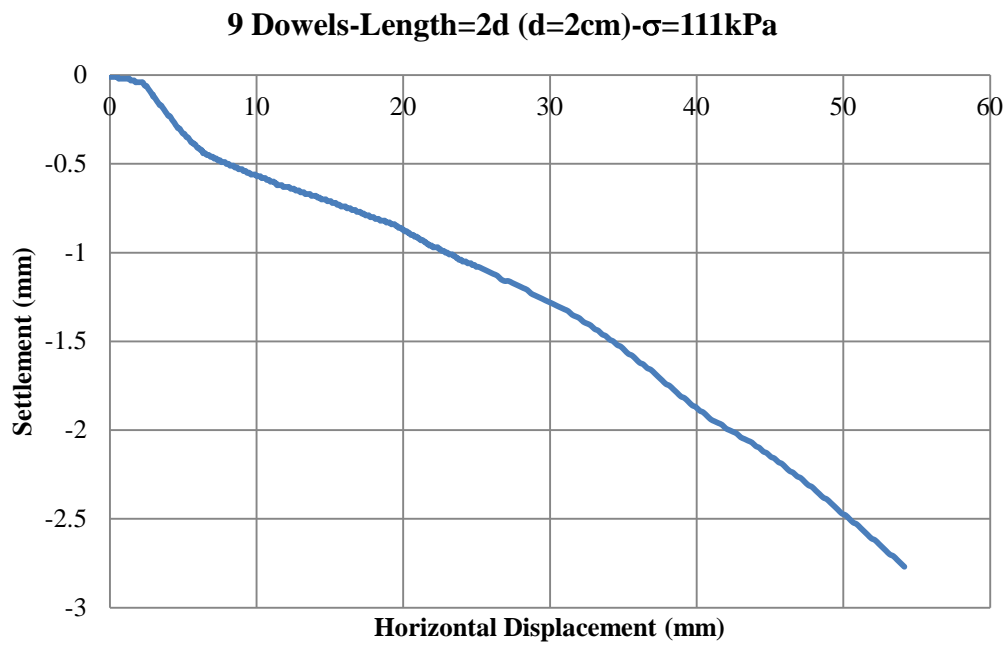


Figure C.35 Settlement vs. Displacement Graph-Experiment 18

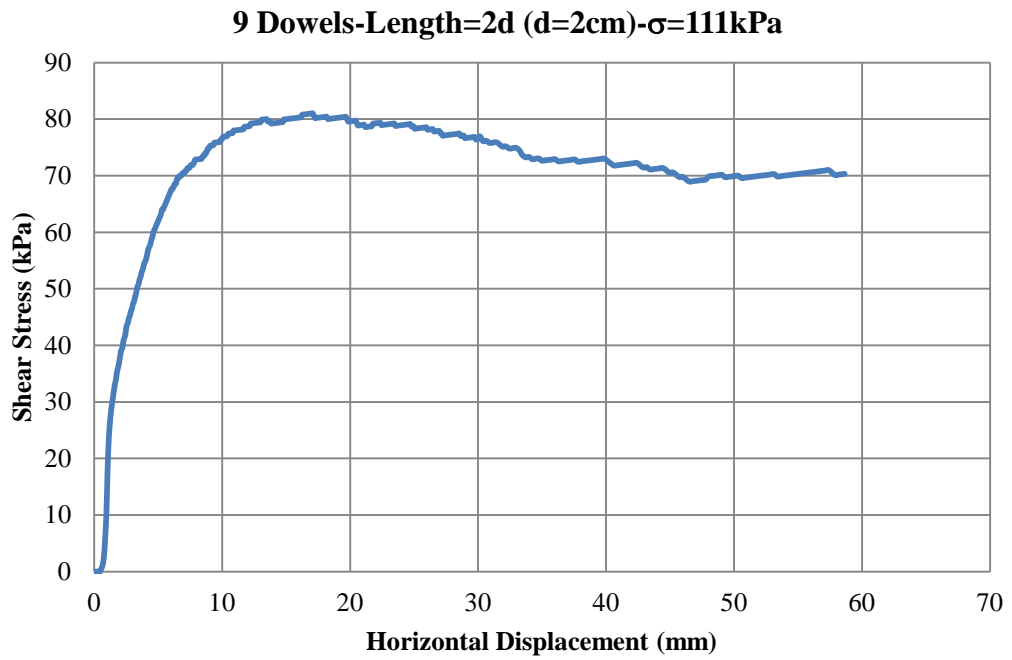


Figure C.36 Shear Stress vs. Displacement Graph-Experiment 19

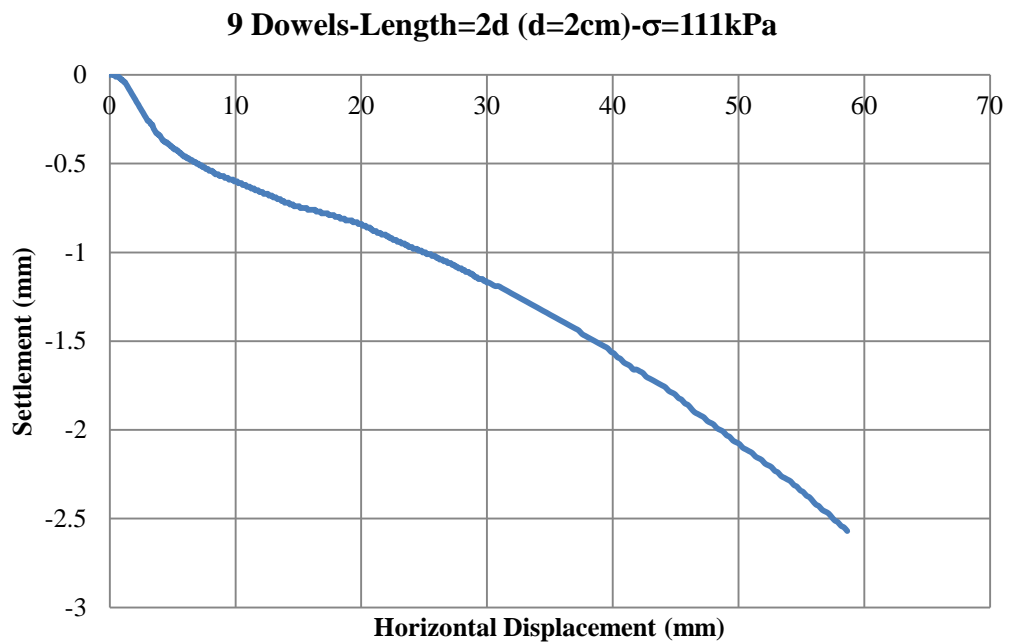


Figure C.37 Settlement vs. Displacement Graph-Experiment 19

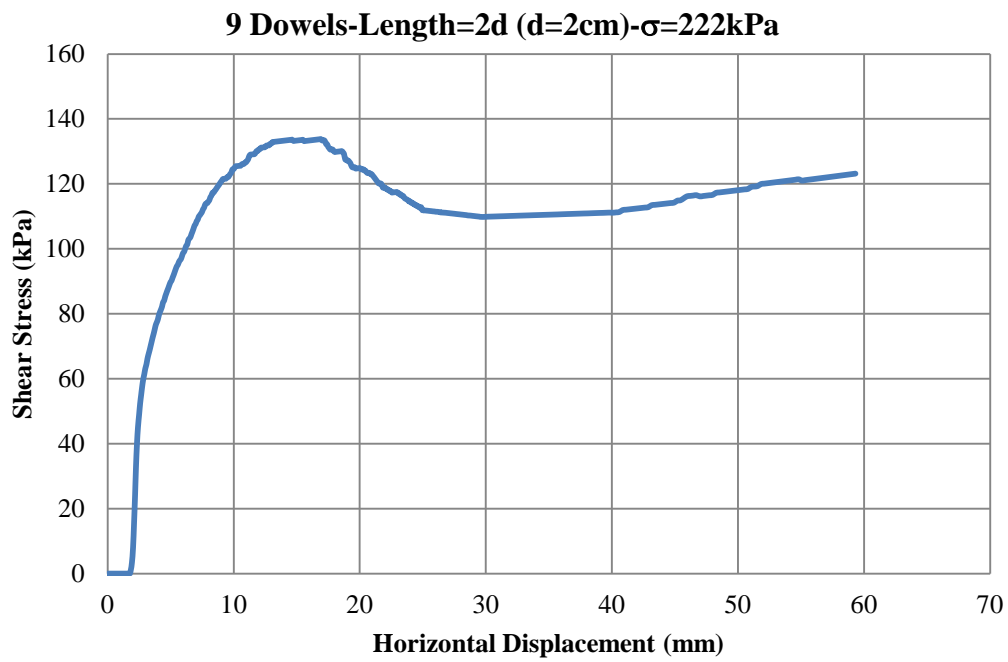


Figure C.38 Shear Stress vs. Displacement Graph-Experiment 20

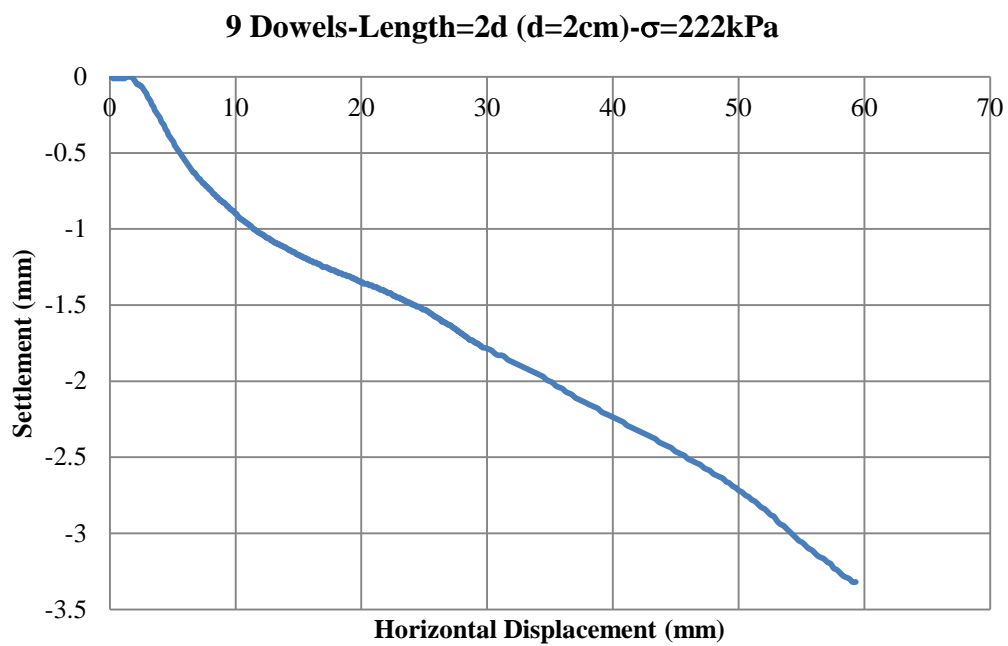


Figure C.39 Settlement vs. Displacement Graph-Experiment 20

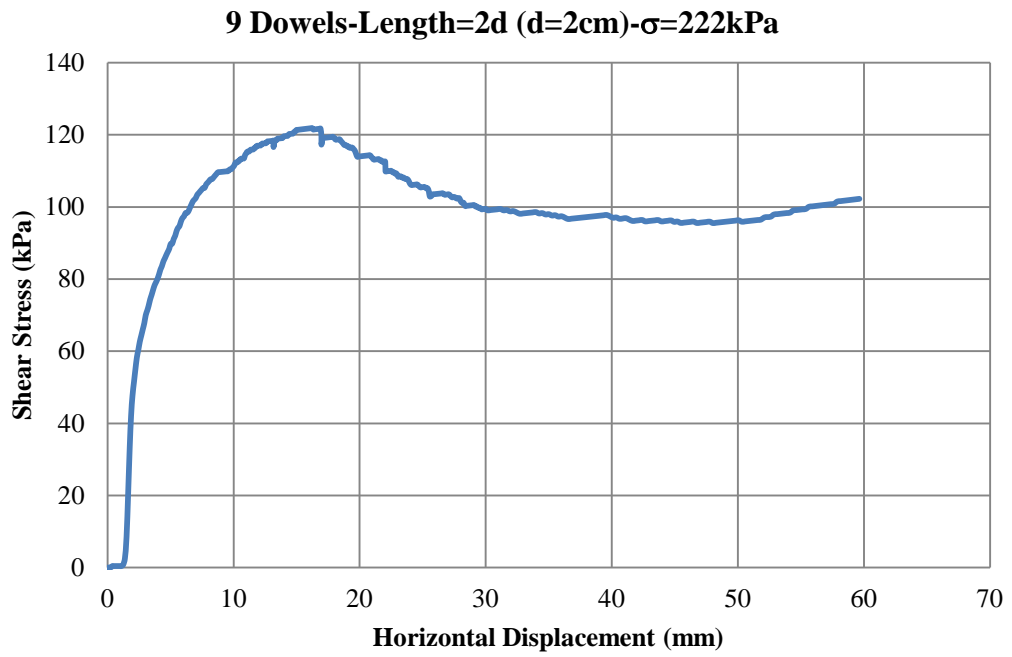


Figure C.40 Shear Stress vs. Displacement Graph-Experiment 21

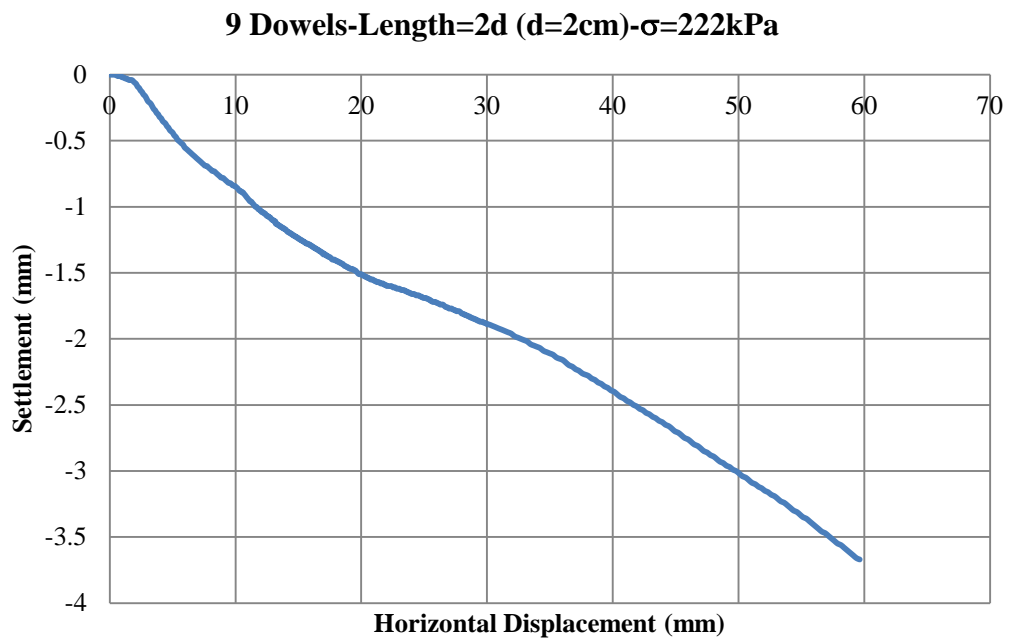


Figure C.41 Settlement vs. Displacement Graph-Experiment 21

5. Improvement Tests- I-5

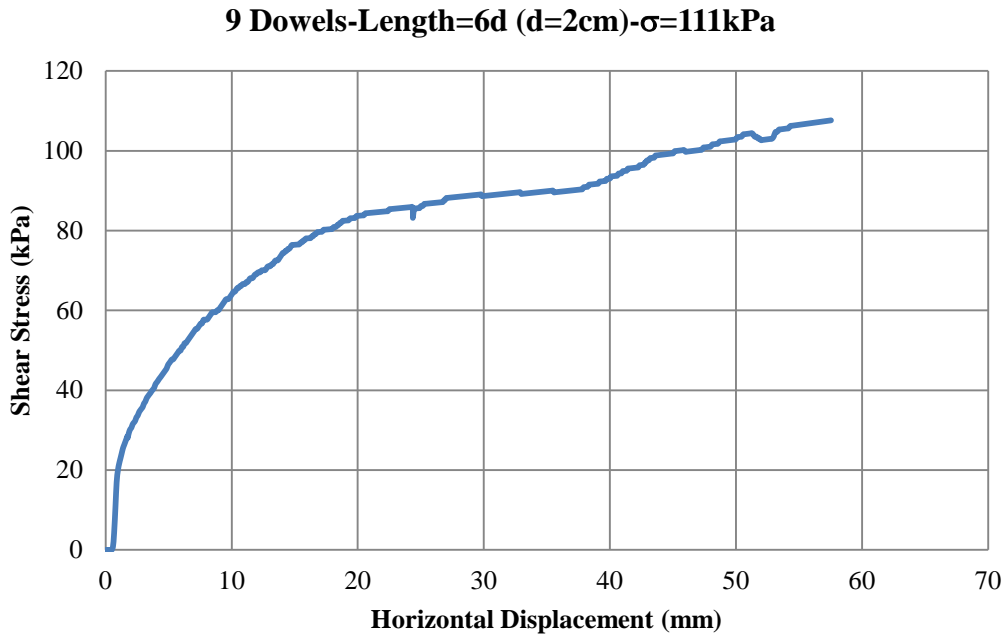


Figure C.42 Shear Stress vs. Displacement Graph-Experiment 22

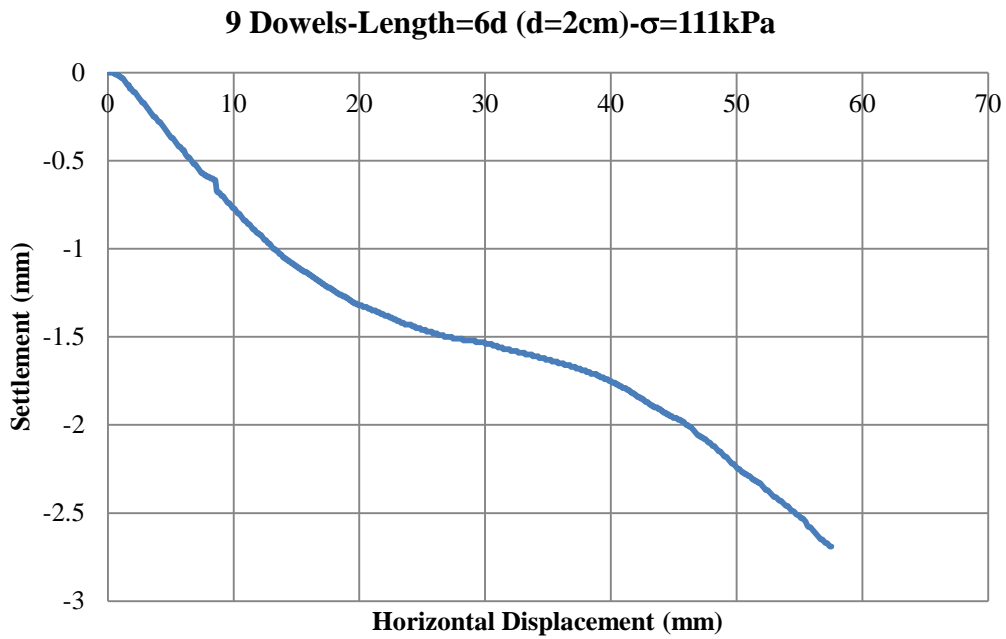


Figure C.43 Settlement vs. Displacement Graph-Experiment 22

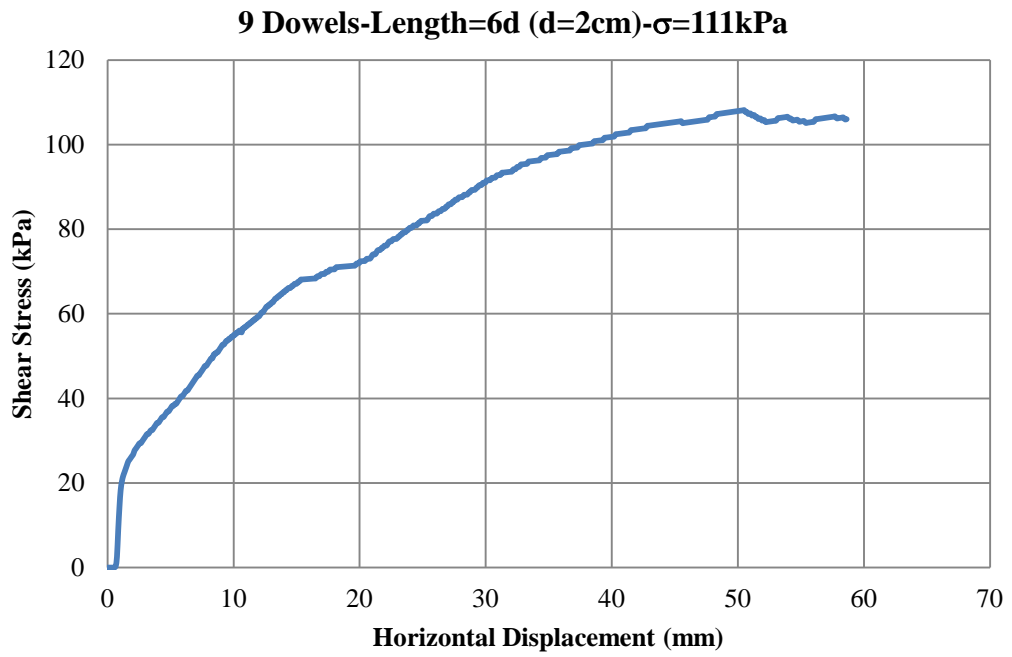


Figure C.44 Shear Stress vs. Displacement Graph-Experiment 23

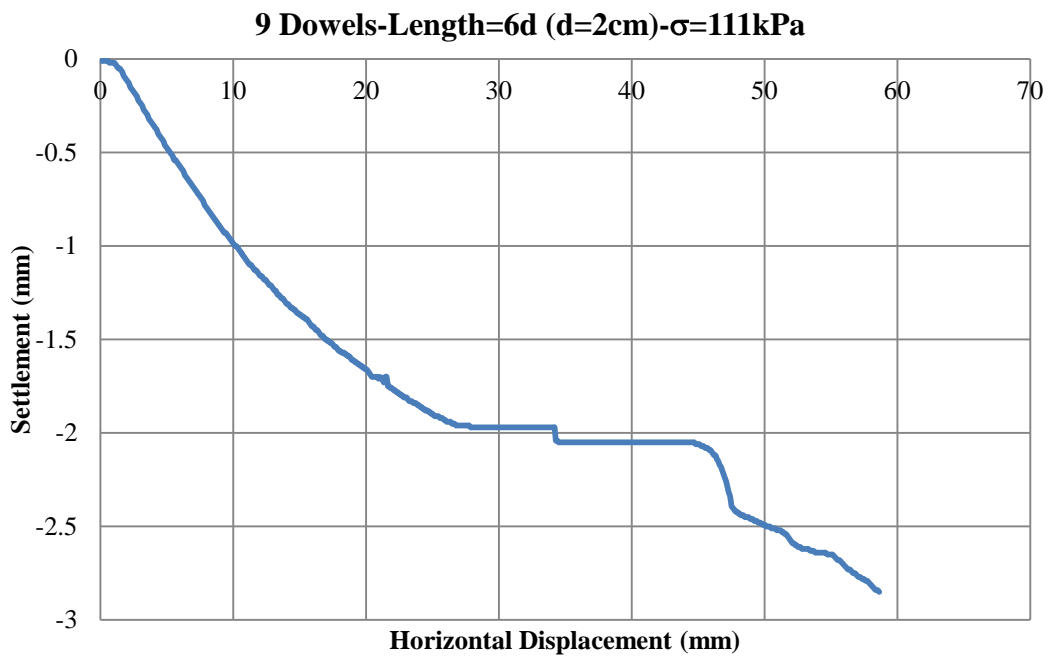


Figure C.45 Settlement vs. Displacement Graph-Experiment 23

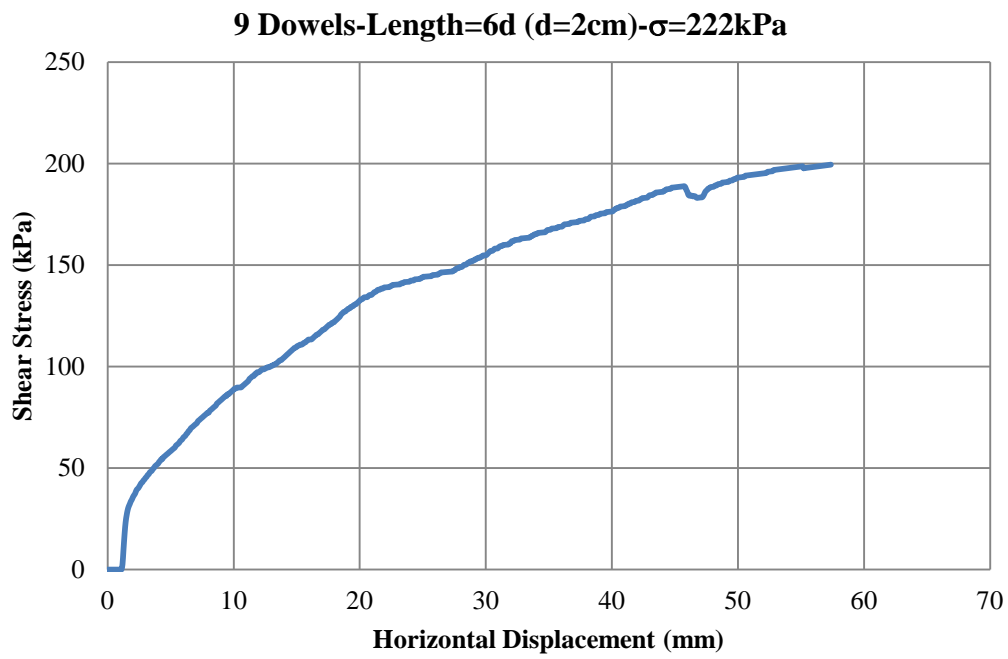


Figure C.46 Shear Stress vs. Displacement Graph-Experiment 24

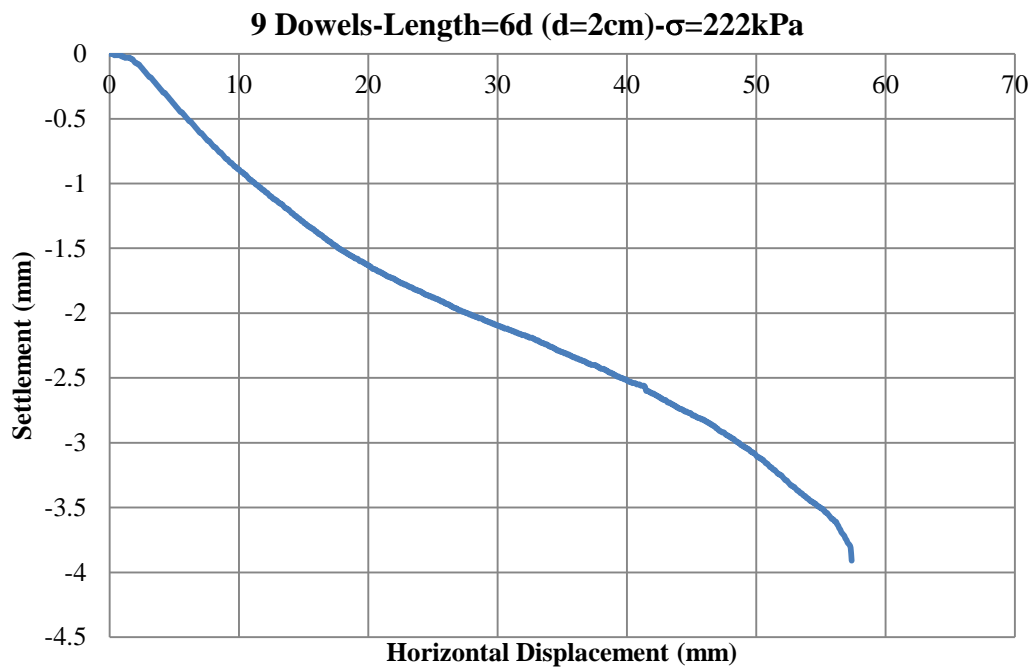


Figure C.47 Settlement vs. Displacement Graph-Experiment 24

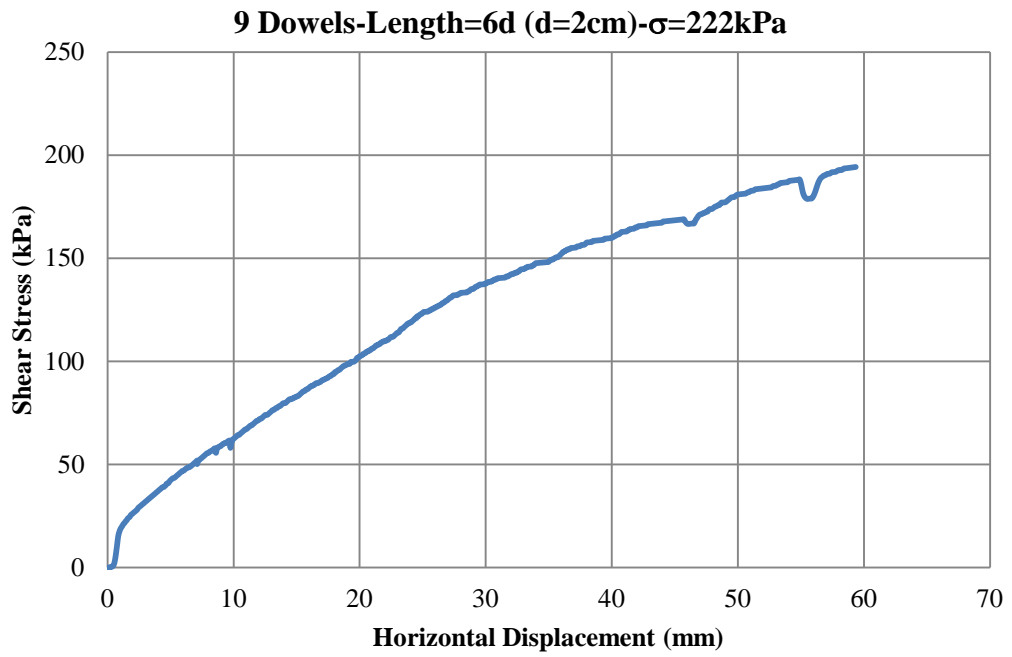


Figure C.48 Shear Stress vs. Displacement Graph-Experiment 25

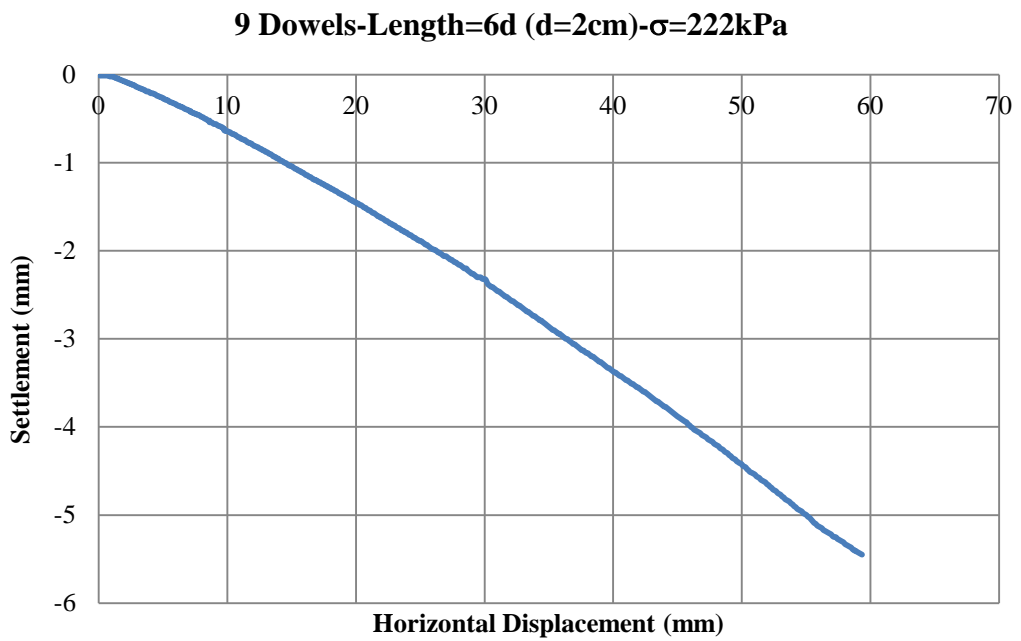


Figure C.49 Settlement vs. Displacement Graph-Experiment 25

## 6. Improvement Tests- I-6

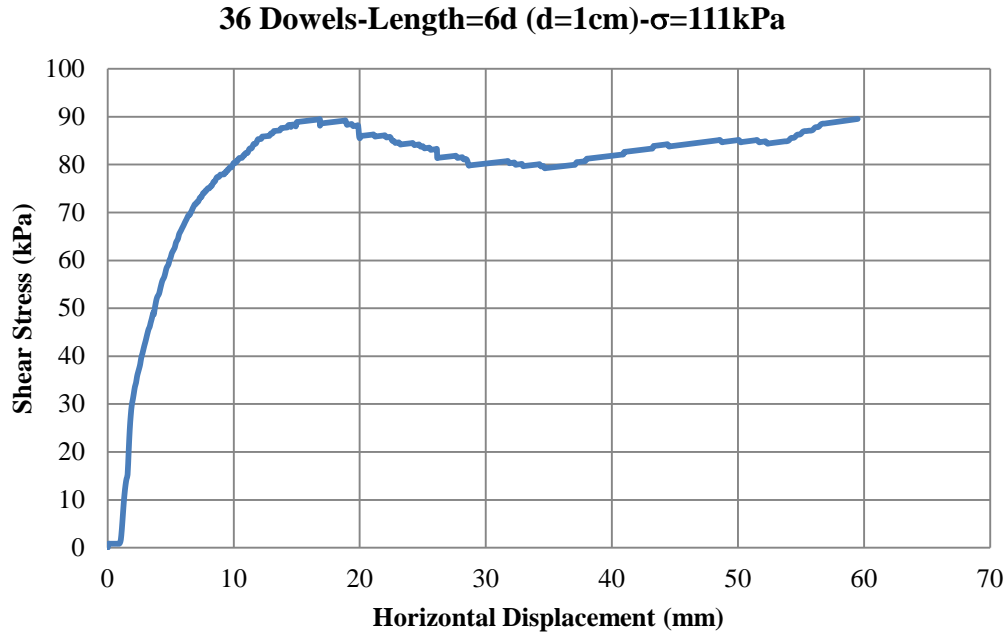


Figure C.50 Shear Stress vs. Displacement Graph-Experiment 26

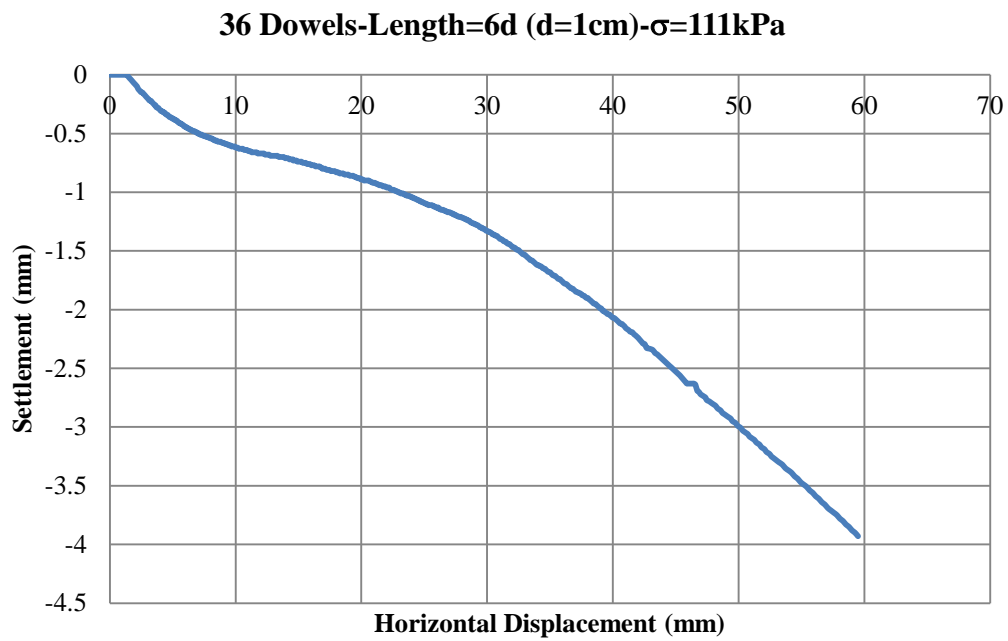


Figure C.51 Settlement vs. Displacement Graph-Experiment 26

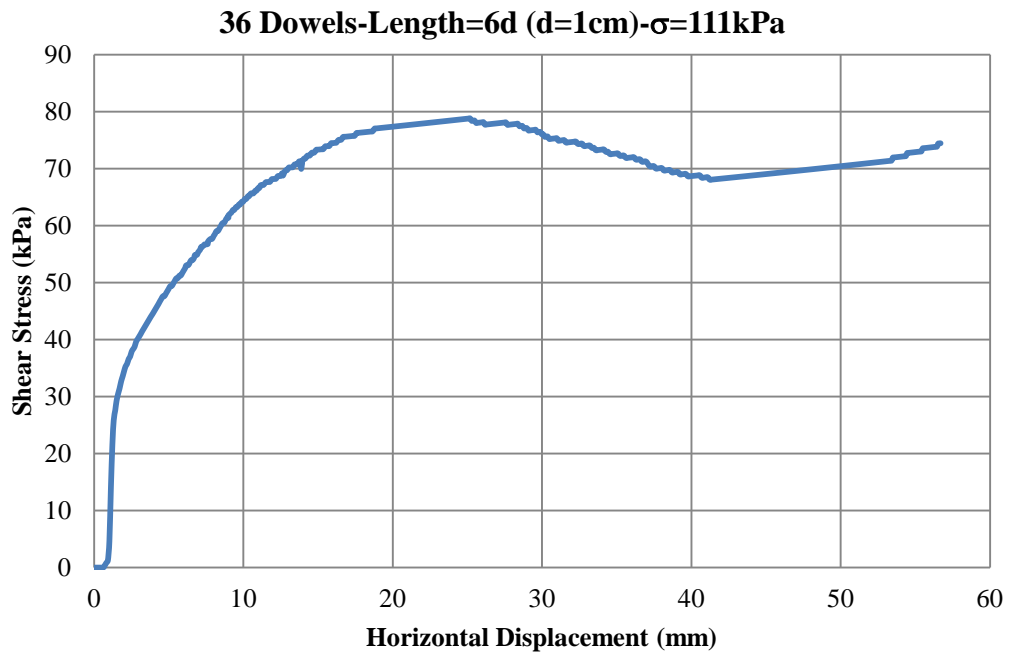


Figure C.52 Shear Stress vs. Displacement Graph-Experiment 27

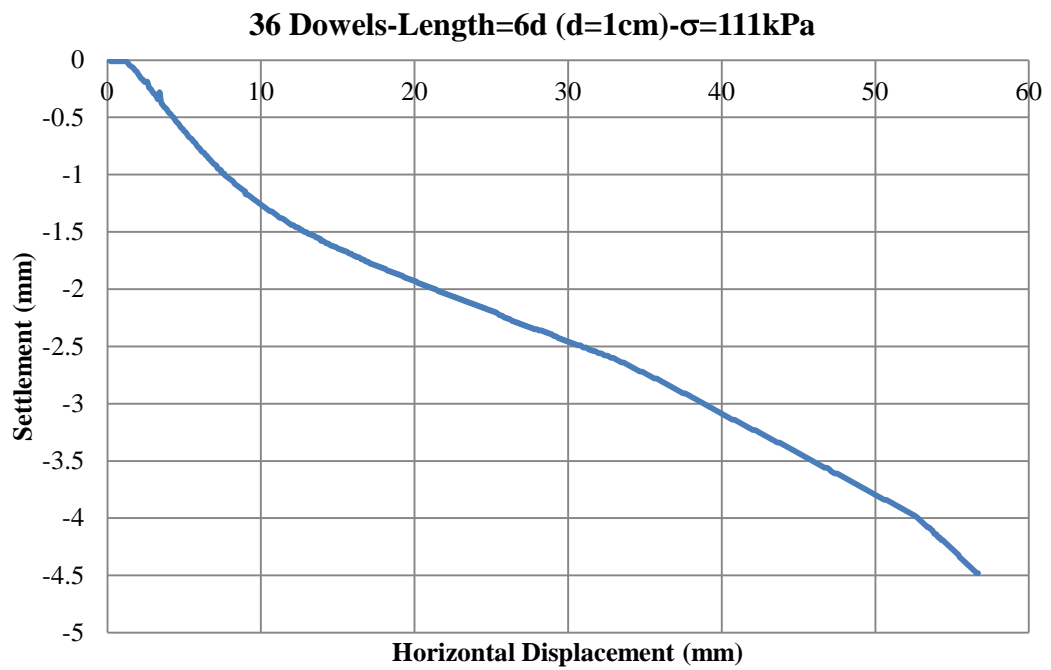


Figure C.53 Settlement vs. Displacement Graph-Experiment 27

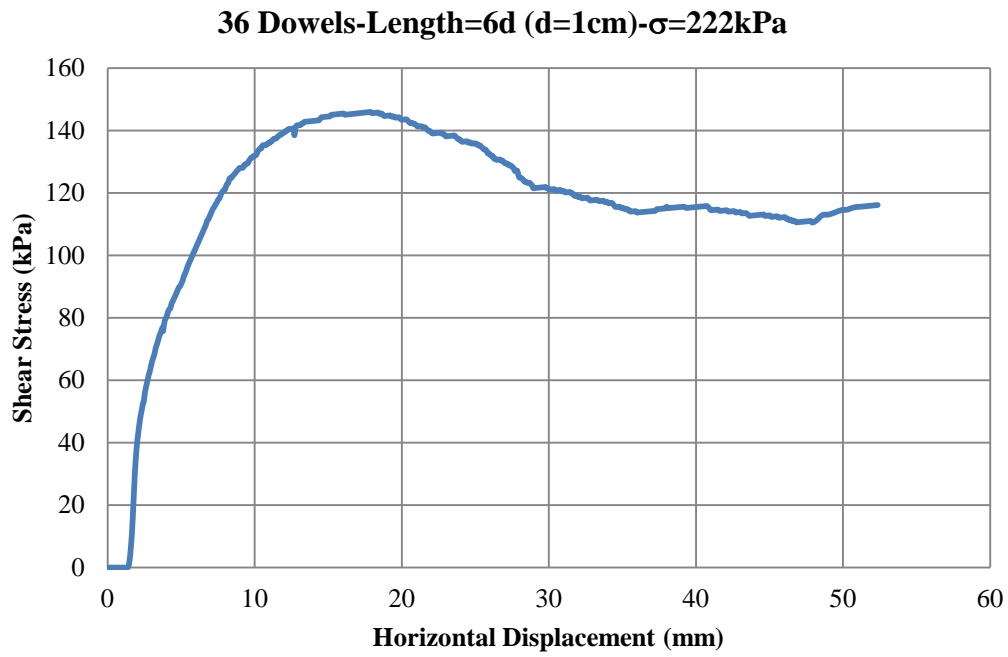


Figure C.54 Shear Stress vs. Displacement Graph-Experiment 28

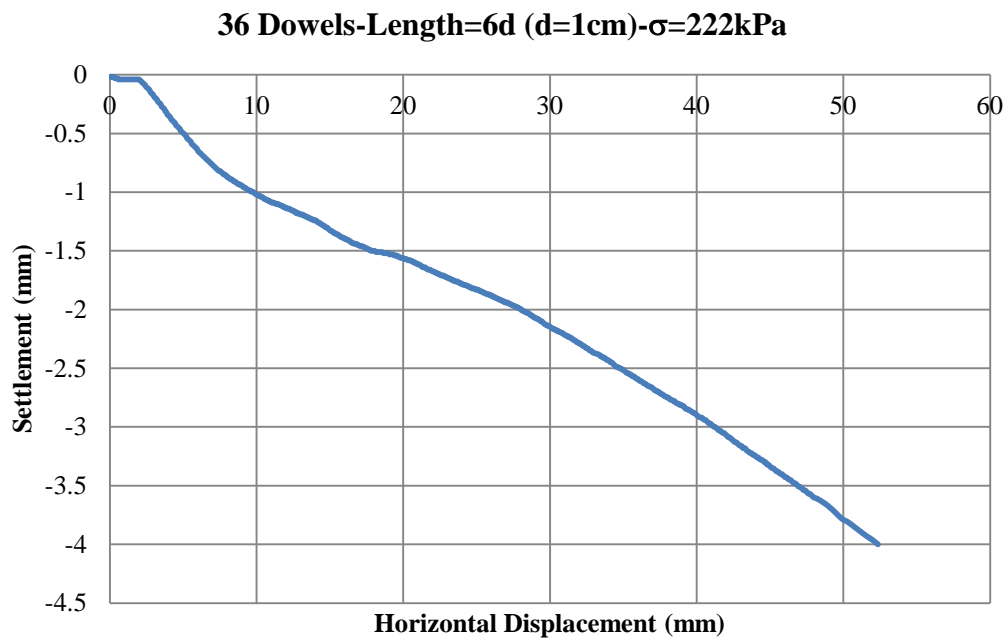


Figure C.55 Settlement vs. Displacement Graph-Experiment 28

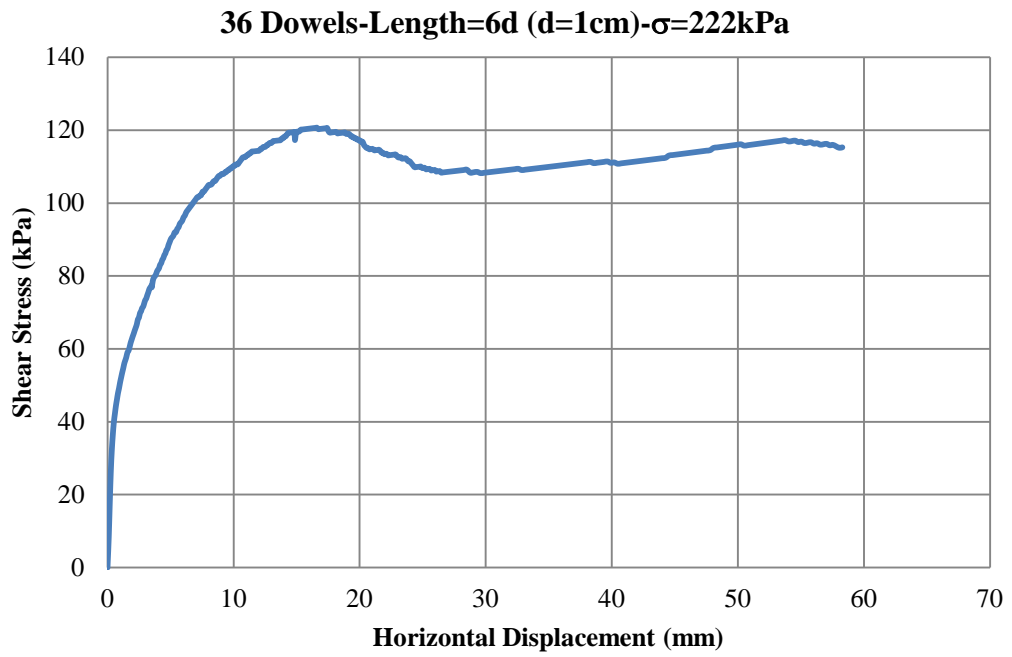


Figure C.56 Shear Stress vs. Displacement Graph-Experiment 29

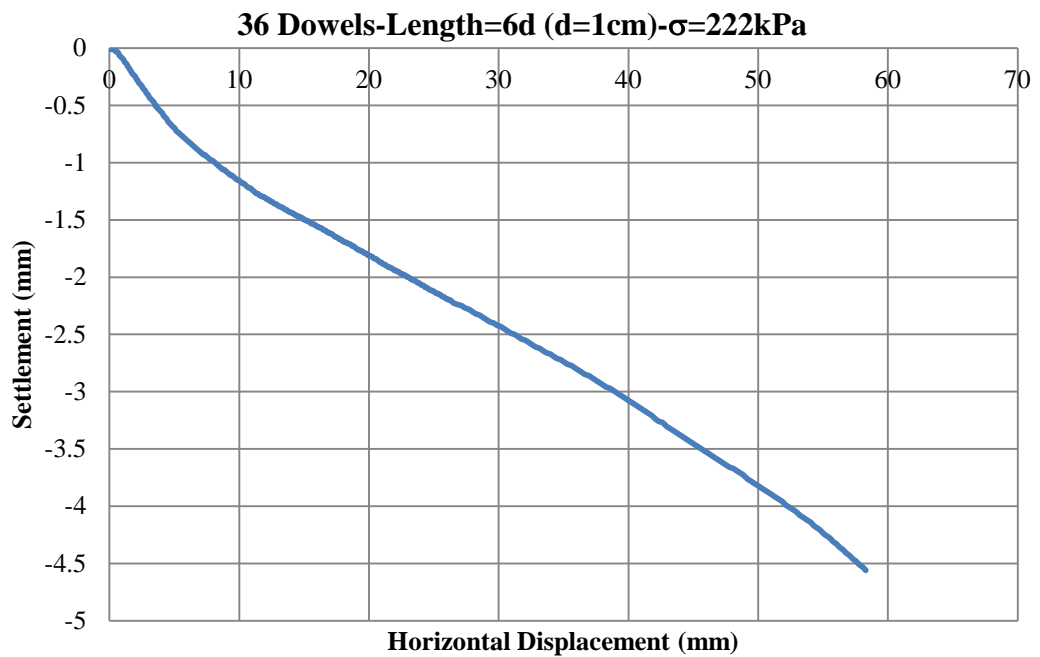


Figure C.57 Settlement vs. Displacement Graph-Experiment 29

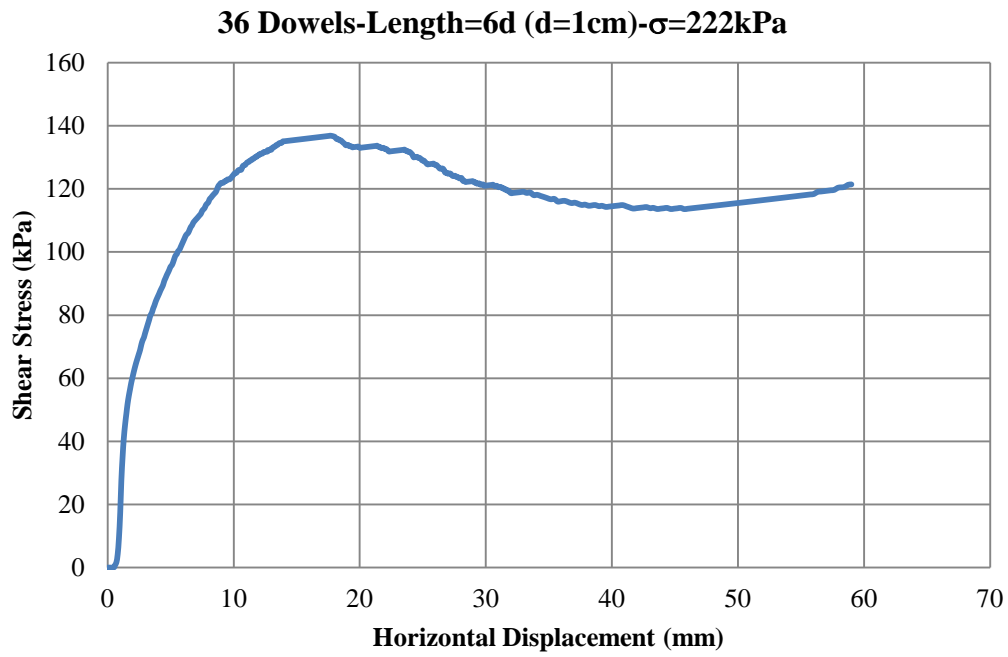


Figure C.58 Shear Stress vs. Displacement Graph-Experiment 30

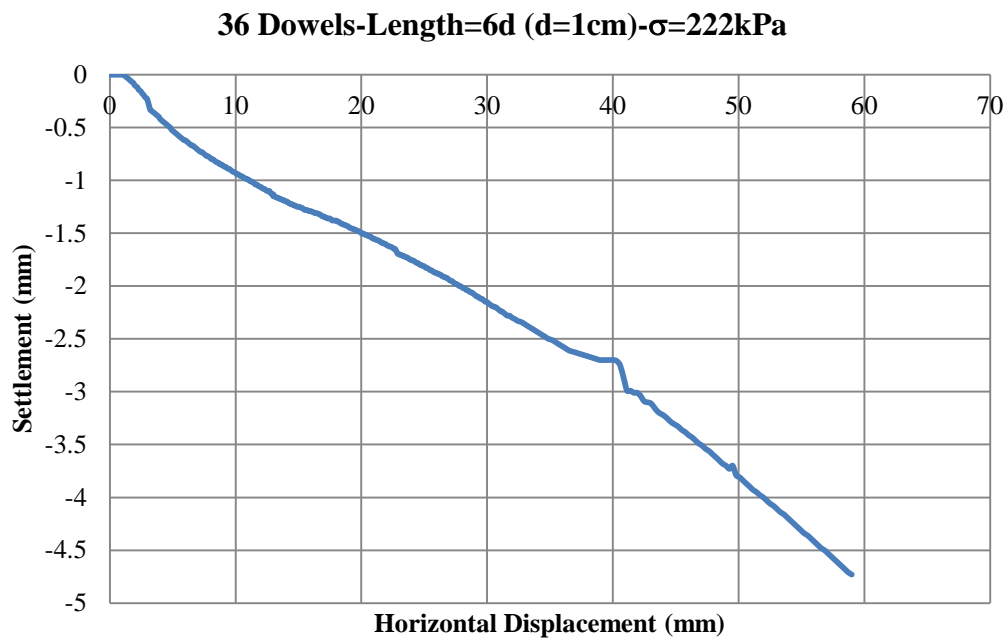


Figure C.59 Settlement vs. Displacement Graph-Experiment 30

## 7. Improvement Tests- I-7

**36 Dowels-Length=12d (d=1cm)- $\sigma$ =111kPa**

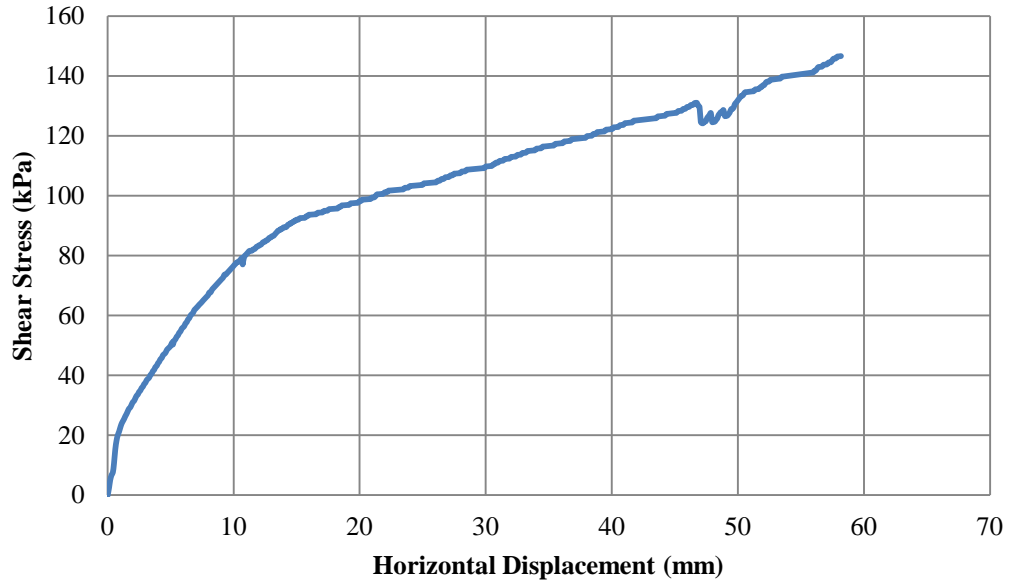


Figure C.60 Shear Stress vs. Displacement Graph-Experiment 31

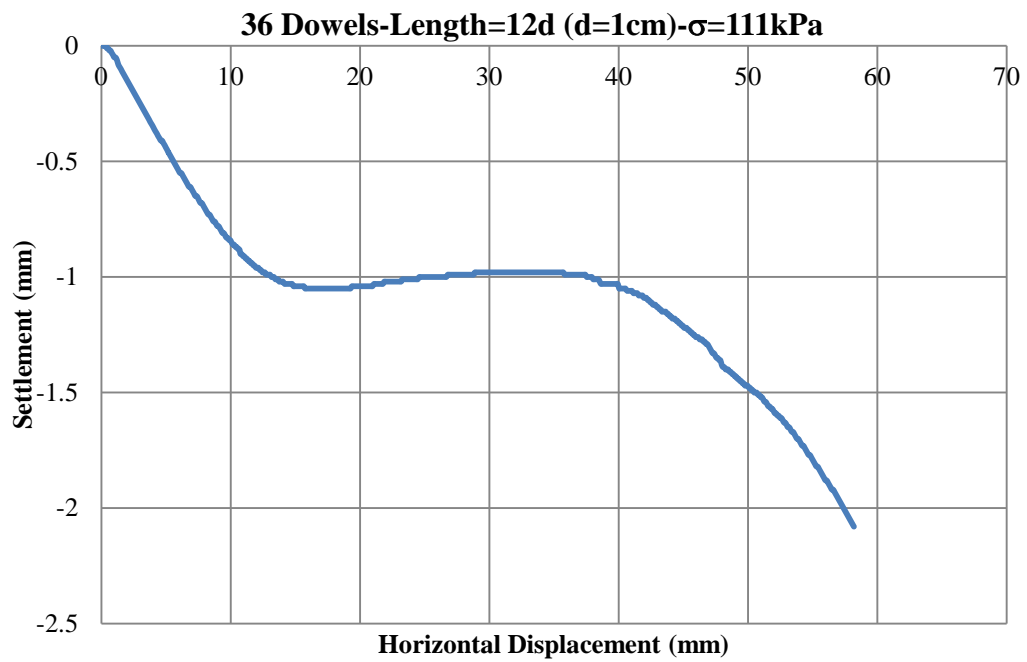


Figure C.61 Settlement vs. Displacement Graph-Experiment 31

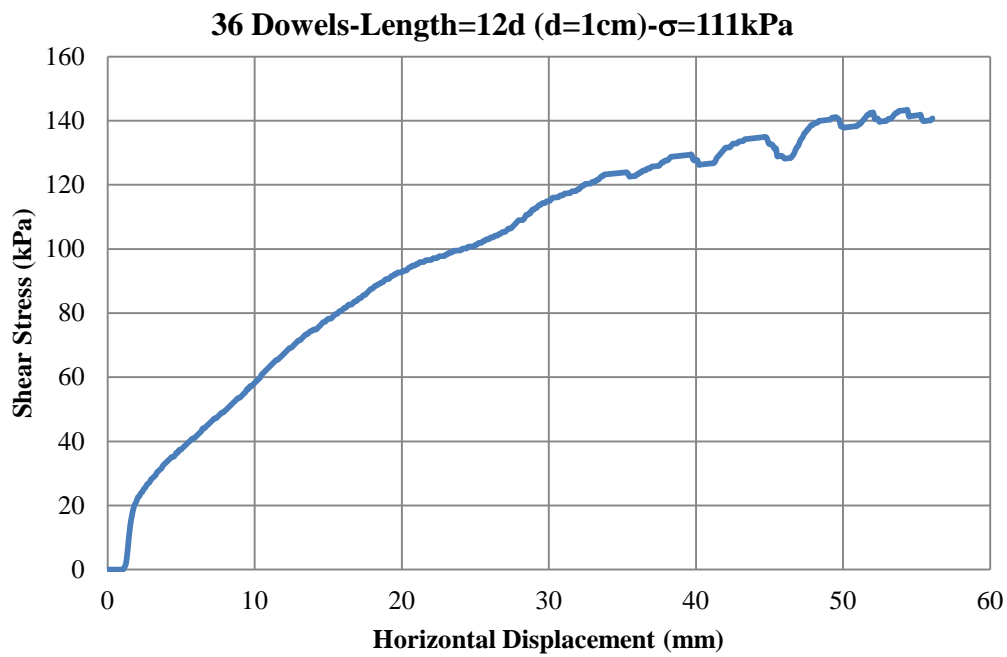


Figure C.62 Shear Stress vs. Displacement Graph-Experiment 32

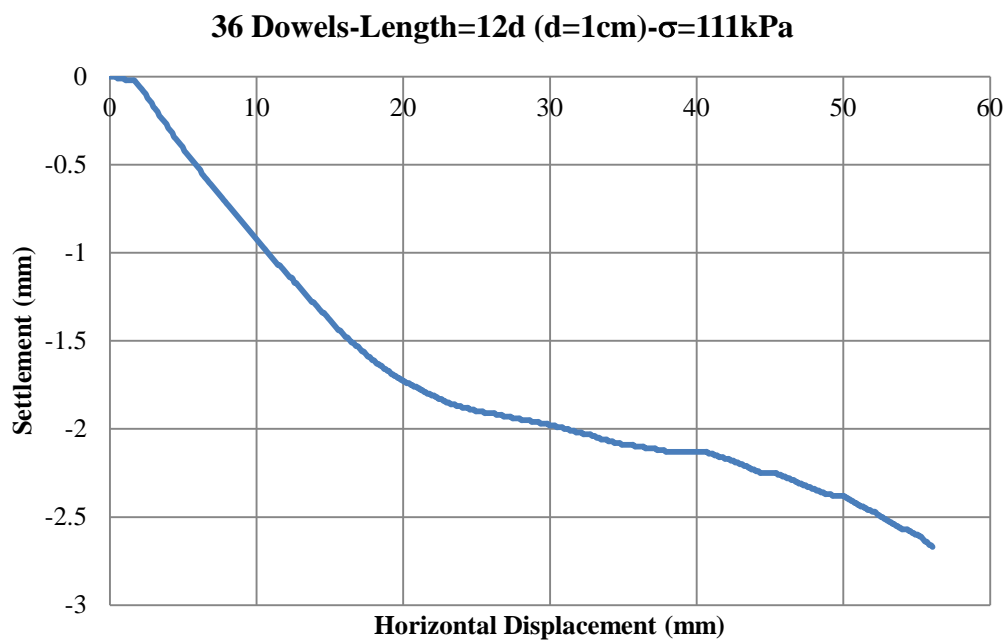


Figure C.63 Settlement vs. Displacement Graph-Experiment 32

**36 Dowels-Length=12d (d=1cm)- $\sigma$ =222kPa**

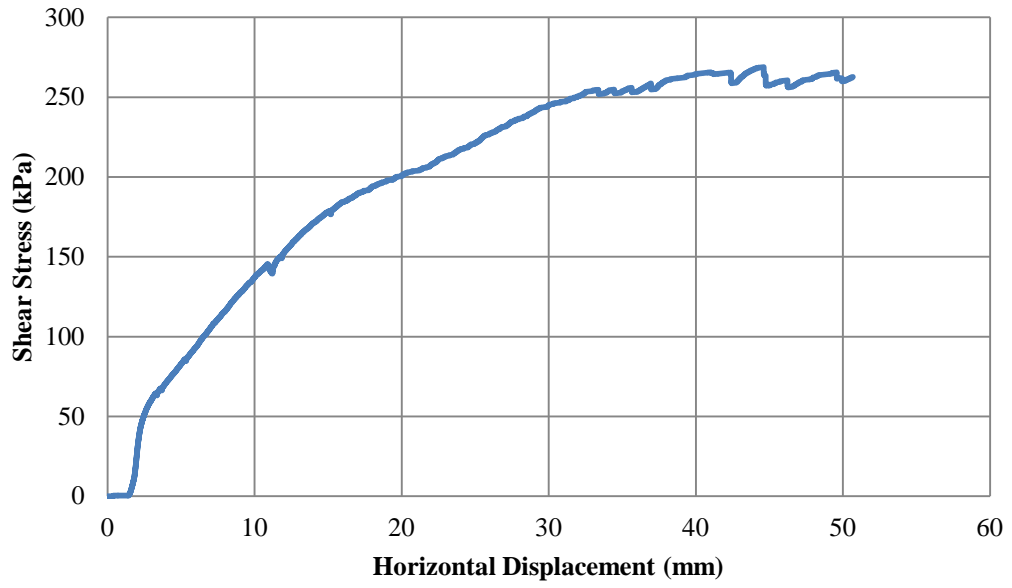


Figure C.64 Shear Stress vs. Displacement Graph-Experiment 33

**36 Dowels-Length=12d (d=1cm)- $\sigma$ =222kPa**

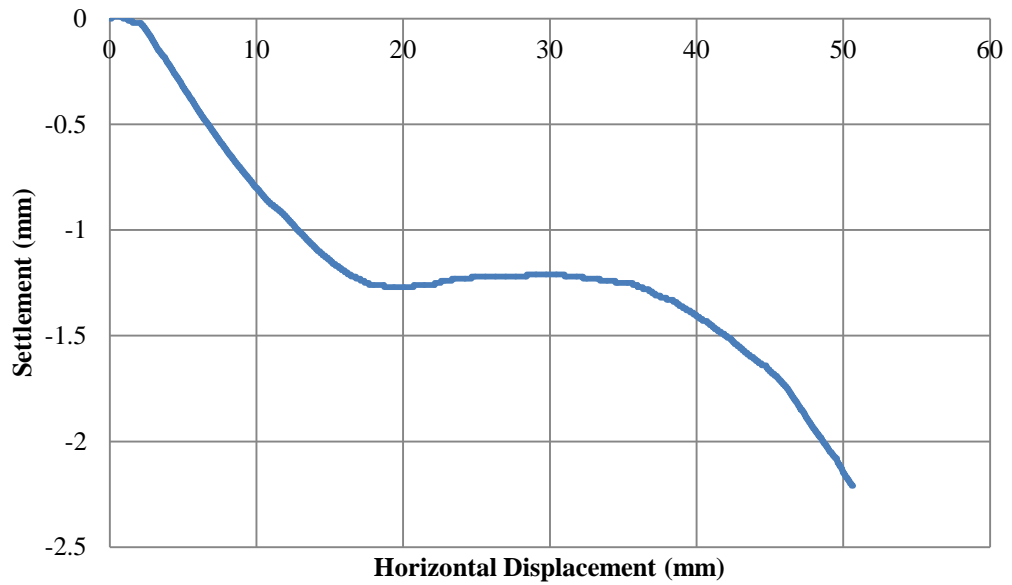


Figure C.65 Settlement vs. Displacement Graph-Experiment 33

**36 Dowels-Length=12d (d=1cm)- $\sigma$ =222kPa**

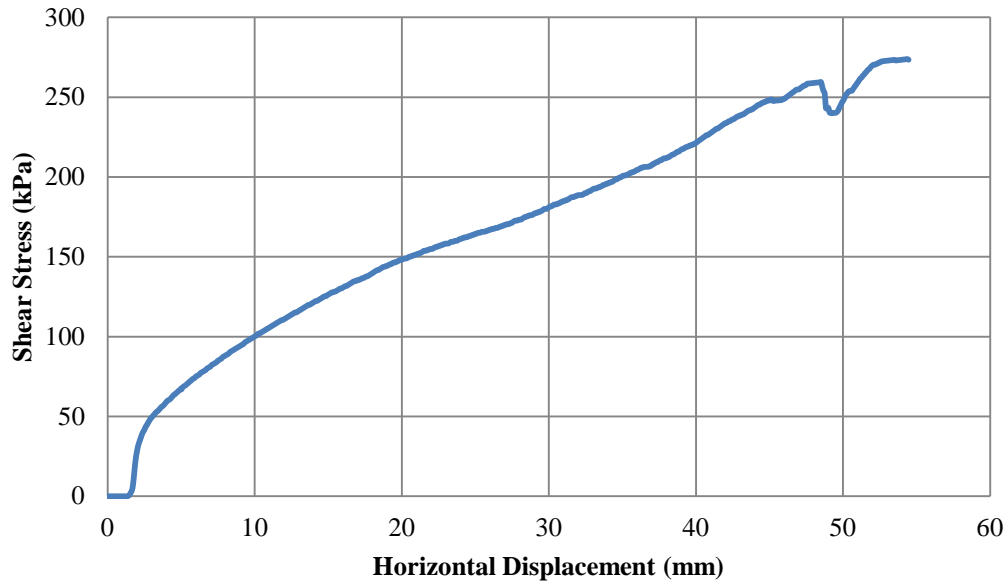


Figure C.66 Shear Stress vs. Displacement Graph-Experiment 34

**36 Dowels-Length=12d (d=1cm)- $\sigma$ =222kPa**

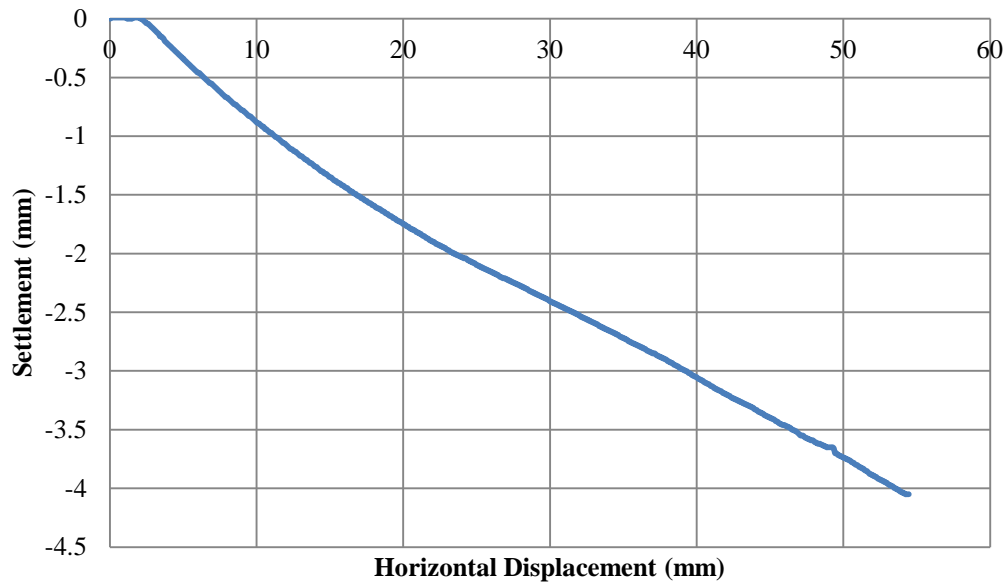


Figure C.67 Settlement vs. Displacement Graph-Experiment 34

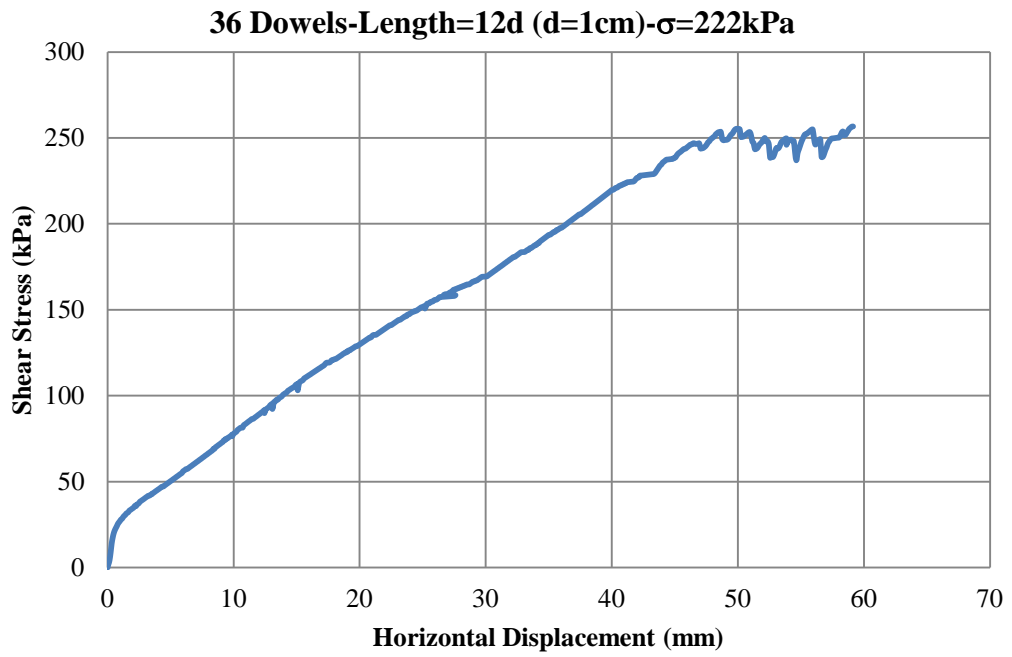


Figure C.68 Shear Stress vs. Displacement Graph-Experiment 35

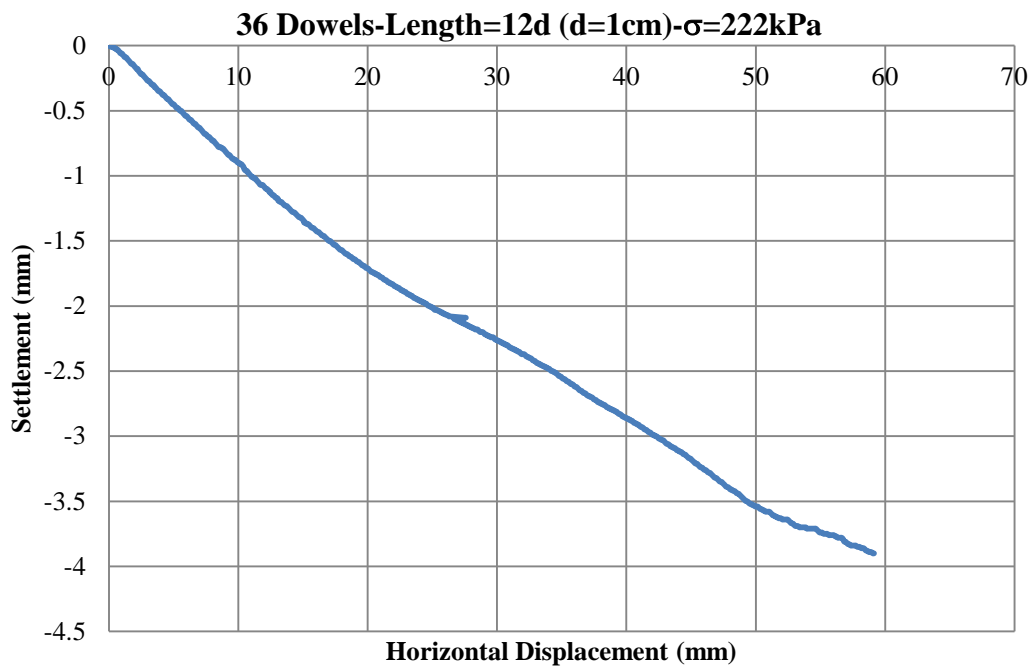


Figure C.69 Settlement vs. Displacement Graph-Experiment 35

## 8. Improvement Tests- W-1

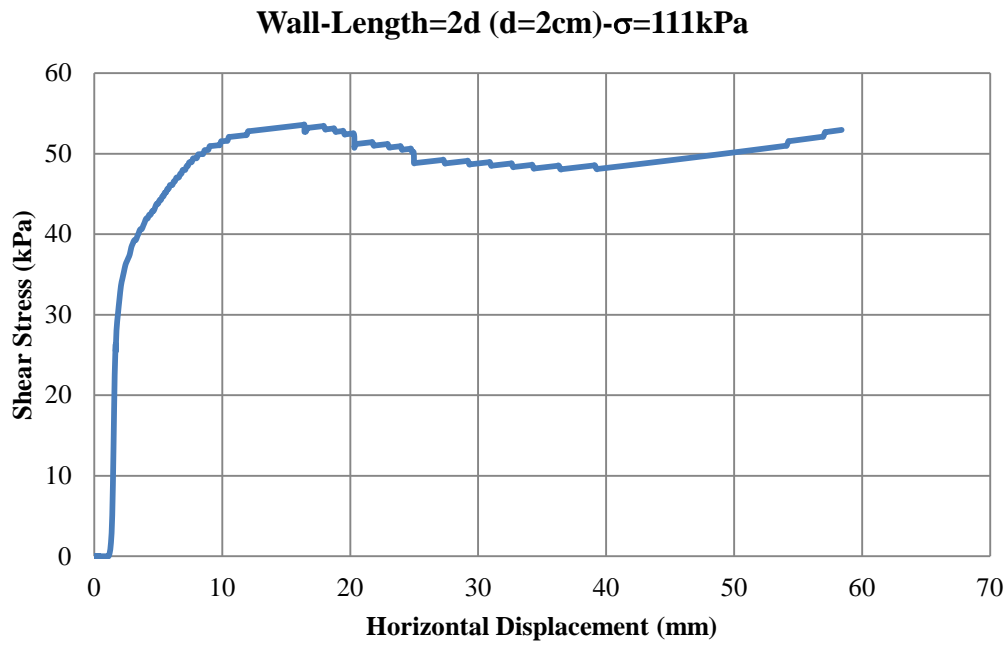


Figure C.70 Shear Stress vs. Displacement Graph-Experiment 1

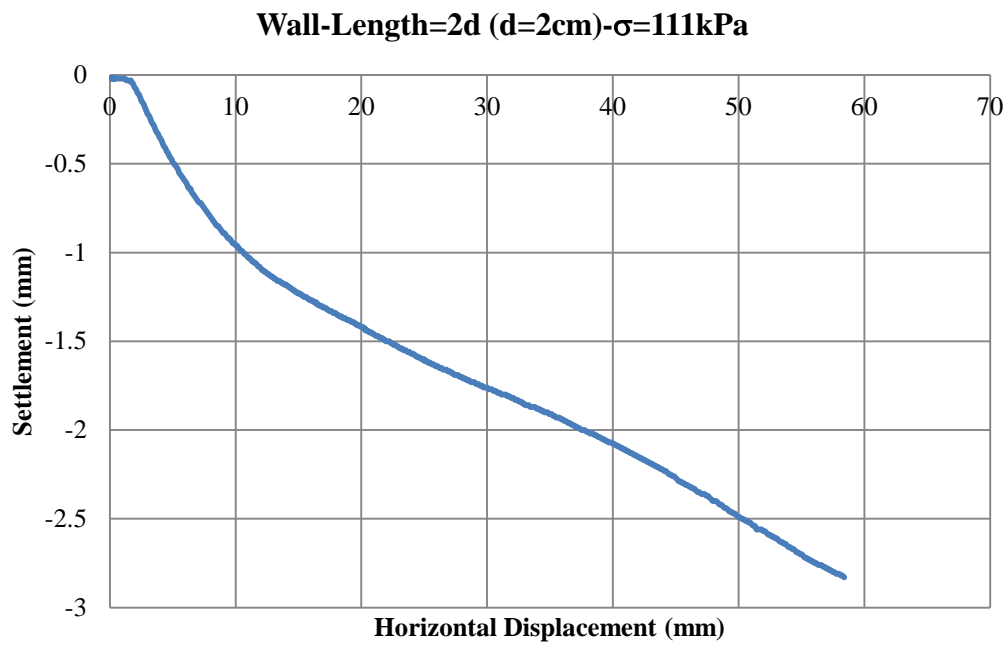


Figure C.71 Settlement vs. Displacement Graph-Experiment 1

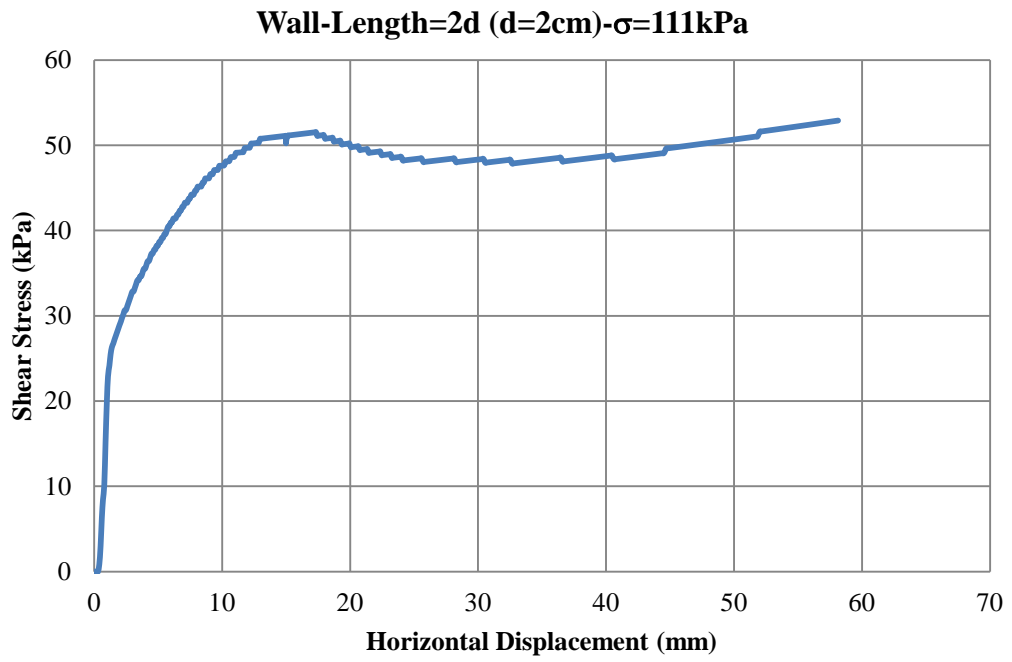


Figure C.72 Shear Stress vs. Displacement Graph-Experiment 2

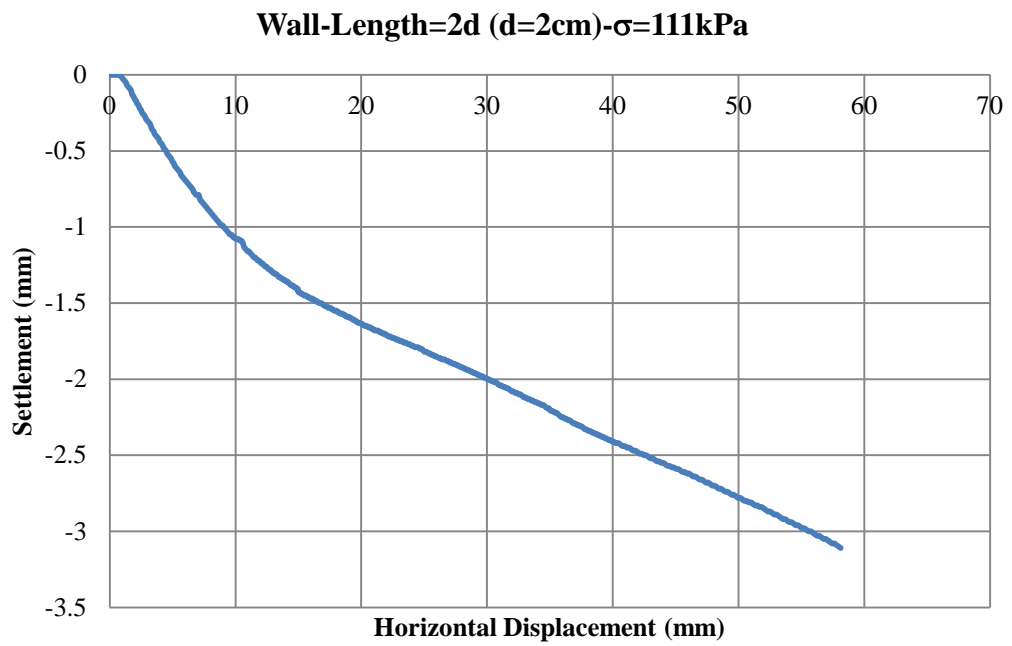


Figure C.73 Settlement vs. Displacement Graph-Experiment 2

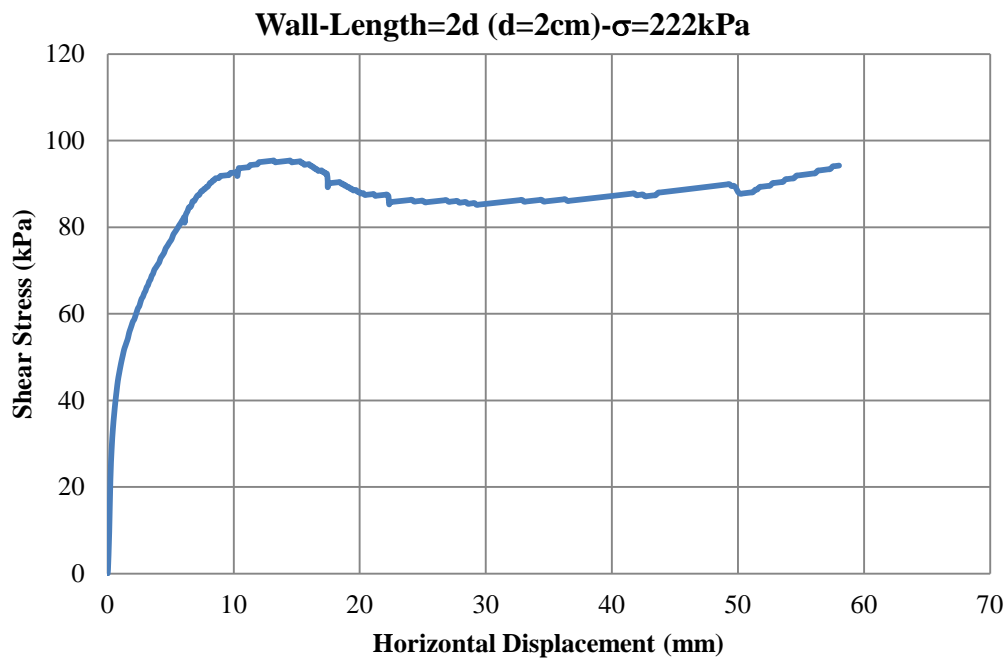


Figure C.74 Shear Stress vs. Displacement Graph-Experiment 3

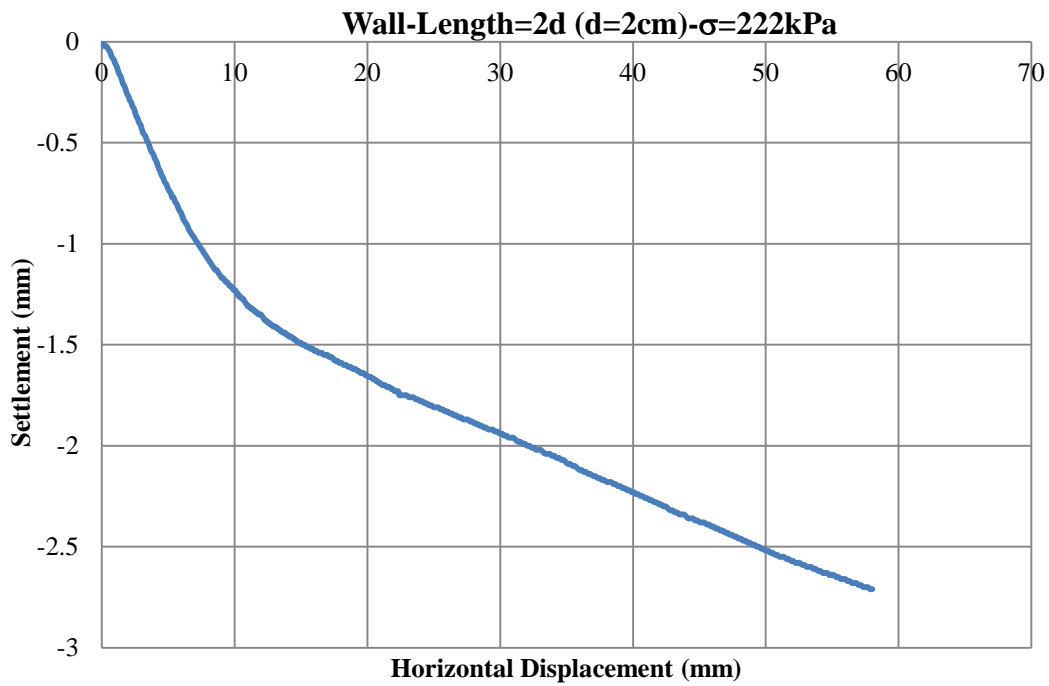


Figure C.75 Settlement vs. Displacement Graph-Experiment 3

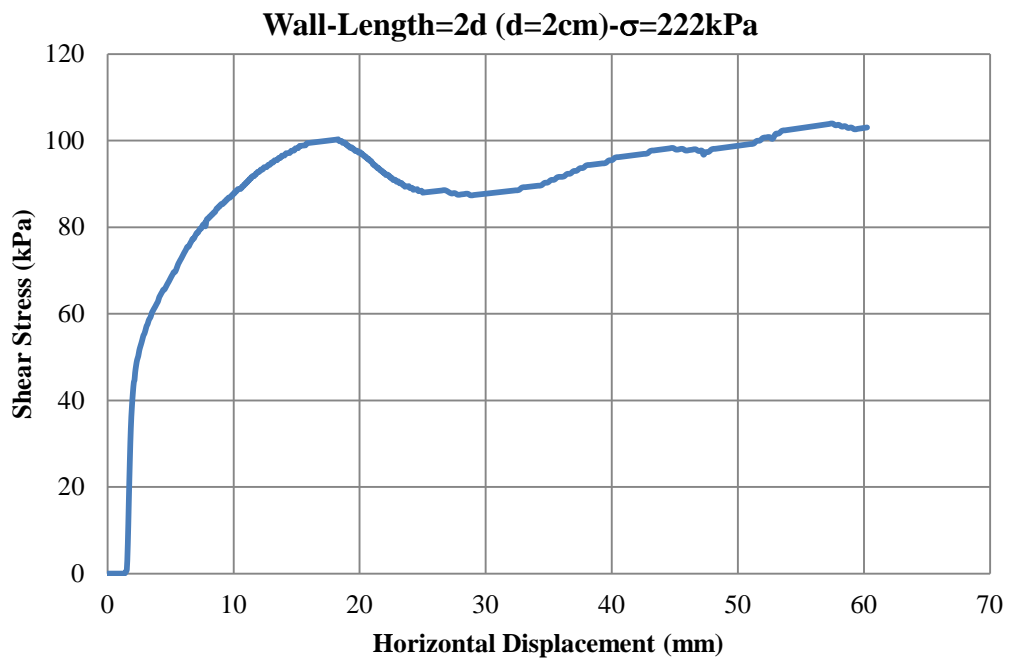


Figure C.76 Shear Stress vs. Displacement Graph-Experiment 4

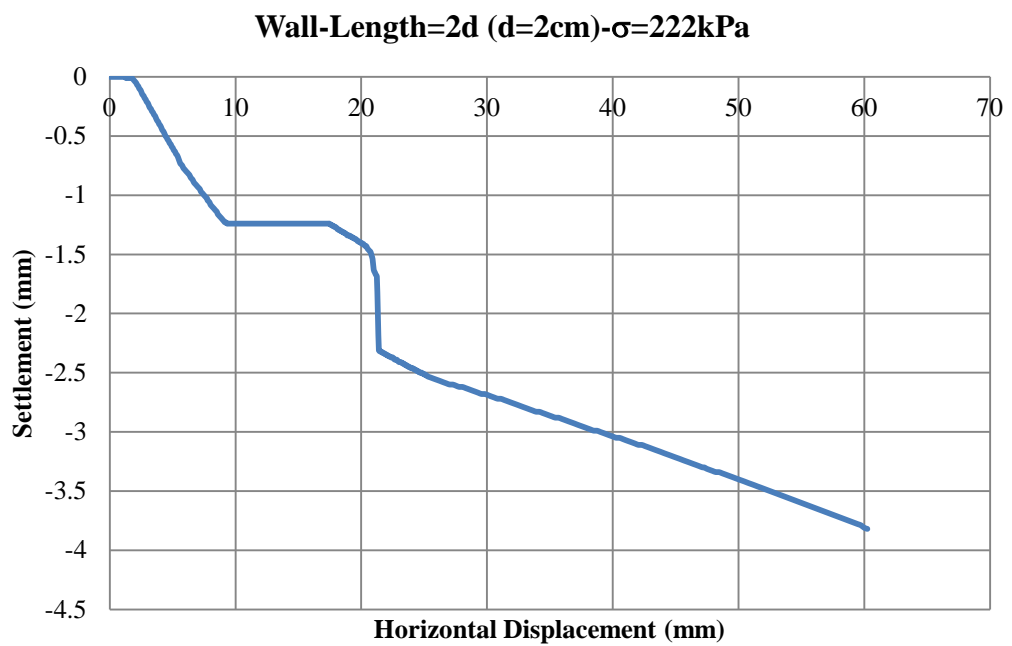


Figure C.77 Settlement vs. Displacement Graph-Experiment 4

## 9. Improvement Tests- W-2

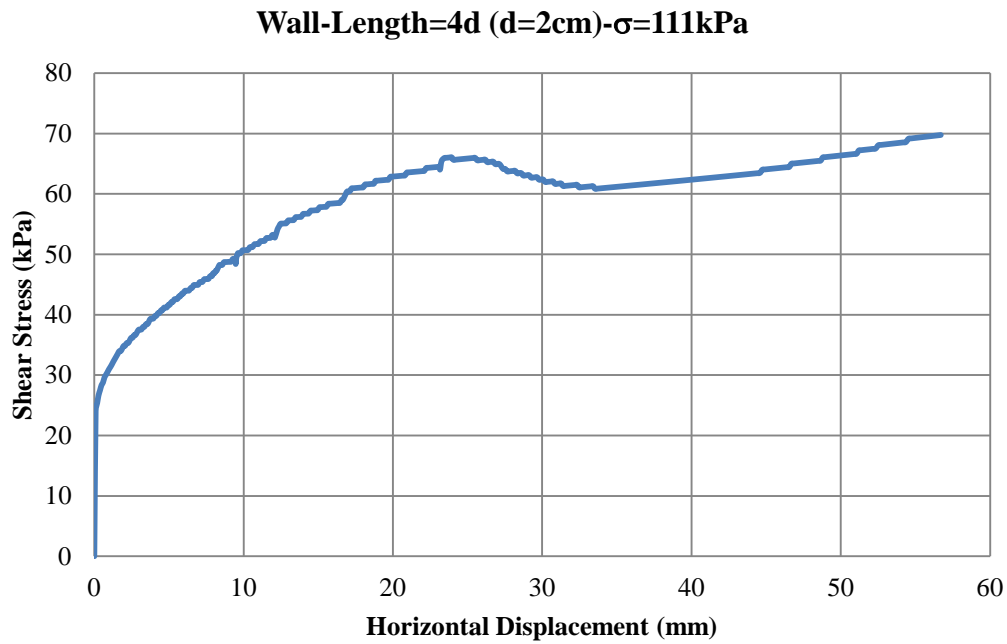


Figure C.78 Shear Stress vs. Displacement Graph-Experiment 5

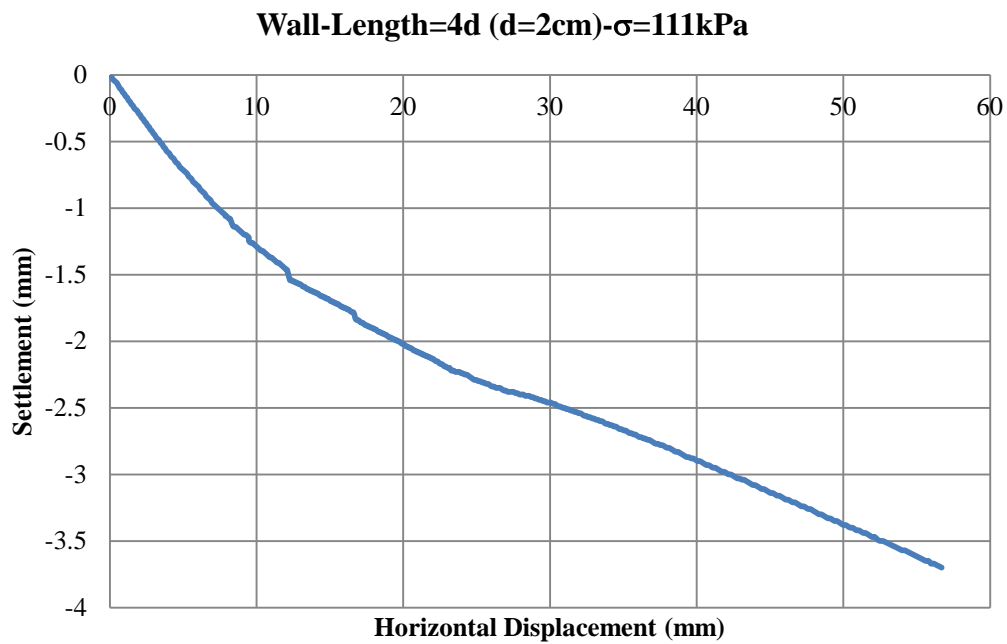


Figure C.79 Settlement vs. Displacement Graph-Experiment 5

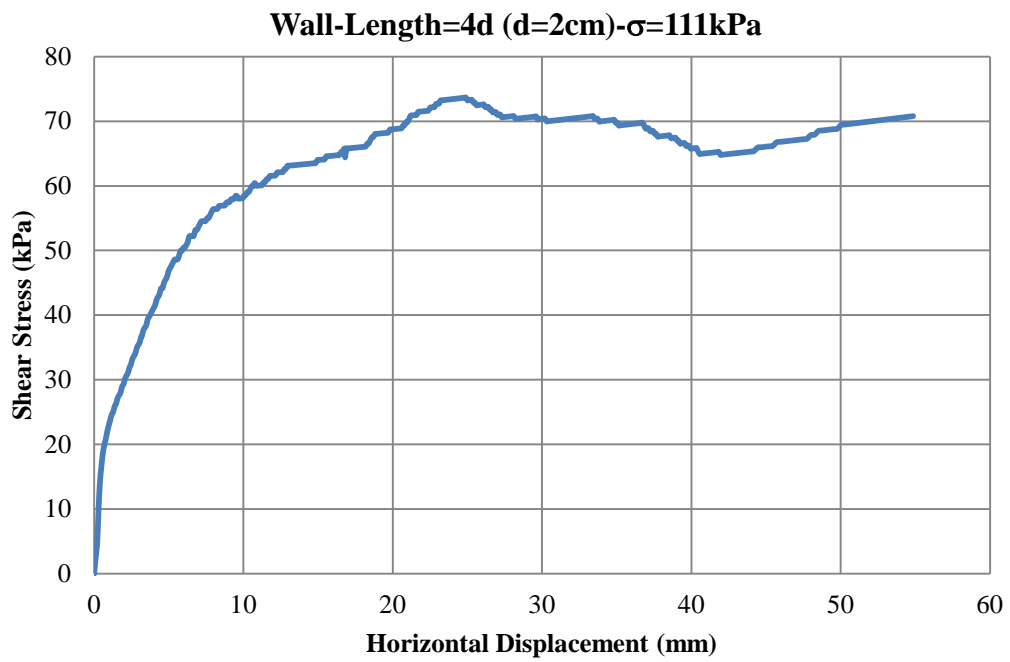


Figure C.80 Shear Stress vs. Displacement Graph-Experiment 6

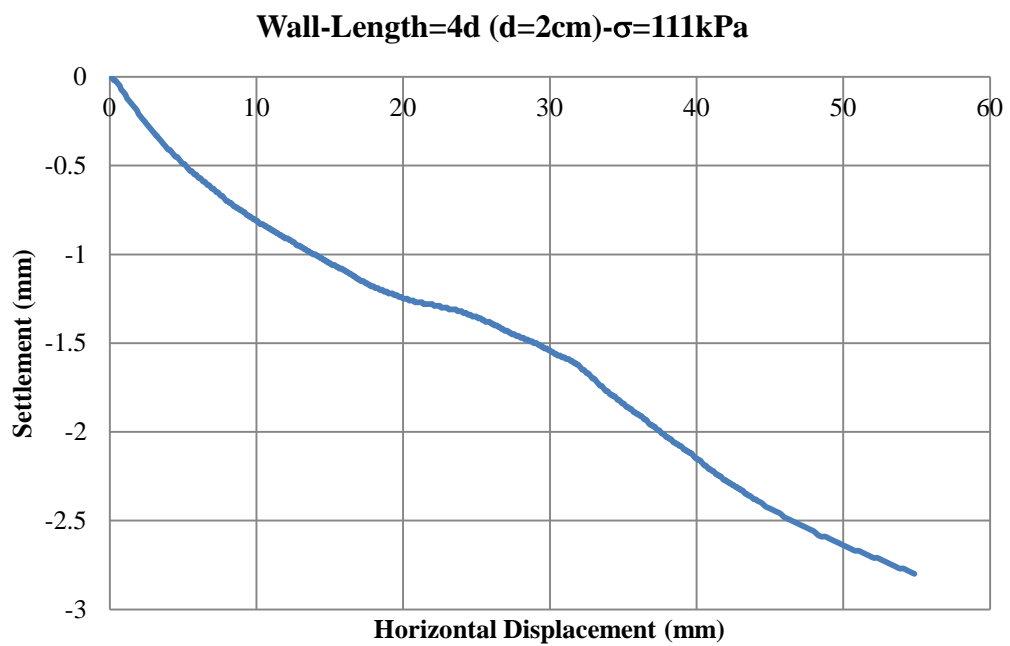


Figure C.81 Settlement vs. Displacement Graph-Experiment 6

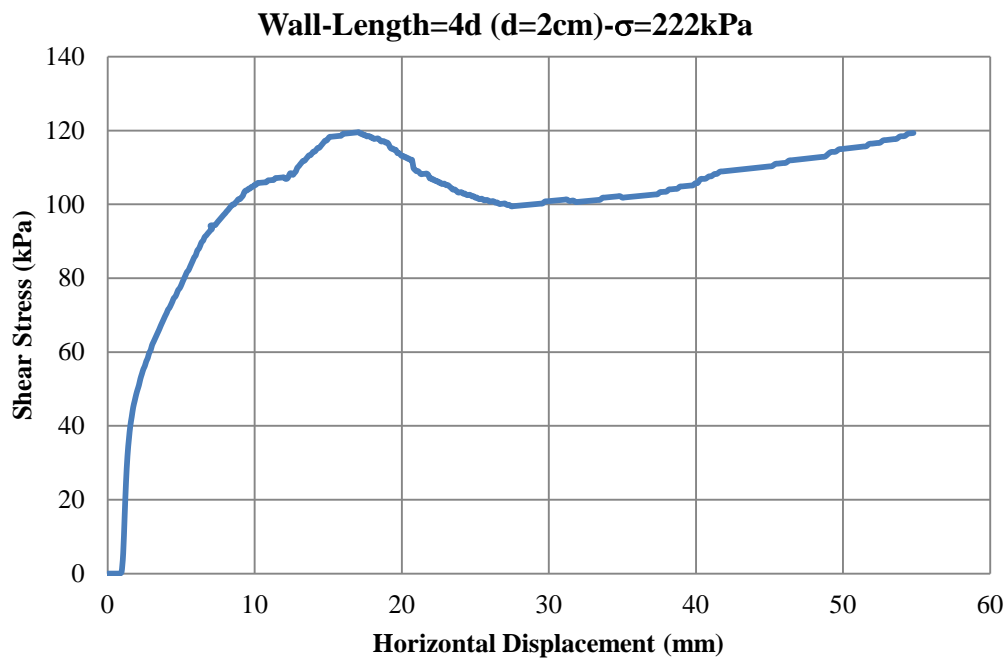


Figure C.82 Shear Stress vs. Displacement Graph-Experiment 7

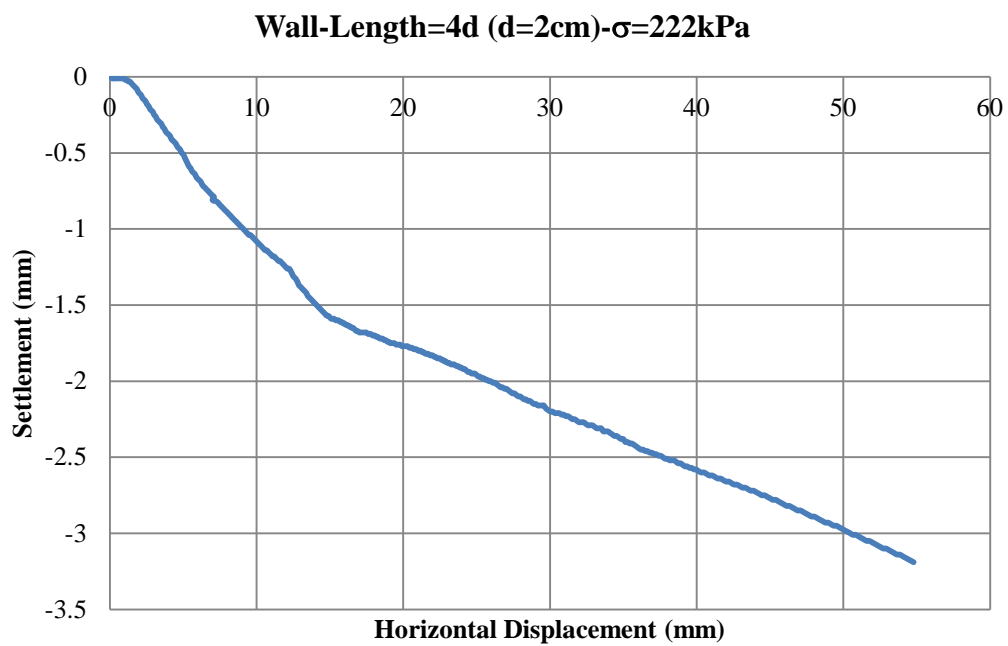


Figure C.83 Settlement vs. Displacement Graph-Experiment 7

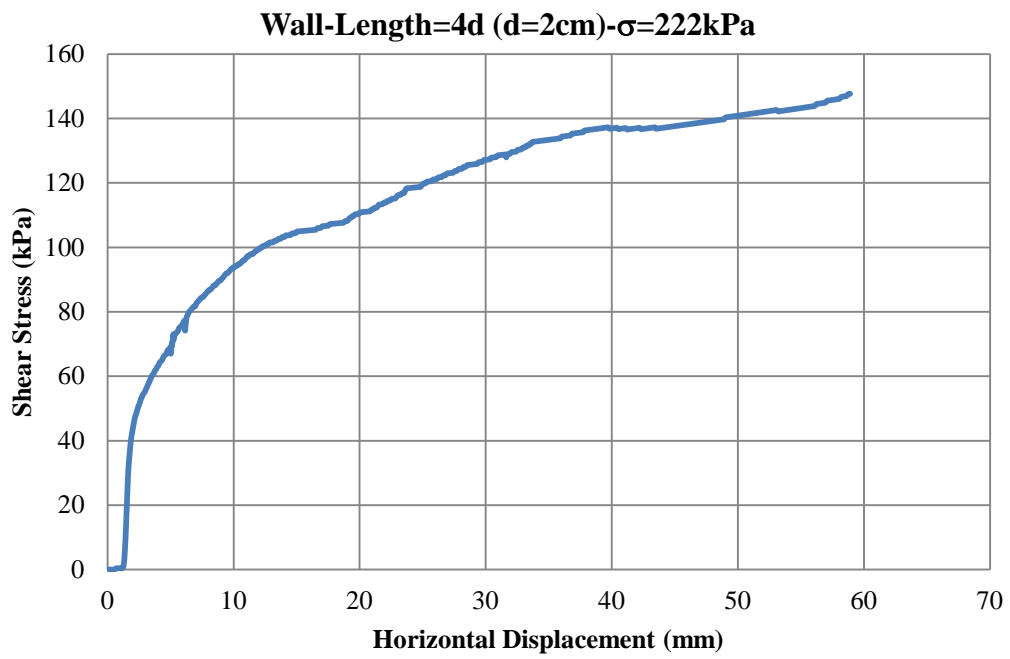


Figure C.84 Shear Stress vs. Displacement Graph-Experiment 8

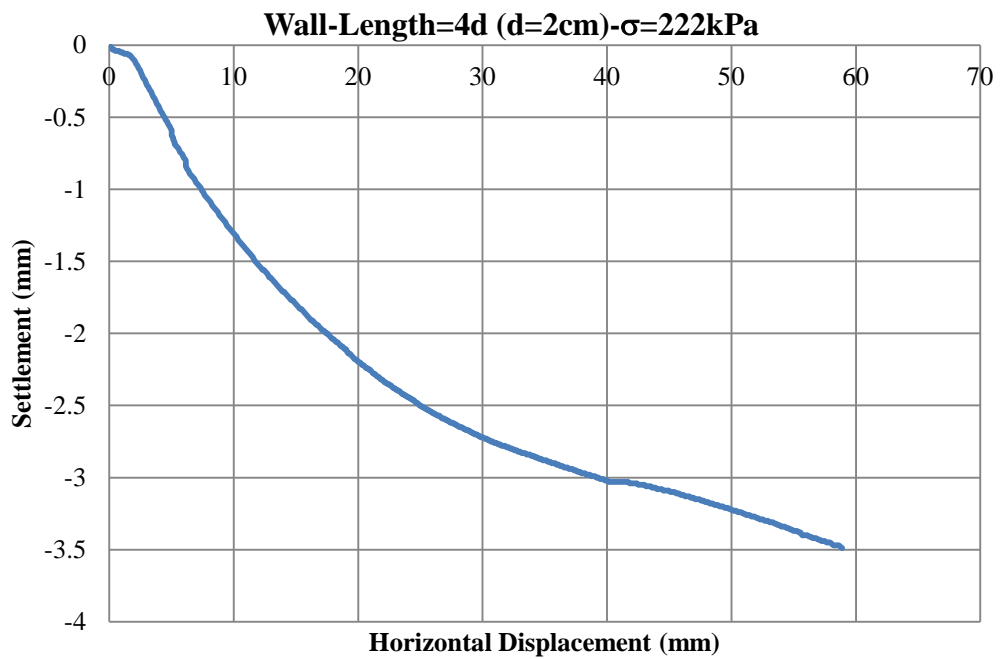


Figure C.85 Settlement vs. Displacement Graph-Experiment 8

### 10. Improvement Tests- W-3

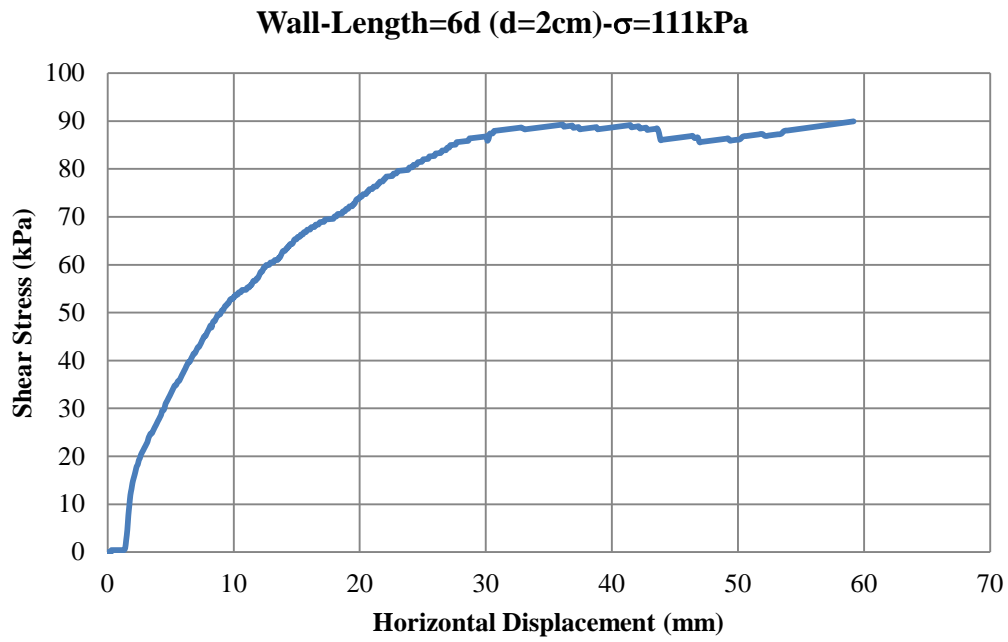


Figure C.86 Shear Stress vs. Displacement Graph-Experiment 9

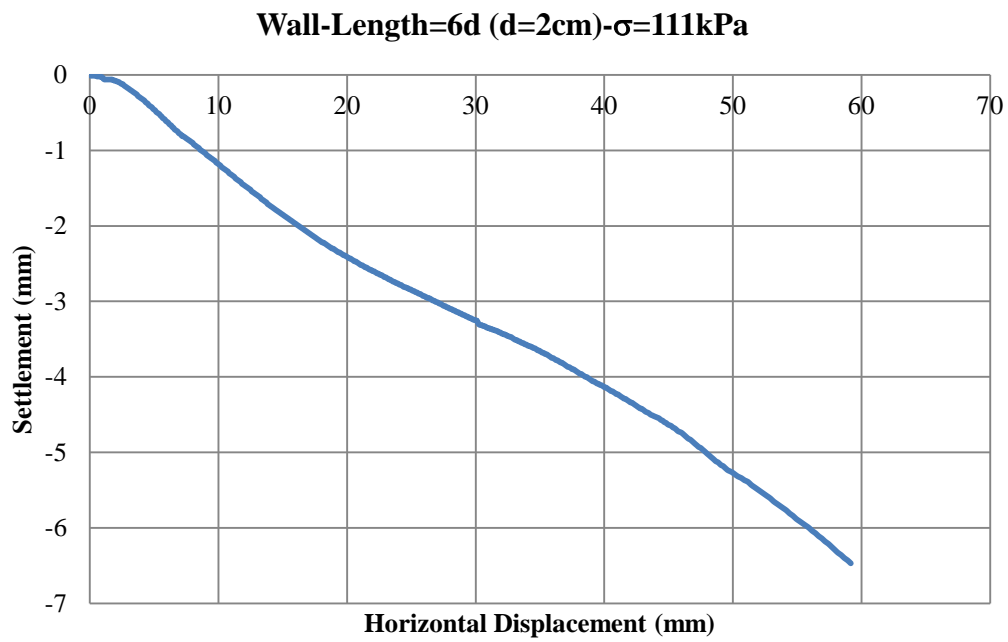


Figure C.87 Settlement vs. Displacement Graph-Experiment 9

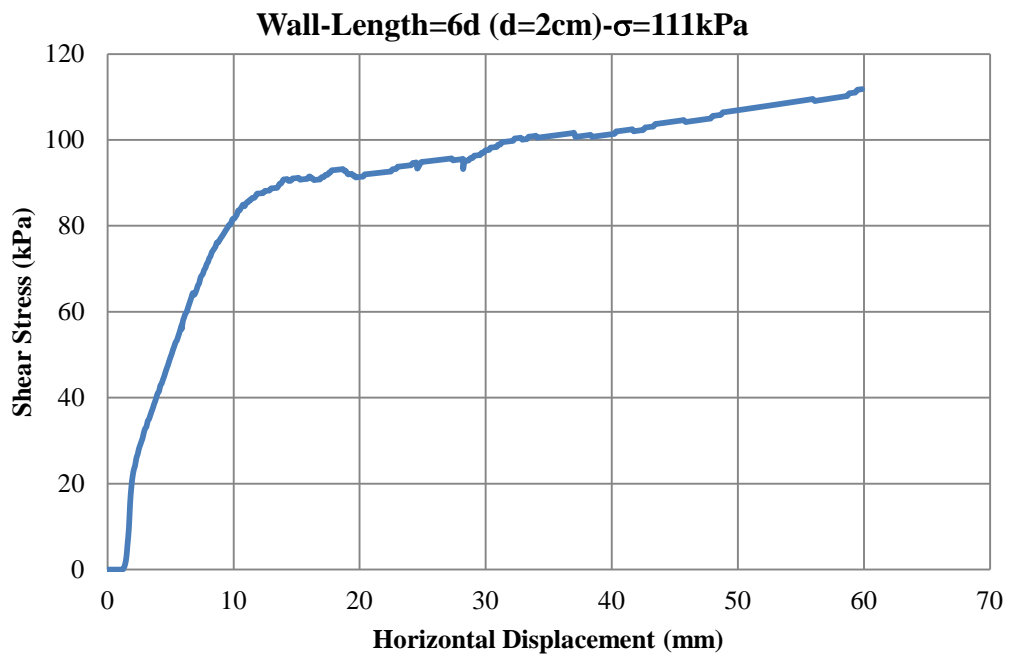


Figure C.88 Shear Stress vs. Displacement Graph-Experiment 10

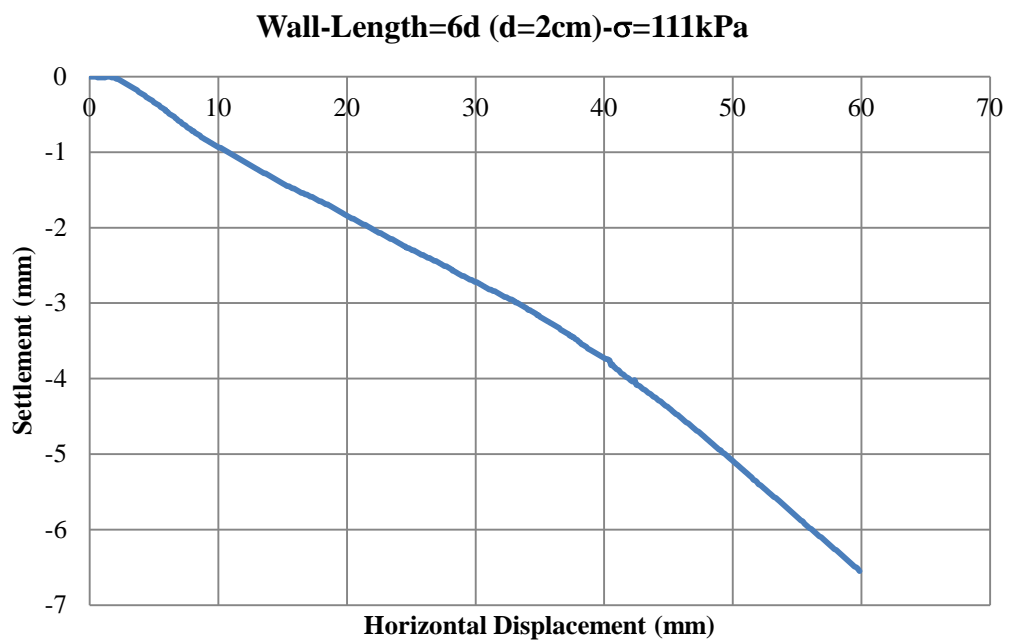


Figure C.89 Settlement vs. Displacement Graph-Experiment 10

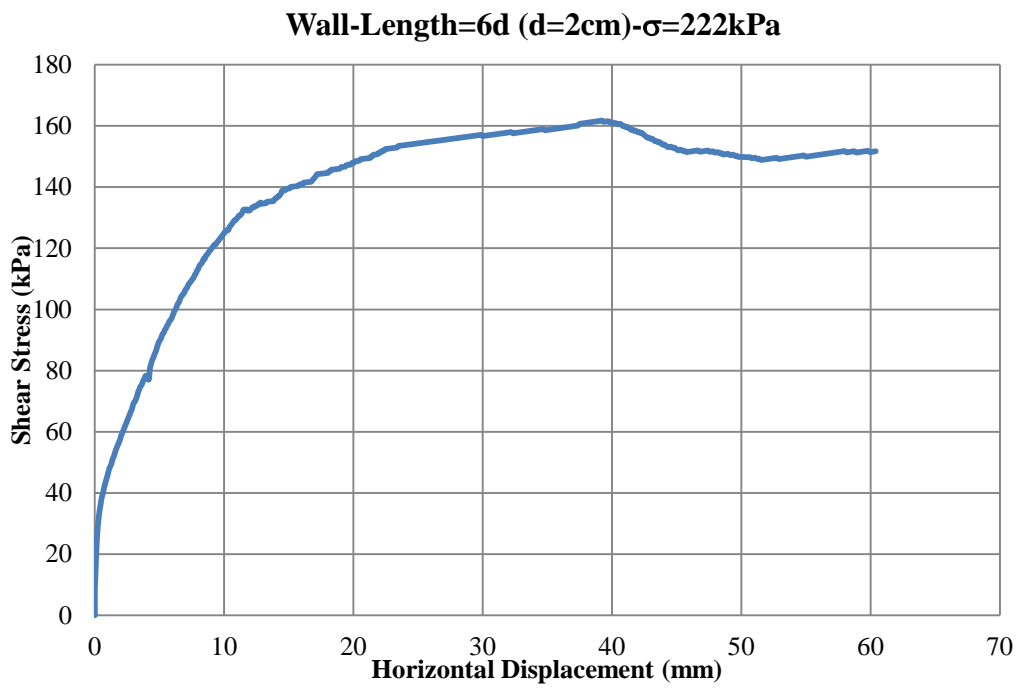


Figure C.90 Shear Stress vs. Displacement Graph-Experiment 11

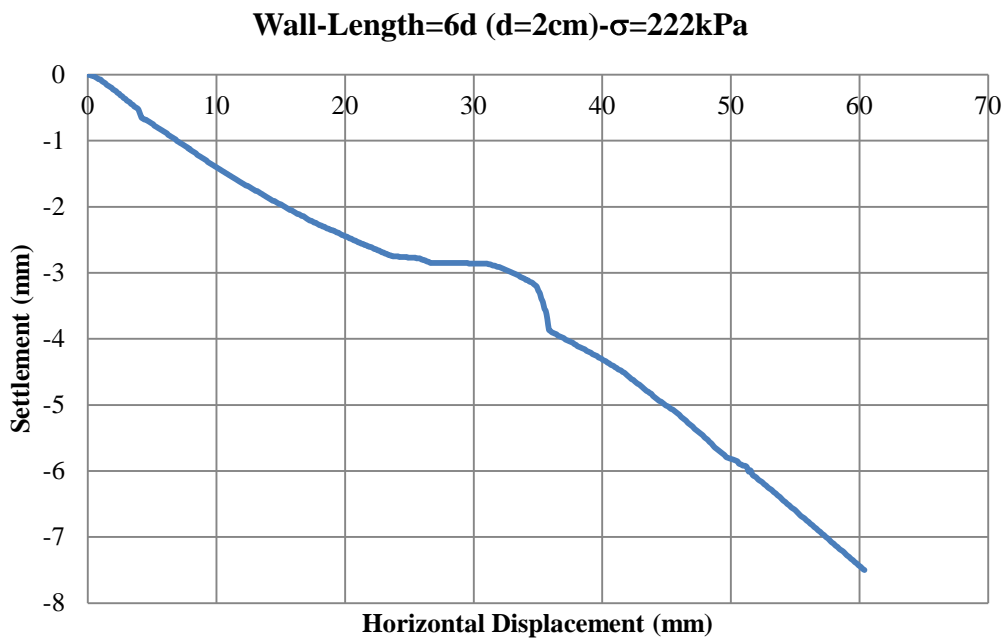


Figure C.91 Settlement vs. Displacement Graph-Experiment 11

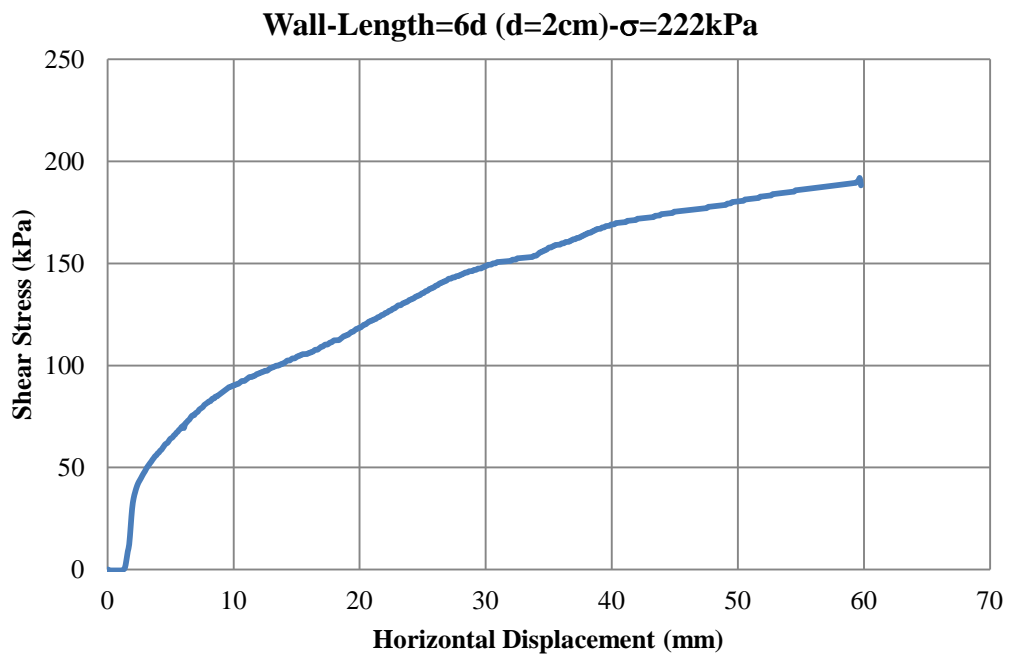


Figure C.92 Shear Stress vs. Displacement Graph-Experiment 12

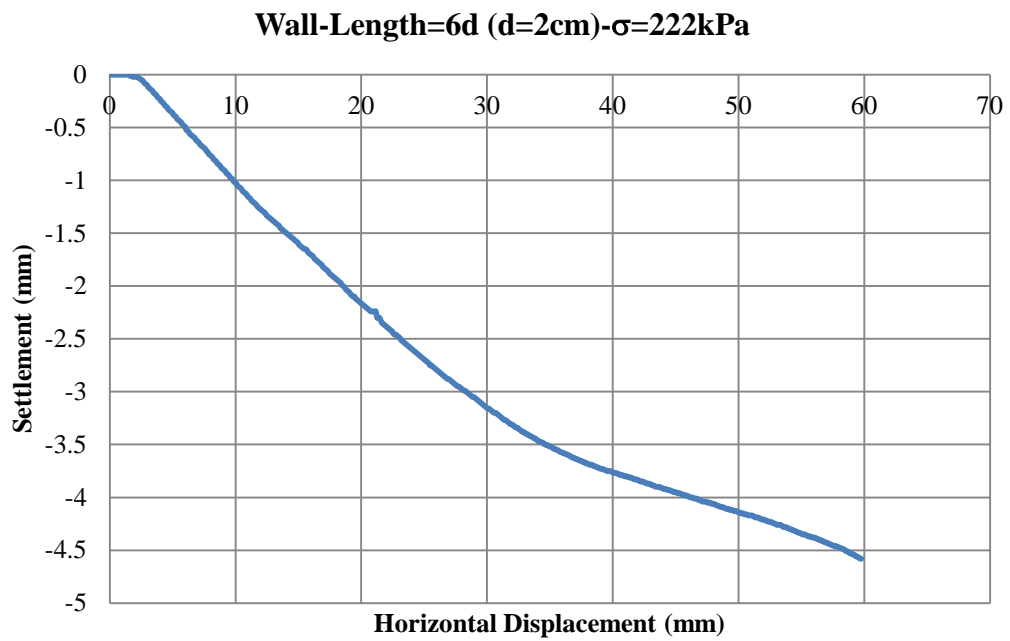


Figure C.93 Settlement vs. Displacement Graph-Experiment 12



## APPENDIX D

### UNCONSOLIDATED UNDRAINED (UU) TESTS OF CLAY (IMPROVEMENT TESTS)

#### 1. Improvement Tests- I-1

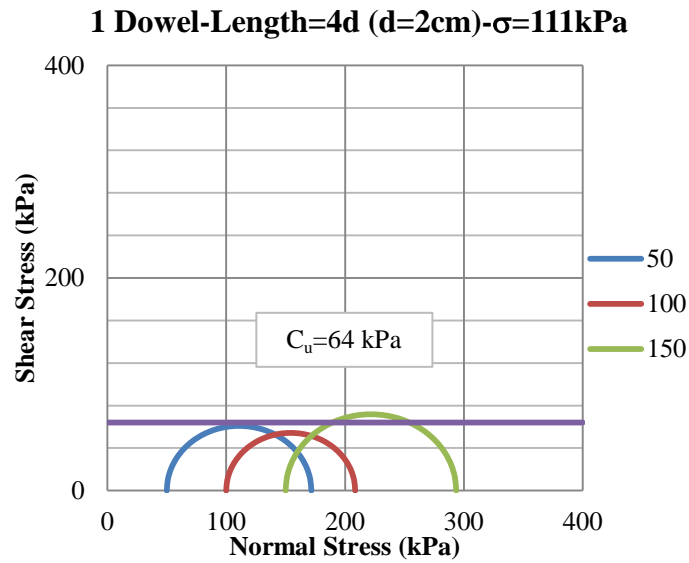


Figure D.1 Mohr Circles of UU Tests Performed-Interface Experiment No: 2

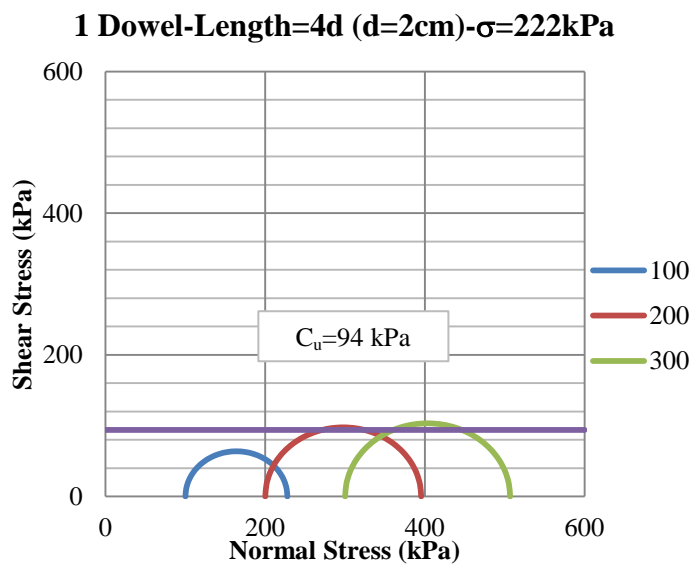


Figure D.2 Mohr Circles of UU Tests Performed-Interface Experiment No: 3

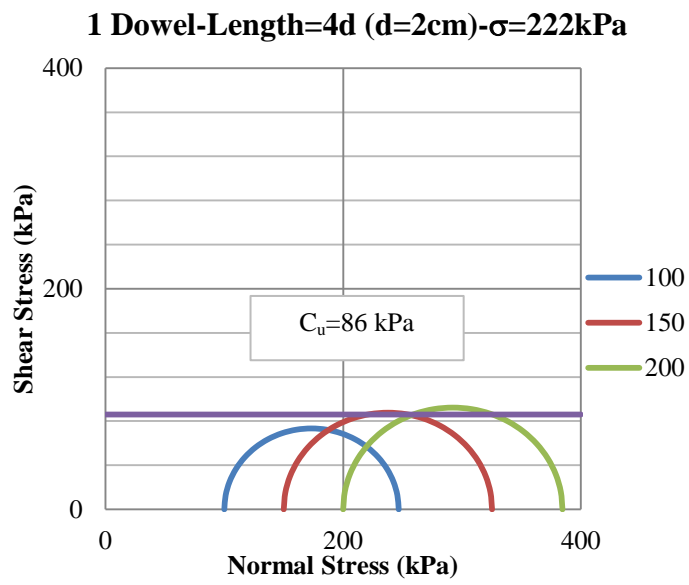


Figure D.3 Mohr Circles of UU Tests Performed-Interface Experiment No: 4

## 2. Improvement Tests- I-2

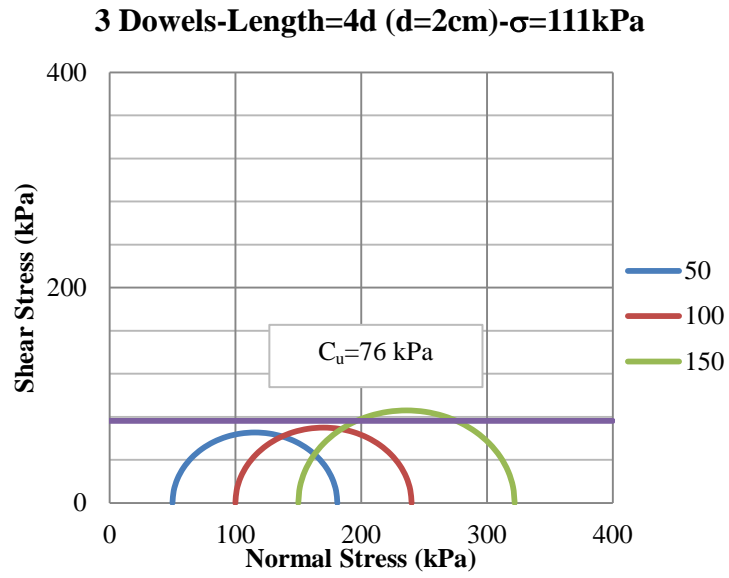


Figure D.4 Mohr Circles of UU Tests Performed-Interface Experiment No: 6

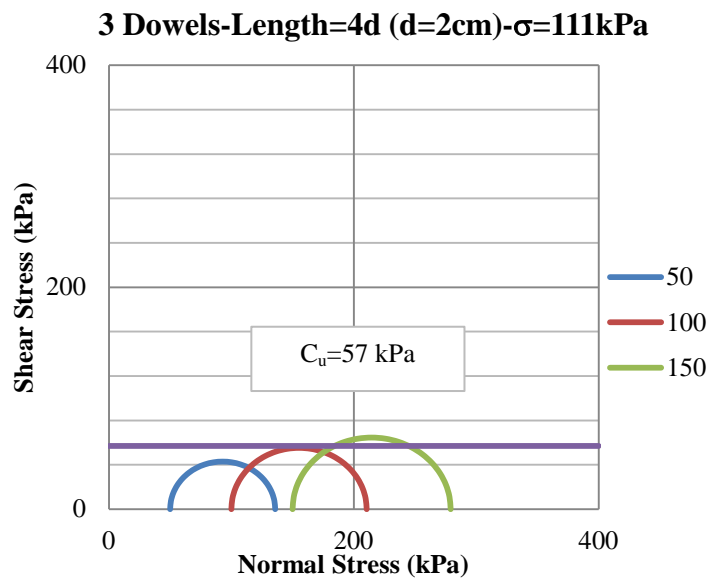


Figure D.5 Mohr Circles of UU Tests Performed-Interface Experiment No: 7

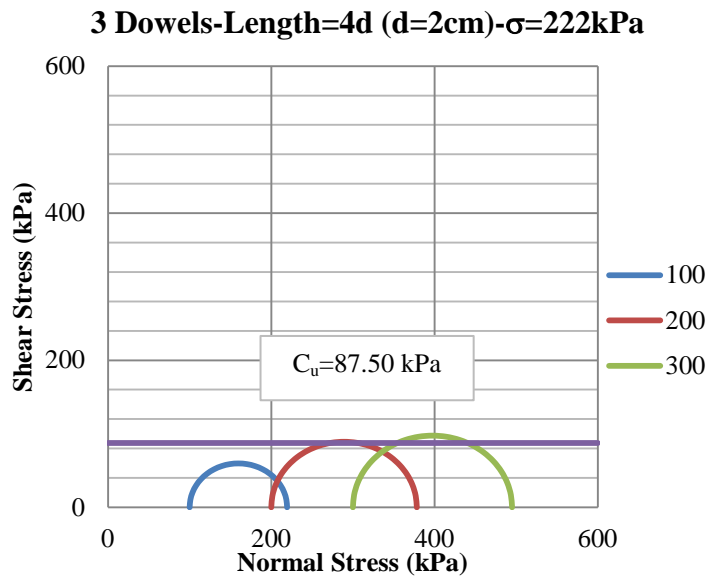


Figure D.6 Mohr Circles of UU Tests Performed-Interface Experiment No: 8

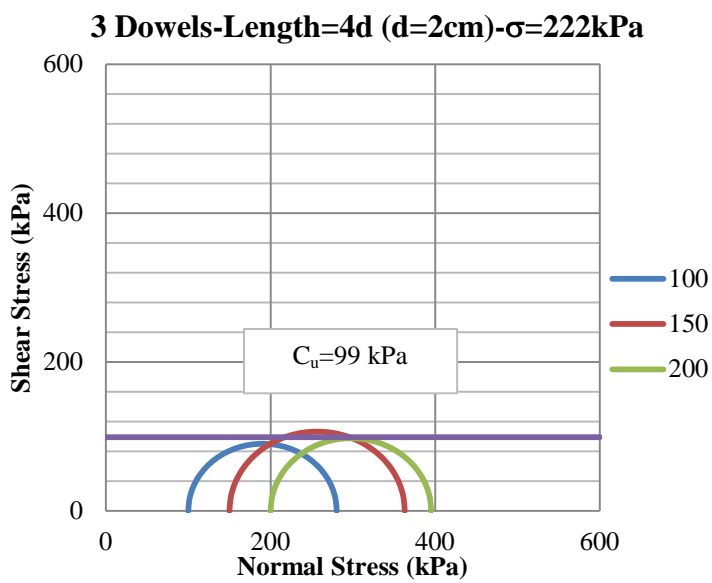


Figure D.7 Mohr Circles of UU Tests Performed-Interface Experiment No: 9

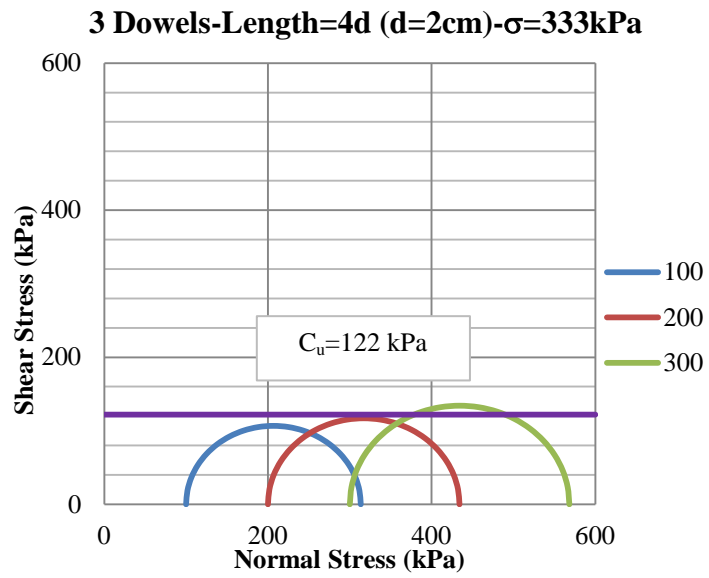


Figure D.8 Mohr Circles of UU Tests Performed-Interface Experiment No: 10

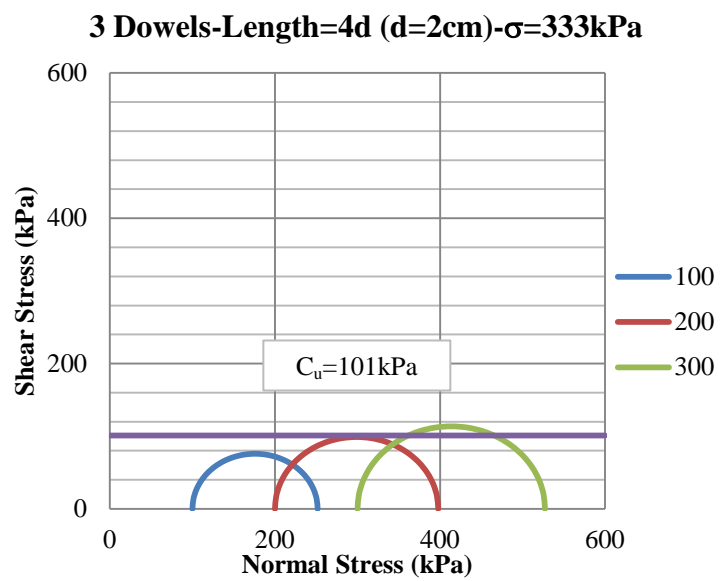


Figure D.9 Mohr Circles of UU Tests Performed-Interface Experiment No: 11

### 3. Improvement Tests- I-3

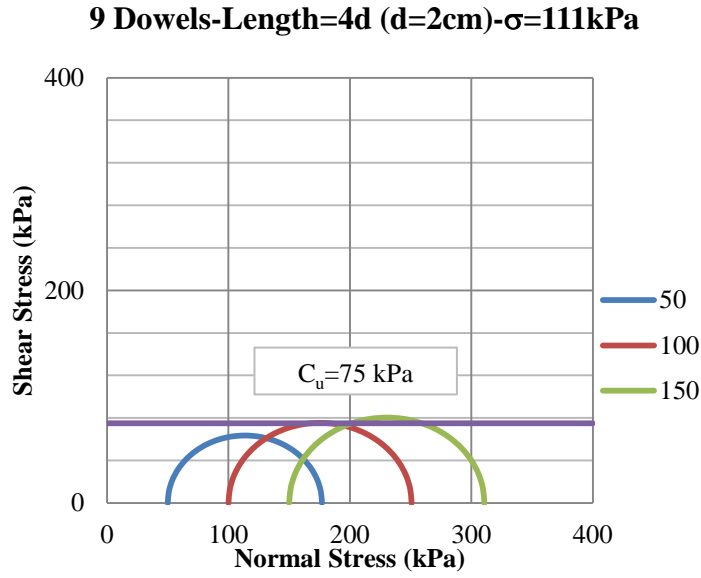


Figure D.10 Mohr Circles of UU Tests Performed-Interface Experiment No: 12

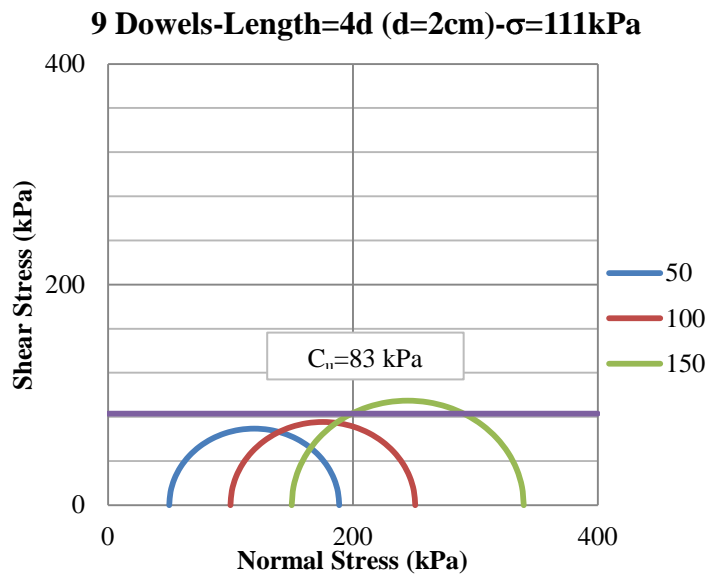


Figure D.11 Mohr Circles of UU Tests Performed-Interface Experiment No: 13

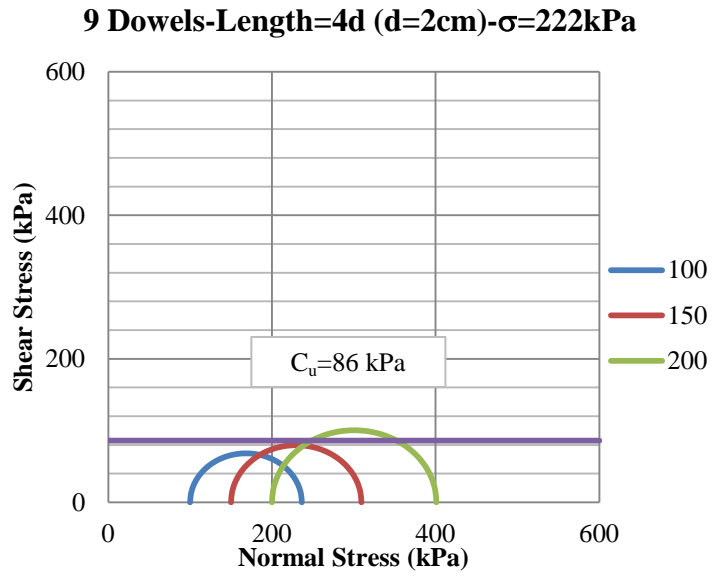


Figure D.12 Mohr Circles of UU Tests Performed-Interface Experiment No: 14

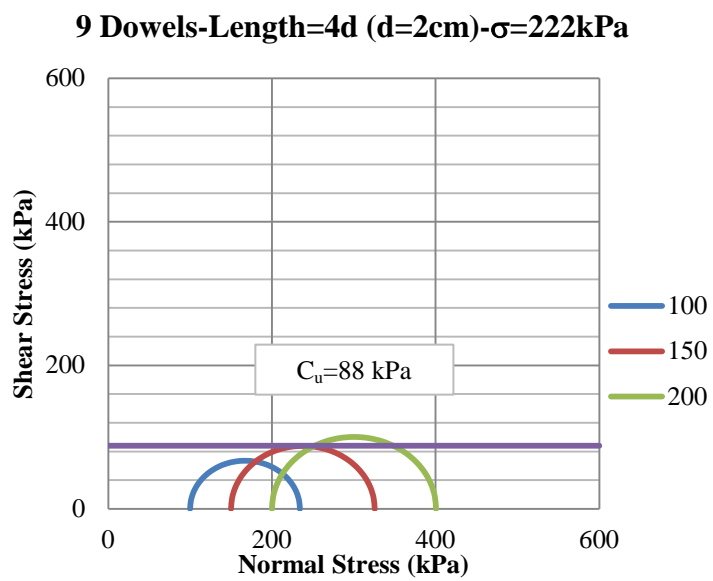


Figure D.13 Mohr Circles of UU Tests Performed-Interface Experiment No: 15

#### 4. Improvement Tests- I-4

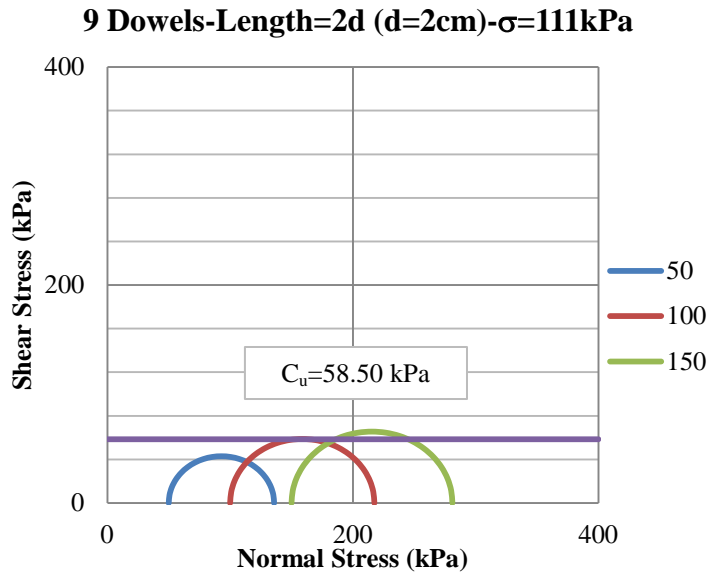


Figure D.14 Mohr Circles of UU Tests Performed-Interface Experiment No: 18

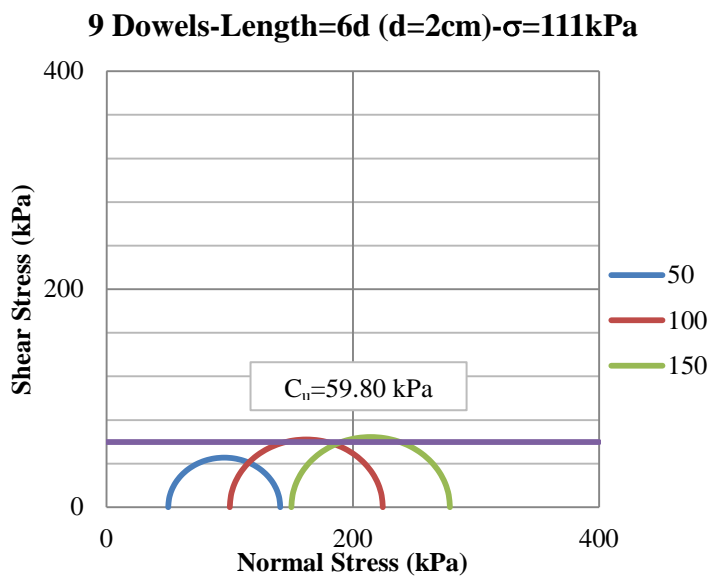


Figure D.15 Mohr Circles of UU Tests Performed-Interface Experiment No: 19

**9 Dowels-Length=2d (d=2cm)- $\sigma=222\text{kPa}$**

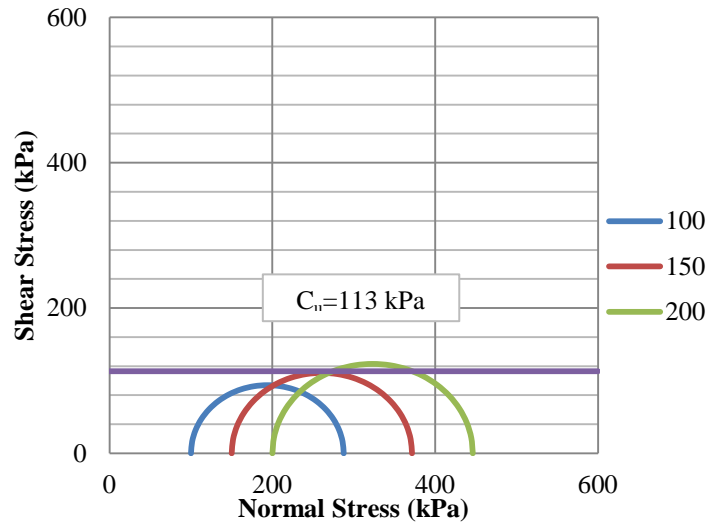


Figure D.16 Mohr Circles of UU Tests Performed-Interface Experiment No: 20



## APPENDIX E

### AREA AND MEMBRANE CORRECTION IN TRIAXIAL TESTS

In triaxial tests, two main corrections were executed for the results of experiments which are area correction and membrane correction. Depending on the failure behavior of specimen, formulation for area correction and membrane correction differs.

In triaxial tests of soft soils, area of the specimen changes according to bulging behavior of the specimen. For stiff soils, a shear plane is formed and area of the specimen changes due to movement along this shear plane. Area correction and membrane correction formulations for two different failure mechanisms are given below.

#### Corrected Area for Bulging Behavior:

$$A = A_c \frac{(1-\varepsilon_v)}{(1-\varepsilon_a)} \quad (\text{E.1})$$

where;

$A_c$  = Area after consolidation

$\varepsilon_v$  = Volumetric strain

$\varepsilon_a$  = Axial strain

#### Corrected Area for Shear Plane Behavior:

$$A = \frac{d_0^2}{4} \left( \frac{\pi\theta}{180} - \sin \theta \right) \quad (\text{E.2})$$

where;

$$\theta = 2\cos^{-1} (2\delta/\tan\alpha)$$

$$\delta = \Delta h/h$$

$\Delta h$  = Decrease of height to the plane shearing movement

$h$  = Height at the start point of shear plane movement

$d_0$  = Initial diameter of specimen

Membrane Correction for Bulging Behavior:

$$\sigma = \frac{4M\varepsilon_a}{d_0} \quad (E.3)$$

where

$\sigma$  = Deviator stress correction

$M$  = Modulus of membrane

$\varepsilon_a$  = Axial strain

$d_0$  = Initial diameter of specimen

Membrane Correction for Shear Plane Behavior:

$$\sigma A_c = 1.5\pi d_0 \sqrt{Mf d_0 \delta} \quad (E.4)$$

where

$\sigma$  = Deviator stress correction

$A_c$  = Area of specimen

$M$  = Modulus of membrane

$f$  = Unit friction between soil and membrane =  $\sigma_3 \tan \phi$

$d_0$  = Initial diameter of specimen

$$\delta = \Delta h/h$$

$\Delta h$  = Decrease of height to the plane shearing movement

$h$  = Height at the start point of shear plane movement

The area correction formulation given above for bulging type of failure based on assumption of cylindrical deformation of the specimen. La Rochelle et al. (1967) concluded that this approximate formula was satisfactory since difference of this approximation from other calculations is small. Other formulations were based on assumptions being not more realistic from the assumption of the given formula above according to La Rochelle et al (1967).

For interface experiments (clay-clay, gravel-clay and sand-clay), both of two failure mechanisms are valid. Initially specimen undergoes a bulging type of failure and then upper specimen starts to move on the lower clay part along the interface resulting in plane shearing failure. Therefore both of two different area correction methodologies given above are valid for interface experiments conducted. However, it is difficult to observe the starting time of transition of failure mode during experiments. Since the sliding along the interface could not be measured exactly after each test, transition point was not estimated from back calculations based on measurements.

Chandler (1966) conducted triaxial tests on clay-clay interfaces and concluded that movement along shear plane started after maximum stress on plane was approached. The reduction in volume was observed to be reduced as movement continued. Meehan et al. (2011) also considered peak stresses and volume reduction as indication of transition point for failure mechanism.

Considering abovementioned conclusions of early researchers and observations during experiments, the transition point for failure mode for clay-clay interface experiments was chosen to be the point where peak deviator stresses obtained. In area correction and membrane correction of clay-clay experiments, formulas given for bulging type of failure were used up to peak deviator stresses were reached and after that point formulas given for shear plane failure were used.

For sand-clay and gravel-clay interfaces, observed movement due to shear plane behavior is small. Also axial load measured were generally constant after peak

value reached. The correction used in clay-clay experiments (only shear plane correction after peak point) lead to increase in deviator stresses for sand-clay and gravel-clay interfaces which is not a realistic soil behavior. Another observation was the spreading of sand or gravel on lower clay specimen while moving along the shear plane. Due to these facts, shear plane correction was not applied to sand-clay and gravel-clay interfaces.

In gravel-clay and sand-clay interfaces only bulging type of corrections were applied as discussed above. Axial strain given and volume change observed during experiments are distributed to upper granular material (sand or gravel) and lower clay according to behaviors observed in individual triaxial tests of granular material and clay.

## CURRICULUM VITAE

### PERSONAL INFORMATION

Surname, Name: Öztürk, Şevki

Nationality: Turkish (TC)

Date and Place of Birth: 27 May 1981, Çankırı

Phone: +90 312 219 72 58

Mobile: +90 542 653 35 44

e-mail: sevkice@gmail.com

### EDUCATION

Degree	Institution	Year of Graduation
MS	METU Civil Engineering	2009
BS	METU Civil Engineering	2003
High School	Çankırı Anatolian High School	1999

### WORK EXPERIENCE

Year	Place	Enrollment
2014-Present	GEOCE Geotechnical Co.	Partner-Geot.Eng.
2009 – 2014	METU Civil Eng. Dept.	Research Assistant
2004-2009	TİNSA Construction Co.	Project Man. Chief
2003-2004	ALİZE Co.	Site Engineer

## **FOREIGN LANGUAGES**

Advanced English, Fluent German

## **PUBLICATIONS**

1. Şengör M., Tekin M., Pekcan O., Öztürk Ş., and Ergun M.U. (2012). Settlement of Foundations on Soils Improved by Columns. Proceedings of ACE 2012 Congress, METU, Ankara.
2. Öztürk Ş., and Ergun M.U. (2010). Distribution of Bending Moments in Laterally Loaded Passive Pile Groups. 13rd National Conference on Soil Mechanics and Foundation Engineering, İKÜ, İstanbul.